Oxidative Medicine and Cellular Longevity

Natural Bioactive Products with Antioxidant Properties Useful in Neurodegenerative Diseases

Lead Guest Editor: Francisco J.B. Mendonça Júnior
Guest Editors: Luciana Scotti, Marcus T. Scotti, Anuraj Nayarisseri, and Ernestine N. Zondegoumba

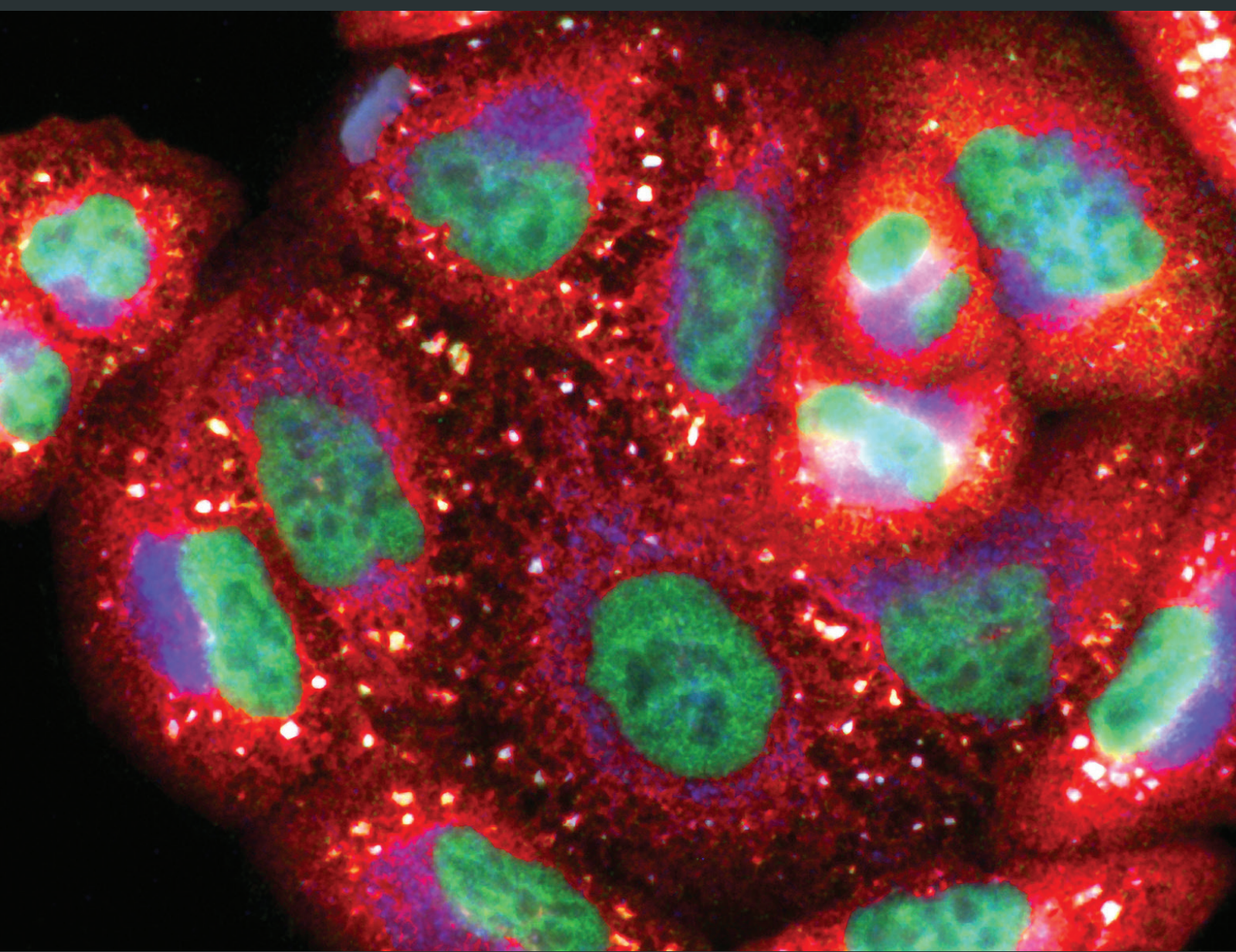

Natural Bioactive Products with Antioxidant Properties Useful in Neurodegenerative Diseases

Oxidative Medicine and Cellular Longevity

Natural Bioactive Products with Antioxidant Properties Useful in Neurodegenerative Diseases

Lead Guest Editor: Francisco J.B. Mendonça Júnior
Guest Editors: Luciana Scotti, Marcus T. Scotti, Anuraj Nayarisseri, and Ernestine N. Zondegoumba

Editorial Board

Contents

Hindawi
Oxidative Medicine and Cellular Longevity
Volume 2019, Article ID 7151780, 2 pages
https://doi.org/10.1155/2019/7151780

Editorial

Natural Bioactive Products with Antioxidant Properties Useful in Neurodegenerative Diseases

Francisco J. B. Mendonça-Junior,[1,2] **Marcus T. Scotti**,[1] **Anuraj Nayarisseri**,[3,4] **Ernestine N. T. Zondegoumba**,[5] **and Luciana Scotti**[1,6]

[1]*Postgraduate Program in Natural and Synthetic Bioactive Products, Federal University of Paraíba, João Pessoa, PB, Brazil*
[2]*Laboratory of Synthesis and Drug Delivery, Department of Biological Science, State University of Paraiba, João Pessoa, PB, Brazil*
[3]*In Silico Research Laboratory, Eminent Biosciences, Indore, 452010 Madhya Pradesh, India*
[4]*Bioinformatics Research Laboratory, LeGene Biosciences Pvt. Ltd., Indore, 452010 Madhya Pradesh, India*
[5]*Department of Organic Chemistry, Faculty of Science, University of Yaoundé I, PO Box 812, Yaoundé, Cameroon*
[6]*Teaching and Research Management-University Hospital, Federal University of Paraíba, João Pessoa, PB, Brazil*

Correspondence should be addressed to Francisco J. B. Mendonça-Junior; franciscojbmendonca@yahoo.com.br

Received 12 March 2019; Accepted 13 March 2019; Published 9 May 2019

Neurodegenerative diseases (NDs) constitute a large group of pathological conditions, characterized by a progressive loss of neuronal cells, which compromise motor and/or cognitive functions. The most common NDs are Alzheimer's disease (AD), amyotrophic lateral sclerosis (ALS), Parkinson's disease (PD), and Huntington's disease (HD). The causes of these pathologies are multifactorial and not fully understood, but it is well known that factors related to aging and to the overproduction of free radical and reactive oxygen species lead to oxidative stress and to cell death, which are extremely related. Whereas oxidative stress plays an unquestionable and central role in NDs, the control of free radicals and reactive oxygen species levels represents an interesting and promising strategy to delay neurodegeneration and attenuate the associated symptoms.

In this context, several natural bioactive compounds isolated from plants, fungi, and algae, among others, and also synthetic compounds inspired by natural scaffolds, which present antioxidant properties, including vitamins C and E, anthocyanins, and phenolic compounds, are extensively described as potential palliative agents of neurodegenerative symptoms. *In vitro* and *in vivo* studies, performed with extracts and fractions of plants and with isolated natural bioactive compounds, provide evidence of the role of these substances in the modulation of the cellular redox balance and in the reduction of the formation of reactive oxygen species originating from oxidative stress, thereby demonstrating their great value as antioxidant agents and cellular protectors.

In this special issue, articles were selected that address new therapeutic alternatives on the antioxidant and anti-inflammatory role and the consequent neuroprotetor of natural (or inspired) bioactive compounds in the prevention/-treatment or improvement of neurodegenerative diseases. This special issue compiles fifteen (15) manuscripts including three (3) reviews and twelve (12) research papers, which show recent research about the discovery of plant-derived antioxidants with application in neurodegenerative diseases.

The review by R. Avila-Sosa et al. describes the antioxidant effects of main bioactive components isolated from Amazonian fruits. Among other activities, the authors highlight antioxidants, immunomodulatory, anticancer, anti-inflammatory, and antidepressant properties of phenolic compounds, unsaturated fatty acids, carotenoids, phytosterols, and tocopherols.

The review by X. Zhao et al. highlights the benefits of vitamin supplementation in the treatment or improvement of the clinical symptoms of Parkinson's disease. The authors summarized the biological correlations between vitamins and

PD as well as the underlying pathophysiological mechanisms, demonstrating that the antioxidant properties and the regulatory gene expression promoted by vitamins are beneficial for the treatment/prevention of PD.

Due to the fact that many diseases that affect the central nervous system also promote blood-brain barrier (BBB) destruction, consequently increasing BBB permeability, in the third review, Z. Chen et al. carry out a systematic review of about the evidence of possible neuroprotective borneol (terpenoid) effects for ischemic stroke. The authors have found much evidence that borneol exerted a significant decrease of BBB permeability, thus acting as a neuroprotector.

Ten of the eleven research articles deal with the proof of antioxidant, anti-inflammatory, and neuroprotective activities in *in vitro* and/or *in vivo* models, of plant and/or cyanobacteria extracts, and natural products isolated or chemically modified. The only article that eludes this theme is the work of A. F. M. Monteiro et al. which carried out *in silico* studies aimed at the identification of potentially useful flavonoids for *in vitro*/*in vivo* screening in Parkinson and Alzheimer models.

G. Oboh et al.'s group found that the alkaloid extract from the African Jointfir (*Gnetum africanum*) is capable to counteract the Mn-induced elevation in AChE activity, NO, and ROS levels. I. K. Martins et al. observed the neuroprotective effect of the methanolic fraction of *Anacardium microcarpum* (from Brazil). This fraction was able to prevent neurodegeneration through the chelating properties toward ROS species, which is dependent on ERK1/2 and AKT phosphorylation; however, it does not prevent mitochondrial damage by 6-OHDA.

K. Adamczyk et al. evaluated the antihyaluronidase, anti-acetylcholinestarase, and anti-DPPH activities of several *Eleutherococcus* species cultivated in Poland. The methanolic extract was shown to be rich in polyphenols and promoted a reduction in DPPH in a time-dependent mode. *E. gracilistylus* and *E. sessiliflorus* showed the highest inhibition of AChE, and *E. henryi* was the best hyaluronidase inhibitor. R. B. de Oliveira Caland et al. observed the neuroprotective and antioxidative effect of pasteurized orange juice (*Citrus sinensis L.*) rich in carotenoids. The authors observed reduction in ROS production and upregulation of the expression of antioxidant and chaperonin genes, generating greater resistance to oxidative stress.

I.-C. Chen et al. evaluated the neuroprotective effects of formulated Chinese herbal medicines in a cell model of tauopathy. Shaoyao Gancao Tang (*P. lactiflora* and *G. uralensis* in a 1 : 1 ratio) presented the best antioxidative and anti-inflammatory results, reducing the tau misfolding and the production of the reactive oxygen species (ROS) level, especially nitric oxide (NO). In the research article by D. Nuzzo et al.'s group, the authors observed the neuroprotective effect of the cyanobacteria extract (Klamin®). Klamin® interferes with Aβ aggregation kinetics, exerts a protective role against beta amyloid (Aβ), and promotes activation of IL-6 and IL-1β inflammatory cytokines.

Y.-J. Wang et al. observed the antioxidant and neuroprotective activities of the extract of *Centipeda minima* and four isolated sesquiterpenoids. They found that the extract reduces glutamate and *tert*-butyl hydroperoxide-induced neuronal death, ROS production, and mitochondria dysfunction. Among the isolated sesquiterpenoids, 6-*O*-Angeloylplenolin and arnicolide D were the most active and responsible for the activation of the Nrf2 pathway and inhibition of ROS production. The study conducted by K. K. S. Narasimhan et al. has demonstrated that scopoletin (one of the main components from *Morinda citrifolia*) prevents oxidative injury and mitigates protein aggregation by the markedly upregulated DJ-1/Nrf2/ARE pathway.

L. Subedi et al. observed the antioxidant and anti-inflammatory effects of sulforaphane-enriched broccoli sprouts (SEBS) which lead to their neuroprotective effects. SEBS has protective effects of neuroinflammatory conditions by inhibition of the LPS-induced activation of the NF-κB signaling pathway, by the secretion of inflammatory proteins (inhibition of inflammatory cascade), and least by the upregulation of the expression of Nrf2 and HO-1, improving the scopolamine-induced memory impairment in mice. Y. Lee et al. verified that γ-mangostin (one of the major constituents from *Garcinia mangostana* fruits) reduces the oxidative neurotoxicity through the inhibition of H_2O_2-induced DNA fragmentation, ROS generation, lipid peroxidation, and DPPH radical formation, which is associated with the protection against H_2O_2-induced oxidative neuronal death. Orally, *in vivo*, γ-mangostin also improved scopolamine-induced memory impairment in mice. And finally, J.-S. Ye et al. observe the neuroprotective effect of Honokiol (a lignan isolated from the *Magnolia* genus) in postoperative cognitive change. Honokiol-mediated mitophagy inhibits the activation of the NLRP3 inflammasome and neuroinflammation in the hippocampus by increasing the expression of LC3-II, Beclin-1, Parkin, and PINK-1 at protein levels and through attenuation of mitochondrial structure damage and reduction of mtROS and MDA generation.

This compilation of articles gives us an up-to-date sample of the therapeutic potential of natural products in providing potential drugs and/or plant candidates to treat, prevent, or ameliorate the oxidative stress associated with neurodegenerative diseases including, but not limited to, Parkinson's and Alzheimer's diseases. We are sure that the information available in this issue will be very useful and will contribute to the future success of new therapies for neurodegenerative diseases.

Conflicts of Interest

The authors declare that there is no conflict of interest regarding the publication of this article.

Acknowledgments

We would like to thank all the authors, reviewers, and editorial staff who contributed to the organization of this special issue.

Francisco J. B. Mendonça-Junior
Marcus T. Scotti
Anuraj Nayarisseri
Ernestine N. T. Zondegoumba
Luciana Scotti

Hindawi
Oxidative Medicine and Cellular Longevity
Volume 2019, Article ID 2761041, 13 pages
https://doi.org/10.1155/2019/2761041

Research Article

Morinda citrifolia and Its Active Principle Scopoletin Mitigate Protein Aggregation and Neuronal Apoptosis through Augmenting the DJ-1/Nrf2/ARE Signaling Pathway

Kishore Kumar S. Narasimhan,[1,2] Deepthy Jayakumar,[1] Prema Velusamy,[1] Ashokkumar Srinivasan,[1] Thangarajeswari Mohan,[1] Divya Bhavani Ravi,[1] Saraswathi Uthamaraman,[1] Yogesh Kanna Sathyamoorthy,[3] Namakkal Soorappan Rajasekaran,[2] and Kalaiselvi Periandavan[1]

[1]*Department of Medical Biochemistry, Dr. ALM Post Graduate Institute for Basic Medical Sciences, University of Madras, Chennai, India*
[2]*Cardiac Aging & Redox Signaling Laboratory, Division of Molecular & Cellular Pathology, Department of Pathology, University of Alabama, Birmingham, AL 35294, USA*
[3]*Department of Anatomy, Dr. ALM Post Graduate Institute for Basic Medical Sciences, University of Madras, Chennai, India*

Correspondence should be addressed to Namakkal Soorappan Rajasekaran; rajnsr@uabmc.edu
and Kalaiselvi Periandavan; pkalaiselvi2011@gmail.com

Received 1 October 2018; Revised 16 January 2019; Accepted 12 February 2019; Published 2 May 2019

Guest Editor: Luciana Scotti

Given the role of oxidative stress in PD pathogenesis and off-target side effects of currently available drugs, several natural phytochemicals seem to be promising in the management of PD. Here, we tested the hypothesis that scopoletin, an active principle obtained from *Morinda citrifolia* (MC), efficiently quenches oxidative stress through DJ-1/Nrf2 signaling and ameliorates rotenone-induced PD. Despite reducing oxidative stress, the administration of MC extract (MCE) has lessened protein aggregation as evident from decreased levels of nitrotyrosine and α-synuclein. *In vitro* studies revealed that scopoletin lessened rotenone-induced apoptosis in SH-SY5Y cells through preventing oxidative injury. Particularly, scopoletin markedly upregulated DJ-1, which then promoted the nuclear translocation of Nrf2 and transactivation of antioxidant genes. Furthermore, we found that scopoletin prevents the nuclear exportation of Nrf2 by reducing the levels of Keap1 and thereby enhancing the neuronal defense system. Overall, our findings suggest that scopoletin acts through DJ-1-mediated Nrf2 signaling to protect the brain from rotenone-induced oxidative stress and PD. Thus, we postulate that scopoletin could be a potential drug to treat PD.

1. Introduction

Although the causal mechanisms of Parkinson's disease (PD) remain elusive, excess production of reactive oxygen species (ROS), mitochondrial dysfunction, neuroinflammation, and environmental toxins are reported to promote the loss of dopaminergic neurons in PD [1]. Oxidative stress has been shown to induce misfolding, aggregation, and accumulation of such aggregates leading to the pathogenesis of many neurodegenerative diseases including PD [2]. Intracellular inclusions known as Lewy bodies (LBs) are regarded as a hallmark of common pathological manifestation in both familial and sporadic PD patients with α-synuclein (α-Syn) serving as the main component of LB [3]. α-Syn is natively unfolded and is prone to form fibrils during oxidative stress [4], indicating that redox signaling may play a significant role in the aggregation of α-Syn.

Previous studies have reported that the loss of antioxidant defense aggravates PD progression [5, 6]. A key example includes DJ-1/PARK7, a molecular chaperone known to regulate Keap1-Nrf2 signaling, which is the primary sensor for reactive electrophiles activating Nrf2 nuclear translocation and transactivation of the antioxidant response element (ARE) in a battery of cytoprotective genes facilitating protection from oxidative stress pathogenesis [7] including experimental models of PD [8]. Thus, pharmacological activation of the Nrf2 in the brain is likely to preserve neuronal health. Therefore, exploration for therapeutic compounds with lesser neurotoxic effects that activates Nrf2 signaling would be promising to treat PD.

In this context, identifying potential principles from medicinal plants would be ideal as plant extracts have been reported to have several therapeutic benefits, due to the synergistic effect of various natural ingredients [9]. However, such plant sources have not been in clinical practice or in global market due to the lack of scientific validation. *Morinda citrifolia* fruit extract (MCE) has potential antioxidant properties due to the presence of several active constituents (including scopoletin and quercetin) and protects skeletal muscle from apoptosis [10] and also prevents striatal degeneration [11] in experimental Parkinsonian rats. Here, we hypothesized that MCE and scopoletin prevent rotenone-induced oxidative stress and apoptosis through the activation of DJ-1/Nrf2 signaling and investigated its neuroprotective effects using *in vivo* (Sprague-Dawley rats) and *in vitro* (SH-SY5Y cells) models of PD.

2. Materials and Methods

2.1. Animals, Intranigral Rotenone Infusion, and Treatment. Adult male Sprague-Dawley rats were used in this study. All experiments were performed in accordance with the guidelines approved by the Institutional Animal Ethical Committee *(IAEC No. 01/09/12)*. Rats were divided into five groups ($n = 10$/gp). Group I served as control, while groups II to V were subjected to stereotaxic surgery. Group II served as sham controls and groups III-V were stereotaxically infused with rotenone to induce Parkinsonism. Briefly, rats were anaesthetized with ketamine hydrochloride and xylazine (80 mg/kg and 10 mg/kg; i.p.) and placed on a small animal stereotaxic frame (Stoelting, IL, USA). Rotenone dissolved in DMSO (1 μg/1 μl) was infused into the right ventral tegmental area (VTA, anterior-posterior (AP): 5.0 mm; laterally (L): 1.0 mm; dorso-ventral (DV): 7.8 mm) and into the right substantia nigra pars compacta (SNPc, AP: 5.0 mm; L: 2.0 mm; DV: 8.0 mm) at a flow rate of 0.2 μl/min using a Hamilton 26-gauge needle [10, 11]. The infusion needle was left in place for additional five minutes for complete diffusion of the drug. Sham controls were infused with DMSO and polyethylene glycol in the ratio of 1 : 1 during stereotaxic surgery. Two weeks postsurgery, rats in groups IV and V were treated with levodopa (LD, 100 mg/kg with 25 mg/kg benserazide [12]) and ethyl acetate extract of *Morinda citrifolia* fruit (MCE, 150 mg/kg body weight), respectively, for the next 30 days. To determine the efficiency of intranigral infusion of rotenone, animals were subjected to behavioural analysis [11].

2.2. In Vitro Studies Using SH-SY5Y Cells. SH-SY5Y cells were initially grown in 1 : 1 mixture of DMEM and F12K Medium supplemented with 10% fetal bovine serum (*v*/*v*), 100 U/ml penicillin, and 100 μg/ml streptomycin in a 25 cm^2 and 75 cm^2 vented culture flasks. The cultures were incubated at 37°C in 5% CO_2/95% humidified air. When cells had reached 80–90% confluence in the flask, they were trypsinized and seeded onto 96-well plates or 6-well plates. Rotenone and scopoletin were dissolved in dimethyl sulfoxide (DMSO, final concentration of DMSO was 0.01%). Rotenone (500 nM) was used for 24 h to induce cell damage [13]. Preliminary studies were carried out with different concentrations (1 μM, 10 μM, 30 μM, 50 μM, and 100 μM) and different time intervals (0 h, 1 h, 3 h, and 6 h) of scopoletin to fix the time of exposure and dosage using MTT assay and the optimal concentration was found to be 30 μM pretreated for 3 h (Supplementary Figure 2). To investigate whether scopoletin protects cells from rotenone-induced cell death, cells were divided into three groups: control group, rotenone group (treated with rotenone for 24 h), and scopoletin group (pretreated with 30 μM scopoletin for 3 h followed by exposure to rotenone).

2.3. Analysis of Apoptotic Cells by Flow Cytometry. The different stages of apoptosis in control and treated SH-SY5Y cells were analyzed by flow cytometry using annexin V-FITC/PI double staining kit (Cayman Chemicals, Carlsbad, USA). After the incubation period, cells were washed with cold phosphate buffered saline (PBS), centrifuged twice at 1500 rpm for 5 min, and suspended in 500 μl of binding buffer. FITC-labeled annexin V (5 μl) and propidium iodide (PI, 5 μl) were added and incubated with the cells at room temperature for 15 min. Apoptotic cells were measured using a FACSCalibur flow cytometer (Becton Dickinson, NJ, USA). Annexin V-positive, PI-negative cells were scored as early apoptotic cells. Cells that were positive for both annexin V and PI were considered as late apoptotic cells.

2.4. mRNA Expression Studies by Reverse Transcription-Polymerase Chain Reaction (RT-PCR). Total RNA was isolated from the striatal tissue using total RNA isolation reagent (TRIZOL, Invitrogen, Carlsbad, CA, USA). Oligonucleotide primer sequences (Supplementary Table 1) of the selected genes for reverse transcription-polymerase chain reaction (RT-PCR) were synthesized by Sigma-Aldrich (St. Louis, MO, USA) and Eurofins Genomics (India). The amplified products were separated by electrophoresis on 1-2% agarose gel. Specificity was confirmed by the size of the amplified products with reference to 100 bp DNA ladder (BioVision, USA) and the band intensities were quantified by Quantity One Software (Bio-Rad, USA).

2.5. Western Blotting. Striatal tissue lysates (50 μg protein) and SH-SY5Y cell lysates were separated by SDS-PAGE on 10–12% polyacrylamide gels and transferred to polyvinylidene difluoride membranes. The membranes were incubated with specific primary antibodies and the antibodies used were DJ-1, Nrf2, phosphoS40-Nrf2 (Abcam 1 : 1000 dilution), Keap1, NQO1, Cullin3, PKC-δ (Pierce Antibodies,

1 : 1000 dilution), γGCLC, HO-1, nitrotyrosine (Santa Cruz Biotech, 1 : 1000 dilution), α-synuclein, and iNOS (Cell Signaling Technology, 1 : 1000 dilution). To verify the uniformity of protein load and transfer efficiency across the test samples, membranes were reprobed with β-actin and Lamin B (Cell Signaling Technology, 1 : 1000 dilution). Immunoreactive bands were developed with Immobilon Western Chemiluminescent HRP substrate (Millipore Corporation, Billerica, USA) and visualized by using an enhanced chemiluminescence system (ChemiDoc, Bio-Rad, USA) and presented in comparison to β-actin/Lamin B expression.

2.6. Statistical Analysis. Data are presented as mean ± standard error of mean (SEM) of the results obtained from the average of at least three to six independent experiments. Results were analyzed by one-way analysis of variance (ANOVA) using the SPSS software package for Windows (Version 20.0; SPSS Inc., Chicago, IL, USA) and p values were determined using the Student-Newman-Keuls and least significant difference post hoc test. Differences among means were considered statistically significant when the p value was less than 0.05.

3. Results

3.1. Impact of MCE on Nigrostriatal Tyrosine Hydroxylase (TH) Immunoreactivity. Immunohistochemical localization of TH-positive neurons in the striatum as well as the substantia nigra pars compacta (SNPc) of control and experimental rats is presented in Figure 1(a). Histochemical analysis of SNPc along with the striatum makes it convenient to understand the efficacy of the MCE treatment. The striatum ipsilateral to the side of infusion showed significant loss of TH immunostaining. TH immunoreactivity of the ipsilateral striatum shows a remarkable refurbishment of dopaminergic neurons seen in MCE-administered rats. Rotenone-infused SNPc showed less number of TH-positive cells as compared to control animals. MCE treatment in these animals restored, to a great extent, the loss of these cells. While there was a 43% decrease in TH-positive neurons in response to rotenone administration, MCE treatment curtailed this to 30% (Figure 1(b)).

3.2. MCE Counteracts Rotenone-Induced Oxidative Stress in Experimental PD Rats. Analyses of various oxidative stress markers indicated that MCE was an efficacious treatment to reduce oxidative stress in rotenone-induced PD rats. We first determined the levels of nitric oxide (NO) which was significantly increased ($p < 0.05$) in the striatum of rotenone-infused PD rats and this was blunted in response to MCE treatment. Next, quantification of lipid peroxidation (LPO) and protein carbonyls (PC) revealed that rotenone infusion increased the levels of these oxidative byproducts to 22 and 41%, respectively, in relation to sham controls (Figure 1(c)). However, upon treating with MCE, LPO and PC content was significantly decreased.

3.3. MCE Protects from Rotenone-Induced Protein Aggregation. Considering the interrelationships between nitric oxide, oxidative stress, and protein aggregation [14], we further determined the impact of MCE on the levels of iNOS and nitrotyrosine as the former is involved in the synthesis of NO and the latter is a marker for protein aggregation. Rotenone-infused Parkinsonian rats showed a significant ($p < 0.05$) increase in the protein levels of iNOS and nitrotyrosine when compared with controls (Figure 1(d)). Treatment with MCE significantly ameliorated rotenone-mediated NO production through diminishing the levels of iNOS. As a result, we also found that MCE was particularly efficient in blocking the formation of nitrotyrosine adducts (i.e. α-synuclein), which are the primary events in the process of protein aggregation that occurs in response to oxidative insults, such as those triggered by rotenone.

To further confirm the suppression of protein aggregation by MCE, we analyzed both the protein levels and the immunostaining for α-synuclein (α-Syn), a pathological protein that is aggregated in PD. While immunostaining showed a significant increase in α-Syn aggregation (Figures 2(a) and 2(b)) in the striatum of rotenone-induced rats which correlates with the increase in the nitrotyrosine levels, MCE treatment abolished these changes and significantly reduced the aggregation of α-Syn suggesting that oxidative stress promotes the aggregation of α-Syn. Moreover, rotenone-infused Parkinsonian rats exhibited a significant ($p < 0.05$) increment in the protein levels of α-Syn by 79% (Figure 2(c)), which further aggravated the aggregation of α-Syn in these rats.

3.4. MCE Prevents Rotenone-Induced Oxidative Stress by Augmenting the Antioxidant Defense. We postulated that the antioxidative potential of MCE might be associated with diminished oxidative stress. A significant decline ($p < 0.05$) in the activities of antioxidant enzymes, namely, superoxide dismutase (SOD), catalase, glutathione peroxidase (GPx), glutathione reductase (GR), and glutathione-S-Transferase (GST), was observed (Table 1(a)) in the rotenone-induced Parkinsonian rats when compared with controls. However, upon supplementing with MCE, a significant augmentation in the activities of SOD, CAT, and GST was observed with a maximum improvement in the SOD activity (36%). However, there were no significant changes in the activities of other enzymatic antioxidants GPx, GR. In addition, the levels of reduced glutathione (GSH), a vital ubiquitous antioxidant thiol, decreased in response to rotenone-induced oxidative stress. MCE supplementation significantly increased the levels of GSH back to near normal when compared with the rotenone-infused rats. Because the Nrf2 pathway transcriptionally activates glutathione-biosynthesizing enzymes, we next assessed whether GSH changes were mechanistically linked to Nrf2 signaling in the MCE-treated animals.

3.5. MCE Induces Nrf2/ARE Pathway and Suppresses Rotenone-Induced Oxidative Stress. The downregulation of the Nrf2/ARE pathway exacerbates oxidative stress which potentiates dopaminergic degeneration and pathogenesis of PD [15]. As we noticed a significant alteration in cellular redox status, elevated α-Syn expression, and aggregation in the current study, we further analyzed the levels of Nrf2

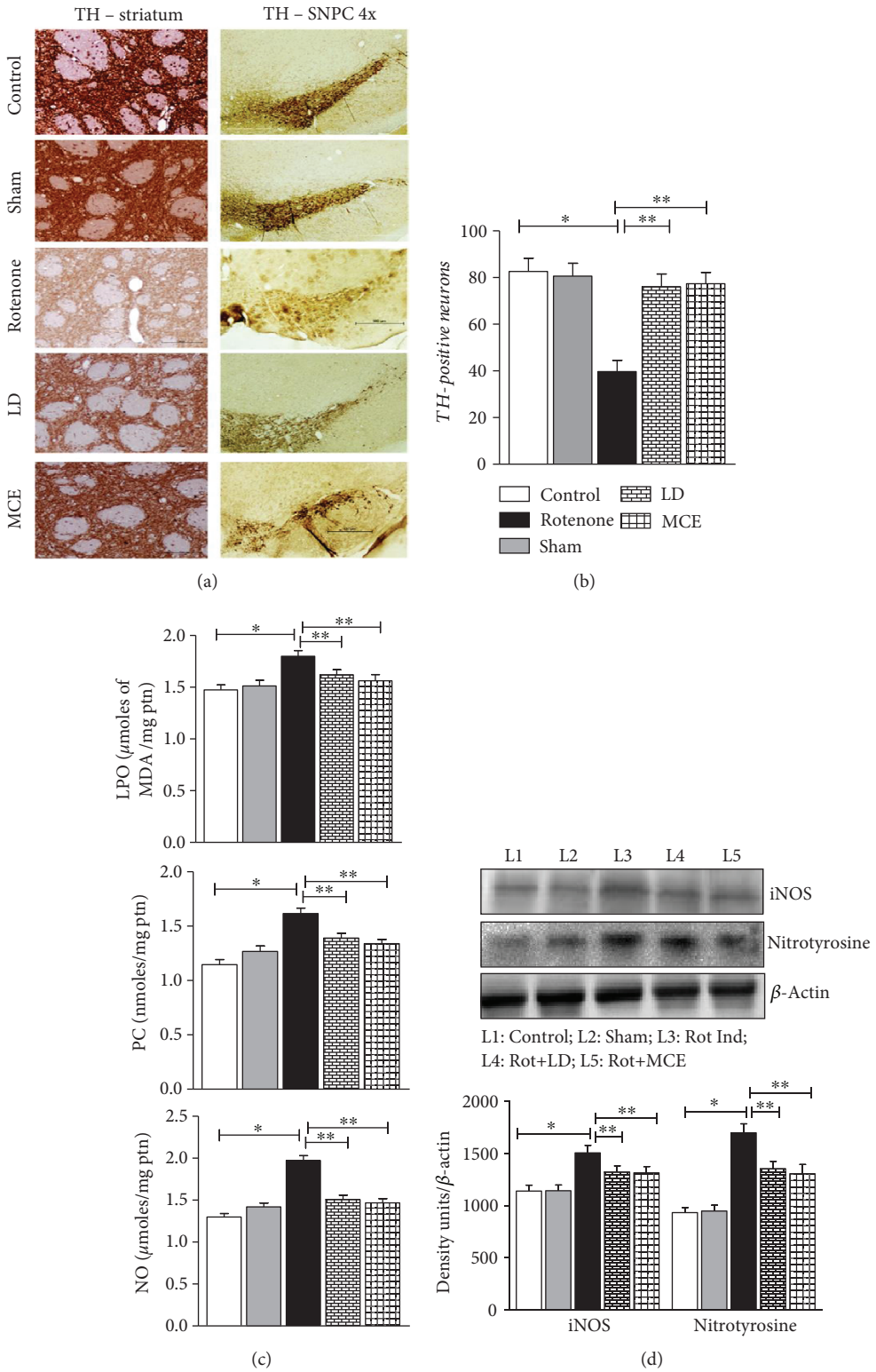

Figure 1: (a) Photographic representation of the TH-positive neurons in the striatum and in SNPc. (b) Quantification of relative intensity of TH staining in the striatum using the densitometry protocol through ImageJ was performed to substantiate the potentials of salvaging activity of MCE. (c) Impact of MCE on rotenone-induced oxidative stress: values are expressed as for six animals in each group. (d) Immunoblot analysis of iNOS and nitrotyrosine (i.e. α-synuclein) and representative densitometry quantification. Statistical significance ($p < 0.05$) was calculated by Student-Newman-Keuls and least significant difference post hoc test, where * represents control vs. other groups, ** represents rotenone vs. LD, MCE.

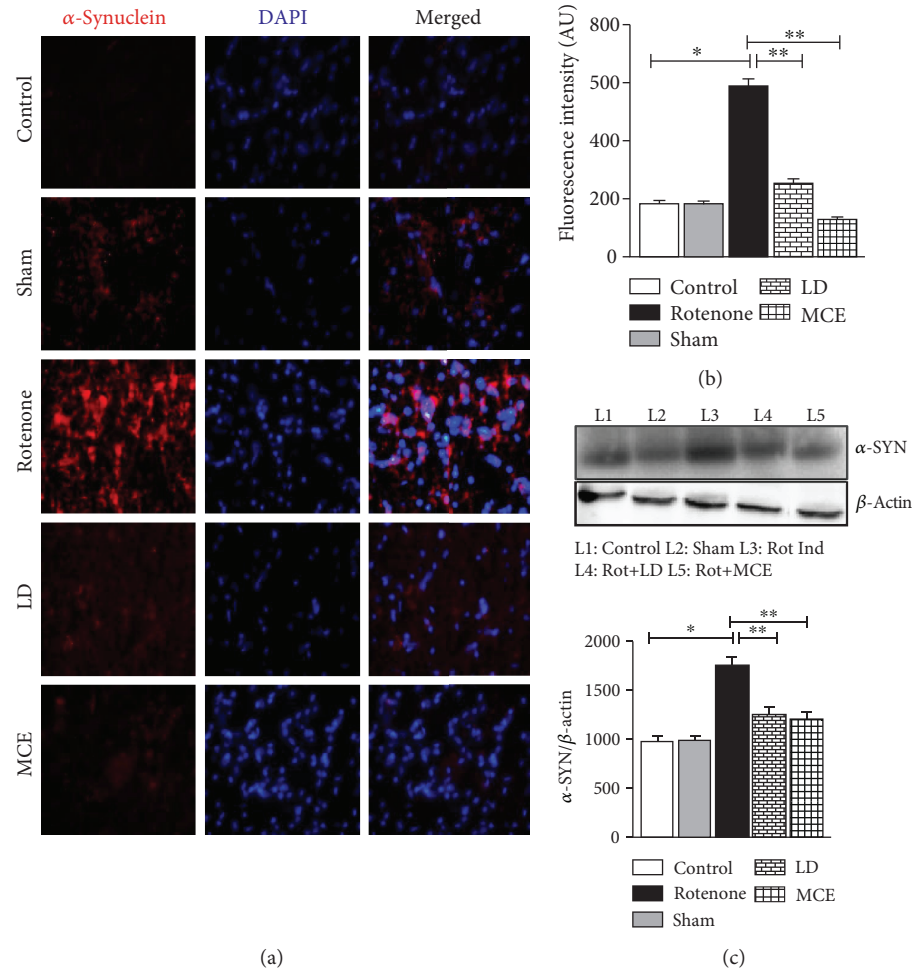

Figure 2: Rotenone-induced aggregation of α-synuclein (α-Syn) measured by immunofluorescence analysis. (a) The cells were visualized using fluorescence microscopy and images captured using 20x magnification. The control and sham groups show very low level of expression; however, the expression is punctate and high in the rotenone-induced group; the expression is meager in levodopa; on the contrary, expression in the MCE groups is comparable with that in the control group. (b) Relative fluorescence intensity was calculated. (c) Immunoblot analysis of α-Syn and representative densitometry quantification. Statistical significance ($p < 0.05$) was calculated by Student-Newman-Keuls and least significant difference post hoc test, where * represents control vs. other groups, ** represents rotenone vs. LD, MCE.

and its interacting proteins to test the hypothesis that the MCE-mediated augmentation of antioxidative system occurs through the activation of Nrf2/ARE signaling.

Immunoblotting analysis revealed that rotenone infusion significantly decreased Nrf2 protein levels. In compounding fashion, Keap1 and Cullin3, scaffold and adaptor proteins responsible for cytosolic sequestration and proteasomal degradation of Nrf2, respectively, were significantly increased in rotenone-infused rats. Interestingly, MCE treatment significantly rescued the levels of Nrf2 and reversed the rotenone-induced increase in Keap1 and Cullin3 (Figure 3(a)). Recent reports indicate that nuclear translocation of Nrf2 is not only mediated by phosphorylation by PKC-δ but also by intact DJ-1, which binds and stabilizes the Nrf2 and favours its translocation to the nucleus [16]. Next, we extended our immunoblotting analyses to DJ-1; similar to that of Nrf2, the DJ-1 is also downregulated in rotenone-infused rats and this was reversed upon MCE administration (Figure 3(a)). To delineate the difference in total protein expression, we performed the immunoblotting of Nrf2 and Keap1 in nuclear and cytosolic fractions (Figure 3(b)). Our results indeed confirmed that rotenone infusion significantly repressed the translocation of Nrf2 from the cytosol to the nucleus as evident from decreased levels of nuclear Nrf2 in rotenone versus control rats. Hence, rotenone infusion not only decreases total Nrf2 protein levels but also impairs its nuclear translocation by downregulating DJ-1 and augmenting cytosolic Keap1 levels. As such, supplementation with MCE significantly augmented the nuclear translocation of Nrf2 as evident from increased levels of nuclear Nrf2 (83%) by augmenting the DJ-1 and decreasing the nuclear Keap1 levels when compared with rotenone-infused rats.

3.6. MCE Augments Nrf2/ARE Downstream Genes. Nrf2, a member of Cap'n'Collar family of basic region-leucine zipper (bZIP) transcription factors, plays an important role in ARE-mediated gene expression through the transcriptional

Table 1: (a) Impact of MCE on antioxidant defense system. Values are expressed as mean ± SEM for six animals in each group. SOD: units/mg protein. One unit is equal to the amount of enzyme that inhibits the pyrogallol autoxidation by 50%; CAT: μmoles of H_2O_2 consumed/min/mg protein; GPx: μg of GSH consumed/min/mg protein; GR: nmoles of NADPH oxidized/min/mg protein; GST: μmoles of CDNB conjugate formed/minute/mg protein; GSH: nmoles/mg protein. (b) Impact of MCE on the activities of Nrf2/ARE downstream enzymes. Values are expressed as mean ± SEM for six animals in each group. γGCLC: millimoles of NADH oxidized/min/mg protein; NQO1: nmoles DCPIP utilized/min/mg protein; HO-1: nmoles of bilirubin/h/mg protein. Statistical significance ($p < 0.05$) was calculated by Student-Newman-Keuls and least significant difference post hoc test, where * represents control vs. other groups, ** represents rotenone vs. LD, MCE.

(a) Impact of MCE on antioxidant defense system

Parameter	Control	Sham control	Rotenone induced	LD	MCE
SOD	0.58 ± 0.018	0.52 ± 0.017	0.33 ± 0.015*	0.41±0.016**	0.45±0.014**
CAD	17.43 ± 0.60	16.36 ± 0.36	12.13 ± 0.38*	14.21±0.32**	15.22±0.41**
GPx	8.25 ± 0.37	8.22 ± 0.32	5.66 ± 0.23*	6.59±0.31**	6.64±0.20**
GR	5.16 ± 0.25	5.12 ± 0.22	3.90 ± 0.15*	4.47±0.19**	4.48±0.15**
GST	9.08 ± 0.394	9.01 ± 0.468	6.38 ± 0.271*	7.75±0.298**	7.86±0.241**
GSH	1.93 ± 0.055	1.76 ± 0.048	1.28 ± 0.058*	1.61±0.059**	1.65±0.062**

(b) Impact of MCE on the activities of Nrf2/ARE downstream enzymes

Parameter	Control	Sham control	Rotenone induced	LD	MCE
γGCL	2.54 ± 0.084	2.46 ± 0.083	1.35 ± 0.051*	1.90±0.071**	2.01±0.068**
NQO1	5.88 ± 0.193	5.85 ± 0.193	3.15 ± 0.111*	4.57±0.151**	4.82±0.153**
HO-1	0.81 ± 0.026	0.80 ± 0.026	0.48 ± 0.016*	0.63±0.021**	0.65±0.018**

activation of antioxidant genes such as heme oxygenase-1 (*Ho-1*), gamma-glutamyl cysteine ligase (γ*Gclc*), and NAD(P)H:quinone oxidoreductase 1 (*Nqo1*). As we observed a significant decline in Nrf2 protein levels, we further assayed transcript and protein levels for Nrf2 gene targets. Consistent with our observation of oxidative insult and Nrf2 pathway antagonism, rotenone treatment was associated with a prominent decline in the mRNA (Figure 4(a)) and protein (Figure 4(b)) levels of several ARE targets with a maximum decrease being observed in *Ho-1* (45%). However, supplementation with MCE significantly enhanced the levels of these proteins both at the transcriptional and translational levels by an average of 40%. The improved protein levels are reflected in the activities of these enzymes (Table 1(b)).

After characterizing the neuroprotective effect of MCE in an *in vivo* model of PD and confirming its ability to augment Nrf2 signaling and reverse oxidative insult, we further examined the neuroprotective efficacy of scopoletin, a major and active principle of MCE using SH-SY5Y cells. To choose an optimal concentration of scopoletin for this study, we pretreated SH-SY5Y neuroblastoma cells with different doses of scopoletin ranging from 1 to 100 μM at different time intervals (from 0 hours to 6 hours). Until 50 μM scopoletin, there was no toxicity observed in SH-SY5Y cells. Maximum viability was achieved at the concentration of 30 μM scopoletin (Supplementary Figure 2). Hence, further studies were carried out using 30 μM scopoletin.

3.7. Scopoletin Prevented Rotenone-Induced Cell Death. SH-SY5Y cells undergoing various stages of apoptosis (early, midstage, and late stage) were analyzed by flow cytometry using annexin V and propidium iodide (PI) dual staining. Treatment of SH-SY5Y cells with rotenone (500 nM for 24 h) resulted in 40% cell death, which was attenuated by pretreating the cells with 30 μM scopoletin for 3 h (Figures 5(a) and 5(b)). These data indicate that scopoletin protects SH-SY5Y from rotenone-induced cell death.

3.8. Scopoletin-Mediated Neuroprotective Effects Were Associated with the Translocation of Nuclear p40Nrf2 and Upregulation of DJ-1. The activation of the Nrf2/ARE pathway is known to confer resistance to oxidative stress-induced cell death [17]. As scopoletin prevented rotenone-induced cell death, we further assessed Nrf2 pathway constituents. Along these lines, both the unphosphorylated (total/cytosolic form) and the serine 40-phosphorylated Nrf2 (pNrf2S40) levels were measured by immunoblotting. Consistent with animal studies demonstrating that MCE improves nuclear levels of Nrf2, scopoletin also increased the nuclear translocation of Nrf2 as evident from the increased nuclear levels of pNrf2 (S40) (Figure 5(d)). This increase in the nuclear levels of Nrf2 may be attributed to the phosphorylation of Nrf2 by PKC-δ which is also augmented upon pretreating with scopoletin (Figure 5(c)). Concomitant with the animal studies, both the total and nuclear levels of Keap1 were significantly elevated in rotenone-treated SH-SY5Y cells when compared with untreated control cells. Furthermore, rotenone treatment also increased the levels of E3 ubiquitin ligase Cullin3 (Figure 5(c)) by 46%.

In order to determine whether DJ-1 plays an important role in scopoletin-mediated Nrf2 translocation, we further

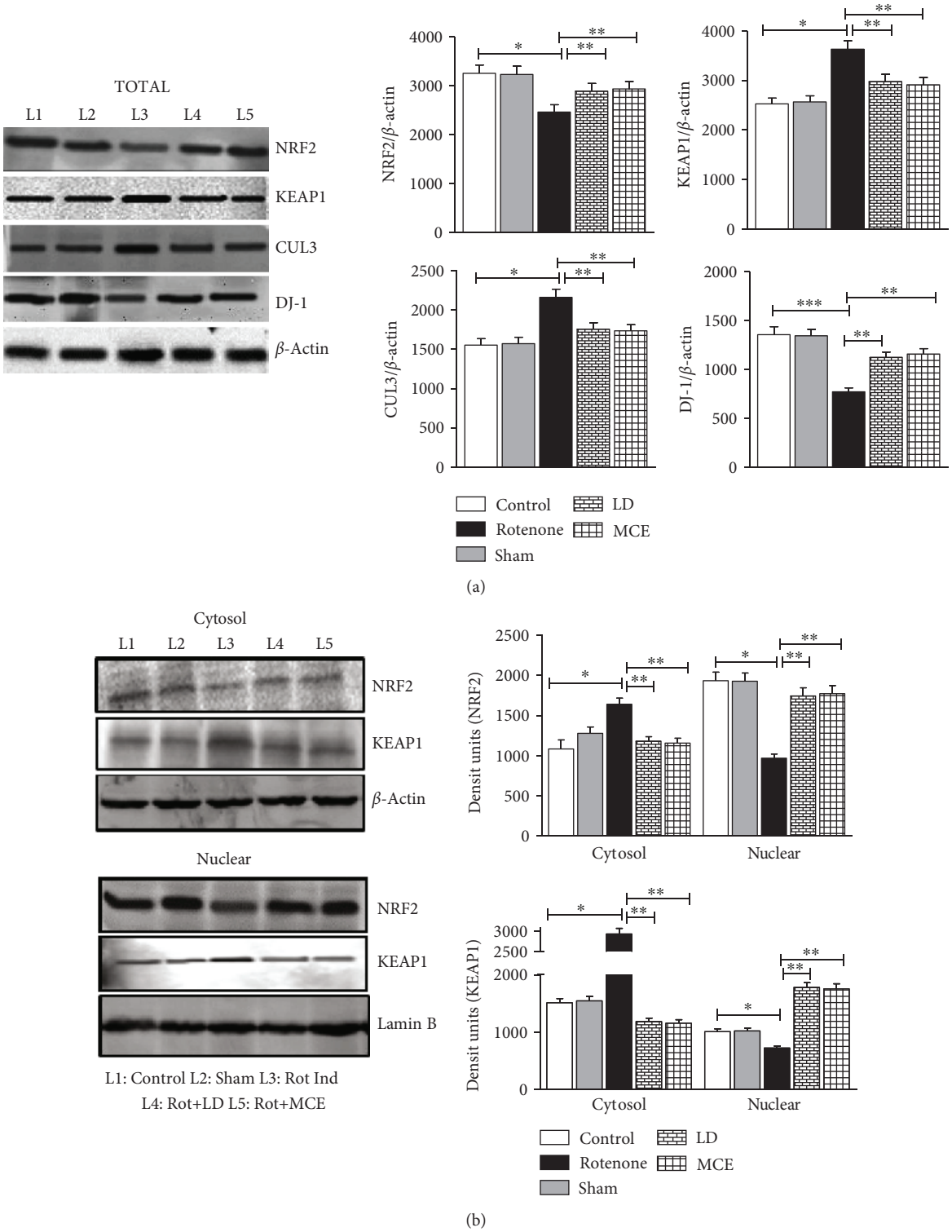

Figure 3: Immunoblot analysis of Nrf2 and its negative regulators Keap1 and Cullin3 in the striatum of rotenone-induced PD rats. (a) The total protein levels of Nrf2, Keap1, Cullin3, and DJ-1. (b) The protein levels of Nrf2 and Keap1 in cytosolic and nuclear compartment of striatal neuronal cells. Statistical significance ($p < 0.05$) was calculated by Student-Newman-Keuls and least significant difference post hoc test, where * represents control vs. other groups, ** represents rotenone vs. LD, MCE.

analyzed the levels of DJ-1 in rotenone-induced SH-SY5Y cells pretreated with or without scopoletin. Rotenone-treated cells exhibited a relative decrease in the protein levels of DJ-1 (Figure 5(c)) which may be attributed to the impaired Nrf2 nuclear translocation in these cells. Conversely, scopoletin-pretreated cells showed an augmented

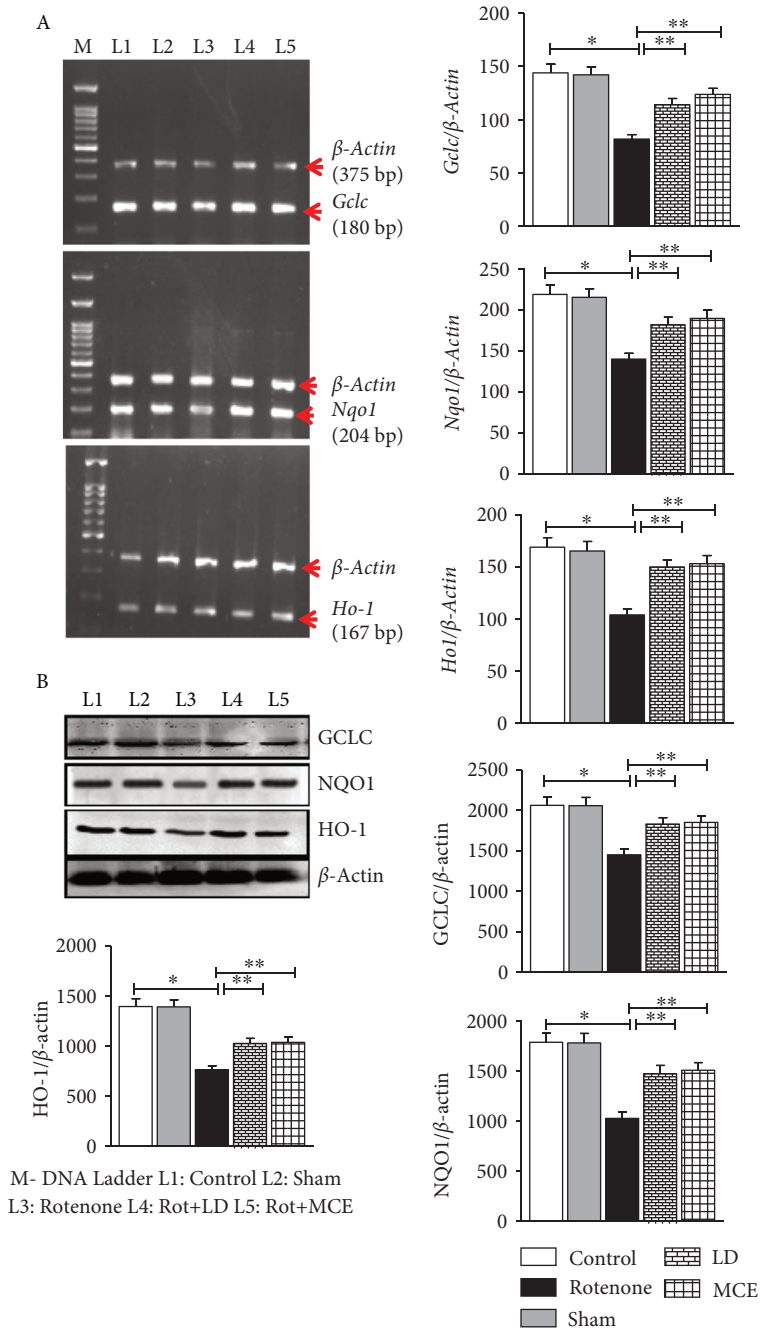

Figure 4: Increased Nrf2 regulated antioxidant genes in response to MCE supplementation in rotenone-induced PD rats. (a) The mRNA levels of Nrf2 downstream genes γGCLC, NQO1, and HO-1. (b) The protein levels of γGCLC, NQO1, and HO-1. Statistical significance ($p < 0.05$) was calculated by Student-Newman-Keuls and least significant difference post hoc test, where * represents control vs. other groups, ** represents rotenone vs. LD, MCE.

expression of DJ-1 (46%), suggesting that DJ-1 may be vital for scopoletin-mediated neuroprotective effects. From these observations, it is clear that scopoletin augments the Nrf2/ARE pathway by increasing levels of DJ-1 and concomitantly prevents the cytosolic degradation of Nrf2 by reducing the levels of its negative regulators Keap1 and Cullin3.

4. Discussion

Increasing interest has been focused on identifying dietary supplements and phytoconstituents that can inhibit ROS-mediated protein aggregation and neuronal cell death and thereby reverse the multifaceted pathophysiological events underlying PD. Here, we investigated whether *Morinda*

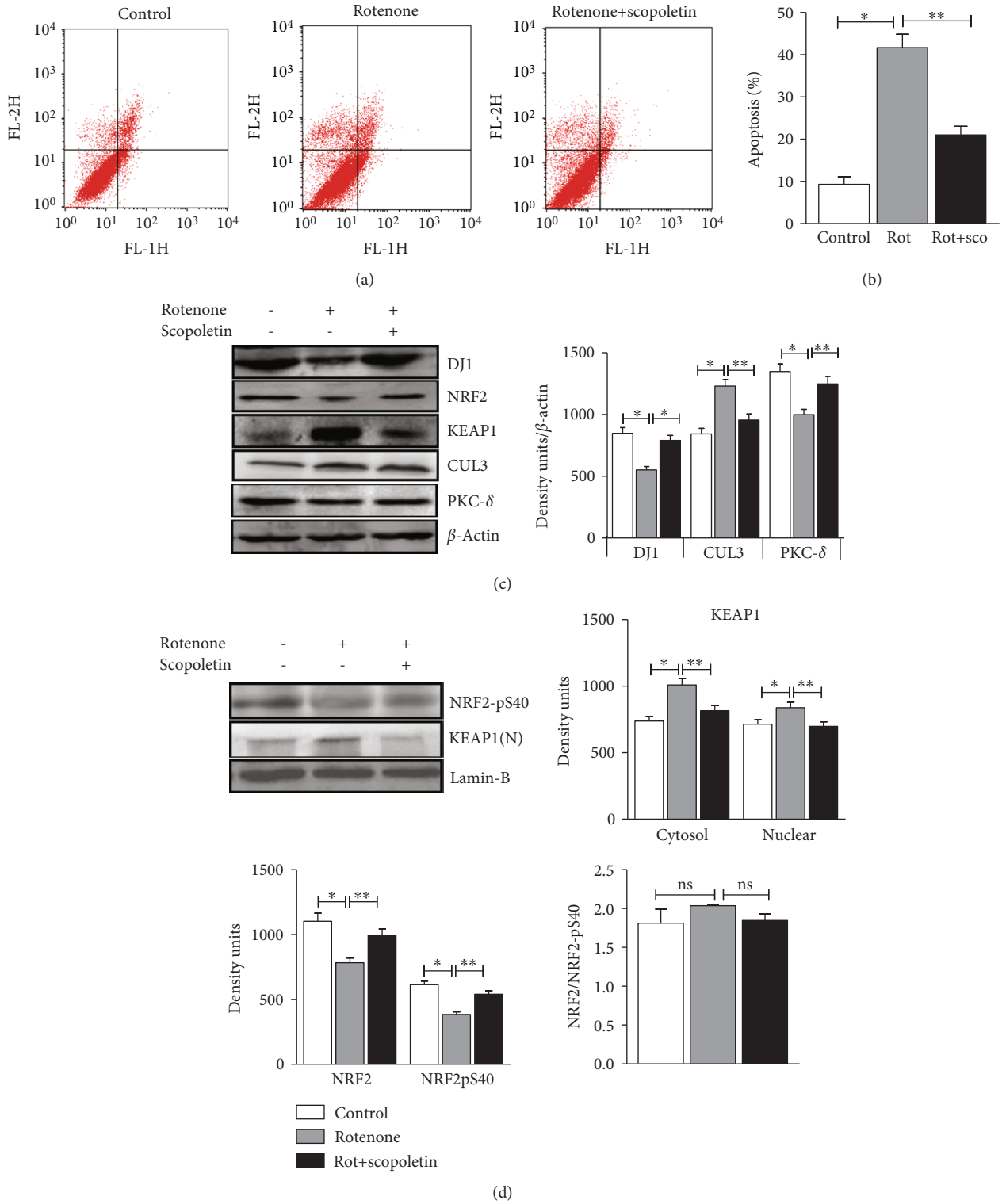

Figure 5: (a) Rotenone-induced apoptosis is counteracted by scopoletin in SH-SY5Y cells. At the end of the experiment, cells were stained with annexin V/FITC and read immediately by flow cytometry to measure the extent of apoptosis; x-axis FL-1H denotes the FITC and y -axis FL-2H denotes the PI. (b) Quantification of percentage dead cells. (c) Immunoblot analysis of several proteins involved in Nrf2/ARE pathway is performed in SH-SY5Y cells treated with/without rotenone and scopoletin. (d) Immunoblot analysis of phospho (S40) Nrf2 and nuclear Keap1 in SH-SY5Y cells. Statistical significance ($p < 0.05$) was calculated by Student-Newman-Keuls and least significant difference post hoc test, where * represents control vs. other groups, ** represents rotenone vs. scopoletin.

citrifolia fruit extract attenuates rotenone-induced oxidative stress by activating the Nrf2-dependent antioxidant response and tested whether this mechanism may prevent the loss of dopaminergic neurons. After confirming its neuroprotective effect *in vivo*, we elucidated the mechanism of action for scopoletin, a major compound present in the MCE, *in vitro* using SH-SY5Y cells and identified that the therapeutic effect of scopoletin is facilitated through the activation of the DJ-1/Nrf2/ARE signaling cascade.

While the pathogenic mechanism of PD is poorly known, it is believed that oxidative stress involving the imbalance of nitric oxide (NO) signaling is a major player in the prognosis of PD [14]. A significant increase in the levels of NO in the striatum of rotenone-infused Parkinsonian rats is in line with previous reports [18]. However, supplementation of MCE reduced the levels of NO in the striatum of PD-induced rats. Recent reports documented that the ethyl acetate extract of noni fruit is shown to reduce oxidative and nitrosative stress in the brain [19]. As NO homeostasis is significantly impaired in response to rotenone infusion, our further analysis revealed an increase in the levels of iNOS in the striatal tissues in these rats. Thus, the increased iNOS might have been responsible for increased nitric oxide levels. The administration of MCE safeguarded the striatum from the deleterious effect of nitric oxide by attenuating the iNOS expression induced by rotenone (Figure 1).

As protein aggregation is a common event underlying neurodegenerative diseases including PD, wherein α-synuclein (α-Syn) comprises the bulk of Lewy bodies [20, 21], further investigations were directed to assess the rate of α-Syn aggregation. α-Syn expression and its aggregation were increased in the striatum of rotenone-infused rats when compared with the control rats (Figure 2). This increased aggregation of α-Syn might also be due to NO-mediated oxidative stress in PD rats (Table 1(a)), as it has been previously shown that fibrillary α-Syn aggregates with perinuclear localization were formed in cells exposed to NO [22]. Interestingly, treatment with MCE reduced the α-Syn aggregation which might be due to the reduction in the levels of NO and the consequent tyrosine nitration in MCE-treated rats.

Intracellular defense is maintained through a variety of antioxidant enzymes and low molecular weight antioxidants such as glutathione to combat the deleterious effects of ROS overproduction and oxidative damage [23]. Elevated ROS production, in the absence of increased antioxidant defenses, will exacerbate oxidative damage and oxidative stress [24]. In the current study, an overall decline in the activities of antioxidant enzymes such as superoxide dismutase (SOD), catalase (CAT), glutathione peroxidase (GPx), glutathione reductase (GR), and glutathione-s-transferase (GST) was noticed along with significantly decreased glutathione (GSH) content in the striatum of intranigrally rotenone-infused rats when compared with control rats. Notably, MCE supplementation restored the overall antioxidant status, rescuing glutathione levels in the striatum of rotenone-infused PD rats. These results support recent work demonstrating that the ethyl acetate extract of *Morinda citrifolia* fruit boosts SOD, GPx, and GR enzymatic activity in β-amyloid-induced cognitive dysfunction in mice [25] and in the skeletal muscle of rotenone-infused hemi-Parkinsonian rats [10].

In the present investigation, the total protein level of Nrf2 was significantly reduced in rotenone-induced rats while Keap1 and Cullin3, negative regulators of Nrf2, were markedly elevated. High levels of oxidative stress may reduce the activity of Nrf2, although the molecular mechanism for this defect is uncertain [26]. Interestingly, the administration of MCE reversed the rotenone-mediated increase in Keap1 and Cullin3, thereby preventing the degradation of Nrf2 *in vivo*. Keap1 is capable of restraining Nrf2 activity not only *via* its capacity to target Nrf2 to a cytoplasmic Cullin3-based E3 ligase [27] but also by transiently entering into the nucleus and targeting Nrf2 for ubiquitylation in this compartment under stressed conditions [28]. This instigated us to analyze the nuclear levels of Nrf2 and Keap1 which gives us an unblemished picture of the nuclear translocation and activated form of Nrf2.

The nuclear level of Nrf2 was reduced in the striatum of rotenone-infused Parkinsonian rats when compared with the control rats and the opposite trend was observed for Keap1. From these observations, it may be inferred that not only is a lower concentration of Nrf2 protein present in the nucleus but that it also may be bound by Keap1, thereby preventing Nrf2 from binding to AREs. Indeed, this notion is consistent with our observation of a lower antioxidant status in these rats. However, the redox milieu inside the striatal nucleus of PD rats treated with MCE is different, where MCE with its rich phytoconstituents favours the translocation of Nrf2 into the nucleus and detains Keap1 in the cytosol, which is further reflected in the results obtained for antioxidant status in these rats. From these observations, it is clear that MCE increases the nuclear translocation of Nrf2.

Since we observed a significant decline in the transcriptional activity of Nrf2, we further assessed its downstream effectors (γ*Gclc*, *Nqo1* and *Ho-1*) by analyzing the levels of mRNA and protein. Overall, both the mRNA and protein levels of γ*Gclc*, *Nqo1* and *Ho-1* were significantly decreased in the striatum of rats stereotaxically infused with rotenone when compared with the control rats. The consequence of impaired transcription and translation of these proteins was also reflected in the diminished activities of these enzymes on rotenone infusion. However, upon treating with MCE, the activities and mRNA and protein levels of these proteins were significantly increased, likely a downstream effect of enhanced Nrf2 stability and activation.

Overall, from the *in vivo* studies, it is clear that MCE, with its antioxidant property, scavenges the free radicals, and it also reduces the expression of iNOS and prevents rotenone-induced aggregation of α-synuclein. MCE also augments the total levels of Nrf2 and subsequently translocates Nrf2 to the nucleus by preventing its degradation mediated by Keap1/Cullin3 complex which in turn leads to transcription and enhanced activities of its downstream effectors γ*Gclc*, *Ho-1* and *Nqo1*. This neuroprotective effect of MCE might be attributed to the presence of identified phytoconstituents

quercetin, rutin, and scopoletin and also other unidentified constituents [10]. However, as scopoletin is the biomarker for *Morinda citrifolia* [29] while other compounds such as rutin and quercetin are commonly present in most of the plants [30, 31], further emphasis was given to scopoletin, and its mechanism of action in boosting DJ-1/Nrf2/ARE pathway was studied in *in vitro* cell culture using SH-SY5Y dopaminergic cells, in order to delineate the ability of the phytochemical derived from *Morinda citrifolia* on dopaminergic neuronal cell survival.

We observed a significant reduction in cell viability on rotenone-exposed SH-SY5Y cells (data not shown), which was attenuated by pretreatment with scopoletin. Hence, we further analyzed the status of cellular apoptosis using annexin V/propidium iodide staining. Rotenone exposure of SH-SY5Y cells shows a significant increase in the proportion of early apoptotic cells compared with the controls. Our observation is in coherence with the previous reports by Jang et al. [32], who have stated that rotenone at a concentration of 200 nM induces apoptosis in SH-SY5Y cells by generating ROS. However, this shift is reversed when the cells are pretreated with scopoletin, and the possible explanation for this effect would be scopoletin with its antioxidant potential [33] should have ameliorated rotenone-induced apoptosis by quenching free radicals. To the best of our knowledge, this is the first study to show that scopoletin prevents apoptosis in an *in vitro* rotenone exposure unless otherwise like literature which poses it as a potent proapoptotic agent in various cancer cell lines [34–36].

In light of our observations on MCE-mediated Nrf2 activation, we examined the capacity of scopoletin to influence the Nrf2 signaling by aiding the nuclear translocation of Nrf2. We analyzed the levels of phospho-Nrf2 and PKC-δ that phosphorylate serine 40 of Nrf2, thereby aiding in its nuclear translocation, in SH-SY5Y cells exposed to rotenone. Pretreatment with scopoletin augmented the nuclear levels of phospho-Nrf2 which may be associated with our observation of increased PKC-δ expression. Indeed, Nam and Kim [37] have shown that scopoletin influences the expression of reprogramming genes and exerts antiaging effects by regulating the transcription factor Nrf2 (Figure 5). Previous reports have shown that DJ-1 stabilizes Nrf2 and promotes its nuclear translocation [38]. Intriguingly, mutations in DJ-1 are associated with the risk of developing PD [39]. Hence, we further evaluated the effect of scopoletin on DJ-1 levels in SH-SY5Y cells. We found that rotenone exposure of cells resulted in diminished levels of DJ-1. Angeline et al. [40] have reported that chronic exposure to rotenone reduced the cytoprotective proteins Parkin, Hsp70, and DJ-1. However, on pretreating with scopoletin, DJ-1 protein levels were augmented, subsequently conferring protection against rotenone-induced oxidative stress, as overexpression of DJ-1 rescued MN9D cells exposed to rotenone, indicating that DJ-1 protected nigral DA neurons from rotenone-induced cell death [41].

5. Conclusions

This study has provided evidence that MCE prevented α-synuclein aggregation through augmenting Nrf2 antioxidant signaling, leading to the suppression of oxidative stress. Notably, scopoletin, the active component from MCE, seems to be responsible for stabilizing Nrf2/ARE pathway by augmenting the phosphorylation of Nrf2 and its nuclear translocation, in a DJ-1-dependent manner. Thus, we propose that DJ-1 might be a potential target for scopoletin-based therapeutic strategy against neurodegenerative diseases.

Abbreviations

DMSO: Dimethyl sulfoxide
F-12K: Kaighn's modification of Ham's F-12 medium
FBS: Fetal bovine serum
GSH: Reduced glutathione
HO-1: Heme oxygenase-1
Keap1: Kelch-like erythroid cell-derived protein with CNC (Cap "n" Collar) homology (ECH) protein1
LD: Levodopa
LPO: Lipid peroxidation
MCE: Ethyl acetate extract of *Morinda citrifolia* fruit
NO: Nitric oxide
NQO1: NAD(P)H:quinone oxidoreductase 1
Nrf2: Nuclear factor erythroid 2-related factor 2
PC: Protein carbonyl
PD: Parkinson's disease
PKC-δ: Protein kinase C delta
ROS: Reactive oxygen species
Rot Ind: Rotenone induced
SH-SY5Y: Neuroblast-like subclone of SK-N-SH
SNPc: Substantia nigra pars compacta
VTA: Ventral tegmental area
γGCLC: Catalytic subunit of gamma glutamate cysteine ligase.

Data Availability

The data supporting the findings of this study are available within the article [and/or] its supplementary materials.

Ethical Approval

All experiments were performed in accordance with the guidelines approved by the Institutional Animal Ethical Committee (IAEC No. 01/09/12, 01/09/12 Extension).

Conflicts of Interest

The authors declare that they have no potential conflict of interest including any financial and personal relationships with other people or organizations.

Authors' Contributions

Kishore Kumar S. Narasimhan, the first author, designed and executed the experimental work; collected, analyzed, and interpreted the data; and drafted the manuscript. Deepthy Jayakumar and Saraswathi Uthamaraman assisted with key experiments and were involved in data collection. Kishore Kumar S. Narasimhan, Prema Velusamy, and Ashokkumar Srinivasan were responsible for the in vitro and flow

cytometry experiments. Thangarajeswari Mohan, Divya Bhavani Ravi, and Yogesh Kanna Sathyamoorthy were responsible for immunofluorescence analysis and quantification and language editing. Namakkal Soorappan Rajasekaran revised the article and provided important directions for interpreting the results and discussion. Kalaiselvi Periandavan conceived the idea, provided directions for designing the experiments, and supervised the entire work.

Acknowledgments

The financial assistance to Dr. Kishore Kumar S Narasimhan, Department of Medical Biochemistry, from the Indian Council of Medical Research (ICMR) in the form of ICMR Senior Research Fellow (SRF), New Delhi, Government of India, is gratefully acknowledged. Authors greatly appreciate Dr. Gobinath Shanmugam for assisting with artwork (figures) and Mr. Justin Quiles for his editorial assistance.

Supplementary Materials

The supplementary materials (SM) provided along with this manuscript details about the methods we used to determine the levels of oxidative stress markers, activities of antioxidant defense systems/downstream enzymes of Nrf2/ARE signaling pathway, immunofluorescence of α-synuclein, and sequence of the primers used in the PCR protocol. In addition, the SM also provides a data for behavioural analysis (Supplementary Figure 1) and dose determination of scopoletin using MTT assay (Supplementary Figure 2). *(Supplementary Materials)*

References

[1] B. J. Ryan, S. Hoek, E. A. Fon, and R. Wade-Martins, "Mitochondrial dysfunction and mitophagy in Parkinson's: from familial to sporadic disease," *Trends in Biochemical Sciences*, vol. 40, no. 4, pp. 200–210, 2015.

[2] X. Chen, C. Guo, and J. Kong, "Oxidative stress in Neurodegenerative diseases," *Neural Regeneration Research*, vol. 7, no. 5, pp. 376–385, 2012.

[3] T. Tamura, M. Yoshida, Y. Hashizume, and G. Sobue, "Lewy body-related α-synucleinopathy in the spinal cord of cases with incidental Lewy body disease," *Neuropathology*, vol. 32, no. 1, pp. 13–22, 2012.

[4] S. Shendelman, A. Jonason, C. Martinat, T. Leete, and A. Abeliovich, "DJ-1 is a redox-dependent molecular chaperone that inhibits α-synuclein aggregate formation," *PLoS Biology*, vol. 2, no. 11, article e362, 2004.

[5] L. Gan and J. A. Johnson, "Oxidative damage and the Nrf2-ARE pathway in neurodegenerative diseases," *Biochimica et Biophysica Acta (BBA) - Molecular Basis of Disease*, vol. 1842, no. 8, pp. 1208–1218, 2014.

[6] F. Jin, Q. Wu, Y. F. Lu, Q. H. Gong, and J. S. Shi, "Neuroprotective effect of resveratrol on 6-OHDA-induced Parkinson's disease in rats," *European Journal of Pharmacology*, vol. 600, no. 1-3, pp. 78–82, 2008.

[7] J. A. Johnson, D. A. Johnson, A. D. Kraft et al., "The Nrf2–ARE pathway," *Annals of the New York Academy of Sciences*, vol. 1147, no. 1, pp. 61–69, 2008.

[8] Y. Masaki, Y. Izumi, A. Matsumura, A. Akaike, and T. Kume, "Protective effect of Nrf2–ARE activator isolated from green perilla leaves on dopaminergic neuronal loss in a Parkinson's disease model," *European Journal of Pharmacology*, vol. 798, pp. 26–34, 2017.

[9] V. Sharma and A. Agarwal, "Physicochemical and antioxidant assays of methanol and hydromethanol extract of ariel parts of *Indigofera tinctoria* Linn," *Indian Journal of Pharmaceutical Sciences*, vol. 77, no. 6, pp. 729–734, 2015.

[10] K. K. S. Narasimhan, L. Paul, Y. K. Sathyamoorthy et al., "Amelioration of apoptotic events in the skeletal muscle of intra-nigrally rotenone-infused Parkinsonian rats by *Morinda citrifolia* – up-regulation of Bcl-2 and blockage of cytochrome c release," *Food & Function*, vol. 7, no. 2, pp. 922–937, 2016.

[11] S. N. Kishore Kumar, J. Deepthy, U. Saraswathi et al., "*Morinda citrifolia* mitigates rotenone-induced striatal neuronal loss in male Sprague-Dawley rats by preventing mitochondrial pathway of intrinsic apoptosis," *Redox Report*, vol. 22, no. 6, pp. 418–429, 2017.

[12] C. E. Adams, A. F. Hoffman, J. L. Hudson, B. J. Hoffer, and S. J. Boyson, "Chronic treatment with levodopa and/or selegiline does not affect behavioral recovery induced by fetal ventral mesencephalic grafts in unilaterally 6-hydroxydopamine-lesioned rats," *Experimental Neurology*, vol. 130, no. 2, pp. 261–268, 1994.

[13] Y. N. Deng, J. Shi, J. Liu, and Q. M. Qu, "Celastrol protects human neuroblastoma SH-SY5Y cells from rotenone-induced injury through induction of autophagy," *Neurochemistry International*, vol. 63, no. 1, pp. 1–9, 2013.

[14] K. J. Barnham, C. L. Masters, and A. I. Bush, "Neurodegenerative diseases and oxidative stress," *Nature Reviews Drug Discovery*, vol. 3, no. 3, pp. 205–214, 2004.

[15] A. Jazwa, A. I. Rojo, N. G. Innamorato, M. Hesse, J. Fernández-Ruiz, and A. Cuadrado, "Pharmacological targeting of the transcription factor Nrf2 at the basal ganglia provides disease modifying therapy for experimental Parkinsonism," *Antioxidants & Redox Signaling*, vol. 14, no. 12, pp. 2347–2360, 2011.

[16] M. S. Bitar, C. Liu, A. Ziaei, Y. Chen, T. Schmedt, and U. V. Jurkunas, "Decline in DJ-1 and decreased nuclear translocation of Nrf2 in Fuchs endothelial corneal dystrophy," *Investigative Ophthalmology & Visual Science*, vol. 53, no. 9, pp. 5806–5813, 2012.

[17] J. W. Yao, J. Liu, X. Z. Kong et al., "Induction of activation of the antioxidant response element and stabilization of Nrf2 by 3-(3-pyridylmethylidene)-2-indolinone (PMID) confers protection against oxidative stress-induced cell death," *Toxicology and Applied Pharmacology*, vol. 259, no. 2, pp. 227–235, 2012.

[18] Y. He, S. Z. Imam, Z. Dong et al., "Role of nitric oxide in rotenone-induced nigro-striatal injury," *Journal of Neurochemistry*, vol. 86, no. 6, pp. 1338–1345, 2003.

[19] S. D. Pachauri, P. R. P. Verma, A. K. Dwivedi et al., "Ameliorative effect of Noni fruit extract on streptozotocin-induced memory impairment in mice," *Behavioural Pharmacology*, vol. 24, no. 4, pp. 307–319, 2013.

[20] L. Stefanis, "α-Synuclein in Parkinson's disease," *Cold Spring Harbor Perspectives in Medicine*, vol. 2, no. 2, article a009399, 2011.

[21] A. Oczkowska, W. Kozubski, M. Lianeri, and J. Dorszewska, "Mutations in PRKN and SNCA genes important for the progress of Parkinson's disease," *Current Genomics*, vol. 14, no. 8, pp. 502–517, 2013.

[22] E. Paxinou, Q. Chen, M. Weisse et al., "Induction of α-synuclein aggregation by intracellular nitrative insult," *Journal of Neuroscience*, vol. 21, no. 20, pp. 8053–8061, 2001.

[23] R. I. López-Cruz, T. Zenteno-Savín, and F. Galván-Magaña, "Superoxide production, oxidative damage and enzymatic antioxidant defenses in shark skeletal muscle," *Comparative Biochemistry and Physiology Part A: Molecular & Integrative Physiology*, vol. 156, no. 1, pp. 50–56, 2010.

[24] B. Poljsak, D. Šuput, and I. Milisav, "Achieving the balance between ROS and antioxidants: when to use the synthetic antioxidants," *Oxidative Medicine and Cellular Longevity*, vol. 2013, Article ID 956792, 11 pages, 2013.

[25] P. Muralidharan, V. R. Kumar, and G. Balamurugan, "Protective effect of *Morinda citrifoliafruits* on β-amyloid (25–35) induced cognitive dysfunction in mice: an experimental and biochemical study," *Phytotherapy Research*, vol. 24, no. 2, pp. 252–258, 2010.

[26] N. Mercado, R. Thimmulappa, C. M. R. Thomas et al., "Decreased histone deacetylase 2 impairs Nrf2 activation by oxidative stress," *Biochemical and Biophysical Research Communications*, vol. 406, no. 2, pp. 292–298, 2011.

[27] S. B. Cullinan and J. A. Diehl, "PERK-dependent activation of Nrf2 contributes to redox homeostasis and cell survival following endoplasmic reticulum stress," *Journal of Biological Chemistry*, vol. 279, no. 19, pp. 20108–20117, 2004.

[28] T. Nguyen, P. J. Sherratt, P. Nioi, C. S. Yang, and C. B. Pickett, "Nrf2 controls constitutive and inducible expression of ARE-driven genes through a dynamic pathway involving nucleocytoplasmic shuttling by Keap1," *Journal of Biological Chemistry*, vol. 280, no. 37, pp. 32485–32492, 2005.

[29] S. Mahattanadul, W. Ridtitid, S. Nima, N. Phdoongsombut, P. Ratanasuwon, and S. Kasiwong, "Effects of *Morinda citrifolia* aqueous fruit extract and its biomarker scopoletin on reflux esophagitis and gastric ulcer in rats," *Journal of Ethnopharmacology*, vol. 134, no. 2, pp. 243–250, 2011.

[30] A. Wach, K. Pyrzynska, and M. Biesaga, "Quercetin content in some food and herbal samples," *Food Chemistry*, vol. 100, no. 2, pp. 699–704, 2007.

[31] J. Kalinova and E. Dadakova, "Rutin and total quercetin content in amaranth (*Amaranthus* spp.)," *Plant Foods for Human Nutrition*, vol. 64, no. 1, pp. 68–74, 2009.

[32] W. Jang, H. J. Kim, H. Li et al., "1,25-Dyhydroxyvitamin D_3 attenuates rotenone-induced neurotoxicity in SH-SY5Y cells through induction of autophagy," *Biochemical and Biophysical Research Communications*, vol. 451, no. 1, pp. 142–147, 2014.

[33] R. Mogana, K. Teng-Jin, and C. Wiart, "Anti-inflammatory, anticholinesterase, and antioxidant potential of scopoletin isolated from *Canarium patentinervium* Miq. (Burseraceae Kunth)," *Evidence-Based Complementary and Alternative Medicine*, vol. 2013, Article ID 734824, 7 pages, 2013.

[34] E. K. Kim, K. B. Kwon, B. C. Shin et al., "Scopoletin induces apoptosis in human promyeloleukemic cells, accompanied by activations of nuclear factor κB and caspase-3," *Life Sciences*, vol. 77, no. 7, pp. 824–836, 2005.

[35] P. Zhao, Y. Dou, L. Chen et al., "SC-III3, a novel scopoletin derivative, induces autophagy of human hepatoma HepG2 cells through AMPK/mTOR signaling pathway by acting on mitochondria," *Fitoterapia*, vol. 104, pp. 31–40, 2015.

[36] Y. M. Tabana, L. E. A. Hassan, M. B. K. Ahamed et al., "Scopoletin, an active principle of tree tobacco (*Nicotiana glauca*) inhibits human tumor vascularization in xenograft models and modulates ERK1, VEGF-A, and FGF-2 in computer model," *Microvascular Research*, vol. 107, pp. 17–33, 2016.

[37] H. Nam and M. M. Kim, "Scopoletin has a potential activity for anti-aging via autophagy in human lung fibroblasts," *Phytomedicine*, vol. 22, no. 3, pp. 362–368, 2015.

[38] C. M. Clements, R. S. McNally, B. J. Conti, T. W. Mak, and J. P. Y. Ting, "DJ-1, a cancer-and Parkinson's disease-associated protein, stabilizes the antioxidant transcriptional master regulator Nrf2," *Proceedings of the National Academy of Sciences*, vol. 103, no. 41, pp. 15091–15096, 2006.

[39] B. Björkblom, A. Adilbayeva, J. Maple-Grødem et al., "Parkinson disease protein DJ-1 binds metals and protects against metal-induced cytotoxicity," *Journal of Biological Chemistry*, vol. 288, no. 31, pp. 22809–22820, 2013.

[40] M. S. Angeline, P. Chaterjee, K. Anand, R. K. Ambasta, and P. Kumar, "Rotenone-induced parkinsonism elicits behavioral impairments and differential expression of parkin, heat shock proteins and caspases in the rat," *Neuroscience*, vol. 220, pp. 291–301, 2012.

[41] H. Gao, W. Yang, Z. Qi et al., "DJ-1 protects dopaminergic neurons against rotenone-induced apoptosis by enhancing ERK-dependent mitophagy," *Journal of Molecular Biology*, vol. 423, no. 2, pp. 232–248, 2012.

Hindawi
Oxidative Medicine and Cellular Longevity
Volume 2019, Article ID 5046280, 13 pages
https://doi.org/10.1155/2019/5046280

Research Article

Pasteurized Orange Juice Rich in Carotenoids Protects *Caenorhabditis elegans* against Oxidative Stress and β-Amyloid Toxicity through Direct and Indirect Mechanisms

Ricardo Basílio de Oliveira Caland,[1,2] Cesar Orlando Muñoz Cadavid,[1] Lourdes Carmona,[3] Leandro Peña,[3,4] and Riva de Paula Oliveira[1,5]

[1]*Rede Nordeste de Biotecnologia (RENORBIO), Universidade Federal do Rio Grande do Norte, Natal, RN, Brazil*
[2]*Instituto Federal de Educação, Ciência e Tecnologia do Piauí-IFPI, Brazil*
[3]*Fundo de Defesa da Citricultura (Fundecitrus), Araraquara, SP, Brazil*
[4]*Instituto de Biología Molecular y Celular de Plantas, Valencia, Spain*
[5]*Departamento de Biologia Celular e Genética, Universidade Federal do Rio Grande do Norte, Natal, RN, Brazil*

Correspondence should be addressed to Riva de Paula Oliveira; rivaoliveira@cb.ufrn.br

Received 4 October 2018; Revised 28 December 2018; Accepted 17 January 2019; Published 18 April 2019

Guest Editor: Luciana Scotti

'Cara Cara' is a red orange (*Citrus sinensis* (L.) Osbeck) variety originally from Venezuela characterized by a significantly higher and diversified carotenoid content including higher-concentration lycopene, *all*-E-β-carotene, phytoene, and other carotenoids when compared with the carotenoid profile of its isogenic blond counterpart 'Bahia', also known as Washington navel. The exceptionally high carotenoid content of 'Cara Cara' is of special interest due to its neuroprotective potential. Here, we used the nematode *Caenorhabditis elegans* to analyze the antioxidant effect and the protection against β-amyloid-induced toxicity of pasteurized orange juice (POJ) obtained from 'Cara Cara' and compare to that from 'Bahia'. POJ treatment reduced the endogenous ROS levels and increased the worm's survival rate under normal and oxidative stress conditions. POJ treatment also upregulated the expression of antioxidant (*gcs-1*, *gst-4*, and *sod-3*) and chaperonin (*hsp-16.2*) genes. Remarkably, ROS reduction, gene expression activation, oxidative stress resistance, and longevity extension were significantly increased in the animals treated with 'Cara Cara' orange juice compared to animals treated with 'Bahia' orange juice. Furthermore, the body paralysis induced by β-amyloid peptide was delayed by both POJs but the mean paralysis time for the worms treated with 'Cara Cara' orange juice was significantly higher compared to 'Bahia' orange juice. Our mechanistic studies indicated that POJ-reduced ROS levels are primarily a result of the direct scavenging action of natural compounds available in the orange juice. Moreover, POJ-induced *gst-4*::*GFP* expression and –increased stress resistance was dependent of the SKN-1/Nrf2 transcription factor. Finally, the transcription factors SKN-1, DAF-16, and HSF-1 were required for the POJ-mediated protective effect against Aβ toxicity. Collectively, these results suggest that orange juice from 'Cara Cara' induced a stronger response against oxidative stress and β-amyloid toxicity compared to orange juice from 'Bahia' possibly due to its higher carotenoid content.

1. Introduction

Citrus sinensis L. Osbeck orange juice is considered an excellent dietary source of several bioactive compounds with beneficial properties for human health due to its high content of flavonoids, carotenoids, sugars, minerals, and fiber. Numerous epidemiological and intervention studies have provided substantial evidence to support an inverse correlation between orange juice intake and the occurrence of cardiovascular disease, cancer, and aging-related disorders [1, 2].

Among sweet oranges, there is increasing interest in *C. sinensis* Osbeck cv. 'Cara Cara', a bud mutation originated from 'Bahia' navel orange, also known as 'Washington' navel orange. 'Cara Cara' orange pulp is characterized by

a bright red coloration due to a significantly higher and diversified carotenoid content compared to 'Bahia' juice, with a mixture of (Z)-isomers of lycopene, *all*-E-β-carotene, phytoene, and phytofluene isomers [3]. Total flavanone content as well as hesperidin levels are usually comparable in 'Cara Cara' and 'Bahia' pasteurized juice [1]. On the other hand, 'Bahia' presents a higher ascorbic acid content compared to 'Cara Cara' [1]. The exceptionally high carotenoid content of 'Cara Cara' may be of special interest due to recent nutritional studies that have demonstrated its association with the prevention and treatment of various diseases, including neurodegenerative diseases (ND) [4].

Carotenoids are the main pigments responsible for the color of the peel and pulp of citrus fruits. They have been indicated as important dietary nutrients having antioxidant, anti-inflammatory, antimutagenic, anticarcinogenic, and autophagy-modulatory activities [4, 5]. In addition to their direct antioxidant activities, carotenoids can protect cells from oxidative stress by activating the antioxidant network enzymes, including superoxide dismutase (SOD) and catalase (CAT) [4].

Given that oxidative damage and increased neuroinflammation are critically related with the pathogenesis of and neuronal loss in neurodegenerative diseases, the neuroprotective effect of carotenoids has been of specific interest in the search for effective treatments for these diseases. The beneficial effects of dietary carotenoids such as lycopene, astaxanthin, crocin, crocetin, and fucoxanthin on neurodegenerative diseases have been recently studied in animal and cell culture models for Alzheimer's disease (AD) [4]. In a recent paper, Hwang et al. [6] showed that lycopene significantly inhibited intracellular β-amyloid accumulation and reduced mitochondrial ROS levels and apoptotic cell death in human neuronal SH-SY5Y cells. In the rodent models, administration of certain types of carotenoids, including lycopene, successfully attenuated not only cellular-level phenotypes such as mitochondrial oxidative damage and increased neuroinflammation but also organism-level phenotypes such as memory impairment and locomotive defects [7]. Despite these studies, there is a substantial lack of AD animal models to show the therapeutic potential of carotenoids against neurodegenerative disease [8–11].

The nematode worm *Caenorhabditis elegans* is an established model organism to study aging and age-related disorders [12–14] and an attractive platform for rapidly screening drug safety and efficacy [15]. It has been demonstrated that lutein supplementation in *C. elegans* is able to suppress the ROS generation induced by the hepatotoxin microcystin-LR (MIC-LR) and restore the levels of the antioxidant enzyme CAT, as well as their survival rate [16]. Pons et al. [17] showed that transgenic β-carotene-enriched orange increases *C. elegans* survival under oxidative stress induced by hydrogen peroxide. Furthermore, a delay of paralysis in a β-amyloid peptide transgenic *C. elegans* strain was induced by lycopene [18], while fucoxanthin, but not β-carotene, provided positive effects on the *C. elegans* lifespan [19].

A number of genes and pathways have been identified to modulate lifespan, stress resistance, and proteostasis in *C. elegans* [20, 21]. These highly conserved pathways include the transcription factors heat shock factor 1 homologue HSF-1, the FOXO homologue DAF-16, and the Nrf-1/2 homologue SKN-1. HSF-1 controls the inducible transcription of a family of genes encoding heat shock proteins (HSPs), many of which are molecular chaperones. The DAF-16/FOXO target genes include specific *hsps* and other stress response/longevity genes. SKN-1 mediates the expression of genes involved in a wide range of detoxification processes, as well as in immunity, proteostasis, and metabolism. Collectively, these transcription factors orchestrate the expression of genes that contribute to longevity.

Up to date, there are no data demonstrating the antioxidant and neuroprotective capacity of pasteurized orange juice (POJ). Here in this work, we assessed and compared the antioxidant capacity and the protective effect against the β-amyloid peptide of pasteurized orange juice from 'Cara Cara' with respect to that from the 'Bahia' counterpart using the nematode *C. elegans*.

2. Materials and Methods

2.1. Chemicals, Reagents, and Strains. *tert*-Butyl hydroperoxide (TBHP), fluorodeoxyuridine (FUdR), and 2,7-dichlorodihydrofluorescein diacetate (H_2DCFDA) were purchased from Sigma-Aldrich (St. Louis, MO, USA).

The following *Caenorhabditis elegans* strains were used: N2 (wild-type strain), EU40 (*skn-1(zu129) IV/nT1 [unc-?(n754) let-?]*) (*IV;V*), CF1038 (*daf-16(mu86) I*), PS3551 (*hsf-1(sy441) I*), CL2006 (*dvIs2[pCL12(unc-54/human Abeta peptide 1-42 minigene) + pRF4]*), CF1553 (*muIs84 [pAD76(sod-3::GFP)]*), CL2166 (*dvls19[pAF15(gst-4::GFP::NLS)]*), LD1171 (*ldIs3[gcs-1p::GFP + rol-6(su1006)]*), and TJ375 (*gpls[hsp-16.2::GFP]*).

2.2. Pasteurized Orange Juice (POJ) Preparation. Pasteurized orange juices obtained from *C. sinensis* L. Osbeck cv. 'Cara Cara' and cv. 'Bahia' were provided by Citrosuco (Matão, São Paulo, Brazil). Oranges from both cultivars were collected on June 7th 2016 in Araraquara (São Paulo, Brazil) located in southeastern São Paulo at 23°23′19″ S and 48°43′22″ W with an elevation of 600 m above sea level. Orange juices were obtained by cutting and squeezing, using an industrial extractor (model 391, JBT). The pasteurization process was achieved in an industrial pasteurizer (UHT/HTST Lab-25-DH, Micro-Thermics) at 92– 94°C for 17 s (750 mL/min). After processing, the juices were filled into 1 L plastic flasks and cooled to 1°C. All juices were immediately stored at −20°C.

2.3. POJ Characterization. Determination of °Brix/acidity ratio: juice acidity was determined by titration with phenolphthalein and 0.1 N NaOH and was expressed as mg citric acid per 100 g. The soluble solid content (°Brix) was estimated by refractometry, using an Atago® refractometer. The maturity index is expressed as the ratio of °Brix/acidity.

Determination of limonin and vitamin C: limonin extraction was performed by centrifugation of orange juice (50 mL) for 15 min at 5000 rpm. Subsequently, a volume of 2 mL of juice sample was passed through a C18 Sep-Pak

cartridge (Waters), and water was added to the concentrated sample and eluted with vacuum using acetonitrile. Finally, the elution was filtered and prepared for HPLC analysis [22]. Vitamin C content was evaluated by the titration method described by Stevens [23].

Carotenoids were extracted as is described in Alquezar et al. [24]. UPLC analysis of individual carotenoids: the carotenoid composition of each sample was analyzed by UPLC with a Nexera X2 Shimadzu liquid chromatography system equipped with a LC-30AD pump and a SPD-M20A photodiode array detector, as well as LabSolutions software (version 5.57 SP1). An Acquity BEH C18 carotenoid column (100 mm × 2.1 mm, 1.8 μm) coupled to a C18 guard column (20 mm × 2.1 mm) (Waters, USA) was used. Samples were prepared for UPLC by dissolving the dried carotenoid extracts in $CHCl_3$: MeOH : acetone (3 : 2 : 1, $v : v : v$). For carotenoid separation, a binary gradient elution was adapted from the ternary described by Alquezar et al. [24] by using the Gradient Method Calculator (Thermo Scientific). The initial solvent composition consisted of 100% MeOH : water (90 : 5, v/v) and 5% methyl tert-butyl ether (MTBE). The solvent composition changed in a linear fashion to 95% MeOH : water and 5% MTBE at 0.91 min. During the next minute, the solvent composition was changed to 86% MeOH : water and 14% MTBE. After reaching this concentration, the solvent was gradually changed to 75% MeOH : water and 25% MTBE at 2.28 min, 50% MeOH : water and 50% MTBE 50% at 3.8 min, and 25% MeOH : water and 75% MTBE at 5.32 min. The initial conditions were reached at 6 min, and the column was equilibrated for 2 min before the next injection. The flow rate was 0.5 mL min^{-1}, column temperature was set to 27°C, and the injection volume was 3 μL. The photodiode array detector was set to scan from 250 to 800 nm, and for each elution a MaxPlot chromatogram was obtained, which plots each carotenoid peak at its corresponding maximum absorbance wavelength. Carotenoids were identified by their retention time, absorption, and fine spectra [25–29]. The carotenoid peaks were integrated at their individual maxima wavelength, and their contents were calculated using calibration curves of β-carotene (Sigma) for α- and β-carotene; β-cryptoxanthin (Extrasynthese) for β-cryptoxanthin; zeaxanthin (Extrasynthese) for zeaxanthin; lutein (Sigma) for violaxanthin isomers, mutatoxanthin and antheraxanthin; lycopene (Sigma) for lycopene; and phytoene (Sigma) for phytoene and phytofluene.

2.4. C. elegans Culture Conditions. For all the experimental procedures, *C. elegans* were cultured at 20°C on Nematode Growth Medium (NGM) plates [30] seeded with *Escherichia coli* OP50. For treatment, worms were cultivated on NGM plates containing 1, 2, 5, or 10% POJ of either 'Bahia' or 'Cara Cara'. The control group was prepared in the same manner but without POJ. Tests were also performed with heat-killed *E. coli* OP50 (OP50-HK). Heat-killed bacteria were prepared by incubating liquid cultures of *E. coli* OP50 to 75°C for 1 hour. Synchronized populations were obtained by either bleach treatment or egg-laying.

RNA interference (RNAi) was carried out using the feeding method described previously [31]. Briefly, RNAi clones were grown with 12.5 μg/mL tetracycline and 100 μg/mL ampicillin. On the following day, cultures were diluted in LB supplemented with 60 μg/mL ampicillin and grown to an OD600 of 1. This culture was used to seed plates containing ampicillin and 1 mM IPTG and left to dry for 2 days at room temperature. Synchronized L1 larvae were then placed at 20°C on *E. coli* HT115 that expressed target gene RNAi or control RNAi (empty vector pL4440) for 48 h, until they reached the L4 stage. *skn-1* RNAi efficiency was verified by the absence of F1 larvae. For *daf-16*, RNAi efficiency was confirmed by the suppression of GFP emission on *DAF-16::GFP* transgenic line (TJ356). For *hsf-1*, RNAi efficiency was confirmed by the worms reduced survival at 35°C.

2.5. Quantification of Intracellular ROS. N2 wild-type animals synchronized at first-stage larvae (L1) were cultivated on NGM with different concentrations of POJ for 48 h. The experiments were performed under standard and stress conditions as described previously by de Freitas Bonomo et al. [32] with modification. For the stress condition, the animals were exposed to 10 mM *tert*-butyl hydroperoxide (TBHP) in M9 medium for 1 hour. Subsequently, 20 to 40 worms per group were collected in PBS+ 1% Tween-20, washed twice, and transferred to a 96-well microtiter plate, to which 50 μM H_2DCF-DA was added. Measurements were performed in triplicate in a multilabel microplate reader GloMax®-Multi Detection System (Promega, Wisconsin, USA), with excitation at 490 nm and emission at 510-570 nm, and the mean values were calculated. Readings were performed every 30 min for 4 h.

2.6. Reporter Gene Analysis. Transgenic lines expressing *gcs-1::GFP*, *gst-4::GFP*, *sod-3::GFP*, and *hsp-16.2::GFP* were treated with 2% POJ for 48 h at 20°C since L1 until the L4 stage. The experiments were performed under standard and stress conditions. For *gcs-1::GFP*, *gst-4::GFP*, and *sod-3::GFP* animals, the stress condition was induced by incubating in 10 mM TBHP in M9 medium for 1 hour. For *hsp-16.2::GFP*, the stress condition was induced for 1 h at 35°C. Images of 25 worms from each group were acquired using the optic microscope Olympus BX51 (Tokyo, Japan) and fluorescent signals were measured with NIH ImageJ software.

2.7. Lifespan and Stress Resistance Assays. The lifespan assay was performed with synchronized N2 wild-type animals treated with 2% POJ starting at the L4 stage. We analyzed approximately 90 animals per group divided into 3 NGM plates containing FUdR to prevent progeny growth. The survival analysis consisted of scoring dead/alive animals every day beginning at the first day of adulthood ($t0$ = day 1) at 25°C. The animals were determined to be dead if no movement was shown with or without stimulation, and those animals with hatched eggs internally, extruded parts, or those who went missing, were excluded from analysis.

To evaluate the resistance to oxidative stress, L4 larval stage of wild-type animals and *skn-1(zu129)*, *daf-16(mu86)*, and *hsf-1(sy441)* mutants were treated with 2% POJ for 48 h on NGM plates containing FUdR seeded with either *E. coli* OP50 (OP50) or heat-killed *E. coli* OP50 (OP50-HK). After that, they were exposed to 10 mM TBHP. Approximately 50 animals were analyzed for each experimental group. Survival fractions were scored every three hours until all animals were considered dead, without pumping or pharyngeal movement. The oxidative stress resistance test was performed three times.

2.8. Bioassays for β-Amyloid-Induced Paralysis. CL2006 strains, which constitutively express Aβ1–42 peptide in the body wall muscle tissue, were treated since L1 until L4 stage on NGM plates with *E. coli* OP50 for 48 hours at 20°C. Animals were then transferred to new plates containing 2% POJ seeded with either *E. coli* OP50 or OP50-HK for another 48 hours at 20°C. The paralysis phenotype was accelerated by transferring the worms to 35°C. Paralysis was scored at 1 h intervals for up to 12 h. The worms were scored as "paralyzed" based on either the failure of the worms to move their body with the touch of a platinum loop or the formation of a halo on the bacterial lawn indicating a paralyzed condition. Each experiment was performed using at least 30 worms. The data represents mean of three different experiments.

2.9. Statistical Analyses. All experiments were performed three times. Statistical analyses were performed using GraphPad Prism (v. 5.0) software (CA, USA). Data were analyzed by Kolmogorov-Smirnov test for normality. For normally distributed data, Student's *t* test was used to compare pairs of groups, whereas a one-way ANOVA followed by Tukey's posttest was used to compare three or more groups. Nonparametric data were analyzed using the Mann–Whitney test when comparing two groups and the Kruskal-Wallis test followed by Dunn's posttest for comparing three or more groups. Survival curves were analyzed by the log-rank (Mantel-Cox) test. For all tests, statistical significance was determined as $p < 0.05$.

3. Results and Discussion

3.1. Quality and Phytochemical Characterization of Pasteurized Juice from 'Cara Cara' and 'Bahia' Oranges. After pasteurization, we compared some quality and phytochemical compounds of the 'Bahia' sweet orange juice and its spontaneous red-fleshed mutant 'Cara Cara', which contains large proportions of linear carotenes. Pasteurized 'Bahia' juice (PBJ) was more acidic than pasteurized 'Cara Cara' juice (PCJ) (Table 1). A higher content of ascorbic acid and limonin was recorded in PBJ compared to PCJ (Table 1). As expected, the total carotenoid content was significantly higher in 'Cara Cara' juice compared to 'Bahia', especially *Z*-violaxanthin, zeaxanthin, phytoene, phytofluene, lycopene, and β-carotene (Table 2). These results are comparable essentially to those of the previous studies by Brasili et al. [1] and Lee [3], which showed that lycopene and β-carotene accumulated at high levels in PCJ but their concentrations were very low or undetectable in PBJ.

Table 1: Quality parameters of pasteurized juices from 'Bahia' and 'Cara Cara' oranges.

Parameters	Bahia	Cara Cara
°Brix	10.8 ± 0.2	9.5 ± 0.1
Acidity (g/100 g)	0.8 ± 0.0	0.5 ± 0.0
Ratio °Brix/acidity	14.1 ± 0.3	18.6 ± 0.1
Vitamin C (mg/L)	424.9 ± 20.7	215.7 ± 9.8
Limonin (mg/L)	7.4 ± 1.4	2.7 ± 0.3

Table 2: Content of carotenoids in pasteurized juices from 'Bahia' and 'Cara Cara' oranges.

Carotenoid (ng/mL)	Bahia	Cara Cara
E-violaxanthin	Tr.	Tr.
Z-Luteoxanthin[a]	34.52 ± 5.26	n.d.
all-E-Luteoxanthin[a]	271.89 ± 32.79	n.d.
Z-Violaxanthin	815.68 ± 26.42	1021.94 ± 109.94
Zeaxanthin[a]	Tr.	195.01 ± 48.78
Anteraxanthin	20.82 ± 8.27	n.d.
Mutatoxanthin[a]	66.09 ± 9.92	n.d.
Zeinoxanthin[a]	196.31 ± 10.6	n.d.
β-Cryptoxanthin	456.50 ± 14.08	351.07 ± 4.69
Phytoene	n.d.	6172.03 ± 113.78
Phytofluene	n.d.	2661.61 ± 136.84
Lycopene	n.d.	469.05 ± 26.55
α-Carotene[a]	n.d	Tr.
β-Carotene	n.d.	228.89 ± 78.47
Total[b]:	1564.81 ± 70.41	11099.25 ± 158.88

n.d.: not detected. Tr.: traces. [a]Identified tentatively, [d]total carotenoids calculated as the sum of all the carotenoids identified individually.

3.2. POJ Treatment Reduces Intracellular ROS Accumulation Primarily as a Result of Direct Scavenging. In order to determine the antioxidant capacity of POJ from 'Bahia' and 'Cara Cara' orange, we investigated the influence of the POJ treatment on the intracellular accumulation of ROS in *C. elegans*. Under standard condition, wild-type worms treated with 1, 2, 5, and 10% of either 'Bahia' or 'Cara Cara' juice displayed reduced ROS levels compared to the control group of untreated worms ($p < 0.0001$) (Figure 1(a)). Interestingly, ROS levels were significantly lower in the animals treated with 2% 'Cara Cara' juice compared to those from worms treated with 2% 'Bahia' juice ($p = 0.0026$) (Figure 1(a)). Similar results were also observed when the worms were treated with POJ and then subjected to stress conditions (Figure 1(b)). All concentrations tested of POJ were able to reduce ROS production under stress

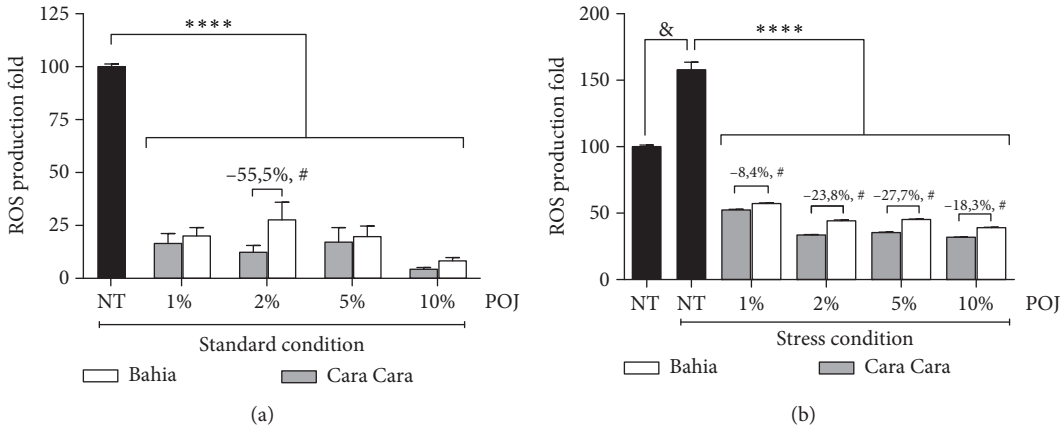

Figure 1: Effect of pasteurized juice from 'Bahia' and 'Cara Cara' oranges on intracellular ROS accumulation in *C. elegans*. (a) Wild-type animals were treated with either 1, 2, 5, or 10% of 'Bahia' or 'Cara Cara' juice for approximately 48 h since L1. ROS production was measured using the dye H_2DCFDA. Results are expressed as H_2DCFDA fluorescence levels. $^{****}p < 0.0001$ compared to respective not treated (NT) control and $^{\#}p = 0.0026$ comparing 2% 'Bahia' with 2% 'Cara Cara' juice by 2-way ANOVA. (b) Wild-type animals were treated with either 1, 2, 5, or 10% of 'Bahia' or 'Cara Cara' juices for approximately 48 h since L1 and then incubated on 10 mM TBHP for 1 hour to induce oxidative stress. Results are expressed as mean H_2DCFDA fluorescence levels ± SEM of values. $^{\&}p < 0.0001$ compared to NT under standard conditions by a two-tailed Student's *t*-test, $^{****}p < 0.0001$ compared to respective NT control under stress and $^{\#}p < 0.0001$ comparing 'Bahia' orange with 'Cara Cara' juice in each concentration by 2-way ANOVA. Percentage difference (%) between 'Bahia' and 'Cara Cara' juices are indicated for those with $^{\#}$statistically significance.

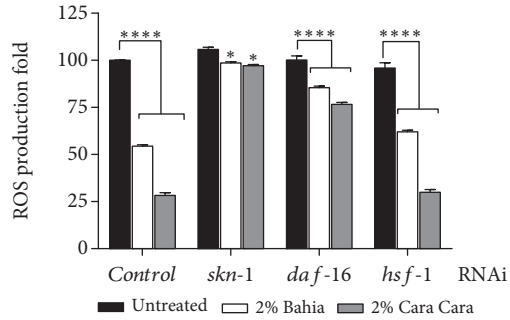

Figure 2: Contribution of SKN-1, DAF-16, and HSF-1 on ROS accumulation in POJ-treated worms. RNAi animals were treated with 2% POJ for approximately 48 h since L1. ROS production was measured using the dye H_2DCFDA. Results are expressed as mean H_2DCFDA fluorescence levels ± SEM of values. $^{****}p < 0.0001$, $^{**}p < 0.0016$, and $^{*}p < 0.0111$ compared to respective untreated RNAi by 2-way ANOVA.

conditions to a level below to those observed in the animals subjected to standard condition ($p < 0.0001$) (Figure 1(b)). Under stress conditions, 'Cara Cara' juice reduced ROS production more efficiently than 'Bahia' juice did in all concentrations tested ($p < 0.0001$). Since 2% 'Cara Cara' juice was the only concentration that showed better results than 'Bahia' juice under standard conditions, we performed all following assays using 2% POJ treatment.

Phytochemicals have the potential to modulate intracellular oxidative stress directly by scavenging free radicals. Besides that, they are also able to modulate oxidative stress indirectly by upregulating antioxidant and phase II detoxification enzymes which are the major enzymatic line of defense against electrophilic toxicants and oxidative stress. The induction of these adaptive systems by phytochemicals may be related to the fact that they function as xenobiotics in animals [33, 34]. The metabolism of xenobiotics/phytochemicals can produce reactive species, reactive intermediates, and metabolites that can act as prooxidants [35]. Therefore, phytonutrients would play a role as a mild stress trigger leading to the activation of defense mechanisms for their own detoxification, which in turn could induce organisms' resistance to a more severe oxidative stress condition. In *C. elegans*, these defense mechanisms are at least partly a result of the activation of three transcription factors, DAF-16, SKN-1, and HSF-1 [36].

In order to elucidate whether ROS reduction was related to POJ direct or an indirect mechanism of action, we performed ROS quantification in animals submitted to RNAi for the SKN-1, DAF-16, and HSF-1 transcription factors. Under standard conditions, knockdown of *skn-1*, *daf-16*, and *hsf-1* significantly reduced the ROS production in the worms treated with 2% of either 'Bahia' or 'Cara Cara' juices (Figure 2) suggesting that ROS reduction induced by POJ may be independent of these transcription factors. Interestingly, quantification of ROS levels showed that the lowest reduction was on *skn-1(RNAi)* animals (Figure 2). The ROS level diminished only by 6.75 and 8.18% on *skn-1(RNAi)* worms treated with 2% 'Bahia' and 2% 'Cara Cara' juices, respectively. Meanwhile, ROS reduction was 14.48% and 23.35% on *daf-16(RNAi)* animals and 33.88% and 66% on *hsf-1(RNAi)* animals treated with 2% 'Bahia' or 'Cara Cara' juices, respectively. This result suggests that ROS reduction promoted by POJ treatment was primarily a result of the direct scavenging action of the carotenoids and other phytonutrients present in the orange juice and secondly an outcome of the transcription factor SKN-1 indirect action.

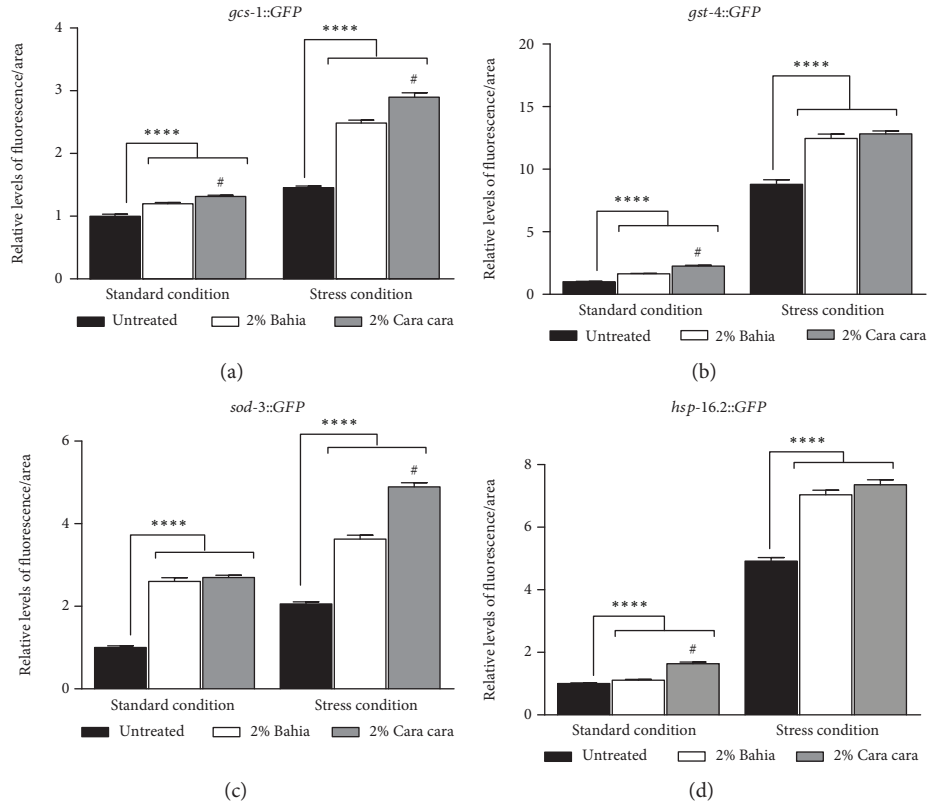

Figure 3: Effect of pasteurized juice from 'Bahia' and 'Cara Cara' oranges on the expression of antioxidant and detoxification genes. Analysis of *gcs-1::GFP* (a), *gst-4::GFP* (b), *sod-3::GFP* (c), and *hsp-16.2::GFP* (d) fluorescent expression levels. Transgenic worms were treated or not with 2% 'Bahia' or 2% 'Cara Cara' juice for 48 h. After this period, animals were submitted to stress conditions. For *gcs-1::GFP* (a), *gst-4::GFP* (b), and *sod-3::GFP* (c); the stress condition was incubation for 1 h on 10 mM TBHP. For *hsp-16.2::GFP*, the stress condition was incubation for 1 h at 35°C. Photographs were taken on a fluorescence microscope, and GFP fluorescence signals were measured using NIH ImageJ software. The results represent mean GFP levels ± SEM of values. $^{****}p < 0.0008$ by a two-tailed Student's *t*-test compared to the untreated group, $^{\#}p < 0.0003$ by a two-tailed Student's *t*-test for 2% 'Bahia' with 2% 'Cara Cara' juice.

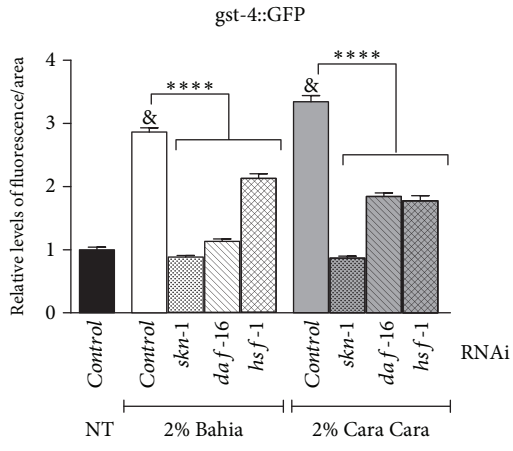

Figure 4: Contribution of SKN-1, DAF-16, and HSF-1 on *gst-4::GFP* expression induced by POJ treatment. RNAi animals were treated with 2% POJ for approximately 48 h since L1. Photographs were taken on a fluorescence microscope, and GFP fluorescence signals were measured using NIH ImageJ software. The results represent mean GFP levels ± SEM of values. $^{\&}p < 0.0001$ compared to untreated (NT) *control(RNAi)* under standard conditions and $^{****}p < 0.0001$, compared to respective POJ-treated *control(RNAi)* by 1-way ANOVA.

3.3. POJ Treatment Induces the Expression of Antioxidant, Detoxification, and Chaperonin Genes. To better characterize the molecular responses associated with the direct and indirect antioxidant effects of POJ in *C. elegans*, we analyzed the gene expression of four reporter genes related to stress resistance, detoxification, and longevity. We selected *γ*-glutamyl cysteine synthetase (*gcs-1*) and glutathione-s-transferase-4 (*gst-4*), two SKN-1 target genes [37, 38], superoxide dismutase 3 (*sod-3*), a well-known DAF-16 target gene [39], and the chaperone *hsp-16.2::GFP* whose expression is regulated by DAF-16 and HSF-1 [40]. The fluorescence signals of *gcs-1::GFP*, *gst-4::GFP*, *sod-3::GFP*, and *hsp-16.2::GFP* animals were significantly increased after 2% POJ treatment with either 'Bahia' or 'Cara Cara' juices compared to untreated worms, both at standard and stress conditions (Figures 3(a)–3(d)). Interestingly, the expression signal of *gcs-1::GFP* (Figure 3(a)), *gst-4::GFP* (Figure 3(b)), and *hsf-16.2::GFP* (Figure 3(d)) from the animals treated with 2% 'Cara Cara' juice were significantly higher than that of the animals treated with 2% 'Bahia' juice under standard conditions. Under stress conditions, the treatment with 2% 'Cara Cara' juice significantly increased the expression of *gcs-1::GFP* and *sod-3::GFP*.

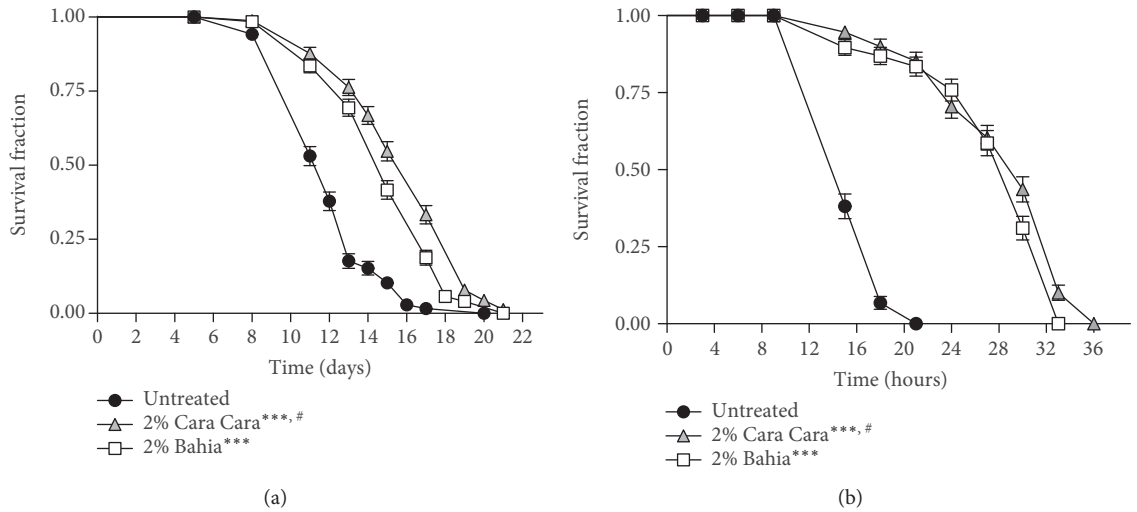

Figure 5: Effect of pasteurized juice from 'Bahia' and 'Cara Cara' oranges on *C. elegans* stress resistance and longevity. (a) Survival curves of wild-type (N2) animals under standard laboratory conditions. Worms were treated with either 2% 'Bahia' or 2% 'Cara Cara' juice beginning at L4. Survival was verified every day at 25°C. $^{****}p < 0.0001$ compared to respective controls and $^{\#}p = 0.0003$ comparing animals treated with 2% 'Bahia' with 2% 'Cara Cara' juice by log-rank (Mantel-Cox) test. (b) Survival curves of wild-type (N2) animals under oxidative stress conditions. Worms were treated with either 2% 'Bahia' or 2% 'Cara Cara' juice beginning at L4 and transferred to plates with 10 mM TBPH. Survival was verified every 3 hours at 20°C. $^{****}p < 0.0001$ compared to the untreated control group and $^{\#}p = 0.0134$ comparing animals treated with 2% 'Bahia' with 2% 'Cara Cara' juice by log-rank (Mantel-Cox) test.

Table 3: Effect of pasteurized juice from 'Bahia' and 'Cara Cara' oranges on *C. elegans* lifespan.

Condition	Maximum survival (days ± SEM)	Mean survival (days ± SEM)	% mean survival time variation vs. untreated	p value (log rank) POJ[a] vs. untreated[b]	p value (log rank) PBJ[c] vs. PCJ[b,d]	N[e]
Untreated	17.33 ± 2.31	12.11 ± 0.13				243 (3)
2% Bahia	19.00 ± 1.73	14.75 ± 0.17	22.0	<0.0001		255 (3)
2% Cara Cara	19.33 ± 2.31	15.64 ± 0.18	29.5	<0.0001	0.0003	234 (3)

[a]POJ, pasteurized orange juice, [b]comparisons were performed using log-rank (Mantel-Cox) test. [c]PBJ, pasteurized 'Bahia' orange juice, [d]PCJ, pasteurized 'Cara Cara' orange juice, [e]total number of animals analyzed. The number in parentheses indicates the number of independent trials.

The POJ induction, rather than an inhibition, of the antioxidant and detoxification genes indicates that the phytonutrients present in the POJ were not only directly scavenging ROS but also acting as prooxidants and inducing a mild cellular stress response [41, 42]. This phenomenon is also referred as hormesis since the phytochemicals are toxic and protect plants against insects and other harmful organisms and stresses. However, at the subtoxic doses, the phytochemicals involve kinases and transcription factors in order to induce the expression of genes that encode antioxidant enzymes, protein chaperones, phase-2 enzymes, neurotrophic factors, and other cytoprotective proteins [41, 42].

Since *gst-4::GFP* showed the strongest expression after POJ treatments, we assessed whether it was dependent on SKN-1, DAF-16, and HSF-1. RNAi of all three transcription factors reduced significantly *gst-4::GFP* expression induced by the POJ treatments suggesting that they all contribute to its activation (Figure 4). Moreover, knocking down of *skn-1* caused the greatest reduction on *gst-4::GFP* expression induced by the POJ treatments. The fluorescent levels of *gst-4::GFP* in the worms treated with 'Bahia' juice were 3.26 times lower on *skn-1(RNAi)* animals compared to *control(RNAi)* animals while the reduction was 2.54 and 1.34 times lower on *daf-16(RNAi)* and *hsf-1(RNAi)* animals, respectively. This result suggests that SKN-1 seemed to play a more important role on *gst-4* expression compared to DAF-16 or HSF-1.

3.4. POJ Treatment Increases Longevity and Oxidative Stress Resistance. To explore whether POJ antioxidant properties have a protective effect *in vivo*, we tested whether POJ could affect the lifespan of *C. elegans* under standard laboratory conditions. We determined the lifespan of N2 worms with and without 2% POJ treatment. The maximum and mean lifespan of N2 worms fed with either 2% pasteurized 'Bahia' or 'Cara Cara' juice was significantly increased compared to untreated worms (Figure 5(a), Table 3). Remarkably, animals treated with 2% 'Cara Cara' juice showed an increased lifespan compared to animals treated with 2% 'Bahia' juice ($p = 0.0003$) (Table 3).

Table 4: Effect of pasteurized juice from 'Bahia' and 'Cara Cara' oranges on *C. elegans* stress resistance.

Strains and conditions	Maximum survival (hours ± SEM)	% maximum survival time variation vs. untreated	Mean survival (hours ± SEM)	% mean survival time variation vs. untreated	p value (log rank) POJ[a] vs. untreated[b]	p value (log rank) PBJ[c] vs. PCJ[b,d]	N[e]
WT on *E. coli* OP50							
Untreated	20.33 ± 1.15		16.50 ± 0.16				145 (3)
2% Bahia	32.00 ± 1.73	57.0	27.72 ± 0.47	68.0	<0.0001		144 (3)
2% Cara Cara	35.00 ± 1.73	71.0	28.63 ± 0.47	73.5	<0.0001	0.0134	149 (3)
WT on *E. coli* OP50-HK							
Untreated	20.00 ± 1.00		15.44 ± 0.28				126 (3)
2% Bahia	23.66 ± 0.58	14.0	17.14 ± 0.33	11.0	<0.0001		134 (3)
2% Cara Cara	26.66 ± 0.58	28.0	20.42 ± 0.26	32.0	<0.0001	<0.0001	131 (3)
skn-1(zu67) on *E. coli* OP50							
Control	11.33 ± 0.58		9.08 ± 0.10				150 (3)
2% Bahia	11.00 ± 1.00	0.0	8.90 ± 0.11	-2.0	0.2405		150 (3)
2% Cara Cara	11.67 ± 0.58	0.0	9.14 ± 0.09	1.0	0.7441	0.1396	150 (3)
daf-16(mu86) on *E. coli* OP50							
Control	12.00 ± 1.73		5.84 ± 0.15				146 (3)
2% Bahia	15.00 ± 1.73	21.0	7.26 ± 0.26	24.0	<0.0001		147 (3)
2% Cara Cara	18.00 ± 1.73	42.0	8.30 ± 0.35	42.0	<0.0001	0.0097	148 (3)
hsf-1*(sy441)* on *E. coli* OP50							
Control	18.00 ± 1.73		14.67 ± 0.22				141 (3)
2% Bahia	23.00 ± 0.00	15.0	17.60 ± 0.38	20.0	<0.0001		150 (3)
2% Cara Cara	25.00 ± 1.73	30.0	19.86 ± 0.37	35.0	<0.0001	<0.0001	150 (3)

HK: heat killed. POJ, pasteurized orange juice, [b]comparisons were performed using log-rank (Mantel-Cox) test. [c]PBJ, pasteurized 'Bahia' orange juice, [d]PCJ, pasteurized 'Cara Cara' orange juice, [e]Total number of animals analyzed. The number in parentheses indicates the number of independent trials.

Several studies have shown that lifespan extension is closely associated with enhanced resistance to various forms of environmental stressors [43]. Thus, we assessed the effects of the POJ treatments on *C. elegans* oxidative stress resistance. Oxidative stress assays were performed in wild-type animals treated with 2% POJ for 48 h and then submitted to stress conditions induced by *tert*-butyl hydroperoxide (TBHP). We observed that animals treated with either 2% 'Bahia' or 'Cara Cara' juice showed an increased maximum and mean lifespan, when compared to untreated controls (Figure 5(b), Table 4). Similar to the longevity assay, animals treated with 2% 'Cara Cara' juice showed increased oxidative stress resistance compared to animals treated with 2% 'Bahia' juice ($p = 0.0134$).

We also repeated the oxidative stress resistance assay in *skn-1*, *daf-16*, and *hsf-1* knockout animals. POJ treatment with either 2% 'Bahia' or 'Cara Cara' juices significantly increased the maximum and mean survival time of *daf-16* and *hsf-1* mutants under stress conditions (Table 4). However, treatment with either 2% POJ 'Bahia' or 'Cara Cara' failed to increase *skn-1* mutant survival under stress conditions (Table 4). These results suggest that the oxidative stress resistance induced by POJ could be mediated by the transcription factor SKN-1. In this work, POJ antioxidant capacity was positively related to an increase in survival under standard and oxidative stress conditions which would be in agreement with the free radical theory of aging.

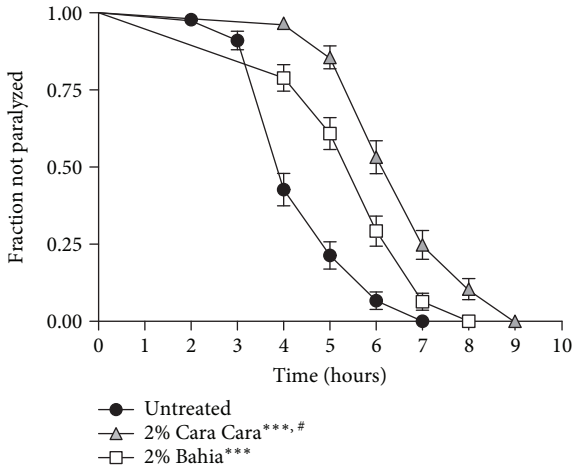

FIGURE 6: Effect of pasteurized juice from oranges cv. 'Bahia' and cv. 'Cara Cara' treatment on the β-amyloid induced paralysis in *C. elegans* transgenic model of Alzheimer's disease. Paralysis curves for *C. elegans* strain CL2006 which expresses β-amyloid peptide constitutively in the muscle. Worms were treated beginning at L4 with 2% POJ for 48 h at L4 stage. Paralysis was verified at 1 h intervals at 35°C. $^{****}p < 0.0001$ compared to untreated control and $^{\#}p < 0.0001$ comparing 2% 'Bahia' with 2% 'Cara Cara' juice by log-rank (Mantel-Cox) test.

Together, these results indicate that pasteurized juice treatment improves *C. elegans* antioxidant capacity, which is associated with the upregulation of antioxidant and chaperonin genes and increased lifespan and stress resistance. It is noteworthy that the treatment with 'Cara Cara' orange juice provided better results on all parameters analyzed here compared to 'Bahia' orange juice with the only exception for the expression of *sod-3::GFP* (Figure 3(c)) under standard conditions and for *gst-4::GFP* (Figure 3(b)) and *hsp-16.2* (Figure 3(d)) under stress conditions. The beneficial effects of 'Cara Cara' orange juice could be related to its higher carotenoid content, especially *Z*-violaxanthin, phytoene, phytofluene, lycopene, and β-carotene, even though 'Bahia' juice has higher levels of vitamin C and limonin (Table 2). However, the additional effects of 'Cara Cara' orange juice compared to 'Bahia' orange juice are either moderate or small to be explained solely based on the total carotenoid difference between these two varieties.

3.5. POJ Treatment Delays Paralysis Induced by β-Amyloid (Aβ) Expression. The oxidative stress state has an important role in the development of neurodegenerative diseases such as Alzheimer's disease (AD). Accumulation of ROS and deposition of toxic amyloid species have been proposed to exacerbate the symptoms observed in AD patients [44, 45]. The observation that POJ has antioxidant properties *in vivo* led us to ask whether POJ could protect against β-amyloid-induced toxicity in a *C. elegans* model for Alzheimer's disease. The expression of human Aβ1–42 in the muscle of transgenic CL2006 strain promotes a paralysis that can be monitored over time. We observed that the onset of paralysis was significantly delayed in POJ-treated animals (Figure 6). The mean paralysis time for worms treated with 2% 'Bahia' and 2% 'Cara Cara' juices was increased by 25.0% and 46.0%, respectively, compared to untreated worms (Figure 6, Table 5).

Various studies have shown that the protective effect of flavonoids and carotenoids against amyloid-induced neurotoxicity is due to their antioxidant properties. Other possible mechanisms could be attenuation of Aβ aggregation *in vivo* by downregulating the expression level of β-amyloid precursor protein (APP) [18] and/or activation of protein degradation pathways [46]. In the present study, the POJ treatment delayed Aβ1–42-induced paralysis in worms suggesting that POJ may be able to attenuate the development of AD by altering Aβ aggregate states *in vivo*. Most importantly, our results indicate that 'Cara Cara' juice, with higher carotenoid contents, provides a superior protection against Aβ1–42-induced paralysis over that provided by Bahia.

We also evaluated the role of SKN-1, DAF-16, and HSF-1 in POJ-mediated protection against Aβ1-42 toxicity. To this end, we examined the effect of POJ on CL2006 worms using RNAi to knock down *skn-1*, *daf-16*, and *hsf-1* expression. POJ treatment significantly delayed the paralysis rate of CL2006 worms with *control(RNAi)* (Table 5). In contrast, RNAi of *skn-1* and *daf-16* in CL2006 worms completely abolished POJ-mediated beneficial effects on delaying the progression of paralysis (Table 5). RNAi of *hsf-1* in CL2006 worms only prevented the beneficial effect against β-amyloid paralysis for those animals treated with 2% 'Cara Cara' juice (Table 5). Together, these findings suggest that the transcription factors SKN-1, DAF-16, and HSF-1 are required for POJ-mediated protective effect against Aβ toxicity.

Taking these data together, our mechanistic studies indicated that POJ improves the antioxidant status of a whole organism by direct and indirect mechanisms. POJ-reduced ROS levels were primarily a result of the direct scavenging action of natural compounds available in the orange juice and secondly an outcome of the transcription factor SKN-1 indirect action. POJ promotes *gst-4::GFP* expression and oxidative stress resistance mainly through SKN-1 although DAF-16 and HSF-1 also contribute to a less extent to these effects. Finally, POJ delayed Aβ-induced onset paralysis on a SKN-1-, DAF-16-, and HSF-1-dependent manner. Previous studies in the nematode reported that DAF-16, SKN-1, and HSF-1 play pivotal roles in regulating longevity and ameliorating Aβ [12]. Since these transcription factors are key regulators of many important biological processes, including lifespan, stress responses, and proteostasis, we reasoned that POJ treatments might protect worms against Aβ1–42 toxicity by increasing antioxidant capacity and proteostasis.

3.6. POJ Protection against Oxidative Stress and Aβ Toxicity Is Partially Related to Antimicrobial Effect. Since *E. coli* has a pathogenic effect on *C. elegans*, which may alter its longevity, resistance to stress, and Aβ1–42-induced paralysis [47, 48], we investigated whether the POJ protective effects could be a secondary response of a possible POJ antimicrobial

Table 5: Effect of pasteurized juice from 'Bahia' and 'Cara Cara' oranges on *C. elegans* paralysis induced by β-amyloid expression.

Strain and conditions	Mean paralysis time (hours ± SEM)	% mean paralysis time variation vs. control	p value (log rank) POJ[a] vs. untreated[b]	p value (log rank) PBJ[c] vs. PCJ[b,d]	N[e]
CL2006 on *E. coli* OP50					
Untreated	4.59 ± 0.11				84 (3)
2% Bahia	5.75 ± 0.12	25.0	<0.0001		85 (3)
2% Cara Cara	6.70 ± 0.13	46.0	<0.0001	<0.0001	84 (3)
CL2006 on *E. coli* OP50-HK[a]					
Untreated	5.29 ± 0.16				86 (3)
2% Bahia	6.50 ± 0.18	23.0	<0.0001		80 (3)
2% Cara Cara	7.82 ± 0.22	48.0	<0.0001	<0.0001	82 (3)
CL2006 on *control(RNAi)*					
Untreated	4.80 ± 0.10				88 (3)
2% Bahia	5.48 ± 0.12	14.0	<0.0001		89 (3)
2% Cara Cara	5.54 ± 0.16	15.0	<0.0001	0.5562	89 (3)
CL2006 on *skn-1(RNAi)*					
Untreated	4.20 ± 0.07				87 (3)
2% Bahia	3.95 ± 0.07	-6.0	0.0191		88 (3)
2% Cara Cara	3.94 ± 0.07	-6.1	0.0151	0.8555	89 (3)
CL2006 on *daf-16(RNAi)*					
Untreated	4.09 ± 0.07				89 (3)
2% Bahia	4.13 ± 0.08	0.9	0.6016		88 (3)
2% Cara Cara	4.17 ± 0.08	1.9	0.4024	0.8582	89 (3)
CL2006 on *hsf-1(RNAi)*					
Untreated	4.26 ± 0.08				88 (3)
2% Bahia	4.57 ± 0.08	7.2	0.0069		89 (3)
2% Cara Cara	3.84 ± 0.07	-9.8	<0.0001	<0.0001	89 (3)

HK: heat killed, [a]POJ, pasteurized orange juice, [b]comparisons were performed using log-rank (Mantel-Cox) test. [c]PBJ, pasteurized 'Bahia' orange juice, [d]PCJ, pasteurized 'Cara Cara' orange juice, [e]total number of animals analyzed. The number in parentheses indicates the number of independent trials.

property. First, we repeated the oxidative stress resistance assay in animals treated with POJ on dead bacteria. We observed that wild-type animals treated with 2% POJ still showed increased survival on 10 mM TBHP compared to untreated controls ($p < 0.0001$) (Figure 7(a), Table 4). However, the mean survival variation observed for the POJ-treated animals on dead bacteria was considerably lower compared to the, respectively, POJ-treated animals on live bacteria (Table 4). The mean survival variation was 11 and 68% for the animals treated with 2% 'Bahia' juice on dead and live bacteria, respectively. Likewise, the mean survival variation was 32 and 73.5% for the animals treated with 2% 'Cara Cara' juice on dead and living bacteria, respectively (Table 4).

The role of bacterial in affecting longevity of aging *C. elegans* is well known [49]. Much experimental evidence

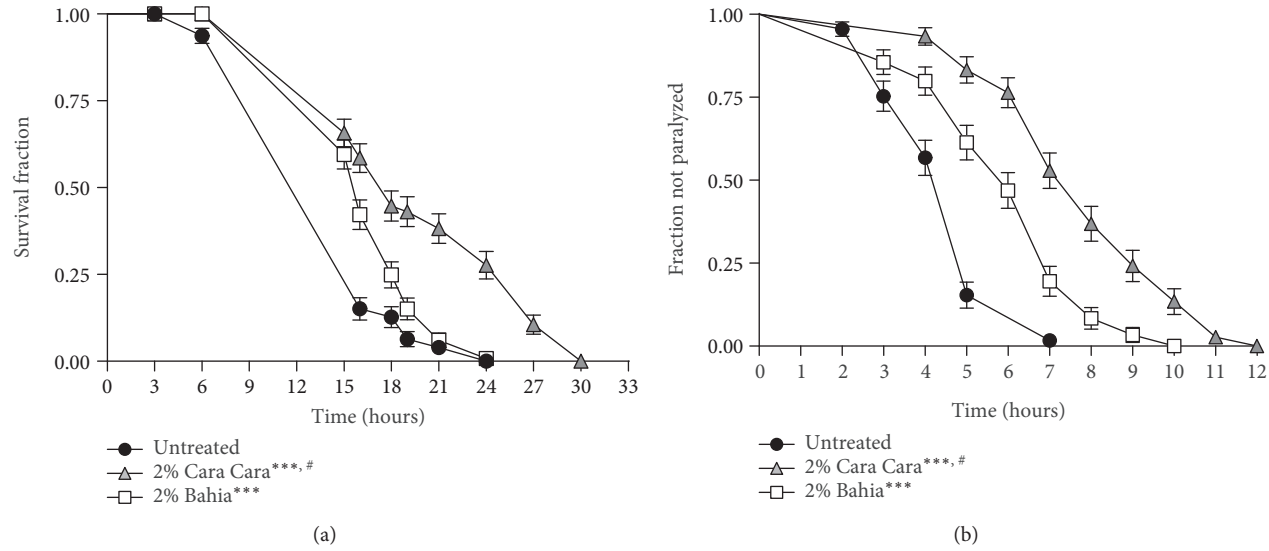

Figure 7: Effect of POJ on oxidative stress resistance and Aβ1-42-induced paralysis on *C. elegans* grown on dead bacteria. (a) Stress resistance assay on bacteria dead bacteria. Worms were treated with 2% POJ on *E. coli* OP50 heat-killed beginning at L4 and transferred to plates with 10 mM TBPH. Survival was verified every 3 hours at 20°C. $^{****}p < 0.0001$ compared to the untreated control group, log-rank (Mantel-Cox) test. (b) Paralysis profile of CL2006 transgenic animals fed with 2% POJ mixed with OP50 heat-killed. Paralysis was verified at 1 h intervals at 35°C. $^{****}p < 0.0001$ compared to untreated control by log-rank (Mantel-Cox) test.

supports bacterial infection and proliferation within the intestine of adults as a potential pathogen that triggers innate immune and stress host responses which may contribute as a double-edged effect to tissue damage and aging [47]. The conserved PMK1-p38 mitogen-activated protein kinase (MAPK) pathway is the major mediator of innate immunity in *C. elegans*. Interestingly, the PMK-1 pathway is also required for the activation of the transcription factor SKN-1 under stress conditions [50]. Thus, any intervention that attenuates bacterial pathogenicity and toxicity extends lifespan and stress resistance. The reduction of the variation survival time on stress when the POJ-treated animals were fed on bacterial previously killed by heat indicates that part of the survival extension observed on POJ-treated animals fed on live bacteria is due to its antimicrobial effect. It is also reasonable to suppose that this reduction of the variation survival time on stress could be a result of the animals acquiring less antioxidant buffer from their living bacterial food source [49]. Another possibility could be related to the fact that in the absence of pathogenic bacteria, the PMK-1-SKN-1 signaling pathway is also diminished and therefore the defense mechanisms activation is attenuated.

Next, we performed the Aβ1-42-induced paralysis assay also using bacteria killed by heat. Interestingly, the mean variation observed for the Aβ1-42-induced paralysis was not particularly different between the POJ treatments on dead or living bacteria (Figure 7(b), Table 5). The mean paralysis time variation for the animals treated with 2% 'Bahia' juice on dead bacteria was 23% compared to untreated animals while the variation for the same treatment on living bacteria was 25% (Table 5). For 'Cara Cara' juice treatment, the mean paralysis time variation was 48% compared to untreated animals on dead bacteria and 46% compared to untreated animals on living bacteria (Table 5).

Although the onset paralysis in the CL2006 animals grown on live OP50 was faster compared to those grown on dead OP50 as expected, we did not observe any significant difference of the paralysis time variation on the POJ-treated animals fed on dead bacteria compared to those fed on live bacteria (Table 5). This result suggests that the beneficial effect of POJ against Aβ toxicity is independent of the bacterial pathogenicity. This observation seems contradictory since many studies have shown a link between food source and proteotoxicity [48, 51]. Steinkraus et al. [51] showed that bacterial food deprivation suppresses proteotoxicity in Aβ worms through an *hsf-1*-dependent mechanism. It would be interesting for further studies to shed light on the possible relationship between POJ protection against Aβ in the absence of bacteria depends on HSF-1.

4. Conclusions

In this work, we investigated the *in vivo* effects of POJ from the 'Bahia' and 'Cara Cara' varieties using the *C. elegans* model. Treatment with POJ reduced the endogenous levels of ROS and increased the rate of survival of the worms under normal and stress conditions. Our mechanistic studies indicated that POJ promotes resistance to oxidative stress by acting through the transcription factor SKN-1. We observed that POJ treatments increased the expression of the antioxidant genes (*gcs-1*, *gst-4*, and *sod-3*) and chaperonin (*hsp-16.2*), which are known to be regulated by the transcription of SKN-1, DAF-16, and HSF-1 factors. In addition, POJ treatments delayed β-amyloid-induced paralysis in the transgenic model *C. elegans* in a manner requiring SKN-1, DAF-16, and HSF-1. Noteworthy, the treatment with the two juice types produced excellent

results; however, 'Cara Cara' juice induced significantly better responses than 'Bahia' juice did in almost all experiments, possibly due to its higher content of carotenoids such as *Z*-violaxanthin, zeaxanthin, phytoene, phytofluene, lycopene, and β-carotene.

Data Availability

All data used to support the findings of this study are available from the corresponding author upon request.

Conflicts of Interest

The authors declare that there is no conflict of interests regarding the publication of this paper.

Acknowledgments

This study was supported by Fundecitrus, São Paulo, Brazil, and Universidade Federal do Rio Grande do Norte (UFRN). Research fellowships were sponsored by CNPq (Oliveira, R. P.). We thank the *Caenorhabditis* Genetics Center (CGC), which is funded by the NIH National Center for Research Resources (NCRR), and Dr. T. Keith Blackwell for supplying the *C. elegans* strains. We thank Citrosuco (Matão, São Paulo, Brazil) for providing access to their farms and processing the orange juices used in this study.

References

[1] E. Brasili, D. F. Seixas Chaves, A. A. O. Xavier, A. Z. Mercadante, N. M. A. Hassimotto, and F. M. Lajolo, "Effect of pasteurization on flavonoids and carotenoids in Citrus sinensis (L.) Osbeck cv. 'Cara Cara' and 'Bahia' juices," *Journal of Agricultural and Food Chemistry*, vol. 65, no. 7, pp. 1371–1377, 2017.

[2] A. Milani, M. Basirnejad, S. Shahbazi, and A. Bolhassani, "Carotenoids: biochemistry, pharmacology and treatment," *British Journal of Pharmacology*, vol. 174, no. 11, pp. 1290–1324, 2017.

[3] H. S. Lee, "Characterization of carotenoids in juice of red navel orange (Cara Cara)," *Journal of Agricultural and Food Chemistry*, vol. 49, no. 5, pp. 2563–2568, 2001.

[4] K. S. Cho, M. Shin, S. Kim, and S. B. Lee, "Recent advances in studies on the therapeutic potential of dietary carotenoids in neurodegenerative diseases," *Oxidative Medicine and Cellular Longevity*, vol. 2018, Article ID 4120458, 13 pages, 2018.

[5] M. Obulesu, M. R. Dowlathabad, and P. V. Bramhachari, "Carotenoids and Alzheimer's disease: an insight into therapeutic role of retinoids in animal models," *Neurochemistry International*, vol. 59, no. 5, pp. 535–541, 2011.

[6] S. Hwang, J. Lim, and H. Kim, "Inhibitory effect of lycopene on amyloid-β-induced apoptosis in neuronal cells," *Nutrients*, vol. 9, no. 8, p. 883, 2017.

[7] M. Qu, L. Li, C. Chen et al., "Protective effects of lycopene against amyloid β-induced neurotoxicity in cultured rat cortical neurons," *Neuroscience Letters*, vol. 505, no. 3, pp. 286–290, 2011.

[8] Y. Ding, A. Qiao, Z. Wang et al., "Retinoic acid attenuates beta-amyloid deposition and rescues memory deficits in an Alzheimer's disease transgenic mouse model," *The Journal of Neuroscience*, vol. 28, no. 45, pp. 11622–11634, 2008.

[9] A. B. Goodman, "Retinoid receptors, transporters, and metabolizers as therapeutic targets in late onset Alzheimer disease," *Journal of Cellular Physiology*, vol. 209, no. 3, pp. 598–603, 2006.

[10] A. B. Goodman and A. B. Pardee, "Evidence for defective retinoid transport and function in late onset Alzheimer's disease," *Proceedings of the National Academy of Sciences*, vol. 100, no. 5, pp. 2901–2905, 2003.

[11] M. Maden, "Retinoic acid in the development, regeneration and maintenance of the nervous system," *Nature Reviews Neuroscience*, vol. 8, no. 10, pp. 755–765, 2007.

[12] A. Antebi, "Genetics of aging in Caenorhabditis elegans," *PLoS Genetics*, vol. 3, no. 9, pp. 1565–1571, 2007.

[13] Y. Luo, "Long-lived worms and aging," *Redox Report*, vol. 9, no. 2, pp. 65–69, 2004.

[14] C. A. Wolkow, K. D. Kimura, M. S. Lee, and G. Ruvkun, "Regulation of C. elegans life-span by insulin-like signaling in the nervous system," *Science*, vol. 290, no. 5489, pp. 147–150, 2000.

[15] M. Artal-Sanz, L. de Jong, and N. Tavernarakis, "Caenorhabditis elegans: a versatile platform for drug discovery," *Biotechnology Journal*, vol. 1, no. 12, pp. 1405–1418, 2006.

[16] P. R. Augusti, A. V. S. Brasil, C. Souto et al., "Microcystin-LR exposure induces oxidative damage in Caenorhabditis elegans: protective effect of lutein extracted from marigold flowers," *Food and Chemical Toxicology*, vol. 109, Part 1, pp. 60–67, 2017.

[17] E. Pons, B. Alquezar, A. Rodriguez et al., "Metabolic engineering of β-carotene in orange fruit increases its in vivo antioxidant properties," *Plant Biotechnology Journal*, vol. 12, no. 1, pp. 17–27, 2014.

[18] W. Chen, L. Mao, H. Xing et al., "Lycopene attenuates Aβ1–42 secretion and its toxicity in human cell and Caenorhabditis elegans models of Alzheimer disease," *Neuroscience Letters*, vol. 608, pp. 28–33, 2015.

[19] E. Lashmanova, E. Proshkina, S. Zhikrivetskaya et al., "Fucoxanthin increases lifespan of Drosophila melanogaster and Caenorhabditis elegans," *Pharmacological Research*, vol. 100, pp. 228–241, 2015.

[20] M. Dimitriadi and A. C. Hart, "Neurodegenerative disorders: insights from the nematode Caenorhabditis elegans," *Neurobiology of Disease*, vol. 40, no. 1, pp. 4–11, 2010.

[21] J. Li and W. Le, "Modeling neurodegenerative diseases in Caenorhabditis elegans," *Experimental Neurology*, vol. 250, pp. 94–103, 2013.

[22] Anon, *FMC Food Tech. The Laboratory Manual. Procedures for Analysis of Citrus Products. Manual No. 054R11990*, John Bean Technologies Corporation, Inc, Lakeland, FL, USA, 2000.

[23] J. W. Stevens, "Estimation of Ascorbic Acid in Citrus Juices," *Industrial & Engineering Chemistry Analytical Edition*, vol. 10, no. 5, pp. 269–271, 1938.

[24] B. Alquezar, M. J. Rodrigo, and L. Zacarías, "Regulation of carotenoid biosynthesis during fruit maturation in the red-fleshed orange mutant Cara Cara," *Phytochemistry*, vol. 69, no. 10, pp. 1997–2007, 2008.

[25] G. Britton, "Overview of carotenoid biosynthesis," in *Biosynthesis and Metabolism*, G. Britton, S. Liaaen-Jensen, and H. Pfander, Eds., pp. 13–148, Birkhäuser Verlag, Basel, 1998.

[26] L. Carmona, L. Zacarías, and M. J. Rodrigo, "Stimulation of coloration and carotenoid biosynthesis during postharvest storage of 'Navelina' orange fruit at 12 ˚C," *Postharvest Biology and Technology*, vol. 74, pp. 108–117, 2012.

[27] M. J. Rodrigo, J. F. Marcos, F. Alferez, M. D. Mallent, and L. Zacarias, "Characterization of Pinalate, a novel Citrus sinensis mutant with a fruit-specific alteration that results in yellow pigmentation and decreased ABA content," *Journal of Experimental Botany*, vol. 54, no. 383, pp. 727–738, 2003.

[28] M. J. Rodrigo, J. F. Marcos, and L. Zacarias, "Biochemical and molecular analysis of carotenoid biosynthesis in flavedo of orange (Citrus sinensis L.) during fruit development and maturation," *Journal of Agricultural and Food Chemistry*, vol. 52, no. 22, pp. 6724–6731, 2004.

[29] R. L. Rouseff, L. Raley, and H. J. Hofsommer, "Application of diode array detection with a C-30 reversed phase column for the separation and identification of saponified orange juice carotenoids," *Journal of Agricultural and Food Chemistry*, vol. 44, no. 8, pp. 2176–2181, 1996.

[30] S. Brenner, "The genetics of Caenorhabditis elegans," *Genetics*, vol. 77, no. 1, pp. 71–94, 1974.

[31] F. A. Paiva, L. de Freitas Bonomo, P. F. Boasquivis et al., "Carqueja (Baccharis trimera) protects against oxidative stress and beta-amyloid-induced toxicity in Caenorhabditis elegans," *Oxidative Medicine and Cellular Longevity*, vol. 2015, Article ID 740162, 15 pages, 2015.

[32] L. de Freitas Bonomo, D. N. Silva, P. F. Boasquivis et al., "Açaí (Euterpe oleracea Mart.) modulates oxidative stress resistance in Caenorhabditis elegans by direct and indirect mechanisms," *PLoS One*, vol. 9, no. 3, article e89933, 2014.

[33] A. M. Gonzalez-Paramas, B. Ayuda-Duran, S. Martinez, S. Gonzalez-Manzano, and C. Santos-Buelga, "The mechanisms behind the biological activity of flavonoids," *Current Medicinal Chemistry*, vol. 25, 2018.

[34] A. Murakami, "Non-specific protein modifications may be novel mechanism underlying bioactive phytochemicals," *Journal of Clinical Biochemistry and Nutrition*, vol. 62, no. 2, pp. 115–123, 2018.

[35] S. Y. Tang and B. Halliwell, "Medicinal plants and antioxidants: what do we learn from cell culture and Caenorhabditis elegans studies?," *Biochemical and Biophysical Research Communications*, vol. 394, no. 1, pp. 1–5, 2010.

[36] K. Koch, S. Havermann, C. Buchter, and W. Watjen, "Caenorhabditis elegansas model system in pharmacology and toxicology: effects of flavonoids on redox-sensitive signalling pathways and ageing," *Scientific World Journal*, vol. 2014, article 920398, 15 pages, 2014.

[37] J. H. An and T. K. Blackwell, "SKN-1 links C. elegans mesendodermal specification to a conserved oxidative stress response," *Genes & Development*, vol. 17, no. 15, pp. 1882–1893, 2003.

[38] L. A. Khan, T. Yamanaka, and N. Nukina, "Genetic impairment of autophagy intensifies expanded polyglutamine toxicity in Caenorhabditis elegans," *Biochemical and Biophysical Research Communications*, vol. 368, no. 3, pp. 729–735, 2008.

[39] C. T. Murphy, S. A. McCarroll, C. I. Bargmann et al., "Genes that act downstream of DAF-16 to influence the lifespan of Caenorhabditis elegans," *Nature*, vol. 424, no. 6946, pp. 277–283, 2003.

[40] E. Guisbert, D. M. Czyz, K. Richter, P. D. McMullen, and R. I. Morimoto, "Identification of a tissue-selective heat shock response regulatory network," *PLoS Genetics*, vol. 9, no. 4, article e1003466, 2013.

[41] V. Murugaiyah and M. P. Mattson, "Neurohormetic phytochemicals: an evolutionary-bioenergetic perspective," *Neurochemistry International*, vol. 89, pp. 271–280, 2015.

[42] T. G. Son, S. Camandola, and M. P. Mattson, "Hormetic dietary phytochemicals," *Neuromolecular Medicine*, vol. 10, no. 4, pp. 236–246, 2008.

[43] K. I. Zhou, Z. Pincus, and F. J. Slack, "Longevity and stress in Caenorhabditis elegans," *Aging*, vol. 3, no. 8, pp. 733–753, 2011.

[44] S. J. Choi, J. K. Kim, S. H. Suh et al., "Ligularia fischeri extract protects against oxidative-stress-induced neurotoxicity in mice and pc12 cells," *Journal of Medicinal Food*, vol. 17, no. 11, pp. 1222–1231, 2014.

[45] H. R. Jeong, Y. N. Jo, J. H. Jeong, H. J. Kim, M.-J. Kim, and H. J. Heo, "Blueberry (Vaccinium virgatum) leaf extracts protect against Aβ-induced cytotoxicity and cognitive impairment," *Journal of Medicinal Food*, vol. 16, no. 11, pp. 968–976, 2013.

[46] P. F. Boasquivis, G. M. M. Silva, F. A. Paiva, R. M. Cavalcanti, C. V. Nunez, and R. de Paula Oliveira, "Guarana (Paullinia cupana) extract protects Caenorhabditis elegans models for Alzheimer disease and Huntington disease through activation of antioxidant and protein degradation pathways," *Oxidative Medicine and Cellular Longevity*, vol. 2018, Article ID 9241308, 16 pages, 2018.

[47] D. H. Kim, "Bacteria and the aging and longevity of Caenorhabditis elegans," *Annual Review of Genetics*, vol. 47, no. 1, pp. 233–246, 2013.

[48] F. Munoz-Lobato, M. J. Rodriguez-Palero, F. J. Naranjo-Galindo et al., "Protective role of DNJ-27/ERdj5 in Caenorhabditis elegans models of human neurodegenerative diseases," *Antioxidants & Redox Signaling*, vol. 20, no. 2, pp. 217–235, 2014.

[49] D. Garigan, A.-L. Hsu, A. G. Fraser, R. S. Kamath, J. Ahringer, and C. Kenyon, "Genetic analysis of tissue aging in Caenorhabditis elegans: a role for heat-shock factor and bacterial proliferation," *Genetics*, vol. 161, no. 3, pp. 1101–1112, 2002.

[50] H. Inoue, N. Hisamoto, J. H. An et al., "The C. elegans p38 MAPK pathway regulates nuclear localization of the transcription factor SKN-1 in oxidative stress response," *Genes & Development*, vol. 19, no. 19, pp. 2278–2283, 2005.

[51] K. A. Steinkraus, E. D. Smith, C. Davis et al., "Dietary restriction suppresses proteotoxicity and enhances longevity by an hsf-1-dependent mechanism in Caenorhabditis elegans," *Aging Cell*, vol. 7, no. 3, pp. 394–404, 2008.

Hindawi
Oxidative Medicine and Cellular Longevity
Volume 2019, Article ID 9421037, 16 pages
https://doi.org/10.1155/2019/9421037

Research Article

Ethanol Extract of *Centipeda minima* Exerts Antioxidant and Neuroprotective Effects via Activation of the Nrf2 Signaling Pathway

Yi-Jie Wang,[1] Xin-Yue Wang,[2] Xu-Yi Hao,[1] Yong-Ming Yan,[3] Ming Hong,[1] Su-Fen Wei,[1] Yi-Le Zhou,[1] Qi Wang,[1] Yong-Xian Cheng,[3] and Yong-Qiang Liu[1]

[1]*Institute of Clinical Pharmacology, Guangzhou University of Chinese Medicine, Guangzhou 510405, China*
[2]*Sun Yat-sen University Cancer Center, Guangzhou 510060, China*
[3]*School of Pharmaceutical Sciences, Shenzhen University Health Science Center, Shenzhen 518060, China*

Correspondence should be addressed to Qi Wang; wangqi@gzucm.edu.cn, Yong-Xian Cheng; yxcheng@szu.edu.cn, and Yong-Qiang Liu; liuyq@gzucm.edu.cn

Received 5 October 2018; Revised 3 January 2019; Accepted 20 January 2019; Published 3 April 2019

Guest Editor: Francisco Jaime B. Mendonça Júnior

Oxidative stress is implicated in the pathogenesis of neurodegeneration and other aging-related diseases. Previous studies have found that the whole herb of *Centipeda minima* has remarkable antioxidant activities. However, there have been no reports on the neuroprotective effects of *C. minima*, and the underlying mechanism of its antioxidant properties is unclear. Here, we examined the underlying mechanism of the antioxidant activities of the ethanol extract of *C. minima* (ECM) both *in vivo* and in *vitro* and found that ECM treatment attenuated glutamate and tert-butyl hydroperoxide (tBHP)-induced neuronal death, reactive oxygen species (ROS) production, and mitochondria dysfunction. tBHP-induced phosphorylation of p38 mitogen-activated protein kinase (p38 MAPK) and c-Jun N-terminal kinases (JNK) was reduced by ECM, and ECM sustained phosphorylation level of extracellular signal regulated kinase (ERK) in SH-SY5Y and PC12 cells. Moreover, ECM induced the activation of nuclear factor erythroid 2-related factor 2 (Nrf2) and the upregulation of phase II detoxification enzymes, including heme oxygenase-1 (HO-1), superoxide dismutase-2 (SOD2), and NAD(P)H quinone oxidoreductase-1 (NQO-1) in both two cell types. In a D-galactose (D-gal) and aluminum muriate ($AlCl_3$)-induced neurodegenerative mouse model, administration of ECM improved the learning and memory of mice in the Morris water maze test and ameliorated the effects of neurodegenerative disorders. ECM sustained the expression level of postsynaptic density 95 (PSD95) and synaptophysin (SYN), activated the Nrf2 signaling pathway, and restored the levels of cellular antioxidants in the hippocampus of mice. In addition, four sesquiterpenoids were isolated from *C. minima* to identify the bioactive components responsible for the antioxidant activity of *C. minima*; 6-*O*-angeloylplenolin and arnicolide D were found to be the active compounds responsible for the activation of the Nrf2 signaling pathway and inhibition of ROS production. Our study examined the mechanism of *C. minima* and its active components in the amelioration of oxidative stress, which holds the promise for the treatment of neurodegenerative disease.

1. Introduction

Aging is a complex molecular process that is associated with many life-threatening diseases, such as neurodegenerative disease, diabetes, and cardiovascular disease [1, 2]. The hippocampus is the most vulnerable region in the central nervous system (CNS), as it can be severely affected by the aging process [3]; neurodegeneration can be induced in the hippocampus and can result in cognitive dysfunction, which has a close relationship with the pathological progression of Alzheimer's disease and markedly decreases quality of life [4–6]. Various drugs have been developed to ameliorate neurodegenerative diseases. Donepezil is one of the most commonly used drugs approved for dementia; however,

adverse side effects could be induced by long-term and high-dose treatment [7–9]. Development of novel drugs for the prevention and treatment of neurodegenerative diseases is urgently needed.

Oxidative damage, mitochondrial dysfunction, and carbonyl toxification have been widely accepted as the primary causes for the development of aging processes, especially the pathogenesis of most neurodegenerative disorders [10, 11]. Previous research has shown that high levels of ROS and abnormal redox changes can markedly induce neuronal death and potentiate the pathogenesis of neurodegenerative disease [12]. Excessive free radicals can attack biological macromolecules, including nucleic acids, lipids, and proteins through peroxidation, which induces malonyl dialdehyde (MDA) production, nucleic acid crosslinking, and antioxidative enzyme overconsumption, consequently leading to neurological senescence in the hippocampus and cortex [13–15]. Several signaling pathways have been reported to protect normal tissues from oxidative damage, and compelling evidence has demonstrated that the phase II detoxification systems exert neuroprotective effects against carcinogens and oxidants via the Nrf2 signaling pathways [16, 17]. Nrf2 is a pivotal regulator that can activate genes in the CNS, such as HO-1, NQO-1, SOD1, glutathione peroxidase, thioredoxins, and glutathione S-transferase (GST) [18–20]. Several studies have shown that HO-1 and NQO-1 exert neuroprotective effects by directly reducing oxidative stress and maintaining the integrity of the mitochondria [21, 22]. Meanwhile, altered levels of HO-1 and NQO-1 expression have been found in the temporal cortex and hippocampus of patients with dementia [23, 24]. Furthermore, Nrf2 overexpression has been shown to protect against neurotoxicity caused by amyloid fibrils [25, 26], indicating that phase II detoxification enzymes have an indispensable role in alleviating the pathogenesis of neurodegenerative disease. Therefore, stimulation of the Nrf2 signaling pathway could be a valuable tool for amelioration of oxidative stress and treatment of neurodegenerative diseases.

Traditional Chinese medicine (TCM) has been widely used for the treatment of aging diseases based on its antioxidant properties. The crude extracts and active components in TCM exert antioxidant activities either by directly scavenging free radical or enhancing the function of the antioxidant enzymes [27]. *C. minima* is widely distributed over the areas of East and Southeast Asia, is well known as a medicinal herb that has antibacterial and antiprotozoal activities, and is used for the treatment of nasal allergy, headache, cough, malaria, and asthma in China and Korea [28–31]. Both the aqueous and hydroalcoholic extracts of *C. minima* have been reported to attenuate oxidative stress by increasing the activities of antioxidant enzymes, which suggests that *C. minima* may contain bioactive components that have antioxidant properties [32]. Several compounds, including sesquiterpene lactones and terpenoids, have been isolated from *C. minima* and tested for antiproliferation activity in cancer cells [33–37]. However, the role of *C. minima* in treating neurodegenerative diseases remains unknown, and the bioactive components of *C. minima* and their antioxidant activities have never been reported. Here, we examined the neuroprotective effects of ECM against oxidative stress and explored its underlying mechanism both *in vivo* and *in vitro*. We also tested the antioxidant activity of the sesquiterpene lactones isolated from ECM. Our results suggest that *C. minima* and its isolated bioactive compounds hold the promise as antioxidant agents for the treatment of aging-related neurodegenerative diseases.

2. Materials and Methods

2.1. Materials. tBHP, D-gal, $AlCl_3$, and glutamate were purchased from Sigma-Aldrich (St. Louis, MO). Kits used for MDA, SOD, glutathione (GSH), the bicinchoninic acid (BCA) protein assay, the ROS assay, and mitochondrial membrane potential detection were purchased from Beyotime (Shanghai, China). Antibodies against Nrf2, HO-1, SOD2, NQO-1, and Lamin B1 were obtained from Abcam (Cambridge, MA). Antibodies against β-actin, phospho-p38, p38, phospho-ERK, ERK, phospho-JNK, GAPDH, SYN, PSD95, Bcl-2, and Bax were purchased from Cell Signaling Technology (Beverly, MA). All secondary antibodies (horseradish peroxidase-conjugated anti-rabbit IgG and anti-mouse IgG) were purchased from Cell Signaling Technology (Beverly, MA). All reagents used were of the highest grade available commercially.

2.2. Centipeda minima Extract Preparation. The *C. minima* powders were extracted by 95% EtOH with ultrasound (twice in 6-fold solvent for 1 h each) followed by concentration *in vacuo* and lyophilization to produce a 10.3% yield dried extract. The ECM was stored at 4°C until use. For the cell treatment, the ECM sample was dissolved in DMSO to make a stock concentration of 20 mg/ml. For the animal experiments, the ECM sample was dissolved in a solution of 10% ethanol in normal saline to the concentrations of 20, 40, and 80 mg/ml, which corresponded to the low-, middle-, and high-dose groups of ECM, respectively. The compound 6-*O*-angeloylplenolin, referred to as EBSC-26A, was purified from the ethanol extract of *C. minima* as previously described [37]. We separated and enriched the EBSC-26A by high-performance liquid chromatography (HPLC) and also got the other three compounds EBSC-26B–EBSC-26D (see Supplementary Information). The structures of EBSC-26A to EBSC-26D with HPLC grade purity were identified as 6-*O*-angeloylplenolin, arnicolide D, arnicolide C, and microhelenin C by spectroscopic methods as well as comparison with literature data [28, 38] (Supplementary Figures S2–S9). The samples were dissolved in DMSO at a stock solution of 20 mmol/l.

2.3. Cell Culture and Treatment. The human neuroblastoma cell line SH-SY5Y was purchased from the cell bank Interlab Cell Line Collection (Genova, Italy). The highly differentiated mouse pheochromocytoma line PC12 was obtained from American Type Culture Collection (Rockville, MD). Cells were cultured in DMEM medium (Gibco, CA) contained with 10% fetal bovine serum (Gibco, CA), penicillin (100 U/ml, Gibco, CA), and streptomycin (100 mg/ml, Gibco, CA) in a humidified incubator containing 95% air

and 5% CO_2 at 37°C. For the experiments, the cells were pretreated with the indicated concentrations of ECM (0.5, 1, or 2 μg/ml) or the compounds EBSC-26A–EBSC-26D (0.5, 1, or 2 μM) for 2 h prior to the addition of tBHP (300 μM) and glutamate (10 mM), and vitamin E was used as a positive control for investigation of antioxidant activity of ECM.

2.4. Animals. All experiments in this study were approved by and performed in accordance with the guidelines of the Animal Ethics Committee of Guangzhou University of Chinese Medicine. Six-week-old male Kunming mice were purchased from Shanghai Laboratory Animal Research Center (Shanghai, China). The mice were kept for a minimum of one week prior to the experiments at a temperature of 23 ± 1°C on a 12 h light/-dark cycle with access to water and food *ad libitum*. The mice were randomly divided into six groups (n = 10 per group): (1) vehicle control (solvent: 10% ethanol in normal saline); (2) D-gal (120 mg/kg)/$AlCl_3$ (20 mg/kg); (3) D – gal/$AlCl_3$ + EC M (100, 200, or 400 mg/kg); (4) D-gal/$AlCl_3$ + vitamin E (80 mg/kg); Vitamin E (16 mg/ml, dissolved with 10% ethanol in normal saline) was used as apositive control. The experimental groups were treated with D-gal (hypodermic injection, 120 mg/kg/d, Sigma-Aldrich, St. Louis, MO) and $AlCl_3$ (intragastric administration, 20 mg/kg/d, Sigma-Aldrich, St. Louis, MO) for 90 days to establish a subacute aging model. After treatment with D-gal and $AlCl_3$ for an uninterrupted 60 days, ECM and vitamin E were administrated intragastrically to each of the treatment group every day for 30 d. At the end of the treatment period, behavioral tests were performed at regular intervals to assess learning and memory of the mice.

2.5. Cell Viability. MTT assay was used to detect the viability of SH-SY5Y and PC12 cells in 96-well plates. 1×10^4 cells per well were pretreated with ECM or EBSC-26A–EBSC-26D at the indicated concentrations for 2 h and further incubated with tBHP (300 μM) for 6 h or glutamate (10 mM) for 24 h. The cell morphology was observed using a Leica optical microscope at the end of treatment. 10 μl of an MTT working solution containing 5 mg/ml MTT was added into each well and incubated for 3 h at 37°C. The supernatant was then replaced with 100 μl of DMSO, and the absorbance was detected at 490 nm using a microplate reader (Thermo Fisher, Waltham, MA). The results were expressed as the mean percentage of absorbance (treated versus control cells).

2.6. Determination of ROS Production. The intracellular ROS levels were measured using a 2′,7′-dichlorofluorescin diacetate (DCFH-DA) fluorescent probe as previously described [39]. Briefly, SH-SY5Y and PC12 cells were washed with ice-cold PBS and incubated with 5 μM DCFH-DA in phenol red-free DMEM medium for 30 min at 37°C in the dark. The cells were then washed with PBS and stained with Hoechst 33342 for 5 min. DCFH-DA will be cleaved by intracellular esterases and be oxidized into the highly fluorescent dichlorofluorescein (DCF) by ROS. ROS-positive cells were monitored using a fluorescence microscope (Spectra MAX, Gemini EM, Molecular Devices, Sunnyvale, CA).

2.7. Measurement of MDA, GSH, and SOD Activities. The contents of the MDA and GSH, and the activities of SOD were determined as described previously [40]. Briefly, the cells were harvested and lysed in 0.2 ml of lysis buffer (1% Triton X-100 in PBS, pH 7.0) with sonication on ice. The homogenate was centrifuged at 13,200×g for 10 min at 4°C, and the supernatant was collected to determine the activity of SOD and the contents of MDA and GSH using assay kits (Beyotime, Shanghai). For the *in vivo* tests, the hippocampus and cortex were homogenized in ice-cold saline. The homogenate was centrifuged at 13,200×g for 10 min at 4°C. The supernatant was collected for the measurement of the activity of SOD and the contents of MDA and GSH according to the manufacturer's instructions. The total protein concentration of the supernatant was determined using a BCA Protein Assay.

2.8. Determination of Mitochondrial Membrane Potential (MMP). The fluorescent probe JC-1 exists as a green fluorescent monomer in cells at low MMP and forms red fluorescent aggregates at high MMP and can be used to measure MMP as previously described [41]. In brief, the cell culture medium was removed and the cells were further incubated with 500 μl of Hank's solution containing 10 mg/ml JC-1 for 20 min at 37°C. After removal of the Hank's solution, the cells were washed with PBS. The green fluorescence of the JC-1 monomer and the red fluorescence of the JC-1 oligomer were observed using fluorescence microscopy.

2.9. Extracting Cytoplasmic and Nuclear Proteins. The cultured cells were harvested and washed twice with cold PBS. The cytoplasmic and nuclear protein fractions were extracted using a Nuclear and Cytoplasmic Extraction Kit (Thermo Fisher Scientific, Rockford, IL) according to the manufacturer's protocol.

2.10. Morris Water Maze Test. The Morris water maze test was performed according to the method described by Morris [42]. The water maze equipment (Guangzhou Feidi Biology Technology Co. Ltd., Guangzhou, China) consists of a black circular pool, black platform, and recording system. The pool was divided into four imaginary quadrants (target, opposite, left, and right) by a computerized tracking/image analysis system. A circular, transparent escape platform (10 cm diameter) was placed 2 cm below the surface of the water in the target quadrant of the pool. The learning and memory abilities of the mice were assessed using the Morris water maze test in a dark room. The mice were given a place navigation test on five consecutive days. Each daily trial consisted of four sequential training trials that began with placing the animal in the water facing the wall of the pool. The drop location changed for each trial at random. The recording system started to record the time upon placement of the animal in the water. The escape latency was recorded at the time required for the mice to find the platform. If the mice failed to find the platform within 90 s, it would be guided to the platform by the trainer and was allowed to remain there for 10 s; in this instance, the escape latency was recorded as 90 s. On the sixth day, the mice were allowed to swim freely in the pool for 90 s without the platform,

and the number of crossing through the original platform position was recorded.

2.11. Western Blotting. At the end of treatment, the cells and tissues were harvested and lysed using RIPA lysis buffer. Equal amounts of protein per sample were loaded in each lane and separated by 12% SDS-PAGE and then transferred to PVDF membranes. The membranes were blocked with 5% skimmed milk for 2 h at room temperature and incubated with the indicated antibodies overnight at 4°C. The PVDF membranes were further incubated with HRP-conjugated secondary antibodies for 2 h at room temperature. The protein bands were visualized using a Super Signal West Pico Chemiluminescent Substrate Trial Kit (Pierce, Rockford, IL). Images were obtained using a ChemiDoc XRS system with Quantity One software (Bio-Rad, Richmond, CA). The results were obtained from a minimum of three independent experiments.

2.12. Statistical Analyses. The data are presented as the mea n ± SD unless noted otherwise. Unpaired *t*-tests or one-way analysis of variance (ANOVA) followed by Dunnett's post hoc tests were performed to determine the statistical significance of the differences. $P < 0.05$ was considered statistically significant (error bars, SEM). Data handling and statistical processing were performed using GraphPad Prism 7.0 (GraphPad Software, San Diego, CA). All experiments were performed at least three times.

3. Results

3.1. ECM Attenuates Oxidative Stress-Induced Cell Death. To determine the neuroprotective effects of ECM against oxidative stress, the well-known ROS inducers tBHP and glutamate were used to generate excessive ROS in neuronal SH-SY5Y and PC12 cells. First, a cell viability assay was performed to examine the toxic effects of ECM on neuronal cells. No obvious cytotoxicity of ECM was observed at the indicated concentrations (Figure 1(a)), suggesting that ECM is safe for neuronal cells. We then tested the neuroprotective effects of ECM. tBHP and glutamate treatment reduced the cell viability of SH-SY5Y and PC12 cells to 30-50% at the indicated time points. However, ECM pretreatment protected the cells against oxidative damage, as the ratio of viable cells of SH-SY5Y and PC12 increased to nearly 90% (Figures 1(b) and 1(c)). Cell morphological changes were examined to detect the neuroprotective effects of ECM. SH-SY5Y and PC12 cells shrank and became round after treatment with tBHP and glutamate, suggesting that massive cytotoxicity had been induced by excessive oxidative stress. ECM pretreatment reversed the morphological changes, with the cells treated with ECM at a high dose almost returning to normal in comparison with the control cells (Figures 1(d) and 1(e)). These results indicated that ECM exerted neuroprotective effects through the attenuation of oxidative stress.

3.2. ECM Inhibits ROS Production and Mitochondria Dysfunction in Neuronal Cells. To confirm the neuroprotective effect of ECM via the amelioration of oxidative stress, we detected the ROS scavenging activity of ECM in SH-SY5Y and PC12 cells using the oxidation-sensitive fluorescent probe DCFH-DA. The results showed that tBHP significantly increased intracellular ROS generation in SH-SY5Y and PC12 cells relative to the control cells that the effect could be reversed by ECM and vitamin E treatment, and that ECM treatment at a high dose had a ROS scavenging activity comparable to vitamin E (Figures 2(a) and 2(b)). Moreover, MDA production was increased, and the levels of GSH and SOD activities were decreased after tBHP treatment (Figures 2(c) and 2(e)), indicating that intracellular antioxidative capacity had been reduced. ECM and vitamin E pretreatment significantly decreased the level of MDA and increased the level of GSH and SOD activities in SH-SY5Y and PC12 cells (Figures 2(c) and 2(e)).

Excessive ROS generation can induce depolarization of mitochondria and changes in the MMP, which accelerate ROS-induced neuronal damage. Moreover, Bcl-2 family proteins are major regulators of MMP, Bcl-2 possesses antiapoptotic activity, whereas Bax exerts proapoptotic effect, and the Bcl-2/Bax ratio is of particular interest in assessing mitochondria-mediated cell death. To determine the role of ECM in mitochondrial protection, we detected MMP by JC-1 staining and further examined the ratio of Bcl-2/Bax expression by Western blot. The control cells with normal MMP exhibited red fluorescence after JC1 staining; however, tBHP treatment for 6 h significantly increased the ratio of green/red fluorescence (Figure 2(f)), representing a decline in MMP in the SH-SY5Y cells. Meanwhile, ECM and vitamin E treatment markedly attenuated the tBHP-induced collapse of MMP, as indicated by an increased red/green florescence ratio (Figure 2(f)). Consistently, exposure to tBHP decreased the ratio of Bcl-2/Bax expression in comparison with control cells, whereas ECM treatment increased the ratio of Bcl-2/Bax (Figures 2(g) and 2(h)), suggesting that ECM sustained MMP and protected mitochondrial function from oxidant-induced damage, thus exerting neuroprotective effects.

3.3. ECM Attenuates tBHP-Induced Oxidative Stress through Modulation of the MAPK and Nrf2 Signaling Pathways. It has previously been demonstrated that oxidative stress can activate members of MAPK family such as p38 MAPK and JNK, which are critical in mediating intracellular stress. We further assessed whether ECM exerts antioxidant effects via regulation of the MAPK kinase pathway. We found that tBHP exposure for 1 h caused a significant increase in the phosphorylation levels of p38 MAPK and JNK in SH-SY5Y and PC12 cells. However, preincubation with ECM markedly attenuated the tBHP-induced p38 MAPK and JNK phosphorylation (Figures 3(a) and 3(b)). In contrast, the phosphorylation level of ERK was significantly decreased in cells exposed to tBHP, while ECM pretreatment increased the phosphorylation level of ERK (Figures 3(a) and 3(b)). These results suggest that alteration of the phosphorylation level of MAPK kinase can mediate the antioxidant activity of ECM, and that p38 MAPK and ERK may play different role in mediating the antioxidant effects of ECM.

ERK has been reported to regulate Nrf2 nuclear translocation and the antioxidative response, and numerous studies have demonstrated that natural products can improve the

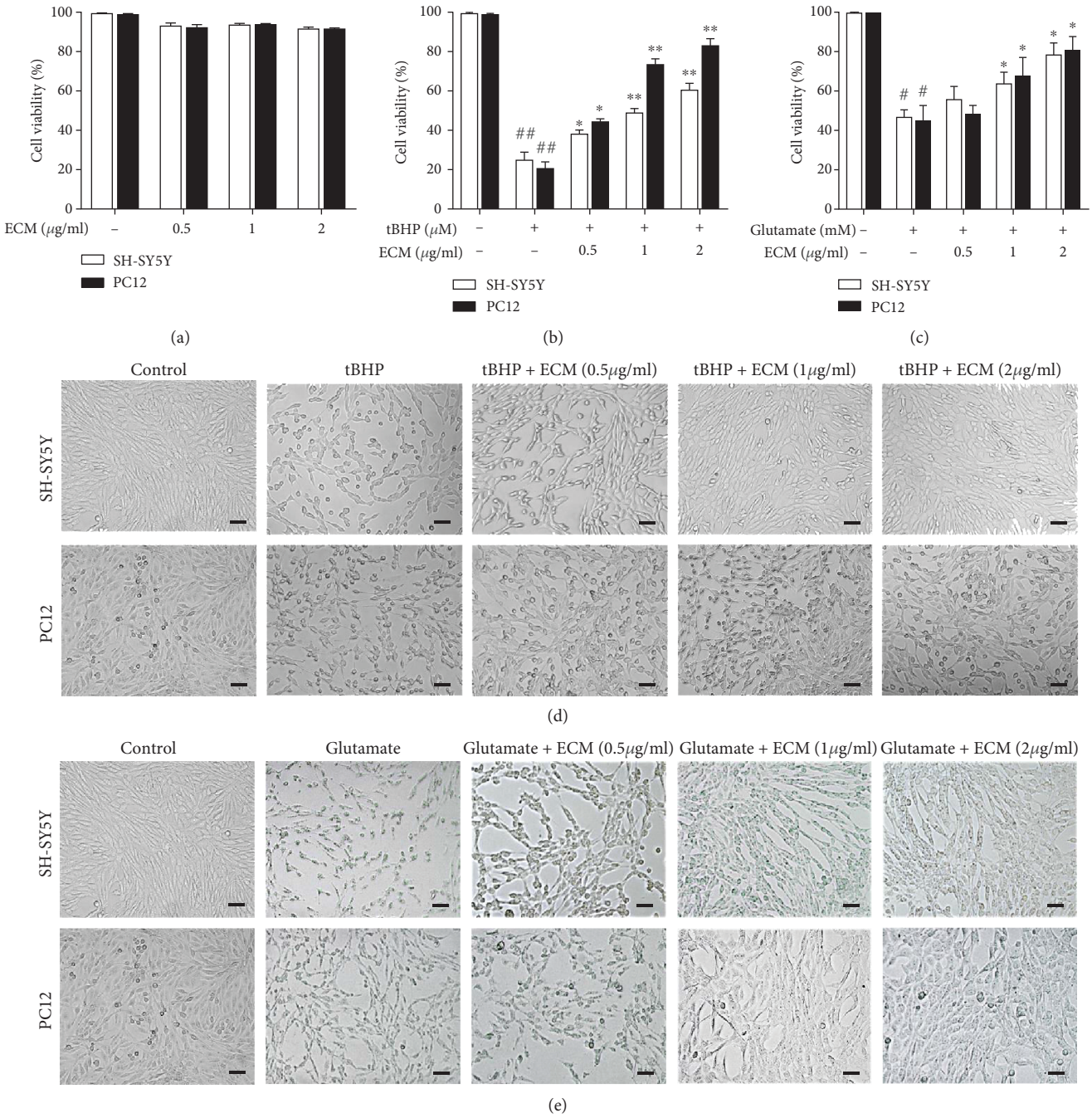

Figure 1: ECM inhibits oxidative stress-induced cell death. (a) Relative viability of SH-SY5Y and PC12 cells treated with 0.5-2 μg/ml ECM at 37°C for 24 h. (b) Relative viability of SH-SY5Y and PC12 cells pretreated with 0.5-2 μg/ml ECM for 2 h and then exposed to 300 μM tBHP for an additional 6 h. (c) Relative viability of SH-SY5Y and PC12 cells pretreated with 0.5-2 μg/ml ECM for 2 h and then exposed to 10 mM glutamate for an additional 24 h. Cells were pretreated with ECM and then treated with 300 μM tBHP for 4 h (d) or 10 mM glutamate for 18 h (e). The morphological changes were observed in the bright field of microscope. Scale bar, 50 μm. All data are normalized to control cells and presented as the mean ± SEM of three independent experiments. $^{\#}p < 0.05$ and $^{\#\#}p < 0.01$ in comparison with control cells. $^{*}p < 0.05$ and $^{**}p < 0.01$ in comparison with the cells exposed to glutamate (b) or tBHP (c) alone.

antioxidant capacity by increasing the level of phase II detoxification enzymes. We examined whether ECM improved the intracellular antioxidant capacity via regulation of the Nrf2 signaling pathway. SH-SY5Y and PC12 cells were pretreated with ECM for 2 h before exposing them to tBHP for an additional 6 h. We found that ECM treatment obviously increased the nuclear level of Nrf2 in the presence of tBHP, while the cytoplasmic part of Nrf2 did not change (Figures 3(c) and 3(e)), suggesting that ECM inhibited Nrf2 degradation and induced Nrf2 nuclear translocation. Further, the expression levels of the Nrf2 downstream proteins, the phase II detoxification enzymes, were checked by Western blot. tBHP treatment alone slightly altered the expression levels of HO-1, SOD2, and NQO-1. However, pretreatment with ECM

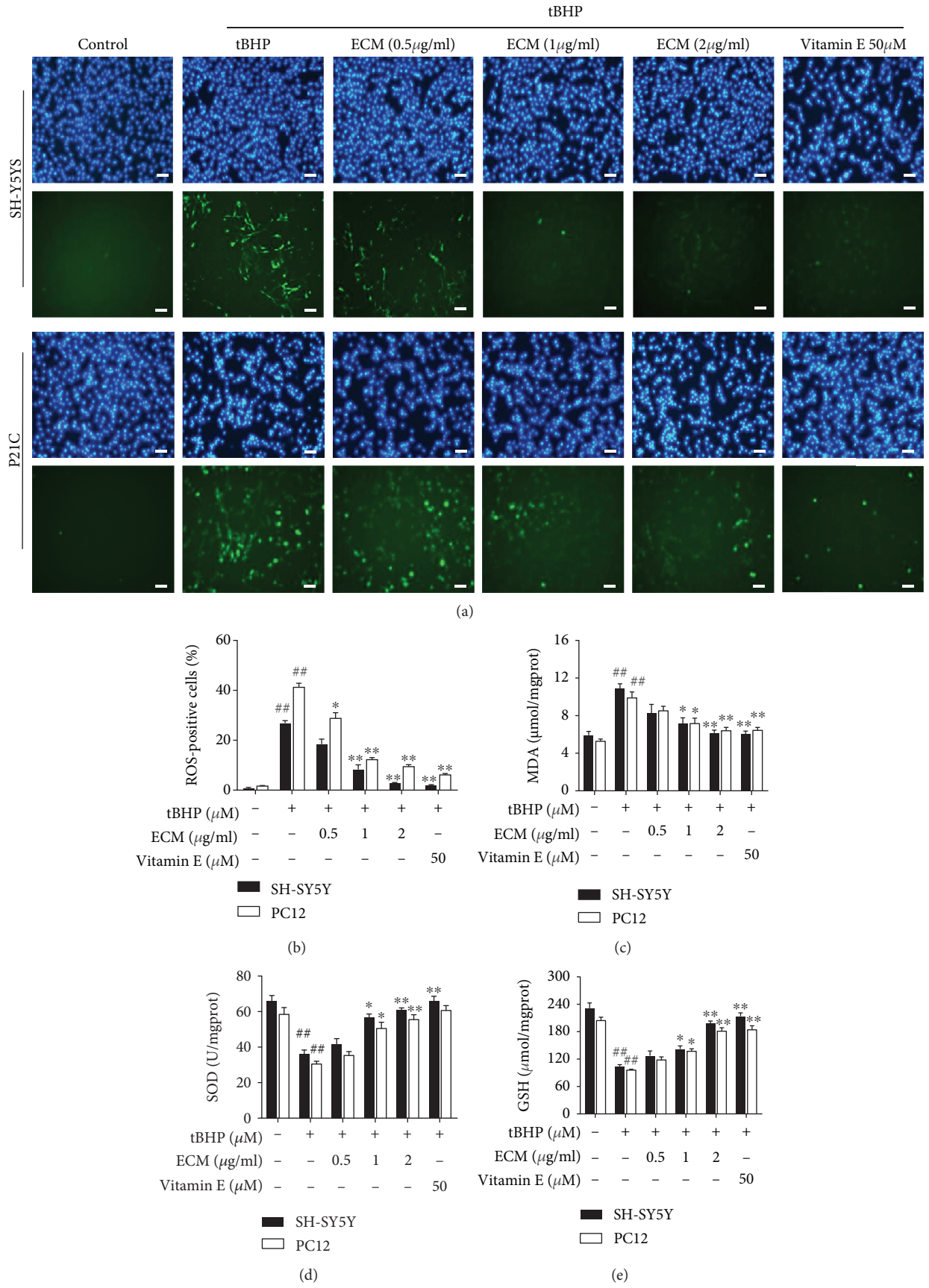

Figure 2: Continued.

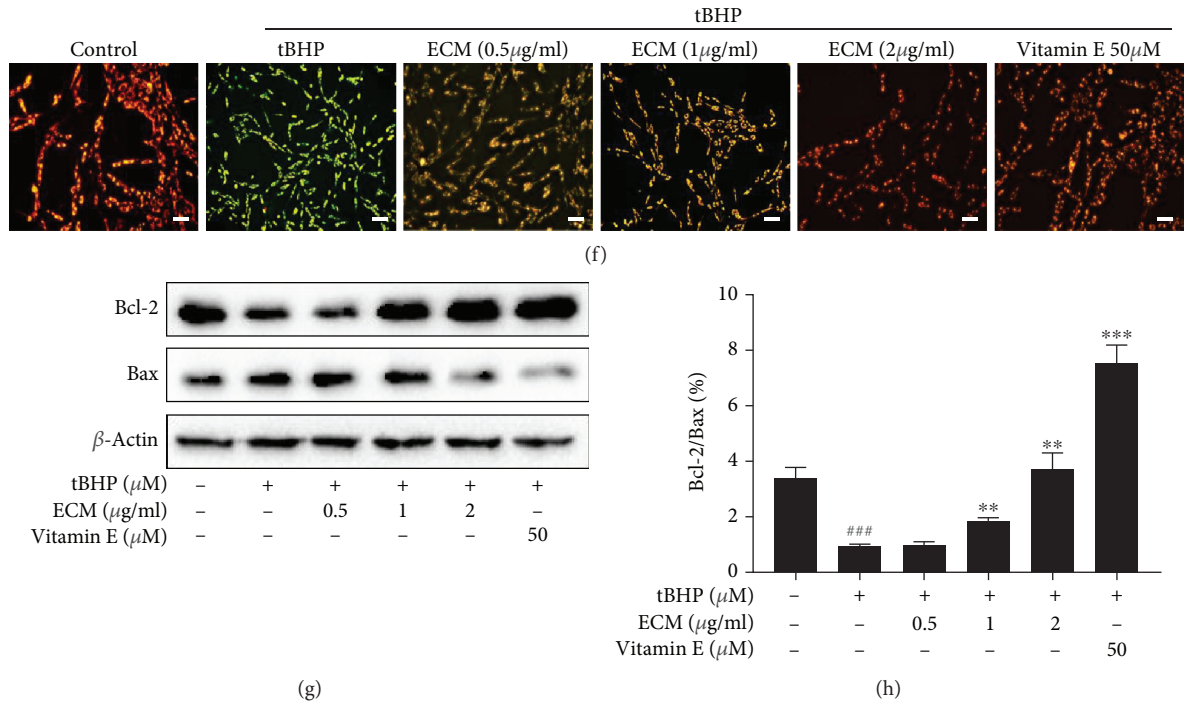

Figure 2: ECM attenuates oxidative stress-induced mitochondrial dysfunction. The cells were pretreated with 0.5-2 μg/ml ECM and 50 μM vitamin E for 2 h and then exposed to 300 μM tBHP for an additional 6 h. (a) SH-SY5Y (upper panel) or PC12 cells (lower panel) were treated with DCFH-DA for 30 min; Hoechst 33342 was used to counterstain cell nuclei. Scale bar, 50 μm. (b) The percentage of ROS-positive cells among cultured SH-SY5Y or PC12 cells was quantified and was shown as histogram. Intracellular MDA content (c), SOD activity (d), and GSH levels (e) were detected using a kit assay and are presented as a histogram. (f) SH-SY5Y cells were pretreated with 0.5-2 μg/ml ECM for 2 h and then exposed to 300 μM tBHP for an additional 6 h. The mitochondrial membrane potential was determined using the JC-1 fluorescence probe, and representative pictures have been shown for comparison. (g) Western blot analysis was performed using antibodies against Bax and Bcl-2, and β-actin was used as a loading control. (h) The ratio of Bcl-2 to Bax was quantified by densitometry and is shown as a histogram. The results are shown as the mean ± SEM of three independent experiments. $^{\#\#}p < 0.01$ in comparison with control cells. $^{*}p < 0.05$ and $^{**}p < 0.01$ in comparison with the cells exposed to tBHP alone.

significantly upregulated the expression levels of HO-1, SOD2, and NQO-1 in the presence of tBHP (Figures 3(d) and 3(e)). Our results indicated that ECM has a role in attenuating ROS production via the enhancement of intracellular antioxidant capacity.

3.4. Active Compounds in ECM Alleviate tBHP-Induced Oxidative Stress through the Nrf2 Signaling Pathway. Recently, several sesquiterpene lactones have been isolated from *C. minima*. However, the active compounds that contribute to the antioxidative properties of *C. minima* have never been reported. In order to identify the active components that exert neuroprotective effects, we isolated a series of sesquiterpenoids from the ethanol extracts of *C. minima*, including 6-*O*-angeloylplenolin, arnicolide D, arnicolide C, and microhelenin C, referred to as EBSC-26A–EBSC-26D, respectively. We first tested the antioxidative activities of these compounds. None of the compounds showed obvious cytotoxicity towards SH-SY5Y or PC12 cells at indicated concentrations (Figure 4(a), upper panel). Intriguingly, the compounds protected the neuronal cells from the oxidative damage induced by tBHP (Figure 4(a), lower panel). In particular, EBSC-26A and EBSC-26B significantly reverse the cytotoxic effects induced by tBHP at lower-dose treatment. Meanwhile, the tBHP-induced ROS production was also attenuated by EBSC-26A and EBSC-26B (Figures 4(b) and 4(c)). We then examined whether EBSC-26A and EBSC-26B exerted antioxidant effects via the Nrf2 signaling pathway. SH-SY5Y cells were pretreated with EBSC-26A and EBSC-26B for 2 h before tBHP treatment for an additional 6 h. We found that both EBSC-26A and EBSC-26B markedly increased the nuclear levels of Nrf2 and subsequently upregulated the expression levels of HO-1, NQO-1, and SOD2 (Figures 4(d) and 4(e)), suggesting that the sesquiterpenoids in *C. minima* act as the active compounds that attenuate oxidative stress, and that 6-*O*-angeloylplenolin and arnicolide D are the potent antioxidant compounds in *C. minima*.

3.5. ECM Improves Learning and Memory Ability in a D-gal/$AlCl_3$-Induced Mouse Model. D-gal can produce oxidative stress and induce neurodegeneration and memory impairment. $AlCl_3$ is also frequently used to reduce neuronal viability in the hippocampus and promote memory impairment. Thus, we evaluated the therapeutic potential of ECM in a D-gal/$AlCl_3$-induced neurodegenerative mouse model. The mice were treated with D-gal/$AlCl_3$ for 3 months to induce neurodegeneration. ECM was administrated during the final month of D-gal/$AlCl_3$ treatment, and the Morris

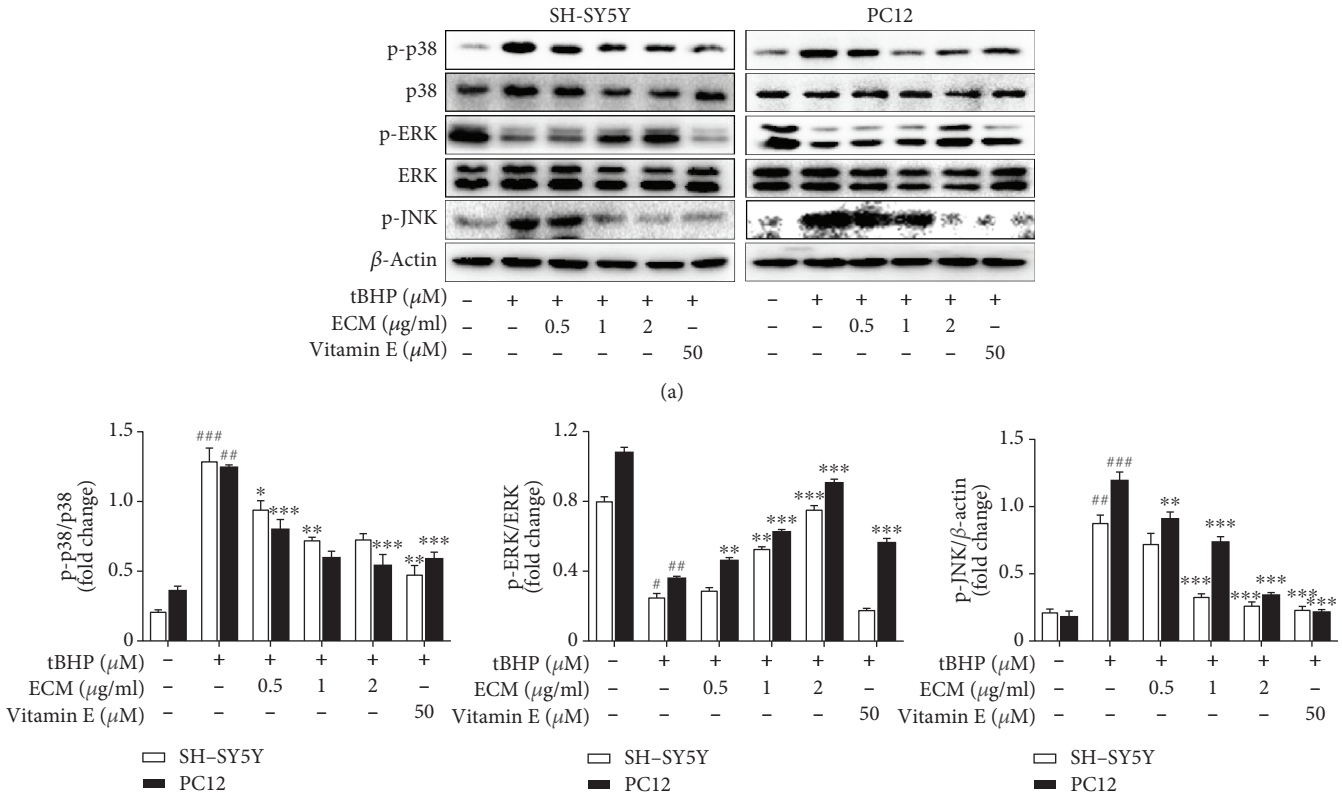

Figure 3: Continued.

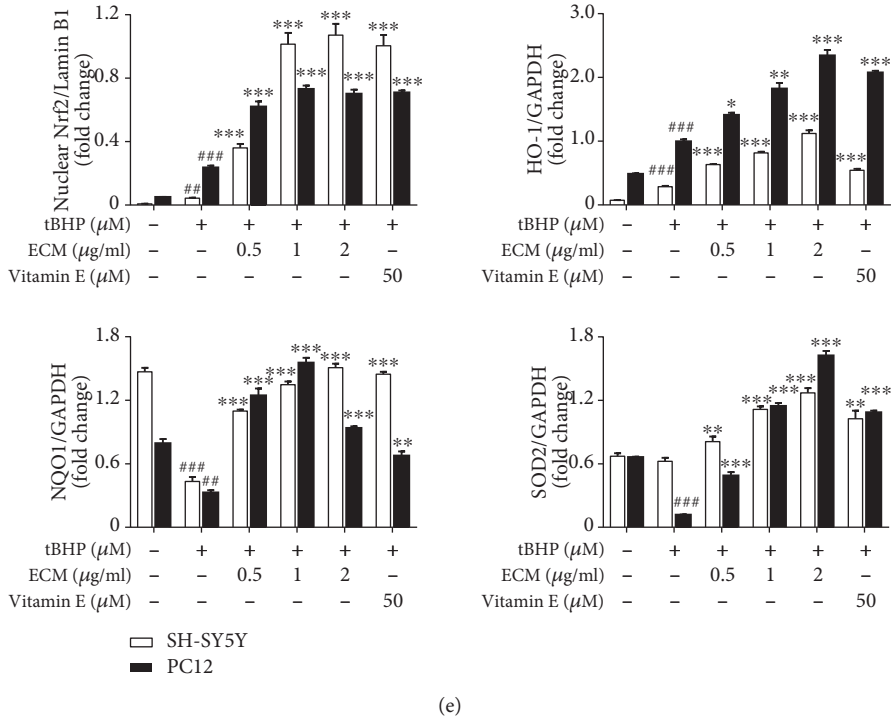

(e)

Figure 3: ECM inhibits oxidative stress via the regulation of the MAPK and Nrf2 signaling pathways. The cells were pretreated with 0.5-2 μg/ml ECM and 50 μM vitamin E for 2 h and then exposed to 300 μM tBHP for an additional 1 h. Western blot analysis was performed using antibodies against p-p38, p38, p-ERK, ERK, p-JNK, and GAPDH; β-actin was used as a loading control in SH-SY5Y (a) and PC12 cells (b). Nuclear and cytoplasmic proteins were extracted after treatment, and Nrf2 was detected using Western blot analysis in SH-SY5Y (c) and PC12 cells (d); GAPDH and Lamin B1 were used as loading controls. Western blot analysis was performed using antibodies against HO-1, NQO1, and SOD2 in SH-SY5Y (e) and PC12 cells (f); GAPDH was used as a loading control.

water maze test was performed to assess learning and memory. During the five days of spatial acquisition training, we found that the time required for the mice to find the hidden platform decreased progressively (Figure 5(a)). The D-gal/$AlCl_3$ group exhibited significantly longer escape latency than the vehicle control group. ECM or vitamin E treatment decreased the escape latency (Figure 5(a)). The ECM or vitamin E treatment group had a shorter swimming path to the platform than the D-gal/$AlCl_3$ group (Figure 5(b)). Subsequently, the platform was removed on day 6, the spatial probe test was performed, and the number of crossings over the position of the removed platform was recorded (Figure 5(c)). The ECM or vitamin E treatment group had significantly more platform crossings than the mice in the D-gal/$AlCl_3$ group (Figure 5(c)), indicating that ECM could improve learning and memory.

The synaptic proteins, PSD95 and SYN, play critical roles in synaptic plasticity and cognitive function [43, 44]. Oxidative stress can induce a decrease of the expression of PSD95 and SYN in the hippocampus, leading to cognitive impairment and development of neurodegenerative diseases [45, 46]. Thus, we examined the neuroprotective effects of ECM on the hippocampus. In D-gal/$AlCl_3$-treated mice, we found that the expression levels of PSD95 and SYN were decreased in the hippocampal tissues (Figure 5(d)); meanwhile, the neurons in the hippocampus were remarkably shrunken and irregularly arranged, and the pyknotic nuclei were also increased based on H&E staining (Supplementary Figure 1), indicating that oxidative stress contributes to neuronal damage in the hippocampus. However, ECM and vitamin E treatment groups exhibited tightly packed and regularly arranged neurons (Supplementary Figure 1). In line with this, ECM or vitamin E treatment sustained the expression levels of PSD95 and SYN (Figures 5(d) and 5(e)). The results indicate that ECM could protect neurons against oxidative stress in a D-gal/$AlCl_3$-induced neurodegenerative mouse model.

3.6. ECM Protects Hippocampus Neurons from Oxidative Stress via the Nrf2 Signaling Pathway. To determine the antioxidant effects of ECM, we first detected the levels of MDA, GSH, and SOD activities in the brain. In the hippocampus and cortex of D-gal/$AlCl_3$-treated mice, the level of MDA was significantly higher, and the SOD activity and GSH level were lower than those of the control group (Figure 6(a)); these levels were markedly reversed by ECM treatment. In particular, the levels in the high-dose ECM group were comparable to those in the vitamin E group (Figure 6(a)). These results indicate that ECM exerts neuroprotective effects via alleviation of oxidative stress in a D-gal/$AlCl_3$ mouse model.

To determine whether ECM ameliorates oxidative stress via the MAPK and Nrf2 signaling pathways in D-gal/$AlCl_3$-challgened mice, the levels of phosphorylated p38 MAPK and ERK and phase II detoxification enzymes in the

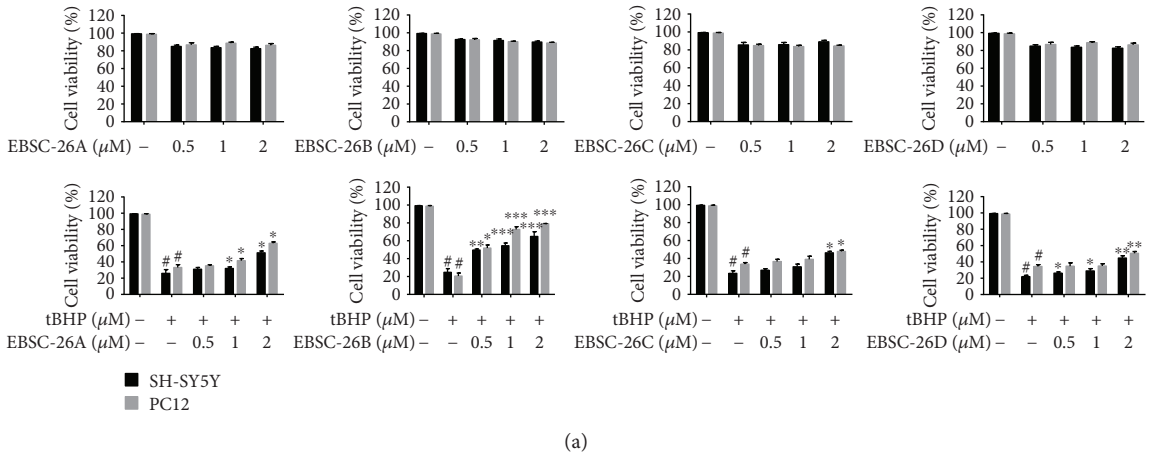

(a)

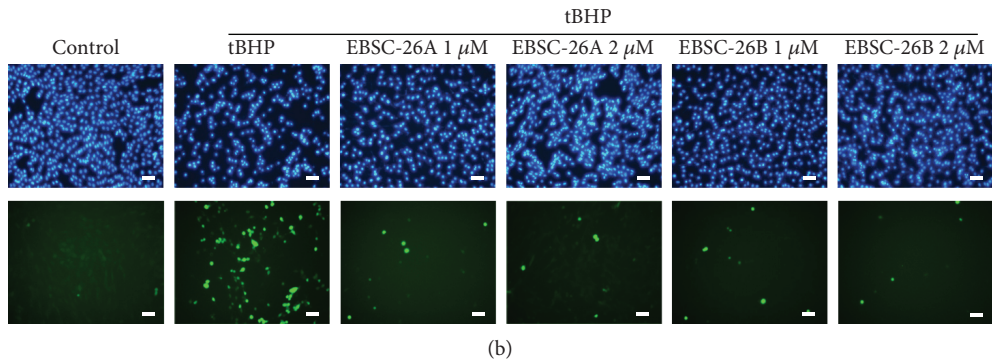

(b)

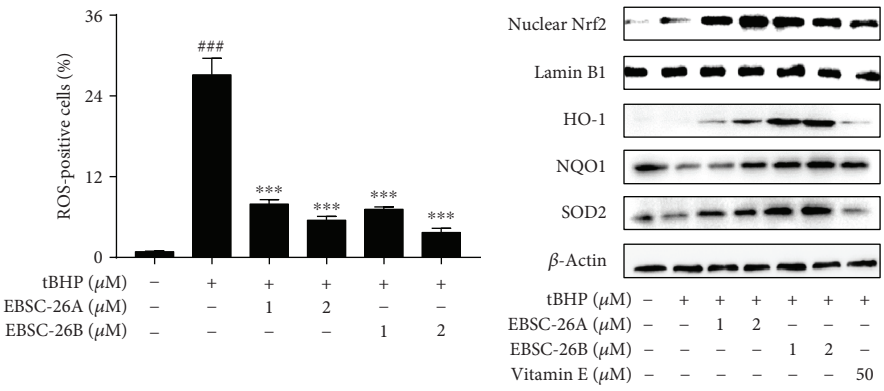

(c) (d)

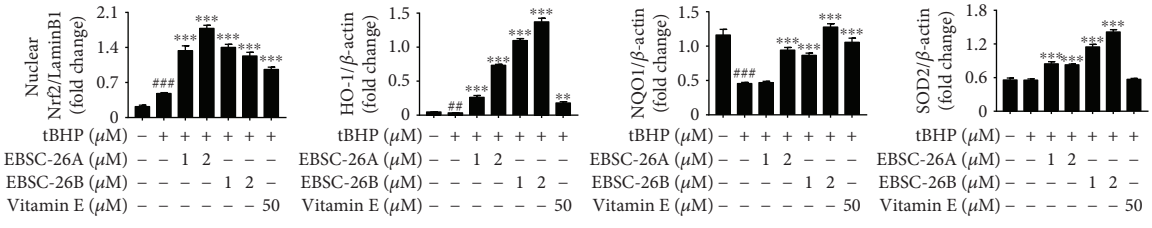

(e)

Figure 4: The active compounds EBSC-26A–EBSC-26D ameliorate oxidative stress. (a) SH-SY5Y and PC12 cells were treated with 0.5-2 μM EBSC-26A–EBSC-26D at 37°C for 24 h (upper panel) or pretreated with 0.5-2 μM EBSC-26A–EBSC-26D for 2 h and then exposed to 300 μM tBHP for an additional 6 h (lower panel); the relative viability of cells was measured by MTT assay. (b, c) SH-SY5Y cells were probed with DCFH-DA (b) and the percentage of ROS-positive cells among culture cells was quantified (c). Scale bar, 50 μm. (d) After pretreatment with 1-2 μM EBSC-26A, EBSC-26B, and vitamin E for 2 h, SH-SY5Y cells were exposed to 300 μM tBHP for an additional 6 h, and then nuclear Nrf2, HO-1, NQO-1, and SOD2 levels were detected by Western blot; β-actin was used as a loading control. (e) Relative protein levels were quantified by densitometry and normalized to Lamin B or β-actin. The results are shown as the mean ± SEM of three independent experiments. $^{\#}p < 0.05$ in comparison with control cells. $^{*}p < 0.05$ and $^{**}p < 0.01$ in comparison with the cells exposed to tBHP alone.

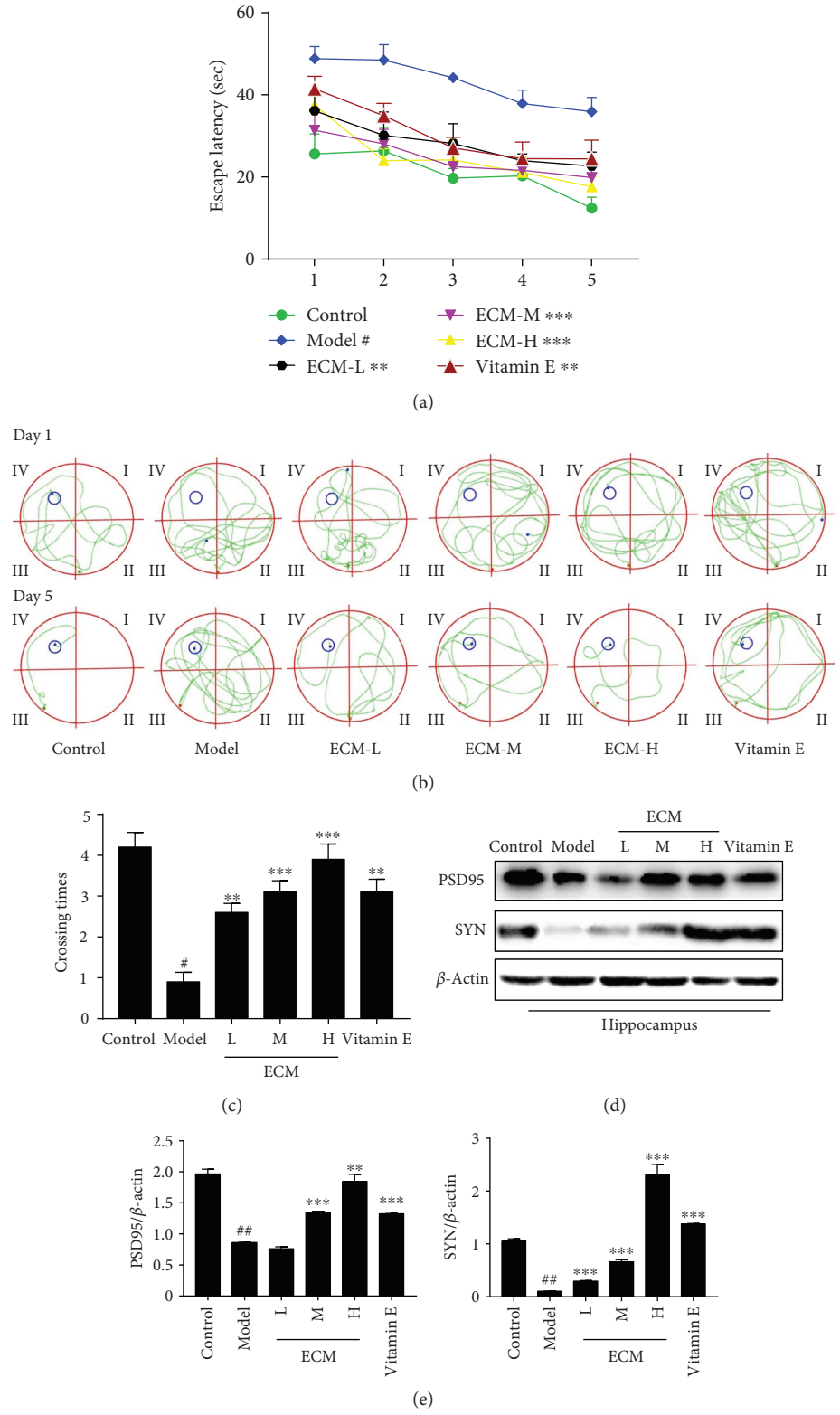

Figure 5: ECM improves learning and memory in a neurodegenerative mouse model. (a) Escape latency on five consecutive days of testing. (b) The swimming paths of the respective groups on the first and fifth days. (c) The crossing times in the probe trial. (d) Western blot analysis of PSD95 and SYN; β-actin was used as a loading control in the hippocampus. (e) Relative protein levels were quantified by densitometry and normalized to β-actin. Control: vehicle control; ECM-L: D – gal/$AlCl_3$ + ECM (100 mg/kg/d); ECM-M: D – gal/$AlCl_3$ + ECM (200 mg/kg/d); ECM-H: D – gal/$AlCl_3$ + ECM (400 mg/kg/d); vitamin E: D – gal/$AlCl_3$ + vitamin E (80 mg/kg/d). Data represent mean ± SEM ($n = 10$ per group). $^{\#}p < 0.05$ and $^{\#\#}p < 0.01$ in comparison with control group; $^{*}p < 0.05$, $^{**}p < 0.01$, and $^{***}p < 0.001$ in comparison with the model group.

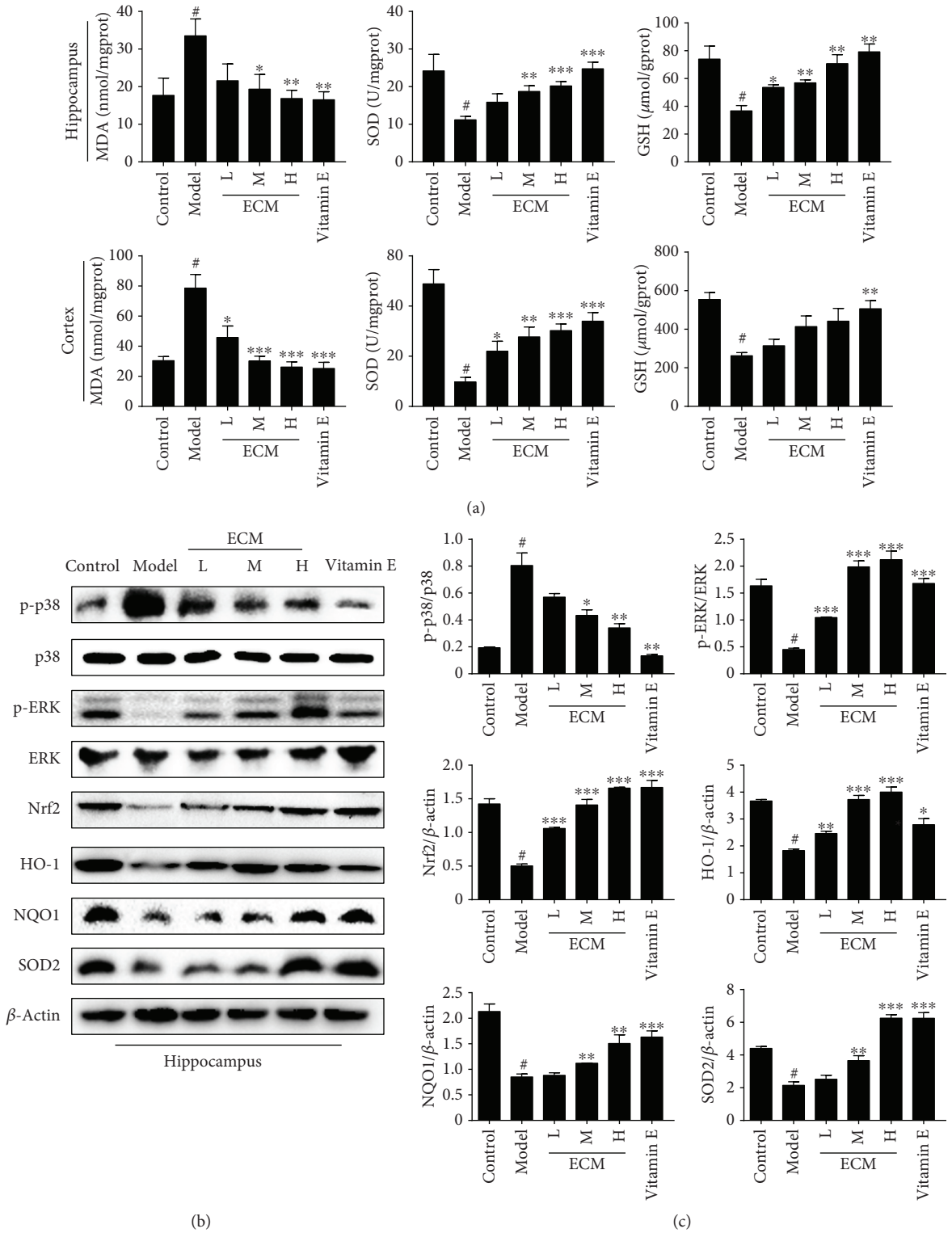

Figure 6: ECM inhibits oxidative stress via the MAPK and Nrf2 signaling pathways in the CNS. The homogenate of the hippocampus and cortex was used for the assay, and the lysate of the hippocampus was used for Western blot. (a) The content of MDA and the activities of SOD and GSH in the hippocampus (upper panel) and cortex (lower panel) were measured using a kit assay. (b) Western blot analysis of p-p38, p38, p-ERK, ERK, Nrf2, HO-1, NQO-1, and SOD2; β-actin was used as a loading control in the hippocampus. (c) Relative protein levels were quantified by densitometry and normalized to β-actin. Control: vehicle control; ECM-L: D – gal/$AlCl_3$ + ECM (100 mg/kg/d); ECM-M: D – gal/$AlCl_3$ + ECM (200 mg/kg/d); ECM – H : D – gal/$AlCl_3$ + ECM (400 mg/kg/d); vitamin E: D – gal/$AlCl_3$ + vitamin E (80 mg/kg/d). Data are represented as the mean ± SEM ($n = 10$ per group). $^{\#}p < 0.05$ and $^{\#\#}p < 0.01$ in comparison with the control group; $^{*}p < 0.05$, $^{**}p < 0.01$, and $^{***}p < 0.001$ in comparison with the model group.

hippocampus were examined by Western blot. In line with the *in vitro* results, phosphor-p38 MAPK was increased, while phosphor-ERK was decreased, in the hippocampus of D-gal/$AlCl_3$-treated mice (Figures 6(b) and 6(c)). However, ECM and vitamin E treatment reduced the phosphorylation of p38 MAPK and increased the phosphorylation of ERK, especially in the high-dose ECM and vitamin E treatment groups (Figures 6(b) and 6(c)). We then detected the expression levels of Nrf2 and its downstream proteins. Nrf2, HO-1, SOD2, and NQO-1 had relatively lower expression levels in the D-gal/$AlCl_3$ model group than those in the control group, whereas ECM or vitamin E treatment significantly increased the levels of Nrf2, HO-1, SOD2, and NQO-1 (Figures 6(b) and 6(c)), which was consistent with the *in vitro* results. These data suggest that ECM treatment can activate the Nrf2 signaling pathway and induce the expression of phase II detoxification enzymes, which are responsible for ameliorating oxidative stress and improving neurodegenerative diseases.

4. Discussion

Numerous reports have indicated that natural products harbor great chemical diversity, in turn exhibiting multiple biological activities. Increasing evidence has demonstrated that some natural products contain antioxidants that protect against oxidative stress in chronic disease, especially aging-related diseases. Identification of safe therapeutic regimens for oxidative stress-related diseases has attracted great attention. *C. minima* has been used as a medicinal herb to treat a number of diseases. Both aqueous and hydroalcoholic extracts of *C. minima* have been reported to scavenge free radicals and ameliorate oxidative stress, and the hydroalcoholic extracts express higher antioxidant activity [32]. However, the underlying mechanism of *C. minima* as an antioxidant agent was previously unknown. In this study, we examined the therapeutic potential and underlying mechanism of ECM in the treatment of oxidative stress-induced neurodegenerative disease and found that the ethanol extracts of *C. minima* exhibited significant antioxidant activity both *in vitro* and *in vivo*, mainly through upregulating nonenzymatic and enzymatic antioxidants. In this study, we also found that ECM protected mitochondrial function through the reduction of oxidative stress and by sustaining the Bcl-2/Bax ratio. Therefore, ECM could protect neurons in the brain from oxidative stress, which in turn attenuates the process of neurodegeneration and improves learning and memory capacity in a D-gal/$AlCl_3$-induced mouse model.

Although polyphenol and flavonoids are thought to be responsible for the antioxidant activity of *C. minima*, the active compounds had not been identified. A series of sesquiterpene lactones have been isolated from *C. minima*, with 6-*O*-angeloylplenolin found to be one of the most abundant compounds in ECM; 6-*O*-angeloylplenolin has been reported to exhibit antiallergy, antibacterial, and antiproliferative effects [34–37]. Arnicolide D and arnicolide C have also been shown to have antibacterial and antiproliferative effects [28, 36]. However, the antioxidant effects of these sesquiterpenoids in *C. minima* have never been reported. Therefore, we examined whether the sesquiterpenoids mediated the antioxidant activity of ECM. Intriguingly, we found that all four sesquiterpenoids had antioxidant activity, as they inhibited the neuronal death induced by tBHP, with 6-*O*-angeloylplenolin and arnicolide D exhibiting antioxidant activity even at low concentrations. Meanwhile, 6-*O*-angeloylplenolin and arnicolide D markedly induced the expression of phase II detoxification enzymes responsible for alleviating oxidant stress. Moreover, we analyzed the concentration of the compounds in ECM and found that both 6-*O*-angeloylplenolin and arnicolide D were highly concentrated in the extract of *C. minima* (see Supplementary Material), further indicating that 6-*O*-angeloylplenolin and arnicolide D act as active compounds that exhibit antioxidant properties. Our results suggest that sesquiterpenoids could be considered the active compounds in *C. minima* responsible for ameliorating oxidative stress; therefore, the therapeutic potential of sesquiterpenoids in treating neurodegenerative diseases warrants further investigation. The compound 6-*O*-angeloylplenolin and arnicolide D have been reported to exhibit antiproliferative activities against cancer cells; however, no obvious cytotoxicity was observed in our study, which may be due to that the compounds were used at lower concentrations than that used for antiproliferation studies, indicating that the compounds exert different activities at different concentrations. We will further examine the toxic effects of 6-*O*-angeloylplenolin and arnicolide D *in vivo*.

Increasing evidence has demonstrated that the transcription factor Nrf2 plays a key role in antagonizing oxidative stress, with Nrf2 exerting cytoprotective effects via the upregulation of a series of phase II detoxification enzymes. Recently, certain Nrf2 inducers have been studied clinically, and Nrf2 has been considered an emerging therapeutic target [47]. Nrf2 activation is under strict regulation; usually, Nrf2 is retained in the cytoplasm by Kelch-like ECH-associated protein 1 (Keap1) and tends to be degraded. Certain kinases, including ERK, protein kinase C, and AKT, regulate Nrf2 activation, and multiple natural products have been reported to regulate Nrf2 activation and nuclear translocation. Vitamin E and sulforaphane have been extensively examined for the ability to attenuate oxidative stress via the regulation of the Nrf2 signaling pathway. In this study, we used vitamin E as a positive agent for attenuating oxidative stress and found that ECM ameliorated oxidative stress both *in vitro* and *in vivo*, mainly through the activation of ERK and induction of Nrf2 nuclear translocation. The active compounds 6-*O*-angeloylplenolin and arnicolide D also markedly induced activation of Nrf2. Our results suggest that the ECM-induced activation of Nrf2 may occur, at least in part, through the induction of ERK activation. It is also possible that the active compounds in ECM directly disrupt the binding interface between Nrf2 and Keaps. Therefore, the role of the active compounds of *C. minima* in Nrf2 activation requires further investigation.

5. Conclusion

In summary, we found that the ethanol extract of *C. minima* is able to protect neuronal cells against oxidative stress-induced neurodegeneration through activation of the Nrf2

signaling pathway. We also found that 6-*O*-angeloylplenolin and arnicolide D are the potential active compounds in *C. minima*, which provides strong evidence that *C. minima* has a therapeutic potential in ameliorating neurodegenerative diseases. *C. minima* could be used as a source of antioxidant and neuroprotective compounds.

Abbreviations

ECM: Ethanol extract of *C. minima*
tBHP: tert-Butyl hydroperoxide
D-gal: D-Galactose
$AlCl_3$: Aluminum chloride
ROS: Reactive oxygen species
JNK: c-Jun N-terminal kinases
ERK: Extracellular signal-regulated kinases
MDA: Malonyl dialdehyde
GST: Glutathione S-transferase
MAPK: Mitogen-activated protein kinase
Nrf2: Nuclear factor erythroid 2-related factor 2
HO-1: Heme oxygenase-1
NQO-1: NAD(P)H: quinone oxidoreductase-1
SOD: Superoxide dismutase
GSH: Glutathione
PSD95: Postsynaptic density protein 95
SYN: Synaptophysin
HPLC: High-performance liquid chromatography
DCFH-DA: 2′,7′-Dichlorofluorescin diacetate.

Data Availability

All data used to support the findings of this study are included within the article.

Conflicts of Interest

The authors declare no conflicts of interest.

Authors' Contributions

Yi-Jie Wang and Xin-Yue Wang contributed equally to this work.

Acknowledgments

This work was supported by the Guangzhou Science Technology and Innovation Commission Technology Research Projects (201805010005), the National Natural Science Foundation of China (81473740 and 81802776), the National Science Fund for Distinguished Young Scholars (81525026), and the National Key Research and Development Program of China "Research and Development of Comprehensive Technologies on Chemical Fertilizer and Pesticide Reduction and Synergism" (2017YFD0201402).

Supplementary Materials

Material and Method for extraction and isolation of EBSC-26A–EBSC-26D and 9 figures. Supplementary Figure 1: ECM exerts neuroprotective effects in the hippocampus. Supplementary Figure 2–9: 1H NMR and 13C NMR spectra of EBSC-26A–EBSC-26D. *(Supplementary Materials)*

References

[1] J. R. Hodges, "Decade in review-dementia: a decade of discovery and disappointment in dementia research," *Nature Reviews Neurology*, vol. 11, no. 11, pp. 613-614, 2015.

[2] B. Maloney and D. K. Lahiri, "Epigenetics of dementia: understanding the disease as a transformation rather than a state," *The Lancet Neurology*, vol. 15, no. 7, pp. 760–774, 2016.

[3] S. J. Lupien, R. P. Juster, C. Raymond, and M. F. Marin, "The effects of chronic stress on the human brain: from neurotoxicity, to vulnerability, to opportunity," *Frontiers in Neuroendocrinology*, vol. 49, pp. 91–105, 2018.

[4] D. M. Lipnicki, J. D. Crawford, R. Dutta et al., "Age-related cognitive decline and associations with sex, education and apolipoprotein E genotype across ethnocultural groups and geographic regions: a collaborative cohort study," *PLoS Medicine*, vol. 14, no. 3, article e1002261, 2017.

[5] J. C. Jurado-Coronel, R. Cabezas, M. F. Avila Rodriguez, V. Echeverria, L. M. Garcia-Segura, and G. E. Barreto, "Sex differences in Parkinson's disease: features on clinical symptoms, treatment outcome, sexual hormones and genetics," *Frontiers in Neuroendocrinology*, vol. 50, pp. 18–30, 2018.

[6] B. A. Kent and R. E. Mistlberger, "Sleep and hippocampal neurogenesis: implications for Alzheimer's disease," *Frontiers in Neuroendocrinology*, vol. 45, pp. 35–52, 2017.

[7] A. Adlimoghaddam, M. Neuendorff, B. Roy, and B. C. Albensi, "A review of clinical treatment considerations of donepezil in severe Alzheimer's disease," *CNS Neuroscience & Therapeutics*, vol. 24, no. 10, pp. 876–888, 2018.

[8] B. T. Winslow, M. K. Onysko, C. M. Stob, and K. A. Hazlewood, "Treatment of Alzheimer disease," *American Family Physician*, vol. 83, pp. 1403–1412, 2011.

[9] L. Letra, T. Rodrigues, P. Matafome, I. Santana, and R. Seica, "Adiponectin and sporadic Alzheimer's disease: clinical and molecular links," *Frontiers in Neuroendocrinology*, vol. 52, pp. 1–11, 2019.

[10] D. Yin and K. Chen, "The essential mechanisms of aging: irreparable damage accumulation of biochemical side-reactions," *Experimental Gerontology*, vol. 40, no. 6, pp. 455–465, 2005.

[11] J. Lv, S. Jiang, Z. Yang et al., "PGC-1α sparks the fire of neuroprotection against neurodegenerative disorders," *Ageing Research Reviews*, vol. 44, pp. 8–21, 2018.

[12] V. Calabrese, R. Sultana, G. Scapagnini et al., "Nitrosative stress, cellular stress response, and thiol homeostasis in patients with Alzheimer's disease," *Antioxidants & Redox Signaling*, vol. 8, no. 11-12, pp. 1975–1986, 2006.

[13] E. E. Devore, F. Grodstein, F. J. A. van Rooij et al., "Dietary antioxidants and long-term risk of dementia," *Archives of Neurology*, vol. 67, no. 7, pp. 819–825, 2010.

[14] N. Dragicevic, N. Copes, G. O'Neal-Moffitt et al., "Melatonin treatment restores mitochondrial function in Alzheimer's mice: a mitochondrial protective role of melatonin membrane receptor signaling," *Journal of Pineal Research*, vol. 51, no. 1, pp. 75–86, 2011.

[15] C. A. Massaad, R. G. Pautler, and E. Klann, "Mitochondrial superoxide: a key player in Alzheimer's disease," *Aging*, vol. 1, no. 9, pp. 758–761, 2009.

[16] M. Zhang, C. An, Y. Gao, R. K. Leak, J. Chen, and F. Zhang, "Emerging roles of Nrf2 and phase II antioxidant enzymes in neuroprotection," *Progress in Neurobiology*, vol. 100, pp. 30–47, 2013.

[17] K. Dasuri, L. Zhang, and J. N. Keller, "Oxidative stress, neurodegeneration, and the balance of protein degradation and protein synthesis," *Free Radical Biology & Medicine*, vol. 62, pp. 170–185, 2013.

[18] R. K. Thimmulappa, K. H. Mai, S. Srisuma, T. W. Kensler, M. Yamamoto, and S. Biswal, "Identification of Nrf2-regulated genes induced by the chemopreventive agent sulforaphane by oligonucleotide microarray," *Cancer Research*, vol. 62, no. 18, pp. 5196–5203, 2002.

[19] J. A. Rubiolo, G. Mithieux, and F. V. Vega, "Resveratrol protects primary rat hepatocytes against oxidative stress damage: activation of the Nrf2 transcription factor and augmented activities of antioxidant enzymes," *European Journal of Pharmacology*, vol. 591, no. 1-3, pp. 66–72, 2008.

[20] A. Loboda, M. Damulewicz, E. Pyza, A. Jozkowicz, and J. Dulak, "Role of Nrf2/HO-1 system in development, oxidative stress response and diseases: an evolutionarily conserved mechanism," *Cellular and Molecular Life Sciences*, vol. 73, no. 17, pp. 3221–3247, 2016.

[21] J. Kwon, E. Han, C. B. Bui et al., "Assurance of mitochondrial integrity and mammalian longevity by the p62–Keap1–Nrf2–Nqo1 cascade," *EMBO Reports*, vol. 13, no. 2, pp. 150–156, 2012.

[22] Y. Yang, S. Jiang, J. Yan et al., "An overview of the molecular mechanisms and novel roles of Nrf2 in neurodegenerative disorders," *Cytokine & Growth Factor Reviews*, vol. 26, no. 1, pp. 47–57, 2015.

[23] H. Schipper, D. Bennett, A. Liberman et al., "Glial heme oxygenase-1 expression in Alzheimer disease and mild cognitive impairment," *Neurobiology of Aging*, vol. 27, no. 2, pp. 252–261, 2006.

[24] Y. Wang, K. Santa–Cruz, C. DeCarli, and J. A. Johnson, "NAD(P)H:quinone oxidoreductase activity is increased in hippocampal pyramidal neurons of patients with Alzheimer's disease," *Neurobiology of Aging*, vol. 21, no. 4, pp. 525–531, 2000.

[25] I. Buendia, P. Michalska, E. Navarro, I. Gameiro, J. Egea, and R. Leon, "Nrf2–ARE pathway: an emerging target against oxidative stress and neuroinflammation in neurodegenerative diseases," *Pharmacology & Therapeutics*, vol. 157, pp. 84–104, 2016.

[26] K. Kanninen, T. M. Malm, H. K. Jyrkkanen et al., "Nuclear factor erythroid 2-related factor 2 protects against beta amyloid," *Molecular and Cellular Neurosciences*, vol. 39, no. 3, pp. 302–313, 2008.

[27] C. Y. Shen, J. G. Jiang, L. Yang, D. W. Wang, and W. Zhu, "Anti-ageing active ingredients from herbs and nutraceuticals used in traditional Chinese medicine: pharmacological mechanisms and implications for drug discovery," *British Journal of Pharmacology*, vol. 174, no. 11, pp. 1395–1425, 2017.

[28] R. S. L. Taylor and G. H. N. Towers, "Antibacterial constituents of the Nepalese medicinal herb, *Centipeda minima*," *Phytochemistry*, vol. 47, no. 4, pp. 631–634, 1998.

[29] H. Liang, F. Bao, X. Dong et al., "Antibacterial thymol derivatives isolated from *Centipeda minima*," *Molecules*, vol. 12, no. 8, pp. 1606–1613, 2007.

[30] S. Schwikkard and F. R. van Heerden, "Antimalarial activity of plant metabolites," *Natural Product Reports*, vol. 19, no. 6, pp. 675–692, 2002.

[31] G. François, C. Passreiter, H. Woerdenbag, and M. van Looveren, "Antiplasmodial activities and cytotoxic effects of aqueous extracts and sesquiterpene lactones from *Neurolaena lobata*," *Planta Medica*, vol. 62, no. 2, pp. 126–129, 1996.

[32] S. S. Huang, C. S. Chiu, T. H. Lin et al., "Antioxidant and anti-inflammatory activities of aqueous extract of *Centipeda minima*," *Journal of Ethnopharmacology*, vol. 147, no. 2, pp. 395–405, 2013.

[33] H. M. On, B. M. Kwon, N. I. Baek et al., "Inhibitory activity of 6-*O*-angeloylprenolin from *Centipeda minima* on farnesyl protein transferase," *Archives of Pharmacal Research*, vol. 29, no. 1, pp. 64–66, 2006.

[34] Y. Q. Liu, X. L. Wang, X. Cheng et al., "Skp1 in lung cancer: clinical significance and therapeutic efficacy of its small molecule inhibitors," *Oncotarget*, vol. 6, no. 33, pp. 34953–34967, 2015.

[35] Y. Liu, X. Q. Chen, H. X. Liang et al., "Small compound 6-*O*-angeloylplenolin induces mitotic arrest and exhibits therapeutic potentials in multiple myeloma," *PLoS One*, vol. 6, no. 7, article e21930, 2011.

[36] P. Wu, M. X. Su, Y. Wang et al., "Supercritical fluid extraction assisted isolation of sesquiterpene lactones with antiproliferative effects from *Centipeda minima*," *Phytochemistry*, vol. 76, pp. 133–140, 2012.

[37] L. F. Ding, Y. Liu, H. X. Liang, D. P. Liu, G. B. Zhou, and Y. X. Cheng, "Two new terpene glucosides and antitumor agents from *Centipeda minima*," *Journal of Asian Natural Products Research*, vol. 11, no. 8, pp. 732–736, 2009.

[38] Y. Imakura, K. H. Lee, D. Sims et al., "Antitumor agents XXXVI: structural elucidation of sesquiterpene lactones microhelenins-A, B, and C, microlenin acetate, and plenolin from *Helenium microcephalum*," *Journal of Pharmaceutical Sciences*, vol. 69, no. 9, pp. 1044–1049, 1980.

[39] L. Xiao, H. Li, J. Zhang et al., "Salidroside protects *Caenorhabditis elegans* neurons from polyglutamine-mediated toxicity by reducing oxidative stress," *Molecules*, vol. 19, no. 6, pp. 7757–7769, 2014.

[40] Q. Wang, Y. Huang, C. Qin et al., "Bioactive peptides from *Angelica sinensis* protein hydrolyzate delay senescence in *Caenorhabditis elegans* through antioxidant activities," *Oxidative Medicine and Cellular Longevity*, vol. 2016, Article ID 8956981, 10 pages, 2016.

[41] S. T. Smiley, M. Reers, C. Mottola-Hartshorn et al., "Intracellular heterogeneity in mitochondrial membrane potentials revealed by a J-aggregate-forming lipophilic cation JC-1," *Proceedings of the National Academy of Sciences of the United States of America*, vol. 88, no. 9, pp. 3671–3675, 1991.

[42] E. Himeno, Y. Ohyagi, L. Ma et al., "Apomorphine treatment in Alzheimer mice promoting amyloid-β degradation," *Annals of Neurology*, vol. 69, no. 2, pp. 248–256, 2011.

[43] M. Audrain, R. Fol, P. Dutar et al., "Alzheimer's disease-like APP processing in wild-type mice identifies synaptic defects as initial steps of disease progression," *Molecular Neurodegeneration*, vol. 11, no. 1, p. 5, 2016.

[44] D. T. Proctor, E. J. Coulson, and P. R. Dodd, "Reduction in post-synaptic scaffolding PSD-95 and SAP-102 protein levels in the Alzheimer inferior temporal cortex is correlated with disease pathology," *Journal of Alzheimer's Disease*, vol. 21, no. 3, pp. 795–811, 2010.

[45] M. A. Ansari, K. N. Roberts, and S. W. Scheff, "Oxidative stress and modification of synaptic proteins in hippocampus after

traumatic brain injury," *Free Radical Biology & Medicine*, vol. 45, no. 4, pp. 443–452, 2008.

[46] S. W. Scheff, M. A. Ansari, and E. J. Mufson, "Oxidative stress and hippocampal synaptic protein levels in elderly cognitively intact individuals with Alzheimer's disease pathology," *Neurobiology of Aging*, vol. 42, pp. 1–12, 2016.

[47] I. M. Copple, A. T. Dinkova-Kostova, T. W. Kensler, K. T. Liby, and W. C. Wigley, "NRF2 as an emerging therapeutic target," *Oxidative Medicine and Cellular Longevity*, vol. 2017, Article ID 8165458, 2 pages, 2017.

Hindawi
Oxidative Medicine and Cellular Longevity
Volume 2019, Article ID 3549274, 19 pages
https://doi.org/10.1155/2019/3549274

Research Article

Sulforaphane-Enriched Broccoli Sprouts Pretreated by Pulsed Electric Fields Reduces Neuroinflammation and Ameliorates Scopolamine-Induced Amnesia in Mouse Brain through Its Antioxidant Ability via Nrf2-HO-1 Activation

Lalita Subedi,[1] **KyoHee Cho**,[1] **Yong Un Park**,[2] **Hyuk Joon Choi**,[2] **and Sun Yeou Kim**[1]

[1]*Laboratory of Pharmacognosy, College of Pharmacy, Gachon University, #191, Hambakmoero, Yeonsu-gu, Incheon 21936, Republic of Korea*
[2]*BK Bio Co. Ltd., 2706-38, Iljudong-ro, Gujwa-eup, Jeju-si, Jeju-do, Republic of Korea*

Correspondence should be addressed to Sun Yeou Kim; sunnykim@gachon.ac.kr

Received 19 September 2018; Revised 12 November 2018; Accepted 21 November 2018; Published 27 March 2019

Guest Editor: Francisco J.B. Mendonça Júnior

Activated microglia-mediated neuroinflammation plays a key pathogenic role in neurodegenerative diseases, such as Alzheimer's disease, Parkinson's disease, multiple sclerosis, and ischemia. Sulforaphane is an active compound produced after conversion of glucoraphanin by the myrosinase enzyme in broccoli (*Brassica oleracea* var) sprouts. Dietary broccoli extract as well as sulforaphane has previously known to mitigate inflammatory conditions in aged models involving microglial activation. Here, we produced sulforaphane-enriched broccoli sprouts through the pretreatment of pulsed electric fields in order to trigger the biological role of normal broccoli against lipopolysaccharide-activated microglia. The sulforaphane-enriched broccoli sprouts showed excellent potency against neuroinflammation conditions, as evidenced by its protective effects in both 6 and 24 h of microglial activation *in vitro*. We further postulated the underlying mechanism of action of sulforaphane in broccoli sprouts, which was the inhibition of an inflammatory cascade *via* the downregulation of mitogen-activated protein kinase (MAPK) signaling. Simultaneously, sulforaphane-enriched broccoli sprouts inhibited the LPS-induced activation of the NF-κB signaling pathway and the secretions of inflammatory proteins (iNOS, COX-2, TNF-α, IL-6, IL-1β, PGE2, etc.), which are responsible for the inflammatory cascades in both acute and chronic inflammation. It also upregulated the expression of Nrf2 and HO-1 in normal and activated microglia followed by the lowered neuronal apoptosis induced by activated microglia. Based on these results, it may exhibit anti-inflammatory effects via the NF-κB and Nrf2 pathways. Interestingly, sulforaphane-enriched broccoli sprouts improved the scopolamine-induced memory impairment in mice through Nrf2 activation, inhibiting neuronal apoptosis particularly through inhibition of caspase-3 activation which could lead to the neuroprotection against neurodegenerative disorders. The present study suggests that sulforaphane-enriched broccoli sprouts might be a potential nutraceutical with antineuroinflammatory and neuroprotective activities.

1. Introduction

Neuroinflammation plays a key role in the regulation of aging, Alzheimer's disease (AD), Parkinson's disease (PD), Huntington's disease (HD), multiple sclerosis (MS), stroke, depression, dementia, and metabolic disorders such as hypertension and diabetes [1]. Neuroinflammation is also the pathogenic hallmark of aging-related neurodegenerative conditions [1, 2]. Therefore, anti-inflammatory strategies could be efficient prophylactic and therapeutic management strategies for a number of central nervous system (CNS) disorders [3, 4]. CNS disorders may develop owing to chronic microglial activation. Glial cells, particularly microglia, are immune cells in the CNS that are responsible for the maintenance of normal homeostasis as well as repair after injury in the brain [5]. Although activated microglia are required for

host defense and debris clearance in the brain, chronic microglial activation is toxic to the CNS [6]. Conversion of normal microglia to the toxic microglial phenotype (known as the M1 phenotype) is responsible for the initiation of inflammatory cascades in the CNS, particularly the production of reactive oxygen species (ROS), nitric oxide (NO), proteases, arachidonic acids, excitatory amino acids, and cytokines [7]. These neurotoxic substances trigger the oxidative stress and are responsible for the disruption of the architecture and functions of neurons, consequently leading to synaptic degeneration and neurodegeneration [8]. These neuroinflammatory and neurotoxic cascades are responsible for the hippocampal neuronal damage leading to cognitive dysfunction [9]. Inhibition of the neuroinflammation or activation of the endogenous antioxidant system might be a better alternative for the repairment of this damage. Particularly, activation of the Nrf2 and its mediated antioxidant enzyme, HO-1, can not only inhibit the inflammatory cascades but also increase the neuronal survival and hippocampal neurogenesis [10]. Extensive neuropharmacology research has succeeded in finding novel drug candidates for the treatment of CNS disorders. However, they have failed to prove their efficacy in human biological systems during clinical trials. Potential reasons for these failures were suggested to be differences in tissue physiology of the CNS, unstable pharmacokinetics, or difficulty in crossing the blood-brain barrier (BBB) [11, 12]. Given the lack of proper allopathic medications to treat neuroinflammatory disorders, there is a growing interest in complementary and alternative medication, including nutraceuticals. Consumption of dietary nutraceuticals with neuroprotection could prevent CNS diseases, overcoming the limitations of allopathic drug delivery to the CNS.

Previous reports highlight the beneficial effects of broccoli and its active compound, sulforaphane, in neurodegenerative disorders. Although broccoli has a mild effect against age-related neuroinflammation, it does not show a significant effect against lipopolysaccharide- (LPS-) induced inflammatory conditions [13]. Another independent study has revealed that sulforaphane can reverse the hyperammonemia-induced glial activation, neuroinflammation, and disturbances in neurotransmitter receptors in the hippocampus that impaired spatial learning [14]. The anti-inflammatory effect of sulforaphane has also been previously reported in rat primary microglia [15]. These previous studies suggest that bioconversion of glucoraphanin in the broccoli may increase the yield of sulforaphane. It could lead to better health benefits for patients with neuroinflammatory disorders. Either the induction of myrosin production or the increase in myrosinase activity can increase the bioconversion of glucoraphanin into sulforaphane [16]. The presence of some other proteins, such as epithiospecifier protein (ESP), can also convert glucoraphanin to sulforaphane nitrile, without affecting sulforaphane's anti-inflammatory effects [17]. An increase in myrosinase activity with reduced ESP activity can selectively enhance sulforaphane yield in the broccoli sprout, making it a better candidate for the treatment of several pathological conditions, including cancer, inflammation, neurodegeneration, and aging [18]. Pharmacokinetic studies have revealed that, in mice, sulforaphane has good absorption and distribution patterns, in various tissues of the body, including the brain, lungs, heart, liver, kidneys, and muscles, after oral administration [19]. Previous reports suggest that sulforaphane and its metabolites do not readily cross the BBB [20]. However, the disruption of the BBB during neuroinflammation and neurodegenerative conditions allows sulforaphane to permeate the BBB and enhances its anti-inflammatory effects along the brain axis [20].

Former reports have revealed that activation of myrosinase in steamed broccoli sprouts can enhance the yield of sulforaphane [20]. Similarly, pulsed electric field (PEF) pretreatment enhances the production of glucosinolate in the broccoli flower and stalk. It also increased anthocyanin's production in red cabbage [21, 22]. Thus, we postulated that PEF might also be effective in enhancing the production of sulforaphane in broccoli sprouts.

In the current study, we are to reveal whether PEF treatment can increase the sulforaphane yield in broccoli sprouts or not. We also try to figure out the difference in the biological activity of broccoli sprout before and after PEF treatment. To determine the molecular mechanism underlying the sulforaphane-enriched broccoli sprout-mediated neuroprotective effect, we assessed the effect of sulforaphane-enriched broccoli sprouts on lipopolysaccharide- (LPS-) induced proinflammatory responses in both acute and chronic microglial activation *in vitro*. *In vivo* study will be done whether sulforaphane-enriched broccoli sprouts improve the scopol amine-induced memory impairment in mice or not.

2. Materials and Methods

2.1. Reagents. The pulsed electric field (PEF) was purchased from HVP 5 (Elea, DIL, Quakenbrueck, Germany). Lipopolysaccharide (LPS) and sulforaphane were purchased from Sigma Chemical (St. Louis, MO). Dulbecco's modified Eagle medium (DMEM), Fetal bovine serum (FBS), and penicillin-streptomycin were purchased from Invitrogen (Carlsbad, CA, USA). Antibodies for cyclooxygenase 2 (COX-2), β-actin, GAPDH, and histone-3 were obtained from Santa Cruz Biotechnology (Dallas, Texas, United States). The antibody of inducible nitric oxide synthase (iNOS) was purchased from Abcam (Cambridge, UK). The primary antibody for α-tubulin, C-Jun N-terminal kinase (JNK), p38, extracellular signal-regulated kinases (ERK), NF-κB, I-κB, pI-κB, C-Jun, pC-Jun, C-Fos, and pC-Fos were purchased from Cell Signaling (Beverly, MA, USA). Various ELISA kits like interleukin-6 (IL-6), prostaglandin E2 (PGE2), tumor necrosis factor alpha (TNF-α), and interleukin-β (IL-1β) were acquired from R&D Systems (Minneapolis, MN, USA).

2.2. Animals. Male ICR mice (6 weeks; 25-30 g) were purchased from Orient Bio, Seoul, Korea. Four or five mice were placed in each cage and acclimatized for one week in laboratory conditions with food and water ad libitum. They were maintained under temperature ($23 \pm 1^{\circ}$C) and relative humidity ($60 \pm 10\%$) conditions and in a 12/12 h light and dark cycle. Animal handling and experimental procedures were conducted in accordance with the Principles of Laboratory Animal Care (GIACUC-R2017016) and the Animal

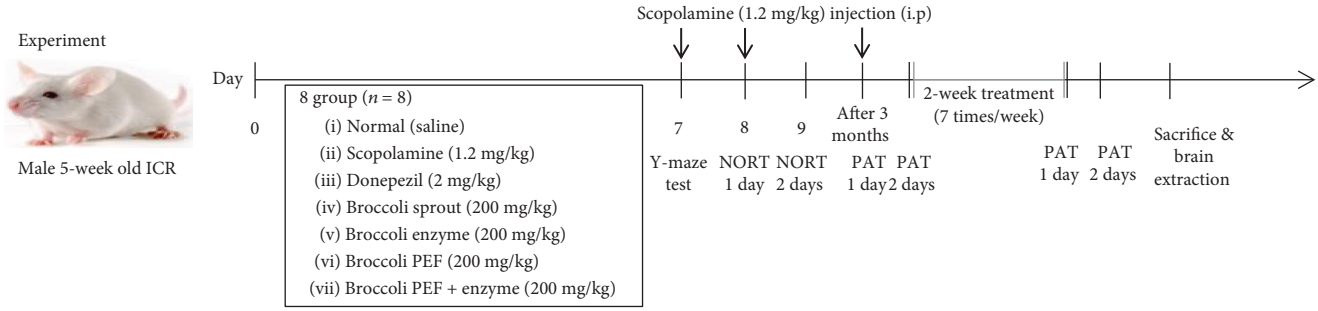

Scheme 1: Experimental design for the *in vivo* experiment.

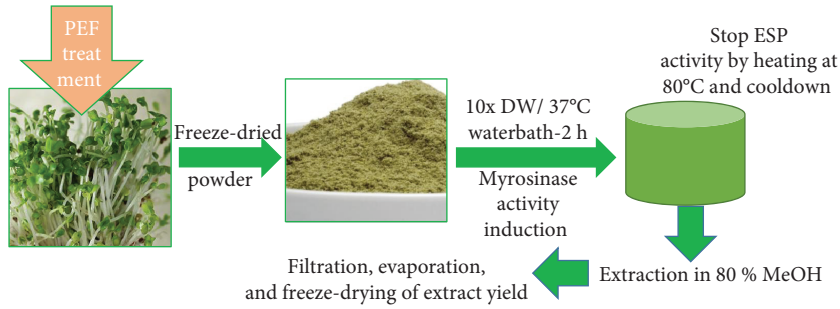

Scheme 2: Preparation of PEF-treated broccoli sprout powder.

Care and Use Guidelines of Gachon University, Korea. The experimental protocol is shown in Scheme 1.

2.3. PEF-Broccoli Preparation and Extraction. Broccoli sprout extraction was performed according to a previous study with slight modifications [23]. Each whole broccoli sprout (SB) as well as the hypocotyl (H), cotyledon (C), and radicle (R) were treated with PEF, at 0–7 kJ, for 3 s each, followed by freeze-drying and grinding to make fine powder ready for myrosinase activity induction. The powdered broccoli or its parts were incubated with 10x volume of distilled water, and the suspension was kept at 37°C for a total of 2 h for the induction of myrosinase activity, yielding a greater amount of glucoraphanin to sulforaphane as a final product. During this conversion, sulforaphane nitrile could also be formed with the help of epithiospecifier protein (ESP). This conversion was prevented by placing/heating the mixture at 80°C for 10 min. The mixture was cooled down by keeping it in the ice. As a final step, the suspension was mixed with methanol making the solvent as 70% methanol in total and the extraction was performed. Extraction was performed with continuous stirring and sonication for about 3 h in total. We used each sample as the following; broccoli sprout cotyledons (C) or sprout cotyledons with both PEF and myrosinase activity (C-P) and hypocotyls from broccoli sprouts (H) or hypocotyls from broccoli sprouts treated with both PEF and myrosinase activity (H-P). The supernatant was filtered (HYUNDAI Micro No. 20 filter paper, Korea) and evaporated using a rotary evaporator to remove the methanol. The extract was free-dried, and the lyophilized powder was used for subsequent experiments. Preparation of PEF-broccoli samples is shown in Scheme 2.

2.4. Broccoli Extract HPLC Standardization. High-performance liquid chromatography (HPLC) analysis was performed to measure the sulforaphane content in the broccoli sprout extract. The HPLC analysis was performed using a Waters system (Waters Corp., Milford, MA), consisting of a separation module (e2695) with an integrated column heater, autosampler, and photodiode array detector (2998). The UV absorbance was monitored at 200–400 nm. Quantification was conducted by integrating the peak areas at 235 nm. The injection volume was 10 μL. A column (250 × 4.6 mm; particle size, 5 μm; Phenomenex, USA) was installed in a column oven and maintained at 25°C. The mobile phase was composed of water containing 1% acetic acid (solvent A) and acetonitrile (solvent B). The flow rate was 0.5 mL/min. The gradient was 0.0 min, 10% B; 5 min, 20% B; 15.0 min, 40% B; 25.0 min, 60% B; 35.0 min, 90% B; and 40.0 min, 10% B. The re-equilibration time between runs was 20 min.

2.5. Cell Culture. The murine microglia cell (BV2) was used as a representative cell of brain microglia. The neuroblastoma cell (N2a) was used as a representative cell line of the neuron [24]. BV2 cells were kindly obtained by Dr. E. Choi at Korea University (Seoul, Korea), while N2a cells were obtained from the Korean Cell Line Bank (Seoul, Korea). BV2 & N2a cells were maintained in high-glucose DMEM supplemented with 10% heat-inactivated FBS and 1% penicillin (1×10^5 U/L) and streptomycin (100 mg/L), in a humidified incubator with 5% CO_2 at 37°C.

2.6. Cell Treatment and Cytotoxicity Assay. Cytotoxicity of the samples was evaluated through 3-(4,5-dimethylthiazol-2-yl)-2,5-diphenyltetrazolium bromide (MTT) assay also

called the cell viability assay [25]. BV2 cells were seeded in 96-well plates overnight, and they were treated (pre/post) with different concentrations of broccoli extract with or without LPS. LPS (100 ng/mL) was added 30 min after sample treatment in case of pretreatment of prophylactic treatment condition. LPS activation in the seeded cells occurred 30 min before the sample treatment in case of posttreatment/therapeutic treatment strategy. Cells were incubated for 24 h after LPS activation, for the nitrite and cell viability assays. In case of neuronal cell viability, conditioned media from 24 h treated BV2 cells were transferred to the seeded N2a cells and incubated for another 24 h as described previously [26]. Treated cells were incubated for an hour with the MTT solution of 0.5 mg/mL concentration that will stain the viable cells into a blue color. The MTT solution was suctioned out, and 200 μL of dimethyl sulfoxide was added to each well that converts the blue-stained cells to a purple-colored solution. The optical density (OD) was measured using a plate reader at 570 nm. The results were expressed as a percentage of the LPS-treated cells (LPS-treated group).

2.7. Nitric Oxide (NO) Measurement. Nitric oxide production inhibition by the treatment of broccoli extract and sulforaphane on LPS-stimulated BV2 cells was performed through Griess assay as described previously with slight modification [27]. BV2 cells were seeded in a 96-well plate (4×10^4 cells/well) and activated with 100 ng/mL LPS, in the presence or absence of different concentrations of broccoli extract or sulforaphane, for 24 h. The nitrite level in the culture media was measured using Griess reagent (1% sulfanilamide and 0.1% N-1-napthylethylenediamine dihydrochloride in 5% phosphoric acid). A total of 50 μL of supernatant was mixed with an equal volume of Griess reagent, and OD was measured at 570 nm. NG-Mono--methyl-L-arginine (L-NMMA), a well-known nitric oxide synthase (NOS) inhibitor, was used as a positive control. The pretreatment and posttreatment conditions were performed to evaluate its effect for prophylactic and therapeutic purposes.

2.8. Measurement of TNF-α, IL-1β, IL-6, and PGE2 Production. Cells were plated in a 6-well plate at a density of 1.5×10^6 cells/well in DMEM and incubated for 24 h, to measure TNF-α, IL-1β, PGE2, and IL-6 production. The cultures were prepared and stimulated with LPS in the presence or absence of sample. After a 24 h incubation, the supernatant from the culture medium was harvested. The levels of PGE2, TNF-α, IL-1β, and IL-6 were measured. PGE2 was measured using a competitive enzyme immunoassay kit (Cayman Chemical, Ann Arbor, MI, USA), and TNF-α, IL-1β, and IL-6 were measured using ELISA development kits (R&D Systems, Minneapolis, MN, USA). The % of CV was set below 10 for every ELISA assay.

2.9. NF-κB Assay. Nuclear and cytosolic extracts from treated microglial cells were prepared using a Nuclear/Cytosolic Extraction Kit (Active Motif, Carlsbad, CA) according to the manufacturer's protocol. Protein levels of NF-κB, histone-3, I-κB, and pI-κB were determined using western blot analysis. Expression of nucleolic and cytosolic NF-κB was measured using histone-3 and β-actin as loading controls, respectively. The expressions of I-κB and pI-κB in the cytosolic fraction were observed. The absence of β-actin expression in the neucleolic fraction suggested the clear separation of the neucleolic and cytosolic fractions during fractionation, without any contamination. Densitometry analysis of the bands was performed using ImageMaster™ 2D Elite software (version 3.1, Amersham Pharmacia Biotech, Buckinghamshire, UK).

2.10. Western Blot Analysis. Western blot analysis was conducted as previously described [26], with slight modification. Proteins obtained from BV2 cells (6×10^5 cells/well), which were seeded in a 6-well plate, were used for western blot analysis. Total proteins (30 μg) from each group were separated by 10% SDS-PAGE gel electrophoresis, transferred to nitrocellulose membranes, and incubated with primary antibodies against tubulin, iNOS, COX-2, ERK, pERK, JNK, pJNK, p38, pp38, NF-κB, histone-3, β-actin, I-κB, pI-κB, C-Fos, pC-Fos, C-Jun, pC-Jun, and α-tubulin. Membranes were incubated with horseradish peroxidase-conjugated secondary antibodies, and protein bands were visualized using ECL Western Blotting Detection Reagents (Amersham Pharmacia Biotech). Densitometry analysis of the bands was performed using ImageMaster™ 2D Elite software (version 3.1, Amersham Pharmacia Biotech).

2.11. Y-Maze Test. The Y-maze test was performed to evaluate the spatial memory or perception of the mice after scopolamine-induced neuronal injury. The Y-shaped maze having 5 : 20 : 10 of width : length : height was prepared, and the three arms of Y shape were allocated as A, B, and C. Mice were trained in the Y-maze before the start of the experiment. Mice were randomly divided into groups of saline, donepezil (2 mg/kg, p.o.), and different extracts of the broccoli sprout (200 mg/kg, p.o.). Mice for the donepezil and extract-administered groups were challenged with scopolamine (1.2 mg/kg, i.p.) 30 min after drug administration. Donepezil is a well-known acetylcholine esterase inhibitor and is widely used as a positive control for the scopolamine-induced memory impairment model [28, 29]. Scopolamine-administered and sample treated mice were kept in the center of the maze, and the mice were allowed to enter into the arms of the maze. Mice were let to habituate for 2 min, and their entry in the arms for 8 min was evaluated. Mouse entry is set when the mouse body (from nose to tail) was fully entered into the arms. Only the entry of the mouse in all the 3 different arms consecutively was assigned with point 1 for each arm entered. Alternation behavior was defined as 3 consecutive entries into 3 different arms of the maze. Spatial perception ability was calculated according to the formula below [30].

$$\text{Voluntary alternation behavior rate } (\%) = \frac{N_{\text{alteration}}}{N_{\text{entries}} - 2} \times 100, \quad (1)$$

where $N_{\text{alterations}}$ is the number of times alternation behavior was observed (scored by points), and N_{entries} is the total number of arm entries.

2.12. Novel-Object Recognition Test (NORT). In order to determine the role of the broccoli sprout extract enriched with sulforaphane in memory boost, a novel object recognition test (NORT) was performed. The mouse was placed into a 45 cm × 45 cm × 50 cm box containing the novel object for about 5 minutes to habituate in the testing environment. Following the habituation, response of the mouse (time) for object recognition was recorded for 3 minutes. On the third day of testing, 1 of the objects was replaced with a new object, and the response time for the new object recognition was recorded. The concentration of mouse to recognize the new object was evaluated by the recognition index (%) as follows:

$$\text{Recognition index}(\%) = [\text{time novel}/\text{time novel} + \text{time familiar})] \times 100. \quad (2)$$

Here, time novel is the time spent exploring the novel object, and time familiar is the time spent exploring the familiar object.

2.13. Passive Avoidance Task. A passive avoidance test was performed using identical boxes which are illuminated or nonilluminated of the size (20 × 20 × 20 cm), separated by a guillotine door (5 × 5 cm) as described elsewhere [31]. The illuminated compartment contained a 50 W bulb, and the floor of the nonilluminated compartment (20 × 20 × 20 cm) was composed of 2 mm stainless steel rods spaced 1 cm apart. For an acquisition trial, mice were placed in the illuminated compartment and, after 10 s, the door between the two compartments was opened. When mice entered the dark compartment, the door automatically closed and an electric foot shock (0.25 mA) was delivered for 3 s through the stainless steel rods. Twenty-four hours after the acquisition trial, the retrieval trial was conducted by placing the mice in the illuminated compartment. The latency to enter the dark compartment after opening the door was recorded. Cut-off latency was set at 600 s to avoid ceiling effects.

2.14. Acetylcholinesterase Activity Assay. Colorimetric assay was performed to determine the acetylcholinesterase activity using acetylthiocholine enzyme and acetylthiocholine iodide substrate as described previously [32], with slight modifications. The mouse brains were quickly harvested after CO_2 euthanasia and well homogenized in a homogenization buffer (12.5 mM sodium phosphate buffer, pH 7.0, 400 mM NaCl) using a glass Teflon homogenizer (EYELA, Japan), and the supernatant was used for the acetylthiocholine activity assay as described previously [32]. In brief, 0.02% Tanshinone congeners were prepared in dimethyl sulfoxide and mixed with acetylthiocholine iodide solution (75 mM), buffered Ellman's reagent (10 mM), 5,5′-dithio-bis(2-nitrobenzoic acid), and 15 mM sodium bicarbonate. The total mixture was incubated for 30 min for reaction at room temperature. Absorbance was measured at 410 nm immediately after adding the enzyme source to the reaction mixtures, and readings were taken at 30 s intervals for 5 min. Donepezil was used as a positive control.

2.15. Data and Statistical Analysis. All results are expressed as mean ± standard error of the mean (SEM). Statistical significance between experimental groups was determined by using one-way analysis of variance (ANOVA) followed by the Tukey post hoc test using GraphPad Prism 5 (GraphPad Software Inc., La Jolla, CA, USA). Statistical significance was set at $P < 0.05$. Each experiment was performed in triplicate.

3. Results

3.1. PEF Exposure Enriched Sulforaphane Content in Broccoli Sprouts. We confirmed the content of sulforaphane as a surrogate marker, using HPLC, for the quality control of broccoli sprouts. Figure 1 shows the chromatogram of broccoli sprouts compared to that of sulforaphane. The linearity of the compound was calculated using five concentrations. The sulforaphane content of adult broccoli is found to be almost 4.5-fold lesser than that of the broccoli sprouts. Enzymatic activation of broccoli sprouts increased the sulforaphane content almost 1.2-fold more than that of the normal broccoli sprout. Sulforaphane content was increased by 2.5-fold in a broccoli sample treated with PEF only. When the enzymatically activated broccoli sprout was treated with PEF, sulforaphane yield was 4.2-fold, in particular in the cotyledon, in comparison to the broccoli sprouts. Our experiment revealed that the sulforaphane content of broccoli sprouts, particularly in the hypocotyls and cotyledons, was increased to the highest extent with the combined treatment of PEF and enhanced enzymatic activity. The radicle of the broccoli had the lowest amount of sulforaphane, which was not altered, even with exposure to PEF and enzymatic activity. Compared to broccoli sprouts, adult broccoli contains less amount of sulforaphane, which was increased with activation of enzymatic activity, PEF exposure, and the combination of both conditions as shown in Figure 1. Overall, increased enzymatic activity and PEF exposure showed a synergistic effect in upregulating the amount of sulforaphane in broccoli sprouts.

3.2. Broccoli Sprouts Exposed to PEF Inhibited Nitrite Production in LPS-Activated Microglia. The ability of young and adult broccoli to inhibit NO was more pronounced when the broccoli sprouts were exposed to PEF and enzyme activity. Broccoli plants exposed to this combination were approximately 2-fold more effective at inhibiting nitrite production, compared to those exposed to either PEF or enzymatic activity only. Compared to the hypocotyls, broccoli plant cotyledons exposed to enzyme and PEF showed the highest potency. After confirming the effect of PEF and enzyme activity on broccoli, we evaluated differences in its activity, during pre-treatment and post-treatment, on LPS-activated microglial cells. The pattern of activity, as well as the extent of potency, was similar to its effects on nitrite production during pre- and post-treatment. Broccoli sprout cotyledons (C) exposed with PEF (C-P) showed better potency in

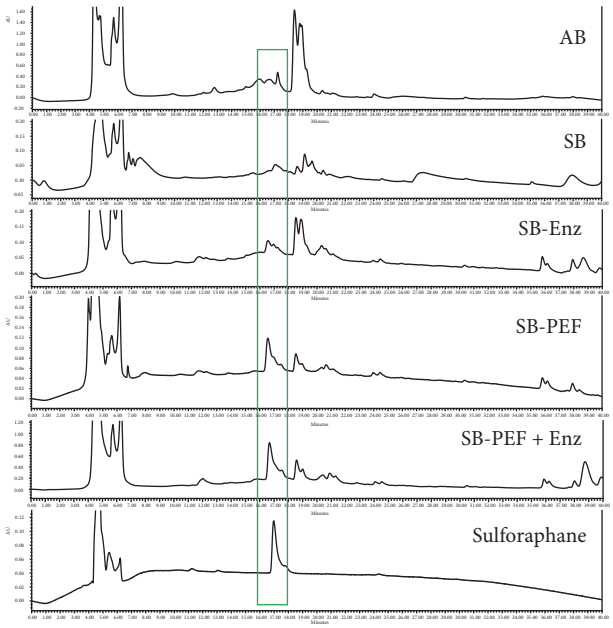

(a)

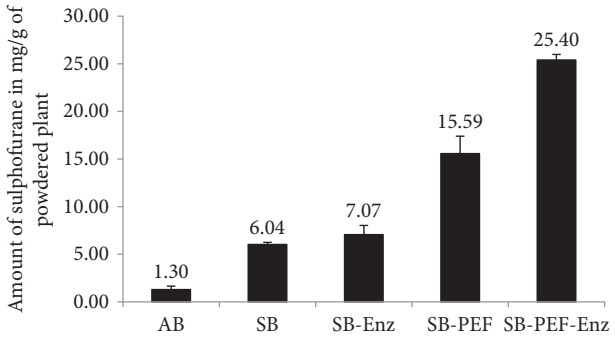

(b)

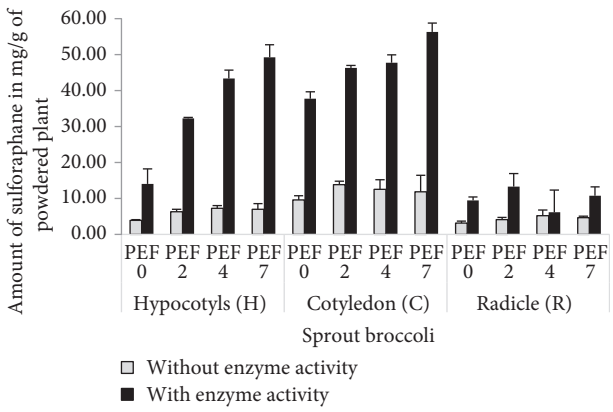

(c)

		PEF amount	Sulforaphane amount
SB-with enzyme activity	Hypocotyls (H)	PEF 0	14.07 ± 4.11
		PEF 2	32.23 ± 0.28
		PEF 4	43.33 ± 2.37
		PEF 7	49.24 ± 3.47
	Cotyledon (C)	PEF 0	37.72 ± 1.92
		PEF 2	46.31 ± 0.64
		PEF 4	47.71 ± 2.21
		PEF 7	56.28 ± 2.51
	Radicle (R)	PEF 0	9.43 ± 0.99
		PEF 2	13.30 ± 3.60
		PEF 4	6.19 ± 6.18
		PEF 7	10.73 ± 2.47
SB-without enzyme activity	Hypocotyls (H)	PEF 0	3.92 ± 0.20
		PEF 2	6.31 ± 0.71
		PEF 4	7.26 ± 0.76
		PEF 7	7.01 ± 1.55
	Cotyledon (C)	PEF 0	9.59 ± 1.14
		PEF 2	13.81 ± 0.98
		PEF 4	12.56 ± 2.64
		PEF 7	11.88 ± 4.54
	Radicle (R)	PEF 0	3.18 ± 0.53
		PEF 2	4.10 ± 0.65
		PEF 4	5.23 ± 1.56
		PEF 7	4.65 ± 0.39

(d)

Figure 1: Pulsed electric field (PEF) and enzyme activity increased sulforaphane content in broccoli sprouts. Broccoli sprout was treated with PEF and extracted followed by the treatment of myrosinase for increased enzyme activity to convert glucoraphane to sulforaphane. High-performance liquid chromatography (HPLC) evaluation of different broccoli extracts was performed. (a, b) Quantitative evaluations of sulforaphane in adult broccoli (AB), broccoli sprouts (SB), broccoli and induced enzyme activity (SB-Enz), sprout broccoli with PEF (SB-PEF), and sprout broccoli with PEF and induced enzyme activity (SB-PEF + Enz), and pure sulforaphane compound samples, using HPLC. (c, d) Amount of sulforaphane in broccoli plants, particularly in the hypocotyls, cotyledons, or radicle, following different PEF concentrations, with or without enzyme activity. All data are presented as mean ± standard error of the mean of three independent experiments.

comparison to normal hypocotyls (H) or PEF-exposed hypocotyls (H-P) as shown in Figure 2. From this screening, we select 100 μg/mL of the concentration of C, C-P, H, and H-P for further experiment and mechanism study.

3.3. Broccoli Sprouts Exposed to PEF Inhibited the Expression of iNOS and COX-2, during 6 and 24 h LPS Activation. LPS-mediated inflammation is mainly characterized by increased nitrite production and the expression of iNOS and COX-2 [27]. The expression of iNOS and COX-2 significantly increased in BV2 cells treated with LPS [26]. The PEF-enzyme activity increased the inhibitory effect of the cotyledons and hypocotyls of broccoli sprouts on the expression of these inflammatory proteins. Further, the expression of these proteins in the BV2 cells returned to almost normal levels with cotyledon and hypocotyl treatment, even in the presence of LPS in microglial cells. Sprout broccoli cotyledons (C) and cotyledon-P (C-P) were less effective at inhibiting the expression of COX-2 than that of iNOS. However, C-P and H-P significantly inhibited COX-2 expression after LPS activation as shown in Figure 3. Interestingly, normal broccoli H showed a higher potency to inhibit COX-2 expression 24 h following microglial activation. Taken together, untreated broccoli plants as well as those exposed to PEF effectively inhibited LPS-induced iNOS and COX-2 expression.

3.4. Broccoli Sprout Cotyledons/Hypocotyls Exposed to PEF Modulated Effector Signaling, Specifically ERK and p38 Phosphorylation. MAPK effector signaling pathways control the production of inflammatory mediators and proinflammatory cytokines. The activation (phosphorylation) of MAPK proteins (i.e., p38, JNK, and ERK) is responsible for controlling transcription factors and ultimately the production of inflammatory mediators [33]. LPS significantly increased JNK, ERK, and p38, and this effect was inhibited by C-P. C-P inhibited the phosphorylation of ERK and p38 to an unexpectedly high extent as shown in Figure 4.

3.5. Broccoli Sprout Cotyledons/Hypocotyls Exposed to PEF Modulated Effector Signaling Short-Term and Chronic LPS Activation in BV2 Microglial Cells. Both 6 h and 24 h LPS activation sufficiently activated MAPK phosphorylation, which was slightly or significantly altered by C, C-P, H, and H-P treatment. Although both C-P and H-P extensively inhibited ERK phosphorylation during the 6 h (short-term) and 24 h (chronic) LPS activation, the inhibitory effect of cotyledons was weak. H samples, however, increased ERK phosphorylation during chronic activation. The inhibitory effect of C and C-P treatment on p38 was very promising during the 6 h short-term activation and 24 h chronic activation as shown in Figure 5. Tubulin was used as a loading control for these experiments.

3.6. Broccoli Sprout Cotyledons Exposed to PEF Inhibited NF-κB- and AP-1-Mediated Transcription of Inflammatory Proteins. NF-κB and AP-1 are the major transcription factors that are responsible for altering the production of inflammatory proteins and proinflammatory cytokines in LPS-activated BV2 cells. Both the cotyledons and hypocotyls of broccoli sprouts can inhibit NF-κB activity; however, this effect was more prominent following exposure to PEF. LPS treatment significantly upregulated nuclear NF-κB and decreased cytosolic NF-κB. This effective translocation was necessary for further transcription. However, this cascade was reversed by PEF-treated broccoli sprout treatment. In addition to inhibiting NF-κB translocation, broccoli C-P and H-P also inhibited the phosphorylation of I-κB and increased its inactive form. Histone-3 was used as a loading control for nuclear proteins, while B-actin was used for cytosolic proteins as shown in Figure 6. No significant changes were measured in AP-1 signaling after broccoli treatment.

3.7. Broccoli Sprout Cotyledons Exposed to PEF Inhibited Production of Proinflammatory Cytokines and Inhibited Neuronal Death Induced by Activated Microglia. Next, we evaluated the effects of broccoli cotyledons and hypocotyls on the production of inflammatory cytokines. The cotyledons and hypocotyls of normal broccoli sprouts, as well as those exposed to PEF and enzyme, significantly inhibited the production of proinflammatory cytokines, such as TNF-α, IL-6, IL-1β, and PGE2. We demonstrated that broccoli plants showed the highest effect inhibiting IL-6 and IL-1β production and the lowest efficacy in inhibiting TNF-α and PGE2 production. The low potency by that in inhibiting COX-2 production is due to weak potency in inhibiting PGE2 production as shown in Figure 7. After confirming the anti-inflammatory potential of C and C-P, we checked its role in the neuronal survival against activated microglia-induced toxicity to neurons. LPS-induced activation of the microglia resulted in the production of various inflammatory mediators which are lethal to neuronal cells, but treatment of C and C-P to the activated microglia lowered the inflammatory cascades and hence made it possible to inhibit neuronal death by lowering the Bax/Bcl2 ration and expression of cleaved caspase-3. In both of the cases, C-P showed a slightly higher potential to that of C alone. This result provides a strong cue that C and C-P might prevent neuronal death, and hence, they can prevent neurodegeneration induced either by neuroinflammation/activated microglia or by other toxicities.

3.8. Broccoli Samples with or without PEF Increased the Nuclear Factor Erythroid 2–Related Factor 2 (Nrf2) and Heme Oxygenase- (HO-) 1 Expression in the Normal BV2 Cells and against Scopolamine-Induced Amnesia in Mouse Brain Tissue Samples. Sulforaphane is known as an Nrf2 activator; in our study, we also observed that treatment of C and C-P significantly increased the expression of Nrf2 and antioxidant protein HO-1 in normal as well as LPS-activated microglia as shown in Figure 8. The increased HO-1 and Nrf2 are higher in the case of the PEF-exposed sample, and it must be because of the increased sulforaphane content in it. This suggests that the better potency of C-P to induce Nrf2/HO-1 activation in direct as well as LPS-activated microglia not only can show its antioxidant effect directly in the brain cells but also can lower the activated microglia-induced inflammatory cascades. In addition to this, SB-PEF or SB-Enz-PEF has the highest amount of sulforaphane,

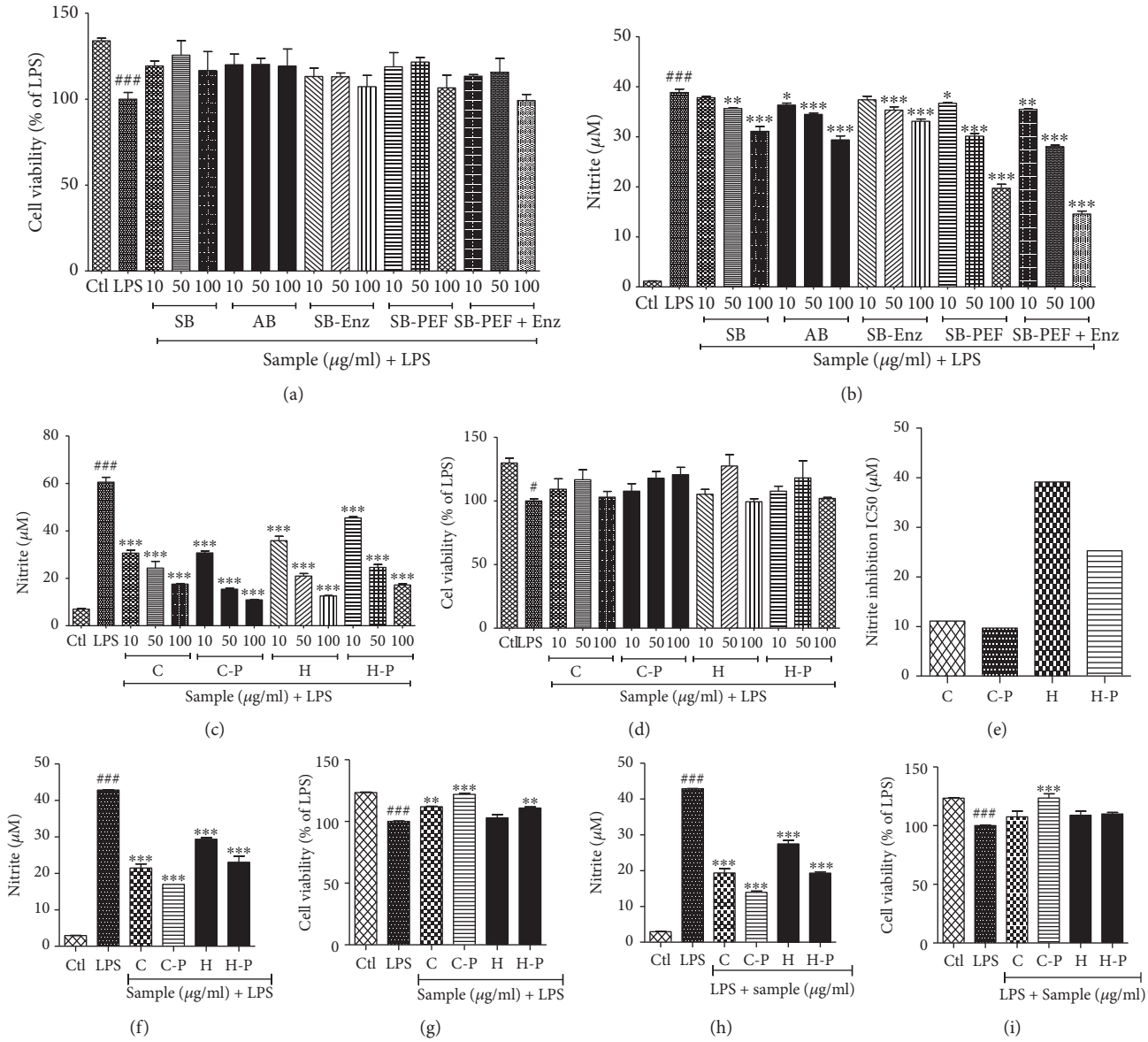

Figure 2: Pulsed electric field (PEF) and enzyme activity-treated broccoli sprouts inhibited nitrite production in lipopolysaccharide- (LPS-) activated BV2 microglial cells. BV2 microglial cells were pretreated with broccoli extracts, and LPS (100 ng/mL) stimulation was performed after 30 min. (a, b) Nitrite production and cell viability after different types of broccoli sample treatment. (c, d) Nitrite production and cell viability of LPS-activated microglia following pretreatment of broccoli samples. (e) IC50 value for the nitrite inhibition by C, C-P, H, and H-P treatment in LPS-activated microglia. (f-i) Nitrite inhibition and cell viability after C, C-P, H, and H-P pre- and post-treatment in LPS-activated microglia. All data are presented as mean ± standard error of the mean of three independent experiments. $^{*}P < 0.05$, $^{**}P < 0.01$, and $^{***}P < 0.001$ indicate significant differences compared with treatment with LPS alone, while $^{\#}P < 0.05$ and $^{\#\#\#}P < 0.001$ indicate the significant differences compared with an untreated control group. Ctl: control; LPS: lipopolysaccharide; SB: sprout broccoli; AB: adult broccoli; SB-Enz: broccoli sprouts with induced enzyme activity; SB-PEF: broccoli sprouts with PEF treatment; SB-PEF + Enz: broccoli sprouts with PEF treatment and induced enzyme activity; C: cotyledons; C-P: cotyledons exposed with PEF + enzyme activity; H: hypocotyls; H-P: hypocotyls exposed with PEF + enzyme activity.

which is responsible for the inhibition of the neuroinflammation and neurodegeneration against scopolamine toxicity. In the animal brain, we clearly noticed that SB-Enz-PEF showed a sharp increase in Nrf2 expression (Figure 8) suggesting that increased Nrf2 was responsible for the improved memory, cognition, and increased latency time in the passive avoidance test.

3.9. Sprout Broccoli Samples Repair the Scopolamine-Induced Memory and Cognitive Impairment In Vivo. Oral administration of the sprout broccoli sample 30 min before scopolamine administration significantly inhibited the spontaneous alteration almost 3-fold in comparison to the untreated control group (Figure 9). The sprout broccoli treated with PEF and sprout broccoli with enzyme activation and PEF treatment

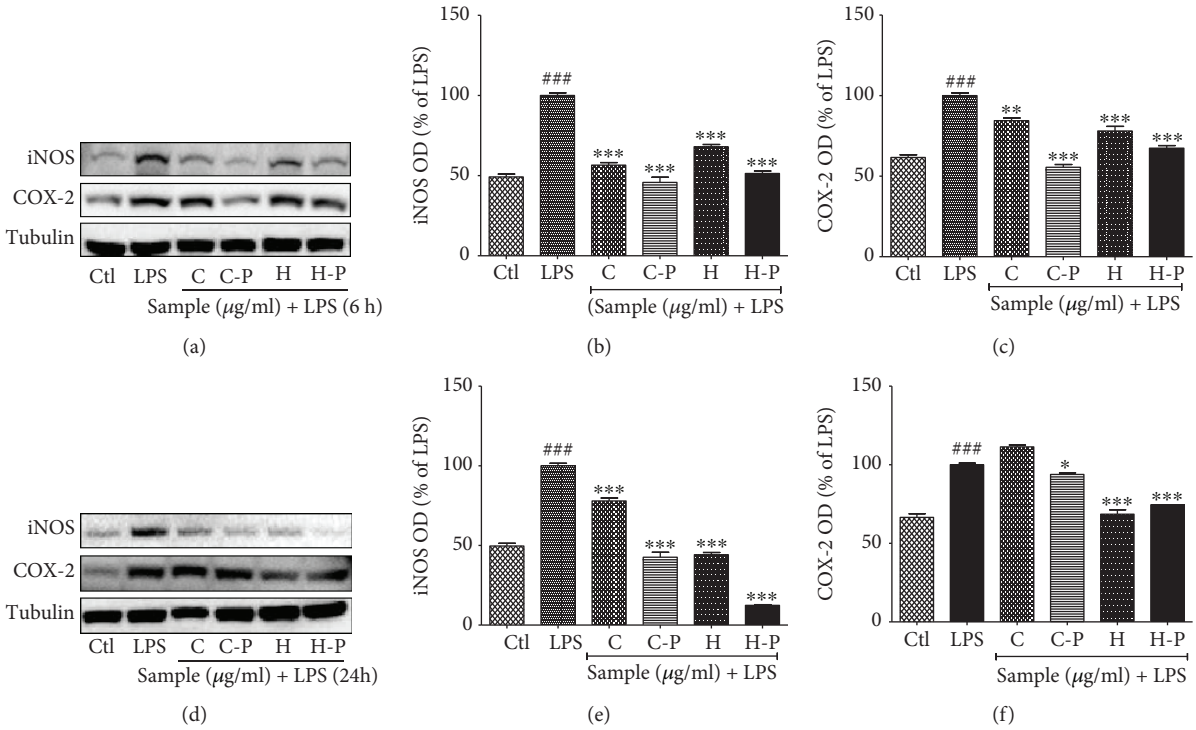

Figure 3: Pulsed electric field (PEF) and enzyme activity-treated broccoli sprouts inhibited expression of inducible nitric oxide synthase (iNOS) and cyclooxygenase 2 (COX-2) in lipopolysaccharide- (LPS-) activated BV2 microglial cells. BV2 microglial cells were pretreated with broccoli extracts; LPS (100 ng/mL) stimulation was performed after 30 min. (a-c) iNOS and COX-2 expression and band intensity observed in LPS-activated BV2 microglial cells after a 6 h sample treatment and LPS activation. (d-f) iNOS and COX-2 expression and band intensity observed in a 24 h sample and LPS activation in BV2 cells. All data are presented as mean ± standard error of the mean of three independent experiments. $^{*}P < 0.05$, $^{**}P < 0.01$, and $^{***}P < 0.001$ indicate significant differences compared with treatment with LPS alone, while $^{\#\#\#}P < 0.001$ indicates the significant differences compared with an untreated control group. Ctl: control; LPS: lipopolysaccharide; C: cotyledons; C-P: cotyledons exposed with PEF + enzyme activity; H: hypocotyls; H-P: hypocotyls exposed with PEF + enzyme activity.

showed the highest and significant ability to repair the memory impairment. SB-PEF and SB-Enz-PEF bring the value of spontaneous alteration almost similar to that of untreated control mice. The role of SB-PEF and SB-Enz-PEF on memory impairment was reaffirmed through the NORT assay. The broccoli samples showed a significantly improved ability to recognize the novel object compared to that of scopolamine-administered mice. Interestingly, the effects of SB-Enz and SB-Enz-PEF for the novel object recognition were higher than that of the well-known positive control, donepezil. Additionally, acetylcholine esterase activity in the brain samples revealed that only the sprout broccoli with enhanced enzyme activity and SB-Enz-PEF significantly inhibited the level of AchE in the brain which might be responsible for the memory improvement against scopolamine toxicity. Beside these changes, normal/PEF broccoli further improved the cognitive ability of mice against scopolamine-induced memory impairment as evidenced by the passive avoidance test in scopolamine-induced acute and chronic models of memory impairment. Scopolamine dramatically reduced the latency time while the sprout broccoli with PEF and SB-Enz-PEF treatment remarkably recovered the latency time in the acute model. In case of chronic impairment, the broccoli samples increased the latency time suggesting their capacity to inhibit scopolamine toxicity. In both cases, SB-PEF and SB-Enz-PEF showed better potency than did the positive control donepezil (Figure 9). Donepezil and all the broccoli samples lowered the Bax/Bcl2 ration while only the broccoli samples lowered the expression of cleaved caspase-3 suggesting that the broccoli sample, especially SB-Enz-PEF, possesses higher potency to increase cell survival and decrease neuronal death in the dementia model like scopolamine treatment. Inhibition of the apoptosis-related proteins in SB-ENZ, SB-PEF, and especially SB-Enz-PEF further clarified that inhibition of neuronal death induced survival which could also take part in the higher potency to improve the cognitive function against scopolamine-induced amentia mice.

4. Discussion

Sulforaphane is an active compound of broccoli, *Brassica oleracea* var. italic, which is produced after conversion of glucoraphanin in the presence of the myrosinase enzyme [34]. Increased amounts of glucoraphanin or myrosinase activity can enhance sulforaphane production in broccoli or broccoli sprouts. We selected broccoli sprout for the current study since it contains more glucoraphanin than does the adult broccoli [16]. Previous studies suggested that steaming broccoli sprouts increases the enzymatic conversion of glucoraphanin to sulforaphane by lowering sulforaphane nitrile [35]. PEF pretreatment promotes the production of

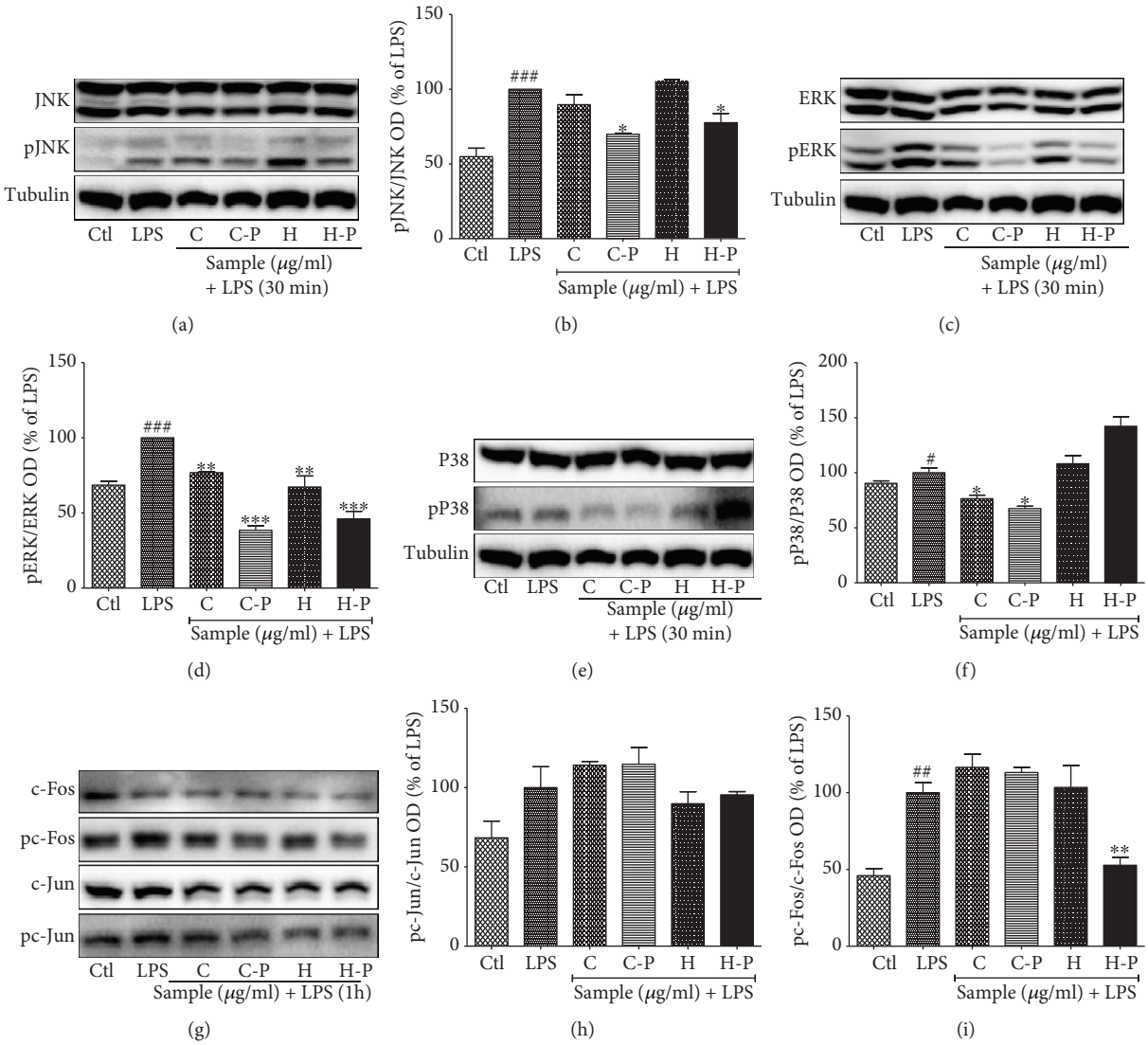

Figure 4: Pulsed electric field (PEF) and enzyme activity-treated broccoli sprouts modulated mitogen-activated protein kinase (MAPK) effector signaling in a 30 min lipopolysaccharide (LPS) activation. BV2 microglial cells were pretreated with broccoli extracts; LPS (100 ng/mL) stimulation was performed after 30 min. MAPK expression was measured after a 30 min LPS activation. The expression and band intensities of (a, b) JNK and pJNK, (c, d) ERK and pERK, and (e, f) p38 and pp38 in LPS-activated BV2 microglia are shown. (g-i) AP-1 signaling in LPS-activated BV2 microglia. All data are presented as mean ± standard error of the mean of three independent experiments. $^{*}P < 0.05$, $^{**}P < 0.01$, and $^{***}P < 0.001$ indicate significant differences compared with treatment with LPS alone, while $^{\#}P < 0.05$, $^{\#\#}P < 0.01$, and $^{\#\#\#}P < 0.001$ indicate significant differences compared with an untreated control group. Ctl: control; LPS: lipopolysaccharide; C: cotyledons; C-P: cotyledons exposed with PEF + enzyme activity; H: hypocotyls; H-P: hypocotyls exposed with PEF + enzyme activity.

glucosinolate, including glucoraphanin, in broccoli flowers and stalk [21]. Thus, we exposed broccoli sprouts to PEF and myrosinase and evaluated its effect on sulforaphane production. The amount of sulforaphane was increased after enzymatic activity, which was further elevated following PEF exposure. In this study, the elevated sulforaphane content in the broccoli sprout showed better anti-inflammatory activities than did the untreated control, emphasizing the importance of enzymatic activation and PEF treatment.

Accumulating evidences regarding the anti-inflammatory potential of natural products and their isolated compounds focus on the scavenging of oxidative stress and downregulating the inflammatory cascades [36]. One of the key molecules participating in such inflammatory disease conditions, especially in neuroinflammatory disorders, is NO [37]. NO in the inflammatory condition is produced by iNOS, which mainly exaggerates oxidative stress in the neurons leading to their degeneration [38]. Inhibition of iNOS or NO production, therefore, could mitigate oxidative stress and further inflammatory cascades in neurodegenerative diseases. Previous studies reported that broccoli sprout inhibited inflammation in endothelial cells [39] and in LPS-treated mice [13]. Additionally, sulforaphane inhibited iNOS-mediated NO production in activated microglia [40]. Along with iNOS-mediated NO production, COX-2-mediated prostaglandin release is also the key pathogenic event in various

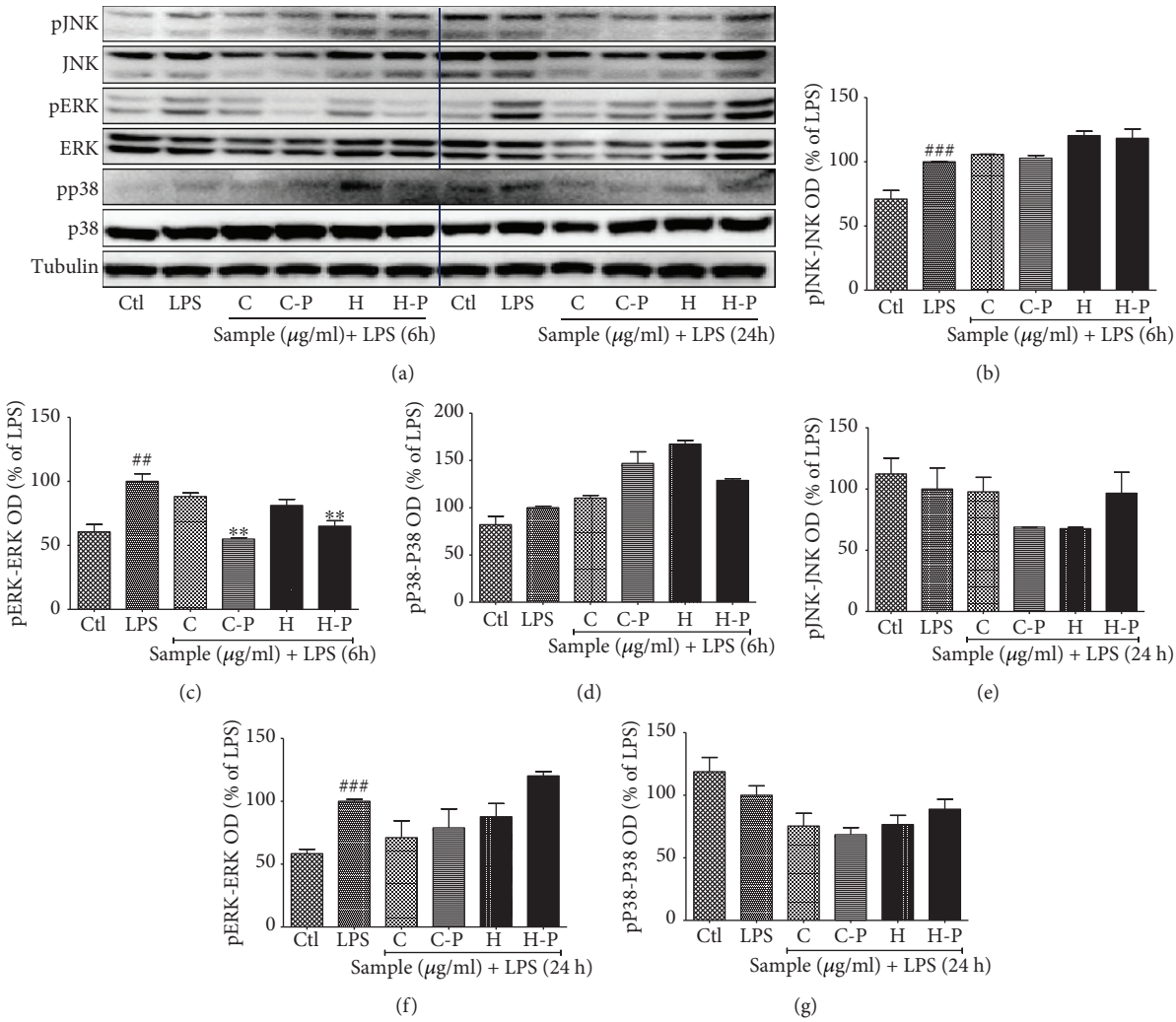

Figure 5: Pulsed electric field (PEF) and enzyme activity-treated broccoli sprouts modulated mitogen-activated protein kinase (MAPK) effector signaling after 6 and 24 h of lipopolysaccharide (LPS) activation. BV2 microglial cells were pretreated with broccoli extracts; LPS (100 ng/mL) stimulation was performed after 30 min. MAPK modulation was observed after 6 and 24 h of LPS activation. (a) MAPK expression in 6 h and 24 h LPS activation. (b-d) JNK and pJNK, ERK and pERK, and p38 and pp38 band intensity in 6 h LPS-activated BV2 microglia. (e-g) JNK and pJNK, ERK and pERK, and p38/pp38 band intensity in 24 h LPS-activated BV2 microglia. All data are presented as mean ± standard error of the mean of three independent experiments. $^{*}P < 0.05$, $^{**}P < 0.01$, and $^{***}P < 0.001$ indicate significant differences compared with treatment with LPS alone, while $^{\#}P < 0.05$, $^{\#\#}P < 0.01$, and $^{\#\#\#}P < 0.001$ indicate significant differences compared with an untreated control group. Ctl: control; LPS: lipopolysaccharide; C: cotyledons; C-P: cotyledons exposed with PEF + enzyme activity; H: hypocotyls; H-P: hypocotyls exposed with PEF + enzyme activity.

inflammatory conditions [41]. Elevated expression of iNOS and COX-2 can occur with toxin exposure and in neuroinflammatory diseases. The chronic overexpression of iNOS and COX-2 is typical in AD, PD, neuropathic pain, etc., in which overexpression of these proteins mainly occurs in microglia [42, 43]. Therefore, minimizing the activation of COX in neuroinflammatory conditions is a desirable approach to achieving the neuroprotective effects. In the current study, enhanced expression of sulforaphane in broccoli sprout dramatically downregulated the COX-2-mediated PGE2 production in activated microglia. Although C-P did not significantly alter the expression of COX-2 in long-term microglial activation, its potency in inhibiting iNOS was much better in long-term LPS exposure than that in short-term microglial activation. Previously, sulforaphane is reported to downregulate COX-2 expression [44]. Our study not only confirms these existing evidences but also provides noble insights exploring that PEF treatment further increased the NO inhibiting potential of broccoli sprout through elevated sulforaphane content.

MAPK effector signaling is responsible for altering the expression and secretion of inflammatory mediators as well as proinflammatory cytokines [45]. MAPK proteins such as ERK, JNK, and p38 play essential roles in neuroinflammation [46]. P38, in particular, is responsible for the induction of apoptosis, differentiation, and regulation of inflammatory responses. LPS activates p38 downstream from TLR4 activation, promoting proinflammatory cytokines, such as TNF-α, IFN-γ, IL-1β, IL-12, IL-6, and IL-23, which are responsible for neuroinflammation [47, 48]. Similarly, JNK pathways can further phosphorylate c-Jun and respond to cytokines,

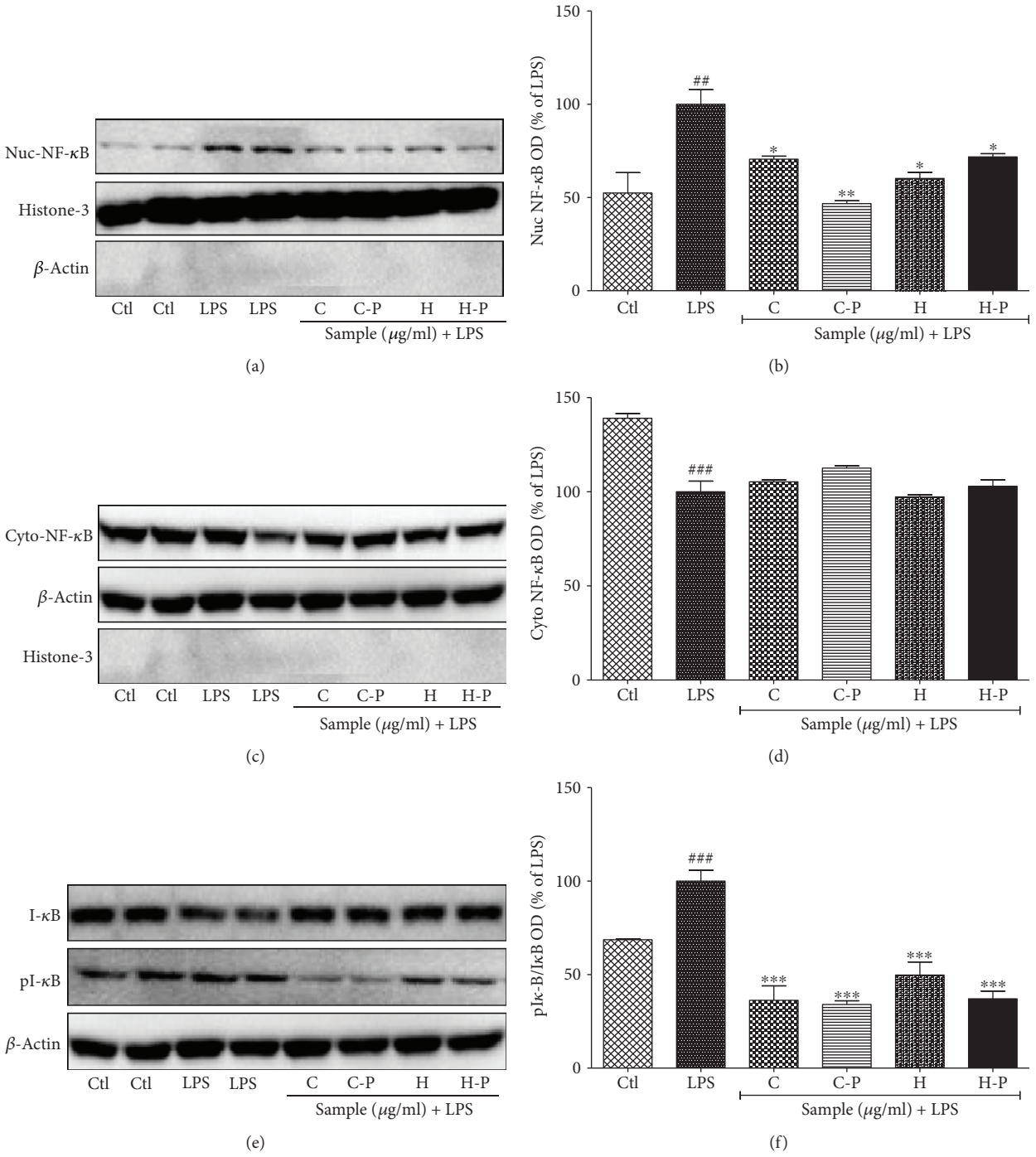

Figure 6: Pulsed electric field (PEF) and enzyme activity-treated broccoli sprouts inhibited NF-κB translocation and I-κB phosphorylation in lipopolysaccharide- (LPS-) activated BV2 cells. BV2 microglial cells were pretreated with broccoli extracts; LPS (100 ng/mL) stimulation was performed after 30 min. NF-κB, I-κB, and pI-κB expression was observed after 1 h of LPS activation. (a, b) Nuclear NF-κB expression and band intensity. Histone-3 was used as loading control. (c, d) Cytosolic NF-κB expression and band intensity. β-Actin was used as loading control. (e, f) Cytosolic I-κB and pI-κB expression and band intensity. β-Actin was used as loading control. All data are presented as mean ± standard error of the mean of three independent experiments. $^{*}P < 0.05$, $^{**}P < 0.01$, and $^{***}P < 0.001$ indicate significant differences compared with treatment with LPS alone, while $^{\#}P < 0.05$, $^{\#\#}P < 0.01$, and $^{\#\#\#}P < 0.001$ indicate significant differences compared with an untreated control group. Ctl: control; LPS: lipopolysaccharide; C: cotyledons; C-P: cotyledons exposed with PEF + enzyme activity; H: hypocotyls; H-P: hypocotyls exposed with PEF + enzyme activity.

like TNF-α and IL-1β, and growth factors [49]. The activation of JNK pathways plays a significant role in Tau pathology; therefore, inhibition of JNK/NF-κB pathways is beneficial for AD and other neuroinflammatory conditions [50]. A growing body of evidences also suggests that MEK/ERK pathways are responsible for the elevated level of

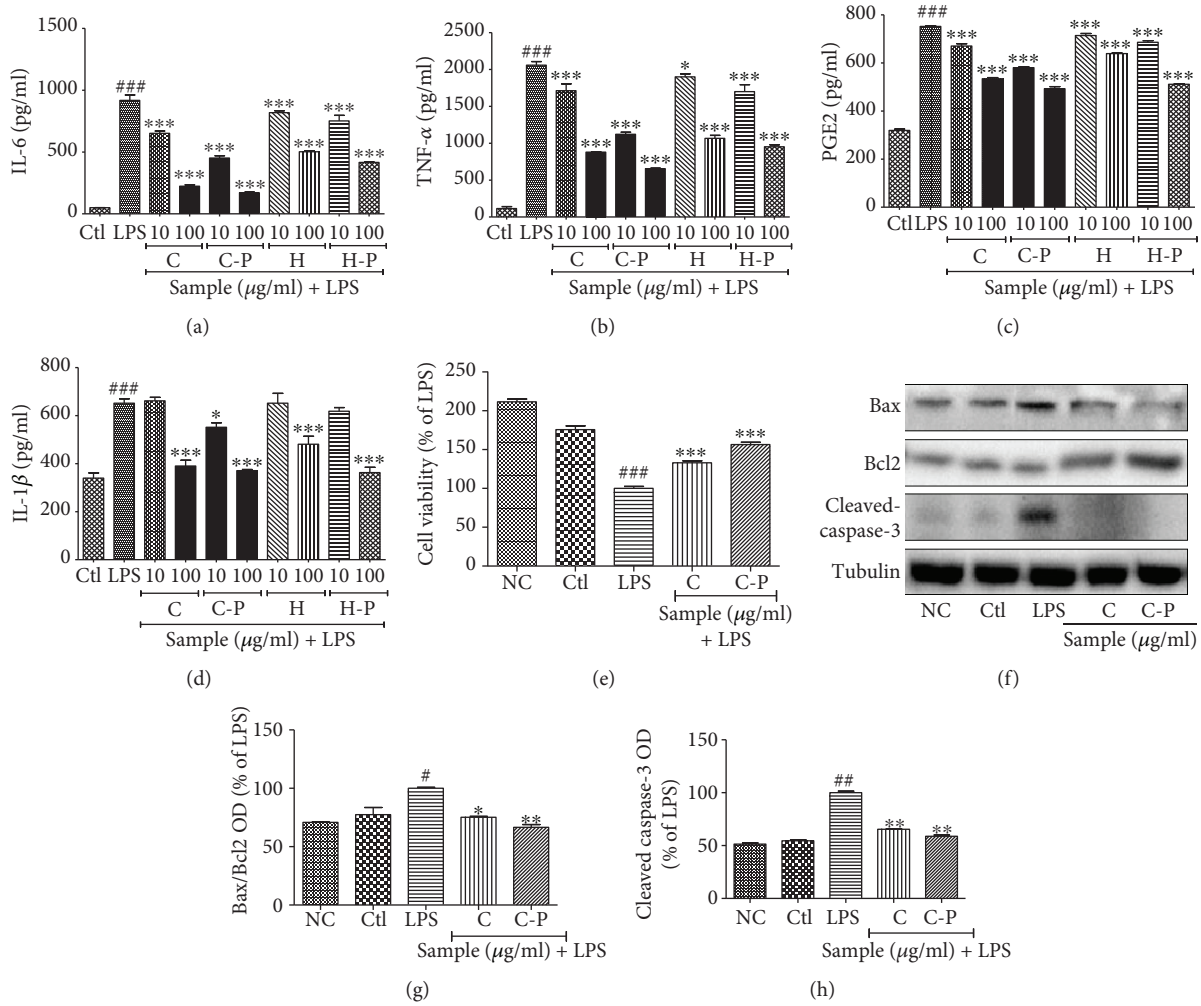

Figure 7: Pulsed electric field (PEF) and enzyme activity-treated broccoli sprouts inhibited proinflammatory cytokine production in LPS-activated microglia and also reduced the neuronal death caused by activated microglia. BV2 microglial cells were pretreated with broccoli extracts; LPS (100 ng/mL) stimulation was performed after 30 min. Proinflammatory cytokines were measured in the conditioned medium of the treated cells using enzyme-linked immunosorbent assays after 24 h of LPS activation. (a) Interleukin- (IL-) 6 production. (b) Tumor necrosis factor- (TNF-) α secretion. (c) Prostaglandin E2 (PGE2) secretion. (d) IL-1β secretion. Similarly treated BV2 cells in the conditioned medium were transferred to seeded N2a cells in the 6-well plate. Cell viability and proteins expression in the N2a cells were evaluated after 24 h of CM treatment. (f) N2a cell viability after activated microglial CM treatment. (f-h) Apoptosis-related protein expression in BV2 CM-treated N2a cells and their quantification. All data are presented as mean ± standard error of the mean of three independent experiments. $^{*}P < 0.05$, $^{**}P < 0.01$, and $^{***}P < 0.001$ indicate significant differences compared with treatment with LPS alone, while $^{\#}P < 0.05$, $^{\#\#}P < 0.01$, and $^{\#\#\#}P < 0.001$ indicate significant differences compared with the untreated control group. NC: normal control; Ctl: control; LPS: lipopolysaccharide; C: cotyledons; C-P: cotyledons exposed with PEF + enzyme activity; H: hypocotyls; H-P: hypocotyls exposed with PEF + enzyme activity.

TNF-α, IL-1β, IL-6, and iNOS following ischemia, which further highlights their neuroinflammatory role [50]. Thus, modulation of p38, JNK, and ERK could be the potential therapeutic strategy in various inflammatory and neurodegenerative conditions in the brain. In the present study, the broccoli sprouts exposed to PEF enzyme significantly inhibited the phosphorylation of ERK, JNK, and p38, during the 30 min and 6 h LPS activation; p38 activation alone was maintained for 24 h of LPS activation. The sulforaphane-enriched broccoli did not change in the activation (phosphorylation) of c-Jun. However, H-P showed the significant inhibition of C-Fos in LPS-activated microglia. This result suggests that PEF-exposed broccoli hypocotyls might have a role in inhibiting pC-Fos-mediated signaling for inflammatory cascades.

MAPK signaling controls NF-κB-mediated transcription of inflammatory mediators such as cytokines and chemokines. NF-κB/AP-1 and MAPK pathways play a key role in the production of cytokines such as TNF-α, IL-6, and IL-8 in BV2 microglial cells [51, 52]. In our study, C-P significantly inhibited the phosphorylation of ERK, JNK, and P38 nonspecifically, during the 30 min, 6 h, and 24 h LPS-induced microglial activation. This alteration might induce the significant inhibition of nuclear NF-κB while increasing cytosolic NF-κB. The inhibition of NF-κB-mediated transcription of inflammatory proteins was further confirmed

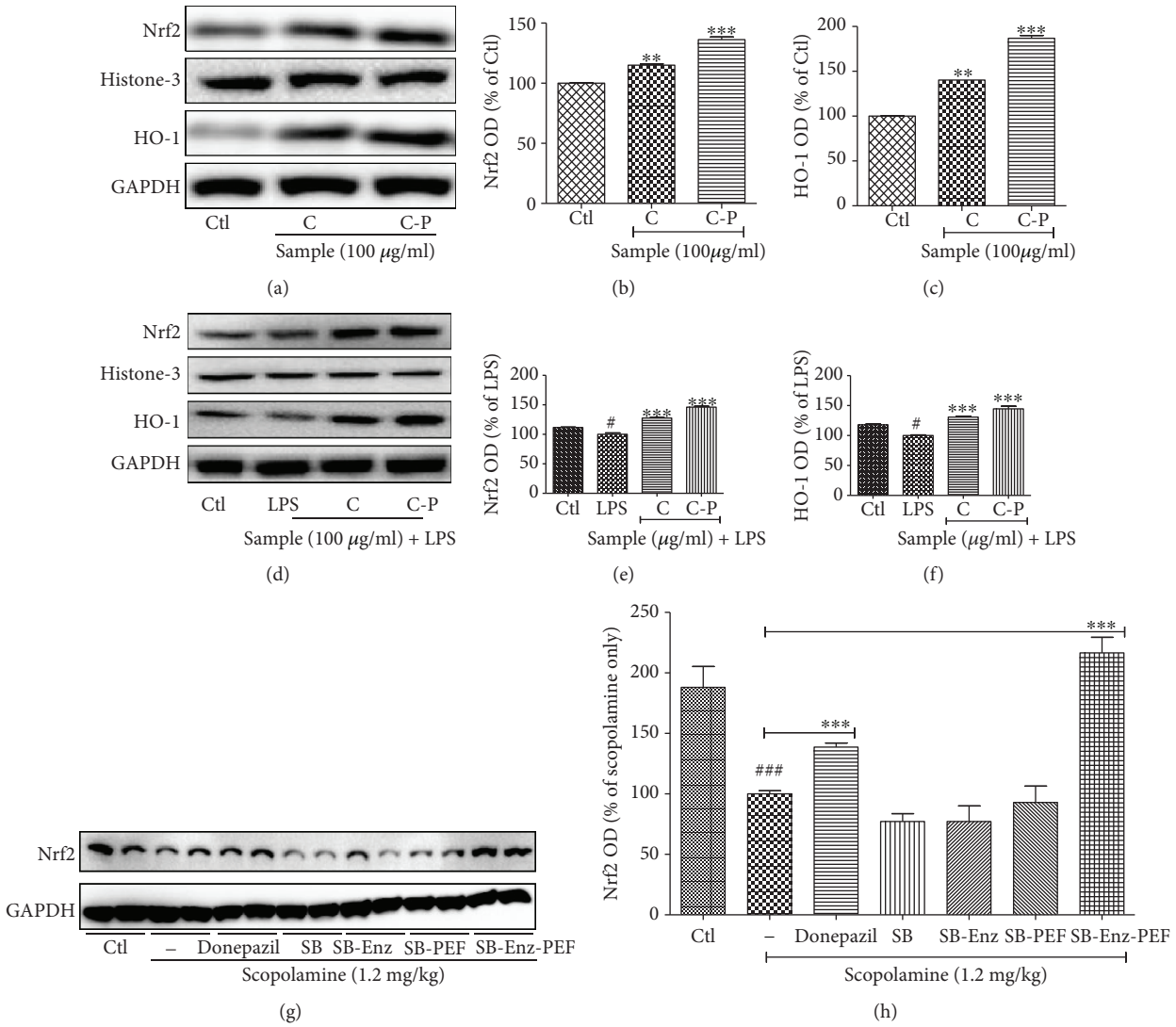

Figure 8: Broccoli sample treatment increased the Nrf2-HO-1 expression showing antioxidant effect in microglial cells (normal and LPS-activated conditions) as well as against a scopolamine-induced amnesia model in mice. BV2 microglial cells were treated with the broccoli sample itself. (a-c) Nrf2-HO-1 expression in normal microglia after broccoli cotyledon treatment and their quantifications. (d-f) Nrf2-HO-1 expression in LPS-activated microglia after broccoli cotyledon treatment and their quantifications. Mice were continuously exposed with scopolamine and broccoli samples for two weeks' period. Animal were sacrifices, and the brain samples were homogenized and tissue lysates were separated using the western blot technique. (g, h) Nrf2 expression and its quantification in the mouse whole brain sample. Histone-3 and GAPDH were used as a loading control for respective proteins. All data are presented as mean ± standard error of the mean of three independent experiments. $^{*}P < 0.05$, $^{**}P < 0.01$, and $^{***}P < 0.001$ indicate significant differences compared with the untreated control group in (c, d) and only scopolamine-treated group in (f) while $^{\#}P < 0.05$ and $^{\#\#\#}P < 0.001$ indicate significant differences compared with the untreated control group. C: cotyledons; C-P: cotyledons exposed with PEF and enzyme activity; SB: sprout broccoli; SB-Enz: sprout broccoli with induced enzyme activity; SB-PEF: sprout broccoli with PEF treatment; SB-Enz-PEF: sprout broccoli with activated enzyme activity and PEF treatment.

by the increased and decreased expression of I-κB and pI-κB, respectively. The inhibition of MAPK-NF-κB was further characterized by the significant inhibition of TNF-α and IL-6 production in LPS-activated BV2 microglial cells. C-P showed the highest potency for all these events, and this might be due to the higher amount of sulforaphane.

Previously, broccoli sprout extract and sulforaphane are reported as activators of well-known antioxidant molecules Nrf2/HO-1 [53]. Treatment of C and C-P activated the expression of Nrf2 and HO-1 as did by the sulforaphane treatment in normal and LPS-activated microglial cells. This effect of broccoli extract and sulforaphane can further inhibit the inflammatory cascades either through inhibiting TLR4-mediated inflammatory cascades or by their antioxidant potentials. Therefore, it is thought to be a potential mechanism that indicates the antineuroinflammatory effect of sulforaphane. Nrf2 inhibits the neuroinflammation as well as neurodegeneration against various models of brain disorders

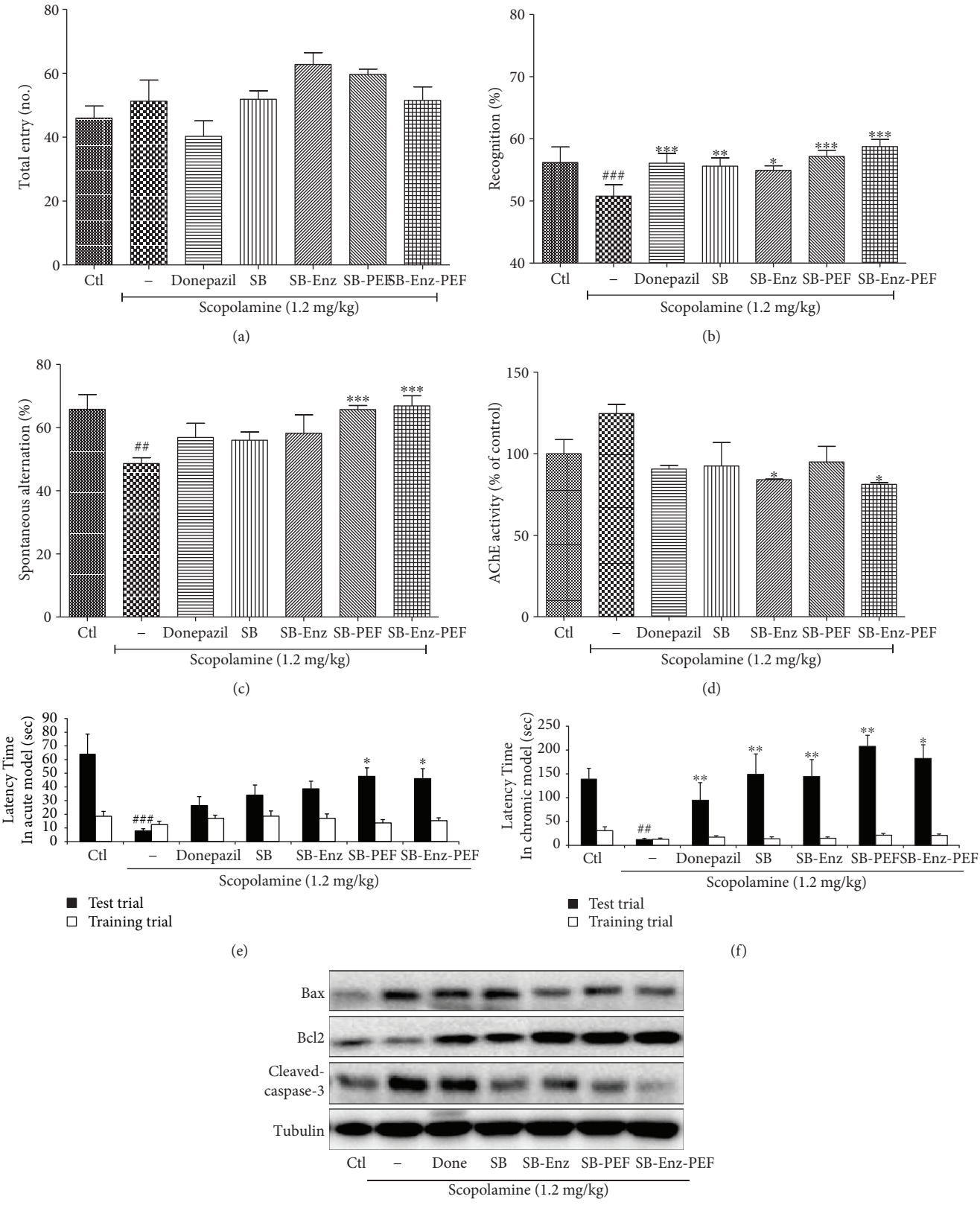

Figure 9: Continued.

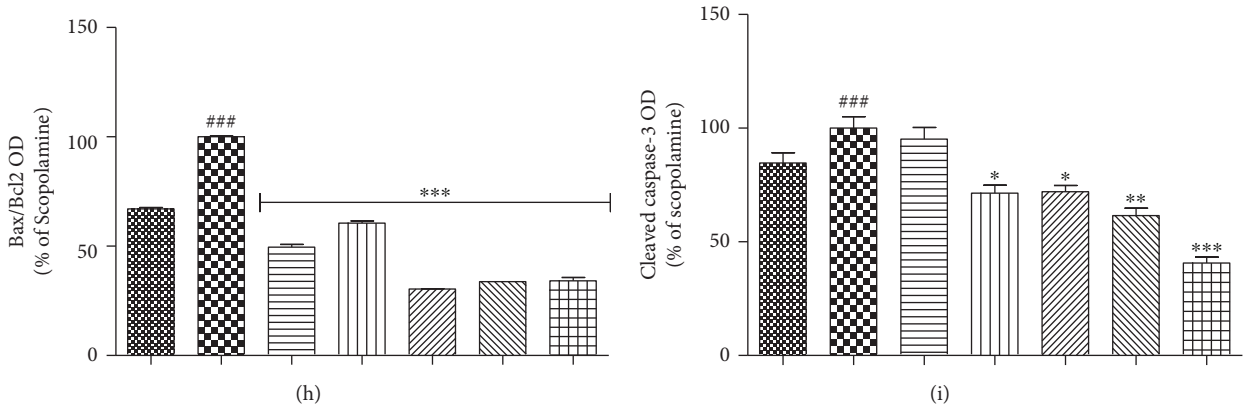

FIGURE 9: Broccoli sprout extract repaired the memory impairment by inhibiting neuronal apoptosis against scopolamine induced toxicity *in vivo*. Experimental animals were exposed with 1.2 mg/kg scopolamine and 2 mg/kg of donepezil for the donepezil group and 200 mg/kg broccoli samples. The treated animal's spatial memory was evaluated by the (a, b) Y-maze test, (c) novel object recognition test (NORT), (d) acetylcholine esterase activity assay in animal brain, (e, f) passive avoidance test in acute condition (one time per-oral treatment and toxicity induction) and chronic condition (two weeks' per-oral treatment and toxicity induction). After sacrifice, mouse whole brains were collected and homogenized with tissue lysis buffer and western blot analysis was performed. (g-i) Bax, Bcl2, and cleaved caspase-3 expression and their quantification. All data are presented as mean ± standard error of the mean of three independent experiments. $^{*}P < 0.05$, $^{**}P < 0.01$, and $^{***}P < 0.001$ indicate significant differences compared with treatment with scopolamine alone while $^{\#\#}P < 0.01$ and $^{\#\#\#}P < 0.001$ indicate the significant differences compared with an untreated control group. Ctl: control; SB: sprout broccoli; SB-Enz: sprout broccoli with induced enzyme activity; SB-PEF: sprout broccoli with PEF treatment; SB-Enz-PEF: sprout broccoli with activated enzyme activity and PEF treatment.

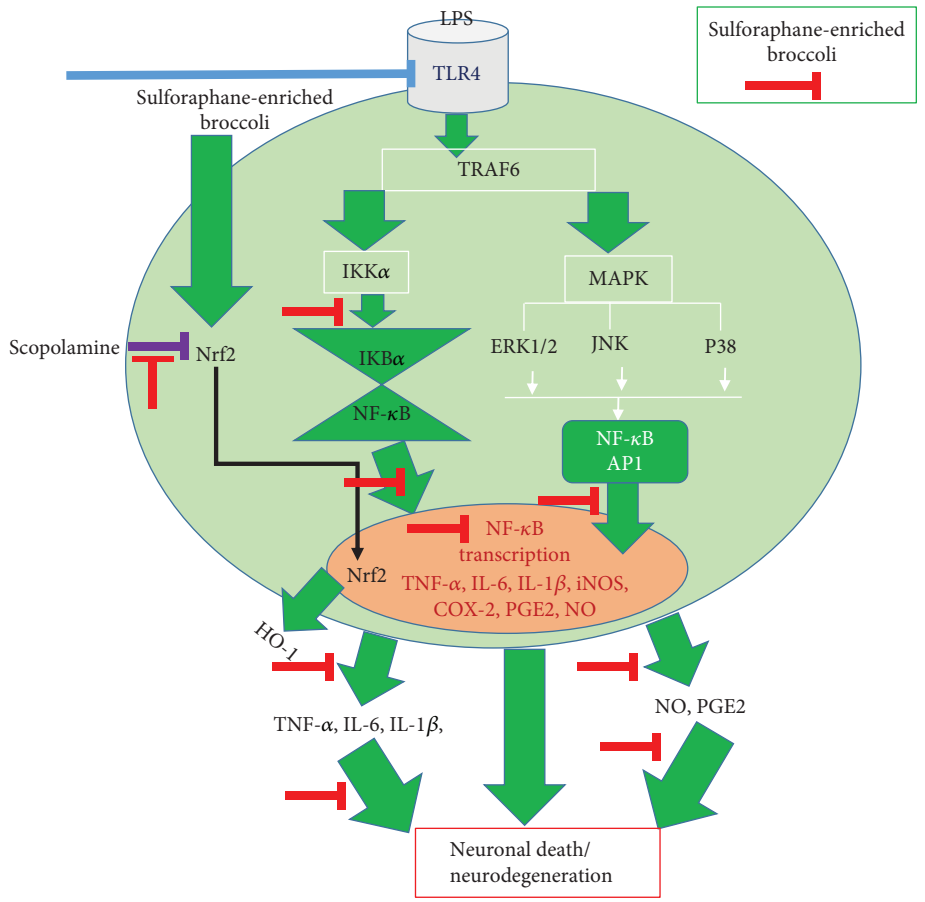

FIGURE 10: Schematic diagram for the antineuroinflammatory and antiamnesic effects of broccoli sprout extract treated with PEF.

in both *in vitro* and *in vivo* experimental models [54, 55]. Previous reports suggested that sulforaphane protected neurons against rotenone-induced toxicity in an *in vivo* model which is mediated through the activation of the Nrf2 pathway [56]. In this study, SB-Enz-PEF significantly improved the scopolamine-induced spontaneous alteration as determined by the Y-maze test, novel object recognition test, and AchE activity inhibition test indicating that sulforaphane could improve memory impairment in different neurological disorders. SB-Enz-PEF also increased latency time in PAT assay. Moreover, through *in vitro* analysis, we found that the SB-Enz-PEF-treated conditioned medium from LPS-stimulated BV2 cells not only increased the neuronal cell survival but also attenuated the apoptotic proteins in neurons. Our data demonstrated that the protective effects of SB-ENZ-PEF are mediated through the Nrf2 signaling pathway; however, the overall neuroprotection of broccoli and sulforaphane might be mediated through the antiapoptotic effects, in particular downregulating caspase-3 activation. Sulforaphane-enriched broccoli extract, therefore, could mediate the neuroprotection in various neurodegenerative models, and the plausible pathway for the neuroprotection could be due to the combination of Nrf2 activation and its antiapoptotic effects.

Taken together, in this study, we provided the new insight of increased-sulforaphane-mediated protective effects in neuroinflammatory models. Being multifunctional, identification of a particular therapeutic target for phytochemicals/nutraceuticals to show desired biological activity is a key issue for the new drug development [57, 58]. However, the technique that increased the particular bioactive compounds, as PEF-induced sulforaphane in this study, could enhance the therapeutic benefit of phytochemicals. Additionally, a time point study of iNOS/COX-2 and MAPK signaling in this study could be the magnificent cues for the further *in vivo* experiment including both acute (such as ischemia, traumatic brain injury) and chronic (such as AD, PD) inflammatory conditions. Our findings demonstrated that sulforaphane-enriched broccoli sprout showed antineuroinflammatory and neuroprotective effects *in vitro* and showed the protective effects in mice against scopolamine-induced amnesia *in vivo* through Nrf2 activation. Finally, in most studies, the biological activity of sulforaphane, specifically of (−)L-isothiocyanato-4R-(methyl-sulfinyl)-butane, is demonstrated using the racemic mixture, despite the fact that humans are exposed only to the R-enantiomer through their diet. Therefore, it would be tempting to determine the role of R- and S-sulforaphane as future independent studies. The overall findings of our current study are summarized in Figure 10.

Data Availability

All the data have been included in the manuscript and it can also be provided by the corresponding author on request.

Conflicts of Interest

No competing financial interests exist.

Authors' Contributions

Hyuk Joon Choi, Sun Yeou Kim, and Lalita Subedi hypothesized and designed the experiment; Lalita Subedi, KyoHee Cho, and Young Un Park performed the experiment; and Lalita Subedi wrote the manuscript. Hyuk Joon Choi and Sun Yeou Kim revised and finalized the manuscript.

Acknowledgments

This work was supported by the National Research Foundation of Korea (NRF) grant funded by the Korea government (MSIT) (NRF-2014M3A9B6069338) and also by a grant from BK bio (R0005491), Republic of Korea.

References

[1] W. W. Chen, X. Zhang, and W. J. Huang, "Role of neuroinflammation in neurodegenerative diseases (review)," *Molecular Medicine Reports*, vol. 13, no. 4, pp. 3391–3396, 2016.

[2] H. Hong, B. S. Kim, and H. I. Im, "Pathophysiological role of neuroinflammation in neurodegenerative diseases and psychiatric disorders," *International Neurourology Journal*, vol. 20, Supplement 1, pp. S2–S7, 2016.

[3] D. L. Krause and N. Muller, "Neuroinflammation, microglia and implications for anti-inflammatory treatment in Alzheimer's disease," *International Journal of Alzheimer's Disease*, vol. 2010, article 732806, 9 pages, 2010.

[4] M. W. Salter and B. Stevens, "Microglia emerge as central players in brain disease," *Nature Medicine*, vol. 23, no. 9, pp. 1018–1027, 2017.

[5] A. D. Kraft and G. J. Harry, "Features of microglia and neuroinflammation relevant to environmental exposure and neurotoxicity," *International Journal of Environmental Research and Public Health*, vol. 8, no. 7, pp. 2980–3018, 2011.

[6] L. Alvarez-Erviti, Y. Couch, J. Richardson, J. M. Cooper, and M. J. A. Wood, "Alpha-synuclein release by neurons activates the inflammatory response in a microglial cell line," *Neuroscience Research*, vol. 69, no. 4, pp. 337–342, 2011.

[7] J. D. Cherry, J. A. Olschowka, and M. O'Banion, "Neuroinflammation and M2 microglia: the good, the bad, and the inflamed," *Journal of Neuroinflammation*, vol. 11, no. 1, p. 98, 2014.

[8] A. I. Ramirez, R. de Hoz, E. Salobrar-Garcia et al., "The role of microglia in retinal neurodegeneration: Alzheimer's disease, Parkinson, and glaucoma," *Frontiers in Aging Neuroscience*, vol. 9, p. 214, 2017.

[9] D. B. McKim, A. Niraula, A. J. Tarr, E. S. Wohleb, J. F. Sheridan, and J. P. Godbout, "Neuroinflammatory dynamics underlie memory impairments after repeated social defeat," *The Journal of Neuroscience*, vol. 36, no. 9, pp. 2590–2604, 2016.

[10] J. Seo, B. Kim, J. Oh, and J.-S. Kim, "Soybean-derived phytoalexins improve cognitive function through activation of Nrf 2/HO-1 signaling pathway," *International Journal of Molecular Sciences*, vol. 19, no. 1, 2018.

[11] S. J. Enna and M. Williams, "Challenges in the search for drugs to treat central nervous system disorders," *The Journal of Pharmacology and Experimental Therapeutics*, vol. 329, no. 2, pp. 404–411, 2009.

[12] T. M. Barchet and M. M. Amiji, "Challenges and opportunities in CNS delivery of therapeutics for neurodegenerative diseases," *Expert Opinion on Drug Delivery*, vol. 6, no. 3, pp. 211–225, 2009.

[13] B. E. Townsend, Y. J. Chen, E. H. Jeffery, and R. W. Johnson, "Dietary broccoli mildly improves neuroinflammation in aged mice but does not reduce lipopolysaccharide-induced sickness behavior," *Nutrition Research*, vol. 34, no. 11, pp. 990–999, 2014.

[14] V. Hernandez-Rabaza, A. Cabrera-Pastor, L. Taoro-Gonzalez et al., "Hyperammonemia induces glial activation, neuroinflammation and alters neurotransmitter receptors in hippocampus, impairing spatial learning: reversal by sulforaphane," *Journal of Neuroinflammation*, vol. 13, no. 1, p. 41, 2016.

[15] L. O. Brandenburg, M. Kipp, R. Lucius, T. Pufe, and C. J. Wruck, "Sulforaphane suppresses LPS-induced inflammation in primary rat microglia," *Inflammation Research*, vol. 59, no. 6, pp. 443–450, 2010.

[16] J. W. Fahey, Y. Zhang, and P. Talalay, "Broccoli sprouts: an exceptionally rich source of inducers of enzymes that protect against chemical carcinogens," *Proceedings of the National Academy of Sciences of the United States of America*, vol. 94, no. 19, pp. 10367–10372, 1997.

[17] N. V. Matusheski, R. Swarup, J. A. Juvik, R. Mithen, M. Bennett, and E. H. Jeffery, "Epithiospecifier protein from broccoli (Brassica oleracea L. ssp. italica) inhibits formation of the anticancer agent sulforaphane," *Journal of Agricultural and Food Chemistry*, vol. 54, no. 6, pp. 2069–2076, 2006.

[18] T. A. Shapiro, J. W. Fahey, A. T. Dinkova-Kostova et al., "Safety, tolerance, and metabolism of broccoli sprout glucosinolates and isothiocyanates: a clinical phase I study," *Nutrition and Cancer*, vol. 55, no. 1, pp. 53–62, 2006.

[19] Y. Li, T. Zhang, X. Li, P. Zou, S. J. Schwartz, and D. Sun, "Kinetics of sulforaphane in mice after consumption of sulforaphane-enriched broccoli sprout preparation," *Molecular Nutrition & Food Research*, vol. 57, no. 12, pp. 2128–2136, 2013.

[20] J. D. Clarke, A. Hsu, D. E. Williams et al., "Metabolism and tissue distribution of sulforaphane in Nrf 2 knockout and wild-type mice," *Pharmaceutical Research*, vol. 28, no. 12, pp. 3171–3179, 2011.

[21] I. Aguilo-Aguayo, M. Suarez, L. Plaza et al., "Optimization of pulsed electric field pre-treatments to enhance health-promoting glucosinolates in broccoli flowers and stalk," *Journal of the Science of Food and Agriculture*, vol. 95, no. 9, pp. 1868–1875, 2015.

[22] T. Gachovska, D. Cassada, J. Subbiah, M. Hanna, H. Thippareddi, and D. Snow, "Enhanced anthocyanin extraction from red cabbage using pulsed electric field processing," *Journal of Food Science*, vol. 75, no. 6, pp. E323–E329, 2010.

[23] D. J. Kliebenstein, J. Kroymann, P. Brown et al., "Genetic control of natural variation in Arabidopsis glucosinolate accumulation," *Plant Physiology*, vol. 126, no. 2, pp. 811–825, 2001.

[24] C. S. Kim, L. Subedi, S. Y. Kim, S. U. Choi, K. H. Kim, and K. R. Lee, "Diterpenes from the trunk of Abies holophylla and their potential neuroprotective and anti-inflammatory activities," *Journal of Natural Products*, vol. 79, no. 2, pp. 387–394, 2016.

[25] S. Y. Lim, L. Subedi, D. Shin, C. S. Kim, K. R. Lee, and S. Y. Kim, "A new neolignan derivative, balanophonin isolated from Firmiana simplex delays the progress of neuronal cell death by inhibiting microglial activation," *Biomolecules & Therapeutics*, vol. 25, no. 5, pp. 519–527, 2017.

[26] L. Subedi, B. P. Gaire, M. H. Do, T. H. Lee, and S. Y. Kim, "Anti-neuroinflammatory and neuroprotective effects of the Lindera neesiana fruit in vitro," *Phytomedicine*, vol. 23, no. 8, pp. 872–881, 2016.

[27] L. Subedi, E. Ji, D. Shin, J. Jin, J. Yeo, and S. Kim, "Equol, a dietary daidzein gut metabolite attenuates microglial activation and potentiates neuroprotection in vitro," *Nutrients*, vol. 9, no. 3, 2017.

[28] A. T. Mugwagwa, L. L. Gadaga, W. Pote, and D. Tagwireyi, "Antiamnesic effects of a hydroethanolic extract of Crinum macowaniion scopolamine-induced memory impairment in mice," *Journal of Neurodegenerative Diseases*, vol. 2015, Article ID 242505, 9 pages, 2015.

[29] S. A. A. El-Marasy, R. M. Abd-Elsalam, and O. A. Ahmed--Farid, "Ameliorative effect of silymarin on scopolamine-induced dementia in rats," *Open Access Macedonian Journal of Medical Sciences*, vol. 6, no. 7, pp. 1215–1224, 2018.

[30] H. E. Lee, Y. W. Lee, S. J. Park et al., "4-Hydroxybenzyl methyl ether improves learning and memory in mice via the activation of dopamine D1 receptor signaling," *Neurobiology of Learning and Memory*, vol. 121, pp. 30–38, 2015.

[31] E. Kim, H. J. Ko, S. J. Jeon et al., "The memory-enhancing effect of erucic acid on scopolamine-induced cognitive impairment in mice," *Pharmacology, Biochemistry, and Behavior*, vol. 142, pp. 85–90, 2016.

[32] G. L. Ellman, K. D. Courtney, V. Andres Jr, and R. M. Featherstone, "A new and rapid colorimetric determination of acetylcholinesterase activity," *Biochemical Pharmacology*, vol. 7, no. 2, pp. 88–95, 1961.

[33] L. Subedi, T. H. Lee, H. M. Wahedi, S. H. Baek, and S. Y. Kim, "Resveratrol-enriched rice attenuates UVB-ROS-induced skin aging via downregulation of inflammatory cascades," *Oxidative Medicine and Cellular Longevity*, vol. 2017, Article ID 8379539, 15 pages, 2017.

[34] D. Angelino, E. B. Dosz, J. Sun et al., "Myrosinase-dependent and -independent formation and control of isothiocyanate products of glucosinolate hydrolysis," *Frontiers in Plant Science*, vol. 6, 2015.

[35] G. C. Wang, M. Farnham, and E. H. Jeffery, "Impact of thermal processing on sulforaphane yield from broccoli (Brassica oleracea L. ssp. italica)," *Journal of Agricultural and Food Chemistry*, vol. 60, no. 27, pp. 6743–6748, 2012.

[36] P. Arulselvan, M. T. Fard, W. S. Tan et al., "Role of antioxidants and natural products in inflammation," *Oxidative Medicine and Cellular Longevity*, vol. 2016, Article ID 5276130, 15 pages, 2016.

[37] G. Gelders, V. Baekelandt, and A. Van der Perren, "Linking neuroinflammation and neurodegeneration in Parkinson's disease," *Journal of Immunology Research*, vol. 2018, Article ID 4784268, 12 pages, 2018.

[38] J. E. Yuste, E. Tarragon, C. M. Campuzano, and F. Ros-Bernal, "Implications of glial nitric oxide in neurodegenerative diseases," *Frontiers in Cellular Neuroscience*, vol. 9, 2015.

[39] A. Sotokawauchi, Y. Ishibashi, T. Matsui, and S. I. Yamagishi, "Aqueous extract of glucoraphanin-rich broccoli sprouts inhibits formation of advanced glycation end products and attenuates inflammatory reactions in endothelial cells,"

Evidence-based Complementary and Alternative Medicine, vol. 2018, Article ID 9823141, 6 pages, 2018.

[40] E. Eren, K. U. Tufekci, K. B. Isci, B. Tastan, K. Genc, and S. Genc, "Sulforaphane inhibits lipopolysaccharide-induced inflammation, cytotoxicity, oxidative stress, and miR-155 expression and switches to Mox phenotype through activating extracellular signal-regulated kinase 1/2–nuclear factor erythroid 2-related factor 2/antioxidant response element pathway in murine microglial cells," *Frontiers in Immunology*, vol. 9, 2018.

[41] L. Minghetti, "Role of COX-2 in inflammatory and degenerative brain diseases," *Sub-Cellular Biochemistry*, vol. 42, pp. 127–141, 2007.

[42] A. R. Patel, R. Ritzel, L. D. McCullough, and F. Liu, "Microglia and ischemic stroke: a double-edged sword," *International Journal of Physiology, Pathophysiology and Pharmacology*, vol. 5, no. 2, pp. 73–90, 2013.

[43] E. Badoer, "Microglia: activation in acute and chronic inflammatory states and in response to cardiovascular dysfunction," *The International Journal of Biochemistry & Cell Biology*, vol. 42, no. 10, pp. 1580–1585, 2010.

[44] W. J. Choi, S. K. Kim, H. K. Park, U. D. Sohn, and W. Kim, "Anti-inflammatory and anti-superbacterial properties of sulforaphane from Shepherd's purse," *The Korean Journal of Physiology & Pharmacology*, vol. 18, no. 1, pp. 33–39, 2014.

[45] B. Kaminska, A. Gozdz, M. Zawadzka, A. Ellert-Miklaszewska, and M. Lipko, "MAPK signal transduction underlying brain inflammation and gliosis as therapeutic target," *The Anatomical Record: Advances in Integrative Anatomy and Evolutionary Biology*, vol. 292, no. 12, pp. 1902–1913, 2009.

[46] G. Ramesh, "Novel therapeutic targets in neuroinflammation and neuropathic pain," *Inflammation and Cell Signaling*, vol. 1, no. 3, 2014.

[47] D. N. Krementsov, T. M. Thornton, C. Teuscher, and M. Rincon, "The emerging role of p 38 mitogen-activated protein kinase in multiple sclerosis and its models," *Molecular and Cellular Biology*, vol. 33, no. 19, pp. 3728–3734, 2013.

[48] H. K. Koul, M. Pal, and S. Koul, "Role of p 38 MAP kinase signal transduction in solid tumors," *Genes & Cancer*, vol. 4, no. 9-10, pp. 342–359, 2013.

[49] P. K. Roy, F. Rashid, J. Bragg, J. A. Ibdah, and Division of Gastroenterology and Hepatology, University of Missouri School of Medicine, Columbia, Missouri, United States, "Role of the JNK signal transduction pathway in inflammatory bowel disease," *World Journal of Gastroenterology*, vol. 14, no. 2, pp. 200–202, 2008.

[50] F. Zhang and L. Jiang, "Neuroinflammation in Alzheimer's disease," *Neuropsychiatric Disease and Treatment*, vol. 11, pp. 243–256, 2015.

[51] L. Neff, M. Zeisel, J. Sibilia, M. Scholler-Guinard, J. P. Klein, and D. Wachsmann, "NF-kappaB and the MAP kinases/AP-1 pathways are both involved in interleukin-6 and interleukin-8 expression in fibroblast-like synoviocytes stimulated by protein I/II, a modulin from oral streptococci," *Cellular Microbiology*, vol. 3, no. 10, pp. 703–712, 2001.

[52] J. Zhu, L. Jiang, Y. Liu et al., "MAPK and NF-κB pathways are involved in bisphenol A-induced TNF-α and IL-6 production in BV2 microglial cells," *Inflammation*, vol. 38, no. 2, pp. 637–648, 2015.

[53] Z. Xu, S. Wang, H. Ji et al., "Broccoli sprout extract prevents diabetic cardiomyopathy via Nrf 2 activation in db/db T2DM mice," *Scientific Reports*, vol. 6, no. 1, article 30252, 2016.

[54] S. A. Onasanwo, R. Velagapudi, A. El-Bakoush, and O. A. Olajide, "Inhibition of neuroinflammation in BV2 microglia by the biflavonoid kolaviron is dependent on the Nrf2/ARE antioxidant protective mechanism," *Molecular and Cellular Biochemistry*, vol. 414, no. 1-2, pp. 23–36, 2016.

[55] P. Deshmukh, S. Unni, G. Krishnappa, and B. Padmanabhan, "The Keap1-Nrf2 pathway: promising therapeutic target to counteract ROS-mediated damage in cancers and neurodegenerative diseases," *Biophysical Reviews*, vol. 9, no. 1, pp. 41–56, 2017.

[56] Q. Zhou, B. Chen, X. Wang et al., "Sulforaphane protects against rotenone-induced neurotoxicity in vivo: involvement of the mTOR, Nrf2, and autophagy pathways," *Scientific Reports*, vol. 6, no. 1, article 32206, 2016.

[57] L.-X. Liao, X.-M. Song, L.-C. Wang et al., "Highly selective inhibition of IMPDH2 provides the basis of antineuroinflammation therapy," *Proceedings of the National Academy of Sciences of the United States of America*, vol. 114, no. 29, pp. E5986–E5994, 2017.

[58] J. A. Beutler, "Natural products as a foundation for drug discovery," *Current Protocols in Pharmacology*, vol. 46, p. 9, 2009.

Hindawi
Oxidative Medicine and Cellular Longevity
Volume 2019, Article ID 3640753, 14 pages
https://doi.org/10.1155/2019/3640753

Research Article

Inhibition of Oxidative Neurotoxicity and Scopolamine-Induced Memory Impairment by γ-Mangostin: *In Vitro* and *In Vivo* Evidence

Youngmun Lee, Sunyoung Kim, Yeonsoo Oh, Young-Mi Kim, Young-Won Chin, and Jungsook Cho

College of Pharmacy, Dongguk University-Seoul, Goyang, Gyeonggi-do 10326, Republic of Korea

Correspondence should be addressed to Jungsook Cho; neuroph@dongguk.edu

Youngmun Lee and Sunyoung Kim contributed equally to this work.

Received 4 October 2018; Revised 14 December 2018; Accepted 9 January 2019; Published 24 March 2019

Guest Editor: Luciana Scotti

Among a series of xanthones identified from mangosteen, the fruit of *Garcinia mangostana* L. (Guttifereae), α- and γ-mangostins are known to be major constituents exhibiting diverse biological activities. However, the effects of γ-mangostin on oxidative neurotoxicity and impaired memory are yet to be elucidated. In the present study, the protective effect of γ-mangostin on oxidative stress-induced neuronal cell death and its underlying action mechanism(s) were investigated and compared to that of α-mangostin using primary cultured rat cortical cells. In addition, the effect of orally administered γ-mangostin on scopolamine-induced memory impairment was evaluated in mice. We found that γ-mangostin exhibited prominent protection against H_2O_2- or xanthine/xanthine oxidase-induced oxidative neuronal death and inhibited reactive oxygen species (ROS) generation triggered by these oxidative insults. In contrast, α-mangostin had no effects on the oxidative neuronal damage or associated ROS production. We also found that γ-mangostin, not α-mangostin, significantly inhibited H_2O_2-induced DNA fragmentation and activation of caspases 3 and 9, demonstrating its antiapoptotic action. In addition, only γ-mangostin was found to effectively inhibit lipid peroxidation and DPPH radical formation, while both mangostins inhibited β-secretase activity. Furthermore, we observed that the oral administration of γ-mangostin at dosages of 10 and 30 mg/kg markedly improved scopolamine-induced memory impairment in mice. Collectively, these results provide both *in vitro* and *in vivo* evidences for the neuroprotective and memory enhancing effects of γ-mangostin. Multiple mechanisms underlying this neuroprotective action were suggested in this study. Based on our findings, γ-mangostin could serve as a potentially preferable candidate over α-mangostin in combatting oxidative stress-associated neurodegenerative diseases including Alzheimer's disease.

1. Introduction

The generation of reactive oxygen species (ROS) including superoxide anion ($\cdot O_2^-$), hydroxyl radical (·OH), and hydrogen peroxide is recognised as a key factor in oxidative stress to the cells [1]. The accumulation of ROS in neuronal cells causes lipid peroxidation as well as damage to the structure and function of proteins and DNA molecules, ultimately leading to cell death [2]. The brain is known to be particularly susceptible to oxidative stress, due to its relative deficiency of endogenous antioxidant defence mechanisms, enriched levels of transition metals and unsaturated lipids, and high utilisation of oxygen [3]. Consequently, oxidative stress-induced neuronal damage has been recognised as an important mechanism involved in many neurodegenerative diseases, including Alzheimer's disease (AD) and Parkinson's disease [4, 5].

AD is characterised by the progressive impairment of cognition which is strongly correlated with neuronal degeneration and death. One of the hallmarks of AD is the appearance of senile plaques generated through the extracellular deposition of β-amyloid (A_β) peptide, which is derived from amyloid precursor protein (APP) upon enzymatic cleavage by β- and

γ-secretases [6, 7]. A_β peptide can induce oxidative damage through the production of ROS, potentially triggering neurotoxic events. Furthermore, it has been suggested that an augmentation in the cellular level of ROS and free radicals produces more A_β peptide, which in turn exerts further oxidative stress and toxic insults on neurons [8]. With the accumulative evidence for oxidative stress as an important factor in AD, antioxidants that reduce ROS and prevent oxidative stress-induced neuronal death have been intriguing potential candidates to prevent or treat AD [4, 5]. However, the results from many clinical studies have been rather disappointing so far. Nonetheless, various approaches considering heterogeneous and multifactorial characteristics of AD are attempted to explore favorable efficacy of antioxidant therapy in AD [9].

Mangosteen, *Garcinia mangostana* L. (*G. mangostana,* Guttifereae), is a tree cultivated in Southeast Asia including Indonesia, Philippines, and India. Its fruit is edible and also known to have medicinal benefits. The pericarp of the fruit has been traditionally used in these countries to treat infection, wounds, inflammation, and diarrhea [10]. In addition, mangosteen products in the form of juice or tablets account for some of the best-selling dietary supplements in the U.S. market [11]. The major bioactive secondary metabolites of mangosteen have been found to be xanthone derivatives, among which α-mangostin is the most studied xanthone [12, 13]. Using cell-free *in vitro* assays, α-mangostin was reported to scavenge singlet oxygen and superoxide anion, while it was shown to be unable to scavenge hydroxyl radicals and hydrogen peroxide [14]. Additionally, using primary cultures of cerebellar granule neurons, α-mangostin was found to exhibit ROS scavenging and neuroprotective effects against the mitochondrial toxin 3-nitropropionic acid or iodoacetate, an inhibitor of the glycolytic enzyme glyceraldehyde-3-phosphate dehydrogenase inducing metabolic inhibition in neurons [14, 15]. Moreover, α-mangostin has been demonstrated to attenuate β-amyloid oligomers-induced neurotoxicity by inhibiting amyloid aggregation and also to decrease A_β production via modulation of the amyloidogenic pathway [16, 17]. Together, these findings suggest that α-mangostin may serve as a multifunctional therapeutic intervention to combat the multiple pathological processes of AD [18, 19].

Unlike α-mangostin, however, there have only been limited findings supporting the neuroprotective effects of γ-mangostin. It has been reported that γ-mangostin, along with other xanthones from *G. mangostana*, inhibits glutamate-induced cell death in the HT22 hippocampal neuronal cell line and self-induced $A_{\beta 42}$ aggregation *in vitro* [18]. These findings also suggest that, in addition to α-mangostin, γ-mangostin could be a promising compound for AD therapy [18].

In order to confirm and further characterise the neuroprotective actions of these mangostins, the present study evaluated the effect of γ-mangostin on the oxidative insults using primary cultured rat cortical cells as a model and compared it to that of α-mangostin. To elucidate the probable action mechanism(s) underlying the neuroprotective effect, we next investigated the effects on the H_2O_2-induced DNA fragmentation and activation of caspases. Their antioxidant properties and effects on β-secretase activity were further examined using cell-free *in vitro* assays. In order to provide *in vivo* evidence of its therapeutic potential in AD, we finally evaluated the memory enhancing effect of orally administered γ-mangostin in a mouse model of scopolamine-induced memory impairment using the passive avoidance test.

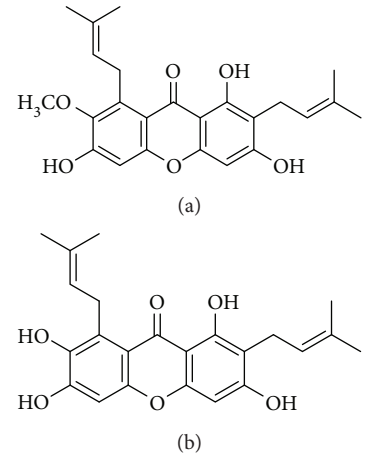

Figure 1: Chemical structures of α-mangostin (a) and γ-mangostin (b) isolated from *G. mangostana*.

2. Materials and Methods

2.1. Materials. *G. mangostana* fruits were collected from Indonesia, and their pericarps were extracted with methanol. Further separation and identification of α- and γ-mangostins were performed according to the method described previously [20]. Spectroscopic data for α- and γ-mangostins are depicted in Supplementary Materials (available here), and their chemical structures are shown in Figure 1. The purification yields of α- and γ-mangostins were 0.57% (w/w) and 0.06% (w/w), respectively, based on the total weight of mangosteen pericarp. The purity of these compounds as determined by HPLC-UV analysis was >95%. Minimum essential medium (MEM, supplemented with Earle's salt), fetal bovine serum (FBS), horse serum (HS), and antibiotic-antimycotic agent were procured from Invitrogen (Carlsbad, CA, USA). Laminin, poly-L-lysine, glucose, L-glutamine, 3-(4,5-dimethylthiazol-2-yl)-2,5-diphenyltetrazolium bromide (MTT), 2′,7′-dichlorofluorescin diacetate (DCFH-DA), H_2O_2, xanthine (X), xanthine oxidase (XO), cytosine arabinoside, 2-thiobarbituric acid (TBA), 1,1-diphenyl-2-picrylhydrazyl (DPPH), and anti-β-actin antibody (monoclonal) were obtained from Sigma-Aldrich (St. Louis, MO, USA). Polyethylene glycol (PEG) was from Yakuri Pure Chemicals Co. Ltd. (Kyoto, Japan). Anti-caspase 3 (8G10), anti-caspase 9 (Asp353), and horseradish peroxidase- (HRP-) linked anti-rabbit or anti-mouse immunoglobulin G (IgG) antibodies were purchased from Cell Signaling Technology (Danvers, MA, USA).

2.2. Animals. Timed-pregnant Sprague-Dawley (SD) rats and ICR mice were procured from Daehan Biolink (Chungbuk, Korea). Animals were maintained under conditions of controlled temperature ($22 \pm 2^\circ$C) and relative humidity (40-60%) with a 12 h light-dark cycle. They were given access to a standard chow diet and water *ad libitum*. All experimental procedures including the use, care, and handling of

animals were conducted following the international guidelines (Guide for the Care and Use of Laboratory Animals, Institute of Laboratory Animal Resources, Commission on Life Sciences, National Research Council; National Academy Press: Washington D.C., 1996). Prior to the study, the rationale, design, and protocols of the experiments were approved by the Institutional Animal Ethical Committee of Dongguk University (approval numbers: IACUC-2013-0005 and IACUC-2016-035-2).

2.3. Cell Culture. Primary culture of rat cerebrocortical cells containing neuronal and nonneuronal cells was carried out as previously described [21, 22]. Briefly, pregnant SD rats on the 17th day of gestation were sacrificed using anesthesia, and their uteri were promptly removed. Embryos were harvested, and their cerebral cortices were excised and mechanically dissociated into single cells by triturating with fire-polished Pasteur pipettes. The isolated cells were then seeded on either 35 mm culture dishes (6×10^6 cells/dish) or 24-well culture plates (6×10^5 cells/well) precoated with the mixture of poly-L-lysine and laminin in MEM (containing Earle's salt) supplemented with 2 mM glutamine, 25 mM glucose, 5% FBS, 5% HS, and 1% antibiotic-antimycotic agent. The cultures plated on 35 mm dishes were employed for Western blotting analysis, and those on 24-well plates were for the remaining experiments. The cells were maintained in the same medium in an incubator at 37°C with a humidified atmosphere of 95% air/5% CO_2. On day 7 of plating, the cultures were treated with 10 μM cytosine arabinoside in order to arrest the proliferation of nonneuronal cells. Finally, the neuronal cells were used for experimentation on days 10-11 of culturing.

2.4. Treatment of Cells and Assessment of Cell Viability. Before starting any treatment, the cultured cortical cells were washed with HEPES-buffered control salt solution (HCSS, 20 mM HEPES, pH 7.4; 120 mM NaCl; 5.4 mM KCl; 1.6 mM $MgCl_2 \cdot 6H_2O$; 2.3 mM $CaCl_2 \cdot 2H_2O$; 15 mM glucose; 10 mM NaOH). To assess the potential cytotoxic effects of α- or γ-mangostin, the HCSS-washed cultured cells were treated with these compounds at the concentrations of 0.3~10 μM in MEM supplemented with 25 mM glucose (MEMG) for 24 h. To induce oxidative damage, the cultured cells were exposed to 100 μM H_2O_2 for 5 min or 0.5 mM X and 10 mU/ml XO for 10 min in MEMG, washed with HCSS, and then incubated in MEMG for 18-20 h [23]. For each experiment, the control cells were exposed to the vehicle (MEMG) without any agent.

In order to evaluate the protective effects of α- or γ-mangostin on the oxidative neuronal damage elicited by the above-mentioned inducers, the cultured cells were simultaneously treated with mangostin compounds at the concentrations of 0.3~10 μM with the respective insults.

Following the termination of desired treatments, the viability of cells was determined by the MTT reduction assay, as previously described [22, 23]. In brief, MTT was added to the treated cells at a final concentration of 1.0 mg/ml and incubated for 3 h at 37°C. Upon completion of the MTT reaction, the culture media were carefully removed, and 500 μl DMSO was added. Following the incubation of cells for 15 min to dissolve the formazan crystal products, the absorbance was measured at 550 nm using a microplate reader (SpectraMax M2^e, Molecular Devices, Sunnyvale, CA, USA). The viability of control cells in terms of absorbance was expressed as 100%.

2.5. Determination of Intracellular ROS. The effect of α- or γ-mangostin on the generation of intracellular ROS was measured spectrofluorometrically using DCFH-DA fluorogenic dye as a probe [22]. Briefly, after washing with HCSS, the cultured cells were treated with DCFH-DA at a final concentration of 10 μM in MEMG for 30 min at 37°C, washed with HCSS, and then treated with the corresponding insults (100 μM H_2O_2 or 0.5 mM X in combination with 10 mU/ml XO) in MEMG for 2 h in the absence or presence of α- or γ-mangostin at the concentrations of 0.3~10 μM. Intracellular ROS generation was determined by the fluorescence detection of 2′,7′-dichlorofluorescein on a microplate reader (SpectraMax M2^e, Molecular Devices) with excitation and emission wavelengths at 490 nm and 520 nm, respectively, and expressed as % control.

2.6. Fluorescence Microscopy. The effect of α- or γ-mangostin on the H_2O_2-induced ROS generation in the cultured cells was further confirmed by fluorescence microscopy using DCFH-DA fluorogenic dye as a probe. Briefly, following DCFH-DA probing and subsequent treatment with 100 μM H_2O_2 in the absence or presence of either α- or γ-mangostin (10 μM) as described above, the intracellular ROS was visualised under a Nikon Eclipse Ti-U inverted microscope (Nikon, Tokyo, Japan) with excitation and emission wavelengths of 495 and 530 nm, respectively [24].

2.7. Terminal Deoxynucleotidyl Transferase-Mediated Deoxyuridine Triphosphate (dUTP) Nick End-Labeling (TUNEL) Assay. The effect of α- or γ-mangostin at 10 μM on H_2O_2-treated apoptotic cells was evaluated by detection of fragmented DNA using a TUNEL assay kit (DeadEnd™ Colorimetric TUNEL System, Promega, Madison, WI, USA), performed according to the manufacturer's instructions [22]. Briefly, the cells were treated, washed with PBS, and fixed for 25 min in 4% paraformaldehyde. The cells were then washed with PBS and incubated for 5 min with 0.2% Triton X-100 for permeabilisation. Following washing and incubation in equilibration buffer for 10 min at room temperature, the cells were transferred into terminal deoxynucleotidyl transferase reaction mixture containing biotinylated nucleotide mix and then incubated for 60 min at 37°C to permit the nick end-labeling reaction. After terminating the reaction, the cells were immersed in saline sodium citrate solution and subsequently incubated with streptavidin-conjugated HRP. After washing with PBS, the cells were finally stained with diaminobenzidine. The cells were washed twice with PBS, and the TUNEL-positive cells stained as dark brown color were detected using a TS-100 inverted microscope (Nikon, Tokyo, Japan).

2.8. Western Blotting. The immunodetection of the cleaved caspases 3 and 9 was performed by Western blotting as

previously described [25]. Briefly, the cultured cells were serum-starved overnight, exposed to either α- or γ-mangostin for 30 min in serum-free medium prior to cotreatment with 100 μM H_2O_2 for 2 h, and then the cells were lysed for 30 min on ice in the lysis buffer (10 mM Tris-HCl, pH 7.4; 150 mM NaCl; 2 mM EDTA; 4.5 mM sodium pyrophosphate; 10 mM β-glycerophosphate; 1 mM NaF; 1 mM Na_3VO_4; 1% (v/v) Triton X-100; 0.5% (v/v) NP-40; and one tablet of protease inhibitor cocktail (Roche Diagnostic GmbH, Mannheim, Germany)). The resultant lysates were then centrifuged at 14,000 rpm for 30 min at 4°C, and the supernatants were collected. The protein concentrations of the supernatants were determined using a Bio-Rad D_C protein assay kit (Bio-Rad, Hercules, CA, USA). Equal amounts of lysate proteins (30 μg) were then resolved by sodium dodecyl sulfate-polyacrylamide gel electrophoresis on 12% gels and electrophoretically transferred to nitrocellulose membranes (Whatman, Clifton, NJ, USA) for 1.5 h at 100 V. After blocking for 1.5 h with Tris-buffered saline (TBS) containing 0.1% Tween 20 (TBST) and 5% nonfat dry milk (BD Falcon, Sparks, MD, USA), the membranes were incubated overnight at 4°C with anti-caspase 3 or 9 antibodies in TBST containing 5% bovine serum albumin (USB, Canton, OH, USA). Next, the membranes were washed three times with TBST and incubated for 1.5 h with HRP-conjugated anti-rabbit IgG secondary antibody. The immunoreactive bands in the membranes were detected by a Bio-Rad ChemiDoc XRS imaging system (Bio-Rad) using Super Signal West Pico ECL reagent (Thermo Fisher Scientific, San Jose, CA, USA). In order to detect β-actin as an internal control, the membranes were stripped and incubated with anti-β-actin antibody.

2.9. Determination of DPPH Radical Scavenging Activity. The effect of α- or γ-mangostin on DPPH radicals was measured as previously described [26]. Briefly, the reaction mixture containing α- or γ-mangostin at the concentrations of 0.3~30 μM and methanolic solution of DPPH (150 μM) was incubated at 37°C for 30 min. The absorbance was then measured at 520 nm on a microplate reader (SpectraMax M2^e, Molecular Devices). The radical scavenging activity of the samples was determined as % inhibition of DPPH absorbance using the following equation:

$$\text{Inhibition}(\%) = 100 \times \frac{\left(\text{Abs}_{\text{control}} - \text{Abs}_{\text{sample}}\right)}{\text{Abs}_{\text{control}}}, \quad (1)$$

where $\text{Abs}_{\text{control}}$ represents the absorbance of the control (without test sample) and $\text{Abs}_{\text{sample}}$ denotes the absorbance in the presence of the test sample.

2.10. Assay of Lipid Peroxidation (LPO) in Rat Brain Homogenates. The effect of α- or γ-mangostin on LPO initiated by Fe^{2+} (10 μM) and L-ascorbic acid (100 μM) in the rat forebrain homogenates was measured as previously described [26]. Briefly, the reaction mixture was incubated at 37°C for 1 h in the absence (control) or presence of α- or γ-mangostin at the concentrations of 0.3~30 μM. After stopping the reaction by adding trichloroacetic acid (28%w/v) and TBA (1%w/v), the mixture was heated at 100°C for 15 min and centrifuged to remove the precipitates. The absorbance of the supernatant was read at 532 nm on a microplate reader (SpectraMax M2^e, Molecular Devices), and the percent inhibition of LPO was calculated using the above formula.

2.11. Assay of In Vitro β-Secretase Activity. The effect of α- or γ-mangostin on the β-secretase activity was determined using a β-secretase fluorescence resonance energy transfer (FRET) assay kit (Invitrogen, Carlsbad, CA, USA) following the manufacturer's instructions with some modifications [22]. In brief, a 10 μl aliquot of assay buffer containing α- or γ-mangostin at the concentrations of 0.3~10 μM was mixed with 20 μl of the substrate (750 nM) in a 96-well plate. Subsequently, 10 μl of β-secretase enzyme (1.0 U/ml) was added and incubated for 2 h at room temperature. The fluorescence was measured on a microplate reader (SpectraMax M2^e, Molecular Devices) with excitation and emission wavelengths set at 545 and 585 nm, respectively.

2.12. Passive Avoidance Test. The passive avoidance test was performed as previously described [27, 28] on six-week-old ICR mice (28~30 g body weight) using two identical compartments (lighted and dark compartments) with an automated guillotine door in between them (Gemini Avoidance System, San Diego Instruments Inc., San Diego, CA, USA). For the acquisition trial, the animals were placed in the lighted chamber, and the guillotine door was opened 15 s later. After the animals entered into the dark compartment, the door was automatically shut down, and an electrical foot shock (0.5 mA for 5 s) was delivered to the animals through the grid floor. Twenty-four hours after the acquisition trial, the animals were again placed in the lighted compartment in order to conduct a retention trial. The duration of each trial was 300 s, and the time latency for entry into the dark compartment was measured.

The animals were orally administered with γ-mangostin (5, 10, and 30 mg/kg in 40%v/v PEG in water), donepezil (10 mg/kg), or vehicle (for control and scopolamine groups). After 30 min of administration, memory impairment was induced by intraperitoneal administration of scopolamine (3 mg/kg, prepared in normal saline); the control group received normal saline only. Following 30 min of scopolamine injection, the acquisition trial was initiated as described above.

2.13. Statistical Analysis. All experiments were performed individually at least three times. Quantitative data are expressed as the mean ± S.E.M. Statistical analyses were performed by one-way ANOVA followed by Tukey's post hoc test using SigmaPlot 12.5 software (Systat Software, San Jose, CA, USA). A $P < 0.05$ was considered to be significant.

3. Results

3.1. Effects of α- and γ-Mangostins on Neuronal Cell Viability in Primary Cultured Rat Cortical Cells. Exposure of the primary cultured rat brain cortical cells to either α- or γ-mangostin at concentrations ranging from 0.3~10 μM for 24 h did not produce any cytotoxicity (Figure 2). Accordingly,

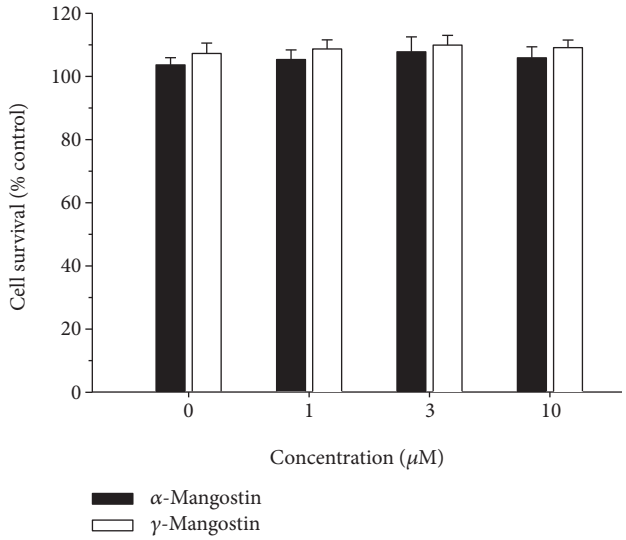

Figure 2: Effects of α- and γ-mangostins on neuronal cell viability in primary cultured rat cortical cells. Cells were exposed to the indicated concentrations of α- or γ-mangostin for 24 h. The control cells were treated with vehicle (DMSO) only. Cell viability was determined by the MTT reduction assay, as described in Materials and Methods. The viability of control cells treated with vehicle only was considered to be 100%, and the data were expressed as percentages of the control. Each point represents the mean ± S.E.M. from at least three independent experiments, performed in duplicate.

upcoming experiments with α- or γ-mangostin were performed using this concentration range.

3.2. Effects of α- and γ-Mangostins on the H_2O_2- or X/XO-Induced Oxidative Neuronal Damage and ROS Generation in Primary Cultured Rat Cortical Cells. In agreement with the previous reports [22, 26], treatment of the cultured cells with 100 μM of H_2O_2 for 5 min caused approximately 80% or more cell death and approximately 200% increase in intracellular ROS production (Figures 3(a) and 3(b), respectively (#, $P < 0.05$ vs. vehicle-treated control cells without H_2O_2, α-mangostin, or γ-mangostin treatment)). The reduced viability of the H_2O_2-treated cells was completely reversed by γ-mangostin at the concentration of 10 μM (Figure 3(a) (*, $P < 0.05$ vs. H_2O_2-treated cells without α- or γ-mangostin)). Since its protective effect against the H_2O_2-induced oxidative damage was so dramatic, we further tested the effect of γ-mangostin at the concentrations between 3 and 10 μM. As shown in Figure 3(a) (inset), 5 and 7 μM of γ-mangostin also exhibited dramatic increases in the viability of H_2O_2-treated cells. In addition, the H_2O_2-induced ROS production was significantly inhibited by γ-mangostin at 3~10 μM concentrations (Figure 3(b) (*, $P < 0.05$ vs. H_2O_2-treated cells without α- or γ-mangostin)), which was confirmed by fluorescence microscopy (Figure 3(c)). In contrast, α-mangostin showed no significant effects on H_2O_2-induced oxidative damage or ROS production at the concentrations tested in this study (Figures 3(a)–3(c)).

Treatment of the cultured cells with 0.5 mM X and 10 mU/ml XO caused approximately 80% or more cell death and a 300% increase in ROS production (Figures 3(d) and 3(e), respectively (#, $P < 0.05$ vs. vehicle-treated control cells without X/XO, α-mangostin, or γ-mangostin treatment)). The decreased viability of the X/XO-treated cells was totally reversed by γ-mangostin at the concentration of 10 μM (Figure 3(d) (*, $P < 0.05$ vs. X/XO-treated cells without α- or γ-mangostin)). Similarly, the X/XO-induced ROS production was significantly suppressed by γ-mangostin at 3 and 10 μM concentrations (Figure 3(e) (*, $P < 0.05$ vs. X/XO-treated cells without α- or γ-mangostin)). However, α-mangostin showed no significant effects on X/XO-induced oxidative damage or ROS production at the concentrations tested (Figures 3(d) and 3(e)).

3.3. Effects of α- and γ-Mangostins on the H_2O_2-Induced Apoptosis in Primary Cultured Rat Cortical Cells. In order to elucidate the probable mechanism(s) underlying the neuroprotective role of γ-mangostin, we next examined the effect of this compound on H_2O_2-induced apoptosis and compared it to that of α-mangostin. In agreement with the previous report [29], the exposure of cultured cells to H_2O_2 caused DNA fragmentation, an important hallmark of apoptosis, as reflected by a dramatic increase in the TUNEL-positive cell population (Figures 4(a) (B and F) and Figure 4(b) (#, $P < 0.05$ vs. vehicle-treated control cells without α- or γ-mangostin treatment)). The H_2O_2-induced DNA fragmentation was remarkably inhibited by γ-mangostin at 10 μM (Figure 4(a) (G) and Figure 4(b) (*, $P < 0.05$ vs. H_2O_2-treated cells without α- or γ-mangostin treatment)). We also examined their effects on the H_2O_2-induced activation of caspases, another important molecular event during the apoptotic process. As illustrated in Figures 4(c) and 4(d), γ-mangostin significantly attenuated the H_2O_2-induced activation of both caspases 3 and 9. In contrast, α-mangostin neither prevented DNA fragmentation nor inhibited caspase activities in the H_2O_2-treated cells (Figure 4).

3.4. Effects of α- and γ-Mangostins on DPPH Radical Formation and Lipid Peroxidation. The antioxidant properties of α- and γ-mangostins were further substantiated by evaluating their radical scavenging activities using stable free radical DPPH as a probe (Figure 5(a)). In addition, their ability to inhibit LPO initiated by Fe^{2+} and L-ascorbic acid in rat brain homogenate was also examined (Figure 5(b)). Our results demonstrated that γ-mangostin considerably attenuated the formation of DPPH radicals and effectively inhibited lipid peroxide formation in concentration-dependent manners. In contrast, α-mangostin showed no DPPH radical scavenging activity with only a minimal inhibition of LPO at the concentrations tested (Figures 5(a) and 5(b), respectively). Vit. C and BHA were used as reference compounds to validate the assay procedures for DPPH radical scavenging activity and inhibition of LPO, respectively (grey bars).

3.5. Effects of α- and γ-Mangostins on In Vitro β-Secretase Enzyme Activity. Since β-secretase plays a vital role in the generation of the A_β peptide from APP [6, 7], we also examined the impact of α- and γ-mangostins on the activity of this enzyme using the *in vitro* β-secretase FRET assay

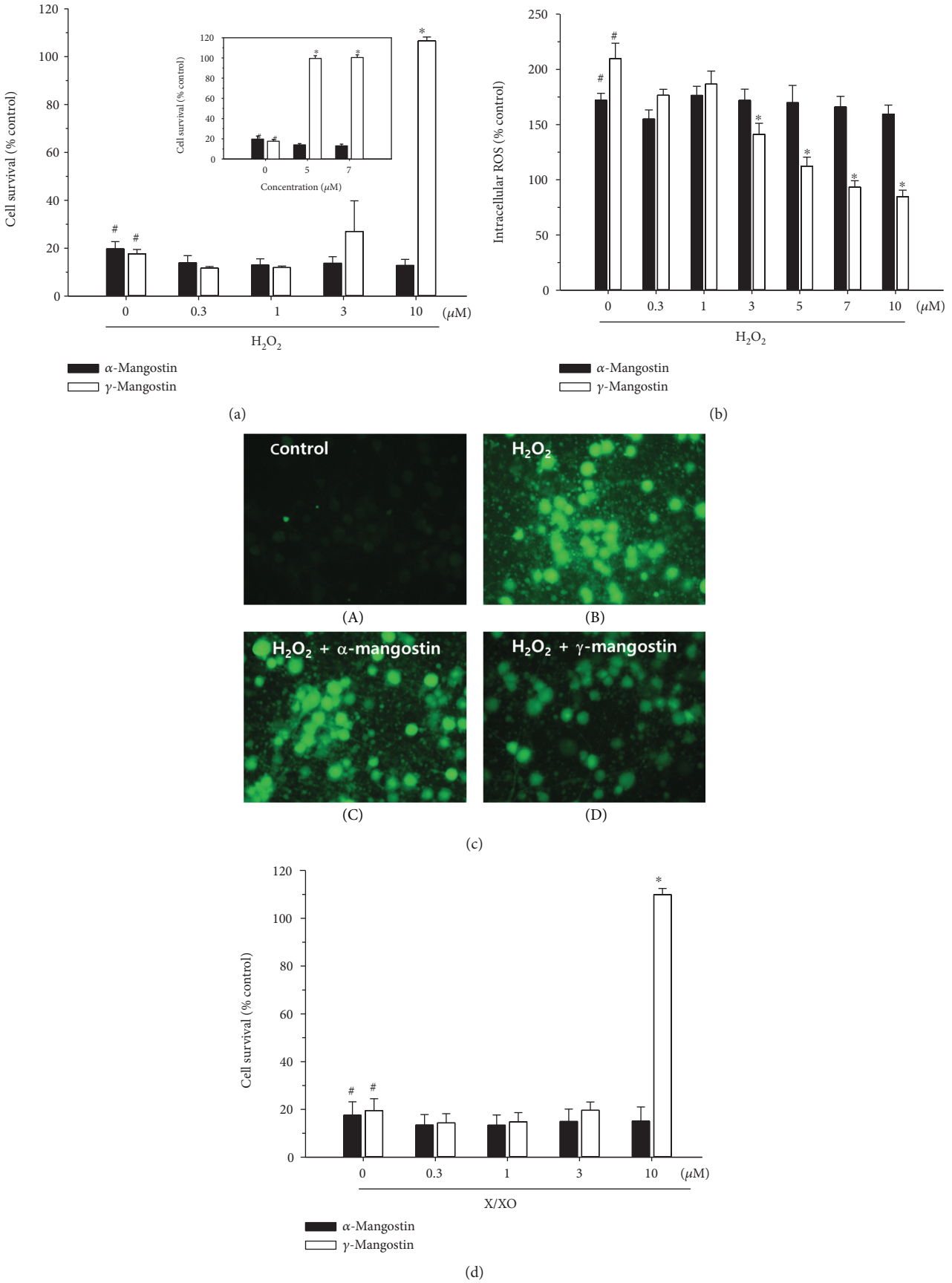

Figure 3: Continued.

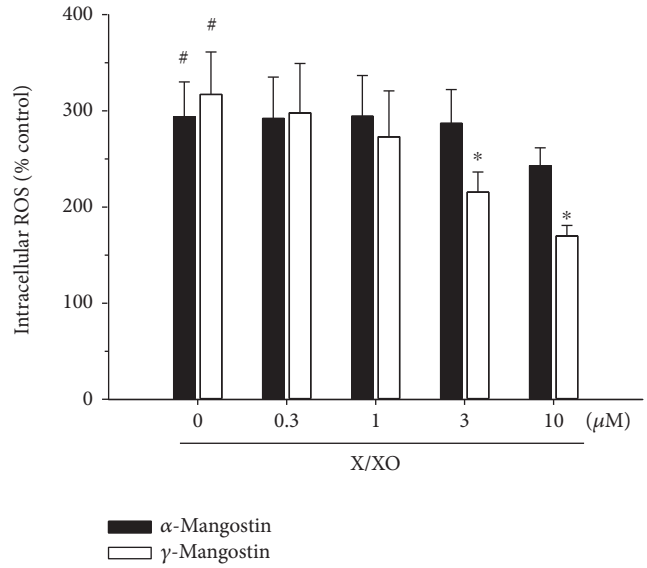

(e)

Figure 3: Effects of α- and γ-mangostins on H_2O_2- or X/XO-induced oxidative neurotoxicity and ROS generation in primary cultured rat cortical cells. (a and d) The cells were exposed to 100 μM H_2O_2 for 5 min (a) or 0.5 mM X in combination with 10 mU/ml XO for 10 min (d) in the absence or presence of either α- or γ-mangostin at various concentrations as indicated. Cell viability was determined by the MTT reduction assay at 18-20 h after exposure, as described in Materials and Methods. The cell survival was expressed as percentages of the control treated with vehicle only. (b and e) The cells were preincubated with 10 μM DCFH-DA for 30 min at 37°C in the dark, then treated with 100 μM H_2O_2 for 2 h (b) or 0.5 mM X in combination with 10 mU/ml XO for 2 h (e) in the absence or presence of either α- or γ-mangostin at various concentrations as indicated. The generation of intracellular ROS was measured as described in Materials and Methods. The ROS levels were expressed as percentages of the control treated with vehicle only. Each data point represents the mean ± S.E.M. from at least three independent experiments, performed in duplicate ($^{\#}P < 0.05$ vs. vehicle-treated control cells without α- or γ-mangostin treatment; $^{*}P < 0.05$ vs. H_2O_2- or X/XO-treated cells). (c) Fluorescence microscopic images showing the inhibition of H_2O_2-induced ROS generation by γ-mangostin in primary cultured rat cortical cells. The cells were preincubated with 10 μM DCFH-DA for 30 min at 37°C in the dark and treated with 100 μM H_2O_2 in the absence (B) or presence of 10 μM α-mangostin (C) or γ-mangostin (D) for 2 h. The control cells were treated with vehicle only without α- or γ-mangostin (A). Following the desired treatment, ROS levels were imaged using epifluorescence microscopy as described in Materials and Methods. Representative photomicrographs from three independent experiments are shown.

kit. We found that both α- and γ-mangostins potently inhibited β-secretase activity in concentration-dependent fashion (Figure 6).

3.6. Effect of γ-Mangostin on the Scopolamine-Induced Memory Impairment in Mice. Using cell-based and cell-free *in vitro* assays, our findings demonstrated that γ-mangostin showed more potent antioxidant and neuroprotective activities than α-mangostin, although both compounds showed similar degrees of inhibition against β-secretase activity. Based on these findings, we selected γ-mangostin to examine whether it could improve scopolamine-induced memory impairment in mice using the passive avoidance test.

As illustrated in Figure 7, the acquisition trials did not show significant differences in the time latency of all groups (black bars). During the retention trials (white bars), the scopolamine-treated group (without γ-mangostin or donepezil administration) showed marked reduction of the time latency than the control group treated with vehicle only (#, $P < 0.05$ vs. vehicle-treated control group), indicating that significant memory impairment was induced by scopolamine injection. The groups administered with γ-mangostin at the dosages of 10 and 30 mg/kg significantly restored the scopolamine-induced decrease in time latency (*, $P < 0.05$ vs. scopolamine-treated amnesia group). Donepezil, a well-known cholinesterase inhibitor clinically used for the treatment of AD, was employed as a reference drug to validate our experimental procedures and compare its effect with that of γ-mangostin. The reduced time latency by scopolamine injection was also recovered by the oral administration of donepezil at the dosage of 10 mg/kg (*, $P < 0.05$ vs. scopolamine-treated amnesia group). The inhibition of scopolamine-induced memory impairment by γ-mangostin administration (10 and 30 mg/kg of dosage) was nearly comparable to that of the donepezil-treated group (Figure 7). However, administration of γ-mangostin at the dosage of 5 mg/kg did not show a significant effect on reversing scopolamine-induced memory impairment in mice.

4. Discussion

Oxidative stress-induced cell damage is known to be involved in a number of neurodegenerative diseases such as AD, Parkinson's disease, and stroke [4, 5], where ROS such as superoxide anion, hydroxyl radical, and hydrogen peroxide play pivotal roles. It has been demonstrated that H_2O_2 can

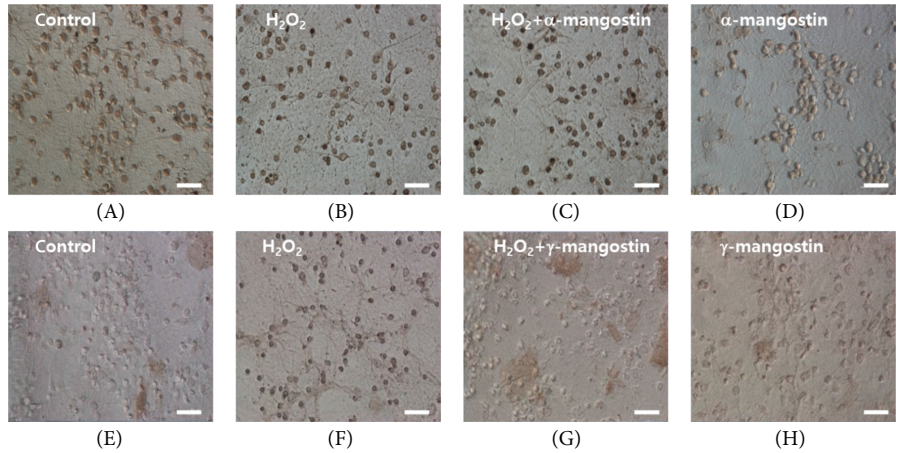

(a)

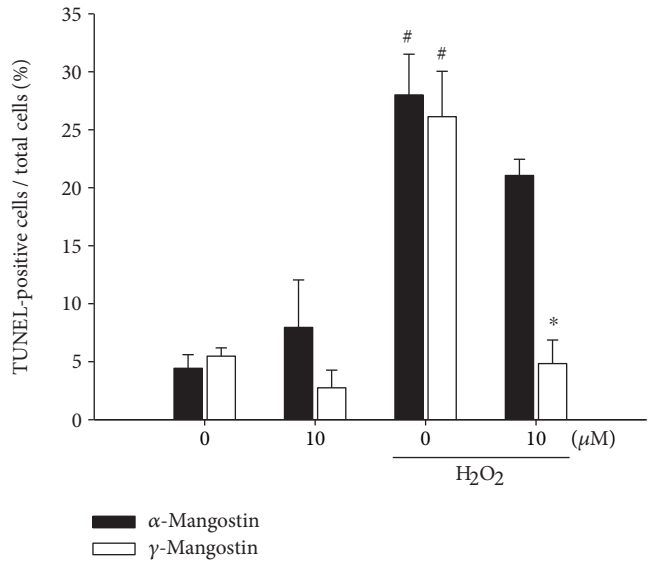

(b)

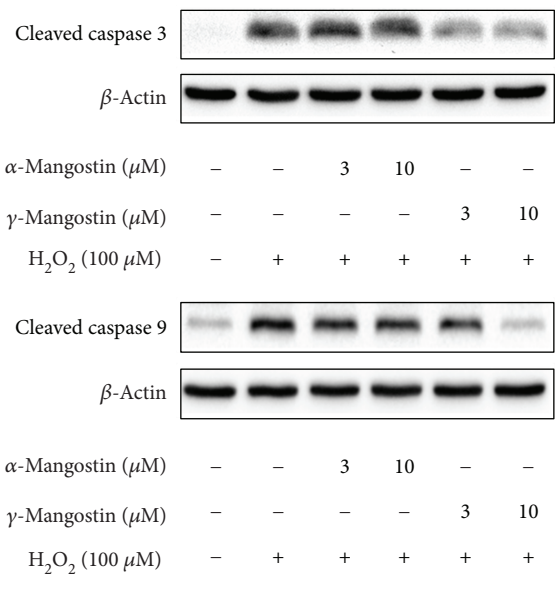

(c)

Figure 4: Continued.

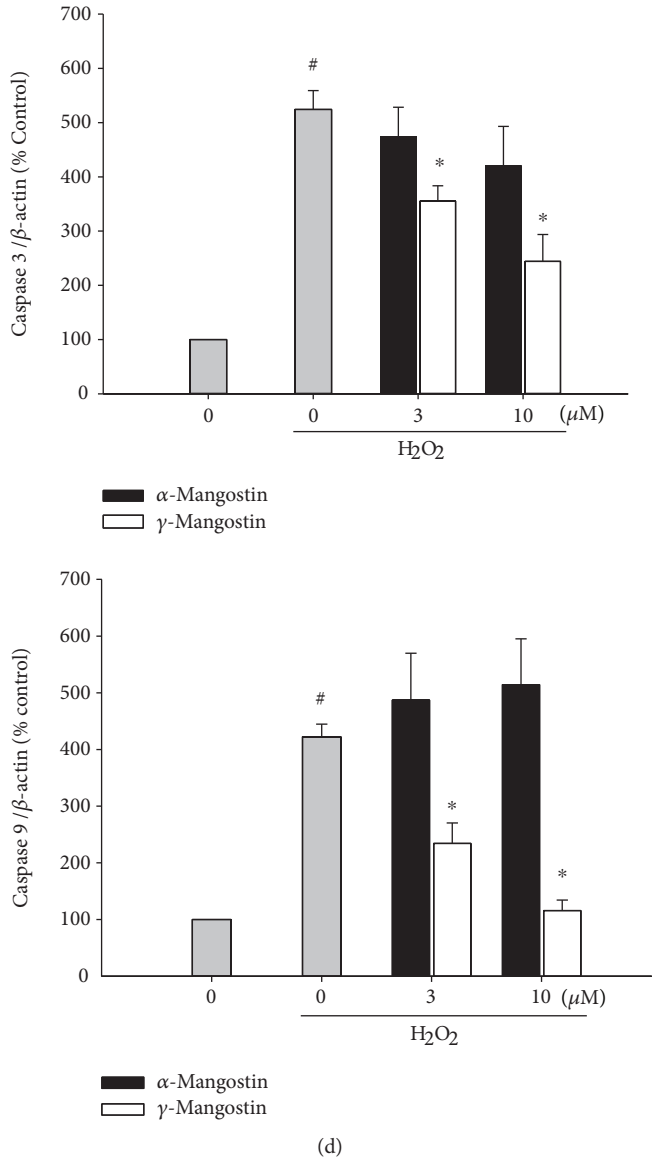

Figure 4: Effects of α- and γ-mangostins on H_2O_2-induced apoptosis in primary cultured rat cortical cells. (a and b) Inhibition of H_2O_2-induced DNA fragmentation by γ-mangostin. Cells were treated with 100 μM H_2O_2 for 2 h with or without α- or γ-mangostin at the concentration of 10 μM, and the TUNEL assay was carried out as described in Materials and Methods. Representative microscopic images from at least three individual experiments are shown (a). (A and E) Control cells were treated with vehicle only; (B and F) cells were treated with 100 μM H_2O_2 for 2 h; (C and G) cells were treated for 2 h with either 10 μM α-mangostin (C) or γ-mangostin (G) in combination with 100 μM H_2O_2; (D and H) cells were treated with 10 μM α-mangostin (D) or γ-mangostin for 2 h without H_2O_2 (H). Scale bar = 10 μm. Quantitative analyses of the TUNEL-positive cells from at least three independent experiments are shown (b) ($^{\#}P < 0.05$ vs. vehicle-treated control cells without α- or γ-mangostin treatment; $^{*}P < 0.05$ vs. H_2O_2-treated cells without α- or γ-mangostin). (c and d) Inhibition of the H_2O_2-induced activation of caspases 3 and 9 by γ-mangostin. Cells were treated with 100 μM H_2O_2 for 2 h in the absence or presence of either α- or γ-mangostin at 3 and 10 μM. The expression of cleaved caspases 3 and 9 was assessed by Western blotting as described in Materials and Methods. Representative blots from at least three individual experiments are shown (c). The intensities of the bands from at least three independent experiments were quantified by densitometric analyses and normalised to β-actin (d) ($^{\#}P < 0.05$ vs. vehicle-treated control cells without α- or γ-mangostin treatment; $^{*}P < 0.05$ vs. H_2O_2-treated cells without α- or γ-mangostin).

readily cross the cell membrane and cause injuries to the tissues through a number of different mechanisms, including the production of hydroxyl radicals and destabilisation of the oxidant/antioxidant pathway, ultimately leading to apoptotic and/or necrotic cell death [30]. The oxidation of X by XO also serves as an important source of ROS, generating H_2O_2 and superoxide anions that are known to contribute to the onset of neuronal damage in many neurodegenerative diseases [31, 32]. Taking critical roles of these ROS into account, we treated the primary cultured rat cortical cells with either H_2O_2 or X and XO in this study to induce oxidative neuronal damage as well as ROS generation and tested

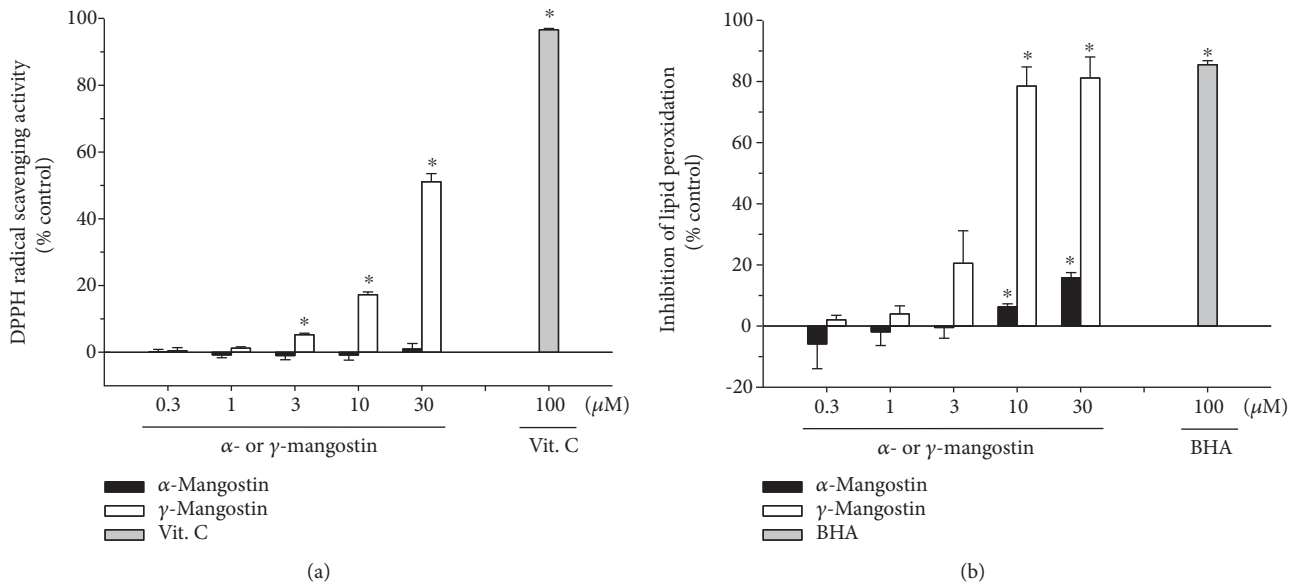

Figure 5: Effects of α- and γ-mangostins on DPPH radical formation and lipid peroxidation (LPO). Inhibition of DPPH radical (a) and LPO induced by Fe^{2+} (10 μM) and L-ascorbic acid (100 μM) in rat forebrain homogenate (b) by α- or γ-mangostin at the indicated concentrations were measured as described in Materials and Methods. Each data point represents the mean ± S.E.M. from at least three independent experiments, performed in duplicate ($^*P < 0.05$ vs. vehicle-treated control without α- or γ-mangostin treatment). Vit. C and BHA were used as references to validate the assay procedures for DPPH radical scavenging activity and inhibition of LPO, respectively (grey bars). Vit. C: vitamin C; BHA: butylhydroxyanisole.

the effects of α- and γ-mangostins, the two xanthones isolated from the fruit hull of mangosteen, on this oxidative damage and ROS.

Our results demonstrated that the exposure of cultured cells to these oxidative insults produced approximately 80% cell death and marked increases in ROS production (Figures 3(a)–3(e)). We found in this study that only γ-mangostin, not α-mangostin, completely reversed the H_2O_2- or X/XO-induced oxidative neuronal damage and significantly attenuated ROS production. These results are in line with those of an earlier report, demonstrating that, among the sixteen xanthones including α- and γ-mangostins, only γ-mangostin exhibited $HO^{\cdot}$ scavenging activity in an *in vitro* cell-free assay [33].

It has been previously reported that α-mangostin provides ROS scavenging activity and neuroprotective action against 3-nitropropionic acid- or iodoacetic acid-treated primary cultures of cerebellar granule neurons [14, 15]. However, in our study, α-mangostin neither exhibited neuroprotective activity against the H_2O_2- or X/XO-induced oxidative damage nor inhibited associated ROS production at any concentration tested (Figures 3(a)–3(e)). The discrepancies between the earlier reports [14, 15] and our results may be due to the different cell types used in these studies. Another plausible reason for these contradictory results may be due to the different species of radicals generated by the different oxidative inducers used in these studies. According to the report by Pedraza-Chaverrí et al. [14], α-mangostin was able to scavenge superoxide anion and peroxynitrite anion, whereas it was unable to scavenge hydroxyl radicals and hydrogen peroxide. Since α-mangostin was found to inhibit 3-nitropropionic acid-induced neurotoxicity and ROS production, Pedraza-Chaverrí et al. suggested that superoxide radical and peroxynitrite anion may be involved in 3-nitropropionic acid-induced toxicity in cerebellar granule neurons [14]. In our study, however, hydroxyl radicals and hydrogen peroxide were produced in cortical neurons by the treatment with H_2O_2 and X/XO, and α-mangostin did not inhibit the neurotoxicity and ROS production caused by these inducers. Thus, our findings on α-mangostin are entirely in agreement with the observation by Pedraza-Chaverrí et al. It would be interesting to clarify preferable species of ROS, if any, to be scavenged by γ-mangostin under the same experimental conditions employed for α-mangostin. Further study will be required to elucidate underlying mechanisms by which these xanthones distinguish different species of radicals to scavenge. We further confirmed that γ-mangostin exhibits more potent radical scavenging activity and antioxidant effect than α-mangostin using *in vitro* assays for DPPH radical scavenging activity and LPO. Again, unlike γ-mangostin, α-mangostin showed no DPPH radical scavenging activity and only minimal inhibition of LPO (Figure 5).

The action of H_2O_2 as an inducer of apoptosis and DNA damage has been well documented [34, 35]. It has been found that in PC12 cells and SH-SY5Y neuroblatoma cells, H_2O_2 can induce ROS generation and the activation of caspase cascades and ultimately triggers apoptosis [29]. In agreement with these previous reports [29, 34, 35], the exposure of our cultured cells to H_2O_2 also caused DNA fragmentation (Figure 4(a), B and F), as evidenced by the increased number of TUNEL-positive cells (Figure 4(b)). The H_2O_2-induced DNA fragmentation was markedly inhibited by γ-mangostin but not by α-mangostin (Figures 4(a) and

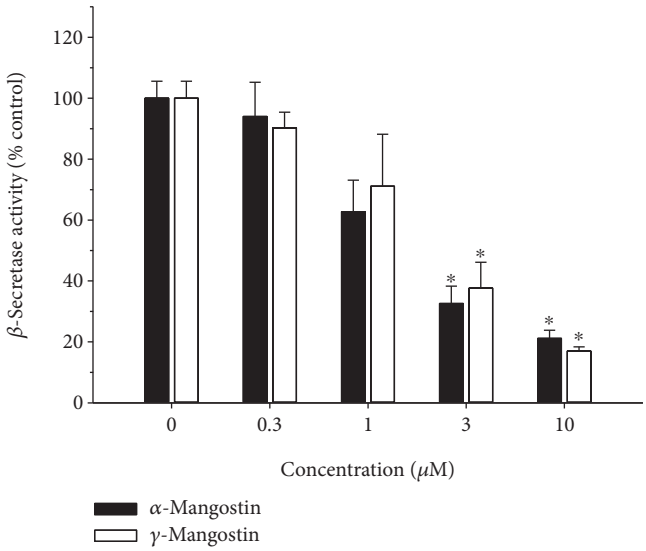

Figure 6: Effects of α- and γ-mangostins on β-secretase activity. The inhibitory effects of α- and γ-mangostins on the enzymatic activity of β-secretase were determined by the β-secretase FRET assay as described in Materials and Methods. The data were expressed as percentages of the control treated without α- or γ-mangostin. Each data point represents the mean ± S.E.M. from at least three independent experiments, performed in duplicate ($^*P < 0.05$ vs. vehicle-treated control without α- or γ-mangostin treatment).

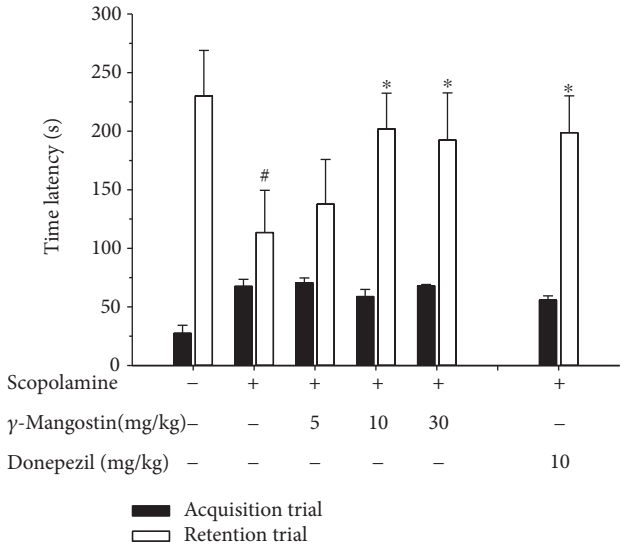

Figure 7: Effect of γ-mangostin on the scopolamine-induced memory impairment in mice. Animals were randomly divided into 6 groups with 6-7 mice in each group. To the 3 groups of animals, γ-mangostin was orally administered at the respective dosages of 5, 10, or 30 mg/kg as indicated. For the reference drug-treated group, donepezil was administered at the dosage of 10 mg/kg. For the control group (the vehicle-treated group without scopolamine, γ-mangostin, or donepezil treatment) and the scopolamine group (the group treated with scopolamine injection, not with γ-mangostin or donepezil treatment), vehicle was only administered. After 30 min of each administration, memory impairment was induced by intraperitoneal injection of scopolamine (3 mg/kg in normal saline) in 5 groups as indicated above in the figure; for the control group, normal saline without scopolamine was injected. Following 30 min of scopolamine or saline injection, the acquisition trial was initiated by delivering a foot shock to the animals. Twenty-four hours after the acquisition trials, the retention trials were performed. The detailed experimental procedures are described in Materials and Methods. The time latency was calculated from three independent experiments. Each data point represents the mean ± S.E.M. ($^\#P < 0.05$ vs. vehicle-treated control group without scopolamine, γ-mangostin, or donepezil treatment; $^*P < 0.05$ vs. scopolamine group treated with scopolamine only without γ-mangostin or donepezil).

4(b)). Furthermore, the H_2O_2 treatment of the cultured cells triggered the activation of caspases 3 and 9, the major molecular events in the apoptotic process. The activated caspases 3 and 9 were significantly suppressed only by γ-mangostin (Figures 4(c) and 4(d)). Recently, γ-mangostin was found to inhibit caspase 3 activity in 6-hydroxy dopamine-treated SH-SY5Y cells [36], which is consistent with our finding. Taken together, it is conceivable that the underlying mechanism(s) for the neuroprotective effect of γ-mangostin against H_2O_2-induced oxidative damage may involve the inhibition of ROS production, as well as its antiapoptotic action inhibiting DNA fragmentation and activation of caspases 3 and 9. Furthermore, the antioxidant activities of γ-mangostin, not α-mangostin, scavenging DPPH radical and inhibiting LPO may also contribute to its neuroprotective action (Figure 5).

Among the diverse pathophysiological factors involved in the onset and development of AD, A_β peptide plays a key role in neuronal cell death [37]. In this study, we found that both α- and γ-mangostins inhibited β-secretase activity, an enzyme involved in the generation of the A_β peptides from APP in the amyloidogenic pathway [6, 7]. Previously, a series of xanthones isolated from *G. mangostana* were reported to modestly inhibit BACE1 activity, exhibiting 60.3 and 42.1% inhibition by α- and γ-mangostins at the concentration of 100 μM, respectively [17]. Our study expanded their findings, illustrating the concentration-dependent inhibition of β-secretase activity by both α- and γ-mangostins at the concentration range of 0.3~10 μM (Figure 6). For some reason, however, the inhibition by α- or γ-mangostin was observed to be much more potent in our study than that shown by a previous report [18], as approximately 60-70% inhibition of β-secretase activity was achieved at the concentration as low as 3 μM of α- or γ-mangostin (Figure 6). One of the possible explanations for this potency discrepancy may be due to the differences in the bioactivities of β-secretase in the assay kits employed in our study and in the previous report. In order to test this possibility, the β-secretase activity has to be reevaluated in the presence of the testing xanthones under the same experimental conditions, using assay kits manufactured by the same company. In any event, our and previous findings strongly support that both α- and γ-mangostins may reduce A_β formation from APP through the inhibition of β-secretase activity.

It has been previously reported that α-mangostin concentration dependently attenuated the neurotoxicity induced by $A_{\beta\text{-}(1\text{-}40)}$ or $A_{\beta\text{-}(1\text{-}42)}$ oligomers in primary rat cerebral cortical neurons [16]. Based on molecular docking simulations,

the thioflavin T fluorescence assay and electron microscopy imaging, α-mangostin was found to inhibit and dissociate amyloid aggregation, which could contribute to its effect of attenuating A_β oligomers-induced neurotoxicity [16]. We also attempted to evaluate the effects of α- and γ-mangostins on the neurotoxicity induced in our culture model by $A_{\beta\text{-}(25\text{-}35)}$, the active fragment of A_β, as previously described [22]. We treated the cultured cells with 40 μM of $A_{\beta\text{-}(25\text{-}35)}$ for 24 h in the absence or presence of α- or γ-mangostin at the concentration range of 0.3~10 μM. Both mangostins appeared to exhibit weak protective effect on $A_{\beta\text{-}(25\text{-}35)}$-induced neurotoxicity (data not shown). However, the apparent effects were not statistically significant by one-way ANOVA analysis. Further extensive studies under the same experimental conditions with the same A_β peptides may be necessary to evaluate and compare their effects on the A_β-induced neurotoxicity.

It has long been believed that acetylcholine is one of the most important neurotransmitters in learning and memory processes [38], and thus, cholinergic dysfunction is closely associated with AD pathology [39, 40]. Based on this cholinergic hypothesis, AChE inhibitors such as donepezil are currently used to alleviate the symptoms of AD in clinical situations. Recently, several prenylated xanthones from mangosteen, including α- and γ-mangostins, have been reported to inhibit AChE activity with IC_{50} values of lower than 20.5 μM, as determined by Ellman's colorimetric method [41, 42]. The protein-ligand interactions between AChE and xanthones were confirmed by molecular docking studies [41]. In our study, we also tested the effects of α- and γ-mangostins on AChE activity *in vitro* and verified the previous findings (data not shown). Collectively, based on our results and previous findings [18, 41, 42], both α- and γ-mangostins may reduce A_β formation and improve cholinergic transmission through the inhibition of β-secretase and AChE activities, respectively.

The α- and γ-mangostins are the most extensively studied xanthone derivatives of mangosteen [12]. Although they share a common chemical backbone, their chemical structures differ with respect to the numbers of hydroxyl and methoxy groups (Figure 1). While α-mangostin possesses three hydroxyl groups (at positions 1, 3, and 6) and a methoxy group (at position 7), γ-mangostin has four hydroxyl groups (at positions 1, 3, 6, and 7) without any methoxy group. We observed that only γ-mangostin, not α-mangostin, exhibited marked and potent neuroprotective and antioxidant effects. The exact mechanisms by which the structural discrepancy between these two xanthones can account for such a decisive difference in their neuroprotective and antioxidant effects are not yet understood. The catechol moiety of γ-mangostin or the hydroxyl group itself at position 7 may play crucial role in its neuroprotective and radical scavenging activities. Interestingly, however, the structural difference between α- and γ-mangostins was not reflected in their inhibitory effects on β-secretase and AChE enzyme activities, as both mangostins exhibited similar degrees of inhibition (Figure 6) [41, 42]. It is assumed that the hydroxyl groups at positions 1, 3, and 6 may play important roles in the inhibition of these enzyme activities. The methoxy group at position 7 of α-mangostin may not be directly involved in the interactions with these enzymes. Further studies are needed to explain the basis of such differential or similar pharmacological actions by the two mangostin compounds.

Even though both mangostins exhibited similar inhibition against β-secretase and AChE activities as measured in cell-free *in vitro* assays, γ-mangostin appeared to be a substantially more potent antioxidant and neuroprotective agent than α-mangostin, based on our findings in cell-based as well as cell-free *in vitro* studies. These beneficial pharmacological profiles of γ-mangostin strongly suggest its therapeutic potential for AD and other neurodegenerative diseases associated with oxidative stress.

In order to test this possibility, we next conducted a passive avoidance test using a scopolamine-induced amnesia model in mice to investigate the memory-improving effect of γ-mangostin *in vivo*. It has been previously revealed that memory deficit induced by scopolamine, a nonselective muscarinic receptor antagonist, is associated with oxidative stress [43], an event known to play a vital role in neurodegenerative disorders such as AD [4, 5]. As shown in Figure 7, the memory impairment induced by scopolamine was significantly improved by a single oral administration of γ-mangostin at dosages of 10 and 30 mg/kg. The memory-improving effects of γ-mangostin at these dosages were quite comparable to that of donepezil, a reference drug. Our results are in alignment with those of a previous report, demonstrating the protective effect of the mangosteen extract on scopolamine-induced amnesia [28]. In addition, the ability of γ-mangostin to penetrate the blood-brain barrier and reach CNS targets was predicted *in vitro* using a parallel artificial membrane penetration assay [18]. Taken together, our result and the previous findings suggest that γ-mangostin could be a promising candidate for therapeutic interventions of AD. To the best of our knowledge, our present study is the first report revealing the neuroprotective effect of γ-mangostin against oxidative neurotoxicity, as well as its memory-enhancing effect in mice.

5. Conclusions

The present study demonstrated that γ-mangostin, a xanthone derivative isolated from the fruit hull of mangosteen, exhibited a potent neuroprotective effect against H_2O_2- or X/XO-induced oxidative neuronal damage. The underlying mechanisms for this neuroprotective action may involve the inhibition of ROS generation triggered by these oxidative insults, antioxidant activities as evident by inhibition of DPPH radical formation and LPO, and its antiapoptotic properties as demonstrated by the inhibition of H_2O_2-induced DNA fragmentation and activation of caspases. Unlike γ-mangostin, however, α-mangostin neither exhibited neuroprotective activity nor demonstrated antioxidant properties in our study. Moreover, γ-mangostin was shown to exhibit a potent inhibitory effect on β-secretase activity and strongly improved scopolamine-induced memory deficits in mice. Based on our study providing *in vitro* and *in vivo* evidences, γ-mangostin may be considered to be a promising

candidate in the prevention and treatment of various neurodegenerative diseases including AD.

Abbreviations

A_β:	β-Amyloid
AD:	Alzheimer's disease
APP:	Amyloid precursor protein
DCFH-DA:	2′,7′-Dichlorodihydrofluorescein diacetate
DMSO:	Dimethylsulfoxide
DPPH:	1,1-Diphenyl-2-picrylhydrazyl
FBS:	Fetal bovine serum
FRET:	Fluorescence resonance energy transfer
G. mangostana:	*Garcinia mangostana* L.
HCSS:	HEPES-buffered control salt solution
HRP:	Horseradish peroxidase
HS:	Horse serum
IgG:	Immunoglobulin G
MEM:	Minimum essential medium
MEMG:	MEM supplemented with 25 mM glucose
MTT:	3-(4,5-Dimethylthiazol-2-yl)-2,5-diphenyltetrazolium bromide
ROS:	Reactive oxygen species
SD:	Sprague-Dawley
TBA:	2-Thiobarbituric acid
TBS:	Tris-buffered saline
TBST:	Tris-buffered saline containing 0.1% Tween 20
TUNEL:	Terminal deoxynucleotidyl transferase-mediated deoxyuridine triphosphate nick end-labeling
X:	Xanthine
XO:	Xanthine oxidase.

Data Availability

The data used to support the findings of this study are available from the corresponding author upon request.

Conflicts of Interest

The authors declare that there are no conflicts of interests regarding the publication of this paper.

Authors' Contributions

Y. Lee and S. Kim performed most experiments and analysed the data; Y. Oh performed Western blotting of caspase 9 and statistically analysed the data; Y-M. Kim provided the purification yield of α- and γ-mangostins from the pericarp of mangosteen fruit; Y-W. Chin provided the purified α- and γ-mangostins and their spectroscopic data depicted in Supplementary Materials; and J. Cho designed the study, analysed the data, and wrote the manuscript.

Acknowledgments

This work was supported by the National Research Foundation of Korea (NRF) grant funded by the Korean Government (MSIT) (NRF-2018R1A5A2023127) and by the GRRC Program of Gyeonggi Province (GRRC DONGGUK 2018-B01), Republic of Korea. The authors would like to thank Prof. M. Lee and Dr. J. Park for proving the epifluorescence microscopy facility and helpful assistance for the fluorescence studies.

Supplementary Materials

Spectroscopic data are available as Supplementary Materials. *(Supplementary Materials)*

References

[1] B. Halliwell and J. M. C. Gutteridge, *Free Radicals in Biology and Medicine*, Clarendon Press, Oxford, 1989.

[2] J. Coyle and P. Puttfarcken, "Oxidative stress, glutamate, and neurodegenerative disorders," *Science*, vol. 262, no. 5134, pp. 689–695, 1993.

[3] J. N. Cobley, M. L. Fiorello, and D. M. Bailey, "13 reasons why the brain is susceptible to oxidative stress," *Redox Biology*, vol. 15, pp. 490–503, 2018.

[4] C. Behl and B. Moosmann, "Antioxidant neuroprotection in Alzheimer's disease as preventive and therapeutic approach," *Free Radical Biology & Medicine*, vol. 33, no. 2, pp. 182–191, 2002.

[5] S. Manoharan, G. J. Guillemin, R. S. Abiramasundari, M. M. Essa, M. Akbar, and M. D. Akbar, "The role of reactive oxygen species in the pathogenesis of Alzheimer's disease, Parkinson's disease, and Huntington's disease: a mini review," *Oxidative Medicine and Cellular Longevity*, vol. 2016, Article ID 8590578, 15 pages, 2016.

[6] R. Vassar, "BACE1: the β-secretase enzyme in Alzheimer's disease," *Journal of Molecular Neuroscience*, vol. 23, no. 1-2, pp. 105–114, 2004.

[7] M. A. Findeis, "The role of amyloid β peptide 42 in Alzheimer's disease," *Pharmacology & Therapeutics*, vol. 116, no. 2, pp. 266–286, 2007.

[8] W. R. Markesbery, "Oxidative stress hypothesis in Alzheimer's disease," *Free Radical Biology & Medicine*, vol. 23, no. 1, pp. 134–147, 1997.

[9] T. Persson, B. O. Popescu, and A. Cedazo-Minguez, "Oxidative stress in Alzheimer's disease: Why did antioxidant therapy fail?," *Oxidative Medicine and Cellular Longevity*, vol. 2014, Article ID 427318, 11 pages, 2014.

[10] J. Pedraza-Chaverri, N. Cardenas-Rodriguez, M. Orozco-Ibarra, and J. M. Perez-Rojas, "Medicinal properties of mangosteen (*Garcinia mangostana*)," *Food and Chemical Toxicology*, vol. 46, no. 10, pp. 3227–3239, 2008.

[11] Y. W. Chin and A. Kinghorn, "Structural characterization, biological effects, and synthetic studies on xanthones from mangosteen (*Garcinia mangostana*), a popular botanical dietary supplement," *Mini-Reviews in Organic Chemistry*, vol. 5, no. 4, pp. 355–364, 2008.

[12] D. Obolskiy, I. Pischel, N. Siriwatanametanon, and M. Heinrich, "*Garcinia mangostana* L.: a phytochemical and pharmacological review," *Phytotherapy Research*, vol. 23, no. 8, pp. 1047–1065, 2009.

[13] F. Gutierrez-Orozco and M. Failla, "Biological activities and bioavailability of mangosteen xanthones: a critical review of the current evidence," *Nutrients*, vol. 5, no. 8, pp. 3163–3183, 2013.

[14] J. Pedraza-Chaverrí, L. M. Reyes-Fermín, E. G. Nolasco-Amaya et al., "ROS scavenging capacity and neuroprotective effect of α-mangostin against 3-nitropropionic acid in cerebellar granule neurons," *Experimental and Toxicologic Pathology*, vol. 61, no. 5, pp. 491–501, 2009.

[15] L. M. Reyes-Fermín, S. González-Reyes, N. G. Tarco-Álvarez, M. Hernández-Nava, M. Orozco-Ibarra, and J. Pedraza-Chaverri, "Neuroprotective effect of α-mangostin and curcumin against iodoacetate-induced cell death," *Nutritional Neuroscience*, vol. 15, no. 5, pp. 34–41, 2013.

[16] Y. Wang, Z. Xia, J. R. Xu et al., "α-Mangostin, a polyphenolic xanthone derivative from mangosteen, attenuates β-amyloid oligomers-induced neurotoxicity by inhibiting amyloid aggregation," *Neuropharmacology*, vol. 62, no. 2, pp. 871–881, 2012.

[17] L. X. Zhao, Y. Wang, T. Liu et al., "α-Mangostin decreases β-amyloid peptides production via modulation of amyloidogenic pathway," *CNS Neuroscience & Therapeutics*, vol. 23, no. 6, pp. 526–534, 2017.

[18] S. N. Wang, Q. Li, M. H. Jing et al., "Natural xanthones from Garcinia mangostana with multifunctional activities for the therapy of Alzheimer's disease," *Neurochemical Research*, vol. 41, no. 7, pp. 1806–1817, 2016.

[19] M. H. Wang, K. J. Zhang, Q. L. Gu, X. L. Bi, and J. X. Wang, "Pharmacology of mangostins and their derivatives: a comprehensive review," *Chinese Journal of Natural Medicines*, vol. 15, no. 2, pp. 81–93, 2017.

[20] G. H. Quan, S. R. Oh, J. H. Kim, H. K. Lee, A. D. Kinghorn, and Y. W. Chin, "Xanthone constituents of the fruits of Garcinia mangostana with anticomplement activity," *Phytotherapy Research*, vol. 24, no. 10, pp. 1575–1577, 2010.

[21] J. Cho, J.-Y. Kong, D.-Y. Jeong, K. D. Lee, D. U. Lee, and B. S. Kang, "NMDA recepter-mediated neuroprotection by essential oils from the rhizomes of *Acorus gramineus*," *Life Sciences*, vol. 68, no. 13, pp. 1567–1573, 2001.

[22] S. Kim, Y. Lee, and J. Cho, "Korean red ginseng extract exhibits neuroprotective effects through inhibition of apoptotic cell death," *Biological & Pharmaceutical Bulletin*, vol. 37, no. 6, pp. 938–946, 2014.

[23] J. Cho, H. M. Kim, J. H. Ryu, Y. S. Jeong, Y. S. Lee, and C. Jin, "Neuroprotective and antioxidant effects of the ethyl acetate fraction prepared from *Tussilago farfara* L," *Biological & Pharmaceutical Bulletin*, vol. 28, no. 3, pp. 455–460, 2005.

[24] K. Lee, C. Park, Y. Oh, H. Lee, and J. Cho, "Antioxidant and neuroprotective effects of *N*-((3,4-dihydro-2H-benzo[h]chromen-2-yl)methyl)-4-methoxyaniline in primary cultured rat cortical cells: involvement of ERK-CREB signaling," *Molecules*, vol. 23, no. 3, 2018.

[25] J. Cho and D. L. Gruol, "The chemokine CCL2 activates p38 mitogen-activated protein kinase pathway in cultured rat hippocampal cells," *Journal of Neuroimmunology*, vol. 199, no. 1-2, pp. 94–103, 2008.

[26] J. Cho and H. K. Lee, "Wogonin inhibits excitotoxic and oxidative neuronal damage in primary cultured rat cortical cells," *European Journal of Pharmacology*, vol. 485, no. 1-3, pp. 105–110, 2004.

[27] J. Sattayasai, P. Chaonapan, T. Arkaravichie et al., "Protective effects of mangosteen extract on H_2O_2-induced cytotoxicity in SK-N-SH cells and scopolamine-induced memory impairment in mice," *PLoS One*, vol. 8, no. 12, article e85053, 2013.

[28] M. Moniruzzaman, Y. W. Chin, and J. Cho, "HO-1 dependent antioxidant effects of ethyl acetate fraction from *Physalis alkekengi* fruit ameliorates scopolamine-induced cognitive impairments," *Cell Stress & Chaperones*, vol. 23, no. 4, pp. 763–772, 2018.

[29] L. Chen, L. Liu, J. Yin, Y. Luo, and S. Huang, "Hydrogen peroxide-induced neuronal apoptosis is associated with inhibition of protein phosphatase 2A and 5, leading to activation of MAPK pathway," *The International Journal of Biochemistry & Cell Biology*, vol. 41, no. 6, pp. 1284–1295, 2009.

[30] S. Okuda, N. Nishiyama, H. Saito, and H. Katsuki, "Hydrogen peroxide-mediated neuronal cell death induced by an endogenous neurotoxin, 3-hydroxykynurenine," *Proceedings of the National Academy of Sciences of the United States of America*, vol. 93, no. 22, pp. 12553–12558, 1996.

[31] R. Harrison, "Structure and function of xanthine oxidoreductase: where are we now?," *Free Radical Biology & Medicine*, vol. 33, no. 6, pp. 774–797, 2002.

[32] C. E. Berry and J. M. Hare, "Xanthine oxidoreductase and cardiovascular disease: molecular mechanisms and pathophysiological implications," *The Journal of Physiology*, vol. 555, no. 3, pp. 589–606, 2004.

[33] Y. W. Chin, H. A. Jung, H. Chai, W. J. Keller, and A. D. Kinghorn, "Xanthones with quinone reductase-inducing activity from the fruits of *Garcinia mangostana* (mangosteen)," *Phytochemistry*, vol. 69, no. 3, pp. 754–758, 2008.

[34] J. Chandra, A. Samali, and S. Orrenius, "Triggering and modulation of apoptosis by oxidative stress," *Free Radical Biology & Medicine*, vol. 29, no. 3-4, pp. 323–333, 2000.

[35] A. Barbouti, P. T. Doulias, L. Nousis, M. Tenopoulou, and D. Galaris, "DNA damage and apoptosis in hydrogen peroxide-exposed Jurkat cells: bolus addition versus continuous generation of H_2O_2," *Free Radical Biology & Medicine*, vol. 33, no. 5, pp. 691–702, 2002.

[36] Y. Jaisin, P. Ratanachamnong, C. Kuanpradit, W. Khumpum, and S. Suksamrarn, "Protective effects of γ-mangostin on 6-OHDA-induced toxicity in SH-SY5Y cells," *Neuroscience Letters*, vol. 665, pp. 229–235, 2018.

[37] M. P. Mattson, "Pathways towards and away from Alzheimer's disease," *Nature*, vol. 430, no. 7000, pp. 631–639, 2004.

[38] M. E. Hasselmo, "The role of acetylcholine in learning and memory," *Current Opinion in Neurobiology*, vol. 16, no. 6, pp. 710–715, 2006.

[39] R. Mayeux, "Therapeutic strategies in Alzheimer's disease," *Neurology*, vol. 40, no. 1, pp. 175–180, 1990.

[40] M. Weinstock, "The pharmacotherapy of Alzheimer's disease based on the cholinergic hypothesis: an update," *Neurodegeneration*, vol. 4, no. 4, pp. 349–356, 1995.

[41] K. Y. Khaw, S. B. Choi, S. C. Tan, H. A. Wahab, K. L. Chan, and V. Murugaiyah, "Prenylated xanthones from mangosteen as promising cholinesterase inhibitors and their molecular docking studies," *Phytomedicine*, vol. 21, no. 11, pp. 1303–1309, 2014.

[42] H. W. Ryu, S. R. Oh, M. J. Curtis-Long, J. H. Lee, H. H. Song, and K. H. Park, "Rapid identification of cholinesterase inhibitors from the seedcases of mangosteen using an enzyme affinity assay," *Journal of Agricultural and Food Chemistry*, vol. 62, no. 6, pp. 1338–1343, 2014.

[43] Y. Fan, J. Hu, J. Li et al., "Effect of acidic oligosaccharide sugar chain on scopolamine-induced memory impairment in rats and its related mechanisms," *Neuroscience Letters*, vol. 374, no. 3, pp. 222–226, 2005.

Hindawi
Oxidative Medicine and Cellular Longevity
Volume 2019, Article ID 8673521, 10 pages
https://doi.org/10.1155/2019/8673521

Research Article

Eleutherococcus Species Cultivated in Europe: A New Source of Compounds with Antiacetylcholinesterase, Antihyaluronidase, Anti-DPPH, and Cytotoxic Activities

Kuba Adamczyk,[1] Marta Olech,[2] Jagoda Abramek,[3] Wioleta Pietrzak,[2] Rafał Kuźniewski,[1] Anna Bogucka-Kocka,[3] Renata Nowak,[2] Aneta A. Ptaszyńska,[4] Alina Rapacka-Gackowska,[1] Tomasz Skalski,[1] Maciej Strzemski,[5] Ireneusz Sowa,[5] Magdalena Wójciak-Kosior,[5] Marcin Feldo,[6] and Daniel Załuski[1]

[1]*Department of Pharmacognosy, Ludwik Rydygier Collegium Medicum, Nicolaus Copernicus University, 9 Marie Curie-Skłodowska Street, 85-094 Bydgoszcz, Poland*
[2]*Department of Pharmaceutical Botany, Medical University of Lublin, 1 Chodźki Street, 20-093 Lublin, Poland*
[3]*Department of Biology and Genetics, Medical University of Lublin, 4a Chodźki Street, 20-093 Lublin, Poland*
[4]*Department of Botany and Mycology, Institute of Biology and Biochemistry, Faculty of Biology and Biotechnology, Maria Curie-Skłodowska University, Lublin, Poland*
[5]*Department of Analytical Chemistry, Medical University of Lublin, Chodźki 4a, 20-093 Lublin, Poland*
[6]*Department of Vascular Surgery and Angiology, Medical University of Lublin, Lublin, Poland*

Correspondence should be addressed to Daniel Załuski; daniel_zaluski@onet.eu

Received 5 October 2018; Revised 10 December 2018; Accepted 18 February 2019; Published 10 March 2019

Guest Editor: Luciana Scotti

Secondary metabolites of the roots of *Eleutherococcus* spp. cultivated in Poland, or the bioactivity, are not fully known. The 75% methanol extracts of five *Eleutherococcus* spp. (*E. senticosus*, *E. divaricatus*, *E. sessiliflorus*, *E. gracilistylus*, and *E. henryi*) were examined for the content of polyphenols and phenolic acids as well as for antiacetylcholinesterase, antihyaluronidase, anti-DPPH*, and cytotoxic activities. The richest in polyphenols were the roots of *E. henryi* (10.4 mg/g DW), while in flavonoids the roots of *E. divaricatus* (6.5 mg/g DW). The richest in phenolic acids occurred the roots of *E. henryi* [protocatechuic acid (1865 μg/g DE), caffeic acid (244 μg/g DE), and *p*-coumaric and ferulic acids (55 μg/g DE)]. The highest inhibition of AChE was observed for *E. gracilistylus* and *E. sessiliflorus* (32%), at the concentration of 100 μg/0.19 mL of the reaction mixture, while that of Hyal for the roots of *E. henryi* (40.7%), at the concentration of 100 μg/0.16 mL of the reaction mixture. Among five species tested, the *E. henryi* extract exhibited the strongest HL-60 cell line growth's inhibition (IC_{50} 270 μg/mL). The extracts reduced DPPH* in a time-dependent mode, at the concentration of 0.8 mg/mL. After 90 min from 14.7 to 26.2%, DPPH* was reduced. A phytochemical composition and activity of the *Eleutherococcus* species, cultivated in Poland, are still under research; however, on the basis of the results obtained, it may be concluded that they may become a source of phytochemicals and be useful for Europe's citizens.

1. Introduction

There are at least 250,000 species of higher plants that exist on the planet, but merely 5-10% of these have been investigated so far. Because plants represent an unlimited source of novel chemical entities (NCE) with potential as drug leads, they are still used by herbalists to treat various ailments [1]. The *Eleutherococcus* species are mostly found in eastern Asia and the far eastern areas of the Russian taiga. The species are a source of plant-based chemicals, such as eleutherosides (derivatives of lignans, coumarins, and phenylpropanoids). These compounds are said to be

responsible for antioxidative, immunomodulating, hepatoprotective, antirheumatic, or anti-inflammatory activities [2–8]. One of the best-known worldwide species from this genus is *Eleutherococcus senticosus* (Rupr. et Maxim.) Maxim. that has been used in TCM (Traditional Chinese Medicine) for years to treat combined neurosis, coronary heart disease, inflammation, angina pectoris, stress-induced pathophysiologic changes, and menopausal syndrome. That species has been recognized as an adaptogenic plant. The adaptogen increases the state of nonspecific resistance and is safe in long-term use in the appropriate dose level. In addition to this, the adaptogen should reduce stress reactions in the alarm phase. Some researchers think that eleutherosides are responsible for that activity, whereas the others do not. Nevertheless, there has been a lack of studies on isolated eleutherosides and their adaptogenic activity [3, 5, 9–11].

In the literature, there is no information on an antihyaluronidase (anti-Hyal) activity of *Eleutherococcus* spp., apart from Załuski et al.'s reports [6, 12]. Hyaluronidase is the enzyme that takes part in tumor invasiveness and the development of inflammation. The overexpression of Hyal has an impact, among others, on the development of varicose veins [13, 14]. The Hyal inhibitors used in the treatment have a low inhibitory potency (aescin isolated from *Hippocastani semen*; *Aesculus hippocastanum* L.), and new inhibitors are required in the clinic.

In the TCM, *Eleutherococcus* spp. are used to improve a mental process; however, the biochemical mechanisms of their action are not yet known. In a majority of studies, an inhibitory effect on amyloid β (Aβ) peptide formation is reported, in *in vitro* and *in vivo* models [15, 16]. There are not a lot of reports on the inhibitory activity of *Eleutherococcus* spp. towards acetylcholinesterase (AChE).

Taking into account the above information, the phytochemical and ethnopharmacological knowledge of *Eleutherococcus* spp. should be now confirmed with using new approaches, in *in vitro* and *in vivo* models. A chemical metabolomics strategy is used to identify the potential biomarkers for assessing their action mechanism and searching for the structure-activity relationship. The knowledge about their valuable medicinal properties is based, mainly, on the Traditional Chinese Medicine and scientific investigations done in Asia. The European species have not been investigated in details; therefore, the results of these studies may become an alternative for the species imported from Asia, very often, with poor quality and substituted with *Periploca sepium*.

As part of a program to search for bioactive constituents from *Eleutherococcus* species, the aim of this study was to evaluate whether the 75% methanol extracts from the roots of five *Eleutherococcus* species contain phytochemicals inhibiting the activity of Hyal, AChE, DPPH*, and the HL-60 cell line's growth. The phenolic acid profile has been also determined.

2. Experimental

2.1. Standards and Reagents. Standards of caffeic, ferulic, gallic, protocatechuic, 4-OH-benzoic, salicylic, rosmarinic, vanillic, syringic, *m*-coumaric, *p*-coumaric, and veratric acids and LC grade acetonitrile were provided by Sigma-Aldrich Fine Chemicals (St. Louis, MO, USA). Gentisic and sinapic acid were provided by ChromaDex (Irvine, USA). Folin-Ciocalteu reagent, 1,1-diphenyl-2-picryl-hydrazyl (DPPH), ascorbic acid, DMSO, bovine albumin, hyaluronidase from bovine testes type I-S, *Streptococcus equi* hyaluronic acid, DTNB (5,5′-dithiobis(2-nitrobenzoic acid)), acetylcholinesterase (AChE), ACTI (acetylthiocholine iodide), and sodium phosphate buffer pH 7.0 were obtained from Sigma-Aldrich. $FeCl_3$ and methanol were obtained from POCH (Lublin, Poland). The acetate buffer, pH 4.5, was purchased from J.T.Baker, USA. Liquid chromatography- (LC-) grade methanol (MeOH) and acetonitrile (ACN) were purchased from Merck (Darmstadt, Germany). LC grade water was prepared using a Millipore Direct-Q3 purification system (Bedford, MA, USA). All reagents were of analytical grade.

2.2. Plant Materials. The roots of *E. senticosus* (Rupr. et Maxim.) Maxim., *E. divaricatus* (Siebold et Zucc.) S.Y. Hu, *E. sessiliflorus* (Rupr. et Maxim.) S.Y. Hu, *E. gracilistylus* (W.W. Smith) S.Y. Hu, and *E. henryi* Oliv. were obtained from the arboretum in Rogów (Poland) in October 2017. Voucher specimen was deposited at the Department of Pharmacognosy, Collegium Medicum in Bydgoszcz, Poland (Nr.: ES01/17, ED02/17, ESes04/17, EG05/17, EH06/17). The following are the growth's conditions: geographic data 51° 49′N and 19° 53′E; the average, long-term temperature—20.1°C, the 6bth subclimate (according to USDA Frost Hardiness Zones), and the second zone according to the Kórnik's category. These plants are grown on the acidic, luvic, and sandy soils.

2.3. Dried Material Extraction with 75% Methanol. The air--dried, grinded roots (10 g each) were soaked in 100 mL of 75% methanol for 24 h. Subsequently, the samples were sonificated three times (100, 2 × 50 mL of 75% methanol) in the following conditions: room temperature and time 15 min for each cycle. Finally, 200 mL of each extract was obtained. The solvents were evaporated under vacuum conditions at 45°C and subjected to lyophilisation. The extraction yield was calculated based on the dry weight of the extract (%).

2.4. Total Phenolic Content (TPC). The total phenolic content of extracts was determined using the method of Singleton and Rossi [17]. Gallic acid was used to calculate the calibration curve (20-100 μg/mL; $y = 0.0026x + 0.044$; $r^2 = 0.999$), and TPC was expressed as gallic acid equivalents (GAE/mL). The experiments were done in triplicate.

2.5. Total Flavonoid Content (TFC). The TFC in investigated samples was determined using the $FeCl_3$ method [18]. TFC were expressed as the mean (±S.E.) mg of quercetin equivalent (QEs/mL for $FeCl_3$ method; 20-100 μg/mL; $y = 0.0041x + 0.236$; $r^2 = 0.999$). The experiments were done in triplicate.

2.6. LC-ESI-MS/MS Conditions of Analysis of Phenolic Acids. Phenolic acid profile was determined according to the modified methods of Nowacka et al., [19], Pietrzak et al., [20], and Załuski et al., [12]. In this case, the Agilent 1200 Series HPLC system (Agilent Technologies, USA) connected to a

3200 QTRAP MS/MS (AB Sciex, USA) was used. The separation's conditions were as follows: temperature 25°C, a Zorbax SB-C18 column (2.1 × 50 mm, 1.8 μm particle size; Agilent Technologies. USA), and injection volume 3 μL. Gradient elution was applied using water containing 0.1% HCOOH (A) and methanol (B) with the flow rate of 500 μL/min. The gradient was as follows: 0-1 min 5% B; 2-3 min 20% B; 5-8 min 100% B; and 9-12 min 5% B.

To quantify phenolic acids, the parameters of analysis were optimized. The 3200 QTRAP ESI-MS/MS system in the negative mode was used. The optimal mass spectrometer parameters were as follows: curtain gas 25 psi; capillary temperature 500°C; nebulizer gas 60 psi; and negative ionization mode source voltage -4500 V. Nitrogen was used as a curtain and collision gas. For the quantitative analysis of compounds, the data were processed using Analyst 1.5 software from AB Sciex, USA, and in a multiple reaction monitoring system (MRM). The identification of analytes was done by comparing the retention times and m/z values obtained by MS and MS2 with the mass spectra of the corresponding standards tested under the same conditions. The calibration curves obtained in the MRM mode were used for the quantification of all analytes. The identified compounds were quantified based on their peak areas and comparison with a calibration curve for the corresponding standards. Linearity ranges for calibration curves were specified. The limits of detection (LOD) and quantification (LOQ) for phenolic acids were determined at a signal-to-noise ratio of 3 : 1 and 10 : 1, respectively, by injecting a series of dilute solutions of known concentrations.

2.7. Antihyaluronidase Studies. The modified spectrophotometric method was used to determine the antihyaluronidase (Hyal) activity of the extracts [21]. The extracts (4.6 mg/mL) were dissolved in 10% water ethanol solution, the final concentration in the reaction's mixture was 100 μg/0.16 mL. 50 μL of enzyme (30 U/mg) in acetate buffer pH 4.5, 50 μL of sodium phosphate buffer (50 mM, pH 7.0; with 77 mM NaCl and 1 mg/mL of albumin), and 22 μL of the analyzed samples were combined and next incubated at 37°C for 10 min. After that time, 50 μL of HA (0.3 mg/mL of acetate buffer pH 4.5) was added and incubated at 37°C for 45 min. The unhydrolyzed HA was precipitated with 1 mL acid albumin solution (0.1% bovine serum albumin in 24 mM sodium acetate and 85 mM acetic acid). After 10 min incubation of the mixture at room temperature, the absorbance of the mixture was measured at 600 nm (Multi-Detection Microplate Reader Synergy™ HT, BioTek). Aescin was used as the positive control at the following concentration 0.05, 0.1, 0.2, 0.4, 0.6, and 0.8 mg/0.16 mL, and the absorbance in the absence of enzyme was used as the blind control. All assays were done in triplicate. The percentage of inhibition was calculated as follows:

$$\%\,\text{inhibition} = \frac{(\text{AB} - \text{AE})}{(\text{AS} - \text{AE})} \times 100, \quad (1)$$

where AB is the absorbance of the enzyme+substrate +extract, AE is the absorbance of the enzyme+substrate sample, and AS is the absorbance of the enzyme+substance sample.

2.8. Antiacetylcholinesterase Studies. To determine the ability of the extracts to inhibit AChE, the modified spectrophotometric method of Ellman et al. [22] was applied. The extracts (1.0 mg/mL) were dissolved in 10% water ethanol solution. The final concentration in the reaction's mixture was 100 μg/0.19 mL. Physostigmine was used as the positive control at the following concentrations: 2, 3, 4, 15, 30, and 40 μg/0.19 mL. Every assay was done in triplicate.

2.9. Cytotoxic Activity. Leukemic cells (HL-60-human Caucasian promyelocytic leukemia from American Type Culture Collection (ATCC CCL-240™)) were incubated at the concentration of 5×10^5 cells/mL in 5% CO_2 atmosphere for 24 h at 37°C, in a growing medium [RPMI 1640 medium (Sigma-Aldrich, St. Luis, USA), with 15% fetal bovine serum (Sigma-Aldrich), 2 mM L-glutamine, and antibiotics (100 U/mL penicillin, 100 μM/mL streptomycin, and 2.5 μg/mL amphotericin B; Gibco, Carlsbad, USA)].

The trypan blue test was used to assay the extracts' cytotoxicity. The cell lines were treated with different concentrations of the extracts (from 10 to 500 μg/mL of cell culture) and incubated for 24 h at 37°C in air atmosphere humidified by 5% CO_2. After that, the medium was removed from each plate by aspiration, the cells were washed with PBS and centrifuged at 800 rpm for 10 min, and PBS was removed by aspiration. Then, 10 μL suspension cells were incubated for 5 min with the 10 μL 0.4% trypan blue solution (Bio-Rad Laboratories Inc., Hercules, CA) and analyzed using an Olympus BX41 light microscope. The extracts were dissolved in DMSO. As a positive control, podophyllotoxin was used. The experiments were done in triplicate.

2.10. DPPH Assay. The DPPH* scavenging activity of the extracts was measured by using the modified method of Brand-Williams et al. [23]. The extracts' concentration was 0.8 mg/mL. As a positive control, ascorbic acid was used (1, 10, 20, 40, and 80 μg/mL). A multidetection BioTek spectrophotometer was applied to measurement of absorbance. The experiments were done in triplicate.

2.11. Statistical Analysis. Determinations were performed by triplicate. The Statistica 7.0. programme (StatSoft, Cracow) was used for the statistical analysis. The evaluations were analyzed for one-factor variance analysis. Statistical differences between the treatment groups were estimated by Spearman's (R) and Person's (r) tests. All statistical tests were carried out at significance level of $\alpha = 0.05$.

3. Results and Discussion

3.1. Extraction Yield, TPC, and TFC Contents. The extraction of the roots yielded 5.7 and 10.7%. The extracts were a yellow-brown, odorless powder. The 75% methanol root extracts contained 4.1 to 10.4 mg of polyphenols (mg GAE/g DW) and 1.8 to 6.5 mg of flavonoids (mg QEs/g DW), (Table 1). The richest in polyphenols were the roots of *E. henryi* (10.4 mg/g DW), while in flavonoids the roots of *E.*

Table 1: Yield, TPC, and TFC in 75% methanol extracts from the roots of *Eleutherococcus* spp. (g GAE/g and QEs/g DW*).

Sample	Yield (%)	TPC	TFC
E. gracilistylus	10.7	4.1 ± 1.4	1.8 ± 0.02
E. divaricatus	5.7	9.4 ± 0.9	6.5 ± 1.1
E. senticosus	8.3	7.9 ± 0.3	4.6 ± 0.9
E. henryi	6.4	10.4 ± 1.3	4.8 ± 0.3
E. sessiliflorus	10.7	9.7 ± 0.5	6.2 ± 0.7

*Results are the means ± standard deviation of triplicates.

divaricatus (6.5 mg/g DW). The previous studies of Załuski et al. [24] have shown that the 75% ethanol root extracts contained 6.9 to 10.6 mg/g DW of polyphenols. Those results are in an agreement with those obtained in another study that may suggest that both 75% ethanol and 75% methanol are the good solvents for polyphenol extraction. There is not many literature reports on polyphenols in *Eleutherococcus* spp. growing, e.g., in Asia. Ondrejovič et al. [25] studied the TPC content in the roots of *E. senticosus*, the roots of which contained 6.2 to 21.8 mg/g plant material of polyphenols. The amount was dependent on the ethanol concentration and extraction's temperature. The other studies have revealed that the roots of *E. senticosus* and *E. koreanum*, growing in Korea, contained 44 and 34 mg GAE/g DW of TPC [5]. As may be seen, the TPC is dependent on species, the type of raw material, extraction type, and solvent used. In this case, it is hard to make a reliable comparison; however, this is important that *Eleutherococcus* spp. growing in Poland contain polyphenols. When comparing the *Eleutherococcus* spp. with other medicinal plants, it should be also reported that the content of polyphenols depends on a morphological part of plants. The underground and woody tissues contain less polyphenols than the aerial parts.

3.2. LC-ESI-MS/MS Analysis of Phenolic Acids. To identify phenolic acids, a triple quadrupole tandem mass spectrometer (MS/MS) with multiple-reaction monitoring mode (MRM) spectra was employed (Tables 2 and 3). Among fourteen phenolic acids, just five were qualitatively and quantitatively determined in the roots (Table 4, Figure 1). The content of phenolic acids ranged between 11 and 1865 μg/g DE. Among five identified acids, the richest occurred in the roots of *E. henryi* (protocatechuic acid occurred in the largest amount, 1865 μg/g DE; followed by caffeic acid, 244 μg/g DE; and *p*-coumaric and ferulic acids, 55 μg/g DE, respectively). Protocatechuic acid has been detected in all species as a predominant constituent. The previous studies of Załuski et al. [6] provided that protocatechuic acid has been detected in the 75% ethanol inflorescence extracts from *E. senticosus*, *E. gracilistylus*, and *E. giraldii*, in the amounts of 614.7, 833.4 and 855.6 μg/g DE, respectively. In turn, the 75% ethanol extracts from the fruits of *E. divaricatus* and *E. sessiliflorus* contained 893 and 818 μg/100 g DE of protocatechuic acid. A lower content was quantified in the fruit infusion of these species (270 and 267 μg/100 g DE, respectively) [26].

There are not a lot of reports on phenolic acid content in *Eleutherococcus* species growing in Asia or Russia and in their native habitat. Li et al. [4] studied the content of protocatechuic acid in ten commercial *E. senticosus* samples, purchased from TCM shops of different places in China. The content varied from 3.1 to 23.1 μg/g.

Protocatechuic acid has been determined in many other plants, however, mostly in the aerial parts, which makes it difficult to interpret when compared to underground parts. The aerial parts, usually, contain more phenolic acids.

3.3. Antienzymatic Activity. Acetylcholinesterase is the enzyme located in the nervous system and muscles, which regulates the AChE concentration. It decreases the acetylcholine level which implies the gradual loss of memory and learning ability. By far, the AChE inhibitors galantamine, rivastigmine, and donepezil are commonly used. Because of their unfavorable side effects, bioprospecting studies in searching for AChEIs are still ongoing [27–29].

The *Eleutherococcus* spp. are known for their improvement of the mental ability; therefore, the impact of the extracts, at the concentration of 100 μg/0.19 mL of the reaction mixture, on AChE (5 U/mg) activity was measured (Table 5). The five extracts have been tested, for which the inhibition was established to be between 19.6 and 32%, with the highest inhibitory level for *E. gracilistylus* and *E. sessiliflorus* (32%). Physostigmine, used as a control, inhibited AChE at the level of 30% at concentration 2 μg.

The previous studies of Załuski et al. [30] on the anti-AChE activity of the 75% ethanol extracts from the roots of *Eleutherococcus* spp. have shown 50% inhibition for the extract concentration in the range of 300-1750 μg/mL. The highest activity was observed for *E. sessiliflorus* and *E. setchuenensis* (IC_{50} 300 μg/mL), the lowest for *E. henryi* (IC_{50} 1750 μg/mL). It is very interesting that in the case of two types of solvents used, 75% EtOH and 75% MeOH extracts, the same species (*E. sessiliflorus*) has shown the highest inhibitory activity.

Nino et al. [31] studied 27 methanol extracts from different species collected in Colombia (AChE, 0.3 U/mL). *Solanum leucocarpum* Dunal and *Witheringia coccoloboides* (Damm) have shown the highest inhibition (IC_{50} 204.5 and 220.6 mg/L). Nwidu et al. [32] showed that the methanol, ethyl acetate, and aqueous root fractions from *Carpolobia lutea* G. Don inhibited AChE activity with the IC_{50} value 0.3-3 μg/mL. Kostelnik and Pohanka [33] found out that boldine inhibited AChE (100 U/mg) with an IC_{50} value of 372 μmol/L. A new promising group of AChE inhibitors are compounds found in fungi and bacteria. Thabthimsuk et al. [28] studied the anti-AChE activity of polysaccharide-peptide complexes extracted from 3 types of edible fungi, including white shimeji (*Hypsizygus marmoreus*), brown shimeji (*Hypsizygus marmoreus*), and enokitake (*Flammulina velutipes*). The highest activity to inhibit AChE (0.28 U/mL) was showed by brown shimeji (71.3%). In turn, Tan et al. [27] evaluated the anti-AChE (0.22 U) activity of 55 ethyl acetate extracts from 55 bacterial strains belonging to nine bacterial families (Vibrionaceae, Bacillaceae, Microbacteriaceae, Aerococcaceae, Brevibacteriaceae, Staphylococcaceae,

Table 2: Optimized LC-MS (MRM) parameters for all analytes. Compounds confirmed by comparison with authentic standards.

Compound	Retention time (min)	Q1 (m/z)	Q3 (m/z)	DP[a] (V)	EP[b] (V)	CEP[c] (V)	CE[d] (eV)	CXP[e] (eV)
Gallic acid	1.01	168.7	178.9	-35	-3	-12	-36	0
			124.9	-35	-3	-12	-14	0
Protocatechuic acid	2.16	152.9	80.9	-55	-1	-10	-26	0
			107.8	-55	-1	-10	-38	0
Gentisic acid	3.32	352.9	80	-70	-4	-16	-110	0
			96.9	-70	-4	-16	-52	0
4-OH-benzoic acid	4.25	136.8	92.9	-30	-7	-10	-18	0
Vanillic acid	5.51	166.8	107.9	-35	-4	-12	-18	0
			123	-35	-4	-12	-12	0
Caffeic acid	5.69	178.7	88.9	-30	-6.5	-12	-46	0
			134.9	-30	-6.5	-12	-16	0
Syringic acid	6.34	196.9	122.8	-30	-9	-12	-24	0
			181.9	-30	-9	-12	-12	-2
p-Coumaric acid	6.67	162.8	93	-30	-8	-12	-44	0
			119	-30	-8	-12	-14	0
Ferulic acid	6.83	192.8	133.9	-25	-11.5	-14	-16	0
			177.9	-25	-11.5	-14	-12	-2
Salicylic acid	6.86	136.9	75	-35	-4	-10	-48	0
			93	-35	-4	-10	-16	-2
Veratric acid	6.88	180.7	121.9	-35	-6	-14	-18	0
			136.9	-35	-6	-14	-12	0
Sinapic acid	6.88	222.8	121	-35	-8.5	-10	-36	0
			148.9	-35	-8.5	-10	-20	0
m-Coumaric acid	6.89	162.8	91	-35	-4.5	-12	-36	0
			119	-35	-4.5	-12	-14	0
Rosmarinic acid	7.01	358.7	132.6	-50	-5	-26	-44	0
			160.8	-50	-5	-26	-20	-2

[a]DP: declustering potential; [b]EP: entrance potential; [c]CEP: cell entrance potential; [d]CE: collision energy; [e]CXP: collision cell exit potential.

Table 3: Limit of detection (LOD), limit of quantification (LOQ), and calibration curve parameters for all analytes.

Compound	LOD (ng/μL)	LOQ (ng/μL)	R^2	Linearity range (ng/μL)
Gallic acid	0.05	0.1	0.9991	0.1- 10
Protocatechuic acid	0.01	0.02	0.9967	0.025-25
Gentisic acid	0.008	0.015	0.9993	0.025-25
4-OH-benzoic acid	0.05	0.1	0.9972	0.1-5
Vanillic acid	0.1	0.2	0.9999	0.2-50
Caffeic acid	0.04	0.085	0.9975	0.1-5
Syringic acid	0.05	0.1	0.9997	0.1-50
p-Coumaric acid	0.01	0.025	0.9982	0.05-2.5
Ferulic acid	0.01	0.025	0.9997	0.025-5
Salicylic acid	0.01	0.02	0.9986	0.02-0.7
Veratric acid	0.4	0.7	0.9977	0.5-25
Sinapic acid	0.007	0.025	0.9987	0.025-5
m-Coumaric acid	0.02	0.05	0.9994	0.05-2.5
Rosmarinic acid	0.005	0.01	0.9985	0.025-25

Pseudoalteromonadaceae, Enterobacteriaceae, and Shewanellaceae) isolated from coral reefs in Hainan (China). The highest inhibition was shown by *Vibrio neocaledonicus* (98.9%).

In the next step, the impact of the extract on the Hyal (30 U/mg) inhibition, at the concentration 100 μg/0.16 mL of the reaction mixture, was measured (Table 5). An inhibition ranged from 9.1 to 40.7%. The most active was the extract from the roots of *E. henryi* (40.7%). In Załuski et al.'s previous studies, aescin was used as the standard compound. The 30.1% level of inhibition was obtained for the concentration of 100 μg [12]. It should be noticed that the extract possesses chemical structures that may be used as possible inhibitors of Hyal, showing a stronger potency than aescin.

Kuźniewski et al. [34] have shown that the 75% ethanol extracts from the autumn and spring leaves *E. senticosus*, at the concentration of 22 μg/0.16 mL of the reaction mixture, inhibited Hyal at the level of 74.3 and 33%, respectively. The higher inhibition of the autumn leaves might result from the higher amount of polyphenolic compounds, such as tannins.

Furusawa et al. [35] reported the anti-Hyal activity of the coffee silverskin, a by-product of the roasting procedure for coffee beans. The IC_{50} value was at the level of 0.27 mg/mL. In turn, McCook et al. [36] showed that tannic acid, at the concentration of 0.05 mg/mL, inhibited Hyal at the level of 100%. Liyanaarachchi et al. [37] studied the influence of the 18 ethanol extracts on Hyal (4200 U/mL) activity at the

Table 4: Phenolic acid contents expressed in μg per 1 g of dry weight of extracts. Mean values of three replicate assays with standard deviation.

Phenolic acid	*E. gracilistylus*	*E. divaricatus**	*E. senticosus**	*E. henryi**	*E. sessiliflorus**
Protocatechuic acid	446 ± 1	435.5 ± 5.5	838 ± 12	1865 ± 35	529 ± 1
Salicylic acid	<LOQ	30.6 ± 0.2	16.8 ± 1	<LOQ	41.4 ± 2.6
Caffeic acid	nd	49 ± 0.3	135.5 ± 3.5	244 ± 2	49.1 ± 0.3
p-Coumaric acid	30.6 ± 0.95	12.35 ± 0.12	23.6 ± 0.3	55 ± 0.2	<LOQ
Ferulic acid	64.6 ± 3	46.6 ± 3	43.9 ± 2.4	55 ± 1.8	11 ± 0.3

nd: not detected.

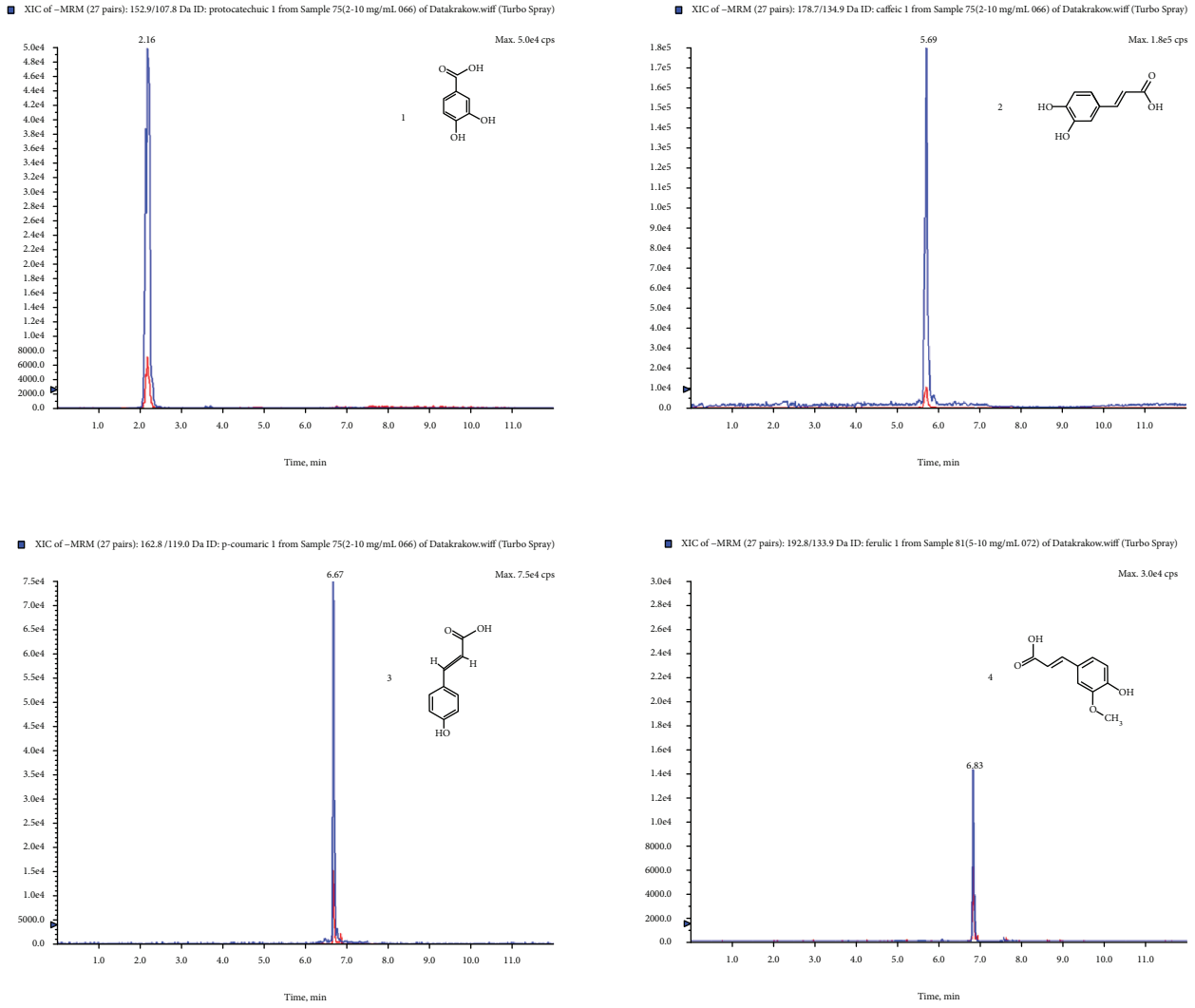

Figure 1: An exemplary chromatogram in the MRM mode of phenolic acids occurring in *E. henryi*: 1—protocatechuic acid; 2—caffeic acid; 3—*p*-coumaric acid; 4—ferulic acid.

concentration of 500 μg/mL. The studies have revealed that only 8 extracts have exhibited such an activity in the range of 34.8 and 95% of inhibition. *Curcuma aromatica* exhibited the best hyaluronidase inhibition activity (95%). Large-scale studies were performed by Hwang et al. [38], in which the inhibitory activity of 500 methanolic extracts of 500 species from medicinal plants was analyzed. Only three MeOH extracts inhibited more than 50% of Hyal activity at a concentration of 2 mg/mL. The level of inhibition for these 3 species, *Styrax japonica* (stem extract), *Deutzia coreana* (stem extract), *Osmanthus insularis* (stem-bark extract), was 57.2, 53.5, and 53.1%, respectively.

Considering the anti-AChE and anti-Hyal activities of different extracts, it is hard to make a reliable comparison because the researchers use the different enzyme activity units and extract concentrations. It is a major problem in

Table 5: Antihyaluronidase and antiacetylcholinesterase activities of extracts.

Sample	Anti-AChE* (% inhibition)	Anti-Hyal*
E. gracilistylus	32 ± 0.8	14.9 ± 0.3
E. divaricatus	23.2 ± 0.9	11 ± 0.2
E. senticosus	26.1 ± 0.05	10.4 ± 0.6
E. henryi	19.6 ± 0.4	40.7 ± 1.1
E. sessiliflorus	32 ± 0.6	9.1 ± 0.05

*Results are the means ± standard deviation of triplicates.

antienzymatic activity assays for which the general protocols for the assay should be developed. When the enzyme activity unit was given, we included it in the manuscript. This problem has been resolved, e.g., in case of cytotoxic activity, where according to the National Cancer Institute (United States) plant screening program, a crude extract is generally considered to have *in vitro* cytotoxic activity if the IC_{50} is <20 μg/mL. For compounds, the limit has been established as 4 μg/mL [39].

3.4. Cytotoxic Activity. About 6 million of people die of cancer each year, and this trend is about to grow in the next decades. Leukemia is a haematological disease caused by persistence of immature white blood cells in different compartments of the organism mainly the bone marrow, lymph node, spleen, and circulating blood. Plant-based chemicals are a promising group of antileukemic agents, especially the polyphenol group [40, 41]. Because *Eleutherococcus* spp. contain polyphenols, we have studied an antileukemic activity of the extracts. The extracts inhibited a HL-60 cell line growth with an IC_{50} value in the range of 270-2000 μg/mL (Table 6). As a positive control, podophyllotoxin was used, with the IC_{50} value of 0.0084 μg/mL. The previous studies of Załuski et al. [42], on the cytotoxic activity of the 75% ethanol extracts from the roots of *Eleutherococcus* spp., have revealed that the IC_{50} values ranged between 49 and 522 μg/mL, with the highest for *E. divaricatus* (49 μg/mL). Comparing the 75% EtOH extracts to the 75% MeOH extracts, it is seen that both types exhibited a weak inhibitory activity.

The higher IC_{50} values have been obtained for the isolated compounds and their derivatives. Hu et al. [43] studied the cytotoxic activities of five stilbenoids isolated from the stem bark of *Acanthopanax leucorrhizus* and six derivatives against HL-60. Among 17 compounds, only two derivatives (E)-3,5-dimethoxy-3′,4′-methylenedioxystilbene and 2-(3′-hydroxy-4′-isopentenyl-5′-methoxyphenyl)-4-hydroxybenzofuran exhibited moderate cytotoxicities against HL-60 cell lines with the lower IC_{50} values of 30.51 ± 5.37 and 40.23 ± 6.12 μM, respectively. In turn, isolates showed a weak inhibitory activity against HL-60, in the range of 98.6-200 μM.

The cytotoxic activity, against HL-60, was also exhibited by the different extracts [petroleum ether, Ch_2Cl_2, EtOAc, EtOH, and EtOH/H_2O (1 : 1 *v*/*v*)] prepared from the aerial parts of *Artemisia biennis* Willd. Nevertheless, high IC_{50} values have been obtained, in the range of 54.3-200 μg/mL [44]. The *n*-hexane, Ch_2Cl_2, EtOAc, EtOH, and EtOH/H_2O (1 : 1 *v*/*v*) extracts from another Artemisia species, *Artemisia turanica* Krasch., have also shown a weak cytotoxic effect with the IC_{50} values of 68.8-450 μg/mL [45]. It should be mentioned that petroleum ether, dichloromethane, ethyl acetate, ethanol, and 50% aqueous ethanol extracts of the aerial parts of *Artemisia ciniformis* inhibited HL60 cell growth with the IC_{50} value of 31.3-200 μg/mL [46].

Teixeira et al. [47] reported on the cytotoxic activity of four flavonoids isolated from the roots of *Tephrosia egregia* Sandwith. Three compounds (pongaflavone, praecansone B, and 12a-hydroxyrotenone) exhibited a high activity against HL-60 cell line with the IC_{50} values of 1.4, 8.1, and 1.9 μg/mL.

Taking into account the antileukemic activity of polyphenols, we noticed that *E. henryi* was the most active towards HL-60 and contains the highest amount of protocatechuic, *p*-coumaric, and caffeic acids. Another observation resulted from this study is that nonpolar extracts are more cytotoxic than polar ones. A moderate/low cytotoxicity in our study may result from a high polarity of extract constituents, for which a cell wall penetration is limited. Further studies are needed to confirm this activity for the isolated compounds.

3.5. The Capacity of DPPH Reduction.* It is known that free radicals are responsible for the development of many diseases, such as Parkinson's disease, Alzheimer's disease, or amyotrophic latera sclerosis. Free radicals are constantly produced in the brain *in vivo*, contributing to oxidative damage of proteins and lipids. For this reason, in searching for new antioxidants, a special attention should be paid to compounds that act as an antioxidant and inhibitor of AChE or BuChE. Nature is a significant source of health-promoting compounds that may be divided into two groups: fruits and vegetables and medicinal plants [48]. Therefore, in the next step, an antioxidative activity of the extracts was examined. The extracts reduced DPPH* in a time-dependent mode, at the concentration of 0.8 mg/mL (Figure 2). After 90 min from 14.7 to 26.2%, DPPH* was reduced. As a positive control, ascorbic acid was used, with an EC_{50} value of 38 μg/mL (after 5 min of incubation). A slow change of antioxidant activity in the time is in agreement with the adaptogen's definition, according to which, adaptogen should act slowly in a long-term mode. It should be noticed that *E. gracilistylus* expressed the highest anti-AChE activity and anti-DPPH* scavenging. Usually, free radicals are associated with the neurodegenerative process development; in this case, we can suppose that *E. gracilistylus* contain both compounds with anti-AChE activity and anti-DPPH*.

Since a few years, the main attention has been paid to fungi as a new source of antioxidants. By far, they were only of culinary interest; however, around 650 species contain therapeutic properties, e.g., *Lentinus edodes*, *Boletus edulis*, or *Grifola frondosa*. They are rich in phenolic acids, such as

Table 6: The cytotoxic impact of the extracts on HL-60 cell line (IC_{50} μg/mL).

E. gracilistylus	*E. divaricatus**	*E. senticosus**	*E. henryi**	*E. sessiliflorus**
890 ± 3.7	650 ± 2.9	450 ± 2.5	270 ± 1.1	2000 ± 3.4

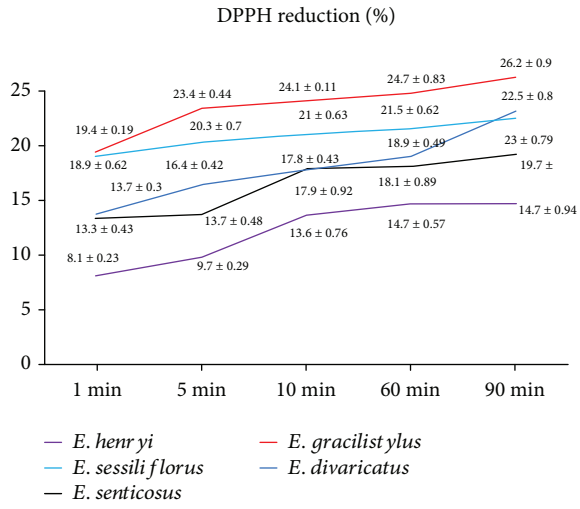

Figure 2: A time-dependent DPPH* reduction (%).

cinnamic, protocatechuic, *p*-hydroxybenzoic, *p*-coumaric, and gallic [48].

The acetonic extracts from *Boletus edulis* and *Boletus aestivalis* have showed a powerful antioxidant activity with the IC_{50} value of 4.72 and 8.63 μg/mL which were similar or greater than those of the standard antioxidants, ascorbic acid (EC_{50} 4.22 μg/mL), BHA (EC_{50} 6.42 μg/mL), and α-tocopherol (EC_{50} 62.43 μg/mL) [49]. Higher values have been obtained for *Agaricus brasiliensis* and *Agaricus bisporus*. The 60% ethanol extracts from those fungi have shown a radical scavenging capability for EC_{50} 1.6 and 2.7 mg/mL. In turn, the aqueous extracts have had the EC_{50} value at the level of 3.8 and 4.5 mg/mL [50].

4. Conclusions

The ethnopharmacological uses of *Eleutherococcus* spp. are now confirmed with an application of new approaches and tools, in *in vitro* and *in vivo* models. Considering the inhibition of an AChE activity and DPPH* reduction, new inhibitors should be searched for in the roots of *E. gracilistylus*, while inhibitors with an anti-Hyal or cytotoxic activity should be searched for in the roots of *E. henryi*. New Hyal inhibitors may have a possible use as ingredients of plant-based products, used, e.g., topically as cosmetics or in treatment of skin diseases. Taking into account the results obtained in this work, a further research should focus on the isolation of single phytochemicals being responsible for the anti-AChE, anti-Hyal, and cytotoxic effects. Further researches are needed to determine the antienzymatic activity with the use of modern approaches, such as the isothermal calorimetric titration (ITC).

Abbreviations

TPC: Total phenolic content
TFC: Total flavonoid content
DNPH: 2,4-Dinitrophenylhydrazine
$FeCl_3$: Iron (III) chloride
GA: Gallic acid
HE: Hesperetin equivalent
QE: Quercetin equivalent
DPPH*: 2,2-Diphenyl-1-picrylhydrazyl
HL-60: Human Caucasian promyelocytic leukemia from American Type Culture Collection (ATCC CCL-240™)
Hyal: Hyaluronidase
AChE: Acetylcholinesterase.

Data Availability

The data used to support the findings of this study are available from the corresponding author upon request.

Consent

Informed consent was obtained from all the participants included in the work.

Conflicts of Interest

The authors declare no competing financial interest.

Acknowledgments

This paper was developed using the equipment purchased within the project "The equipment of innovative laboratories doing research on new medicines used in the therapy of civilization and neoplastic diseases" within the Operational Program Development of Eastern Poland 2007-2013, Priority Axis I Modern Economy, Operations I.3 Innovation Promotion. This work was funded by the financial support of academic research in the Ludwik Rydygier Collegium Medicum in Bydgoszcz, Nicolaus Copernicus University in Toruń.

References

[1] W. Rungsung, K. K. Ratha, S. Dutta, A. K. Dixit, and J. Hazra, "Secondary metabolites of plants in drugs discovery," *World Journal of Pharmaceutical Research*, vol. 4, pp. 604–613, 2015.

[2] Ł. Ciesla, M. Waksmundzka-Hajnos, D. Zaluski, H. D. Smolarz, and M. Hajnos, "HPTLC-densitometric method for determination of eleutherosides B, E, and E1 in different Eleutherococcus species," *Journal of Chromatographic Science*, vol. 49, no. 3, pp. 182–188, 2011.

[3] A. Panossian, "Understanding adaptogenic activity: specificity of the pharmacological action of adaptogens and other phytochemicals," *Annals of the New York Academy of Sciences*, vol. 1401, pp. 49–64, 2017.

[4] Q. Li, Y. Jia, L. Xu et al., "Simultaneous determination of protocatechuic acid, syringin, chlorogenic acid, caffeic acid, liriodendrin and isofraxidin in *Acanthopanax senticosus* Harms by HPLC-DAD," *Biological & Pharmaceutical Bulletin*, vol. 29, pp. 532–534, 2006.

[5] A. Panossian, E. J. Seo, and T. Efferth, "Novel molecular mechanisms for the adaptogenic effects of herbal extracts on isolated brain cells using systems biology," *Phytomedicine*, vol. 50, pp. 257–284, 2018.

[6] D. Załuski, M. Olech, R. Kuźniewski, R. Verpoorte, R. Nowak, and H. D. Smolarz, "LC-ESI-MS/MS profiling of phenolics from *Eleutherococcus* spp. inflorescences, structure-activity relationship as antioxidants, inhibitors of hyaluronidase and acetylcholinesterase," *Saudi Pharmaceutical Journal*, vol. 25, pp. 734–743, 2017.

[7] D. Załuski, E. Mendyk, and H. D. Smolarz, "Identification of MMP-1 and MMP-9 inhibitors from the roots of *Eleutherococcus divaricatus*, and the PAMPA test," *Natural Product Research*, vol. 30, pp. 595–599, 2016.

[8] D. Załuski and Z. Janeczko, "Variation in phytochemicals and bioactivity of the fruits of *Eleutherococcus* species cultivated in Poland," *Natural Product Research*, vol. 29, no. 23, pp. 2207–2211, 2015.

[9] Y. Zhou, C. Cheng, D. Baranenko, J. Wang, Y. Li, and W. Lu, "Effects of *Acanthopanax senticosus* on brain injury induced by simulated spatial radiation in mouse model based on pharmacokinetics and comparative proteomics," *International Journal of Molecular Sciences*, vol. 19, no. 1, p. 159, 2018.

[10] M. X. Lu, Y. Yang, Q. P. Zou et al., "Anti-diabetic effects of Acankoreagenin from the leaves of *Acanthopanax gracilistylus* herb in RIN-m5F cells via suppression of NF-κB activation," *Molecules*, vol. 23, no. 4, p. 958, 2018.

[11] W. Dimpfel, L. Schombert, and A. G. Panossian, "Assessing the quality and potential efficacy of commercial extracts of *Rhodiola rosea* L. by analyzing the salidroside and rosavin content and the electrophysiological activity in hippocampal long-term potentiation, a synaptic model of memory," *Frontiers in Pharmacology*, vol. 9, p. 425, 2018.

[12] D. Załuski, M. Olech, A. Galanty et al., "Phytochemical content and pharma-nutrition study on *Eleutherococcus senticosus* fruits intractum," *Oxidative Medicine and Cellular Longevity*, vol. 2016, Article ID 9270691, 10 pages, 2016.

[13] K. Madan and S. Nanda, "*In-vitro* evaluation of antioxidant, anti-elastase, anti-collagenase, anti-hyaluronidase activities of *safranal* and determination of its sun protection factor in skin photoaging," *Bioorganic Chemistry*, vol. 77, pp. 159–167, 2018.

[14] D. Załuski, Ł. Cieśla, and Z. Janeczko, "The structure-activity relationships of plant secondary metabolites with antimicrobial, free radical scavenging and inhibitory activity towards selected enzymes," in *Studies in Natural Product Chemistry (Bioactive Natural Products)*, A.-u. Rahman, Ed., vol. 45, pp. 217–249, Elsevier science publishers, Amsterdam, the Netherlands, 2015.

[15] C. Tohda, M. Ichimura, and Y. Bai, "Inhibitory effects of *Eleutherococcus senticosus* extracts on amyloid β(25-35)–induced neuritic atrophy and synaptic loss," *Journal of Pharmacological Sciences*, vol. 107, pp. 329–339, 2008.

[16] D. Lee, "Neuroprotective effects of *Eleutherococcus senticosus* bark on transient global cerebral ischemia in rats," *Journal of Ethnopharmacology*, vol. 139, pp. 6–11, 2012.

[17] V. L. Singleton and J. A. Rossi, "Colometry of total phenolics with phosphomolybdic- phospotungstic acid reagents," *American Journal of Enology Viticulture*, vol. 16, pp. 144–158, 1965.

[18] C. C. Chang, M. H. Yang, H. M. Wen, and J. C. Chern, "Estimation of total flavonoid content in propolis by two complementary colorimetric methods," *Journal of Food and Drug Analysis*, vol. 10, pp. 178–182, 2002.

[19] N. Nowacka, R. Nowak, M. Drozd, M. Olech, R. Los, and A. Malm, "Analysis of phenolic constituents, antiradical and antimicrobial activity of edible mushrooms growing wild in Poland," *LWT - Food Science and Technology*, vol. 59, pp. 689–694, 2014.

[20] W. Pietrzak, R. Nowak, U. Gawlik-Dziki, M. K. Lemieszek, and W. Rzeski, "LC-ESI-MS/MS identification of biologically active phenolic compounds in mistletoe berry extracts from different host trees," *Molecules*, vol. 22, no. 4, p. 624, 2017.

[21] Y. A. Yahaya and M. M. Don, "Evaluation of *Trametes lactinea* extracts on the inhibition of hyaluronidase, lipoxygenase and xanthine oxidase activities *in vitro*," *Journal of Physical Science*, vol. 23, no. 2, pp. 1–15, 2012.

[22] G. L. Ellman, K. D. Courtney, V. Andres jr., and R. M. Featherstone, "A new and rapid colorimetric determination of acetylcholinesterase activity," *Biochemical Pharmacology*, vol. 7, no. 2, pp. 88–95, 1961.

[23] W. Brand-Williams, M. E. Cuvelier, and C. Berset, "Use of a free radical method to evaluate antioxidant activity," *LWT - Food Science and Technology*, vol. 28, pp. 25–30, 1995.

[24] D. Załuski, H. D. Smolarz, and U. Gawlik-Dziki, "Bioactive compounds and antioxidative, antileukemic and anti-MMPs activity of Eleutherococcus species cultivated in Poland," *Natural Product Communications*, vol. 7, no. 11, pp. 1483–1486, 2012.

[25] M. Ondrejovič, D. Chmelová, and T. Maliar, "Optimization of the antioxidant extraction from *Eleutherococcus senticosus* roots by response surface methodology," *Nova Biotechnologica et Chimica*, vol. 12, no. 1, pp. 30–38, 2013.

[26] D. Załuski, M. Olech, R. Verpoorte, I. Khan, R. Kuźniewski, and R. Nowak, "Phytoconstituents and nutritional properties of the fruits of *Eleutherococcus divaricatus* and *Eleutherococcus sessiliflorus*: a study of non-European species cultivated in Poland," *Oxidative Medicine and Cellular Longevity*, vol. 2017, Article ID 8374295, 7 pages, 2017.

[27] L. Tan, S. Guo, F. Ma, C. Chang, and I. Gómez-Betancur, "In vitro inhibition of acetylcholinesterase, alphaglucosidase, and xanthine oxidase by bacteria extracts from coral reef in Hainan, South China Sea," *Journal of Marine Science and Engineering*, vol. 6, no. 2, p. 33, 2018.

[28] S. Thabthimsuk, N. Panya, A. Owatworakit, and W. Choksawangkarn, "Acetylcholinesterase inhibition and antioxidant activities of polysaccharide-peptide complexes from edible mushrooms," in *The 6th International Conference on Biochemistry and Molecular Biology*, Thailand, 2018.

[29] M. T. N. S. Lima, L. B. d. Santos, R. W. Bastos, J. R. Nicoli, and J. A. Takahashi, "Antimicrobial activity and acetylcholinesterase inhibition by extracts from chromatin modulated fungi," *Brazilian Journal of Microbiology*, vol. 49, no. 1, pp. 169–176, 2018.

[30] D. Załuski and R. Kuźniewski, "*In vitro* anti-AChE, anti--BuChE, and antioxidant activity of 12 extracts of *Eleutherococcus* species," *Oxidative Medicine and Cellular Longevity*, vol. 2016, Article ID 4135135, 7 pages, 2016.

[31] J. Niño, J. A. Hernández, Y. M. Correa, and O. M. Mosquera, "In vitro inhibition of acetylcholinesterase by crude plant extracts from Colombian flora," *Memórias do Instituto Oswaldo Cruz*, vol. 101, no. 7, pp. 783–785, 2006.

[32] L. L. Nwidu, E. Elmorsy, J. Thornton et al., "Anti-acetylcholinesterase activity and antioxidant properties of extracts and fractions of *Carpolobia lutea*," *Pharmaceutical Biology*, vol. 55, pp. 1875–1883, 2017.

[33] A. Kostelnik and M. Pohanka, "Inhibition of acetylcholinesterase and butyrylcholinesterase by a plant secondary metabolite boldine," *BioMed Research International*, vol. 2018, Article ID 9634349, 5 pages, 2018.

[34] R. Kuźniewski, D. Załuski, M. Olech, P. Banaszczak, and R. Nowak, "LC-ESI-MS/MS profiling of phenolics in the leaves of *Eleutherococcus senticosus* cultivated in the West Europe and anti-hyaluronidase and anti-acetylcholinestarase activities," *Natural Product Research*, vol. 32, pp. 448–452, 2018.

[35] M. Furusawa, Y. Narita, K. Iwai, T. Fukunaga, and O. Nakagiri, "Inhibitory effect of a hot water extract of coffee "silverskin" on hyaluronidase," *Bioscience, Biotechnology, and Biochemistry*, vol. 75, pp. 1205–1207, 2011.

[36] J. McCook, P. Dorogi, D. Vasily, and D. Cefalo, "In vitro inhibition of hyaluronidase by sodium copper chlorophyllin complex and chlorophyllin analogs," *Clinical, Cosmetic and Investigational Dermatology*, vol. 8, pp. 443–448, 2015.

[37] G. D. Liyanaarachchi, J. K. R. R. Samarasekera, K. R. R. Mahanama, and K. D. P. Hemalal, "Tyrosinase, elastase, hyaluronidase, inhibitory and antioxidant activity of Sri Lankan medicinal plants for novel cosmeceuticals," *Industrial Crops and Products*, vol. 111, pp. 597–605, 2018.

[38] S. G. Hwang, A. Yang, S. J. Kim et al., "Screening of hyaluronidase inhibitor in Korean medicinal plants," *Journal of Life Science*, vol. 24, pp. 498–504, 2014.

[39] V. Kuete, B. Wiench, M. E. F. Hegazy et al., "Antibacterial activity and cytotoxicity of selected Egyptian medicinal plants," *Planta Medica*, vol. 78, pp. 193–199, 2012.

[40] S. Taverna and C. Corrado, "Natural compounds: molecular weapons against Leukemia's," *Journal of Leukemia*, vol. 5, no. 1, p. 226, 2017.

[41] Y. Han, A. H. Zhang, Y. Z. Zhang, H. Sun, X. C. Meng, and X. J. Wang, "Chemical metabolomics for investigating the protective effectiveness of *Acanthopanax senticosus* Harms leaf against acute promyelocytic leukemia," *RSC Advances*, vol. 8, no. 22, pp. 11983–11990, 2018.

[42] D. Załuski, H. D. Smolarz, and A. Bogucka-Kocka, "Cytotoxic activity of ethanolic extracts of Eleutherococcus species cultivated in Poland on HL60 leukemia cell line," *Current Issues in Pharmacy and Medical Sciences*, vol. 27, pp. 41–45, 2014.

[43] H. B. Hu, H. P. Liang, H. M. Li et al., "Isolation, modification and cytotoxic evaluation of stilbenoids from *Acanthopanax leucorrhizus*," *Fitoterapia*, vol. 124, pp. 167–176, 2018.

[44] Z. Tayarani-Najaran, F. S. Makki, N. S. Alamolhodaei, M. Mojarrab, and S. A. Emami, "Cytotoxic and apoptotic effects of different extracts of *Artemisia biennis* Willd. on K562 and HL-60 cell lines," *Iranian Journal of Basic Medical Sciences*, vol. 20, no. 2, pp. 166–171, 2017.

[45] Z. Tayarani-Najaran, M. Sareban, A. Gholami, S. A. Emami, and M. Mojarrab, "Cytotoxic and apoptotic effects of different extracts of *Artemisia turanica* Krasch. on K562 and HL-60 cell lines," *The Scientific World Journal*, vol. 2013, Article ID 628073, 6 pages, 2013.

[46] Z. Tayarani-Najaran, Z. Hajian, M. Mojarrab, and S. A. Emami, "Cytotoxic and apoptotic effects of extracts of Artemisia ciniformis Krasch. & Popov ex Poljakov on K562 and HL-60 cell lines," *Asian Pacific Journal of Cancer Prevention*, vol. 15, pp. 7055–7059, 2014.

[47] M. V. S. Teixeira, J. Q. Lima, A. T. A. Pimenta et al., "New flavone and other compounds from *Tephrosia egregia*: assessing the cytotoxic effect on human tumor cell lines," *Revista Brasileira de Farmacognosia*, vol. 28, no. 3, pp. 333–338, 2018.

[48] A. Haseeb, H. Ghulam, and M. Imtiaz, "Antioxidants from natural sources," in *Chapter 1 in Book: Antioxidants in Food and Its Application*, pp. 1–27, IntechOpen Publisher, 2018.

[49] M. Kosanić, B. Ranković, and M. Dašić, "Mushrooms as possible antioxidant and antimicrobial agents," *Iranian Journal of Pharmaceutical Research*, vol. 11, no. 4, pp. 1095–1102, 2012.

[50] C. H. Gan, B. Nurul Amira, and R. Asmah, "Antioxidant analysis of different types of edible mushrooms (*Agaricus bisporous* and *Agaricus brasiliensis*)," *International Food Research Journal*, vol. 20, pp. 1095–1102, 2013.

Hindawi
Oxidative Medicine and Cellular Longevity
Volume 2019, Article ID 8639618, 13 pages
https://doi.org/10.1155/2019/8639618

Research Article

Honokiol-Mediated Mitophagy Ameliorates Postoperative Cognitive Impairment Induced by Surgery/Sevoflurane via Inhibiting the Activation of NLRP3 Inflammasome in the Hippocampus

Ji-Shi Ye,[1] Lei Chen,[2] Ya-Yuan Lu,[2] Shao-Qing Lei,[1] Mian Peng,[2] and Zhong-Yuan Xia[1]

[1]*Department of Anesthesiology, Renmin Hospital of Wuhan University, Wuhan, 430060 Hubei, China*
[2]*Department of Anesthesiology, Zhongnan Hospital of Wuhan University, 169, Donghu Road, Wuhan, 430071 Hubei, China*

Correspondence should be addressed to Zhong-Yuan Xia; xiazhongyuan2005@aliyun.com

Received 5 August 2018; Revised 16 October 2018; Accepted 10 December 2018; Published 24 February 2019

Guest Editor: Luciana Scotti

Background. The potential mechanism of postoperative cognitive impairment is still largely unclear. The activation of NLRP3 inflammasome had been reported to be involved in neurodegenerative diseases, including postoperative cognitive change, and is closely related to mitochondrial ROS and mitophagy. Honokiol (HNK) owns multiple organic protective effects. This study is aimed at observing the neuroprotective effect of HNK in postoperative cognitive change and examining the role of HNK in the regulation of mitophagy and the relationship between these effects and NLRP3 inflammasome activation in mice induced by surgery/anesthesia. *Methods*. In this study, mice were divided into several groups: control group, surgery group, surgery+HNK group, and surgery+HNK+3-methyladenine (3-MA) group. Hippocampal tissue samples were harvested and used for proinflammatory cytokines, mitochondrial ROS, and malondialdehyde (MDA) assay. The process of mitophagy and the activation of NLRP3 inflammasome were observed by Western blot, immunohistochemistry, and transmission electron microscopy. *Results*. The results showed that HNK treatment obviously recovered the postoperative decline and enhanced the expressions of LC3-II, Beclin-1, Parkin, and PINK1 at protein levels after surgery/sevoflurane treatment, which are both an autophagy marker and a mitophagy marker. In addition, HNK attenuated mitochondrial structure damage and reduced mtROS and MDA generation, which are closely associated with NLRP3 inflammasome activation. Honokiol-mediated mitophagy inhibited the activation of NLRP3 inflammasome and neuroinflammation in the hippocampus. Using 3-MA, an autophagy inhibitor, the neuroprotective effects of HNK on mitophagy and NLRP3 inflammasome activation were eliminated. *Conclusion*. These results indicated that HNK-mediated mitophagy ameliorates postoperative cognitive impairment induced by surgery/sevoflurane. This neuroprotective effect may be involved in inhibiting the activation of NLRP3 inflammasome and suppressing inflammatory responses in the hippocampus.

1. Introduction

Surgery/anesthesia is often an inevitable medical intervention in many patients during hospitalization. Postoperative cognitive decline (POCD) describes a cluster of cognitive behavior abnormalities including a relative drop in learning and memory performance on a set of neuropsychological tests from before to after surgery [1]. Dissecting the mechanisms of POCD becomes important, not only because it is a pathophysiological problem that we do not yet illuminate completely but also because it is a common postoperative complication that affects the quality of the patients' daily life and long-term outcome [2]. Like Alzheimer's disease (AD) and other neurodegenerative diseases, the potential pathophysiological mechanism of POCD may also be involved in neuroinflammation, oxidative stress, blood-brain barrier dysfunction, and apoptosis [2–6].

In recent years, several lines of studies have focused their attention on inflammasomes, which are essential components of the innate immune system and play a pivotal role in pro- or anti-inflammatory homeostasis [6–8]. Inflammasomes are intracellular multiprotein complexes that drive the activation of inflammatory responses. Among all types of inflammasomes, such as NLRP1, NLRP3, NLRC4, and AIM2, NLRP3 is the most studied one, especially in the central neural system [9, 10]. NLRP3 inflammasome activation could recruit and activate Caspase-1, leading to the secretion of mature IL-1β and IL-18 and the initiation of a novel form of cell death named pyroptosis [11]. Emerging evidence showed that NLRP3 inflammasomes could be identified in microglia, astrocytes and neurons, which induced neuroinflammation in a series of neurodegenerative diseases [7, 8, 12, 13]. So, in the surgery/sevoflurane model, we can observe whether the NLRP3 inflammasome was activated and could influence the neurological outcome. Moreover, a set of researches have also uncovered that the high levels of reactive oxygen species (ROS) are a common step that is essential for the formation of NLRP3 inflammasome [14]. Mitophagy, an autophagic process that specifically autophagically degrades damaged and free radical-generating mitochondria, regulates the mitochondrial homeostasis and cellular survival [15]. As mitophagy is impaired, the overaccumulation of mitochondrial ROS from the damaged mitochondria could induce NLRP3 inflammasome activation and lead to the inflammatory cascade [16]. Therefore, recent studies have demonstrated that regulation of autophagy/mitophagy may be a novel target for NLRP3-dependent proinflammatory responses in CNS disorders and metabolic inflammation.

Honokiol (HNK) (2-(4-hydroxy-3-prop-2-enyl-phenyl)-4-prop-2-enyl-phenol) is a bioactive compound obtained from *Magnolia grandiflora*, a species of magnolia common in Japan, which possesses multiple properties including antitumor, antiarrhythmic, antithrombocytic, anti-inflammatory, antiangiogenesis, and antioxidative activities in vivo and in vitro [17–21]. In previous studies, we found that honokiol have the protective effect on amyloid β oligomer-induced Alzheimer's disease in mice via attenuating mitochondrial apoptosis [22]. And in our preliminary studies (unpublished), honokiol could also ameliorate the oxidative stress and neuroinflammation in mice induced by surgery/anesthesia. However, the influence of HNK on mitophagy and its relationship with the NLRP3 inflammasome in surgery/sevoflurane models are still unknown.

In the present study, to improve the understanding of the neuroprotective effect of HNK in POCD, we observed the role of HNK in the regulation of mitophagy and the relationship between these effects and NLRP3 inflammasome activation in mice induced by surgery/anesthesia.

2. Materials and Methods

2.1. Animals. The animal use and care protocols were approved by the Animal Ethics Committee of Zhongnan Hospital of Wuhan University, Hubei, China. 4-month-old adult female C57BL/6J mice weighing 20–25 g were purchased from the Beijing Vital River Laboratory. All animals were acclimatized to the laboratory condition for at least 7 days prior to use. The environment of animal housing was under a 12-h/12-h light/dark cycle at 25°C and 50%-65% humidity with free access to food and water.

2.2. Experimental Group and Treatment. Animals were divided into six groups: (1) control group; (2) surgery+vehicle group (mice treated with vehicle for 1 week and underwent surgical operation); (3) surgery+HNK group (mice treated with HNK and underwent surgical operation); (4) surgery+HNK+3-MA group (mice treated with HNK and 3-MA and underwent surgical operation); (5) control+HNK group (control mice pretreated with HNK); and (6) control+HNK+3-MA group (control mice pretreated with HNK and 3-MA). Both honokiol and 3-MA were obtained from Sigma–Aldrich (St. Louis, MO, USA). They were dissolved in 0.5% dimethyl sulfoxide (DMSO). The animals received daily intraperitoneal injections of HNK at a dose of 10 mg/kg, 3-MA at a dose of 2 mg/kg, or DMSO for 7 days before the surgery. The control group mice received daily intraperitoneal injections of equal volume (0.5 mL) 0.5% DMSO for 7 days. Drug dosages were selected based on data from previous studies [23, 24] and preliminary experiments.

After fear conditioning training for 1 day, all animals received surgery/sevoflurane exposure. The open-field test (OFT) was achieved 20 min before each test phase of fear conditioning at postoperative 1, 3, and 7 days. And then the mice performed the fear conditioning test (FCT). After each test, the OFT and the FCT were washed with 75% ethanol to eliminate olfactory cues. The mice were sacrificed for biochemistry detection 1 h after all behavioral evaluations. The detailed study plan is graphically described in Figure 1.

2.3. Anesthesia and Surgery. The mice were subjected to abdominal exploratory surgery under general anesthesia via inhaling sevoflurane. Briefly, animals were anesthetized with 5% sevoflurane and maintained with 3% sevoflurane carried by 5 L/min oxygen. To avoid carbon dioxide retention and deep anesthesia, the concentration of sevoflurane and carbon dioxide was continuously monitored by an anesthesia gas monitor (Dräger Medical GmbH, Lübeck, Germany). Under spontaneous breathing, a 3 cm midline abdominal incision was made in the midline and the abdominal organs were explored gently with sterilized gauze. Using 9/0 Prolene sutures (Ethicon, USA), the incision was closed neatly. Then, a 0.2% lidocaine solution was administered subcutaneously for postoperative analgesia. All processes lasted approximately 50 mins. And a heat pad was utilized to keep the rats' body temperature at ~37°C during the surgery. At the end of the operation, 0.5 mL saline was administered by intraperitoneal injection for fluid supplementation. The mice of the control group did not receive the surgical operation.

2.4. Open-Field Test. To assess the effect of surgery/sevoflurane on locomotor activity of the mice, we performed the open-field test in an open-field chamber ($60 \times 60 \times 40$ cm) under dim light. The floor of a plastic transparent box was divided in 16 equal-sized squares. The center zone was the

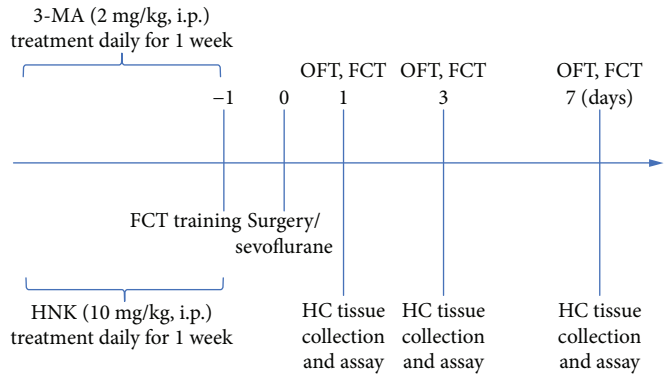

Figure 1: The study plan and schematic diagram of the experimental timeline. HNK: honokiol; FCT: fear conditioning test; OFT: open-field test; HC: hippocampus.

four squares in the center and the periphery was the 12 squares along the walls. Each animal was put into the center of the box and was permitted to travel for 5 min. The total travelled distance and the amount of time spent in the center zone were recorded via the ANY-maze animal tracking system software (Xinruan, Shanghai, China).

2.5. Fear Conditioning Test. Fear conditioning tests (FCT) were performed to assess memory in animals. The freezing behavior times of the mice reflect the capacity of learning and memory. Based on previously published studies, FCT includes two parts: a training phase at 1 day before surgical operation and a test phase at postoperative 1 day and 3 days.

In the training phase, the mice were trained for fear conditioning to establish the long-term memory. All animals were in the same training session and allowed to adapt to the environments (context) for 120 seconds, followed by six cycles of conditional-unconditional stimuli. A cycle of conditional-unconditional stimuli was then applied as a 20 s, 80 dB tone (conditional stimuli)—30 s delay—5 s, 0.75 mA electrical foot shock (unconditional stimuli). The cycles of conditional-unconditional stimuli were separated by random intervals from 45 to 60 seconds.

The context test, which reflects hippocampal-dependent memory, is the part of FCT. 1, 3, and 7 days after surgical operation, all the mice were placed back into the original conditioning box for 5 min, where no tone and no shock were produced. The percentage of time spent not moving (percentage freezing time) was captured and recorded by a video camera mounted above the center of the pool.

2.6. Apoptosis Detection in the Hippocampus. After behavioral tests, the mice were deeply anesthetized with pentobarbital sodium (50 mg/kg). To clear the blood in the circulatory system, the mice underwent a thoracotomy for transcardial perfusion with 0.9% NaCl, followed by 4% paraformaldehyde. Then, the fixed brain was removed and postfixed in 4% paraformaldehyde overnight at 4°C, then embedded in paraffin. Terminal deoxynucleotidyl transferase-mediated dUTP nick-end labeling (TUNEL) staining was performed according to the manufacturer's instruction (Roche, South San Francisco, CA, USA). Neuronal apoptosis was analyzed in the hippocampus sections. The quantification of TUNEL-positiveneurons in the hippocampal CA1 and DG was performed by a pathologist in 3 fields per slide randomly at 200× magnification.

2.7. Immunohistochemistry. The mice were deeply anesthetized with pentobarbital sodium (50 mg/kg) and perfused intracardially with saline followed by 4% paraformaldehyde. Then, the fixed cerebral tissues were postfixed in 4% paraformaldehyde at 4°C for 24 h and embedded in paraffin. The brain sections (4 μm thickness) were incubated overnight at 4°C with a primary antibody against NLRP3. After washing carefully in PBS for about 15 min, the sections were then incubated with a second antibody (1 : 200) and AB work solution (Vector Laboratories, Burlingame, CA, USA) for 30 min at room temperature. DAB solution was used to visualize the staining of NLRP3.

2.8. Transmission Electron Microscopy. 1 mm^3 tissue from the brain tissues from each group of mice was cut and fixed with a solution containing 2% (*v*/*v*) glutaraldehyde and 4% formaldehyde in 0.1 M sodium cacodylate, pH 7.4, for 15 min at room temperature. The fixed samples were then treated at the Wuhan Institute of Virology, Chinese Academy of Sciences, for further steps as previously described. Images were acquired using a Tecnai G^2 20 TWIN transmission electron microscope.

2.9. Western Blot. After behavior tests, the mice were killed and their hippocampal tissues were harvested. Total proteins were separated by SDS-PAGE after denaturation and transferred onto polyvinylidene difluoride (PVDF) membranes. After blocking with 5% skim milk, the membranes were incubated with rabbit anti-mouse monoclonal antibodies against NLRP3 (1 : 200, Novus, USA); Caspase-1 and ASC (1 : 200, Santa Cruz, CA, USA); PINK1, Parkin, and Beclin-1 (1 : 500, 1 : 1000, and 1 : 500, respectively, Abcam, Cambridge, UK); LC-3 (1 : 10000; Cell Signaling, USA); and GAPDH (1 : 1000, Abcam, Cambridge, UK) overnight at 4°C with shaking. Then, the membranes were washed in TBST. After that, the membranes were washed and incubated with secondary antibody anti-rabbit IgG (1 : 2000, Santa Cruz, CA, USA) for 1.5 h at room temperature. All blots were

scanned and analyzed using the Odyssey Infrared Imaging System (LI-COR Biosciences).

2.10. Isolation of Mitochondria from the Hippocampus. The intact mitochondria of the hippocampal region were isolated from the fresh hippocampus by using a tissue mitochondria isolation kit (Beyotime, China). Briefly, the hippocampus tissues were homogenized in an ice-cold buffer as previously described [25]. And then, the homogenate was centrifuged at 6000×g at 4°C for 5 min. After that, the collected supernatant was then centrifuged at 11000×g at 4°C for 10 min to obtain a mitochondrial pellet. Then, the pellet was stored as mitochondria and suspended in the mitochondrial storage fluid provided in the kit.

2.11. Enzyme-Linked Immunosorbent Assay (ELISA). We detected the hippocampal levels of IL-1β and TNF-α at 24 h after isoflurane exposure by ELISA kits (R&D Systems, DY401) following the protocols provided by the manufacturer (Abcam). Readings were normalized to the amount of a standard protein.

2.12. Statistical Analysis. All statistical analyses were performed with SPSS12 (SPSS Inc., Chicago, IL) and GraphPad Prism 5 (GraphPad, San Diego, CA). All data are presented as mean ± standard error of the mean (SEM). Statistical analysis of differences between groups was performed by using a one-way ANOVA followed by a SNK test for post hoc comparisons; $p < 0.05$ was considered statistically significant.

3. Results

3.1. HNK Enhanced Cognitive Recovery in Surgery/Sevoflurane-Treated Mice. Previous and our preliminary studies showed that surgery/anesthesia (sevoflurane or isoflurane) induced behavioral and cognitive impairment in mice.

To evaluate the postoperative cognitive decline in mice induced by surgery/sevoflurane and the protective effect of HNK, we assessed locomotor activity, learning, and memory by using the open-field test and the contextual fear conditioning tests, respectively.

In the open-field test, there are no significant differences in the total distance among the groups at postoperative 1, 3, and 7 days. These data suggested that surgery/sevoflurane, HNK, and 3-MA had no effect on the locomotor activity of the mice.

In the contextual fear conditioning test, there are significant differences among the groups at postoperative 1, 3, and 7 days. Meanwhile, we found that HNK or 3-MA pretreatment alone did not change the cognitive function of the control mice ($p > 0.05$). Besides, we also observed that surgery under sevoflurane anesthesia could reduce the freezing time of the contextual fear response compared with the control group up to postoperative 7 days, indicating the hippocampal impairments with postoperative cognitive decline ($p < 0.05$, Figures 2(d)–2(f)). Notably, HNK prevented the memory impairment from surgical stress and restored freezing behavior, the index for memory retention in mice ($p < 0.05$, Figures 2(d)–2(f)). However, 3-MA, an autophagy and mitophagy inhibitor, abolished the protective effect of HNK ($p < 0.05$, Figures 2(d)–2(f)). These data indicated that HNK may regulate autophagy or mitophagy to provide neuroprotection in postoperative cognitive impairment.

3.2. HNK Improved Mitophagy and Reduced the Levels of Mitochondrial ROS in the Hippocampus of Mice Induced by Surgery/Sevoflurane. To evaluate the levels of autophagy and mitophagy in mice under surgery operation, we examined the expressions of autophagy and mitophagy biomarkers by Western blotting and immunofluorescence. And ultrastructural morphological changes of the mitochondria were observed by transmission electron microscopy (TEM). Surgery under sevoflurane could upregulate the expression levels of autophagy-related proteins, LC3-II, and Beclin-1, compared with the control group up to postoperative 7 days ($p < 0.05$, Figure 3). Intriguingly, pretreatment with HNK could further enhance the expression of autophagy biomarkers compared with the surgery/sevoflurane group ($p < 0.05$, Figure 3). And 3-MA markedly decreased the HNK-induced autophagy enhancement in mice under surgery/sevoflurane ($p < 0.05$, Figure 3).

Double immunofluorescence suggested that Beclin-1 was colocalized with positive staining of Iba-1 and NeuN (microglia and neuron marker, respectively) in the hippocampus at 1 day after surgery/sevoflurane. These results demonstrated that autophagy activation could occur in the two most common types of neuronal cells of mice induced by surgery/sevoflurane. Meanwhile, the expression of microglial marker Iba-1 was upregulated in the hippocampus of the mice in the surgery group on postoperative 1 day compared to the control group (Figure 3, $p < 0.05$). For autophagy, the expression of Beclin-1 was upregulated in the hippocampus of mice at 1 day after surgery/anesthesia compared to the control group, while HNK pretreatment could further augment the Beclin-1 expression in the hippocampus and 3-MA inhibited these results (Figure 3, $p < 0.05$). However, different treatments had no effect on the NeuN expression ($p > 0.05$).

Mitophagy, a process of selective autophagy, removed damaged and superfluous mitochondria from the cell by the Parkin/PINK1 pathway. The mice underwent surgery/sevoflurane and promoted the PINK1 and Parkin protein expression compared with the control group up to postoperative 7 days, whereas HNK pretreatment further improved these expressions ($p < 0.05$, Figures 4(a)–4(c)). Moreover, 3-MA intervention could ameliorate the upregulation of these mitophagy-related proteins ($p < 0.05$, Figures 4(a)–4(c)). Mitochondrial ROS (mtROS) and malondialdehyde (MDA) can also reflect mitochondria function and the degree of oxidative stress. There are significant differences among the groups at postoperative 1, 3, and 7 days (Figures 4(d) and 4(e)). The levels of MDA and mtROS were significantly increased in the surgery/sevoflurane mice compared with the control group, which was consistent with mitochondrial structure damage. And HNK treatment made a marked reduction on mtROS and MDA compared with the control group ($p < 0.05$, Figures 4(d) and 4(e)). Inhibition of mitophagy by 3-MA exaggerated the content of mtROS and

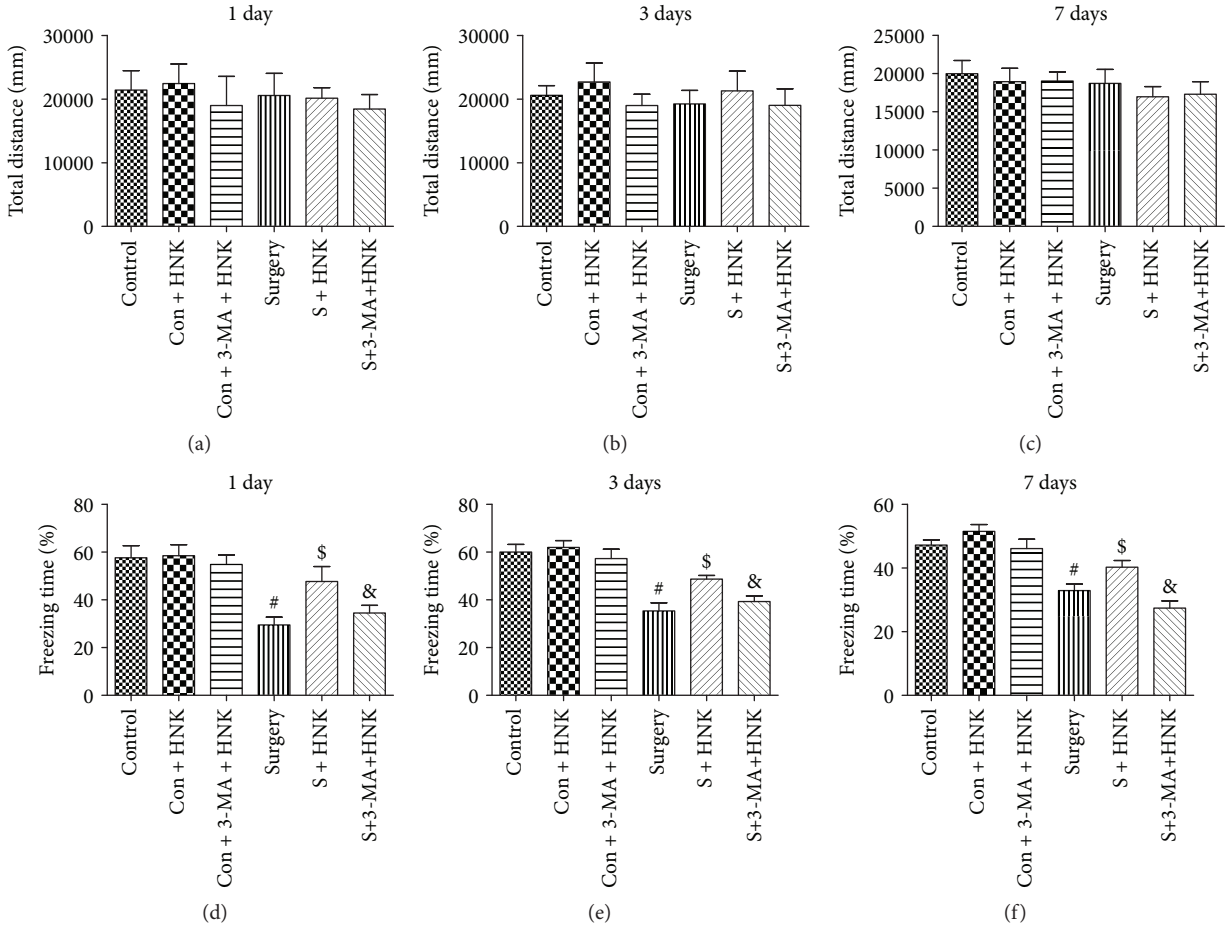

Figure 2: The effects of HNK on cognitive recovery in surgery/sevoflurane-treated mice. (a–c) The total distance traveled during 5 min of open-field exploration at postoperative 1, 3, and 7 days. (d–f) The percentage of freezing time during 5 min in context test (test phase of the FCT) at postoperative 1, 3, and 7 days. The data are presented as the mean ± standard error of the mean for each group ($n = 6$ per group). $^{\#}p < 0.05$ versus the control group; $^{\$}p < 0.05$ versus the surgery+vehicle group; and $^{\&}p < 0.05$ versus the surgery+HNK group.

MDA in the mice which underwent surgical stress up to 7 days ($p < 0.05$, Figures 4(d) and 4(e)).

Based on TEM, we observed that surgery under sevoflurane could induce mitochondrial structure damage at postoperative 1 day (Figure 5). Compared to healthy cellular organelles in the control group, severe cell damage appeared in the surgery/sevoflurane group. Nuclear membrane shrinkage, dark mitochondrial matrix, and structural disorganization of the mitochondrial cristae were found in the hippocampus of the surgery/sevoflurane mice. Besides, other organelles are vague and difficult to recognize; HNK ameliorated the destruction of mitochondria in the hippocampus. However, the protective effects were eliminated in the 3-MA intervention group.

These above results suggested that the augmentation of mitophagy by HNK may contribute to the maintenance of mitochondrial quality following surgery/sevoflurane.

3.3. HNK Alleviates the Activation of NLRP3 Inflammasome and Microglia in the Hippocampus of Mice Treated by Surgery/Sevoflurane. Accumulation of mitochondrial ROS is one of the triggers of NLRP3 inflammasome activation, which exaggerates the inflammatory response and expedites proinflammatory cytokine release.

We determined the effects of surgery and HNK and/or 3-MA pretreatment on the expression of NLRP3, ASC, Caspase-1, IL-1, and IL-8 in the hippocampus of the mice on postoperative days 1, 3, and 7 by Western blotting, ELISA, and immunohistochemistry, respectively. Surgery/anesthesia led a marked increase in the expressions of NLRP3, ASC, and Caspase-1 in the hippocampus on postoperative days 1, 3, and 7 compared to the control group (Figures 6(a)–6(d)). These mice that received HNK pretreatment had downregulated the expression of NLRP3, as well as decreased the hippocampal expression of ASC and Caspase-1 on postoperative days 1, 3, and 7. Additionally, 3-MA eradicated the inhibition effects of HNK on NLRP3 inflammasome activation.

The increased secretion of proinflammatory cytokines, including IL-1β and IL-18, is in parallel with the NLRP3 inflammasome activation. ELISA analysis showed that the concentration of IL-1β and IL-18 increased significantly in the surgery/anesthesia group at postoperative 1, 3, and 7 days, whereas HNK treatment notably suppressed the expressions

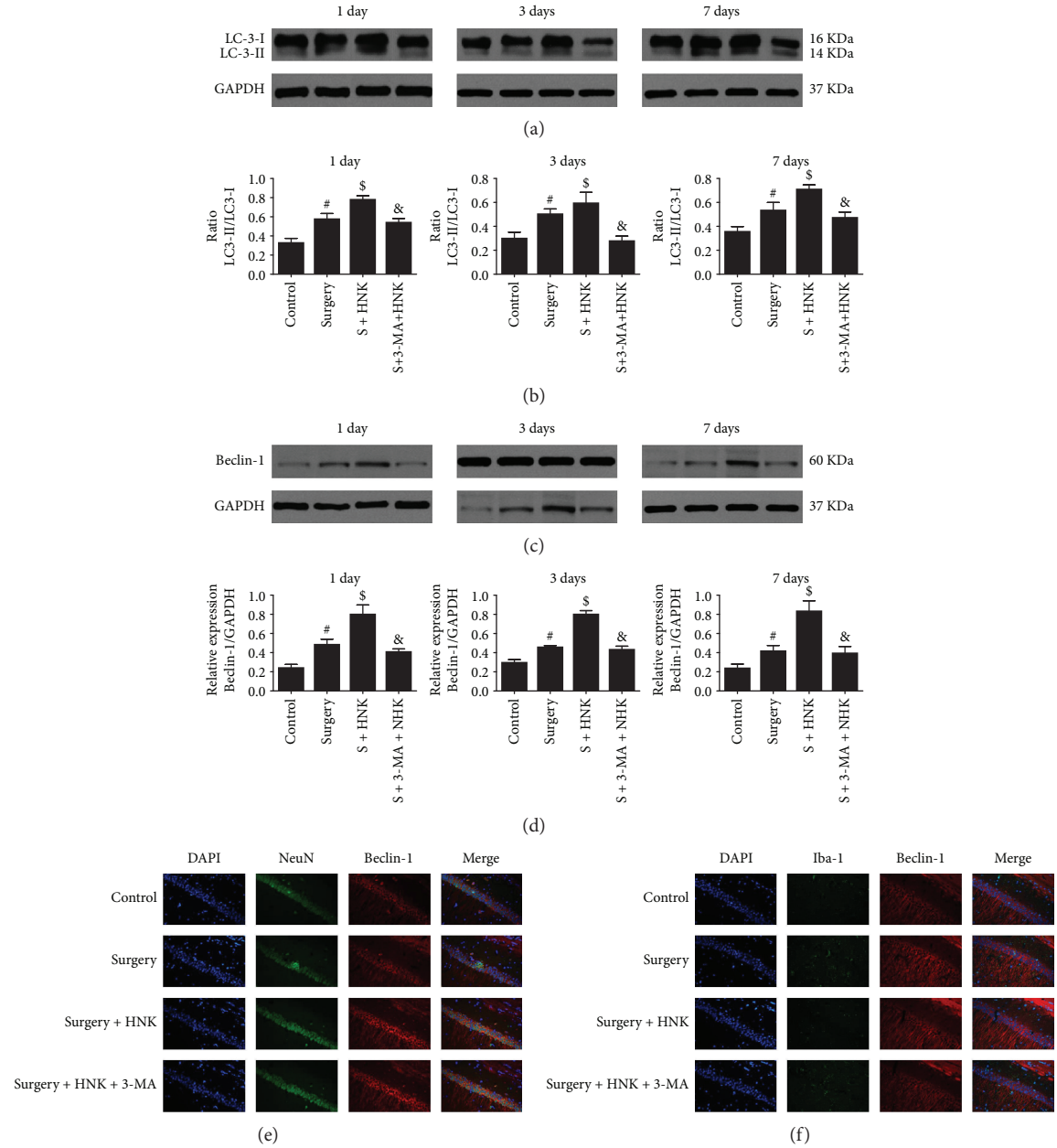

FIGURE 3: The effects of HNK on autophagy in the hippocampus of mice induced by surgery/sevoflurane. (a–d) The Western blot representative blots of autophagy-related proteins, LC3-II, and Beclin-1 ($n = 6$ per group). (e, f) Representative double immunofluorescence labeling of Beclin-1 with NeuN and Iba-1 in the CA1 at 24 h after surgery/sevoflurane. Scale bar = 50 μm. The data are presented as the mean ± standard error of the mean for each group ($n = 6$ per group). $^{\#}p < 0.05$ versus the control group; $^{\$}p < 0.05$ versus the surgery+vehicle group; and $^{\&}p < 0.05$ versus the surgery+HNK group.

of IL-1β and IL-18 compared with the surgery/anesthesia-induced mice (Figures 6(e)–6(g)). Microglia activation also reflects neuroinflammation. Pretreatment with HNK resulted in a decreased Iba-1 expression on postoperative 1 day, while 3-MA treatment could result in an increased Iba-1 expression compared to the surgery group, which indicated the different activation of microglia (Figure 3(f)).

3.4. HNK Suppresses Neuronal Apoptosis in the Hippocampal CA1 and DG Regions of Mice Induced by Surgery/Sevoflurane. To reveal whether mitophagy was associated with the neuronal apoptosis, 3-MA was utilized as described above in the surgery/sevoflurane-induced mice. As shown in Figure 7, TUNEL-positive cells were rarely detected in the control group, whereas there were more TUNEL-positive cells in the surgery/sevoflurane group compared to the control group, suggesting that surgery/sevoflurane led to neuronal damage. HNK pretreatment dramatically deceased the neuronal apoptosis in both the hippocampal CA1 and DG regions compared with the surgery/sevoflurane group. However, 3-MA inhibited the neuroprotection of HNK on neuronal apoptosis.

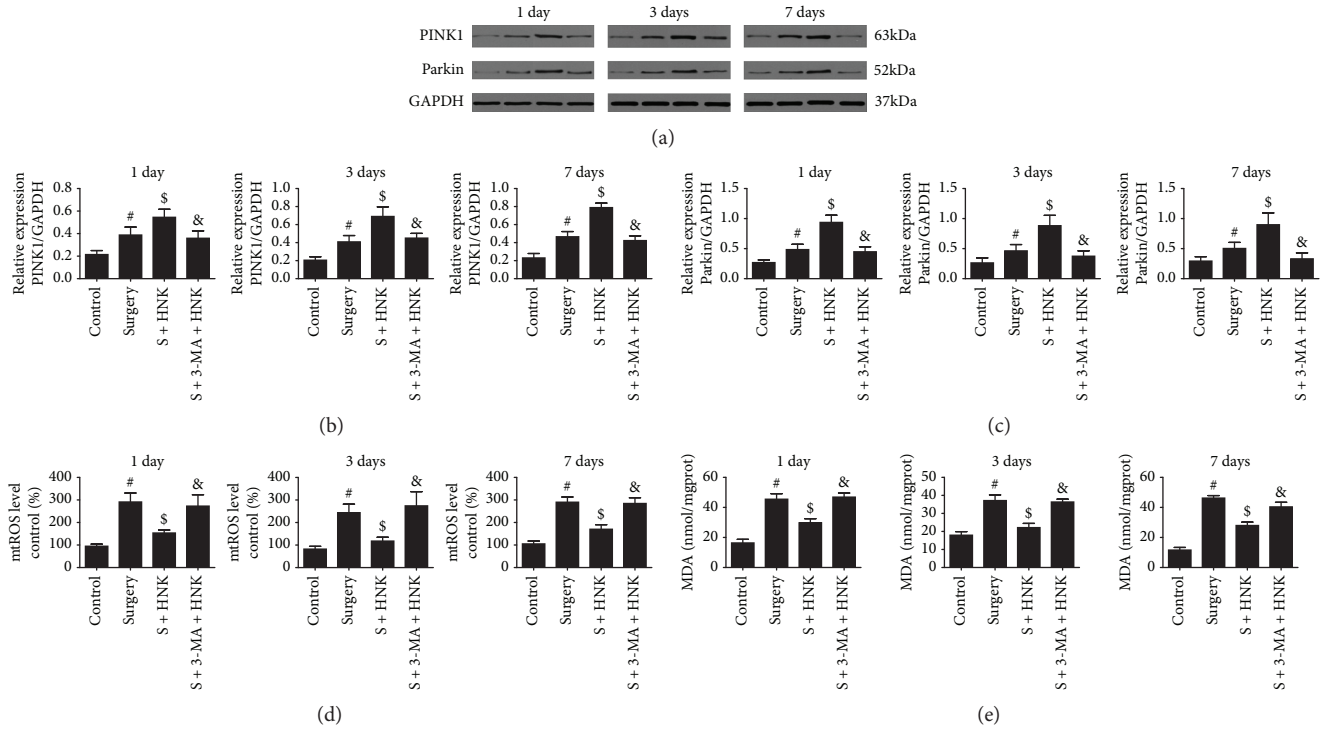

Figure 4: The effects of HNK on mitophagy and oxidative stress in the hippocampus of mice induced by surgery/sevoflurane. (a–c) The Western blot representative blots of mitophagy-related proteins, Parkin, and PINK1 ($n = 6$ per group). (d, e) The oxidative indicators of mtROS levels and MDA in the hippocampus induced by surgery/sevoflurane. The data are presented as the mean ± standard error of the mean for each group. $^{\#}p < 0.05$ versus the control group; $^{\$}p < 0.05$ versus the surgery+vehicle group; and $^{\&}p < 0.05$ versus the surgery+HNK group.

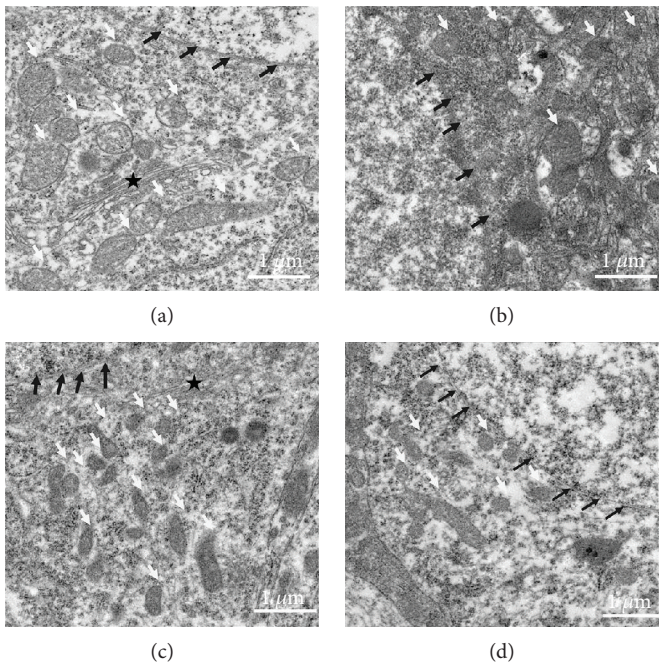

Figure 5: Ultrastructural mitochondrial change in the hippocampus after surgery/sevoflurane exposure: (a) healthy nuclear membrane (black arrowheads), mitochondria (white arrowheads), and cytoplasmic Golgi complexes (black pentagram) in the control group; (b) severe cell damage appeared in the surgery/sevoflurane group: nuclear membrane shrinkage (black arrowheads), mitochondrial matrix appeared darker, structural disorganization of mitochondrial cristae (white arrowheads), and other organelles are vague and difficult to recognize; (c) in the surgery+HNK group, the degree of cellular organelles above were reduced; and (d) in the surgery+HNK+3-MA group, the protective effects of HNK on cellular organelles were reversed (scale bar = 1 μm).

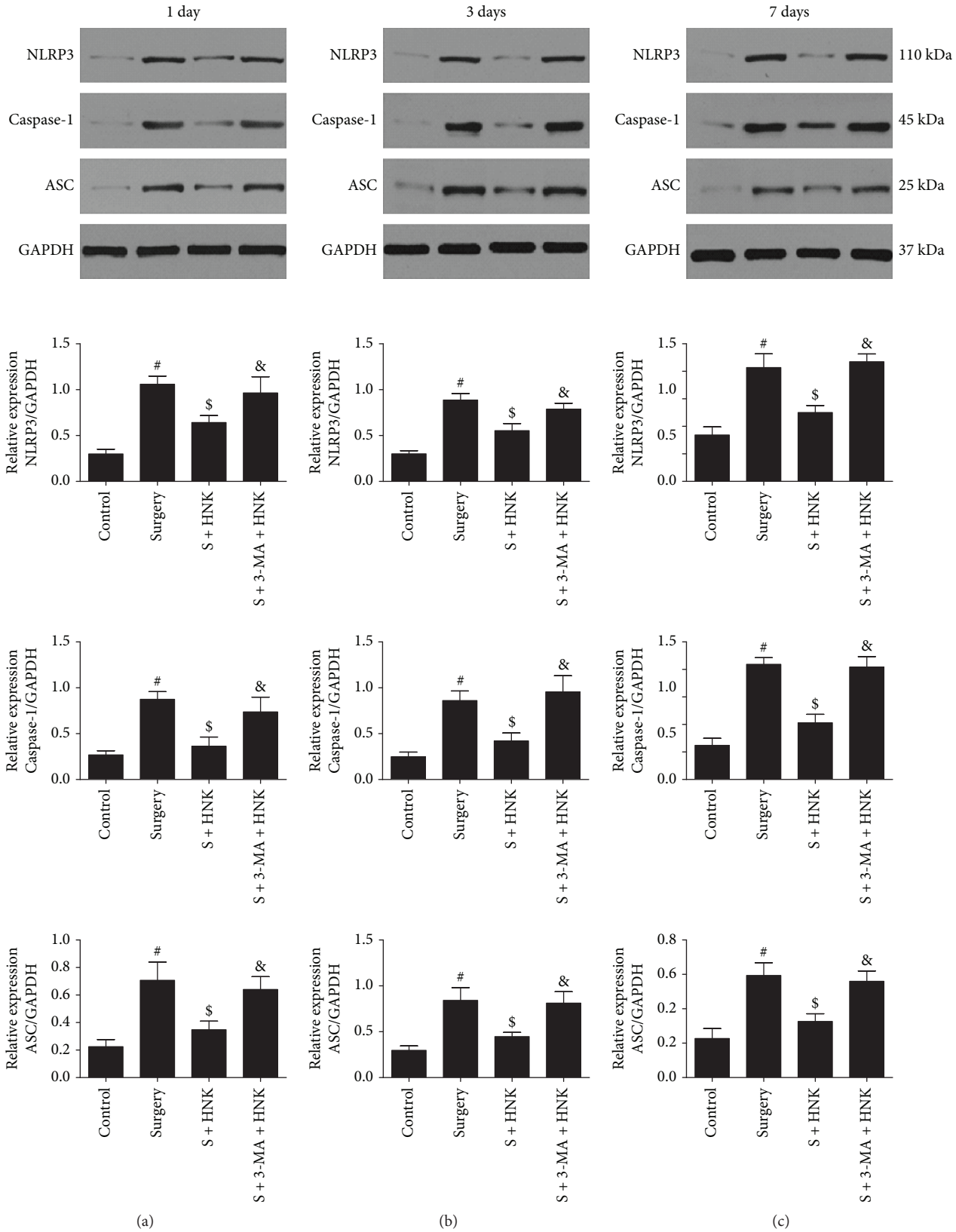

Figure 6: Continued.

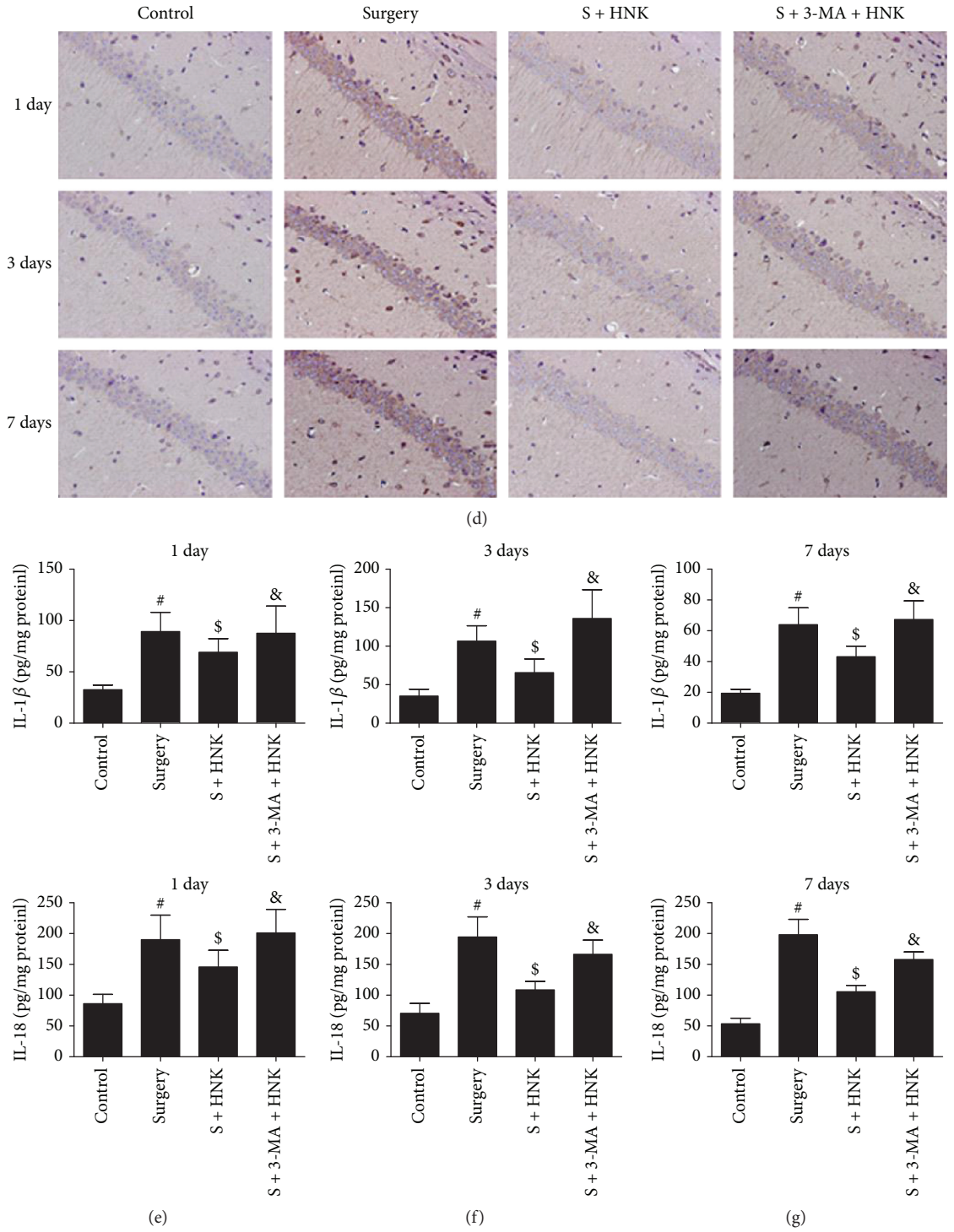

Figure 6: The effects of HNK on NLRP3 inflammasome activation in the hippocampus induced by surgery/sevoflurane. (a–c) The Western blot representative blots of NLRP3, ASC, and Caspase-1 ($n = 6$ per group). (d) The immunohistochemistry of NLRP3 in the hippocampus at 24 h after surgery/sevoflurane. (e–g) The concentration of IL-1β and IL-18 in the hippocampus at postoperative 1, 3, and 7 days. The data are presented as the mean ± standard error of the mean for each group. $^{\#}p < 0.05$ versus the control group; $^{\$}p < 0.05$ versus the surgery+vehicle group; and $^{\&}p < 0.05$ versus the surgery+HNK group.

4. Discussion

POCD can deteriorate surgery and lead to an induction of morbidity and mortality in patients [26]. Revealing the pathogeny and treatments for POCD are beneficial for the increase of hospitalization comfort and improvement of the long-term outcome. In the current study, we first provided evidence that mitophagy or autophagy was involved in postoperative cognitive impairment induced by surgery/sevoflurane in mice. Honokiol could further induce the

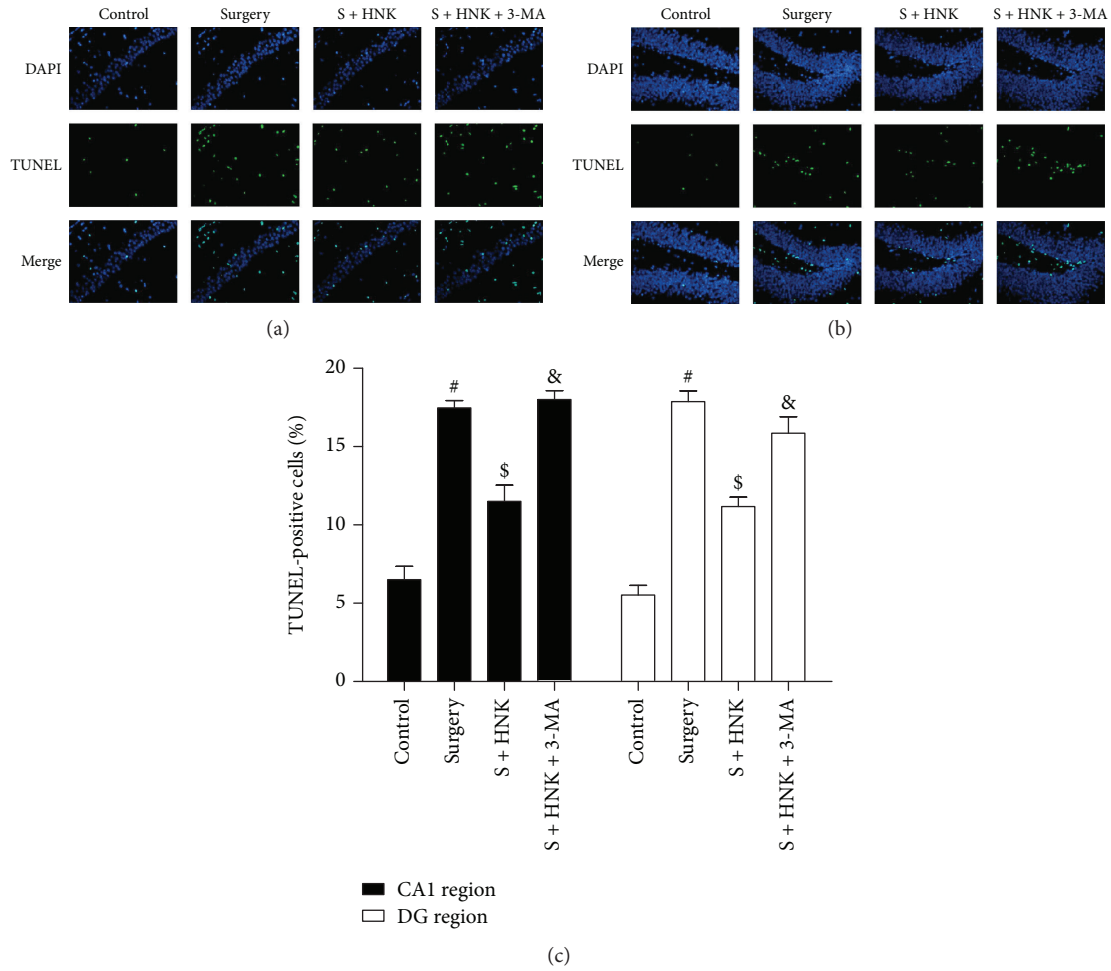

Figure 7: The effects of HNK on neuronal apoptosis in the hippocampal CA1 and DG regions of mice induced by surgery/sevoflurane. (a, b) The representative images showing TUNEL staining in the hippocampal CA1 and DG regions at 24 h after surgery/sevoflurane. The apoptotic cells were detected by TUNEL (green), and the nuclei were detected by DAPI (blue). Scale bar = 50 μm. (c) The percentage of TUNEL-positive cells. The data are presented as the mean ± standard error of the mean for each group ($n = 3$ per group), $^{\#}p < 0.05$ versus the control group; $^{\$}p < 0.05$ versus the surgery+vehicle group; and $^{\&}p < 0.05$ versus the surgery+HNK group.

mitophagy in surgery/sevoflurane-induced mice. Besides, honokiol inhibited the activation of NLRP3 inflammasome after surgery/sevoflurane treatment and alleviated the neuroinflammation in mice. Pretreatment with honokiol could also preserve neuronal apoptosis and alleviate cognitive decline following surgery/sevoflurane treatment. In addition, 3-MA, an autophagy and mitophagy inhibitor, reversed the neuroprotective effect of HNK on the inhibition of NLRP3 inflammasome activation. These results demonstrated that HNK-mediated mitophagy ameliorates postoperative cognitive impairment induced by surgery/sevoflurane in mice via inhibiting the activation of the NLRP3 inflammasome.

Surgical stress and long duration of inhaled anesthetics can then prompt the activation of immune cells which contributes to neuroinflammation and cognitive change [27, 28]. Without effective intervention, the transformation from acute neuroinflammation to chronic neuroinflammation, which was accompanied by neutrophil infiltration and microglia/macrophage activation, may result in neuronal death, disruption of the blood-brain barrier, and brain edema [26, 29–32]. All the time, anti-neuroinflammatory strategies exhibit potential therapeutic effects against surgery/anesthesia exposure and improve cognitive functions after surgery/anesthesia stress. In recent years, the NLRP3 inflammasome became a research focus in a series of diseases, such as diabetes, neurodegenerative disorders, and brain trauma. Previous studies showed that the MPTP mouse model of Parkinson's disease, traumatic brain injury, cerebral ischemia-reperfusion injury, and isoflurane-inducedhippocampal inflammation can induce the NLRP3 inflammasome activation [6, 8, 33]. Moreover, the inhibition of the NLRP3 inflammasome provided robust neuroprotective response in these pathophysiological processes, which was associated with NLRP3-mediated inflammation and reduction of proinflammatory cytokines. Our findings also suggested that HNK could effectively suppress NLRP3 inflammasome activation and subsequent inflammatory cytokine expression. Immunofluorescence results also showed that trends of microglia activation are correlated with the NLRP3 inflammasome expression in surgery/sevoflurane-induced mice, which is consistent with previous studies. Emerging evidences demonstrated that NLRP3 seems

sensitive to the imbalance of cellular homeostasis, so there are a great many of NLRP3 activators, such as low intracellular K^+ concentration, lysosomal lysis, mitochondrial ROS, or mitochondrial DNA released from damaged mitochondria and Ca^2 flux [11]. In our studies, we further detected the levels of mitochondrial ROS and MDA, which could reflect the relationships between oxidative stress and the NLRP3 inflammasome. Our results showed that HNK possessed strongly antioxidant capacity which decreased the levels of mtROS and was critical for the reduction of the NLRP3 inflammasome. This study may be the first to exhibit the bridge between oxidative stress and NLRP3-mediated neuroinflammation in postoperative cognitive decline induced by surgery/sevoflurane.

Mitochondria are the primary platforms for energy production and are hypersensitive to the surgical stress. When mitochondrial function is damaged, the overplus of ROS, especially for mitochondrial ROS, is deleterious for the normal physiological state and could cause oxidative stress and inflammation, which are the basis of a wealth of diseases, such as diabetes and cerebral/myocardial ischemia-reperfusion injury [34, 35]. In the view of mitochondrial morphology and biochemical results, we found that HNK effectively blunted the mitochondrial injury (decrease of swelling mitochondria) and the degrees of oxidative stress. These results provided a novel sight for NLRP3 inflammasome activation in postoperative cognitive decline induced by surgery/sevoflurane.

Mitophagy, as a selective autophagy, is a crucial mediator of the degradation of injured mitochondria. Larger numbers of evidence have indicated that autophagy/mitophagy emerges in response to various conditions, such as nutrient depletion, mitochondrial dysfunction, or red blood cell maturation, and has a significant impact on a series of diseases [36]. Lin et al. showed that inhibition of mitophagy could aggravate the neuroinflammation induced by traumatic brain injury. And melatonin enhanced mitophagy through the mTOR signaling pathway, then ameliorated the TBI-triggered neuroinflammation [37]. And not all mitophagy is processed by the Parkin/PINK1 pathway. Studies of the Bnip3/Nix pathway and the Parkin/PINK1 signaling pathway all have a direct connection between defective mitochondria and mitophagy [36]. The difference is that the Parkin/PINK1 pathway depends on the voltage-dependent inhibition in the autophagosome clearance process [38, 39]. And the dysfunction of the Parkin/PINK1 mechanism may lead to defects in mitochondrial morphology, dynamics, and function and result in an imbalance in mitochondrial fusion and fission. However, mitophagy involved in the Bnip3/Nix pathway may be crucial for maintaining the number and the function of mitochondria during cell differentiation and dedifferentiation [40]. In our studies, we found that HNK increased the mitophagy-related proteins, Parkin/PINK1, and protected the abnormal mitochondrial structure (e.g., fragmented cristae and swollen, distorted mitochondrial morphology) in the surgery/sevoflurane model, suggesting that increased mitophagy may eliminate more damaged and dysfunctional mitochondria and may be helpful in reducing the overproduction of ROS. These signaling pathways may be the upstream of NLRP3 inflammasome activation. And different disease models have demonstrated the assumption above. For example, Kim et al. demonstrated that SESN2/sestrin2, an autophagic inducer, prevents sepsis by inducing mitophagy and inhibiting NLRP3 via an increase of unc-51-like kinase 1 protein activity and levels [41]. Consistent with these outcomes, Zhong et al. observed that the NF-κB signaling pathway can translocate the increased cargo receptor p62 to damaged mitochondria, which are recognized by Parkin-dependent ubiquitin and induce mitophagic clearance. The intrinsic regulatory loop "NF-κB-p62-mitophagy" in the macrophage restrains NLRP3 inflammasome activation and maintains homeostasis [42]. Our findings and these studies indicate that mitophagy is one of the self-limiting systems to protect tissues and organs from hyperinflammation and favor tissue repair.

However, it is noted that there are some limitations in our current study. Firstly, in view of behavior tests, we just performed three timepoints (postoperative 1, 3, and 7 days). Due to lack of behavioral data at postoperative 28 days and continuous monitoring within postoperative 24 hours, we failed to understand the fluctuations of cognitive impairment. Further investigation would observe the long-term postoperative cognitive change. Second, in our studies, we just measured the related indicator only in the hippocampus. Several studies also have reported that other brain regions, such as the prefrontal cortex and amygdaloid nucleus, could participate in cognitive function. So, these regions would be investigated in the future. Third, considering the antianxiety property of HNK and our previous study, we cannot exclude the possibility that the change in anxiety levels by HNK hindered the freezing behavior in the fear conditioning test in mice. Finally, due to the expensive price and limited number, we only used 8-week-old female mice but not the aged mice. However, several studies have shown that surgical stress could also induce cognitive change in female mice. And in the future investigation, we will add the observation of the effects of surgery/sevoflurane on postoperative cognitive decline in mice of different sexes and ages.

5. Conclusions

Taken together, our study deepened the understanding of the neuroprotective effects of HNK on surgery/sevoflurane-induced postoperative cognitive impairment and detected a novel therapeutic target. Our results indicated that honokiol-mediatedmitophagy ameliorates postoperative cognitive impairment induced by surgery/sevoflurane. This neuroprotective effect may be involved in inhibiting the activation of the NLRP3 inflammasome and suppressing inflammatory responses in the hippocampus.

Data Availability

The datasets analyzed during the current study are available from the corresponding author on reasonable request.

Ethical Approval

The experimental protocol was approved by the Animal Ethics Committee of Zhongnan Hospital of Wuhan University, Hubei, China, and all experiments were performed in accordance with the National Institutes of Health Guidelines for the Care and Use of Laboratory Animals.

Conflicts of Interest

The authors declare that they have no competing interests.

Authors' Contributions

JSY designed and performed the experiments, analyzed and interpreted the data, and drafted the manuscript. LC participated in designing the study and interpreting the results. YYL contributed to behavioral testing and biochemical analysis. SQL and MP participated in preparing the animal models. ZYX conceived the study, participated in its design and coordination, secured funding for the project, helped to draft the manuscript, and critically revised the manuscript. All authors read and approved the final manuscript.

Acknowledgments

We thank the Central Laboratory (Renmin Hospital of Wuhan University) for the equipment and excellent technical assistance. This study was supported by the National Natural Science Foundation of China (Grant Nos. 81471844 and 81671891).

References

[1] M. J. Needham, C. E. Webb, and D. C. Bryden, "Postoperative cognitive dysfunction and dementia: what we need to know and do," *British Journal of Anaesthesia*, vol. 119, Supplement 1, pp. i115–i125, 2017.

[2] S. S. Makhani, F. Y. Kim, Y. Liu et al., "Cognitive impairment and overall survival in frail surgical patients," *Journal of the American College of Surgeons*, vol. 225, no. 5, pp. 590–600.e1, 2017.

[3] Z. Cristina, B. Michela, B. Agostino et al., "Post-operative cognitive decline (POCD) after gynaecologic surgery: current opinions and future applications," *Archives of Gynecology and Obstetrics*, vol. 297, no. 3, pp. 551–554, 2018.

[4] X. Feng, M. Valdearcos, Y. Uchida, D. Lutrin, M. Maze, and S. K. Koliwad, "Microglia mediate postoperative hippocampal inflammation and cognitive decline in mice," *JCI insight*, vol. 2, no. 7, article e91229, 2017.

[5] W. Liu, J. Guo, J. Mu, L. Tian, and D. Zhou, "Rapamycin protects sepsis-induced cognitive impairment in mouse hippocampus by enhancing autophagy," *Cellular and Molecular Neurobiology*, vol. 37, no. 7, pp. 1195–1205, 2017.

[6] Z. Wang, S. Meng, L. Cao, Y. Chen, Z. Zuo, and S. Peng, "Critical role of NLRP3-caspase-1 pathway in age-dependent isoflurane-induced microglial inflammatory response and cognitive impairment," *Journal of Neuroinflammation*, vol. 15, no. 1, p. 109, 2018.

[7] T. Wang, D. Nowrangi, L. Yu et al., "Activation of dopamine D1 receptor decreased NLRP3-mediated inflammation in intracerebral hemorrhage mice," *Journal of Neuroinflammation*, vol. 15, no. 1, p. 2, 2018.

[8] X. Xu, D. Yin, H. Ren et al., "Selective NLRP3 inflammasome inhibitor reduces neuroinflammation and improves long-term neurological outcomes in a murine model of traumatic brain injury," *Neurobiology of Disease*, vol. 117, pp. 15–27, 2018.

[9] Q. Guo, Y. Wu, Y. Hou et al., "Cytokine secretion and pyroptosis of thyroid follicular cells mediated by enhanced NLRP3, NLRP1, NLRC4, and AIM2 inflammasomes are associated with autoimmune thyroiditis," *Frontiers in Immunology*, vol. 9, p. 1197, 2018.

[10] K. Vats, D. Sarmah, H. Kaur et al., "Inflammasomes in stroke: a triggering role for acid-sensing ion channels," *Annals of the New York Academy of Sciences*, vol. 1431, no. 1, pp. 14–24, 2018.

[11] T. Tang, X. Lang, C. Xu et al., "CLICs-dependent chloride efflux is an essential and proximal upstream event for NLRP3 inflammasome activation," *Nature Communications*, vol. 8, no. 1, p. 202, 2017.

[12] Y. L. Wang, Q. Q. Han, W. Q. Gong et al., "Microglial activation mediates chronic mild stress-induced depressive- and anxiety-like behavior in adult rats," *Journal of Neuroinflammation*, vol. 15, no. 1, p. 21, 2018.

[13] J. Zheng, L. Shi, F. Liang et al., "Sirt3 ameliorates oxidative stress and mitochondrial dysfunction after intracerebral hemorrhage in diabetic rats," *Frontiers in Neuroscience*, vol. 12, p. 414, 2018.

[14] Y. He, M. Y. Zeng, D. Yang, B. Motro, and G. Núñez, "NEK7 is an essential mediator of NLRP3 activation downstream of potassium efflux," *Nature*, vol. 530, no. 7590, pp. 354–357, 2016.

[15] S. Cao, S. Shrestha, J. Li et al., "Melatonin-mediated mitophagy protects against early brain injury after subarachnoid hemorrhage through inhibition of NLRP3 inflammasome activation," *Scientific Reports*, vol. 7, no. 1, p. 2417, 2017.

[16] M. J. Kim, J. H. Yoon, and J. H. Ryu, "Mitophagy: a balance regulator of NLRP3 inflammasome activation," *BMB Reports*, vol. 49, no. 10, pp. 529–535, 2016.

[17] V. B. Pillai, S. Samant, N. R. Sundaresan et al., "Honokiol blocks and reverses cardiac hypertrophy in mice by activating mitochondrial Sirt3," *Nature Communications*, vol. 6, no. 1, p. 6656, 2015.

[18] T. Hong, H. Min, Z. Hui, L. Yuejian, Y. Lixing, and X. Z. Liang, "Oral administration of honokiol attenuates airway inflammation in asthmatic mouse model," *Pakistan Journal of Pharmaceutical Sciences*, vol. 31, no. 4, pp. 1279–1284, 2018.

[19] P. Tang, J. M. Gu, Z. A. Xie et al., "Honokiol alleviates the degeneration of intervertebral disc via suppressing the activation of TXNIP-NLRP3 inflammasome signal pathway," *Free Radical Biology and Medicine*, vol. 120, pp. 368–379, 2018.

[20] D. Wang, X. Dong, and C. Wang, "Honokiol ameliorates amyloidosis and neuroinflammation and improves cognitive impairment in Alzheimer's disease transgenic mice," *The Journal of Pharmacology and Experimental Therapeutics*, vol. 366, no. 3, pp. 470–478, 2018.

[21] B. Zhang, M. Zhai, B. Li et al., "Honokiol ameliorates myocardial ischemia/reperfusion injury in type 1 diabetic rats by reducing oxidative stress and apoptosis through activating the SIRT1-Nrf2 signaling pathway," *Oxidative medicine and cellular longevity*, vol. 2018, Article ID 3159801, 16 pages, 2018.

[22] M. Wang, Y. Li, C. Ni, and G. Song, "Honokiol attenuates oligomeric amyloid $\beta_{1\text{-}42}$-induced Alzheimer's disease in mice through attenuating mitochondrial apoptosis and inhibiting the nuclear factor kappa-B signaling pathway," *Cellular Physiology and Biochemistry*, vol. 43, no. 1, pp. 69–81, 2017.

[23] Y. F. Xian, S. P. Ip, Q. Q. Mao et al., "Honokiol improves learning and memory impairments induced by scopolamine in mice," *European Journal of Pharmacology*, vol. 760, pp. 88–95, 2015.

[24] A. Jangra, S. Dwivedi, C. S. Sriram et al., "Honokiol abrogates chronic restraint stress-induced cognitive impairment and depressive-like behaviour by blocking endoplasmic reticulum stress in the hippocampus of mice," *European Journal of Pharmacology*, vol. 770, pp. 25–32, 2016.

[25] J. S. Ye, L. Chen, Y. Y. Lu, S. Q. Lei, M. Peng, and Z. Y. Xia, "SIRT3 activator honokiol ameliorates surgery/anesthesia-induced cognitive decline in mice through anti-oxidative stress and anti-inflammatory in hippocampus," *CNS Neuroscience & Therapeutics*, 2018.

[26] J. Bi, W. Shan, A. Luo, and Z. Zuo, "Critical role of matrix metallopeptidase 9 in postoperative cognitive dysfunction and age-dependent cognitive decline," *Oncotarget*, vol. 8, no. 31, pp. 51817–51829, 2017.

[27] A. A. Zurek, J. Yu, D. S. Wang et al., "Sustained increase in α5GABA$_A$ receptor function impairs memory after anesthesia," *The Journal of Clinical Investigation*, vol. 124, no. 12, pp. 5437–5441, 2014.

[28] M. Plas, E. Rotteveel, G. J. Izaks et al., "Cognitive decline after major oncological surgery in the elderly," *European journal of cancer*, vol. 86, pp. 394–402, 2017.

[29] Z. Li, N. Mo, L. Li et al., "Surgery-induced hippocampal angiotensin II elevation causes blood-brain barrier disruption via MMP/TIMP in aged rats," *Frontiers in Cellular Neuroscience*, vol. 10, p. 105, 2016.

[30] D. Ikawa, M. Makinodan, K. Iwata et al., "Microglia-derived neuregulin expression in psychiatric disorders," *Brain, Behavior, and Immunity*, vol. 61, pp. 375–385, 2017.

[31] B. Zheng, R. Lai, J. Li, and Z. Zuo, "Critical role of P2X7 receptors in the neuroinflammation and cognitive dysfunction after surgery," *Brain, Behavior, and Immunity*, vol. 61, pp. 365–374, 2017.

[32] J. Wang, L. Li, Z. Wang et al., "Supplementation of lycopene attenuates lipopolysaccharide-induced amyloidogenesis and cognitive impairments via mediating neuroinflammation and oxidative stress," *The Journal of Nutritional Biochemistry*, vol. 56, pp. 16–25, 2018.

[33] C. Qiao, L. X. Zhang, X. Y. Sun, J. H. Ding, M. Lu, and G. Hu, "Caspase-1 deficiency alleviates dopaminergic neuronal death via inhibiting caspase-7/AIF pathway in MPTP/p mouse model of Parkinson's disease," *Molecular Neurobiology*, vol. 54, no. 6, pp. 4292–4302, 2017.

[34] L. Tilokani, S. Nagashima, V. Paupe, and J. Prudent, "Mitochondrial dynamics: overview of molecular mechanisms," *Essays in Biochemistry*, vol. 62, no. 3, pp. 341–360, 2018.

[35] O. E. Aparicio-Trejo, E. Tapia, L. G. Sánchez-Lozada, and J. Pedraza-Chaverri, "Mitochondrial bioenergetics, redox state, dynamics and turnover alterations in renal mass reduction models of chronic kidney diseases and their possible implications in the progression of this illness," *Pharmacological Research*, vol. 135, pp. 1–11, 2018.

[36] J. Harris, N. Deen, S. Zamani, and M. A. Hasnat, "Mitophagy and the release of inflammatory cytokines," *Mitochondrion*, vol. 41, pp. 2–8, 2018.

[37] C. Lin, H. Chao, Z. Li et al., "Melatonin attenuates traumatic brain injury-induced inflammation: a possible role for mitophagy," *Journal of Pineal Research*, vol. 61, no. 2, pp. 177–186, 2016.

[38] C. T. Chu, "Mechanisms of selective autophagy and mitophagy: implications for neurodegenerative diseases," *Neurobiology of Disease*, vol. 122, 2019.

[39] R. Lan, J. T. Wu, T. Wu et al., "Mitophagy is activated in brain damage induced by cerebral ischemia and reperfusion via the PINK1/Parkin/p62 signalling pathway," *Brain Research Bulletin*, vol. 142, pp. 63–77, 2018.

[40] M. Šprung, I. Dikic, and I. Novak, "Flow cytometer monitoring of Bnip3- and Bnip3L/Nix-dependent mitophagy," in *Mitophagy*, N. Hattori and S. Saiki, Eds., vol. 1759 of Methods in Molecular Biology, Humana Press, New York, NY, USA, 2017.

[41] M. J. Kim, S. H. Bae, J. C. Ryu et al., "SESN2/sestrin2 suppresses sepsis by inducing mitophagy and inhibiting NLRP3 activation in macrophages," *Autophagy*, vol. 12, no. 8, pp. 1272–1291, 2016.

[42] Z. Zhong, A. Umemura, E. Sanchez-Lopez et al., "NF-κB restricts inflammasome activation via elimination of damaged mitochondria," *Cell*, vol. 164, no. 5, pp. 896–910, 2016.

Hindawi
Oxidative Medicine and Cellular Longevity
Volume 2019, Article ID 9426867, 14 pages
https://doi.org/10.1155/2019/9426867

Review Article

Benefits of Vitamins in the Treatment of Parkinson's Disease

Xiuzhen Zhao,[1] Ming Zhang,[2] Chunxiao Li,[3] Xue Jiang,[1] Yana Su,[1] and Ying Zhang[1]

[1]*Department of Neurology and Neuroscience Center, First Hospital of Jilin University, Xinmin Street No. 71, Changchun 130000, China*
[2]*Department of Pharmacology, College of Basic Medical Sciences, Jilin University, 126 Xin Min Street, Changchun, Jilin 130021, China*
[3]*Department of Neurology and Neuroscience Center, The Affiliated Hospital of Qingdao University, Qingdao, Shandong 266000, China*

Correspondence should be addressed to Ying Zhang; zhang_ying99@jlu.edu.cn

Received 4 October 2018; Accepted 4 February 2019; Published 20 February 2019

Guest Editor: Francisco Jaime B. Mendonça Júnior

Parkinson's disease (PD) is the second most common neurodegenerative disease in the elderly, which is clinically characterized by bradykinesia, resting tremor, abnormal posture balance, and hypermyotonia. Currently, the pathogenic mechanism of PD remains unclear. Numerous clinical studies as well as animal and cell experiments have found a certain relationship between the vitamin family and PD. The antioxidant properties of vitamins and their biological functions of regulating gene expression may be beneficial for the treatment of PD. Current clinical evidence indicates that proper supplementation of various vitamins can reduce the incidence of PD in the general population and improve the clinical symptoms of patients with PD; nevertheless, the safety of regular vitamin supplements still needs to be highlighted. Vitamin supplementation may be an effective adjuvant treatment for PD. In this review, we summarized the biological correlations between vitamins and PD as well as the underlying pathophysiological mechanisms. Additionally, we elaborated the therapeutic potentials of vitamins for PD.

1. Introduction

Parkinson's disease (PD) is the second most common neurodegenerative disorder following Alzheimer's disease. Clinically, PD is characterized by resting tremor, hypermyotonia, postural instability, and bradykinesia [1]. Additionally, patients with PD can also manifest with nonmotor symptoms, such as cognitive decline, olfactory dysfunction, constipation, sleep disorders, and autonomic symptoms [2], and these nonmotor symptoms usually occur prior to the onset of motor symptoms [3]. PD severely affects the quality of life of the individual with the disease and also creates a great burden on the caregivers. The typical pathological hallmark of PD is degeneration of dopaminergic neurons in the substantia nigra pars compacta (SNpc) and eosinophilic inclusion bodies (Lewy bodies) in the remaining neurons, which is the major contributor to the deficiency of dopamine in the basal ganglia [4, 5]. The exact pathogenetic mechanisms of PD is not yet fully understood. Current theories regard PD as a multifactorial disease, involving various genetic and environmental factors, among which mitochondrial dysfunction and oxidative stress play an important role in the pathogenesis and development of PD [6, 7]. The treatment for PD is challenging, and the existing therapeutic strategies can only relieve clinical symptoms but fail to control the progression of PD.

Vitamins are natural bioactive products with antioxidant properties, which are necessities for maintaining the normal functions of human organisms. Essential vitamins cannot be endogenously synthesized in the organism and therefore must be obtained through the diet. Clinically, vitamin deficiency is quite common, especially in infants and elderly. Vitamins are generally divided into fat-soluble variants (vitamins A, D, E, and K) and water-soluble variants (vitamins B and C). The former mainly bind to cellular nuclear receptors and affect the expression of specific genes [8]. The latter

mainly constitute a cofactor for the enzyme, affecting the enzymatic activity [9].

Numerous clinical studies as well as animal and cell experiments have found a certain relationship between the vitamin family and PD [10]. The antioxidant properties of vitamins and their biological functions of regulating gene expression may be beneficial for the treatment of PD. Current clinical evidence indicates that proper supplementation of various vitamins can reduce the incidence of PD in the general population and improve the clinical symptoms of patients with PD; nevertheless, the safety of regular vitamin supplements still needs to be highlighted. Vitamin supplementation may represent an effective adjuvant treatment for PD. In this review, we summarized the biological correlations between vitamins and PD as well as the underlying pathophysiological mechanisms. Additionally, we elaborated the therapeutic potentials of vitamins for PD.

2. The Pathogenesis of Oxidative Stress in PD

Oxidative stress refers to the imbalance between the oxidation system and antioxidant system, resulting in excessive accumulation of oxidative substances, such as reactive oxygen species (ROS) and reactive nitrogen species (RNS) [11]. ROS include superoxide anion radical (O_2^-), hydroxyl radical (OH^-), and hydrogen peroxide (H_2O_2); RNS include nitric oxide (NO), nitrogen dioxide (NO_2), and peroxynitrite ($ONOO^-$). The antioxidant system mainly consists of two subtypes: (1) enzymatic antioxidant system, including superoxide dismutase (SOD), catalase (CAT), and glutathione peroxidase (GSH-Px), and (2) nonenzymatic antioxidant system, including vitamin C, vitamin E, glutathione, melatonin, alpha-lipoic acid, carotenoids, and trace elements copper, zinc, and selenium.

Oxidative stress plays an important physiological role in the organism. For example, phagocytic cells kill pathogenic microorganisms, participate in detoxification and enzymatic reactions, and synthesize some essential biologically active substances. Meanwhile, it can as well cause damage to the body, such as cell membrane destruction, protein denaturation, and nucleic acid changes.

There is increasing evidence that oxidative stress represents a pathophysiological characteristic of PD, and the production of reactive oxygen species can result in neuronal death [12, 13]. The mitochondrial respiratory chain is regarded as the major source of ROS [14]. Additionally, previous studies have found that mitochondrial dysfunction exists in the substantia nigra of patients with PD [15]. Reduced glutathione (GSH) can enhance the production of ROS and RNS [16], and oxidation of dopamine and dopamine metabolites such as 3,4-dihydroxyphenylacetic acid (DOPAC) can inhibit the activity of complex I [17]. These findings indicate that the downstream metabolites of dopamine may make dopamine neurons more susceptible. Moreover, iron accumulation in the substantia nigra is common in patients with PD, leading to overproduction of hydrogen peroxide and molecular oxygen in the Fenton reaction from Fe^{2+} to Fe^{3+}; hydrogen peroxide generates a highly toxic hydroxyl radical through the Haber-Weiss reaction in the presence of Fe^{2+}, which causes severe oxidative damage to the cellular components [18]. From the above, the oxidant stress is closely associated with the pathogenesis of PD. Oxidative stress can cause neuronal loss through some underlying intracellular damage, such as protein aggregation, mitochondrial dysfunction, and DNA rupture. Therefore, antioxidant damage has become a potential target for the treatment of PD.

3. Vitamin B and PD

The B family of vitamins is water-soluble, which includes thiamine (vitamin B_1), riboflavin (vitamin B_2), niacin (vitamin B_3), pantothenic acid (vitamin B_5), pyridoxine (vitamin B_6), biotin (vitamin B_7), folate (vitamin B_9), and cobalamin (vitamin B_{12}) [19]. These vitamins play an important role as enzyme cofactors in multiple biochemical pathways in all tissues, such as regulating metabolism, improving the function of the immune system and nervous system, and promoting cell growth and division [20].

Almost all of these B family vitamins are essential variants dependent on diet supply, except niacin which can also be synthesized from tryptophan. Vitamin B deficiencies are frequent in the children, elderly, vegetarians, pregnant women, and patients with gastrointestinal diseases. Recently, the association with vitamin B and PD is getting more and more attention. Herein, we use vitamin B_3 as a representative to discuss the relationship between vitamin B and PD.

3.1. Vitamin B_3. Nicotinamide is the active form of niacin, and it is the precursor of coenzymes NADH and NADPH, which are essential for over 200 enzymatic reactions in the organism, especially the production of adenosine triphosphate (ATP). Meat, fish, and wheat are generally rich in nicotinamide, while vegetables have a low nicotinamide content [21]. Deficiency of nicotinamide/niacin can lead to pellagra, causing dermatitis, diarrhea, and depression [22]. Nicotinamide has neuroprotective and antioxidant functions at low doses but exhibits neurotoxicity, especially dopaminergic toxicity, at high doses [23]. Fukushima also suggests that excessive nicotinamide is related to the development of PD [24]; excessive nicotinamide can induce overproduction of 1-methylnicotinamide (MNA), which is increased in patients with PD [25]. In an *in vitro* study, Griffin et al. found that low-dose nicotinamide (10 mM) has a significant effect on inducing differentiation from embryonic stem cells into neurons; however, higher doses (>20 mM) of nicotinamide induce cytotoxicity and cell death [26]. The definitive protective dose of vitamin B_3 still needs further researches.

3.2. Possible Neuroprotective Mechanisms of Vitamin B_3 in PD. Firstly, numerous studies have demonstrated that mitochondrial dysfunction and cellular energy failure are pathophysiological features of PD. Nicotinamide participates in the biosynthesis of nicotinamide adenine dinucleotide (NAD; oxidized form: NAD^+; reduced form: NADH) via various metabolic pathways [27]. NADH is an essential cofactor assisting the tetrahydrobiopterin functioning in tyrosine

hydroxylase, which can hydroxylate tyrosine and produce dopamine; NADH deficiency is common in PD [28].

Secondly, NADH is indispensable for the physiological function of mitochondrial complex I in ATP synthesis, and the corresponding dysfunction is involved in PD patients and animal models [15, 29, 30]. Nicotinamide mononucleotide (NMN) constitutes one of the key precursors of NAD^+. In previous *in vitro* studies, the scholars have established a cellular model of PD using rotenone-treated PC12 cells, and they found the NMN (0.1 mM or 1 mM) treatment was associated with a significantly higher survival rate in the rotenone-treated (0.5 μm) PC12 cells. NMN is assumed to enhance the intracellular levels of NAD^+ and ATP in the cellular model of PD [31].

In addition, nicotinamide can act a neuroprotective role by inhibiting the oxidative stress. In 1-methyl-4--phenyl-1,2,3,6-tetrahydropyridine- (MPTP-) induced mouse models of PD, nicotinamide (500 mg/kg) was injected before subacute (30 mg/kg/d for 5 days) MPTP administration. This study showed that cotreatment with MPTP and nicotinamide significantly improved the locomotor activity compared to single-agent treatment with MPTP. Nicotinamide administration significantly attenuated the MPTP-induced dopamine depletion (47.11 ± 21.06 vs. 12.77 ± 8.06). Meanwhile, nicotinamide pretreatment markedly inhibited MPTP-induced lactate dehydrogenase (LDH) and NOS activities, which prevented the oxidative stress and alleviated the oxidative damage.

Sirtuins (SIRTs) are NAD^+-dependent protein deacetylases involved in vital biological processes [32]. Recently, sirtuin 5 (SIRT5) has received considerable attention. Liu et al. investigated the role of SIRT5 in MPTP-induced mouse PD models [33]. They found that deletion of SIRT5 exacerbated motor deficits, nigrostriatal dopaminergic degeneration in the compact part of substantia nigra (SNc), and mitochondrial antioxidant activities in the PD models. These findings provide new insight into the therapeutic strategies for PD. However, the protective effects of nicotinamide are still controversial, and further researches are needed to clarify the biological function of vitamin B_3 in PD.

3.3. Clinical Studies regarding Vitamin B_3 in PD. Current existing clinical studies have shown that a high-niacin diet can reduce the risk of PD [34, 35]. A previous case report also demonstrated that oral niacin (500 mg twice daily for three months) significantly improved rigidity and bradykinesia in a patient with idiopathic PD, though the original purpose was to treat hypertriglyceridemia; after the cessation of oral niacin due to obvious adverse effects (unacceptable nightmares and skin rash), the symptoms of rigidity and bradykinesia relapsed [36]. However, other studies failed to notice the remarkable clinical efficacy [37, 38]. Therefore, more clinical observations are warranted to verify the efficacy as well as side effects of niacin in PD.

4. Vitamin C and PD

Vitamin C (ascorbic acid) is another water-soluble, essential vitamin, which is widely distributed in various tissues. This nutriment is abundant in vegetables, fresh fruits, and animal livers. Vitamin C contains two molecular subforms in organisms: the reduced form (ascorbic acid (AA)) and the oxidized form (dehydroascorbic acid (DHA)). Deficiency of vitamin C is common, especially in children and elderly. A long-term lack of vitamin C can cause scurvy. Vitamin C is very important for the physiological function of the nervous system and the antioxidant function by inhibiting oxidative stress, reducing lipid peroxidation, and scavenging free radicals [39]. Moreover, it is also involved in many nonoxidative stress processes, such as synthesis of collagen, cholesterol, carnitine, catecholamines, amino acids, and some peptide hormones [40, 41].

Dopamine metabolism can produce oxidative stress products, which in return induce accumulation of abnormal proteins in PD [42]. Vitamin C has potentials for the treatment of PD considering the following reasons. Firstly, vitamin C is mainly distributed in areas that are rich in neurons [43, 44]. Secondly, vitamin C can be transported to the brain by SVCT2 (vitamin C transporter type 2) [45], and DHA can be transported to the brain by GLUT1 (glucose transporter type 1) and GLUT3 (glucose transporter type 3) [46].

4.1. Possible Neuroprotective Mechanisms of Vitamin C in PD. There is evidence that ascorbic acid can protect against both levodopa toxicity and the MPTP neurotoxicity [47, 48]. Vitamin C can increase the production of dihydroxyphenylalanine (DOPA). Seitz et al. noted overproduction of DOPA in a dose-dependent manner after incubation of the human neuroblastoma cell line SK-N-SH with ascorbic acid (100-500 mM) for 2 hours. Additionally, the gene expression of tyrosine hydroxylase increased threefold after incubation with ascorbic acid (200 mM) for 5days. The scholars speculated that ascorbic acid may be effective in the treatment of early-stage PD [49].

Vitamin C can improve the absorption of levodopa in elderly PD patients with a poor levodopa bioavailability [50]. Previous studies showed that ascorbic acid can reduce the levodopa dosage under the premise of equal efficacy [51]. Combination of anti-PD drugs and vitamin C may be more effective for alleviating the symptoms of PD.

Vitamin C is essential for the brain development. A study showed that ascorbic acid treatment can promote a 10-fold increase of dopaminergic differentiation in CNS precursor cells derived from the E12 rat mesencephalon [52]. Soon after, another *in vitro* study also reported that AA can stimulate the CNS precursor cells differentiating into CNS neurons and glia [53]. Recently, He et al. proposed that vitamin C can greatly enhance the embryonic midbrain neural stem cells differentiating into midbrain dopaminergic neurons in vitro. Vitamin C induces the gain of 5-hydroxymethylcytosine (5HMC) and loss of H3K27m3 in dopaminergic phenotype gene promoters, which are catalysed by ten-eleven translocation 1 methylcytosine dioxygenase 1 (TET1) and histone H3K27 demethylase (JMJD3), respectively. However, subsequent TET1 and JMJD3 knockdown/inhibition experiments did not show this effect of vitamin C, and the epigenetic role of vitamin C

may be associated with the midbrain dopaminergic neuron development [54, 55].

4.2. Clinical Studies regarding Vitamin C in PD. Although vitamin C has many potential positive effects on PD, the serum level of vitamin C in patients with PD remains controversial [56, 57]. Noteworthily, the vitamin C level in lymphocytes has been found significantly lower in patients with severe PD [58]. Theoretically, vitamin C supplementation may be beneficial for the treatment of PD. A cohort study involving 1036 patients with PD supported this hypothesis, which found that dietary vitamin C intake significantly reduced the risk of PD, but this effect is invalid for a 4-year-lag analysis [59]. Controversially, many studies did not support that vitamin C supplementation can reduce the risk of PD [10, 60, 61]. We speculate this contradiction may be related to the timing of vitamin application.

5. Vitamin E and PD

Vitamin E is a fat-soluble vitamin with high antioxidant properties. Natural vitamin E includes two subgroups: tocopherols and tocotrienols; and they can further be divided into four lipophilic molecules, respectively: α-, β-, γ-, and δ-tocopherol (αT, βT, γT, and δT) and α-, β-, γ-, and δ-tocotrienol (αTE, βTE, γTE, and δTE). The major difference between tocopherols and tocotrienols is the side chain. Tocopherols have a saturated phytyl tail, while tocotrienols possess an unsaturated isoprenoid side chain [62]. Because of this unsaturated side chain, the tocotrienol is superior to the tocopherol as an antioxidant by increasing the molecular mobility through lipid membranes and by accepting electrons readily. Overt vitamin E deficiency is relatively rare, mainly in infants and premature babies.

In addition to its potent antioxidant capacity, vitamin E is involved in many physiological processes such as immune function [63], cognitive function, physical performance [64, 65], and regulation of gene expression. In humans, deficiency of vitamin E is clinically characterized by peripheral neuropathy, ataxia, and anemia [66, 67].

5.1. Possible Neuroprotective Mechanisms of Vitamin E in PD. Unilateral 6-hydroxydopamine (6-OHDA) injections into the striatum can cause circling behaviours and biochemical abnormalities in rats. Cadet et al. found that pretreatment with either D-alpha-tocopherol or all-racemic-alpha--tocopherol significantly attenuated these pathological changes [68]. Roghani and Behzadi [69] and Sharma and Nehru [70] also demonstrated the similar phenomenon in 6-OHDA-induced PD models and in rotenone-induced PD models, respectively. However, some studies have shown that vitamin E did not completely protect dopaminergic neurons from MPTP-mediated damage in PD models [71, 72]. The protective effects of vitamin E may be achieved through preventing oxidative stress in cells and inhibiting apoptosis. Moreover, one study has found that tocotrienol participates not only in antioxidant stress but also in estrogen receptor beta (ERβ) signal transduction [73]. Then, Nakaso's team demonstrated a protective effect of vitamin E via this signaling pathway. Firstly, they reported that γ-tocotrienol/δ-tocotrienol exerts neuroprotective effects through the ERβ-PI3K/Akt signaling pathways in SH-SY5Y cells by resisting 1-methyl-4-phenylpyridiniumion- (MPP^+-) induced toxicity [74]. Secondly, they verified this mechanism in a mouse model of PD. Meanwhile, they found δ-tocotrienol administration can reduce the loss of dopaminergic neurons in the substantia nigra and ER inhibitors can attenuate this neuroprotective effect [75]. These findings indicate vitamin E may be potential therapeutic agents for PD.

5.2. Clinical Studies regarding Vitamin E in PD. The DATATOP (Deprenyl and Tocopherol Antioxidative Therapy of Parkinsonism) experiment is a multicentre-controlled clinical trial to investigate the long-term efficacy of treatment with deprenyl and/or copherol (vitamin E) and to explore whether it is possible to extend the time before the application of levodopa treatment. At 28 US and Canadian sites, 800 eligible patients with untreated early-stage PD were enrolled in DATATOP and randomized to four groups: (1) deprenyl 10 mg/d, (2) copherol 2000 IU/d, (3) placebo-controlled, and (4) deprenyl 10 mg/d and copherol 2000 IU/d. Deprenyl can delay the development of functional disorders, delay the application of levodopa, and improve motor symptoms, but vitamin E is disappointing [76]. Similarly, another two population-based studies also did not find the association between vitamin E intake and risk of PD [10, 77].

However, a large community-based study showed that high intake of dietary vitamin E (10 mg/day) may reduce the occurrence of PD [78]. Another pilot trail suggests that long-term treatment with vitamin E may delay the use of levodopa in patients with PD [79]. Further research is needed to verify these results.

Although there seems to be no difference in the level of alpha-tocopherol (vitamin E) in serum, cerebrospinal fluid, and brains between PD and normal controls [80–82], there is evidence showing that high-dose vitamin E (2000 IU/day) can significantly elevate the vitamin E level in cerebrospinal fluid [83]. At present, the protective mechanism of vitamin E in PD is still unclear and may be related to the strong antioxidant effect of vitamin E. Further research is needed to determine whether vitamin E can be used as a potential treatment for PD.

6. Vitamin D and PD

Vitamin D, a steroid hormone, is crucial for calcium homeostasis and skeletal health. This nutriment mainly includes two forms: vitamin D_2 and vitamin D_3; the latter is endogenously produced when skin is exposed to UV-B rays from the sun. Both of the above forms are inactive, and they are transformed into the active form 1,25-dihydroxy vitamin D3 (1,25-$(OH)_2$-D_3) after being hydroxylated twice [84, 85]. 1,25-$(OH)_2$-D_3 were secreted into the blood system by the kidney, having a direct effect on gene regulation by binding to the nuclear vitamin D receptor (VDR) [86, 87]. Vitamin D deficiency is prevalent at all ages, especially in elderly. Vitamin D not only regulates the calcium homeostasis

Table 1: The other clinical study of vitamins and Parkinson's disease.

Vitamins	Authors	Type of study	Patients/controls	Conclusions
Vitamin B_3	Abbott et al. [37]	A Honolulu-Asia Aging Study in Japanese-American	Total 8006 and observed 137 PD	Niacin has no obvious relationship with clinical PD
	Johnson et al. [38]	A case-control study in US	126/432	Niacin has no relationship with PD
	Fall et al. [34]	A case-control study in Sweden	113/263	High-niacin diet can reduce the risk of PD
	Hellenbrand et al. [35]	A case-control study in German	342/342	PD patients with lower intake of niacin than controls
Vitamin C	Yang et al. [61]	A prospective study in Sweden	Total 84,774 and observed 1329 PD cases	Intake of vitamin C has a negative correlation with PD risk in women at borderline significance ($P = 0.04$)
	Hughes et al. [59]	A prospective study in American	Total 129,422 and observed 1036 PD cases	Intake of vitamin C has no relationship with PD risk
	Ide et al. [58]	A case-case study in Japan	62 PD	The severe PD patients with significantly lower lymphocyte vitamin C levels ($P < 0.01$)
	Miyake et al. [60]	A case-control study in Japan	249/368	Intake of vitamin C has no relationship with PD risk
	Zhang et al. [10]	A prospective study in US	Total 124,221 and observed 371 PD cases	Intake of vitamin C has no relationship with PD risk
	Férnandez-Calle et al. [56]	A case-control study in Spain	63/63	Vitamin C has no relationship with PD
	King et al. [127]	A case-control study in United States	27/16	Vitamin C was higher in PD groups
Vitamin E	Yang et al. [61]	A prospective study in Sweden	Total 84,774 and observed 1329 PD cases	Dietary intake of vitamin E has negative correlation with the incidence of PD in women ($P = 0.02$)
	Hughes et al. [59]	A prospective study in American	Total 129,422 and observed 1036 PD cases	Vitamin E has no relationship with PD risk
	Miyake et al. [60]	A case-control study in Japan	249/368	Vitamin E significantly reduced the risk of PD
	Zhang et al. [10]	A prospective study in US	Total 124,221 and observed 371 PD cases	Intaking foods containing more vitamin E can reduce the risk of Parkinson's disease
	Molina et al. [82]	A case-control study in Spain	34/47	CSF and serum vitamin E levels have no difference between two groups
	de Rijk et al. [78]	A cross-sectional study in Netherlands	5342 individuals including 31 PD cases	Intaking 10 mg dietary vitamin E daily may reduce the risk of PD
	Logroscino et al. [77]	A case-control study in USA	110/287	Vitamins A, C, and E were not associated with PD
	Férnandez-Calle et al. [80]	A case-control study in Spain	42/42	Serum levels of alpha-tocopherol (vitamin E) have no difference between two groups
Vitamin D	Kim et al. [128]	A prospective, observational study in Korea	39 PD cases	The level of vitamin D might impact the olfactory dysfunction in PD
	Sleeman et al. [112]	A prospective observational study in England	145/94	Serum 25(OH)D concentrations are often lower in PD patients than controls and relate to the severity of motor symptoms

Table 1: Continued.

Vitamins	Authors	Type of study	Patients/controls	Conclusions
	Wang et al. [110]	A case-control study in China	201/199	The serum 25(OH)D and sunlight exposure inversely correlated with PD occurrence
	Shrestha et al. [129]	A prospective study in USA	Total 12,762 participants and observed 67 PD cases	This study did not suggest that the vitamin D can reduce the risk of PD
	Liu and Zhang [111]	A case-control study in China	229/120	The 25(OH) D levels may be inversely associated with the PD severity
	Lin et al. [130]	A case-control study in China	700/792	They have not found the associations between the genetic variants of VDR and PD occurrence
	Zhu et al. [131]	A case-control study in China	209/210	Outdoor activity and total vitamin D intake may reduce the risk of PD
	Petersen et al. [132]	A case-control study in Denmark	121/235	They have not found the association between PD and vitamin D polymorphisms and/or 25(OH)D levels
	Török et al. [133]	A case-control study in Hungary	100/109	It showed the association between the FokI C allele and PD
	Lv et al. [134]	A case-control study in China	483/498	The study did not support the relationship between VDR gene and PD
	Peterson et al. [135]	A cross-sectional, observational study in USA	40 PD	Serum vitamin D levels are inversely related to the severity of Parkinson's disease and play an important role in balance of PD
	Suzuki et al. [96]	A prospective cohort study in Japan	137 PD	The 25-hydroxyvitamin D levels and the vitamin D receptor FokI CC genotype may be associated with the severity of the PD
	Kenborg et al. [108]	A case-control study in Denmark	3819/19,282	This study supports that working outdoors can reduce the risk of PD
	Evatt et al. [136]	A survey study in USA	199 PD (from DATATOP)	Vitamin D insufficiency is very common in early PD patients
	Miyake et al. [137]	A case-control study in Japan	249/368	The study showed that vitamin D was not related to the PD
	Knekt et al. [106]	The Mini-Finland Health Survey in Finland	Total 3173 and observed 50 PD cases	The serum vitamin D concentrations were inversely correlated with the risk of PD
	Kim et al. [94]	A case-control study in Korea	85/231	Vitamin D receptor gene polymorphism was associated with the PD

and skeletal health but also regulates the physiological and pathological processes, such as cell proliferation and differentiation, immunomodulatory, and antioxidative stress [88–90]. Children with a lack of vitamin D may suffer from rickets, and adults may develop osteomalacia. Additionally, vitamin D deficiency is also associated with cardiovascular diseases, muscle weakness, diabetes mellitus, cancers, and multiple sclerosis [91]. The relationship between vitamin D and PD has gradually attracted attention [92].

6.1. Possible Neuroprotective Mechanisms of Vitamin D in PD. VDR belongs to the intranuclear receptor superfamily, composing of eight coding exons and three alternative 5′ noncoding exons, spanning over 105 kb, on chromosome 12 [93]. The most widely studied biallelic polymorphic sites are BsmI, TaqI, ApaI, and FokI. Substantial researches have been carried out to explore the relationship between these allelic variations and PD. Kim et al. detected VDR gene BsmI polymorphisms in over 300 Korean individuals (85 PD and

Table 2: The clinical intervention trial of vitamins and Parkinson's disease.

Vitamins	Authors	Patients	Treatment	Conclusions
Vitamin C	Nagayama et al. [50]	67 elderly PD patients	200 mg ascorbic acid	Ascorbic acid can improve levodopa absorption in elderly PD patients
Vitamin E	Parkinson Study Group (DATATOP study) [76]	800 untreated and early PD patients	Deprenyl 10 mg/d and/or tocopherol (vitamin E) 2000 IU/d	There was no effect of tocopherol on PD
	Parkinson Study Group (DATATOP study) [124]	800 untreated and early PD patients	Deprenyl 10 mg/d and/or tocopherol (vitamin E) 2000 IU/d	Alpha-tocopherol did not improve clinical features in patients with Parkinson's disease
	Vatassery et al. (DATATOP study) [83]	$n = 18$ (vitamin E group)/$n = 5$ (placebo group)	Tocopherol (vitamin E) 2000 IU/d	Treatment with vitamin E significantly increased the alpha-tocopherol concentrations in cerebrospinal fluid
	Taghizadeh et al. [125]	$n = 30$ (vitamin E group)/$n = 30$ (placebo group)	1000 mg omega-3 fatty acids plus 400 IU vitamin or placebo	Omega-3 and vitamin E cosupplementation in PD patients improved UPDRS compared with the placebo
Vitamin D	Suzuki et al. [113]	$n = 56$ (vitamin D3 group)/$n = 58$ placebo group)	Vitamin D3 1200 IU/d or placebo for 12 months	Vitamin D3 prevented the deterioration of the PD and especially patients with FokI TT genes
	Sato et al. [126]	$n = 43$ (vitamin D group)/$n = 43$ (placebo group)	$1\alpha(OH)D_3$ 1 μg/d or placebo for 12 months	1alpha-hydroxyvitamin D3 supplements can reduce the risk of hip and other nonvertebral fractures in PD patients

231 controls). The frequency of VDR genotype *bb* was significantly increased in the PD patients (84.7%) than that in the controls (72.7%). The *bb* genotype was more common in PD patients with postural instability and gait difficulty than in the PD patients with tremor (94.3% vs. 75.6%) [94]. A meta-analysis showed that VDR BsmI and FokI polymorphisms were associated with the risk of PD [95], and VDR FokI genotype was associated with the severity and cognitive decline of PD [96, 97]. Muscular and motor impairments, which can seriously affect the motor behaviour, were found in the VDR-knockout mice [98], indicating that vitamin D may be involved in the pathogenesis of PD.

Glial cell line-derived neurotrophic factor (GDNF) is a protein that is essential for the maintenance and survival of dopaminergic neurons and can inhibit microglial activation [99]. Many animal studies showed that $1,25\text{-}(OH)_2\text{-}D_3$ could enhance the endogenous GDNF expression in vitro and in vivo and inhibit the glial cell activation to protect dopaminergic neurons from immune inflammation [100–102].

Vitamin D_3 can protect dopaminergic neurons against 6-hydroxydopamine-mediated neurotoxicity and improve the motor performance in the 6-hydroxydopamine-induced PD rat [103]. It may be related to vitamin D's properties of inhibiting oxidative stress and decreasing the production of reactive oxygen species and free radicals [104]. In addition, endothelial dysfunction may be associated with low vitamin D levels in patients with PD [105]. The definitive correlations between vitamin D and PD require more researches.

6.2. Clinical Studies regarding Vitamin D in PD. Substantial epidemiological and clinical studies suggest that vitamin D has a positive effect on PD. In a cohort study, over 7000 Finnish's serum samples were collected for measuring the 25-hydroxy vitamin D level, and meanwhile, the occurrence of PD was instigated over a 30-year follow-up period. The results showed that individuals with higher serum vitamin D concentrations had a lower risk of PD [106]. Evatt et al. also noted consistent findings [107].

As mentioned above, vitamin D_3 can be endogenously synthesized upon sunlight exposure in the skin. In a large case-control study of Danish men, involving 3819 PD patients and 19,282 controls, the scholars proposed that men working outdoors have a lower risk of PD [108]. Another nationwide ecologic study in France also suggests that vitamin D levels are negatively correlated with the risk of PD, but this result needs taking ages into account [109]. Wang et al. not only demonstrated a positive correlation between serum 25-hydroxy vitamin D and sunlight exposure but also noted that lower serum levels of 25-hydroxy vitamin D and sunlight exposure can increase the risk of PD [110].

Furthermore, PD patients with lower 25-hydroxy vitamin D levels may exhibit more severe symptoms compared with normal controls [111, 112]. Unsurprisingly, a randomized, double-blind, placebo-controlled trial found that vitamin D_3 supplementation (1200 IU/day for 12 months) significantly prevented the deterioration of PD [113].

Table 3: The basic study of vitamins in PD.

Vitamin	Authors	Object of study	Treatment	Conclusions
Vitamin B_3 (nicotinamide)	Lu et al. [31]	Rotenone-PC12 cells	NMN (0.1 mM, 1.0 mM, 5 mM, and 10 mM) coculture	Attenuated apoptosis and improved energy metabolism
	Xu et al. [114]	MPTP-C57BL/6 mice	500 mg/kg/day for 5 days i.p.	Nicotinamide can alleviate MPTP-induced damage to dopaminergic neurons through antioxidant stress
	Jia et al. [115]	MPP(+)-SK-N-MC human neuroblastoma cells and alpha-synuclein transgenic Drosophila PD model	Nicotinamide concentration (21, 51, 101, 301, and 501 mg/L and 3, 15, 30, and 60 mg/100 g)	High doses of nicotinamide can reduce oxidative stress and improve mitochondrial function
	Anderson et al. [116]	MPTP-adult male C57Bl/6 mice	Nicotinamide (125, 250, or 500 mg/kg i.p.)	Recovered the striatal DA levels and SNc neurons after accepting nicotinamide
Vitamin C (ascorbic acid)	Khan et al. [117]	PD Drosophila model	L-Ascorbic acid (AA, 11.35×10^{-5} M, 22.71×10^{-5} M, 45.42×10^{-5} M, and 68.13×10^{-5} M for 21 days)	Except 11.35×10^{-5} M, other concentrations of AA attenuated the loss of climbing ability of PD model flies in a dose-dependent manner
	Yan et al. [52]	Mesencephalic precursors from the E12 rat	Ascorbic acid (0.1 μM, 1 μM, 10 μM, 100 μM, and 1 mM)	Ascorbic acid promoted the dopaminergic differentiation
	Seitz et al. [49]	Human neuroblastoma cell line SK-N-SH	Short-term incubation (100–500 μM for 2 h) and long-term incubation (200 μM for 5 days)	Ascorbic acid increased the DOPA production and tyrosine hydroxylase gene expression
	Pardo et al. [47]	Human neuroblastoma cell NB69	10^{-3} M ascorbic acid or 23 and 115×10^{-3} M alpha-tocopherol	Ascorbic acid prevents the levodopa toxicity and quinone formation, but alpha-tocopherol did not
	Sershen et al. [48]	MPTP-BALB/cBy mice	Ascorbic acid 100 mg/kg i.p.	Ascorbic acid may protect against the MPTP neurotoxicity
Vitamin E	Nakaso et al. [75]	MPTP-C57BL/6 mice	δ-Tocotrienol (100 μg/kg for 4 days, p.o.)	δ-Tocotrienol administration inhibited the loss of dopaminergic neurons and improved the motor performance
	Sharma and Nehru [70]	Rotenone-Sprague-Dawley rats	Vitamin E (100 IU/kg/day for 35 days i.m.)	Vitamin E administration significantly improved locomotor activity and increased the dopamine level, GSH, and SOD
	Ortiz et al. [118]	MPTP-C57BL/6 mice	Vitamin E (50 mg/kg/day p.o.)	Vitamin E administration has decreased the COX-2 activity, LPO, and nitrite/nitrate level
	Pasbakhsh et al. [119]	6-OHDA-rat	Alpha-tocopherol acid succinate (24 IU/kg, i.m.)	Vitamin E treatment can protect locus coeruleus neurons in the PD model
	Roghani and Behzadi [69]	6-OHDA – Sprague-Dawley rats	D-α-Tocopheryl acid succinate (24 I.U./kg, i.m.)	Vitamin E treatment improved the rotational behaviour and prevented the reduction of tyrosine hydroxylase-immunoreactive cells

Table 3: Continued.

Vitamin	Authors	Object of study	Treatment	Conclusions
Vitamin D	Lima et al. [120]	6-OHDA-Wistar rats	1,25-$(OH)_2D_3$ (1 μg/kg for 7 days or for 14 days, p.o.)	Vitamin D can protect the dopaminergic neurons by its anti-inflammatory and antioxidant properties
	Calvello et al. [121]	MPTP-male C57BL/6 N mice	Vitamin D (1 μg/kg for 10 days, i.g.)	Vitamin D administration attenuates neuroinflammation and dopaminergic neurodegeneration
	Li et al. [122]	MPTP-C57BL/6 mice	Calcitriol (0.2, 1, and 5 μg/kg/day for 7 days p.o.)	Calcitriol can significantly attenuate the neurotoxicity induced by MPTP
	Jang et al. [104]	Rotenone-SH-SY5Y cells	Calcitriol (0.0 μM, 0.63 μM, 1.25 μM, 2.5 μM, 5 μM, and 10 μM)	1,25-Dyhydroxyvitamin D_3 can induce the autophagy to protect against the rotenone-induced neurotoxicity
	Cass et al. [123]	6-OHDA-male Fischer-344 rats	Calcitriol (0.3 or 1.0 μg/kg/day for 8 days, i.h.)	Calcitriol can promote functional recovery of dopaminergic neurons and release of dopamine
	Sanchez et al. [100]	6-OHDA-Sprague-Dawley rats	1,25(OH)(2)D(3) (1 μg/mL/kg/day for 7 days i.p.)	1,25(OH)(2)D(3) treatment increased the GDNF protein expression and partially restored TH expression
	Kim et al. [102]	6-OHDA Sprague-Dawley rats and MPTP-C57BL/6 mice	1,25-$(OH)_2D_3$ (1 μg/mL at 1 mL/kg/day for 7 days, i.p.)	1,25-$(OH)_2D_3$ can inhibit the microglial activation and protect against nigrostriatal degeneration

LPO: lipid peroxides; COX-2: ciclooxigenase-2; TH: tyrosine hydroxylase; i.p.: intraperitoneal; i.m.: intramuscular; i.g.: intragastrical; i.h.: hypodermic injection; p.o.: peros.

7. Conclusion

In summary, vitamins may play a protective role in PD. Among the fat-soluble vitamins, we briefly summarized the effects of vitamin E and vitamin D. At present, although many studies have shown that vitamin E supplementation can reduce the risk of Parkinson's disease (Table 1), the DATATOP study has showed that vitamin E supplementation is ineffective in Parkinson's disease (Table 2). Many noninterventional studies found that the high levels of serum vitamin D can reduce the risk of PD (Table 1), and several clinical intervention trials also proposed that vitamin D supplementation can attenuate the deterioration of the Parkinson's disease and reduce the occurrence of fractures in patients with PD (Table 2). Among the water-soluble vitamins, we elaborated the functions of vitamin B_3 and vitamin C. There is still a paucity of clinical evidence for determining the pros and cons of vitamin B_3 in PD (Table 2). Vitamin C is vital to the human organism, and it can improve levodopa absorption in elderly PD patients (Table 2); current epidemiological evidence is still insufficient to establish a correlation between the serum level or dietary intakes of vitamin C and the risk of PD (Table 1). Although there have been many researches on the relationship between vitamins and PD (Tables 1–3), there is still lack of a clinical intervention trial explicitly confirming that vitamin supplementation can reduce the incidence of PD and prevent the progression of the disease. Moreover, the individual physical and chemical properties, absorption rate, and bioavailability of vitamins may affect the efficacy. Further studies are still needed to clarify the potentials of vitamins for the treatment of PD.

Conflicts of Interest

The authors have no conflicts of interest to declare.

Authors' Contributions

Xiuzhen Zhao and Ming Zhang equally contributed to this study.

Acknowledgments

This work was supported by the crosswise project from the Ministry of Science and Technology of Jilin Province (Grant No. 3R2168713428) and the Natural Science Foundation of Jilin Province (Grant No. 20180101154JC).

References

[1] W. R. Gibb and A. J. Lees, "The relevance of the Lewy body to the pathogenesis of idiopathic Parkinson's disease," *Journal of Neurology, Neurosurgery, and Psychiatry*, vol. 51, no. 6, pp. 745–752, 1988.

[2] T. K. Khoo, A. J. Yarnall, G. W. Duncan et al., "The spectrum of nonmotor symptoms in early Parkinson disease," *Neurology*, vol. 80, no. 3, pp. 276–281, 2013.

[3] R. B. Postuma, D. Aarsland, P. Barone et al., "Identifying prodromal Parkinson's disease: pre-motor disorders in Parkinson's disease," *Movement Disorders*, vol. 27, no. 5, pp. 617–626, 2012.

[4] P. Goswami, N. Joshi, and S. Singh, "Neurodegenerative signaling factors and mechanisms in Parkinson's pathology," *Toxicology In Vitro*, vol. 43, pp. 104–112, 2017.

[5] M. G. Spillantini, M. L. Schmidt, V. M. Y. Lee, J. Q. Trojanowski, R. Jakes, and M. Goedert, "α-Synuclein in Lewy bodies," *Nature*, vol. 388, no. 6645, pp. 839-840, 1997.

[6] E. Hattingen, J. Magerkurth, U. Pilatus et al., "Phosphorus and proton magnetic resonance spectroscopy demonstrates mitochondrial dysfunction in early and advanced Parkinson's disease," *Brain*, vol. 132, no. 12, pp. 3285–3297, 2009.

[7] W. D. Parker Jr, J. K. Parks, and R. H. Swerdlow, "Complex I deficiency in Parkinson's disease frontal cortex," *Brain Research*, vol. 1189, pp. 215–218, 2008.

[8] D. Sánchez-Hernández, G. H. Anderson, A. N. Poon et al., "Maternal fat-soluble vitamins, brain development, and regulation of feeding behavior: an overview of research," *Nutrition Research*, vol. 36, no. 10, pp. 1045–1054, 2016.

[9] J. Chawla and D. Kvarnberg, "Hydrosoluble vitamins," *Handbook of Clinical Neurology*, vol. 120, pp. 891–914, 2014.

[10] S. M. Zhang, M. A. Hernan, H. Chen, D. Spiegelman, W. C. Willett, and A. Ascherio, "Intakes of vitamins E and C, carotenoids, vitamin supplements, and PD risk," *Neurology*, vol. 59, no. 8, pp. 1161–1169, 2002.

[11] H. Sies, C. Berndt, and D. P. Jones, "Oxidative stress," *Annual Review of Biochemistry*, vol. 86, no. 1, pp. 715–748, 2017.

[12] L. V. Kalia and A. E. Lang, "Parkinson's disease," *The Lancet*, vol. 386, no. 9996, pp. 896–912, 2015.

[13] J. Blesa, I. Trigo-Damas, A. Quiroga-Varela, and V. R. Jackson-Lewis, "Oxidative stress and Parkinson's disease," *Frontiers in Neuroanatomy*, vol. 9, p. 91, 2015.

[14] M. P. Murphy, "How mitochondria produce reactive oxygen species," *The Biochemical Journal*, vol. 417, no. 1, pp. 1–13, 2009.

[15] A. H. Schapira, J. M. Cooper, D. Dexter, P. Jenner, J. B. Clark, and C. D. Marsden, "Mitochondrial complex I deficiency in Parkinson's disease," *The Lancet*, vol. 333, no. 8649, p. 1269, 1989.

[16] J. Sian, D. T. Dexter, A. J. Lees et al., "Alterations in glutathione levels in Parkinson's disease and other neurodegenerative disorders affecting basal ganglia," *Annals of Neurology*, vol. 36, no. 3, pp. 348–355, 1994.

[17] M. R. Gluck and G. D. Zeevalk, "Inhibition of brain mitochondrial respiration by dopamine and its metabolites: implications for Parkinson's disease and catecholamine-associated diseases," *Journal of Neurochemistry*, vol. 91, no. 4, pp. 788–795, 2004.

[18] D. J. Hare and K. L. Double, "Iron and dopamine: a toxic couple," *Brain*, vol. 139, no. 4, pp. 1026–1035, 2016.

[19] H. E. Sauberlich, "Implications of nutritional status on human biochemistry, physiology, and health," *Clinical Biochemistry*, vol. 17, no. 2, pp. 132–142, 1984.

[20] K. Mikkelsen, L. Stojanovska, K. Tangalakis, M. Bosevski, and V. Apostolopoulos, "Cognitive decline: a vitamin B perspective," *Maturitas*, vol. 93, pp. 108–113, 2016.

[21] W. Gehring, "Nicotinic acid/niacinamide and the skin," *Journal of Cosmetic Dermatology*, vol. 3, no. 2, pp. 88–93, 2004.

[22] D. Surjana and D. L. Damian, "Nicotinamide in dermatology and photoprotection," *Skinmed*, vol. 9, no. 6, pp. 360–365, 2011.

[23] A. Williams and D. Ramsden, "Nicotinamide: a double edged sword," *Parkinsonism & Related Disorders*, vol. 11, no. 7, pp. 413–420, 2005.

[24] T. Fukushima, "Niacin metabolism and Parkinson's disease," *Environmental Health and Preventive Medicine*, vol. 10, no. 1, pp. 3–8, 2005.

[25] K. Aoyama, K. Matsubara, M. Kondo et al., "Nicotinamide-N-methyltransferase is higher in the lumbar cerebrospinal fluid of patients with Parkinson's disease," *Neuroscience Letters*, vol. 298, no. 1, pp. 78–80, 2001.

[26] S. M. Griffin, M. R. Pickard, R. P. Orme, C. P. Hawkins, and R. A. Fricker, "Nicotinamide promotes neuronal differentiation of mouse embryonic stem cells in vitro," *Neuroreport*, vol. 24, no. 18, pp. 1041–1046, 2013.

[27] S. Imai, "Nicotinamide phosphoribosyltransferase (Nampt): a link between NAD biology, metabolism, and diseases," *Current Pharmaceutical Design*, vol. 15, no. 1, pp. 20–28, 2009.

[28] S. M. Pearl, M. D. Antion, G. D. Stanwood, J. D. Jaumotte, G. Kapatos, and M. J. Zigmond, "Effects of NADH on dopamine release in rat striatum," *Synapse*, vol. 36, no. 2, pp. 95–101, 2000.

[29] Y. Mizuno, S. Ohta, M. Tanaka et al., "Deficiencies in complex I subunits of the respiratory chain in Parkinson's disease," *Biochemical and Biophysical Research Communications*, vol. 163, no. 3, pp. 1450–1455, 1989.

[30] W. J. Nicklas, I. Vyas, and R. E. Heikkila, "Inhibition of NADH-linked oxidation in brain mitochondria by 1-methyl-4-phenyl-pyridine, a metabolite of the neurotoxin, 1-methyl-4-phenyl-1, 2, 5, 6-tetrahydropyridine," *Life Sciences*, vol. 36, no. 26, pp. 2503–2508, 1985.

[31] L. Lu, L. Tang, W. Wei et al., "Nicotinamide mononucleotide improves energy activity and survival rate in an in vitro model of Parkinson's disease," *Experimental and Therapeutic Medicine*, vol. 8, no. 3, pp. 943–950, 2014.

[32] L. Yang, X. Ma, Y. He et al., "Sirtuin 5: a review of structure, known inhibitors and clues for developing new inhibitors," *Science China Life Sciences*, vol. 60, no. 3, pp. 249–256, 2017.

[33] L. Liu, C. Peritore, J. Ginsberg, J. Shih, S. Arun, and G. Donmez, "Protective role of SIRT5 against motor deficit and dopaminergic degeneration in MPTP-induced mice model of Parkinson's disease," *Behavioural Brain Research*, vol. 281, pp. 215–221, 2015.

[34] P. A. Fall, M. Fredrikson, O. Axelson, and A. K. Granérus, "Nutritional and occupational factors influencing the risk of Parkinson's disease: a case-control study in southeastern Sweden," *Movement Disorders*, vol. 14, no. 1, pp. 28–37, 1999.

[35] W. Hellenbrand, H. Boeing, B. P. Robra et al., "Diet and Parkinson's disease. II: a possible role for the past intake of specific nutrients. Results from a self-administered food-frequency questionnaire in a case-control study," *Neurology*, vol. 47, no. 3, pp. 644–650, 1996.

[36] J. M. Alisky, "Niacin improved rigidity and bradykinesia in a Parkinson's disease patient but also caused unacceptable nightmares and skin rash—a case report," *Nutritional Neuroscience*, vol. 8, no. 5-6, pp. 327–329, 2005.

[37] R. D. Abbott, G. Webster Ross, L. R. White et al., "Environmental, life-style, and physical precursors of clinical

Parkinson's disease: recent findings from the Honolulu-Asia Aging Study," *Journal of Neurology*, vol. 250, Supplement 3, pp. iii30–iii39, 2003.

[38] C. C. Johnson, J. M. Gorell, B. A. Rybicki, K. Sanders, and E. L. Peterson, "Adult nutrient intake as a risk factor for Parkinson's disease," *International Journal of Epidemiology*, vol. 28, no. 6, pp. 1102–1109, 1999.

[39] H. M. Oudemans-van Straaten, A. M. E. Spoelstra-de Man, and M. C. de Waard, "Vitamin C revisited," *Critical Care*, vol. 18, no. 4, p. 460, 2014.

[40] I. B. Chatterjee, A. K. Majumder, B. K. Nandi, and N. Subramanian, "Synthesis and some major functions of vitamin C in animals," *Annals of the New York Academy of Sciences*, vol. 258, pp. 24–47, 1975.

[41] G. Grosso, R. Bei, A. Mistretta et al., "Effects of vitamin C on health: a review of evidence," *Frontiers in Bioscience*, vol. 18, pp. 1017–1029, 2013.

[42] E. Belluzzi, M. Bisaglia, E. Lazzarini, L. C. Tabares, M. Beltramini, and L. Bubacco, "Human SOD2 modification by dopamine quinones affects enzymatic activity by promoting its aggregation: possible implications for Parkinson's disease," *PLoS One*, vol. 7, no. 6, article e38026, 2012.

[43] I. N. Mefford, A. F. Oke, and R. N. Adams, "Regional distribution of ascorbate in human brain," *Brain Research*, vol. 212, no. 1, pp. 223–226, 1981.

[44] K. Milby, A. Oke, and R. N. Adams, "Detailed mapping of ascorbate distribution in rat brain," *Neuroscience Letters*, vol. 28, no. 1, pp. 15–20, 1982.

[45] S. N. Hansen, P. Tveden-Nyborg, and J. Lykkesfeldt, "Does vitamin C deficiency affect cognitive development and function?," *Nutrients*, vol. 6, no. 9, pp. 3818–3846, 2014.

[46] K. Hosoya, G. Nakamura, S. I. Akanuma, M. Tomi, and M. Tachikawa, "Dehydroascorbic acid uptake and intracellular ascorbic acid accumulation in cultured Müller glial cells (TR-MUL)," *Neurochemistry International*, vol. 52, no. 7, pp. 1351–1357, 2008.

[47] B. Pardo, M. A. Mena, S. Fahn, and J. G. de Yébenes, "Ascorbic acid protects against levodopa-induced neurotoxicity on a catecholamine-rich human neuroblastoma cell line," *Movement Disorders*, vol. 8, no. 3, pp. 278–284, 1993.

[48] H. Sershen, M. E. A. Reith, A. Hashim, and A. Lajtha, "Protection against 1-methyl-4-phenyl-1, 2, 3, 6-tetrahydropyridine neurotoxicity by the antioxidant ascorbic acid," *Neuropharmacology*, vol. 24, no. 12, pp. 1257–1259, 1985.

[49] G. Seitz, S. Gebhardt, J. F. Beck et al., "Ascorbic acid stimulates DOPA synthesis and tyrosine hydroxylase gene expression in the human neuroblastoma cell line SK-N-SH," *Neuroscience Letters*, vol. 244, no. 1, pp. 33–36, 1998.

[50] H. Nagayama, M. Hamamoto, M. Ueda, C. Nito, H. Yamaguchi, and Y. Katayama, "The effect of ascorbic acid on the pharmacokinetics of levodopa in elderly patients with Parkinson disease," *Clinical Neuropharmacology*, vol. 27, no. 6, pp. 270–273, 2004.

[51] W. Sacks and G. M. Simpson, "Letter: ascorbic acid in levodopa therapy," *Lancet*, vol. 1, no. 7905, p. 527, 1975.

[52] J. Yan, L. Studer, and R. D. G. McKay, "Ascorbic acid increases the yield of dopaminergic neurons derived from basic fibroblast growth factor expanded mesencephalic precursors," *Journal of Neurochemistry*, vol. 76, no. 1, pp. 307–311, 2001.

[53] J. Y. Lee, M. Y. Chang, C. H. Park et al., "Ascorbate-induced differentiation of embryonic cortical precursors into neurons and astrocytes," *Journal of Neuroscience Research*, vol. 73, no. 2, pp. 156–165, 2003.

[54] X. B. He, M. Kim, S. Y. Kim et al., "Vitamin C facilitates dopamine neuron differentiation in fetal midbrain through TET1- and JMJD3-dependent epigenetic control manner," *Stem Cells*, vol. 33, no. 4, pp. 1320–1332, 2015.

[55] N. Wulansari, E. H. Kim, Y. A. Sulistio, Y. H. Rhee, J. J. Song, and S. H. Lee, "Vitamin C-induced epigenetic modifications in donor NSCs establish midbrain marker expressions critical for cell-based therapy in Parkinson's disease," *Stem Cell Reports*, vol. 9, no. 4, pp. 1192–1206, 2017.

[56] P. Férnandez-Calle, F. J. Jiménez-Jiménez, J. A. Molina et al., "Serum levels of ascorbic acid (vitamin C) in patients with Parkinson's disease," *Journal of the Neurological Sciences*, vol. 118, no. 1, pp. 25–28, 1993.

[57] K. Sudha, A. V. Rao, S. Rao, and A. Rao, "Free radical toxicity and antioxidants in Parkinson's disease," *Neurology India*, vol. 51, no. 1, pp. 60–62, 2003.

[58] K. Ide, H. Yamada, K. Umegaki et al., "Lymphocyte vitamin C levels as potential biomarker for progression of Parkinson's disease," *Nutrition*, vol. 31, no. 2, pp. 406–408, 2015.

[59] K. C. Hughes, X. Gao, I. Y. Kim et al., "Intake of antioxidant vitamins and risk of Parkinson's disease," *Movement Disorders*, vol. 31, no. 12, pp. 1909–1914, 2016.

[60] Y. Miyake, W. Fukushima, K. Tanaka et al., "Dietary intake of antioxidant vitamins and risk of Parkinson's disease: a case-control study in Japan," *European Journal of Neurology*, vol. 18, no. 1, pp. 106–113, 2011.

[61] F. Yang, A. Wolk, N. Håkansson, N. L. Pedersen, and K. Wirdefeldt, "Dietary antioxidants and risk of Parkinson's disease in two population-based cohorts," *Movement Disorders*, vol. 32, no. 11, pp. 1631–1636, 2017.

[62] M. L. Colombo, "An update on vitamin E, tocopherol and tocotrienol-perspectives," *Molecules*, vol. 15, no. 4, pp. 2103–2113, 2010.

[63] A. Beharka, S. Redican, L. Leka, and S. N. Meydani, "[22] Vitamin E status and immune function," *Methods in Enzymology*, vol. 282, pp. 247–263, 1997.

[64] M. Cesari, M. Pahor, B. Bartali et al., "Antioxidants and physical performance in elderly persons: the Invecchiare in Chianti (InCHIANTI) study," *The American Journal of Clinical Nutrition*, vol. 79, no. 2, pp. 289–294, 2004.

[65] A. Cherubini, A. Martin, C. Andres-Lacueva et al., "Vitamin E levels, cognitive impairment and dementia in older persons: the InCHIANTI study," *Neurobiology of Aging*, vol. 26, no. 7, pp. 987–994, 2005.

[66] M. W. Clarke, J. R. Burnett, and K. D. Croft, "Vitamin E in human health and disease," *Critical Reviews in Clinical Laboratory Sciences*, vol. 45, no. 5, pp. 417–450, 2008.

[67] J. M. Aparicio, A. Bélanger-Quintana, L. Suárez et al., "Ataxia with isolated vitamin E deficiency: case report and review of the literature," *Journal of Pediatric Gastroenterology and Nutrition*, vol. 33, no. 2, pp. 206–210, 2001.

[68] J. L. Cadet, M. Katz, V. Jackson-Lewis, and S. Fahn, "Vitamin E attenuates the toxic effects of intrastriatal injection of 6-hydroxydopamine (6-OHDA) in rats: behavioral and biochemical evidence," *Brain Research*, vol. 476, no. 1, pp. 10–15, 1989.

[69] M. Roghani and G. Behzadi, "Neuroprotective effect of vitamin E on the early model of Parkinson's disease in rat: behavioral and histochemical evidence," *Brain Research*, vol. 892, no. 1, pp. 211–217, 2001.

[70] N. Sharma and B. Nehru, "Beneficial effect of vitamin E in rotenone induced model of PD: behavioural, neurochemical and biochemical study," *Experimental Neurobiology*, vol. 22, no. 3, pp. 214–223, 2013.

[71] T. L. Perry, V. W. Yong, S. Hansen et al., "α-Tocopherol and β-carotene do not protect marmosets against the dopaminergic neurotoxicity of *N*-methyl-4-phenyl-1, 2, 3, 6-tetrahydropyridine," *Journal of the Neurological Sciences*, vol. 81, no. 2-3, pp. 321–331, 1987.

[72] C. Heim, W. Kolasiewicz, T. Kurz, and K. H. Sontag, "Behavioral alterations after unilateral 6-hydroxydopamine lesions of the striatum. Effect of alpha-tocopherol," *Polish Journal of Pharmacology*, vol. 53, no. 5, pp. 435–448, 2001.

[73] R. Comitato, K. Nesaretnam, G. Leoni et al., "A novel mechanism of natural vitamin E tocotrienol activity: involvement of ERβ signal transduction," *American Journal of Physiology. Endocrinology and Metabolism*, vol. 297, no. 2, pp. E427–E437, 2009.

[74] K. Nakaso, N. Tajima, Y. Horikoshi et al., "The estrogen receptor β-PI3K/Akt pathway mediates the cytoprotective effects of tocotrienol in a cellular Parkinson's disease model," *Biochimica et Biophysica Acta (BBA) - Molecular Basis of Disease*, vol. 1842, no. 9, pp. 1303–1312, 2014.

[75] K. Nakaso, Y. Horikoshi, T. Takahashi et al., "Estrogen receptor-mediated effect of δ-tocotrienol prevents neurotoxicity and motor deficit in the MPTP mouse model of Parkinson's disease," *Neuroscience Letters*, vol. 610, pp. 117–122, 2016.

[76] "DATATOP: a multicenter controlled clinical trial in early Parkinson's disease: Parkinson Study Group," *Archives of Neurology*, vol. 46, no. 10, pp. 1052–1060, 1989.

[77] G. Logroscino, K. Marder, L. Cote, M. X. Tang, S. Shea, and R. Mayeux, "Dietary lipids and antioxidants in Parkinson's disease: a population-based, case-control study," *Annals of Neurology*, vol. 39, no. 1, pp. 89–94, 1996.

[78] M. C. de Rijk, M. M. Breteler, J. den Breeijen et al., "Dietary antioxidants and Parkinson disease. The Rotterdam Study," *Archives of Neurology*, vol. 54, no. 6, pp. 762–765, 1997.

[79] S. Fahn, "A pilot trial of high-dose alpha-tocopherol and ascorbate in early Parkinson's disease," *Annals of Neurology*, vol. 32, no. S1, pp. S128–S132, 1992.

[80] P. Fernandez-Calle, J. A. Molina, F. J. Jimenez-Jimenez et al., "Serum levels of alpha-tocopherol (vitamin E) in Parkinson's disease," *Neurology*, vol. 42, no. 5, pp. 1064–1066, 1992.

[81] D. T. Dexter, P. Jenner, R. J. Ward et al., "α-Tocopherol levels in brain are not altered in Parkinson's disease," *Annals of Neurology*, vol. 32, no. 4, pp. 591–593, 1992.

[82] J. A. Molina, F. de Bustos, F. J. Jiménez-Jiménez et al., "Cerebrospinal fluid levels of alpha-tocopherol (vitamin E) in Parkinson's disease," *Journal of Neural Transmission*, vol. 104, no. 11-12, pp. 1287–1293, 1997.

[83] G. T. Vatassery, S. Fahn, and M. A. Kuskowski, "Alpha tocopherol in CSF of subjects taking high-dose vitamin E in the DATATOP study: Parkinson Study Group," *Neurology*, vol. 50, no. 6, pp. 1900–1902, 1998.

[84] V. Kulda, "Vitamin D metabolism," *Vnitřní Lékařství*, vol. 58, no. 5, pp. 400–404, 2012.

[85] S. Christakos, P. Dhawan, A. Verstuyf, L. Verlinden, and G. Carmeliet, "Vitamin D: metabolism, molecular mechanism of action, and pleiotropic effects," *Physiological Reviews*, vol. 96, no. 1, pp. 365–408, 2016.

[86] M. R. Haussler, G. K. Whitfield, I. Kaneko et al., "Molecular mechanisms of vitamin D action," *Calcified Tissue International*, vol. 92, no. 2, pp. 77–98, 2013.

[87] C. Carlberg and F. Molnar, "Vitamin D receptor signaling and its therapeutic implications: genome-wide and structural view," *Canadian Journal of Physiology and Pharmacology*, vol. 93, no. 5, pp. 311–318, 2015.

[88] S. Samuel and M. D. Sitrin, "Vitamin D's role in cell proliferation and differentiation," *Nutrition Reviews*, vol. 66, no. 10, Supplement 2, pp. S116–S124, 2008.

[89] M. Myszka and M. Klinger, "The immunomodulatory role of vitamin D," *Postępy Higieny i Medycyny Doświadczalnej*, vol. 68, pp. 865–878, 2014.

[90] K. Kono, H. Fujii, K. Nakai et al., "Anti-oxidative effect of vitamin D analog on incipient vascular lesion in non-obese type 2 diabetic rats," *American Journal of Nephrology*, vol. 37, no. 2, pp. 167–174, 2013.

[91] O. Sahota, "Understanding vitamin D deficiency," *Age and Ageing*, vol. 43, no. 5, pp. 589–591, 2014.

[92] H. L. Newmark and J. Newmark, "Vitamin D and Parkinson's disease—a hypothesis," *Movement Disorders*, vol. 22, no. 4, pp. 461–468, 2007.

[93] K. Köstner, N. Denzer, C. S. Müller, R. Klein, W. Tilgen, and J. Reichrath, "The relevance of vitamin D receptor (VDR) gene polymorphisms for cancer: a review of the literature," *Anticancer Research*, vol. 29, no. 9, pp. 3511–3536, 2009.

[94] J. S. Kim, Y. I. Kim, C. Song et al., "Association of vitamin D receptor gene polymorphism and Parkinson's disease in Koreans," *Journal of Korean Medical Science*, vol. 20, no. 3, pp. 495–498, 2005.

[95] C. Li, H. Qi, S. Wei et al., "Vitamin D receptor gene polymorphisms and the risk of Parkinson's disease," *Neurological Sciences*, vol. 36, no. 2, pp. 247–255, 2015.

[96] M. Suzuki, M. Yoshioka, M. Hashimoto et al., "25-hydroxyvitamin D, vitamin D receptor gene polymorphisms, and severity of Parkinson's disease," *Movement Disorders*, vol. 27, no. 2, pp. 264–271, 2012.

[97] N. M. Gatto, K. C. Paul, J. S. Sinsheimer et al., "Vitamin D receptor gene polymorphisms and cognitive decline in Parkinson's disease," *Journal of the Neurological Sciences*, vol. 370, pp. 100–106, 2016.

[98] T. H. J. Burne, J. J. McGrath, D. W. Eyles, and A. Mackay-Sim, "Behavioural characterization of vitamin D receptor knockout mice," *Behavioural Brain Research*, vol. 157, no. 2, pp. 299–308, 2005.

[99] F. L. Campos, A. C. Cristovão, S. M. Rocha, C. P. Fonseca, and G. Baltazar, "GDNF contributes to oestrogen-mediated protection of midbrain dopaminergic neurones," *Journal of Neuroendocrinology*, vol. 24, no. 11, pp. 1386–1397, 2012.

[100] B. Sanchez, J. L. Relova, R. Gallego, I. Ben-Batalla, and R. Perez-Fernandez, "1, 25-Dihydroxyvitamin D3 administration to 6-hydroxydopamine-lesioned rats increases glial cell line-derived neurotrophic factor and partially restores tyrosine hydroxylase expression in substantia nigra and

striatum," *Journal of Neuroscience Research*, vol. 87, no. 3, pp. 723–732, 2009.

[101] B. Sanchez, E. Lopez-Martin, C. Segura, J. L. Labandeira--Garcia, and R. Perez-Fernandez, "1, 25-Dihydroxyvitamin D_3 increases striatal GDNF mRNA and protein expression in adult rats," *Molecular Brain Research*, vol. 108, no. 1-2, pp. 143–146, 2002.

[102] J. S. Kim, S. Y. Ryu, I. Yun et al., "1α,25-Dihydroxyvitamin D3 protects dopaminergic neurons in rodent models of Parkinson's disease through inhibition of microglial activation," *Journal of Clinical Neurology*, vol. 2, no. 4, pp. 252–257, 2006.

[103] J. Y. Wang, J. N. Wu, T. L. Cherng et al., "Vitamin D_3 attenuates 6-hydroxydopamine-induced neurotoxicity in rats," *Brain Research*, vol. 904, no. 1, pp. 67–75, 2001.

[104] W. Jang, H. J. Kim, H. Li et al., "1,25-Dyhydroxyvitamin D_3 attenuates rotenone-induced neurotoxicity in SH-SY5Y cells through induction of autophagy," *Biochemical and Biophysical Research Communications*, vol. 451, no. 1, pp. 142–147, 2014.

[105] J. H. Yoon, D. K. Park, S. W. Yong, and J. M. Hong, "Vitamin D deficiency and its relationship with endothelial dysfunction in patients with early Parkinson's disease," *Journal of Neural Transmission (Vienna)*, vol. 122, no. 12, pp. 1685–1691, 2015.

[106] P. Knekt, A. Kilkkinen, H. Rissanen, J. Marniemi, K. Sääksjärvi, and M. Heliövaara, "Serum vitamin D and the risk of Parkinson disease," *Archives of Neurology*, vol. 67, no. 7, pp. 808–811, 2010.

[107] M. L. Evatt, M. R. Delong, N. Khazai, A. Rosen, S. Triche, and V. Tangpricha, "Prevalence of vitamin d insufficiency in patients with Parkinson disease and Alzheimer disease," *Archives of Neurology*, vol. 65, no. 10, pp. 1348–1352, 2008.

[108] L. Kenborg, C. F. Lassen, B. Ritz et al., "Outdoor work and risk for Parkinson's disease: a population-based case-control study," *Occupational and Environmental Medicine*, vol. 68, no. 4, pp. 273–278, 2011.

[109] A. Kravietz, S. Kab, L. Wald et al., "Association of UV radiation with Parkinson disease incidence: a nationwide French ecologic study," *Environmental Research*, vol. 154, pp. 50–56, 2017.

[110] J. Wang, D. Yang, Y. Yu, G. Shao, and Q. Wang, "Vitamin D and sunlight exposure in newly-diagnosed Parkinson's disease," *Nutrients*, vol. 8, no. 3, p. 142, 2016.

[111] Y. Liu and B. S. Zhang, "Serum 25-hydroxyvitamin D predicts severity in Parkinson's disease patients," *Neurological Sciences*, vol. 35, no. 1, pp. 67–71, 2014.

[112] I. Sleeman, T. Aspray, R. Lawson et al., "The role of vitamin D in disease progression in early Parkinson's disease," *Journal of Parkinson's Disease*, vol. 7, no. 4, pp. 669–675, 2017.

[113] M. Suzuki, M. Yoshioka, M. Hashimoto et al., "Randomized, double-blind, placebo-controlled trial of vitamin D supplementation in Parkinson disease," *The American Journal of Clinical Nutrition*, vol. 97, no. 5, pp. 1004–1013, 2013.

[114] J. Xu, S. Q. Xu, J. Liang, Y. Lu, J. H. Luo, and J. H. Jin, "Protective effect of nicotinamide in a mouse Parkinson's disease model," *Zhejiang Da Xue Xue Bao. Yi Xue Ban*, vol. 41, no. 2, pp. 146–152, 2012.

[115] H. Jia, X. Li, H. Gao et al., "High doses of nicotinamide prevent oxidative mitochondrial dysfunction in a cellular model and improve motor deficit in a Drosophila model of Parkinson's disease," *Journal of Neuroscience Research*, vol. 86, no. 9, pp. 2083–2090, 2008.

[116] D. W. Anderson, K. A. Bradbury, and J. S. Schneider, "Broad neuroprotective profile of nicotinamide in different mouse models of MPTP-induced parkinsonism," *The European Journal of Neuroscience*, vol. 28, no. 3, pp. 610–617, 2008.

[117] S. Khan, S. Jyoti, F. Naz et al., "Effect of L-ascorbic acid on the climbing ability and protein levels in the brain of *Drosophila* model of Parkinson's disease," *The International Journal of Neuroscience*, vol. 122, no. 12, pp. 704–709, 2012.

[118] G. G. Ortiz, F. P. Pacheco-Moisés, V. M. Gómez-Rodríguez, E. D. González-Renovato, E. D. Torres-Sánchez, and A. C. Ramírez-Anguiano, "Fish oil, melatonin and vitamin E attenuates midbrain cyclooxygenase-2 activity and oxidative stress after the administration of 1-methyl-4-phenyl-1, 2, 3, 6- tetrahydropyridine," *Metabolic Brain Disease*, vol. 28, no. 4, pp. 705–709, 2013.

[119] P. Pasbakhsh, N. Omidi, K. Mehrannia et al., "The protective effect of vitamin E on locus coeruleus in early model of Parkinson's disease in rat: immunoreactivity evidence," *Iranian Biomedical Journal*, vol. 12, no. 4, pp. 217–222, 2008.

[120] L. A. R. Lima, M. J. P. Lopes, R. O. Costa et al., "Vitamin D protects dopaminergic neurons against neuroinflammation and oxidative stress in hemiparkinsonian rats," *Journal of Neuroinflammation*, vol. 15, no. 1, p. 249, 2018.

[121] R. Calvello, A. Cianciulli, G. Nicolardi et al., "Vitamin D treatment attenuates neuroinflammation and dopaminergic neurodegeneration in an animal model of Parkinson's disease, shifting M1 to M2 microglia responses," *Journal of Neuroimmune Pharmacology*, vol. 12, no. 2, pp. 327–339, 2017.

[122] H. Li, W. Jang, H. J. Kim et al., "Biochemical protective effect of 1,25-dihydroxyvitamin D_3 through autophagy induction in the MPTP mouse model of Parkinson's disease," *Neuroreport*, vol. 26, no. 12, pp. 669–674, 2015.

[123] W. A. Cass, L. E. Peters, A. M. Fletcher, and D. M. Yurek, "Calcitriol promotes augmented dopamine release in the lesioned striatum of 6-hydroxydopamine treated rats," *Neurochemical Research*, vol. 39, no. 8, pp. 1467–1476, 2014.

[124] The Parkinson Study Group, "Effects of tocopherol and deprenyl on the progression of disability in early Parkinson's disease," *The New England Journal of Medicine*, vol. 328, no. 3, pp. 176–183, 1993.

[125] M. Taghizadeh, O. R. Tamtaji, E. Dadgostar et al., "The effects of omega-3 fatty acids and vitamin E co-supplementation on clinical and metabolic status in patients with Parkinson's disease: a randomized, double-blind, placebo-controlled trial," *Neurochemistry International*, vol. 108, pp. 183–189, 2017.

[126] Y. Sato, S. Manabe, H. Kuno, and K. Oizumi, "Amelioration of osteopenia and hypovitaminosis D by 1α-hydroxyvitamin D3 in elderly patients with Parkinson's disease," *Journal of Neurology, Neurosurgery, and Psychiatry*, vol. 66, no. 1, pp. 64–68, 1999.

[127] D. King, J. R. Playfer, and N. B. Roberts, "Concentrations of vitamins A, C and E in elderly patients with Parkinson's disease," *Postgraduate Medical Journal*, vol. 68, no. 802, pp. 634–637, 1992.

[128] J. E. Kim, E. Oh, J. Park, J. Youn, J. S. Kim, and W. Jang, "Serum 25-hydroxyvitamin D3 level may be associated with olfactory dysfunction in *de novo* Parkinson's disease," *Journal of Clinical Neuroscience*, vol. 57, pp. 131–135, 2018.

[129] S. Shrestha, P. L. Lutsey, A. Alonso, X. Huang, T. H. Mosley Jr, and H. Chen, "Serum 25-hydroxyvitamin D concentrations in mid-adulthood and Parkinson's disease risk," *Movement Disorders*, vol. 31, no. 7, pp. 972–978, 2016.

[130] C. H. Lin, K. H. Chen, M. L. Chen, H. I. Lin, and R. M. Wu, "Vitamin D receptor genetic variants and Parkinson's disease in a Taiwanese population," *Neurobiology of Aging*, vol. 35, no. 5, pp. 1212.e11–1212.e13, 2014.

[131] D. Zhu, G. Y. Liu, Z. Lv, S. R. Wen, S. Bi, and W. Z. Wang, "Inverse associations of outdoor activity and vitamin D intake with the risk of Parkinson's disease," *Journal of Zhejiang University Science B*, vol. 15, no. 10, pp. 923–927, 2014.

[132] M. S. Petersen, S. Bech, D. H. Christiansen, A. V. Schmedes, and J. Halling, "The role of vitamin D levels and vitamin D receptor polymorphism on Parkinson's disease in the Faroe Islands," *Neuroscience Letters*, vol. 561, pp. 74–79, 2014.

[133] R. Török, N. Török, L. Szalardy et al., "Association of vitamin D receptor gene polymorphisms and Parkinson's disease in Hungarians," *Neuroscience Letters*, vol. 551, pp. 70–74, 2013.

[134] Z. Lv, B. Tang, Q. Sun, X. Yan, and J. Guo, "Association study between vitamin d receptor gene polymorphisms and patients with Parkinson disease in Chinese Han population," *The International Journal of Neuroscience*, vol. 123, no. 1, pp. 60–64, 2013.

[135] A. L. Peterson, M. Mancini, and F. B. Horak, "The relationship between balance control and vitamin D in Parkinson's disease-a pilot study," *Movement Disorders*, vol. 28, no. 8, pp. 1133–1137, 2013.

[136] M. L. Evatt, M. DeLong, M. Kumari et al., "High prevalence of hypovitaminosis D status in patients with early Parkinson disease," *Archives of Neurology*, vol. 68, no. 3, pp. 314–319, 2011.

[137] Y. Miyake, K. Tanaka, W. Fukushima et al., "Lack of association of dairy food, calcium, and vitamin D intake with the risk of Parkinson's disease: a case-control study in Japan," *Parkinsonism & Related Disorders*, vol. 17, no. 2, pp. 112–116, 2011.

Hindawi
Oxidative Medicine and Cellular Longevity
Volume 2019, Article ID 8204129, 11 pages
https://doi.org/10.1155/2019/8204129

Review Article

Antioxidant Properties of Amazonian Fruits: A Mini Review of In Vivo and In Vitro Studies

Raúl Avila-Sosa,[1] **Andrés Felipe Montero-Rodríguez**,[1] **Patricia Aguilar-Alonso**,[1] **Obdulia Vera-López**,[1] **Martin Lazcano-Hernández**,[1] **Julio César Morales-Medina**,[2] **and Addí Rhode Navarro-Cruz**[1]

[1]*Departamento de Bioquímica-Alimentos, Facultad de Ciencias Químicas, Benemérita Universidad Autónoma de Puebla, Puebla, Mexico*
[2]*Research Center for Animal Reproduction, CINVESTAV-UAT, Tlaxcala, Mexico*

Correspondence should be addressed to Addí Rhode Navarro-Cruz; addi.navarro@correo.buap.mx

Received 26 September 2018; Revised 27 November 2018; Accepted 6 December 2018; Published 17 February 2019

Guest Editor: Francisco Jaime B. Mendonça Júnior

Brazil, Colombia, Ecuador, Peru, Bolivia, Venezuela, Suriname, Guyana, and French Guiana share an area of 7,295,710 km^2 of the Amazon region. It is estimated that the Amazonian forest offers the greatest flora and fauna biodiversity on the planet and on its surface could cohabit 50% of the total existing living species; according to some botanists, it would contain about 16-20% of the species that exist today. This region has native fruit trees in which functional properties are reported as antioxidant and antiproliferative characteristics. Amazon plants offer a great therapeutic potential attributed to the content of bioactive phytochemicals. The aim of this mini review is to examine the state of the art of the main bioactive components of the most studied Amazonian plants. Among the main functional compounds reported were phenolic compounds, unsaturated fatty acids, carotenoids, phytosterols, and tocopherols, with flavonoids and carotenoids being the groups of greatest interest. The main beneficial effect reported has been the antioxidant effect, evaluated in most of the fruits investigated; other reported functional properties were antimicrobial, antimutagenic, antigenotoxic, analgesic, immunomodulatory, anticancer, bronchodilator, antiproliferative, and anti-inflammatory, including hypercholesterolemic effects, leishmanicidal activity, induction of apoptosis, protective action against diabetes, gastroprotective activity, and antidepressant effects.

1. Introduction

In the vicinity of the Amazon River, a large number of plants grow. Many of them are slightly known by a large part of the population living in this region. Most of these plant fruits not only are edible but are potentially functional with a variety of beneficial compounds to health. Basically, the problem with native Amazonian fruits is summarized in poor processing technologies and ignorance of their functional compounds and that outside the region, we have very little knowledge of it. The aim of this mini review is to examine the state of the art of the main bioactive components of the most studied Amazonian plants.

2. Methodology

Studies with original data related to the presence of functional activity compounds in Amazonian plants (published between 1999 and 2018) were identified by searching electronic databases and reviewing citations. Among the databases were Elsevier, ScIELO, Dialnet, and Redalyc, including publications in English, Spanish, and Portuguese. Eligible studies for this review included randomized controlled trials in humans, experimental animals, or cell cultures, with prospective, parallel, or crossed designs, with full text, and whose results showed a protective effect against oxidative stress and/or favorable effects on some pathological

Table 1: Biological activity and main responsible compounds of some Amazonian plants.

Botanical name	Functional compounds	Functional properties	Reference
Eugenia stipitata	Phenolic compounds (chlorogenic, gallic, and caffeic acids), carotenoids (xanthophylls and carotenes)	Antioxidant, antimutagenic, and antigenotoxic	[5, 7, 15]
Euterpe oleracea	Phenolic compounds (flavonoids) and carotenoids	Antioxidant, leishmanicide, antimicrobial, immunomodulatory, and antigenotoxic	[14, 16, 18, 19],
Myrciaria dubia	Phenolic compounds (flavonoids), carotenoids, and vitamin C	Antioxidant, antimicrobial, and antigenotoxic	[26–29, 31, 32]
Solanum sessiliflorum	Ascorbic acid, p-coumaric acid, p-hydroxy dihydro coumaric acid, naringenin, methyl salicylate, long chain hydrocarbons, fatty acids, and their methyl and ethyl esters	Antioxidant, hypocholesterolemic, and antigenotoxic	[39, 40]
Theobroma grandiflorum	Theobromine, volatile compounds (aldehydes, ketones and alcohols, ethyl butanoate, ethyl hexanoate, and linalool), unsaturated fatty acids, and flavonoids	Antioxidant, probiotic, and reduction of hypertriglyceridemia	[42, 43, 45, 47]
Mauritia flexuosa	Phenolic compounds (phenolic acids and flavonoids) and carotenoids	Antioxidant and antimicrobial	[46, 48, 49]
Plukenetia volubilis	Polyunsaturated fatty acids, tocopherols, phytosterols, and phenolic compounds	Antioxidant	[52, 53]
Bactris gasipaes	Unsaturated fatty acids (oleic, linoleic, and linolenic), carotenoids (β-carotene, lutein, zeaxanthin, β-cryptoxanthin, and α-carotene), and dietary fiber	Antioxidant, precursor of vitamin A	[54–60]
Paullinia cupana	Phenolic compounds: catechin, epicatechin, and proanthocyanidins; also dietary fiber, theobromine, theophylline, and caffeine	Antioxidant, stimulant, antimicrobial, antihyperglycemic, and cytoprotective effect	[62–64]

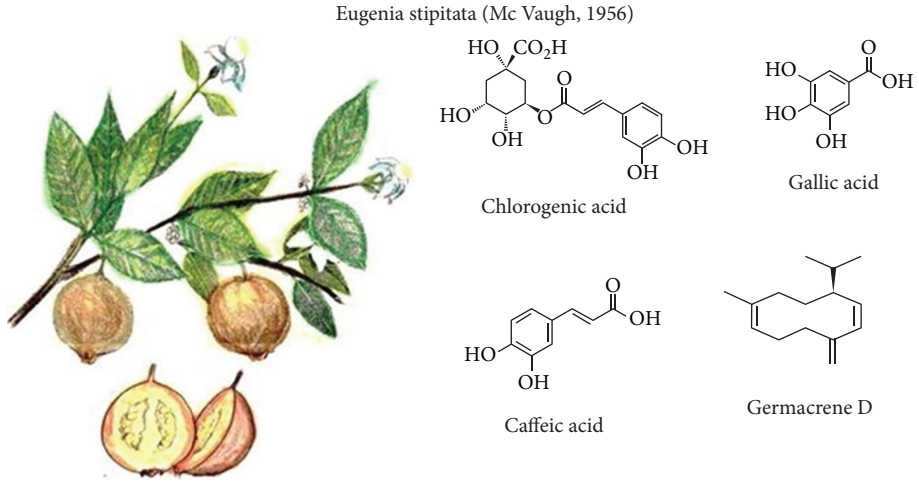

Figure 1: *Eugenia stipitata* McVaugh and its main compounds with functional activity.

conditions. There was no restriction on the type of publication or sample size. Documents whose main information was related to technological processing or could not verify the functional effects of Amazonian plants were excluded. Table 1 shows the main compounds and the biological activities reported for the plants reviewed.

3. Monographs

3.1. Eugenia stipitata (McVaugh, 1956). Also known as quince, Amazonic guava, arazá, or araça in Brazil, it is a climacteric fruit of the Myrtaceae family from the Ecuadorian Amazon region. It grows in deep, fertile, and well-drained soils. It is harvested from 38 days of the transition from flower to fruit with a frequency of three crops per year. It has an oval shape (Figure 1), with a longitudinal diameter and transverse diameter of 5-10 cm and 7-8 cm, respectively, with a yellow pulp and skin and an average weight of 150 g (per fresh fruit). Its epicarp is thin, with fine pubescence and light-green color that turns yellowish or orange at maturity [1, 2].

It has a moisture content of 82-83% and an acidic taste (pH~2.5). It is a delicate and easily decomposable fruit; the postharvest shelf life is shortened as a result of anthracnose

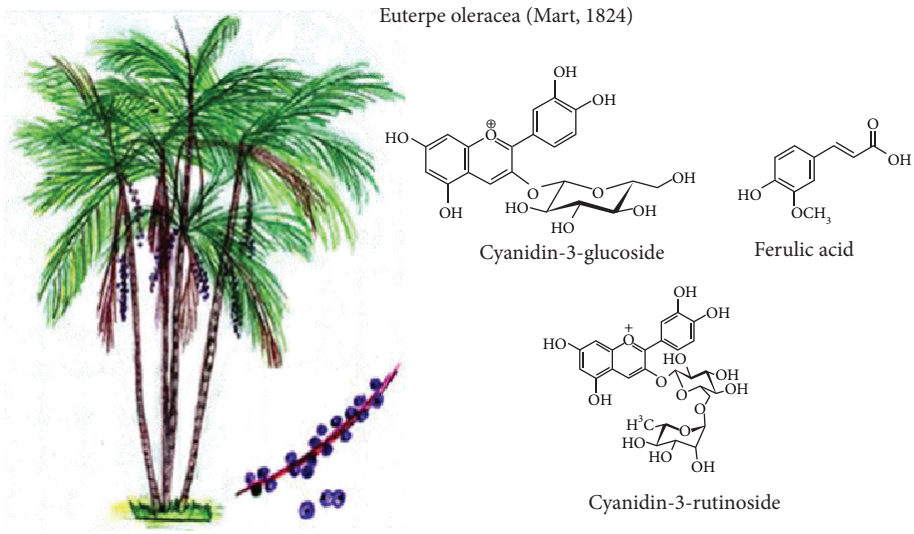

Figure 2: *Euterpe oleracea* Mart and its main compounds with functional activity.

and other decay problems [3]. Protein content and minerals are 11.9 ± 0.5 and 4 ± 0.1, respectively (dry base); soluble sugar content represents around 50% of the dry weight being its main constituent fructose. Total dietary fiber content is high compared to other tropical fruits, reaching about 35% (d/w) [2]. It is rich in volatile terpenes, fiber, and mainly vitamin C. Some studies have shown antioxidant activity and a high phenolic content that differ between different arazá genotypes. Arazá fruit revealed a total phenolic quantity of 184.05 ± 8.25 mg of gallic acid/100 g of extract with antioxidant activity. No cytostatic effects have been demonstrated; however, antimutagenic and antigenotoxic activities were observed at doses of 300 mg of extract/kg of body weight; so, *E. stipitata* could contribute to antimutagenic and antigenotoxic activities [4, 5].

A greater antioxidant activity is showed in the green state. As maturity degree advances, especially in the epicarp, chlorogenic, gallic, and caffeic acids are the major phenols responsible for antioxidant activity [6, 7]. Among the identified carotenoids, lutein and esters with palmitic and myristic acids were identified: lutein dipalmitate, lutein palmitate--myristate, β-cryptoxanthin palmitate, and zeaxanthin palmitate [6]. Essential oils present in tree leaves showed a complex pattern of monoterpenes and sesquiterpenes (69.5%), of which approximately 52% of them being oxygenated. One of these molecules, Germacrene D, could be responsible for the cytotoxic activity on the HCT116 human colon carcinoma cell line [8, 9], as well as its antimicrobial capacity [10].

3.2. Euterpe oleracea (Mart, 1824). It is a widespread palm tree, with an incidence and economic importance in the Amazonian delta flood plains, known by the names of palm of asaí, azaí, huasaí, palma murrapo, naidí, or generally acai. The fruit is produced in clusters from a third-year growth. Each fruit (Figure 2) is a sessile stone fruit with a woody endocarp, round shape, 1-2 cm diameter, and mass that varies from 0.8 to 2.3 g. Its fruits are constituted by a slightly hard seed, surrounded by a greyish and oily pulp, covered by a dark-purple epidermis [11, 12]. Fruits and roots are traditionally being used against diarrhea, jaundice, skin complications (acne, eczema), and parasitic infections (helminths) and as a remedy against influenza, fever, and pain [13].

The polyphenolic profile and antioxidant activity of Colombian acai are different from the one carried out with several Brazilian acai studies. Colombian acai has higher proportions of delphinidin, cyanidin (cyanidin-3-glucoside), and ferulic acid with high antioxidant activity [14, 15]. Proanthocyanidins were detected from acai seed aqueous extract, as well as their bioactivity (antioxidant and cytotoxic activities) depending strongly on their phenolic profile. However, other nonphenolic compounds may be involved in their antioxidant activity [16]. Moreover, in healthy women, it has been observed that the consumption of acai pulp improves the concentration of antioxidant cellular enzymes and serum biomarkers increasing catalase activity, total antioxidant capacity, and the reduction of reactive oxygen species and carbonyl protein concentration [17].

Among other studies, acai showed antiparasitic activity against *L. infantum* and *L. amazonensis* without cytotoxic effects to the host cell [18], reduction of early carcinogenesis in the colon of mice, mitigation of DNA damage induced by azoxymethane [19], antitumorigenic potential in the MCF-7 cell line [20], reduction in selected markers of metabolic disease risk in overweight adults [21], protection against renal damage in diabetic rats [22], inhibition of urinary bladder carcinogenesis in mice [23], improvement of cardiac dysfunction and exercise intolerance in rats subjected to myocardial infarction [24], and prevention of oxidative damage in the brain of rats [25].

3.3. Myrciaria dubia (HBK) (McVaugh). Its common names are camu-camu, caçari, arazá de agua, guayabo, guayabito, or guapuro blanco. It grows near the river and lake margins (Figure 3). Its high phenolic and vitamin C concentration contributes to a high antioxidant capacity and the consequent health benefits [26, 27].

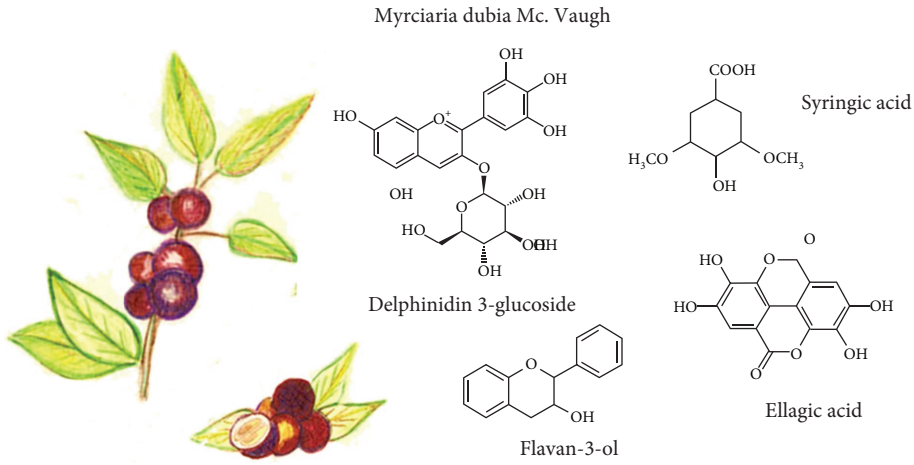

Figure 3: *Myrciaria dubia* McVaugh and its main compounds with functional activity.

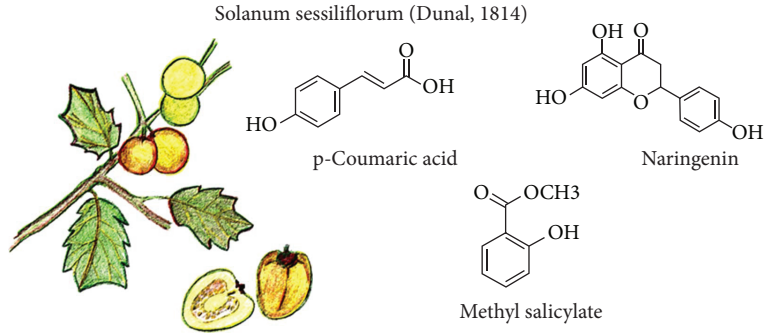

Figure 4: *Solanum sessiliflorum* Dunal and some compounds with functional activity.

Camu-camu is a spherical fruit (with a diameter and length of approximately 1.0-3.2 cm and 1.2-2.5 cm, respectively) [28]. Polyphenolic compounds, antioxidant concentration, and antioxidant capacity depend on their maturity state [28]. Before harvest, carotenoids, flavonoids, and anthocyanins, as well as vitamin C, are in higher concentrations. When the fruit ripens, ascorbic acid concentration decreases, while anthocyanin, flavonol, and flavanol content, as well as the antioxidant capacity, increased [26, 29].

Chemical analysis by HPLC identified the presence of catechin, delphinidin 3-glucoside, cyanidin 3-glucoside, ellagic acid, and rutin. Other phenolic compounds were also present such as flavan-3-ol, flavonol, flavanone, and ellagic acid derivatives. Acid hydrolysis of phenolic fraction revealed the presence mainly of gallic and ellagic acids, which suggests that this fruit has important quantities of hydrolyzed tannins (gallotannins and/or ellagitannins) [29].

It has been observed in rats with diabetes type 1 that camu-camu frozen pulp extracts attenuate hyperlipidemia and lipid peroxidation. This could be due to the presence of flavonoids such as quercetin and myricetin that would be contributing to avoid oxidative damage, relieving diabetic complications in this animal model [30]. Camu-camu juice has an antigenotoxic effect in acute, subacute, and chronic treatments in blood cells of mice. This effect is being observed only in ex vivo studies, with more significant results in juice acute administration, without toxic effects or posttreatment death [31]. Moreover, compounds such as ellagitannins, ellagic acid, quercetin glucosides, syringic acid, and myricetin could be the main reason for a protection effect against microvascular complications (associated with diabetes type 2) and against some bacterial infections; *in vitro* evaluation showed antihyperglycemic, antihypertensive, antimicrobial, and cell rejuvenation activities [32]. Camu-camu residues have also demonstrated antioxidant, antimicrobial, and antienzymatic activities [33].

3.4. Solanum sessiliflorum (Dunal, 1814). Its name is cocona and it is an herbaceous shrub whose fruits vary from almost spherical or ovoid to oval. With a 4 to 12 cm width and a 3 to 6 cm length and a 240 to 250 g weight, it has a color from yellow to reddish (Figure 4). Their hull is soft and is surrounded by a thick, yellow, and watery mesocarp; it has an unusual taste, highly acid. It is consumed in salads and juices [34]. Cocona is slightly known mainly due its small-scale production [35]. However, local population consumes it very frequently as hypocholesterolemic and hypoglycemic remedies and for skin disease treatment [36, 37].

Its components include the presence of p-coumaric acid, p-hydroxydihydrocoumaric acid, naringenin, methyl salicylate, long-chain hydrocarbons, fatty acids, and their methyl and ethyl esters. Some of these compounds accumulate only in fruit epicarp. Chromatographic profile comparison between volatile compounds and different morphotypes

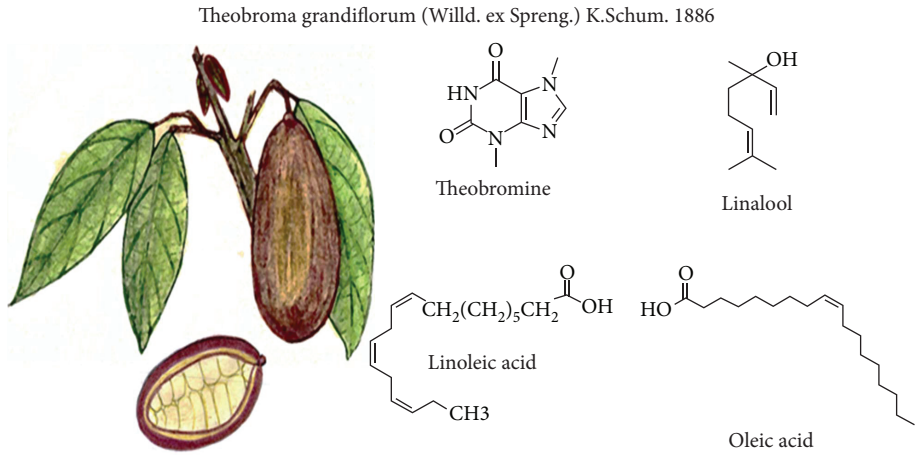

Figure 5: *Theobroma grandiflorum* and its main compounds with functional activity.

(oval, small round, and large round) showed chemical differences; the oval morphotype exhibits greater chemical complexity in terms of volatile and nonvolatile metabolites. Furthermore, cytotoxic, genotoxic, and antigenotoxic potential was evaluated *in vivo*, observing a noncytotoxic effect on bone marrow cells and a nongenotoxic effect on Wistar rats. Cocona antioxidant capacity may contribute to the antigenotoxic effects [38, 39]. Finally, cocona flour administration showed a reduction of total cholesterol concentration, low-density lipoprotein (LDL-c), and liver cholesterol and increasing cholesterol and high-density lipoprotein (HDL-c) fecal excretion in hypercholesterolemic rats [40].

3.5. Theobroma grandiflorum (Willd. ex Spreng.) (K. Schum, 1886). It is a tree that reaches 15-20 m high; it belongs to the *Sterculiaceae* family [41]. Its fruits have different shapes (oblong, round oval), weighing between 200 g and 4000 g (Figure 5) [42]. It is known as copoazú and belongs to the Theobroma genus, like cocoa, and is considered as one of the most popular fruits in the Amazonian market [43].

From copoazú almonds, it is obtained as a cocoa-like liquor, with improved characteristics on unsaturated fatty acid percentages and a smooth and pleasant flavor. It has active antioxidant substances, low percentage of theobromine, and high content of linoleic and oleic unsaturated fatty acids. It is considered a suitable product for cosmetic, chocolate, beverage, liquor, and food industries [44]. Its main components in pulp were detected such as volatile compounds: 24 esters, 13 terpenes, 8 alcohols, 4 carbonyls, 4 acids, 2 lactones and phenol, ethyl butanoate, ethyl hexanoate, and linalool [41].

Polyphenols derived from copoazú were studied evaluating the distribution and metabolism in the gastrointestinal tract of mice and the microbial metabolic conversion of a unique combination of flavonoids (flavan-3-ols, procyanidins, and flavones). These compounds are accumulated mainly in the stomach and small intestine where they could exert local effects. Procyanidin microbial metabolism was different from cocoa that contains procyanidin too [43]. Further, copoazú and cocoa liquors were chronically provided to diabetic rats with streptokin. Copoazú liquor improves their lipid profile and antioxidant status, which could suggest a superior effect of the cocoa liquor [45].

3.6. Mauritia flexuosa L.f. (1782). It is commonly known as canangucha, buriti, or moriche palm. It is considered the most abundant native palm that grows naturally in the Brazilian Amazon biome. Its fruit is highly nutritious with a yellow-orange pulp (Figure 6) and bittersweet taste. Its endocarp is surrounded by a spongy material made of starch and oil, with a hard skin, and contains a small reddish-brown scale-like fruit [46]. It is possible to extract oil from its pulp, whose main components are palmitic (18.7%), stearic (1.5%), oleic (76.7%), linoleic (1.5%), linolenic (0.7%), and arachidic acid (0.5%) [47].

The moriche plant has phenolic compounds mainly flavonoids and glycosylated anthocyanins like the following: catechin, caffeic acid, chlorogenic acid, quercetin, naringenin, myricetin, vitexin, scoparin, rutin, cyanidin-3-rutinoside, cyanidin-3-glucoside, epicatechin, and kaempferol [48]. On the other hand, the fruits show a reasonable amount of phenolic compounds, carotenoids (with predominance of β-carotenes), and antioxidant activity, which confirms the functional potential of moriche [49]. Fruit pulp extracts showed six phenolic acids: p-coumaric, ferulic, caffeic, protocatechuic, chlorogenic, and quinic. Quinic acid is much more abundant than other phenolic acids in pulp; extracts also show seven kinds of flavonoids such as catechin, epicatechin, apigenin, luteolin, myricetin, kaempferol, and quercetin [50]. In leaves, tricine-7-O-rutinoside, apigenin-6-C-arabinoside, 8-C-glucoside (isoschaftoside), kaempferol-3-O-rutinoside (nicotiflorine), quercetin-3-O-rutinoside (rutin), luteolin-8-C-glucoside (orientin), and luteolin-6-C-glucoside (isoorientin) were identified [51]. Leaf extract revealed its great ability to inhibit food pathogens, like *Pseudomonas aeruginosa*, and a moderate antimicrobial activity when applied in fruits [48].

3.7. Plukenetia volubilis L. It is a domesticated grapevine known also as sacha inchi, sacha yuchi, sacha yuchiqui, mountain peanuts, wild peanuts, or inca peanuts among others. It

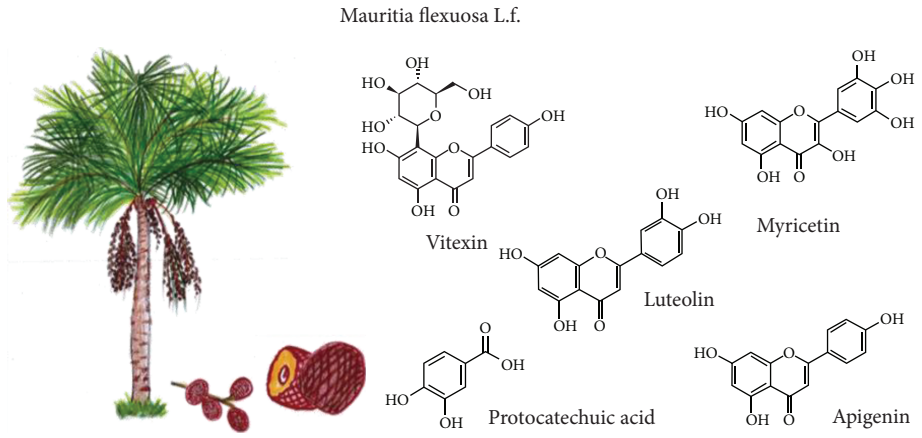

Figure 6: *Mauritia flexuosa* L.f. and some compounds with functional activity.

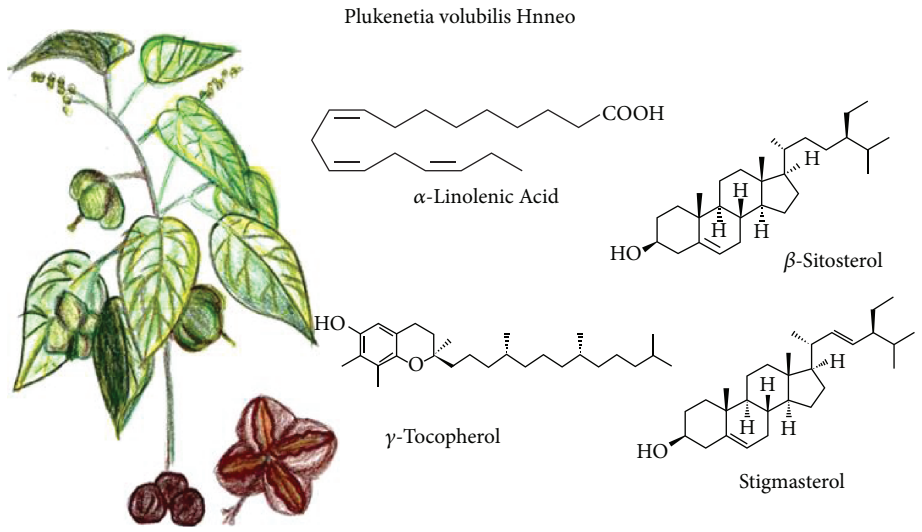

Figure 7: *Plukenetia volubilis* L. and its main compounds with functional activity.

grows in warm climates, at high altitude in the Andean rainforest to the Peruvian Amazon lowlands (Figure 7). Due to its oil content, it is used as food supplement, in skin care, and for wound treatment, insect bites, and skin infections [52].

The most studied and interesting fraction of this fruit is its oil. Fruit seeds are a suitable oil source (35-60%) rich in omega 3 and 6, whose composition varies according to seed varieties. Found were significant contents of α-linolenic acid and a low linolenic acid/linoleic acid ratio, as well as considerable amounts of tocopherols (γ- and δ-tocopherols), phytosterols (β-sitosterol and stigmasterol), and phenolic compounds like ferulic acid. However, no correlations have been found between hydrophilic and lipophilic bioactive compounds and antioxidant capacity. It suggests a complex interaction of different antioxidant compounds with different action modes. Although there are few studies on the sacha inchi oil effects on health, there are evidences that it could act by improving the lipid profile [52]. Regarding its use for skin care, sacha inchi oil was very active as a nonstick (preventive) in keratinocytes and in the detachment of *Staphylococcus aureus* on the adherence to *in vitro* human skin explants [53].

3.8. Bactris gasipaes H. B. Kunth. It is an Amazonian palm grown mainly for fruit production (Figure 8), known as chontaduro, pejiballe, acana, or pupunha [54]. The chontaduro fruit has considerable concentration of proteins and oil [55], with an important content of linoleic and linolenic polyunsaturated fatty acids [56], as well as β-carotenes [57].

Chontaduro flour residues contain different types of carotenoids: violaxanthin, lutein, zeaxanthin, 15-cis β-carotene, 13-cis β-carotene, all-trans β-carotene, 9-cis β-carotene, and α-carotene, as the main carotenoid pigment. Retinol equivalent values found for chontaduro cooked fruit (traditional consumption form) and flour are higher than those reported for popular products such as tomato and papaya [58, 59]. Chontaduro flour carbohydrates are predominantly composed of insoluble fiber, highly esterified homogalacturonan (70% of esterification). It contains linear methyl and minor portions of xylogalacturonan and rhamnogalacturonan that may promote health benefits. Although not very well documented in the literature, probably refer to their antioxidant capacity and their nutritional value since their protein contains eight essential amino acids [60].

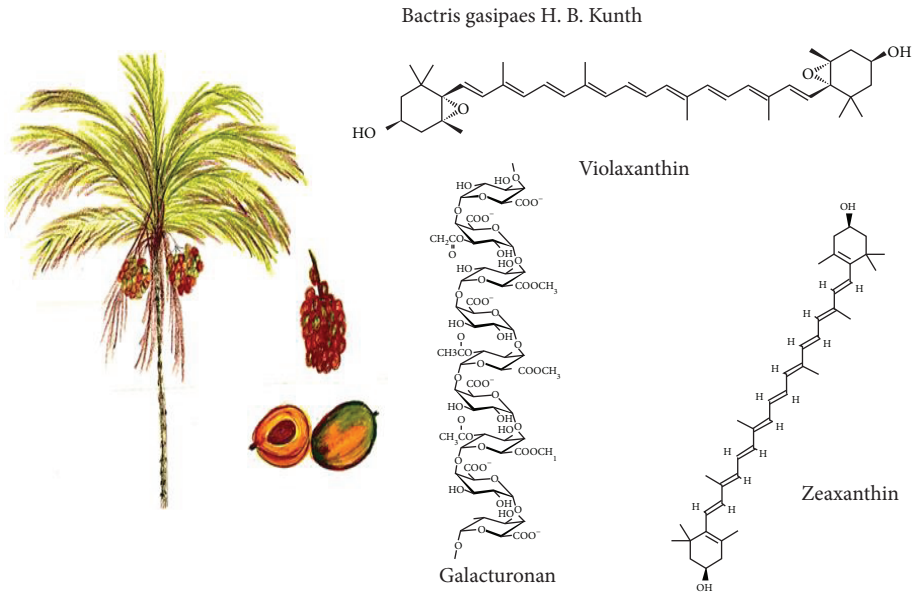

Figure 8: *Bactris gasipaes* H. B. Kunth and its main functional compounds.

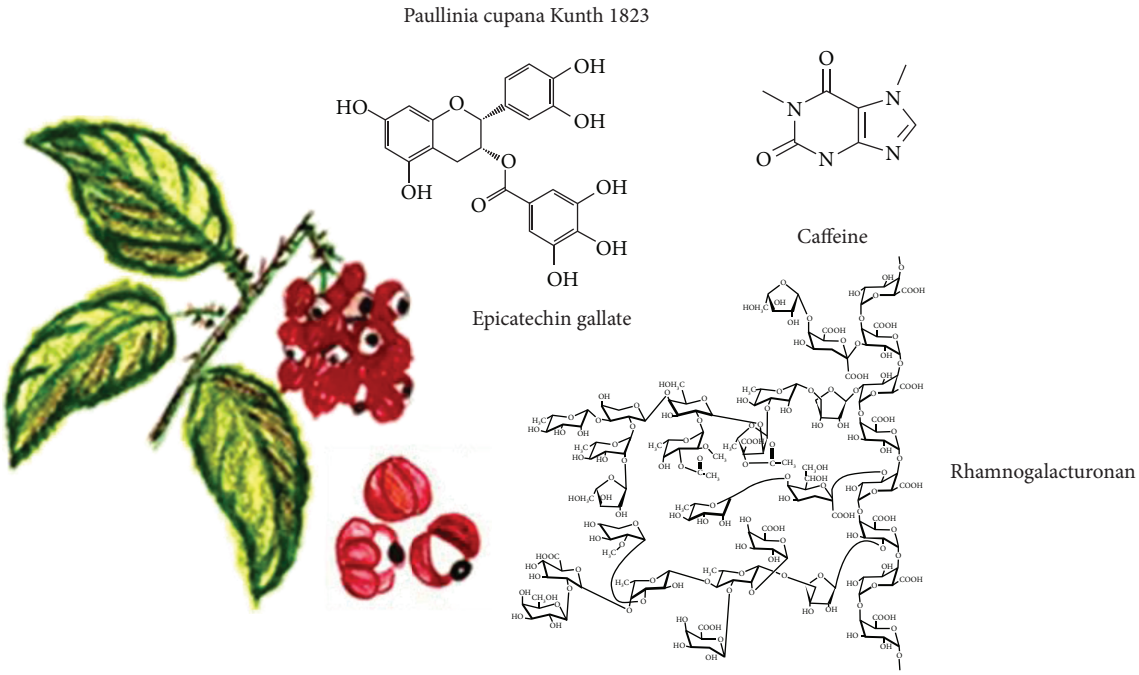

Figure 9: *Paullinia cupana* Kunth, 1823, and some functional compounds.

3.9. Paullinia cupana Kunth (1823). This climbing shrub, better known as guarana, is rich in vitamins and stimulants such as caffeine; so, it is used mainly for consumption as beverage (Figure 9). It is produced mainly in the Brazilian states of Amazonas and Bahia, and approximately 70% of its production is used in soft and energy drink industries [61]. Its seeds are used to produce guarana powder, which is consumed mainly due to its stimulating activity [62]. The main reason so far to study guarana is its caffeine content, and this probably will continue due to the high demand of this alkaloid in the pharmaceutical and cosmetic industries. Semipurified guarana extract shows antidepressant and panicolytic effects [63]. Guarana seed extracts present antimicrobial activity against *Escherichia coli*, *Pseudomonas fluorescens*, *Bacillus cereus*, and spoilage fungi such as *Aspergillus niger*, *Trichoderma viride*, and *Penicillium cyclopium* [64].

All guarana seed extracts have antioxidant activity with high amounts of total phenolic compounds like catechins, such as epicatechin, catechin, and epicatechin gallate. Due to their high antioxidant, antibacterial, and antifungal activities, guarana extracts have a promising potential as natural antioxidants in food, cosmetic, and pharmaceutical industries [64].

Table 2: Antioxidant capacity of native Amazonian fruits.

Name	DPPH	ORAC	ABTS	FRAP	Reference
Eugenia stipitata	IC 500.69 ± 0.23 μg/mL	371.98 ± 11.50 μmol TE/100 g DW	N/R	N/R	[5]
Euterpe oleracea	21,049 ± 3,071.0 μmol TE/100 g DW; 12,420 μmol TE ± 465/100 g DW; 609.1 μmol TE/g DW IC50 : 8.8 ± 0.27 μg/mL	101,336.1 μmol TE/100 g DW; 686.0 μmol TE/100 g DW	24.7 ± 10.6 μmol TE/100 g DW; 40,330 ± 19,656 μmol TE/100 g DW	3,834 ± 56 mg ascorbic acid/100 g DW	[6, 14, 16]
Myrciaria dubia	185 ± 11 (μmol TE/g FW); 1,679 ± 75 (μmol TE/g DW); 2,138.7 μmol TE/g DW IC 50 1,116.87 ± 0.064 μg/mL	1,002 ± 27 (μmol TE/g DW; 3,060.8 μmol TE/g DW	N/R	N/R	[26, 30, 31]
Solanum sessiliflorum	N/R	N/R	N/R	N/R	
Mauritia flexuosa	IC 50 19.58 ± 0.064 mg/mL	N/R	33.02 μmol TE/g FW	280.80 ± 37.99 μmol $FeSO_4 \cdot 7H_2O$ equiv/100 g	[48, 49]
Theobroma grandiflorum	1,913 ± 228 μmol TE/100 g DW	13,628 ± 184 μmol TE/100 g DW	N/R	N/R	[51]
Plukenetia volubilis	N/R	6.5 – 9.8 μmol TE/g	N/R	N/R	[29]
Bactris gasipaes	N/R	N/R	N/R	N/R	
Paullinia cupana	IC50 = 8.5 μg/mL (approximate value taken from the graph)	N/R	N/R	N/R	[63]

TE: Trolox equivalent, VCE: vitamin C equivalent, DW: dry weight; FW: fresh weight; NR: not reported

The presence of dietary fiber, including pectic and hemicellulose polysaccharides has been reported, and a homogalacturonan with rhamnogalacturonan and xylans has also been isolated and characterized. Pectic polysaccharides and methanolic extract exhibited antioxidant activity, and part of the possible antioxidant effects of guarana could be attributed to their pectic component [62].

4. Antioxidant Capacity of Native Amazonian Fruits

In summary, most of the compounds with functional activity correspond to compounds with antioxidant activity; Table 2 shows the different methods used in the references examined in the present mini review. However, the comparisons are extremely complicated so it would be more appropriate to review clinical studies performed on animals, but unfortunately, to date, there are very few of them. The antioxidant capacity methods were DPPH, FRAP, TEAC, ABTS, and ORAC. Comparison of antioxidant capacity between fruits should be made only when the conditions (method, solvent, sampling, expression of results, etc.) analyzed are the same; therefore, results are not comparable with a great disadvantage that presents to compare the antioxidant capacities of various fruits.

5. Conclusion

According to numerous authors, many Amazonian fruits are an adequate source of multiple compounds with potential health benefits, mainly antioxidant effects, which has also been proven through numerous studies such as those detailed in this mini review. However, among its differences in composition, quality, and insufficient in vivo tests, scientific evidence offers challenges and great opportunities in different areas of research (toxicology, food safety, food technology, and processing). Therefore, new trends in functional foods should be conducted considering the enormous potential of these Amazonian fruits in human health.

Conflicts of Interest

The authors declare no conflict of interest.

References

[1] L. C. Neves, J. M. Tosin, R. M. Benedette, and L. Cisneros-Zevallos, "Post-harvest nutraceutical behaviour during ripening and senescence of 8 highly perishable fruit species from the Northern Brazilian Amazon region," *Food Chemistry*, vol. 174, pp. 188–196, 2015.

[2] H. Rogez, R. Buxant, E. Mignolet, J. N. S. Souza, E. M. Silva, and Y. Larondelle, "Chemical composition of the pulp of three typical Amazonian fruits: araça-boi (*Eugenia stipitata*), bacuri (*Platonia insignis*) and cupuaçu (*Theobroma grandiflorum*)," *European Food Research and Technology*, vol. 218, no. 4, pp. 380–384, 2004.

[3] R. Rodríguez Sandoval and P. Bastidas Garzón, "Evaluating the cooking process for obtaining hard candy from araza (*Eugenia stipitata*) pulp," *Ingeniería e Investigación*, vol. 29, pp. 35–41, 2009.

[4] J. P. L. Aguiar, "Araçá-boi (eugenia stiptata, mcvaug) - aspectos e dados preliminares sobre a sua composição química," *Acta Amazonica*, vol. 13, no. 5-6, pp. 953-954, 1983.

[5] I. A. Neri-Numa, L. B. Carvalho-Silva, J. P. Morales et al., "Evaluation of the antioxidant, antiproliferative and antimutagenic potential of araçá-boi fruit (*Eugenia stipitata* Mc Vaugh — Myrtaceae) of the Brazilian Amazon Forest," *Food Research International*, vol. 50, no. 1, pp. 70–76, 2013.

[6] G. A. Garzón, C.-E. Narváez-Cuenca, R. E. Kopec, A. M. Barry, K. M. Riedl, and S. J. Schwartz, "Determination of carotenoids, total phenolic content, and antioxidant activity of Arazá (*Eugenia stipitata* McVaugh), an Amazonian fruit," *Journal of Agricultural and Food Chemistry*, vol. 60, no. 18, pp. 4709–4717, 2012.

[7] F. A. Cuellar, E. Ariza, C. Anzola, and P. Restrepo, "Research of antioxidant capacity of araza (*Eugenia stipitata* Mc Vaugh) during the ripening," *Revista Colombiana de Química*, vol. 42, pp. 21–28, 2013.

[8] A. Guerrini, G. Sacchetti, A. Grandini, A. Spagnoletti, M. Asanza, and L. Scalvenzi, "Cytotoxic effect and TLC bioautography-guided approach to detect health properties of Amazonian *Hedyosmum sprucei* essential oil," *Evidence--Based Complementary and Alternative Medicine*, vol. 2016, Article ID 1638342, 8 pages, 2016.

[9] S. Casiglia, M. Bruno, M. Bramucci et al., "Kundmannia sicula (L.) DC: a rich source of germacrene D," *Journal of Essential Oil Research*, vol. 29, no. 6, pp. 437–442, 2017.

[10] I. Peluso, T. Magrone, D. Villaño Valencia, C. Y. O. Chen, and M. Palmery, "Antioxidant, anti-inflammatory, and microbial-modulating activities of nutraceuticals and functional foods," *Oxidative Medicine and Cellular Longevity*, vol. 2017, Article ID 7658617, 2 pages, 2017.

[11] F. Aguiar, V. Menezes, and H. Rogez, "Spontaneous postharvest fermentation of açai (Euterpe oleracea) fruit," *Postharvest Biology and Technology*, vol. 86, pp. 294–299, 2013.

[12] R. G. Costa, K. Andreola, R. de Andrade Mattietto, L. J. G. de Faria, and O. P. Taranto, "Effect of operating conditions on the yield and quality of açai (*Euterpe oleracea* Mart.) powder produced in spouted bed," *LWT - Food Science and Technology*, vol. 64, no. 2, pp. 1196–1203, 2015.

[13] M. Amsellem-Laufer, "Euterpe oleracea Martius (Arecaceae):Açaï," *Phytothérapie*, vol. 13, no. 2, pp. 135–140, 2015.

[14] B. A. Rojano, I. C. Z. Vahos, A. F. A. Arbeláez, A. J. M. Martínez, F. B. C. Correa, and L. G. Carvajal, "Polifenoles y actividad antioxidante del fruto liofilizado de palma naidi (Açai Colombiano) (Euterpe oleracea Mart)," *Revista Facultad Nacional de Agronomía Medellín*, vol. 64, pp. 6213–6220, 2011.

[15] G. A. Garzón, C. E. Narváez-Cuenca, J. P. Vincken, and H. Gruppen, "Polyphenolic composition and antioxidant activity of açai (*Euterpe oleracea* Mart.) from Colombia," *Food Chemistry*, vol. 217, pp. 364–372, 2017.

[16] L. Barros, R. C. Calhelha, M. J. R. P. Queiroz et al., "The powerful in vitro bioactivity of Euterpe oleracea Mart. seeds and related phenolic compounds," *Industrial Crops and Products*, vol. 76, pp. 318–322, 2015.

[17] P. O. Barbosa, D. Pala, C. T. Silva et al., "Açai (*Euterpe oleracea Mart.*) pulp dietary intake improves cellular antioxidant enzymes and biomarkers of serum in healthy women," *Nutrition*, vol. 32, no. 6, pp. 674–680, 2016.

[18] B. J. M. Da Silva, J. R. Souza-Monteiro, H. Rogez, M. E. Crespo-López, J. L. M. Do Nascimento, and E. O. Silva, "Selective effects of *Euterpe oleracea* (açai) on *Leishmania (Leishmania) amazonensis* and *Leishmania infantum*," *Biomedicine & Pharmacotherapy*, vol. 97, pp. 1613–1621, 2018.

[19] G. R. Romualdo, M. F. Fragoso, R. G. Borguini, M. C. P. de Araújo Santiago, A. A. H. Fernandes, and L. F. Barbisan, "Protective effects of spray-dried açaí (*Euterpe oleracea* Mart) fruit pulp against initiation step of colon carcinogenesis," *Food Research International*, vol. 77, pp. 432–440, 2015.

[20] D. F. Silva, F. C. B. Vidal, D. Santos et al., "Cytotoxic effects of *Euterpe oleracea* Mart. in malignant cell lines," *BMC Complementary and Alternative Medicine*, vol. 14, no. 1, p. 175, 2014.

[21] J. K. Udani, B. B. Singh, V. J. Singh, and M. L. Barrett, "Effects of Açai (*Euterpe oleracea* Mart.) berry preparation on metabolic parameters in a healthy overweight population: a pilot study," *Nutrition Journal*, vol. 10, no. 1, pp. 45–51, 2011.

[22] V. da Silva Cristino Cordeiro, G. F. de Bem, C. A. da Costa et al., "*Euterpe oleracea* Mart. seed extract protects against renal injury in diabetic and spontaneously hypertensive rats: role of inflammation and oxidative stress," *European Journal of Nutrition*, vol. 57, no. 2, pp. 817–832, 2018.

[23] M. F. Fragoso, M. G. Prado, L. Barbosa, N. S. Rocha, and L. F. Barbisan, "Inhibition of mouse urinary bladder carcinogenesis by açai fruit (*Euterpe oleraceae* Martius) intake," *Plant Foods for Human Nutrition*, vol. 67, no. 3, pp. 235–241, 2012.

[24] G. Zapata-Sudo, J. S. da Silva, S. L. Pereira, P. J. C. Souza, R. S. de Moura, and R. T. Sudo, "Oral treatment with *Euterpe oleracea* Mart. (açaí) extract improves cardiac dysfunction and exercise intolerance in rats subjected to myocardial infarction," *BMC Complementary and Alternative Medicine*, vol. 14, no. 1, p. 227, 2014.

[25] F. de Souza Machado, J. Kuo, M. F. Wohlenberg et al., "Subchronic treatment with acai frozen pulp prevents the brain oxidative damage in rats with acute liver failure," *Metabolic Brain Disease*, vol. 31, no. 6, pp. 1427–1434, 2016.

[26] L. C. Neves, V. X. Silva, E. A. Chagas, C. G. B. Lima, and S. R. Roberto, "Determining the harvest time of camu-camu [*Myrciaria dubia* (H.B.K.) McVaugh] using measured pre-harvest attributes," *Scientia Horticulturae*, vol. 186, pp. 15–23, 2015.

[27] A. L. R. Souza, M. M. Pagani, M. Dornier, F. S. Gomes, R. V. Tonon, and L. M. C. Cabral, "Concentration of camu-camu juice by the coupling of reverse osmosis and osmotic evaporation processes," *Journal of Food Engineering*, vol. 119, no. 1, pp. 7–12, 2013.

[28] M. S. Akter, S. Oh, J. B. Eun, and M. Ahmed, "Nutritional compositions and health promoting phytochemicals of camu-camu (*Myrciaria dubia*) fruit: a review," *Food Research International*, vol. 44, no. 7, pp. 1728–1732, 2011.

[29] R. Chirinos, J. Galarza, I. Betalleluz-Pallardel, R. Pedreschi, and D. Campos, "Antioxidant compounds and antioxidant capacity of Peruvian camu camu (*Myrciaria dubia* (H.B.K.) McVaugh) fruit at different maturity stages," *Food Chemistry*, vol. 120, no. 4, pp. 1019–1024, 2010.

[30] A. E. de Souza Schmidt Gonçalves, C. Lellis-Santos, R. Curi, F. M. Lajolo, and M. I. Genovese, "Frozen pulp extracts of camu-camu (*Myrciaria dubia* McVaugh) attenuate the hyperlipidemia and lipid peroxidation of type 1 diabetic rats," *Food Research International*, vol. 64, pp. 1–8, 2014.

[31] F. C. da Silva, A. Arruda, A. Ledel et al., "Antigenotoxic effect of acute, subacute and chronic treatments with Amazonian camu-camu (*Myrciaria dubia*) juice on mice blood cells," *Food and Chemical Toxicology*, vol. 50, no. 7, pp. 2275–2281, 2012.

[32] A. Fujita, K. Borges, R. Correia, B. D. G. M. Franco, and M. I. Genovese, "Impact of spouted bed drying on bioactive compounds, antimicrobial and antioxidant activities of commercial frozen pulp of camu-camu (*Myrciaria dubia* Mc. Vaugh)," *Food Research International*, vol. 54, no. 1, pp. 495–500, 2013.

[33] J. C. S. De Azevêdo, A. Fujita, E. L. de Oliveira, M. I. Genovese, and R. T. P. Correia, "Dried camu-camu (*Myrciaria dubia* H.B.K. McVaugh) industrial residue: a bioactive-rich Amazonian powder with functional attributes," *Food Research International*, vol. 62, pp. 934–940, 2014.

[34] D. F. da Silva Filho, J. S. de Andrade, C. R. Clement, F. M. Machado, and H. Noda, "Correlações fenotípicas, genéticas e ambientais entre descritores morfológicos e químicos em frutos de cubiu (*Solanum sessiliflorum* Dunal) da amazônia[1]," *Acta Amazonica*, vol. 29, no. 4, pp. 503–511, 1999.

[35] C. Agudelo, M. Igual, P. Talens, and N. Martínez-Navarrete, "Optical and mechanical properties of cocona chips as affected by the drying process," *Food and Bioproducts Processing*, vol. 95, pp. 192–199, 2015.

[36] J. Salick, "Cocona (*Solanum sessiliflorum* Dunal), an overview of productions and breeding potentials," in *International Symposium on New Crops for Food Industry*, pp. 125–129, University Southampton, Southampton, 1989.

[37] M. A. Pardo, "Efecto de Solanum sessiliflorum dunal sobre el metabolismo lipídico y de la glucosa," *Ciencia e Investigación*, vol. 7, pp. 43–48, 2004.

[38] L. C. Hernandes, A. F. Aissa, M. R. d. Almeida et al., "*In vivo* assessment of the cytotoxic, genotoxic and antigenotoxic potential of maná-cubiu (*Solanum sessiliflorum* Dunal) fruit," *Food Research International*, vol. 62, pp. 121–127, 2014.

[39] J. E. C. Cardona, L. E. Cuca, and J. A. Barrera, "Determination of some secondary metabolites in three ethnovarieties of cocona (*Solanum sessiliflorum* Dunal)," *Revista Colombiana de Química*, vol. 40, pp. 185–200, 2011.

[40] J. R. P. Maia, M. C. Schwertz, R. F. S. Sousa, J. P. L. Aguiar, and E. S. Lima, "Efeito hipolipemiante da suplementação dietética com a farinha do cubiu (*Solanum sessiliflorum* Dunal) em ratos hipercolesterolêmicos," *Revista Brasileira de Plantas Medicinais*, vol. 17, no. 1, pp. 112–119, 2015.

[41] C. E. Quijano and J. A. Pino, "Volatile compounds of copoazú (*Theobroma grandiflorum* Schumann) fruit," *Food Chemistry*, vol. 104, no. 3, pp. 1123–1126, 2007.

[42] S. d. N. Melo Ramos, W. Danzl, G. Ziegleder, and P. Efraim, "Formation of volatile compounds during cupuassu fermentation: influence of pulp concentration," *Food Research International*, vol. 87, pp. 161–167, 2016.

[43] H. R. d. M. Barros, R. García-Villalba, F. A. Tomás-Barberán, and M. I. Genovese, "Evaluation of the distribution and metabolism of polyphenols derived from cupuassu (*Theobroma grandiflorum*) in mice gastrointestinal tract by UPLC-ESI-Q-TOF," *Journal of Functional Foods*, vol. 22, pp. 477–489, 2016.

[44] J. Criollo, D. Criollo, and A. S. Aldana, "Fermentación de la almendra de copoazú (Theobroma grandiflorum [Willd. ex Spreng.] Schum.): evaluación y optimización del proceso," *Corpoica Ciencia y Tecnología Agropecuaria*, vol. 11, no. 2, p. 107, 2010.

[45] T. B. De Oliveira and M. I. Genovese, "Chemical composition of cupuassu (*Theobroma grandiflorum*) and cocoa (*Theobroma*

cacao) liquors and their effects on streptozotocin-induced diabetic rats," *Food Research International*, vol. 51, no. 2, pp. 929–935, 2013.

[46] J. T. Milanez, L. C. Neves, R. C. Colombo, M. Shahab, and S. R. Roberto, "Bioactive compounds and antioxidant activity of buriti fruits, during the postharvest, harvested at different ripening stages," *Scientia Horticulturae*, vol. 227, pp. 10–21, 2018.

[47] R. Pereira Lima, P. T. Souza da Luz, M. Braga et al., "Murumuru (*Astrocaryum murumuru* Mart.) butter and oils of buriti (*Mauritia flexuosa* Mart.) and pracaxi (*Pentaclethra macroloba* (Willd.) Kuntze) can be used for biodiesel production: physico-chemical properties and thermal and kinetic studies," *Industrial Crops and Products*, vol. 97, pp. 536–544, 2017.

[48] H. H. F. Koolen, F. M. A. da Silva, F. C. Gozzo, A. Q. L. de Souza, and A. D. L. de Souza, "Antioxidant, antimicrobial activities and characterization of phenolic compounds from buriti (*Mauritia flexuosa* L. f.) by UPLC-ESI-MS/MS," *Food Research International*, vol. 51, no. 2, pp. 467–473, 2013.

[49] T. L. N. Candido, M. R. Silva, and T. S. Agostini-Costa, "Bioactive compounds and antioxidant capacity of Buriti (*Mauritia flexuosa* L.f.) from the Cerrado and Amazon biomes," *Food Chemistry*, vol. 177, pp. 313–319, 2015.

[50] G. A. Bataglion, F. M. A. da Silva, M. N. Eberlin, and H. H. F. Koolen, "Simultaneous quantification of phenolic compounds in buriti fruit (*Mauritia flexuosa* L.f.) by ultra-high performance liquid chromatography coupled to tandem mass spectrometry," *Food Research International*, vol. 66, pp. 396–400, 2014.

[51] D. M. De Oliveira, E. P. Siqueira, Y. R. F. Nunes, and B. B. Cota, "Flavonoids from leaves of *Mauritia flexuosa*," *Revista Brasileira de Farmacognosia*, vol. 23, no. 4, pp. 614–620, 2013.

[52] F. Garmendia, R. Pando, and G. Ronceros, "Efecto del aceite de sacha inchi (Plukenetia volúbilis L) sobre el perfil lipídico en pacientes con hiperlipoproteinemia," *Revista Peruana de Medicina Experimental y Salud Pública*, vol. 28, no. 4, pp. 628–632, 2012.

[53] G. Gonzalez-Aspajo, H. Belkhelfa, L. Haddioui-Hbabi, G. Bourdy, and E. Deharo, "Sacha inchi oil (Plukenetia volubilis L.), effect on adherence of Staphylococus aureus to human skin explant and keratinocytes in vitro," *Journal of Ethnopharmacology*, vol. 171, pp. 330–334, 2015.

[54] A. S. Heringer, D. A. Steinmacher, H. P. F. Fraga et al., "Improved high-efficiency protocol for somatic embryogenesis in peach palm (*Bactris gasipaes* Kunth) using RITA® temporary immersion system," *Scientia Horticulturae*, vol. 179, pp. 284–292, 2014.

[55] E. E. Haro, J. A. Szpunar, and A. G. Odeshi, "Dynamic and ballistic impact behavior of biocomposite armors made of HDPE reinforced with chonta palm wood (Bactris gasipaes) microparticles," *Defence Technology*, vol. 14, no. 3, pp. 238–249, 2018.

[56] J. Restrepo, J. A. Estupiñán, and A. J. Colmenares, "Estudio comparativo de las fracciones lipídicas de Bactris gasipaes Kunth (chontaduro) obtenidas por extracción soxhlet y por extracción con CO_2 supercrítico," *Revista Colombiana de Química*, vol. 45, no. 1, pp. 5–9, 2016.

[57] F. A. Espinosa-Pardo, J. Martinez, and H. A. Martinez-Correa, "Extraction of bioactive compounds from peach palm pulp (*Bactris gasipaes*) using supercritical CO_2," *The Journal of Supercritical Fluids*, vol. 93, pp. 2–6, 2014.

[58] C. Rojas-Garbanzo, A. M. Pérez, J. Bustos-Carmona, and F. Vaillant, "Identification and quantification of carotenoids by HPLC-DAD during the process of peach palm (*Bactris gasipaes* H.B.K.) flour," *Food Research International*, vol. 44, no. 7, pp. 2377–2384, 2011.

[59] G. J. Basto, C. W. P. Carvalho, A. G. Soares et al., "Physicochemical properties and carotenoid content of extruded and non-extruded corn and peach palm (*Bactris gasipaes*, Kunth)," *LWT - Food Science and Technology*, vol. 69, pp. 312–318, 2016.

[60] B. C. Bolanho, E. D. G. Danesi, and A. D. P. Beleia, "Carbohydrate composition of peach palm (*Bactris gasipaes* Kunth) by-products flours," *Carbohydrate Polymers*, vol. 124, pp. 196–200, 2015.

[61] F. C. Schimpl, J. F. da Silva, J. F. C. Gonçalves, and P. Mazzafera, "Guarana: revisiting a highly caffeinated plant from the Amazon," *Journal of Ethnopharmacology*, vol. 150, no. 1, pp. 14–31, 2013.

[62] N. Dalonso and C. L. d. O. Petkowicz, "Guarana powder polysaccharides: characterisation and evaluation of the antioxidant activity of a pectic fraction," *Food Chemistry*, vol. 134, no. 4, pp. 1804–1812, 2012.

[63] T. Klein, R. Longhini, M. L. Bruschi, and J. C. P. de Mello, "Microparticles containing Guaraná extract obtained by spray-drying technique: development and characterization," *Revista Brasileira de Farmacognosia*, vol. 25, no. 3, pp. 292–300, 2015.

[64] L. Majhenič, M. Škerget, and Ž. Knez, "Antioxidant and antimicrobial activity of guarana seed extracts," *Food Chemistry*, vol. 104, no. 3, pp. 1258–1268, 2007.

Hindawi
Oxidative Medicine and Cellular Longevity
Volume 2019, Article ID 2936737, 15 pages
https://doi.org/10.1155/2019/2936737

Review Article

Borneol for Regulating the Permeability of the Blood-Brain Barrier in Experimental Ischemic Stroke: Preclinical Evidence and Possible Mechanism

Zi-xian Chen,[1] Qing-qing Xu,[1] Chun-shuo Shan,[1] Yi-hua Shi,[1] Yong Wang,[1] Raymond Chuen-Chung Chang,[2,3] and Guo-qing Zheng[1]

[1]*Department of Neurology, The Second Affiliated Hospital and Yuying Children's Hospital of Wenzhou Medical University, Wenzhou, China*
[2]*Laboratory of Neurodegenerative Diseases, School of Biomedical Sciences, LKS Faculty of Medicine, The University of Hong Kong, Hong Kong*
[3]*State Key Laboratory of Brain and Cognitive Sciences, The University of Hong Kong, Hong Kong*

Correspondence should be addressed to Raymond Chuen-Chung Chang; rccchang@hku.hk
and Guo-qing Zheng; gq_zheng@sohu.com

Received 8 August 2018; Accepted 2 December 2018; Published 4 February 2019

Guest Editor: Luciana Scotti

Borneol, a natural product in the Asteraceae family, is widely used as an upper ushering drug for various brain diseases in many Chinese herbal formulae. The blood-brain barrier (BBB) plays an essential role in maintaining a stable homeostatic environment, while BBB destruction and the increasing BBB permeability are common pathological processes in many serious central nervous system (CNS) diseases, which is especially an essential pathological basis of cerebral ischemic injury. Here, we aimed to conduct a systematic review to assess preclinical evidence of borneol for experimental ischemic stroke as well as investigate in the possible neuroprotective mechanisms, which mainly focused on regulating the permeability of BBB. Seven databases were searched from their inception to July 2018. The studies of borneol for ischemic stroke in animal models were included. RevMan 5.3 was applied for data analysis. Fifteen studies investigated the effects of borneol in experimental ischemic stroke involving 308 animals were ultimately identified. The present study showed that the administration of borneol exerted a significant decrease of BBB permeability during cerebral ischemic injury according to brain Evans blue content and brain water content compared with controls ($P < 0.01$). In addition, borneol could improve neurological function scores (NFS) and cerebral infarction area. Thus, borneol may be a promising neuroprotective agent for cerebral ischemic injury, largely through alleviating the BBB disruption, reducing oxidative reactions, inhibiting the occurrence of inflammation, inhibiting apoptosis, and improving the activity of lactate dehydrogenase (LDH) as well as P-glycoprotein (P-GP) and NO signaling pathway.

1. Introduction

The blood-brain barrier (BBB) is an anatomical and biochemical barrier, consisting of endothelial cells, a basal lamina, and astrocytic end feet [1]. The BBB integrity is of great significance for brain homeostasis, while the dysfunction of BBB can lead to complications of neurological diseases, such as stroke, chronic neurodegenerative disorders, neuroinflammatory disorders, and brain tumor [1–3]. Moreover, a disruption of BBB integrity, characterized by increased permeability, is associated with several neurological pathologies, such as ischemia/hypoxia, hemorrhage, multiple sclerosis, and amyotrophic lateral sclerosis [4]. During the cerebral ischemia/reperfusion injury, changes in BBB structures result in the increase of its permeability and the loss of its protective function, which may deteriorate the tissue injury [5, 6]. Thus, the disruption of BBB is an essential pathological basis of cerebral ischemic injury. The long-lasting BBB disruption can directly contribute to cerebral edema and the influx of immune cell and inflammatory materials, ultimately resulting in the

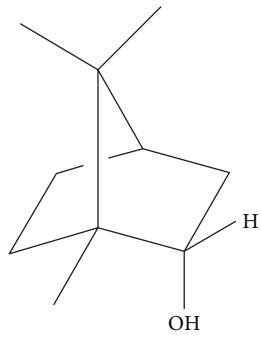

Figure 1: Chemical structures of borneol.

neuronal death, damage to the brain tissue, and neurological deficits, which plays a dominant role in the pathophysiological process of cerebral ischemic injury [7–10]. Further, extravasation of blood-borne albumin due to the increase of BBB permeability is assumed to trigger stroke-related complications like astrocyte-mediated epileptogenesis [11]. Consequently, those findings could provide a key basis that restore BBB integrity or reduce BBB opening is of great importance for the treatments of cerebral ischemic injury.

Borneol (Figure 1), a highly lipid-soluble bicyclic terpene chemical extracted from *Blumea balsamifera* (L.) DC. in the Asteraceae family or *Cinnamomum camphora* (L.) Presl. or chemically transformed based on camphor and turpentine oil [12], is early described in a Chinese herbology volume *The Compendium of Materia Medica* (Bencao Gangmu) during the 16^{th} century. It is widely used as a common ingredient in many traditional Chinese herbal formulas against stroke, such as Angong Niuhuang pill [13]. According to traditional Chinese medicine (TCM) Emperor-Minister-Assistant-Courier theory, borneol is classified as a "courier herb" that guides the herbs upward to target organ, especially in the upper part of the body, such as the brain. Many studies reported that borneol had neuroprotective effects through a variety of mechanisms like antinociception [14], anti-inflammatory [15, 16], antioxidation [16], and antiepilepsy [17]. Here, we conducted a preclinical systematic review to provide the current evidence of borneol for experimental ischemic stroke, mainly through possible mechanisms of regulating the BBB permeability.

2. Methods

2.1. Search Strategy. A comprehensive search strategy was conducted in seven databases, including PubMed, Embase, CENTRAL (the Cochrane Library), China National Knowledge Infrastructure, VIP database, Wanfang database, and Chinese Biomedical Database from their inceptions to July 2018. The search terms were as follows: "(borneol OR camphol) AND (ischemic stroke OR cerebral ischemic injury OR cerebral infarction OR brain infraction)." No restrictions were placed on the date, country, or language of publication. All searches were limited to animal studies.

2.2. Eligibility Criteria

2.2.1. Types of Studies. All *in vivo* studies evaluating the effect of borneol on ischemic stroke were selected, regardless of animal species or publication status. The following eligibility criteria should be met: (1) the administration of borneol was performed on the animal model of ischemic stroke, regardless of its mode, dosage, and frequency; (2) the BBB integrity was assessed by qualitative assessments and/or quantitative evaluations of the brain or both the brain and the blood for a substance remaining stable in the blood or for an agent additionally injected into the blood, including brain water content, drugs used for ischemic stroke, Evans blue (EB), and imaging contrast agents; and (3) the control group receiving vehicle or no adjunct intervention was included in the studies.

2.2.2. Types of Outcome Measures. The primary outcome measures were the brain EB content, the brain water content, and the ultrastructure of BBB. The secondary outcome measures were neurological function score (NFS), triphenyltetrazolium chloride (TTC) staining, measurement of superoxide dismutase (SOD) activity, and malonaldialdehyde (MDA) level.

2.3. Exclusion Criteria. Exclusion criteria were as follows: (1) the study was a case report, clinical trial, review, abstract, comment, editorial, or *in vitro* study; (2) the targeting disease was not ischemic stroke; (3) the intervention was a combination of borneol and another agent with potential effect on ischemic stroke; (4) the effect of borneol was not tested on BBB permeability; and (5) lack of the control group.

2.4. Data Extraction. Two independent reviewers assessed the articles for the eligibility and extracted the following details: (1) author, year, method of anesthesia, and/or model; (2) individual data, including animal species, sex, and weight; (3) the method of administration from both treatment and control groups, including drug, dose, mode, and frequency; and (4) the outcome measures and samples for individual comparison were included. A comparison was defined as the qualitative and/or quantitative assessments of the BBB permeability in the treatment and corresponding control groups after the administration of borneol or vehicle with a given dosage, mode, and frequency. If a drug was used for outcome assessment, both the drug and the method of drug administration were obtained. All available data from quantitative assessments of the BBB integrity were extracted for every comparison including mean outcome and standard deviation.

2.5. Quality of Evidence. Quality of evidence in included studies was conducted by two independent reviewers according to a ten-item modified scale [18, 19]: (1) peer reviewed publication; (2) statement of physiological parameter control, such as temperature; (3) random allocation; (4) blinded conduct of the experiments; (5) blinded assessment of outcome; (6) use of anesthetic without significant intrinsic neuroprotective activity; (7) appropriate animal and/or model (aged, diabetic, or hypertensive); (8) sample size calculation; (9)

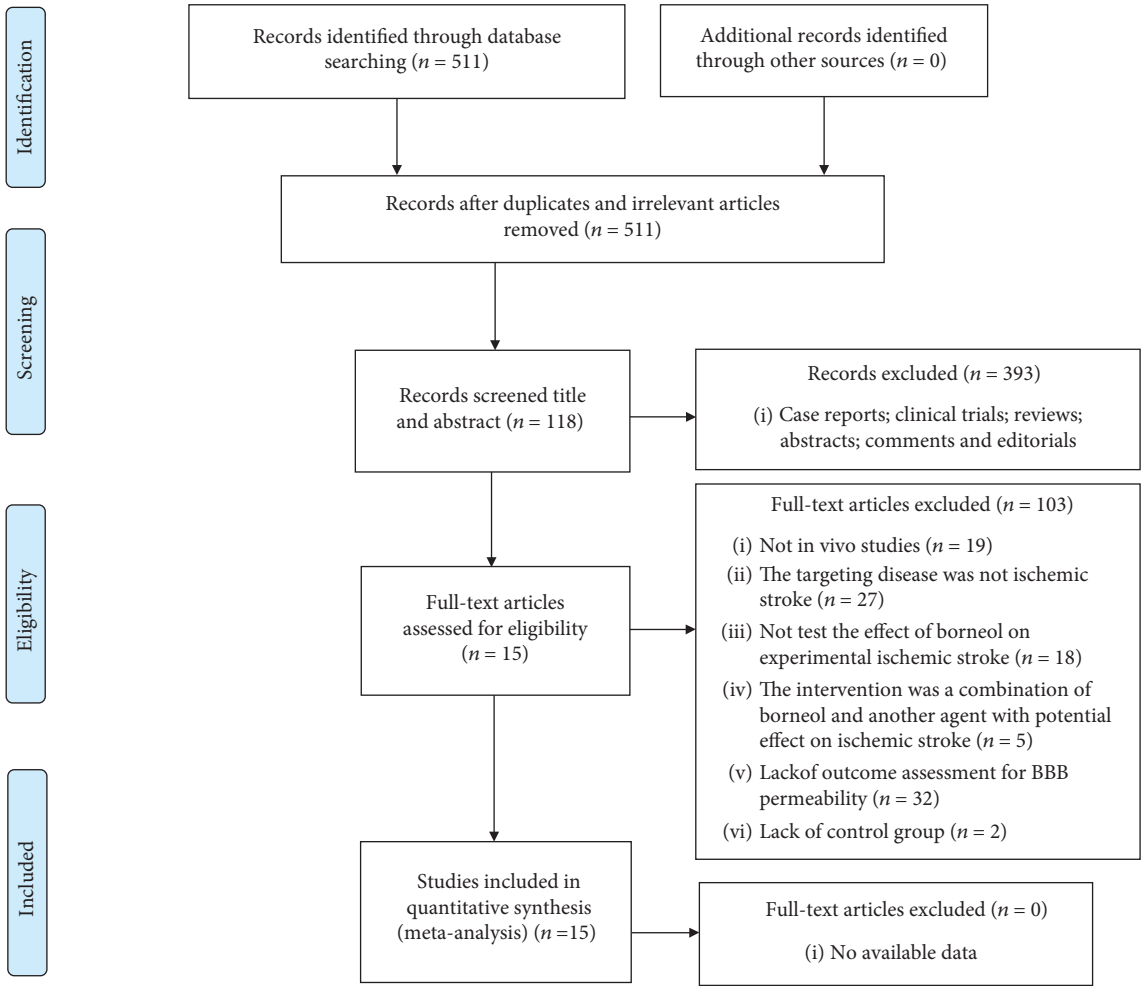

Figure 2: Flow diagram of the search process.

compliance with animal welfare regulations; (10) statement of potential conflict of interests.

2.6. Statistical Analysis. The statistical analysis was conducted via RevMan version 5.3. To estimate the effect of borneol on ischemic stroke, a model of random effect (RE) was applied to estimate pooled effect with 95% confidence intervals (CI) if statistical heterogeneity was found ($P < 0.1$, $I^2 > 50\%$), while a model of fixed effect (FE) was set with 95% CI if no statistical evidence of heterogeneity existed ($p \geq 0.1$, $I^2 \leq 50\%$). The weighted mean difference (WMD) was calculated as a summary statistic if the outcomes were applied the same scale, while standardized mean differences (SMD) was used if the same outcome measurements were measured in a variety of ways. Heterogeneity was assessed via a standard chi-square test and I^2 statistic. A probability value less than 0.05 was considered statistically significant.

3. Results

3.1. Study Selection. After primary search from seven databases, a total of 511 potentially relevant studies were included. By reviewing titles and abstracts, 393 studies that were case reports, clinical trials, reviews, abstracts, comments, or editorials were excluded. After reading the remaining 118 full-text articles for eligibility, 103 studies were removed for at least one of following reasons: (1) not an *in vivo* study; (2) the targeting disease was not ischemic stroke; (3) the study did not access the effects of borneol on the animal model of ischemic stroke; (4) the intervention was a combination of borneol and another agent with potential effect on ischemic stroke; (5) lack of outcome assessments for BBB integrity; and (6) lack of the control group. Ultimately, 15 studies involving 308 animals were selected for quantitative analysis (Figure 2).

3.2. Study Characteristics. Fifteen studies [20–34] involving 308 animals were included. Five species were referred, including SD rats ($n = 225$) [21–23, 25, 27–30, 33, 34], Wistar rats ($n = 24$) [24], ICR mice ($n = 21$) [33], Kunming mice ($n = 14$) [31], and C57 BL/6J mice ($n = 24$) [20]. The weight of rats ranged from 180 g to 400 g, and the weight of mice ranged from 18 g to 25 g. Cerebral ischemic injury in the included studies was induced by temporary middle cerebral artery occlusion (MCAO) for two hours [25–27, 30], permanent MCAO [21, 32], temporary occlusion of bilateral common carotid arteries for a range of 20-60 min [20, 22, 23, 33], transient occlusion of bilateral hemisphere

for 20 min by Pulsinelli-4VO method [24], or permanent ligation of bilateral common carotid arteries [28, 29, 31, 34]. Chloral hydrate was used in twelve studies, while the anesthetic in three study [21, 26, 28] cannot be confirmed from the primary data.

Among all the included studies, one study [21] assessed the effects of L-borneol, D-borneol, and synthetic borneol, one study [23] assessed the effects of synthetic borneol as well as L-borneol, three studies [23, 29, 31] used synthetic borneol, one study [24] used D-borneol, two studies declared the administration of natural borneol [30] but without reporting the type of borneol, and the remaining studies used the borneol without further information provided. The mode of borneol application consisted of oral gavage (14 studies) and intravenous injection (1 study) [34]. The frequency of the treatment varied from once daily for the duration of 3 days [20, 21, 24, 26, 27, 29–31] to 8 days [33]. Two studies applied the borneol to the animals before as well as after the model establishment [20, 25], while the other thirteen studies applied it before the model establishment.

Four studies [23, 26–28] reported the ultrastructure of BBB when six studies performed the quantitative assessments of brain for EB [20, 24, 25, 30, 31], and ten studies performed the quantitative assessments of brain for water content [20, 22–25, 27, 29, 32–34]. More details about the characteristics of the included studies were shown in Table 1.

3.3. Quality of Included Study. The quality scores varied from 2/10 to 5/10 with the average of 3.13. Twelve studies were peer-reviewed publications, while three studies were unpublished master's thesis or PhD thesis. Four studies described the control of temperature. Fourteen studies declared the random allocation. Twelve studies described the use of anesthetic without significant intrinsic neuroprotective activity. Four studies stated the compliance with animal welfare regulations. One study had a statement of potential conflict of interests. None of the included studies reported the masked conduct of experiments, the blinded assessments of outcome, and the application of animal or model with relevant comorbidities or a sample size calculation. The quality scores for the included studies shown in Table 2.

3.4. Effectiveness Assessment

3.4.1. The Brain EB Content. The assessments of the brain EB content were performed in six studies [20, 24, 25, 28, 30, 31] at a time point ranged from 20 min to 72 hours after the induction of the model. Combining available data in a meta-analysis from the above six studies showed the significantly protective effect of borneol on the BBB during cerebral ischemic injury according to the brain EB content [$n_{\text{Treatment}}/n_{\text{Control}}$ (n_T/n_C) = 40/38, WMD -4.16, 95% CI: -4.68~-3.64, $P < 0.00001$; heterogeneity $\chi^2 = 12.34$, df = 5, $I^2 = 59\%$]. After sequentially omitting each study, one outlier study [24] reporting Pulsinelli four-vessel method was considered as the potential sources of the heterogeneity. Meta-analysis of remaining four studies showed a more homogeneous result (n_T/n_C = 34/32, WMD -3.81, 95% CI: -4.39~-3.23, $P < 0.00001$; heterogeneity $\chi^2 = 4.94$, df = 4, $I^2 = 19\%$, Figure 3). It was indicated that the method of model induction may be one possible explanation for the heterogeneity.

3.4.2. The Brain Water Content. Ten studies [20, 22–25, 27, 29, 32–34] with eleven comparisons evaluated the brain water content at a time point ranged from 10 min to 72 hours after the induction of the model. Among them, nine studies assessed brain water content by using dry-wet weight method and showed the significant decreasing of BBB permeability in the treatment of cerebral ischemic injury (n_T/n_C = 72/72, WMD -1.28, 95% CI: -1.93~-0.63, $P = 0.0001$; heterogeneity $\chi^2 = 61.26$, df = 8, $I^2 = 87\%$). After sequential removal of each study, the outlier study [24] with model induced by Pulsinelli four-vessel method was removed. The meta-analysis of eight studies showed a homogeneous result (n_T/n_C = 68/68, WMD -0.92, 95% CI: -1.10~-0.75, $P < 0.00001$; heterogeneity $\chi^2 = 3.96$, df = 7, $I^2 = 0\%$, Figure 4), which also indicated a possible explanation for the heterogeneity. The remaining study [27] with two comparisons reported the rate of cerebral edema based on wet weight and meta-analysis of them showed significant effects of borneol for alleviating BBB permeability during cerebral ischemic injury (n_T/n_C = 16/16, WMD -9.09, 95% CI: -12.11~-6.07, $P < 0.00001$; heterogeneity $\chi^2 = 0.02$, df = 1, $I^2 = 0\%$, Figure 4).

3.4.3. The Ultrastructure of BBB. For cerebral ischemic injury, four studies [21, 23, 26, 27] with seven comparisons assessed the impacts of borneol on the ultrastructure of BBB, involving six comparisons reporting significantly neuroprotective effects and one comparison reporting no difference.

3.4.4. NFS. NFS was reported in two studies [21, 32] with four comparisons, examined according to the five-point scale described previously by Longa et al. (Longa et al., 1989). Meta-analysis showed a significant difference in improving NFS but with substantial heterogeneity (n_T/n_C = 45/45, MD -0.42, 95% CI: -0.65 to -0.20, $P < 0.00001$, heterogeneity $\chi^2 = 300.05$, df = 3, $I^2 = 99\%$). Zhang *et al.* [32] compared administration of borneol (0.4 g per animal, ig, qd) with the same volume of 1% Tween (ig, qd) for 7 days before occlusion and reported no significant difference in NFS between the two groups (n_T/n_C = 9/9). Comparing L-borneol (0.2 g/kg, ig, qd), D-borneol (0.2 g/kg, ig, qd), or synthetic borneol (0.6 g/kg, ig, qd) with the same volume of 5% Tween 80 solution (ig, qd) for 3 days before occlusion, respectively, Dong et al. [21] found that these three comparisons had a significant difference in improving NFS (L-borneol: n_T/n_C = 12/12; D-borneol: n_T/n_C = 12/12; and synthetic borneol: n_T/n_C = 12/12).

3.4.5. TTC Staining. Two studies [21, 32] with four comparisons applied TTC staining to evaluate cerebral infarction area, showing a significant difference but with substantial heterogeneity (n_T/n_C = 24/24, MD -6.64, 95% CI: -12.53 to -0.75, $P < 0.00001$, heterogeneity $\chi^2 = 252.43$, df = 3, $I^2 = 99\%$). Using borneol (0.4 g per animal, ig, qd) for 7 days before occlusion as an experimental administration (n_T/n_C = 9/9), Zhang et al. [32] found that the infarction area was

Table 1: Summary of the efficacy of borneol for ischemic stroke.

Study (author, years)	Species	Weight	Anesthetic	Conditions or model induction	Method of administration		Outcome measures (sample)	Intergroup differences
					Treatment group	Control group		
Chen et al. 2010 [20]	Male, C57 BL/6J mice	18–20 g	Chloral hydrate (300 mg/kg, ip)	Temporary occlusion of bilateral common carotid arteries for 25 min	Borneol, 0.01 g/kg, ig, at 30 min before model and once daily for 2 days after occlusion	Same volume of 10% ethanol, ig, at 30 min before model and once daily for 2 days after occlusion	(1) Brain EB content, 48 h (6/6) (2) Brain water content, 24 h (6/6) (3) Morris water maze test, 4 d (12/12) (4) MDA, SOD, 4 d (6/6) (5) GFAP, 4 d (3/3)	(1) $P < 0.05$ (2) $P < 0.05$ (3) $P > 0.05$ (4) $P > 0.05$
Dong 2018 [21] a	Male, SD rats	230–270 g	NS	Permanent middle cerebral artery occlusion	L-borneol, 0.2 g/kg, ig, once daily for 3 days before occlusion	Same volume of 5% Tween 80 solution, ig, once daily for 3 days before occlusion	(1) Neurological function score, 24 h (12/12) (2) Brain water content, 24 h (8/8) (3) Cerebral infarction rate with TTC staining, 24 h (5/5) (4) The ultrastructure of BBB, NS (5) VEGF levels in the serum, 24 h (7/7) (6) TNF-α levels in the serum, 24 h (7/7) (7) Bax mRNA, 24 h (3/3) (8) Bcl-2 mRNA, 24 h (3/3) (9) Claudin-5 mRNA, 24 h (3/3)	(1) $P < 0.05$ (2) $P < 0.01$ (3) $P < 0.01$ (4) NS (5) $P < 0.01$ (6) $P < 0.01$ (7) $P > 0.05$ (8) $P > 0.05$ (9) $P > 0.05$
Dong 2018 [21] b	Male, SD rats	230–270 g	NS	Permanent middle cerebral artery occlusion	D-borneol, 0.2 g/kg, ig, once daily for 3 days before occlusion	Same volume of 5% Tween 80 solution, ig, once daily for 3 days before occlusion	(1) Neurological function score, 24 h (12/12) (2) Brain water content, 24 h (8/8) (3) Cerebral infarction rate with TTC staining, 24 h (5/5) (4) The ultrastructure of BBB, NS (5) VEGF levels in the serum, 24 h (7/7)	(1) $P > 0.05$ (2) $P > 0.05$ (3) $P > 0.05$ (4) NS (5) $P < 0.01$ (6) $P < 0.01$ (7) $P > 0.05$ (8) $P > 0.05$ (9) $P < 0.05$

Table 1: Continued.

Study (author, years)	Species	Weight	Anesthetic	Conditions or model induction	Method of administration		Outcome measures (sample)	Intergroup differences
					Treatment group	Control group		
Dong 2018 [21] c	Male, SD rats	230–270 g	NS	Permanent middle cerebral artery occlusion	Synthetic borneol, 0.6 g/kg, ig, once daily for 3 days before occlusion	Same volume of 5% Tween 80 solution, ig, once daily for 3 days before occlusion	(6) TNF-α levels in the serum, 24 h (7/7) (7) Bax mRNA, 24 h (3/3) (8) Bcl-2 mRNA, 24 h (3/3) (9) Claudin-5 mRNA, 24 h (3/3) (1) Neurological function score, 24 h (12/12) (2) Brain water content, 24 h (8/8) (3) Cerebral infarction rate with TTC staining, 24 h (5/5) (4) The ultrastructure of BBB, NS (5) VEGF levels in the serum, 24 h (7/7) (6) TNF-α levels in the serum, 24 h (7/7) (7) Bax mRNA, 24 h (3/3) (8) Bcl-2 mRNA, 24 h (3/3) (9) Claudin-5 mRNA, 24 h (3/3)	(1) $P > 0.05$ (2) $P < 0.01$ (3) $P < 0.01$ (4) $P < 0.01$ (5) $P < 0.01$ (6) $P < 0.01$ (7) $P < 0.05$ (8) $P > 0.05$ (9) $P < 0.01$
Fang et al. 2004 [22]	Male and female, SD rats	200–300 g	10% chloral hydrate (300 mg kg, ip)	Temporary occlusion of bilateral common carotid arteries for 60 min	Borneol, 0.2 g/kg, ig, once daily for 7 days before occlusion	Same volume of normal saline, ig, once daily for 7 days before occlusion	(1) Brain water content, NS (10/10) (2) BAX, NS (10/10) (3) BCL-XL, NS (10/10)	(1) $P < 0.001$ (2) $P < 0.001$ (3) $P < 0.05$
Huang et al. 2000 [23]	Male and female, SD rats	180–200 g	NS	Temporary obstruction of bilateral common carotid arteries for 45 min	Synthetic borneol, 1 g/kg, ig, once daily for 7 days before model establishment	Same volume of distilled water, ig, once daily for 7 days before model establishment	(1) Brain water content, 1 h (10/10) (2) The ultrastructure of BBB, 1 h (10/10)	(1) $P > 0.05$ (2) NS

Table 1: Continued.

Study (author, years)	Species	Weight	Anesthetic	Conditions or model induction	Method of administration		Outcome measures (sample)	Intergroup differences
					Treatment group	Control group		
Jia 2014 [24]	Male, Wistar rats	240–280 g	10% chloral hydrate (NS, ip)	Transient occlusion of bilateral hemisphere for 20 min (Pulsinelli-4VO method)	D-borneol, 0.2 g/kg, ig, once daily for 3 days before occlusion	Same volume of 70% ethanol, ig, once daily for 3 days before occlusion	(1) Brain EB content, 72 h (6/6) (2) Brain water content, 72 h (6/6) (3) ZO-1, 72 h (6/6)	(1) $P < 0.05$ (2) $P < 0.05$ (3) $P < 0.05$
Liu et al. 2007 [25]	Male and female, SD rats	260–300 g	10% chloral hydrate (350 mg/kg, ip)	Temporary middle cerebral artery occlusion for 2 h	Borneol, 0.003 g/kg, ig, at 12 h, 30 min before model and at 12 h, 24 h after occlusion	Same volume of 1% Tween, ig, at 12 hr, 30 min before model and at 12 hr, 24 hr after occlusion	(1) Brain EB content, 24 h (5/5) (2) Brain water content, 24 h (5/5)	(1) $P < 0.01$ (2) $P > 0.05$
Ni et al. 2011 [26]	Male, SD rats	280–320 g	10% chloral hydrate (350 mg/kg, ip)	Temporary middle cerebral artery occlusion for 2 h	Borneol, 0.2 g/kg, ig, once daily for 3 days before occlusion	Same volume of 5% Tween, ig, once daily for 3 days before occlusion	(1) The ultrastructure of BBB, 22 h (NS/NS) (2) VEGF, 22 h (8/8) (3) MMP-9, 22 h (8/8)	(1) NS (2) $P < 0.05$ (3) $P > 0.05$
Tian 2013 [27] a	Male, SD rats	280–350 g	10% chloral hydrate (350 mg/kg, ip)	Temporary middle cerebral artery occlusion for 2 h	L-borneol, 0.20 g/kg, ig, once daily for 3 days before occlusion	Same volume of normal saline, ig, once daily for 3 days before occlusion	(1) Rate of cerebral edema, 22 h (8/8) (2) MDA, 22 h (8/8) (3) SOD, 22 h (8/8) (4) P-GP, 22 h (8/8) (5) The ultrastructure of BBB, 22 h (2/2)	(1) $P < 0.01$ (2) $P < 0.05$ (3) $P < 0.01$ (4) $P < 0.01$ (5) NS
Tian 2013 [27] b	Male, SD rats	280–350 g	10% chloral hydrate (350 mg/kg, ip)	Temporary middle cerebral artery occlusion for 2 h	Synthetic borneol, 0.20 g/kg, ig, once daily for 3 days before occlusion	Same volume of normal saline, ig, once daily for 3 days before occlusion	(1) Rate of cerebral edema, 22 h (8/8) (2) MDA, 22 h (8/8) (3) SOD, 22 h (8/8) (4) P-GP, 22 h (8/8) (5) The ultrastructure of BBB, 22 h (2/2)	(1) $P < 0.01$ (2) $P < 0.05$ (3) $P < 0.01$ (4) $P < 0.01$ (5) NS
Shao 2018 [28]	Male & female, SD rats	300–400 g	NS	Permanent ligation of bilateral common carotid arteries	Borneol, 0.5 g/kg, ig, once daily for 7 days before model establishment	Same volume of normal saline, ig, once daily for 7 days before model establishment	(1) Brain EB content, 24 h (10/10) (2) SOD, NS (10/10) (3) MPO, NS (10/10) (4) TNF-α, NS (10/10)	(1) $P < 0.01$ (2) $P < 0.01$ (3) $P < 0.01$ (4) NS
Wang 2011 [29]	Male and female, SD rats	180–220 g	10% chloral hydrate (300 mg/kg, ip)	Permanent ligation of bilateral common carotid arteries	Synthetic Borneol, 0.2 g/kg, ig, once daily for 3 days before model establishment	Same volume of normal saline, ig, once daily for 3 days before model establishment	(1) Brain water content, 3 h (9/10) (2) SOD, Na^+-K^+-ATPase, 3 h (9/10) (3) MDA, 3 h (9/10) (4) LDH, 3 h (9/10)	(1) $P > 0.05$ (2) $P < 0.05$ (3) $P < 0.05$ (4) $P < 0.05$

Table 1: Continued.

Study (author, years)	Species	Weight	Anesthetic	Conditions or model induction	Method of administration		Outcome measures (sample)	Intergroup differences
					Treatment group	Control group		
Xu and Zhang 2015 [30]	Male, SD rats	250 ± 20 g	10% chloral hydrate (NS, NS)	Temporary middle cerebral artery occlusion for 2 h	Natural borneol, 0.028 g/kg, ig, once daily for 3 days before occlusion	Same volume of normal saline, ig, once daily for 3 days before occlusion	(1) Brain EB content, 24 h (5/5) (2) ZO-1, 24 h (5/5) (3) Claudin-5, 24 h (5/5)	(1) $P > 0.05$ (2 $P > 0.05$ (3) $P > 0.05$
Yao et al. 2011 [31]	Male and female, Kunming mice	22 ± 3 g	4% chloral hydrate (400 mg/kg, ip)	Permanent ligation of bilateral common carotid arteries	Synthetic borneol, 0.0666 g/kg, ig, once daily for 3 days before occlusion	Same volume of normal saline, ig, once daily for 3 days before occlusion	Brain EB content, 20 min (8/6)	$P > 0.05$
Zhang et al. 2011 [32]	Male, SD rats	250–280 g	10% chloral hydrate (350 mg/kg, ip)	Permanent middle cerebral artery occlusion	Borneol, 0.4 g per animal, ig, once daily for 7 days before occlusion	Same volume of 1% Tween, ig, once daily for 7 days before occlusion	(1) Brain water content, 24 h (9/9) (2) Neurological function score, NS (9/9) (3) Infarction volume, NS (9/9)	(1) $P > 0.05$ (2) $P > 0.05$ (3) $P > 0.05$
Zhang et al. 2011 [33]	Male and female, ICR mice	18–22 g	4% chloral hydrate (0.4 mg/kg, NS)	Temporary occlusion of bilateral common carotid arteries for 20 min	Borneol, 0.5 g per animal, ig, once daily for 8 days before occlusion	Same volume of 1% Tween, ig, once daily for 8 days before occlusion	(1) Brain water content, 10 min (11/10) (2) SOD, 10 min (11/10) (3) MDA, 10 min (11/10)	(1) $P > 0.05$ (2) $P > 0.05$ (3) $P > 0.05$
Zhu et al. 2007 [34]	Male, SD rats	200–250 g	10% chloral hydrate (400 mg/kg, ip)	Permanent ligation of bilateral common carotid arteries	Borneol, 0.020 g/kg, iv, once daily for 4 days before model establishment	Same volume of normal saline, iv, once daily for 4 days before model establishment	Brain water content, 3 h (8/8)	$P > 0.05$

Note: BBB: the blood-brain barrier; increased: a significantly increasing blood-brain barrier permeability after the administration of borneol; decreased: a significantly decreasing blood-brain barrier permeability after the administration of borneol; ND: no statistical difference between treatment and control groups; Increased? or decreased?: the efficacy result was reported as increasing or decreasing blood brain barrier permeability with the absence of statistical analysis or available original data; ig: intragastric administration; ip: intraperitoneal administration; iv: intravenous injection; NS: not stated; SOD: superoxide dismutase; MDA: malondialdehyde; ET: endothelin; NO: nitric oxide; LDH: lactated hydrogenase; EB: Evans blue; ZO-1: zonula occludens-1; GFAP: gliofibrillar acid protein; BAX: Bcl-2 associated X protein; BCL: B-cell lymphoma; VEGF: vascular endothelial growth factor; MMP-9: matrix metalloproteinase-9; P-GP: P-glycoprotein.

Table 2: Quality assessment of included studies.

Study	A	B	C	D	E	F	G	H	I	J	Total
Chen et al. [20]	+	+	+			+			+		5
Dong et al. [21]	+	+	+						+	+	5
Fang et al. [22]	+		+			+					3
Huang et al.[23]	+		+								2
Jia [24]			+			+			+		3
Liu et al. [25]	+		+			+					3
Ni et al. [26]	+					+			+		3
Tian [27]		+	+			+					3
Shao et al. [28]	+		+								2
Wang [29]			+			+					2
Xu and Zhang [30]	+		+			+					3
Yao et al. [31]	+		+			+					3
Zhang et al. [32]	+	+	+			+					4
Zhang et al. [33]	+		+			+					3
Zhu et al. [34]	+		+			+					3

A: peer-reviewed publication; B: monitoring of physiological parameters such as temperature; C: random allocation; D: blinded conduct of the experiments; E: blinded assessment of outcome; F: use of anesthetic without significant intrinsic neuroprotective activity (e.g., ketamine); G: animal and/or model (aged, diabetic, or hypertensive); H: sample size calculation; I: compliance with animal welfare regulations; J: statement of potential conflict of interests.

statistically similar between the borneol group and the control group (same volume of 1% Tween, ig, qd). Comparing L-borneol (0.2 g/kg, ig, qd), D-borneol (0.2 g/kg, ig, qd), or synthetic borneol (0.6 g/kg, ig, qd) with the same volume of 5% Tween 80 solution (ig, qd) for 3 days before occlusion, respectively, Dong *et al.* [21] found that these three comparisons had a significant difference in alleviating the infarction area (L-borneol: $n_T/n_C = 5/5$; D-borneol: $n_T/n_C = 5/5$; and synthetic borneol: $n_T/n_C = 5/5$).

3.4.6. SOD. Meta-analysis of four studies [20, 28, 29, 33] showed that animals in the borneol group had statistically significant higher SOD activity than the control group ($n_T/n_C = 34/35$, MD 17.22, 95% CI: -10.00 to 24.44, $P < 0.00001$, heterogeneity $\chi^2 = 20.56$, df = 3, $I^2 = 85\%$). Sensitivity analyses were conducted to explore potential sources of heterogeneity after the omissions of each individual study from the original analysis. Sensitivity analyses pointed to one study [28] as a likely source of heterogeneity. After removal of the study, the SOD activity between the two groups had significant difference and the heterogeneity was reduced ($n_T/n_C = 24/25$, MD 14.51, 95% CI: 10.93 to 18.09, $P < 0.00001$, heterogeneity $\chi^2 = 3.65$, df = 2, $I^2 = 45\%$, Figure 5).

3.4.7. MDA. Three studies [20, 29, 33] based on the measurement of MDA level showed no significant difference between the borneol group and the control group but with substantial heterogeneity ($n_T/n_C = 24/24$, WMD -0.39, CI: -6.25~1.63, $P = 0.86$, $I^2 = 66\%$). Sensitivity analyses were conducted to explore potential sources of heterogeneity after the omissions of each individual study from the original analysis. Sensitivity analyses pointed to one study [20] as a likely source of heterogeneity. After removal of the study, the MDA outcomes between the two groups remained similar and the heterogeneity was reduced ($n_T/n_C = 18/18$, WMD -0.32, CI: -0.80~0.16, $P = 0.19$, $I^2 = 0\%$, Figure 6).

3.4.8. Possible Neuroprotective Mechanisms of Borneol. According to the included studies, the possible neuroprotective mechanisms of borneol for ischemic stroke lie in the following aspects: (1) borneol could help alleviate the pathological BBB disruption [21, 23, 24, 26, 27, 30]. (2) Borneol could effectively reduce oxidative reactions through increasing the activity of SOD and decreasing the concentration of MDA [28, 29, 33]. (3) Borneol could inhibit the occurrence of inflammation by decreasing the expression of proinflammatory cytokines such as TNF-α [21, 28]. (4) Borneol could exert antiapoptotic effects, resulting in neuroprotection [21, 22]. (5) Borneol could improve the activity of lactate dehydrogenase (LDH) in brain tissue to inhibit the increase of lactic acid, which reduces the accumulation of lactic acid and exerts neuroprotective effect [29]. (6) Borneol could improve the energy metabolism disorder by upregulating the activity of Na^+-K^+-ATPase [27, 29], Ca^{2+}-Mg^{2+}-ATPase [27], and T-ATPase [27]. (7) Borneol could exert the neuroprotective effect via P-glycoprotein (P-GP) signaling pathway [27]. (8) Borneol exerts the neuroprotective effect via NO signaling pathway [27]. More details were shown in Table 3.

4. Discussion

4.1. Summary of Results. As far as we know, this is the first preclinical systematic review to determine the effects of borneol for experimental ischemic stroke, mainly through possible mechanisms of regulating the BBB permeability. In the present study, thirteen studies with 230 animals were selected for analysis. Borneol were identified to have a decreased impact on pathological BBB permeability from animals with cerebral ischemic injury. The pooled data suggested that borneol exerts a significant protection on the experimental model of ischemic stroke.

4.2. Limitations. First, all the databases we searched were in English or Chinese, which may cause selective bias as studies published in other languages may be left out. Second, the present study found that only one animal species (rodent) was used, which potentially posed a threat to the promotion of the findings. Third, the methodological quality of most included studies was moderate, which was an inherent drawback in the primary study. Methodological flaws in most included studies lie in blinding, sample size calculation, lacking animals with relevant comorbidities, and lacking statement of potential conflict of interests. Thus, the conclusions in the present study should be partially treated with caution.

4.3. Implications. Currently, it is increasingly recognized that the regulation of BBB permeability is a complicated process, which involves multiple components, such as endothelial cells, tight junction, basal lamina, and pericytes [35–38], and a variety of genes. BBB can effectively prevent the entry

Study or subgroup	Borneol Mean	Borneol SD	Borneol Total	Control Mean	Control SD	Control Total	Weight	Mean difference IV, fixed, 95% CI
Chen et al. 2010 [20]	4.57	0.88	6	8.84	1.79	6	13.1%	−4.27 [−5.87, −2.67]
Jia 2014 [24]	72.17	0.75	6	77.83	1.3	6		Not estimable
Liu et al. 2007 [25]	4.87	1.83	5	10.65	3.99	5	2.2%	−5.78 [−9.63, −1.93]
Shao et al. 2018 [28]	5.36	1.02	10	9.13	0.13	10	82.0%	−3.77 [−4.41, −3.13]
Xu and Zhang 2015 [30]	26.79	2.24	5	27.38	3.5	5	2.5%	−0.59 [−4.23, 3.05]
Yao et al. 2011 [31]	30.578	13.449	8	39.659	11.995	6	0.2%	−9.08 [−22.46, 4.30]
Total (95% CI)			34			32	100.0%	−3.81 [−4.39, −3.23]

Heterogeneity: Chi² = 4.94, df = 4 ($P = 0.29$); $I^2 = 19\%$
Test for overall effect: $Z = 12.94$ ($P < 0.00001$)

Mean difference IV, fixed, 95% CI

−20 −10 0 10 20
Favours [borneol] Favours [control]

Figure 3: The forest plots: the borneol group versus the control group on brain Evans blue content under pathological conditions.

Study or subgroup	Borneol Mean	Borneol SD	Borneol Total	Control Mean	Control SD	Control Total	Weight	Mean difference IV, fixed, 95% CI
1.2.1 celebral ischemic injury - brain water sontent 1								
Chen et al. 2010 [20]	79.33	0.18	6	80.43	0.4	6	18.6%	−1.10 [−1.45, −0.75]
Fang et al 2004 [22]	77.3	0.27	10	78.23	0.52	10	18.4%	−0.93 [−1.29, −0.57]
Huang et al. 2000 [23]	82.22	1.84	10	82.14	0.95	10	7.9%	0.08 [−1.20, −1.36]
Liu et al. 2007 [25]	80.79	0.93	5	81.51	0.53	5	11.1%	−0.72 [−1.66, −0.22]
Wang 2011 [29]	78.55	0.19	9	79.45	0.41	10	19.3%	−0.90 [−1.18, −0.62]
Zhang et al. 2011 [32]	82.22	1.24	9	83.05	2.06	9	6.0%	−0.83 [−2.40, −0.74]
Zhang et al. 2011 [33]	80.08	2.02	11	81.13	1.63	10	6.1%	−1.05 [−2.61, −0.51]
Zhu et al. 2007 [34]	79.19	1.13	8	79.79	0.91	8	10.4%	−0.60 [−1.61, −0.41]
Subtotal [95% CI]			68			68	99.7%	−0.92 [−1.10, −0.75]
Heterogeneity: Chi² = 3.96; df = 7 ($P = 0.78$); $I^2 = 0\%$								
Test for overall effect: $Z = 10.21$ ($P < 0.00001$)								
1.2.2 cerebral ischemic injury - brain water content 2								
Tian 2013 [27] a	7.91	3.01	8	17.21	5.15	8	0.2%	−9.30 [−13.43, −5.17]
Tian 2013 [27] b	8.36	3.77	8	17.21	5.15	8	0.2%	−8.85 [−13.27, −4.43]
Subtotal (95% CI)			16			16	0.3%	−9.09 [−12.11, −6.07]
Heterogeneity: Chi² = 0.02; df = 1 ($P = 0.88$); $I^2 = 0\%$								
Test for overall effect: $Z = 5.90$ ($P < 0.00001$)								
Total (95% CI)			84			84	100.0%	−0.95 [−1.13, −0.78]
Heterogeneity: Chi² = 31.97, df = 9 ($P = 0.0002$); $I^2 = 72\%$								
Test for overall effect: $Z = 4.25$ ($P < 0.00001$)								
Test for subgroup difference: Chi² =27.99. df = 1 ($P < 0.00001$), $I^2 = 96.4\%$								

Mean difference IV, fixed, 95% CI

−10 −5 0 5 10
Favours [borneol] Favours [control]

Figure 4: The forest plots: the borneol group versus the control group on brain water content under pathological conditions.

Study or subgroup	Borneol Mean	Borneol SD	Borneol Total	Control Mean	Control SD	Control Total	Weight	Mean difference IV, fixed, 95% CI
Chen et al. 2010 [20]	375.31	30.11	6	344.04	17.83	6	1.6%	31.27 [3.27, 59,27]
Wang 2011 [29]	122.89	2.34	7	107.63	4.96	8	86.5%	15.26 [11,41, 19.11]
Zhang et al. 2011 [33]	105.45	14.58	11	98.68	9.84	11	11.9%	6.77 [−3.62, 17.16]
Total (95% CI)			24			25	100.0%	14.51 [10.93, 18.09]

Heterogeneity: Chi² = 3.65, df = 2 ($P = 0.16$); $I^2 = 45\%$
Test for overall effect: $Z = 7.95$ ($P < 0.00001$)

Mean difference IV, fixed, 95% CI

−100 −50 0 50 100
Favours [control] Favours [borneol]

Figure 5: The forest plots: the borneol group versus the control group on SOD activity under pathological conditions.

of lipophilic potential neurotoxins, protect the brain from most pathogens, and selectively transport essential molecules, which is of great importance in the homeostatic regulation of the brain microenvironment. As common pathological processes in many serious CNS diseases, the BBB destruction and the increasing BBB permeability are especially essential

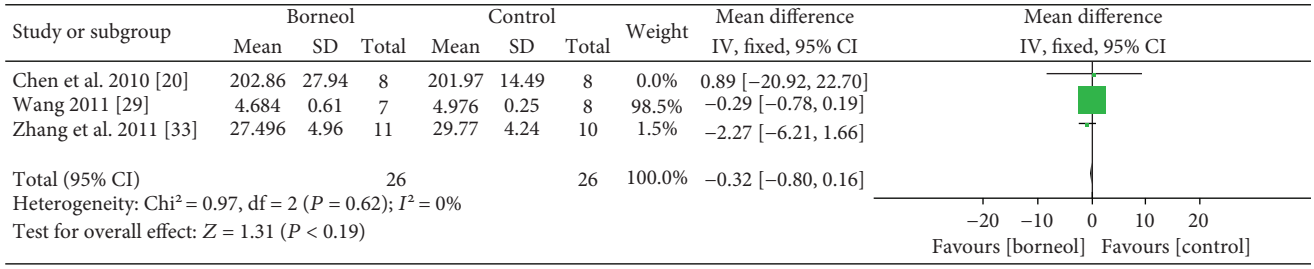

Figure 6: The forest plots: the borneol group versus the control group on MDA level under pathological conditions.

pathological bases of ischemic stroke. The present study demonstrated that the borneol could alleviate the increased BBB permeability by protecting the functions of endothelial cells and maintaining the integrity of the tight junction and basal lamina during cerebral ischemic injury, which exerts potential neuroprotective effect.

The possible neuroprotective mechanisms of borneol for ischemic stroke are summarized as follows: (1) BBB: borneol can alleviate the pathological BBB disruption through protecting the function of endothelial cells, maintaining the integrity of the basal lamina, and reducing the damage of tight junction integrity [23, 24, 26, 27, 30]. (2) Oxidative reactions: borneol can reduce oxidative reactions and the neurotoxicity of free radicals through increasing the activity of SOD and decreasing the concentration of MDA [29, 33]. SOD is a potent natural antioxidant enzyme that plays a bioprotective role by alternately catalyzing the dismutation or partitioning of the superoxide (O_2-) radical into either ordinary molecular oxygen (O_2) or hydrogen peroxide (H_2O_2), which is a prominent antioxidant defense in nearly all living cells exposed to oxygen [39]. As part of the brain ischemic antioxidant defense, an increase of SOD activities can ameliorate the oxidative stress damages [40]. MDA is a main product of lipid peroxidation of polyunsaturated fatty acids [41]. MDA can be overproduced, resulting from an increase in free radicals [42]. Thus, MDA is commonly used as a biomarker to measure the level of oxidative stress [43, 44]. Oxidative stress, including lipid peroxidation, plays an important role in the pathogenesis of acute brain injury and the breakdown of BBB [45]. Lipid peroxidation, mediated by superoxide, could cause alterations of membrane permeability as well as structural and functional impairment of cellular components. Free radicals are generally generated in the ischemic areas during ischemic stroke, leading to neuronal damage by promoting lipid peroxidation, protein breakdown, and DNA damage, which in turn results in cellular apoptosis and BBB permeability [46]. The pooled data showed that borneol significantly increases the activity of SOD and decreases the concentration of MDA which reduced the neurotoxicity of free radicals. (3) Anti-inflammation: borneol can exert anti-inflammation effects by decreasing the expression of proinflammatory cytokine TNF-α [21, 28]. Inflammation has been well recognized as a predominate contributor in ischemic stroke, playing an important role in all stages of the ischemic cascade [47, 48]. After ischemia, proinflammatory cytokines, such as TNF-α, were released, which resulted in BBB breakdown and neuronal death [21]. TNF-α, as a key proinflammatory mediator, plays a critical role in inflammatory responses. The present study indicated that borneol may be a potential anti-inflammatory drug, particularly in respect to cytokine suppression, resulting from the decreased expression of TNF-α induced by ischemic stroke. (4) Antiapoptosis: apoptosis is essential in the pathogenesis of acute and chronic neurodegenerative diseases, such as ischemic stroke, which can cause neuronal death and irreversible cerebral dysfunction [49]. It was found that inhibition of apoptosis could alleviate ischemic injury [50, 51]. The expression of Bcl-2 family plays a predominate role in apoptosis, which could either promote (Bax, Bak, Bad, Bim, and Bid) or prevent (Bcl-2, Bcl-XL, and Bcl-w) apoptosis [52, 53]. The present study revealed that borneol had antiapoptosis effects by decreasing the mRNA expression of Bax [22], increasing the mRNA expression of Bcl-XL [22] and modulating the Bax/Bcl-2 expression at both the mRNA and protein levels [21]. (5) LDH: LDH is an enzyme that is widely distributed in the cytoplasm of neurons and glial cells. LDH is abundant in the brain under physiological condition, which would release into the blood and consequently increase the accumulation of lactic acid during cerebral ischemic injury. The accumulation of lactic acid can cause acidosis in ischemic injury, which increases free radicals and decreases the use of glucose in the brain, ultimately resulting in the oxidative stress and the decrease in ATP levels [29]. Borneol can improve the activity of LDH to inhibit an increase in lactic acid [29]. (6) Energy metabolism: ischemic stroke easily causes the energy metabolism disorder including mitochondria functional impairment and imbalance of ion homeostasis [54]. Borneol can improve the energy metabolism disorder through upregulating the activity of Na^+-K^+-ATPase [27, 29], Ca^{2+}-Mg^{2+}-ATPase [27], and T-ATPase [27]. (7) P-glycoprotein (P-GP): P-GP is an important protein of the cell membrane and more accurately an ATP-dependent efflux pump with broad substrate specificity. P-GP expressed in the capillary endothelial cells composes the BBB [55–57]. Borneol could decrease the expression of P-GP. (8) NO: excessive nitric oxide (NO) generated during the cerebral ischemic stroke may be combined with free radicals, which causes damage to lipid membranes, nucleic acids, and cell protein. Borneol exerts the neuroprotective effect via NO signaling pathway [27]. Borneol could decrease the expression of NO [27]. During cerebral ischemia and reperfusion, signaling cascades can be triggered by cross talk. As mentioned above, BBB disruption, oxidative stress, acidosis, the energy metabolism disorder, P-GP, and NO can affect each other and interact as both cause and effect. The present study showed the neuroprotective mechanism of

Table 3: Characteristics of mechanism studies of borneol on experimental ischemic stroke.

Study	Model	Method of administration (experimental group versus control group)	Possible mechanism
Dong et al. [21]	pMCAO in SD rats	(1) L-borneol versus 5% Tween 80 (2) D-borneol versus 5% Tween 80 (3) Synthetic borneol versus 5% Tween 80	(1) Alleviate the pathological BBB disruption by upregulating tight junction proteins Claudin-5 (2) Accelerate the proliferation of vascular endothelial cells and by initiating angiogenesis. (3) Anti-inflammation by decreasing the expression of TNF-α (4) Antiapoptosis by modulating the Bax/Bcl-2 expression at both the mRNA and protein levels
Fang et al. [22]	BCO/1 h in SD rats	Borneol versus normal saline	Antiapoptosis by decreasing the mRNA expression of Bax and increasing the mRNA expression of Bcl-XL
Huang et al. [23]	BCO/45 min in SD rats	Synthetic borneol versus distilled water	Alleviate the pathological BBB disruption by protecting the function of endothelial cells and maintaining the integrity of the basal lamina
Jia [24]	Occlusion of bilateral hemisphere (Pulsinelli-4VO method)/20 min in Wistar rats	D-borneol versus 70% ethanol	Alleviate the pathological BBB disruption by upregulating tight junction proteins ZO-1
Ni et al. [26]	MCAO/2 h in SD rats	Borneol versus 5% Tween	Alleviate the pathological BBB disruption by downregulating VEGF and MMP-9
Tian [27]	MCAO/2 h in SD rats	(1) L-borneol versus normal saline (2) Synthetic borneol versus normal saline	(1) Alleviate the pathological BBB disruption by alleviating the damage of the BBB tight junction integrity (2) Reduce oxidative reactions by increasing the activity of SOD and decreasing the concentration of MDA (3) Improve the energy metabolism disorder by upregulating the activity of Na^+-K^+-ATPase, Ca^{2+}-Mg^{2+}-ATPase, and T-ATPase (4) Neuroprotection via P-GP signaling pathway (5) Neuroprotection via NO signaling pathway
Shao et al. [28]	Permanent BCO in SD rats	Borneol versus normal saline	(1) Reduce oxidative reactions by increasing the activity of SOD (2) Anti-inflammation by decreasing the expression of TNF-α
Wang [29]	Permanent BCO in SD rats	Synthetic borneol versus 1% Tween	(1) Reduce oxidative reactions by increasing the activity of SOD and decreasing the concentration of MDA (2) Improve the activity of LDH (3) Improve the energy metabolism disorder by upregulating the activity of Na^+-K^+-ATPase

Table 3: Continued.

Study	Model	Method of administration (experimental group versus control group)	Possible mechanism
Xu and Zhang [30]	MCAO/2 h in SD rats	Borneol versus normal saline	Alleviate the pathological BBB disruption by upregulating tight junction proteins ZO-1 and claudin-5
Zhang et al. [33]	BCO/20 min in ICR mice	Borneol versus 1% Tween	Reduce oxidative reactions by increasing the activity of SOD and decreasing the concentration of MDA

Note: BCO, bilateral carotid occlusion; MCAO, middle cerebral artery occlusion; pMCAO, permanent middle cerebral artery occlusion; LDH, lactate dehydrogenase; ZO-1, Zonula occludens-1; VEGF, vascular endothelial cell growth factor; MMP-9matrix metalloproteinase-9; P-GP, P-glycoprotein.

borneol in the treatment of cerebral ischemic injury was mainly attributed to the decrease of BBB permeability. However, cellular and molecular alteration mechanisms of borneol for ischemic stroke have not been clearly elucidated yet, which presented an exciting investigative direction of further research in this field. In addition, the administration of borneol could expand to other diseases with similar pathologies, namely, the increased BBB permeability, which was associated with the development and progression of many CNS diseases, such as multiple sclerosis, Alzheimer's disease, and HIV-associated dementia.

Infarct volume (IV) is a common index for assessing the extent of cerebral ischemic injury. Infarct on imaging is one of the common identified predictors of clinical outcome for ischemic stroke [58]. In addition, IV measurement is clinically helpful in the accurate selection of patients for decompressive surgery and the determination of the time of surgery [59]. Therefore, it is essential for further experimental trails of borneol for ischemic stroke to choose IV as outcome measures.

The methodological quality of the included studies was moderate. In particular, no study estimated the sample size, since inadequate sample size can miss the real intervention effect in an experiment or excessive sample size can result in wasting animals and raising animal ethical issues [60]. No study blindingly assessed outcome, which could attribute to a 27% overestimation of the mean reported effect size [61]. No study used animals with relevant comorbidities, which was rarely like human pathology under the clinical conditions [18]. Thus, it is necessary for further research of borneol for ischemic stroke to take a rigor experimental design into consideration. We recommended that the Animal Research: Reporting of In Vivo Experiments (ARRIVE) [62], a reporting guideline consisting of a 20-item checklist for the introduction, methods, results, and discussion, should be used as guidelines for the design and reporting of further experimental research examining borneol for ischemic stroke, which can extremely help improve the methodological quality.

5. Conclusion

Borneol can alleviate the BBB disruption and plays a protective role on cerebral ischemic injury through multiple signaling pathways. Further relevant molecular mechanisms deserve adequate research.

Conflicts of Interest

The authors declare that there is no conflict of interests regarding the publication of this paper.

Authors' Contributions

ZXC, QQX, CSS, YHS, YW, RCCC, and GQZ designed the study. ZXC, QQX, CSS, YHS, and YW collected the data. ZXC, QQX, CSS, YHS, and YW performed all analyses. ZXC, QQX, and GQZ wrote the manuscript. All authors contributed to writing of this manuscript. Zi-xian Chen and Qing-qing Xu contributed equally to this work.

Acknowledgments

This work was supported by the grant of the National Natural Science Foundation of China (81573750, 81473491, 81173395); the Young and Middle-Aged University Discipline Leaders of Zhejiang Province, China (2013277); and the Zhejiang Provincial Program for the Cultivation of High-level Health Talents (2015).

References

[1] R. Khatri, A. M. McKinney, B. Swenson, and V. Janardhan, "Blood-brain barrier, reperfusion injury, and hemorrhagic transformation in acute ischemic stroke," *Neurology*, vol. 79, 13, Supplement 1, pp. S52–S57, 2012.

[2] R. Daneman and A. Prat, "The blood-brain barrier," *Cold Spring Harbor Perspectives in Biology*, vol. 7, no. 1, article a020412, 2015.

[3] Z. Zhao, A. R. Nelson, C. Betsholtz, and B. V. Zlokovic, "Establishment and dysfunction of the blood-brain barrier," *Cell*, vol. 163, no. 5, pp. 1064–1078, 2015.

[4] G. A. Rosenberg, "Neurological diseases in relation to the blood-brain barrier," *Journal of Cerebral Blood Flow and Metabolism*, vol. 32, no. 7, pp. 1139–1151, 2012.

[5] Y. Shi, R. K. Leak, R. F. Keep, and J. Chen, "Translational stroke research on blood-brain barrier damage: challenges, perspectives, and goals," *Translational Stroke Research*, vol. 7, no. 2, pp. 89–92, 2016.

[6] X. Jiang, A. V. Andjelkovic, L. Zhu et al., "Blood-brain barrier dysfunction and recovery after ischemic stroke," *Progress in Neurobiology*, vol. 163-164, pp. 144–171, 2018.

[7] F. Ju, Y. Ran, L. Zhu et al., "Increased BBB permeability enhances activation of microglia and exacerbates loss of dendritic spines after transient global cerebral ischemia," *Frontiers in Cellular Neuroscience*, vol. 12, p. 236, 2018.

[8] Y. Yang and G. A. Rosenberg, "Blood–brain barrier breakdown in acute and chronic cerebrovascular disease," *Stroke*, vol. 42, no. 11, pp. 3323–3328, 2011.

[9] M. Krueger, I. Bechmann, K. Immig, A. Reichenbach, W. Härtig, and D. Michalski, "Blood—brain barrier breakdown involves four distinct stages of vascular damage in various models of experimental focal cerebral ischemia," *Journal of Cerebral Blood Flow and Metabolism*, vol. 35, no. 2, pp. 292–303, 2015.

[10] R. Prakash and S. T. Carmichael, "Blood-brain barrier breakdown and neovascularization processes after stroke and traumatic brain injury," *Current Opinion in Neurology*, vol. 28, no. 6, pp. 556–564, 2015.

[11] M. Krueger, W. Härtig, C. Frydrychowicz et al., "Stroke-induced blood-brain barrier breakdown along the vascular tree - no preferential affection of arteries in different animal models and in humans," *Journal of Cerebral Blood Flow and Metabolism*, vol. 37, no. 7, pp. 2539–2554, 2017.

[12] State Pharmacopoeia Committee, *The Pharmacopoeia of People's Republic of China*, Chemical Industry Press, Beijing, 2010.

[13] Y. Guo, S. Yan, L. Xu, G. Zhu, X. Yu, and X. Tong, "Use of Angong Niuhuang in treating central nervous system diseases and related research," *Evidence-based Complementary and Alternative Medicine*, vol. 2014, Article ID 346918, 9 pages, 2014.

[14] M. Takaishi, K. Uchida, F. Fujita, and M. Tominaga, "Inhibitory effects of monoterpenes on human TRPA1 and the structural basis of their activity," *The Journal of Physiological Sciences*, vol. 64, no. 1, pp. 47–57, 2014.

[15] H. Y. Wu, Y. Tang, L. Y. Gao et al., "The synergetic effect of edaravone and borneol in the rat model of ischemic stroke," *European Journal of Pharmacology*, vol. 740, pp. 522–531, 2014.

[16] R. Liu, L. Zhang, X. Lan et al., "Protection by borneol on cortical neurons against oxygen-glucose deprivation/reperfusion: involvement of anti-oxidation and anti-inflammation through nuclear transcription factor κappaB signaling pathway," *Neuroscience*, vol. 176, pp. 408–419, 2011.

[17] R. Tambe, P. Jain, S. Patil, P. Ghumatkar, and S. Sathaye, "Antiepileptogenic effects of borneol in pentylenetetrazole-induced kindling in mice," *Naunyn-Schmiedeberg's Archives of Pharmacology*, vol. 389, no. 5, pp. 467–475, 2016.

[18] S. C. Landis, S. G. Amara, K. Asadullah et al., "A call for transparent reporting to optimize the predictive value of preclinical research," *Nature*, vol. 490, no. 7419, pp. 187–191, 2012.

[19] M. R. Macleod, T. O'Collins, D. W. Howells, and G. A. Donnan, "Pooling of animal experimental data reveals influence of study design and publication bias," *Stroke*, vol. 35, no. 5, pp. 1203–1208, 2004.

[20] X. H. Chen, Z. Z. Lin, A. M. Liu et al., "The orally combined neuroprotective effects of sodium ferulate and borneol against transient global ischaemia in C57 BL/6J mice," *Journal of Pharmacy and Pharmacology*, vol. 62, no. 7, pp. 915–923, 2010.

[21] T. Dong, N. Chen, X. Ma et al., "The protective roles of L-borneolum, D-borneolum and synthetic borneol in cerebral ischaemia via modulation of the neurovascular unit," *Biomedicine & Pharmacotherapy*, vol. 102, pp. 874–883, 2018.

[22] Y. Q. Fang, L. Li, Q. D. Wu, Y. Y. Zhou, G. Wei, and S. F. Lin, "Protective effects of β-asarone and borneol in rat model of cerebral ischemia with reperfusion," *Zhongguo Zhong Yi Yao Ke Ji*, vol. 11, no. 6, pp. 353-354, 2004.

[23] P. Huang, Q. Wu, X. Rong et al., "Protective effects of Borneolum combined with rhizoma chuanxiong on cerebral ischemia with reperfusion injury," *Journal of Guangzhou University Traditional Chinese Medicine*, vol. 17, no. 4, pp. 323–326, 2000.

[24] Y. L. Jia, "Effects of borneol on rat's blood brain barrier and zonula occludens-1 after global cerebral ischemia-reperfusion injury, MD dissertation," Xinxiang Medical University, 2014.

[25] Y. M. Liu, X. H. Xia, G. F. Zhao, S. Q. Peng, Q. Y. Xu, and Q. Shen, "Effect of Moschus combined with borneol on brain water content and blood-brain barrier permeability in rat model of cerebral focal ischemia with reperfusion," *Journal of Guangzhou University Traditional Chinese Medicine*, vol. 24, no. 6, pp. 498–501, 2007.

[26] C. Ni, N. Zeng, F. Xu et al., "Effects of aromatic resuscitation drugs on blood brain barrier in cerebral ischemia-reperfusion injury model rats," *Zhongguo Zhong Yao Za Zhi*, vol. 36, no. 18, pp. 2562–2566, 2011.

[27] H. Tian, "Comparative research on mechanism of neuroprotective effect and influence of blood-brain barrier between L-borneolum and borneolum syntheticum, PhD dissertation," Chengdu University of TCM, Sichuan (Chengdu), 2013.

[28] X. R. Shao, K. R. Cai, R. Jia et al., "Effects of borneol on inflammatory reaction and permeability of blood-brain barrier in rats with cerebral ischemic injury," *The Chinese Journal of Clinical Pharmacology*, vol. 34, no. 13, pp. 1558–1560, 2018.

[29] Y. Wang, "The effect of musk, borneol and compatibility of them on the animal models of cerebral isehemia, MD dissertation," Chengdu University of Traditional Chinese Medicine, Sichuan (Chengdu), 2011.

[30] L. Xu and T. J. Zhang, "Effects of borneol combined with breviscapine on blood-brain barrier permeability after ischemia reperfusion injury in rats," *Pharmacology & Clinics of Chinese Materia Medica*, vol. 31, no. 1, pp. 74–76, 2015.

[31] H. W. Yao, J. Wang, Y. Liu, and D. D. Wang, "Effect of Moschus and Borneo camphor in different proportion on blood brain barrier permeability of acute cerebral ischemic model mice," *Journal of Chengdu University of Traditional Chinese Medicine*, vol. 34, no. 4, pp. 62–64, 2011.

[32] X. S. Zhang, E. H. Zhang, X. Shen, and J. R. Chen, "The protective effects of compatibility of dioscin and borneol on the focal cerebral ischemia in rats," *Chinese Journal of Experimental Traditional Medical Formulae*, vol. 17, no. 24, pp. 151–153, 2011.

[33] X. S. Zhang, E. H. Zhang, G. K. Gao, and Y. Q. Ren, "The effect of the compatibility of dioscin and camphol on cerebral ischemia-reperfusion injury in mice," *Western Journal of Traditional Chinese Medicine*, vol. 24, no. 12, pp. 11–13, 2011.

[34] J. R. Zhu, Y. M. Li, W. R. Fang, and S. X. Liu, "Protective effects of scutellarin and borneolum injection on experimental cerebral ischemia in animals," *Journal of China Pharmaceutical University*, vol. 38, no. 35, pp. 456–460, 2007.

[35] A. Armulik, G. Genové, M. Mäe et al., "Pericytes regulate the blood-brain barrier," *Nature*, vol. 468, no. 7323, pp. 557–561, 2010.

[36] R. Daneman, "The blood-brain barrier in health and disease," *Annals of Neurology*, vol. 72, no. 5, pp. 648–672, 2012.

[37] J. Sargento-Freitas, S. Aday, C. Nunes et al., "Endothelial progenitor cells enhance blood-brain barrier permeability in subacute stroke," *Neurology*, vol. 90, no. 2, pp. e127–e134, 2018.

[38] F. Arba, R. Leigh, D. Inzitari et al., "Blood–brain barrier leakage increases with small vessel disease in acute ischemic stroke," *Neurology*, vol. 89, no. 21, pp. 2143–2150, 2017.

[39] J. Azadmanesh and G. E. O. Borgstahl, "A review of the catalytic mechanism of human manganese superoxide dismutase," *Antioxidants*, vol. 7, no. 2, p. 25, 2018.

[40] S. Manzanero, T. Santro, and T. V. Arumugam, "Neuronal oxidative stress in acute ischemic stroke: sources and contribution to cell injury," *Neurochemistry International*, vol. 62, no. 5, pp. 712–718, 2013.

[41] A. Ayala, M. F. Muñoz, and S. Argüelles, "Lipid peroxidation: production, metabolism, and signaling mechanisms of malondialdehyde and 4-hydroxy-2-nonenal," *Oxidative Medicine and Cellular Longevity*, vol. 2014, Article ID 360438, 31 pages, 2014.

[42] I. M. Cojocaru, M. Cojocaru, V. Sapira, and A. Ionescu, "Evaluation of oxidative stress in patients with acute ischemic stroke," *Romanian Journal of Internal Medicine*, vol. 51, no. 2, pp. 97–106, 2013.

[43] D. Tsikas, "Assessment of lipid peroxidation by measuring malondialdehyde (MDA) and relatives in biological samples: analytical and biological challenges," *Analytical Biochemistry*, vol. 524, pp. 13–30, 2017.

[44] S. Jiménez-Fernández, M. Gurpegui, F. Díaz-Atienza, L. Pérez-Costillas, M. Gerstenberg, and C. U. Correll, "Oxidative stress and antioxidant parameters in patients with major depressive disorder compared to healthy controls before and after antidepressant treatment: results from a meta-analysis," *Journal of Clinical Psychiatry*, vol. 76, no. 12, pp. 1658–1667, 2015.

[45] P. T. Ronaldson and T. P. Davis, "Targeting transporters: promoting blood-brain barrier repair in response to oxidative stress injury," *Brain Research*, vol. 1623, pp. 39–52, 2015.

[46] S. Milanizadeh, K. N. N. Zuwarali, A. Aliaghaei, and M. R. Bigdeli, "Therapeutic potential of pretreatment with allograft Sertoli cells transplantation in brain ischemia by improving oxidative defenses," *Journal of Molecular Neuroscience*, vol. 64, no. 4, pp. 533–542, 2018.

[47] M. Gelderblom, M. Gallizioli, P. Ludewig et al., "IL-23 (interleukin-23)-producing conventional dendritic cells control the detrimental IL-17 (interleukin-17) response in stroke," *Stroke*, vol. 49, no. 1, pp. 155–164, 2018.

[48] C. Iadecola and J. Anrather, "The immunology of stroke: from mechanisms to translation," *Nature Medicine*, vol. 17, no. 7, pp. 796–808, 2011.

[49] S. E. Khoshnam, W. Winlow, M. Farzaneh, Y. Farbood, and H. F. Moghaddam, "Pathogenic mechanisms following ischemic stroke," *Neurological Sciences*, vol. 38, no. 7, pp. 1167–1186, 2017.

[50] D. Radak, N. Katsiki, I. Resanovic et al., "Apoptosis and acute brain ischemia in ischemic stroke," *Current Vascular Pharmacology*, vol. 15, no. 2, pp. 115–122, 2017.

[51] N. Wei, L. Xiao, R. Xue et al., "MicroRNA-9 mediates the cell apoptosis by targeting Bcl2l11 in ischemic stroke," *Molecular Neurobiology*, vol. 53, no. 10, pp. 6809–6817, 2016.

[52] P. E. Czabotar, G. Lessene, A. Strasser, and J. M. Adams, "Control of apoptosis by the BCL-2 protein family: implications for physiology and therapy," *Nature Reviews Molecular Cell Biology*, vol. 15, no. 1, pp. 49–63, 2014.

[53] X. Chen, M. Lu, X. He, L. Ma, L. Birnbaumer, and Y. Liao, "TRPC3/6/7 knockdown protects the brain from cerebral ischemia injury via astrocyte apoptosis inhibition and effects on NF-κB translocation," *Molecular Neurobiology*, vol. 54, no. 10, pp. 7555–7566, 2017.

[54] J. P. Zöllner, E. Hattingen, O. C. Singer, and U. Pilatus, "Changes of pH and energy state in subacute human ischemia assessed by multinuclear magnetic resonance spectroscopy," *Stroke*, vol. 46, no. 2, pp. 441–446, 2015.

[55] W. Fang, P. Lv, X. Geng et al., "Penetration of verapamil across blood brain barrier following cerebral ischemia depending on both paracellular pathway and P-glycoprotein transportation," *Neurochemistry International*, vol. 62, no. 1, pp. 23–30, 2013.

[56] W. Abdullahi, T. P. Davis, and P. T. Ronaldson, "Functional expression of P-glycoprotein and organic anion transporting polypeptides at the blood-brain barrier: understanding transport mechanisms for improved CNS drug delivery?," *The AAPS Journal*, vol. 19, no. 4, pp. 931–939, 2017.

[57] Y. Hoshi, Y. Uchida, M. Tachikawa, S. Ohtsuki, and T. Terasaki, "Actin filament-associated protein 1 (AFAP-1) is a key mediator in inflammatory signaling-induced rapid attenuation of intrinsic P-gp function in human brain capillary endothelial cells," *Journal of Neurochemistry*, vol. 141, no. 2, pp. 247–262, 2017.

[58] W. J. Powers, A. A. Rabinstein, T. Ackerson et al., "2018 guidelines for the early management of patients with acute ischemic stroke: a guideline for healthcare professionals from the American Heart Association/American Stroke Association," *Stroke*, vol. 49, no. 3, pp. e46–e110, 2018.

[59] S. Kamran, N. Akhtar, A. Alboudi et al., "Prediction of infarction volume and infarction growth rate in acute ischemic stroke," *Scientific Reports*, vol. 7, no. 1, article 7565, 2017.

[60] W. N. Arifin and W. M. Zahiruddin, "Sample size calculation in animal studies using resource equation approach," *Malaysian Journal of Medical Sciences*, vol. 24, no. 5, pp. 101–105, 2017.

[61] L. Holman, M. L. Head, R. Lanfear, and M. D. Jennions, "Evidence of experimental bias in the life sciences: why we need blind data recording," *PLoS Biology*, vol. 13, no. 7, article e1002190, 2015.

[62] C. Kilkenny, W. J. Browne, I. C. Cuthill, M. Emerson, and D. G. Altman, "Improving bioscience research reporting: the ARRIVE guidelines for reporting animal research," *Osteoarthritis and Cartilage*, vol. 20, no. 4, pp. 256–260, 2012.

Hindawi
Oxidative Medicine and Cellular Longevity
Volume 2018, Article ID 7912765, 21 pages
https://doi.org/10.1155/2018/7912765

Research Article

Computational Studies Applied to Flavonoids against Alzheimer's and Parkinson's Diseases

Alex France M. Monteiro,[1] Jéssika De O. Viana,[1] Anuraj Nayarisseri,[2,3] Ernestine N. Zondegoumba,[4] Francisco Jaime B. Mendonça Junior,[5] Marcus Tullius Scotti,[1] and Luciana Scotti[1,6]

[1]*Postgraduate Program in Natural and Synthetic Bioactive Products, Federal University of Paraíba, João Pessoa, PB, Brazil*
[2]*In Silico Research Laboratory, Eminent Bioscience, Inodre - 452010, Madhya Pradesh, India*
[3]*Bioinformatics Research Laboratory, LeGene Biosciences, Indore - 452010, Madhya Pradesh, India*
[4]*Department of Organic Chemistry, Faculty of Science, University of Yaounde I, PO Box 812, Yaoundé, Cameroon*
[5]*Laboratory of Synthesis and Drug Delivery, Department of Biological Science, State University of Paraiba, João Pessoa, PB, Brazil*
[6]*Teaching and Research Management-University Hospital, Federal University of Paraíba, João Pessoa, PB, Brazil*

Correspondence should be addressed to Luciana Scotti; luciana.scotti@gmail.com

Received 5 October 2018; Revised 12 November 2018; Accepted 14 November 2018; Published 30 December 2018

Academic Editor: Alin Ciobica

Neurodegenerative diseases, such as Parkinson's and Alzheimer's, are understood as occurring through genetic, cellular, and multifactor pathophysiological mechanisms. Several natural products such as flavonoids have been reported in the literature for having the capacity to cross the blood-brain barrier and slow the progression of such diseases. The present article reports on *in silico* enzymatic target studies and natural products as inhibitors for the treatment of Parkinson's and Alzheimer's diseases. In this study we evaluated 39 flavonoids using prediction of molecular properties and *in silico* docking studies, while comparing against 7 standard reference compounds: 4 for Parkinson's and 3 for Alzheimer's. Osiris analysis revealed that most of the flavonoids presented no toxicity and good absorption parameters. The Parkinson's docking results using selected flavonoids as compared to the standards with four proteins revealed similar binding energies, indicating that the compounds 8-prenylnaringenin, europinidin, epicatechin gallate, homoeriodictyol, capensinidin, and rosinidin are potential leads with the necessary pharmacological and structural properties to be drug candidates. The Alzheimer's docking results suggested that seven of the 39 flavonoids studied, being those with the best molecular docking results, presenting no toxicity risks, and having good absorption rates (8-prenylnaringenin, europinidin, epicatechin gallate, homoeriodictyol, aspalathin, butin, and norartocarpetin) for the targets analyzed, are the flavonoids which possess the most adequate pharmacological profiles.

1. Introduction

Neurodegenerative diseases (NDDs) arise as a progressive loss of neuron structure and function, resulting in muscle weakness and deterioration of the body's physiological functions [1, 2]. During this process, postmitotic cells undergo cell death, leading to cellular apoptosis signaling and further oxidative stress [3]. In addition to neuronal loss, other pathological genetic, biochemical, and molecular factors affect the progression of the disease. Recent studies have demonstrated the presence of proteins in the brains of the affected (involved in the process of NDDs), with modified physicochemical properties [4]. NDDs include Alzheimer's disease (AD), Parkinson's disease (PD), Huntington disease (HD), schizophrenia, amyotrophic lateral sclerosis (ALS), seizure disorders, and head injuries along with other systemic disorders [5].

Phytochemicals are a diversified group of naturally occurring bioactive compounds in plants; they include flavonoids, alkaloids, terpenoids, lignans, and phenols. Since they have a wide range of chemical, biochemical, and molecular

characteristics, phytochemicals are of considerable interest for treating NDDs. Phytochemicals are promising candidates for various pathological conditions involving modulation of multiple signal pathways and serving as antioxidant and anti-inflammatory agents [6], agents against cancer and neurodegenerative diseases [7–9], or as antifungal agents [10]. Several studies have addressed the protective activity of natural derivatives such as alkaloids when applied to neurodegenerative diseases such as Alzheimer's and Parkinson's [11]; genistein brings neuroprotective effects [12, 13]; hesperetin presents potent antioxidant and neuroprotective effects [14]; quercetin [15] and xanthones present multifunctional activities against Alzheimer's disease [16].

Flavonoids fit the NDDs profile, and in a process dependent on the suppression of lipid peroxidation, inhibition of inflammatory mediators, modulation of gene expression, and activation of antioxidant enzymes, flavonoids help maintain the endogenous antioxidant status of neurons, protecting them from neurodegeneration [17, 18]. Based on their chemical structure, they are classified into several categories including flavanols, flavonols, flavones, flavanones, isoflavones, anthocyanidins, and chalcones [19].

This article focuses on flavonoids found in the literature for anti-Parkinson and anti-Alzheimer activity, including targets involved in the degenerative process of each disease. Molecular docking studies detail the structural parameters involved that best contribute to the activity of such compounds. This study facilitates knowledge as applied to two NDDs concerning flavonoid structural enhancements and the pharmacophores involved in the receptor-protein complex.

2. Parkinson's Disease

Parkinson's disease (PD) is the second most common neurodegenerative disease globally and has been increasing considerably without evidence of cure [20, 21]. PD is reported as a loss of dopaminergic neurons located in the substantia nigra (SN) and affects 1-2% of people over the age of 60 [22]. Estimates of the disease range from 5 to 35 new cases per 100,000 individuals [23]; this increases with age [24]. The prevalence of PD is increasing considerably, corroborating a doubling by the year 2030 [25].

To characterize PD, progressive degeneration of dopaminergic (DA) neurons causing depletion of striatal dopamine and formation of Lewy bodies in the substantia nigra (SN) are the principal neuropathological correlations of motor damage in PD. The symptoms include resting tremor, rigidity, bradykinesia, gait difficulty, postural instability, and behavioral problems [26]; nonmotor symptoms include depression, anxiety, emotional changes, cognitive impairment, sleep difficulty, and olfactory dysfunction [27]. There are several studies that report neurodegenerative factors such as neuroinflammation [28] and cytotoxic factors such as IL1, NO, ROS, and TNF [29].

The treatment of PD focuses on carbidopa to replace dopamine, levodopa drugs, monoamine oxidase B inhibitors, dopamine agonists, catechol-o-methyltransferase inhibitors, anticholinergics, and amantadine [30]. Levodopa is the single most used drug to treat Parkinson's disease [31]. However, these drugs cause many side effects [32], and they usually lead to other complications, yet without curing or stopping disease progression. The search for new therapeutic agents with few side effects is essential.

The use of natural products against PD has intensified in recent years, chiefly compounds derived from plants, since they are known to have fewer side effects than synthetic compounds [33, 34]. These advances in the treatment of PD give the disease a chance to be administered effectively, leading to symptom control and improvement of patient quality of life, often for decades after onset of the disease.

2.1. Molecular Docking Applied to Natural Products for Parkinson's Disease. Molecular docking studies are based on joining a particular ligand to a receptor region, providing information about conformation, orientation, and organization at the receptor site [35]. Studies using computational chemistry to predict potential inhibitors for neurodegenerative diseases have been reported in the literature [36–38], and studies involving molecular docking have been reported in the literature for Parkinson's disease and flavonoid derivatives [39].

Desideri et al. [40] reported the *in vitro* and *in silico* activity of a series of homo-isoflavonoids as potent inhibitors of human monoamine oxidase-B. Presenting better *in vitro* results than the standard drug, selegiline, (E)-3-(4-(Dimethylamino)benzylidene)chroman-4-one and (E)-5,7-dihydroxy-3-(4-hydroxybenzylidene)chroman-4-one also demonstrated selectivity and high potency during the *in silico* studies, interacting with hydrogen and hydrophobic bonds at the active site.

Our research group applied ligand-based-virtual screening together with structure based-virtual screening (docking) for 469 alkaloids of the Apocynaceae family in a study of human AChE inhibitory activity [41]. As a result, 9 alkaloids presenting better inhibition profiles for both Parkinson's and Alzheimer's (dihydro-cylindrocarpine, 14,19-dihydro-11-methoxycondylocarpine, Di (demethoxycarbonyl) tetrahydrosecamine, tetrahydrosecamine, 16-demethoxycarbonyltetrahydrosecamine, 16-hydroxytetrahydrosecamine, usambarensine, 4′,5′,6′,17-tetrahydro-usambarensine-N-oxide, and 6,7-seco-angustilobine) were selected for future studies.

Baul and Rajiniraja [42] performed a molecular docking study using flavonoids such as quercetin, epigallocatechin gallate (EGCG), and acacetin to predict inhibitory activities and their ability to inhibit the enzyme α-synuclein. The results showed that the flavonoids present low energy value interactions with residues Lys45, Lys43, Lys32, and Val40, being essential for activity in this protein.

In silico studies involving Parkinson's disease anti-inflammatory activity have also been targeted for novel bioactive compounds. As a general rule for anti-inflammatory activity, both hydrogen and π-π hydrophobic interactions between the active site of the macromolecule and the compounds are essential. Madeswaran et al. [43] reported the inhibition activity of nine flavonoids (morin, naringenin, taxifolin, esculatin, daidzein, genistein, scopoletin, galangin, and silbinin) against human lipoxygenase enzyme. The flavonoid interactions especially those of morin were similar to

Azelastine, a flavonoid already reported in the literature for lipoxygenase inhibition activity, thus defining amino acids Tyr359, Gln358, and Gln539 as critical to the activity of these compounds.

2.2. Targets in Parkinson's Disease

2.2.1. Adenosine A_{2A} Receptors. Adenosine receptors are members of the G protein-coupled receptor superfamily and considered potential targets for treatment of numerous diseases. Adenosine binds four types of G-protein receptors known as A_1, A_{2A}, A_{2B}, and A_3 all with distribution in the brain. A_{2A} has a more specific and abundant distribution in the basal ganglia. This selective distribution for receptors can help guarantee fewer adverse effects and make nondopaminergic antagonists more promising for the treatment of PD [44].

The A_{2A} adenosine receptor (A_{2A}AR) is highly expressed in the basal ganglia and depends on Gs and other protein interactions for signal interpretation [45]. In mammals, high expression of this protein is found in the striatum in the basal ganglia, with an important route for the regulation of dopaminergic transmission [46]. The A_{2A} receptor subtype presents signaling involving activation of serine/threonine kinase [47, 48], which modulates phosphorylation of ionotropic glutamate receptors [49, 50]. The A_{2A} receptor may provide improvement in motor abnormalities for patients with PD, by controlling hyperphosphorylation of the glutamatergic receptor.

Indeed, five A_{2A} receptor antagonists are now in clinical trials (phases I to III) for Parkinson's disease, and other antagonists have been reported in the literature [51]. The use of these receptors is due to various preclinical studies which have shown that adenosinergic neuromodulation antagonizes dopaminergic neurotransmission in aspects relevant to motor control. The adenosine A_{2A} receptor activates adenylyl cyclase and certain voltage-sensitive Ca^{2+} channels [52]. These receptors are expressed in the GABAergic neurons and in glutamatergic neuronal terminals [53].

Schwarzschild et al. [54] proposed an anti-Parkinson activity reactive mechanism for the A_{2A} receptor. In the normal state, the dopamine of the neurons is found in the substantia nigra and acts on two receptors: D1 receptors (direct stimulatory pathway) and D2 receptors (indirect inhibitory pathway). Adenosine, which is released by A_{2A} receptors, stimulates neurons at the D2 receptor pathway. In degenerative processes, as is the case in PD, the central nervous system (CNS) degeneration blocks the entry of striatum dopamine, which increases GABA's inhibitory influence, consequently mitigating PD motor deficits.

The restriction of striatum region expression contributes to fewer side effects in PD patients [55–57]. Several studies have reported the activity of nondopaminergic A_{2A} receptor antagonists [58, 59], a good target for the development of anti-Parkinson drugs.

2.2.2. α-Synuclein. A 140 amino acid protein, α-synuclein is commonly located in presynaptic terminals [60, 61]. Alpha-synuclein represents the most abundant protein in Lewy bodies (LB), cytoplasmic inclusions found in PD and in LB dementia (LBD), which have a little understood physiology. The synuclein family has three members, α-synuclein, β-synuclein, and γ-synuclein, ranging from 127 to 140 amino acids, with about 55 to 62% of homologous sequences, and where α and β have an identical carboxy-terminal domain. These proteins are commonly found in nerve terminals, close to synaptic vesicles; β-synucleins are present in almost all nerve cells [62].

Among the factors that influence α-synuclein abnormalities, genetic factors (protein gene, PARK3, and PARK4 locus mutations) and environmental factors (oxidative damages) often lead to errors in the ordering and conformation of α-synuclein filaments [63].

Recent studies report a mutation of alanine to threonine at position 53 of the protein gene causing a rare and familial form of PD in four families [64]. The identification of this mutation in autosomal dominant families of inherited Parkinson's led to the discovery of a new target for PD pathology.

Olanow and Brundin [65] provided evidence of α-synuclein activity in prion-like proteins acting in PD, thus suggesting new studies for the development of inhibitors. Recent studies have reported that a doubling or tripling of the α-synuclein gene leads to a similar type of PD [66, 67]. Mutagenic studies involved in the α-synuclein response associate and reinforce the hypothesis that mutations are involved in the pathogenesis of PD.

2.2.3. Catechol-O-Methyltransferase. The enzyme catechol-O-methyltransferase, also known as COMT, is as an important enzyme involved in biochemistry, pharmacology, and genetic mechanisms. Methylation of endogenous catecholamines, as well as other catechols, is catalyzed by the enzyme catechol-O-methyltransferase (COMT). COMT transfers the methyl group of S-adenosylmethionine (SAM) to the *meta-* or *para*-hydroxyl group present in catechols [68, 69]; COMT is considered a SAM-dependent methyltransferase [70]. COMT substrates involve both endogenous and exogenous catechols, such as dopamine, norepinephrine, and epinephrine. In the brain, COMT is involved in mental processes, as studies have reported for Parkinson's disease [71]. COMT is considered a target for study and development of new anti-Parkinson drugs using coadministration with levodopa [72, 73]. The enzyme has two forms: a soluble form, known as S-COMT, presenting 221 residues; and a second form, known as membrane based (MB-COMT), exhibiting 50 residues at the N-terminus [74]. The COMT active site has a SAM binding site and an S-COMT catalytic site. In addition, the presence of Mg^{2+} in the catalytic site is responsible for converting catechol hydroxyl groups to substrates [68].

The COMT enzyme has the single domain structure containing α and β moieties, where 8 helices are disposed around a central β sheet. The active site of the enzyme is composed of an S-adenosyl-L-methionine-(AdoMet-) binding domain, similar to a Rossmann fold, and present in numerous proteins that interact with nucleotides [68].

The catechol-O-methyltransferase (COMT) gene encodes an enzyme that performs catecholamine (such as dopamine, epinephrine, and norepinephrine) degradation [75]; this process is depressed in patients with PD. The COMT gene is located on chromosome 22q11, which has been reported as one of the major loci related to schizophrenia [76]. Recent studies have shown a polymorphism at codon 158 (Val158-Met, called rs4680) that influences the COMT enzyme, by decreasing its activity [77], and which interferes with executive cognitive performance [78, 79].

2.2.4. Monoamine Oxidase B. The enzyme monoamine oxidase B (MAO-B) has been reported as a therapeutic target for the treatment of Parkinson's disease [80, 81] and is also a brain glial biomarker [82]. Studies have shown that MAO is located in the outer mitochondrial membrane, in the liver, and in the brain [83] and presents FAD as a cofactor in its active site, where irreversible MAO inhibitors bind, such as rasagiline.

MAO's mechanism of reaction involves oxidative deamination of primary, secondary, and tertiary amines, to the corresponding aldehyde, and free amine with the generation of hydrogen peroxide. As for the aldehyde, this is metabolized by the enzyme aldehydedehydrogenase, producing acids such as 5-hydroxyindole acetic acid (5-HIAA) or dihydroxy-phenyl-acetic acid (DOPAC), metabolites used as MAO activity drugs. MAO also produces hydrogen peroxide, leading to oxidative stress and neuronal cell death [84, 85].

MAO can be found in two isoforms, known as isoform A and isoform B, with differences that are of great pharmacological importance [86]. Isoform A is located next to catecholaminergic neurons, whereas the B isoform is located in neurotransmitters. Among the two subtypes, MAO-B is one of the enzymes that oxidize the neurotransmitter dopamine in addition to metabolizing other amines. This enzyme is found in large numbers in astrocytes but is also present in serotonin neuron cell bodies, whereas MAO-A is located in neurons in the brain [87]. Isoform A is inhibited by low concentrations of clorgiline, while MAO-B is inhibited by selegiline and rasagiline [88–90], drugs used to elevate brain dopamine by inhibiting its breakdown and promoting beneficial symptomatic effects for the patient.

Studies have reported the expression of MAO-B in human brains or more precisely in the substantia nigra of patients affected by PD [91, 92]. Human MAO-B presents two cavities in its structure, and the FAD coenzyme is present in the active site. The N5 atom is present in the external region, and the residues Tyr398 and Tyr435 play important roles in hMAO-B catalytic activity [93]. The inhibition of MAO-B using rasagiline may promote increased dopaminergic activity of the striatum, leading to symptomatic benefits due to interference in dopamine degradation. Improvements also result from decreased free radicals as generated from dopamine oxidation. The development of selective and reversible MAO-B inhibitors may reduce undesirable adverse effects and present long-term efficacy in neurodegenerative disease treatment.

3. Alzheimer's Disease

Alzheimer's disease (AD) is a progressive neurodegenerative disease common in older people (from 60 years of age and upwards). It consists in memory loss and gradual impairment of cognitive function due to mainly cholinergic neuron death, which makes accomplishment of daily activities difficult, leading the patient to dependence for the basic activities of their daily routine. Because the neurological impairment compromises the autonomic nervous system (ANS), it eventually leads to death. [94–98].

One of the symptoms of AD is dementia, and according to the World Health Organization (WHO) Bulletin, AD is the main pathology responsible for up to 70% of individuals with dementia. WHO estimates that more than 47 million people suffer from dementia, and more than half are from underdeveloped countries. Alzheimer's has no cure and its treatment consists of trying to slow the progression of the disease and offer symptomatic relief [99, 100].

Alzheimer's is clinically explained by neuronal decreases linked to deficient synthesis of acetylcholine (ACh) involved in memory, learning, and SNA. Thus, studies commonly aim at inhibiting acetylcholinesterase (AChE) to prevent ACh breakdown and consequent loss of memory and cognitive functions [101–104].

3.1. Molecular Docking Applied to Natural Products for Alzheimer's Disease. Bioactive beta-secretase-1 (BACE1) inhibitors are currently being studied as therapeutic targets. BACE1 inhibition prevents the amyloid β-amyloid peptide (Aβ) from increasing, preventing cleavage of localized amyloid precursor protein (APP), and thus portion C99 enters the membrane while the (sAPPβ) portion enters the extracellular environment. Inhibition of BACE1 is a therapeutic alternative that inhibits the evolution of AD. This hypothesis has been known since the 1990s as "amyloid cascade" because it consists of a set of neuropathological events that occur in chain, initiated by the accumulation of Aβ, followed by the dysfunction of Tau proteins (which normally stabilize neuronal microtubules), which results in cell death through the agglomeration of Tau proteins in the cell; this compromises both dendrite and the neuronal cell body functions [105–109].

In a molecular docking study [110] to identify molecules that potentiate Alzheimer's inhibition in the BACE1 target, docking of 14 molecules using Molex Virtual Docker was performed with PDB ID 2XFJ and presented interactions with amino acid residues Thr292, Asp93, Asp289, Thr293, Gln134, Asn294, and Thr133. For the compounds studied, hydrogen bonds and hydrophobic interactions with these residues favored inhibitory activity.

Barai et al. [111] using the GOLD suite v.5 program analyzed molecular docking interactions of bergenin (Figure 1(a)) 2 with the objective of highlighting its neuroprotective effects against AD. The docking data in this study were obtained from interactions of the natural product with acetylcholinesterase (PDB ID 1B41), butyrylcholinesterase (PDB ID 1P0I), Tau protein kinase 1 (PDB ID 1J1B), and BACE-1 (PDB ID 1FKN). The docking results were compared

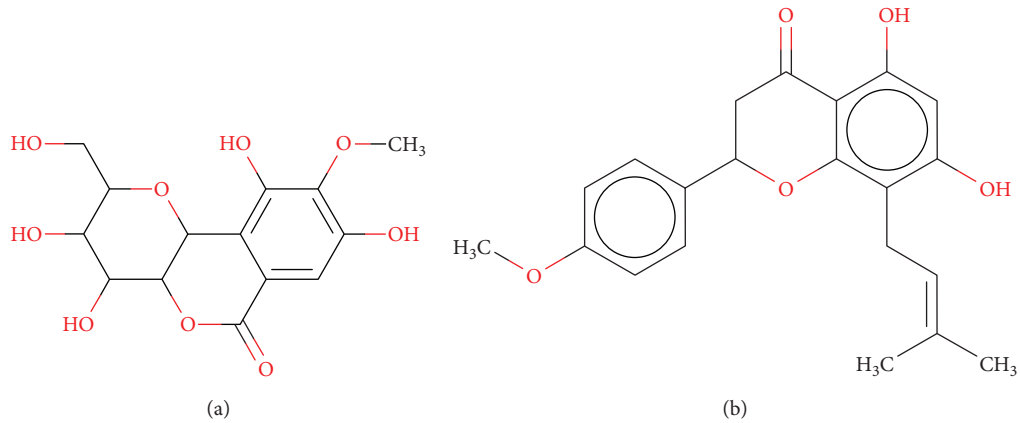

Figure 1: 2D structure of Alzheimer's disease inhibitors. (a) Bergenin. (b) 5,7-dihydroxy-4′-methoxy-8-prenylflavanone.

with the standard drugs donepezil, galantamine, and physostigmine. In the AChE target interactions, hydrogen bonds were present with residues Val340, Gly342, and Phe346; for the BuChE target, hydrogen bond interactions appeared with residues Asn245, Phe278, Val280, and Pro281; for GSK-3β, hydrogen bond interactions appeared with residues Ile62, Gly68, Lys85, Leu132, Asp133, Tyr134, Val135, Arg141, and Asp200, with hydrogen bonds also appearing in most of the residues; and finally for BACE1, hydrogen bond interactions with the amino acids Asp32, Gly34, Asp228, Thr231, and Arg235 were present. In each target, bergenin presented amino acid residue interactions similar to those of the standard drugs studied: Arg24, Lys32, Val340, Gly342, Ala343, and Phe346.

Das et al. [112] performed *in silico* molecular docking studies with 5,7-dihydroxy-4′-methoxy-8-prenylflavanone (Figure 1(b)) using the FlexX of Biosolveit LeadIT program along with the drugs donepezil, galantamine, rivastigmine, tacrine, huperzine, methoxytaxine, and others. The target (PDB ID 5HF6) was chosen with the help of the PharmMapper tool (http://lilab.ecust.edu.cn) and is involved in inhibition of acetylcholinesterase. The aim of this study was to predict anti-Alzheimer activity through molecular docking and QSAR. As a conclusion of this research, the studied flavonoid presented a better ligand-receptor score ($-13.576\,\text{kJ.mol}^{-1}$) than 9 of the 21 controls used for comparison.

3.2. Targets in Alzheimer's Disease

3.2.1. Glycogen Synthase Kinase 3 (GSK3). Glycogen synthase kinase-3 (GSK-3) is a protein responsible for the addition of phosphate molecules to serine and threonine residues [113–115] and is generally encoded by two GSK3α and GSK3β genes. GSK3β phosphorylates the Tau protein and its expression is related to diseases such as Alzheimer's, cancer, and diabetes [113–116].

GSK3β phosphorylates the Tau protein; amino acid residue Tyr216 activates protein kinase, while Ser9 contributes to inhibition. Studies by Nicolia et al. [117] in neuroblastoma cells, analyzing hypomethylation in postmortem frontal cortex, showed that patients with initial AD present inactive GSK3β decreases, whereas patients in the pathological stage V-VI level present large increases in inactive GSK3β.

According to Chinchalongporn et al. [118] who analyzed the inhibitory effect of melatonin on the production of β-amyloid peptide, activation of the GSK3β gene contributes to the formation of Aβ and neuritic plaque and thus a large increase in Tau phosphorylation.

3.2.2. TNF-α Converting Enzyme (TACE). Two factors are associated with the incidence of Alzheimer's, the increase of β-amyloid plaques that form and impede neurotransmissions and the presence of neurofibrillary structures containing Tau in the brain. Tumor necrosis factor-α (TNF-α) is a transmembrane protein that when undergoing TACE (TNF-α converting enzyme) action releases its extracellular domain or soluble TNF-α. TNF$s\alpha$ is a signaling protein; its deregulation is directly related to neuronal degeneration and inflammation [119, 120]. Many studies show that neuroinflammation can trigger pathological processes, including AD. TNF-α is usually maintained at very low concentrations, but with the development of AD the levels increase. [120–123].

3.2.3. Human Angiotensin-Converting Enzyme (ACE). ACE is a zinc metalloenzyme that helps regulate blood pressure and body fluids, by converting the hormone angiotensin I into angiotensin II, a potent vasoconstrictor which is widely used in cardiovascular disease therapies such as degradation of β-amyloid [124–126]. ACE is a peptide and widely distributed as an ectoenzyme in vascular endothelial cell membranes, in epithelial and neuroepithelial cells, and also in its plasma soluble form. Studies have shown that ACE inhibition is a promising therapeutic target for Alzheimer's because angiotensin II in some studies has blocked memory consolidation [127–130].

3.2.4. BACE1 Inhibitor. BACE1, a β-secretase involved in the production of β-amyloid peptide, is the cleavage enzyme of the amyloid precursor protein site 1 and is very important in AD studies. BACE1 has become an increasingly well-studied pharmacological target; many research groups seek bioactives with inhibitory action against this enzyme, yet major problems with inhibitory drugs that cross the blood-

Table 1: Structure, name, structural formula, and molar mass of the flavonoids present in the study.

No.	Structure	Molecular name	Molecular formula	Mass
1	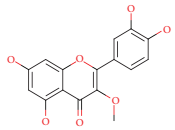	3-O-Methylquercetin	C16H12O7	316.058
2	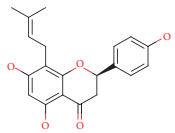	8-Prenylnaringenin	C20H20O5	340.131
3	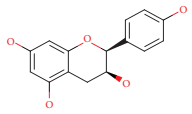	Afzelechin	C15H14O5	274.084
4	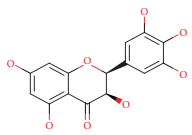	Ampelopsin	C15H12O8	320.053
5	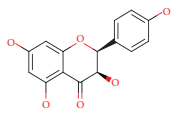	Aromadendrin	C15H12O6	288.063
6	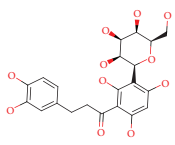	Aspalathin	C21H24O11	452.131
7	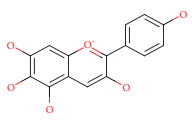	Aurantinidin	C15H11O6	287.055
8	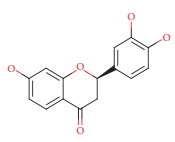	Butin	C15H12O5	272.068
9	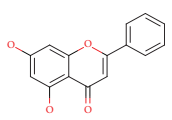	Capensinidin	C18H17O7	345.097
10	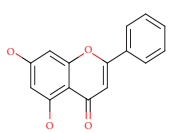	Chrysin	C15H10O4	254.057
11	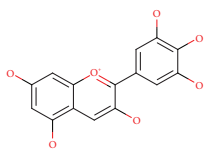	Delphinidin	C15H11O7	303.050

Table 1: Continued.

No.	Structure	Molecular name	Molecular formula	Mass
12	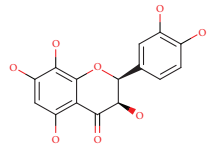	Di-hydrogossypetin	C15H12O8	320.053
13	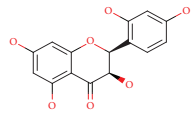	Di-hydromorin	C15H12O7	304.058
14	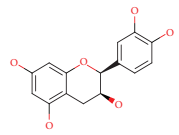	Epicatechin	C15H14O6	290.07
15	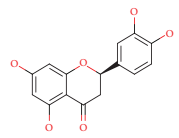	Eriodictyol	C15H12O6	288.063
16	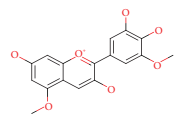	Europinidin	C17H15O7	331.081
17	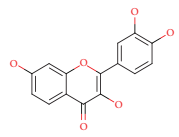	Fisetin	C15H10O6	286.047
18	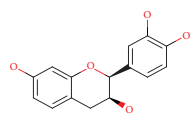	Fisetinidol	C15H14O5	274.084
19	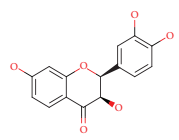	Fustin	C15H12O6	288.063
20	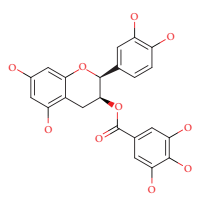	Epicatechin gallate	C22H18O10	442.090
21	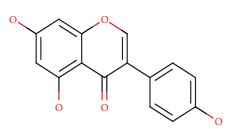	Genistein	C15H10O5	270.052
22	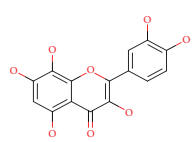	Gossypetin	C15H10O8	318.037

Table 1: Continued.

No.	Structure	Molecular name	Molecular formula	Mass
23	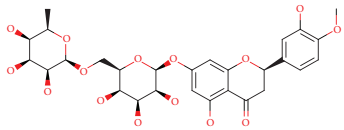	Hesperidin	C28H34O15	610.189
24	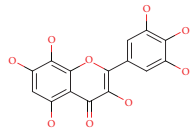	Hibiscetin	C15H10O9	334.032
25	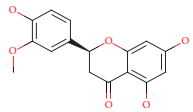	Homoeriodictyol	C16H14O6	302.079
26	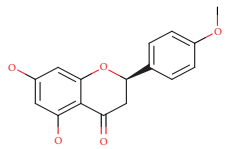	Isosakuranetin	C16H14O5	286.084
27	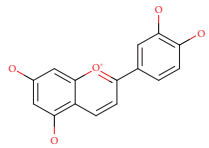	Luteolinidin	C15H11O5	271.060
28	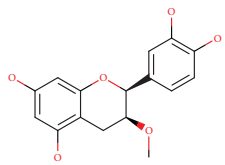	Meciadanol	C16H16O6	304.094
29	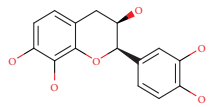	Mesquitol	C15H14O6	290.079
30	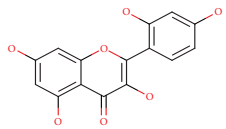	Morin	C15H10O7	302.042
31	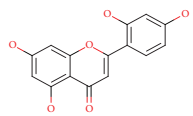	Norartocarpetin	C15H10O6	286.047
32	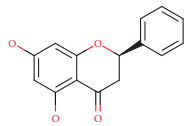	Pinocembrin	C15H12O4	256.073

Table 1: Continued.

No.	Structure	Molecular name	Molecular formula	Mass
33	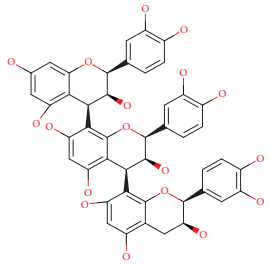	Procyanidins	C45H38O18	866.205
34	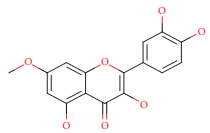	Rhamnetin	C16H12O7	316.058
35	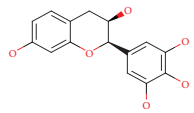	Robinetidinol	C15H14O6	290.079
36	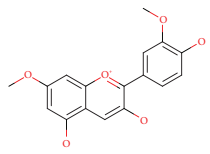	Rosinidin	C17H15O6	315.086
37	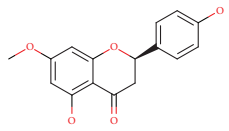	Sakuranetin	C16H14O5	286.084
38	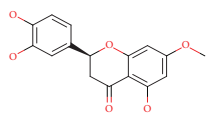	Sterubin	C16H14O6	302.079
39	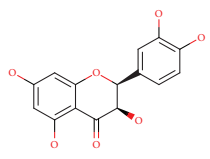	Taxifolin	C15H12O7	304.058
40	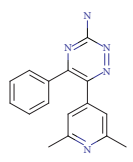	Control 4TG-Aden2A-Parkinson	C17H27N3O15P2	575.357
41	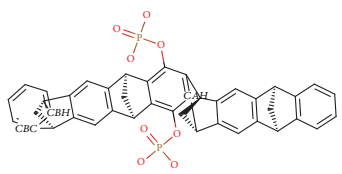	Control CLR01–Parkinson	C42H32O8P2	726.658
42	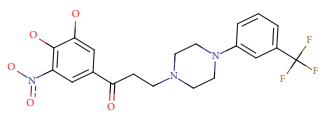	Control BIA–Parkinson	C16H20N4O2	300.360

Table 1: Continued.

No.	Structure	Molecular name	Molecular formula	Mass
43	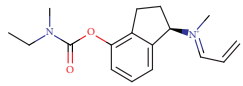	Control ladostigil-Parkinson	C16H20N2O2	272.340
44	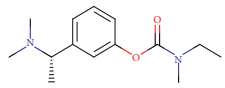	Control rivastigmine-Alzheimer	C14H22N2O2	250.337
45	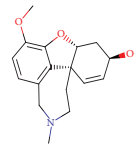	Control galantamine-Alzheimer	C17H21NO3	287.340
46	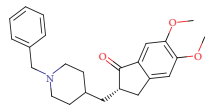	Control donepezil-Alzheimer	C24H29NO3	379.480

brain barrier remain [131–134]. Studies with mice show that BACE1 inhibitors are efficient in combating new Aβ plaques but inefficient against growth of existing plaques, suggesting early treatment with the aim of preventing initial plaque formation [135, 136].

4. Materials and Methods

4.1. Data Set. From the literature, we selected the set of 39 flavonoid structure, known for their antioxidant action. The compounds were submitted to molecular modeling and molecular docking tools to provide their important structural information and activity as multitarget compounds. Data for the physicochemical characteristics of the compounds has been reported (Table 1).

4.2. Molecular Modeling. All of the structures were drawn in HyperChem for Windows v. 8.0.5 (HyperChem, 2009) [137], and their molecular geometries were minimized using the molecular mechanics MM^+ force field, without restrictions for aromatic form conversions, and clean molecular graphing in three dimensions. The optimized structures were subjected to conformational analysis using a random search method with 1000 interactions, 100 cycles of optimization, and the 10 lowest minimum energy conformers. The compounds were saved in the MOL format.

4.3. Quantitative Structure-Activity Relationship: OSIRIS. The cytotoxicity risk study was performed using OSIRIS DataWarrior 4.7.3 [138]. The cytotoxic effects were mutagenicity, carcinogenicity, and irritability to the skin and reproductive system. The TPSA (topological polar surface area) values were used to calculate the rate of absorption (%) of flavonoids and control as drugs by the formula

$$\%\mathrm{ABS} = 109 - (0.345 \times \mathrm{TPSA}). \quad (1)$$

4.4. Molecular Docking. For Parkinson's disease, the structures of human adenosine receptor A_{2A} (PDB ID 3UZA, at a resolution of 3.2 Å), α-synuclein (PDB ID 1XQ8), COMT (PDB ID 1H1D, at a resolution of 2 Å), and MAO-B (PDB ID 2C65, at a resolution of 1.7 Å) were downloaded from the Protein Data Bank (PDB) [139]. The choice of these proteins relied on protein validations reported in the literature, with anti-Parkinson activity as a prerequisite. The adenosine receptor A_{2A}, COMT, and MAO-B proteins, respectively, contained 6-(2,6-dimethylpyridin-4-yl)-5-phenyl-1,2,4-triazin-3-amine (T4G) (an inhibitory drug), 1-(3,4,dihydroxy-5-nitrophenyl)-3-{4-[3-(trifluoromethyl) phenyl] piperazin-1-yl}propan-1-one (BIA), and ladostigil which served as bases for active site labeling and as control compounds for comparing energy values with the flavonoids. As for the α-synuclein protein, the option was chosen to detect 10 possible cavities, admitted as possible active sites on which to run the molecular docking. In order to compare the results of the 39 flavonoids, the docking was also run with the compound CLR01, an α-synuclein inhibitor from the literature.

For Alzheimer's, 4 targets with respect to pathology were analyzed, PDB ID 160 K (resolution of 1.94 Å) the crystal structure of glycogen synthase kinase 3 (GSK-3) with a complexed inhibitor [114], PDB ID 2FV5 (2.1 Å resolution) for the TACE crystal structure complexed with IK682 [140], PDB ID 3BKL (resolution 2.18 Å) for the ACE cocrystal structure with kAW inhibitor [141], and PDB ID 4DJU (resolution 1.8 Å) for the crystalline structure of BACE bound to 2-imino-3-methyl-5,5-diphenylimidazolidin-4-one [142]. The targets were selected based on scientific papers on *in silico* studies of molecules with anti-Alzheimer activity. The inhibitor for GSK-3 complexed together with the crystal structure was N-(4-methoxybenzyl)-N′-(5-nitro-1,3-thiazol-2-yl) urea (TMU), for TACE it was (2R)-N-hydroxy-2-[(3S)-3-methyl-3-{4-[(2-methylquinolin-4-yl)methoxy] phenyl}-2-oxopyrrolidin-1-yl] propanamide (541), and for ACE it was N-{(5S)-4,4-dihydroxy-6-phenyl-5-[(phenylcarbonyl)amino] hexanoyl}-L-tryptophan (kAW).

All 39 flavonoid structures (in MOL format) were submitted to molecular docking using the Molegro Virtual Docker v. 6.0.1 (MVD) [143]. All of the water compounds were deleted from the enzyme structure. For the molecular docking simulation, the bonds for all the compounds and the protein residues in the binding site were set as flexible, with a tolerance of 1.0, strength of 0.80, and with the torsional degrees of freedom for the flexible residues and ligands at 2000 steps of energy minimization. The enzyme and compound structures were prepared using the same default parameter settings in the same software package (score functions: MolDock score; ligand evaluation: internal ES, internal HBond, were all verified; number of runs: 10; algorithm: MolDock SE; maximum interactions: 1500; max. population size: 50; max. steps: 300; neighbor distance factor: 1.00; max. number of poses returned: 5). The docking procedure was performed using a 15 Å radius GRID and 0.30 of resolution to cover the ligand-binding site of the protein. For pose organizer, the MolDock score (GRID) algorithm was used as the score function and the Moldock search algorithm was used.

5. Results and Discussion

5.1. Quantitative Structure-Activity Relationship. Studies in structure-based design have become routine in drug discovery, searching for the best profiles against a disease. Thus, it is possible to analyze and discover various pharmacophoric groups and predict possible activities against a certain target. This study was performed through analysis of the physicochemical properties of drugs, such as TPSA and drug absorption, and using studies related to structure-based protein drug design. Toxicity risks and TPSA data, calculated in Osiris software, are presented in Table 2.

Mutagenicity studies can be used to quantify the role played by various organics in promoting or interfering with the way a drug can associate with DNA. According to the data from the Osiris program, flavonoids present low tendencies to be toxic. There were only six compounds that presented mutagenic toxicity (fisetin, genistein, gossypetin, hibiscetin, morin, and rhamnetin); two presented reproductive toxicity (genistein and procyanidin) and one presented tumor activity (genistein). These compounds present high risk and do not possess good drug profiles.

Table 2: Toxicity data, TPSA, and %ABS calculated on the Osiris tool for flavonoids.

Flavonoids	Toxicity risks	TPSA	%ABS
3-O-methylquercetin	No	116.450	68.824
8-prenylnaringenin	No	86.990	78.9884
Afzelechin	No	90.150	77.8982
Ampelopsin	No	147.680	58.050
Aromadendrin	No	107.220	72.009
Aspalathin	No	208.370	37.112
Aurantinidin	No	101.150	74.103
Butin	No	86.990	78.988
Capensinidin	No	88.380	78.508
Chrysin	No	66.760	85.967
Delphinidin	No	121.380	67.123
Di-hydrogossypetin	No	147.680	58.050
Di-hydromorin	No	127.450	65.029
Epicatechin	No	110.380	70.918
Eriodictyol	No	107.220	72.009
Europinidin	No	99.380	74.713
Fisetin	Mutagenic	107.220	72.009
Fisetinidol	No	90.150	77.898
Fustin	No	107.220	72.009
Epicatechin gallate	No	177.140	47.886
Genistein	Mutagenic/tumor/ reproductive	86.990	78.988
Gossypetin	Mutagenic	147.680	58.050
Hesperidin	No	234.290	28.169
Hibiscetin	Mutagenic	167.910	51.071
Homoeriodictyol	No	96.220	75.804
Isosakuranetin	No	75.990	82.783
Luteolinidin	No	80.920	81.082
Meciadanol	No	99.380	74.713
Mesquitol	No	110.380	70.918
Morin	Mutagenic	127.450	65.029
Norartocarpetin	No	107.220	72.009
Pinocembrin	No	66.760	85.967
Procyanidin	Reproductive	331.140	−5.243
Rhamnetin	Mutagenic	116.450	68.824
Robinetinidol	No	110.380	70.918
Rosinidin	No	92.290	77.159
Sakuranetin	No	75.990	82.783
Sterubin	No	96.220	75.804
Taxifolin	No	127.450	65.029

5.2. Molecular Docking in Parkinson's Disease. The molecular docking studies for the flavonoids and the control drugs with the PD targets are presented in Table 3.

For the enzyme $Aden_{2A}$, it was observed that the three flavonoids (epicatechin gallate, hesperidin, and procyanidin) with respective energy values of −113.727 kcal/mol, −101.446 kcal/mol, and −98.216 kcal/mol presented higher affinities when compared to the PDB ligand (4TG).

The flavonoids pre PDB ligand; hydrogen bonds present in hydroxyl groups with residues Asn253, Ala63, His250, His278, and steric interactions were observed for Asn253, Phe168, Trp246, and Leu249 for the flavonoids which presented higher score values. Key interactions were detected at His278, Leu249, and Asn253, being present in all of the flavonoids studied, principally at residue Asn253, because it is also present for the ligand PDB (Figure 2(a)).

For the enzyme α-synuclein, the observed value of PDB (CLR01 = −147.800 kcal/mol) presented better energy values as compared to flavonoids in the study. However, three of the compounds presented energy values close to that of the PDB ligand; these were procyanidin (−130.002 kcal/mol),

Table 3: Description of energy scores of flavonoids and control compounds on PD target proteins.

Flavonoids	Aden A_{2A}	α-Synuclein	COMT	MAO-B
3-O-methylquercetin	−71.095	−74.901	−53.659	−140.763
8-prenylnaringenin	−83.692	−83.012	−67.998	−145.425
Afzelechin	−61.973	−70.911	−51.278	−107.22
Ampelopsin	−60.848	−74.188	−53.806	−134.626
Aromadendrin	−53.880	−66.701	−45.951	−123.726
Aspalathin	−55.009	−86.361	−56.396	−150.386
Aurantinidin	−67.749	−75.414	−56.591	−117.977
Butin	−68.355	−77.949	−60.034	−124.25
Capensinidin	−84.669	−87.321	−71.529	−140.926
Chrysin	−59.594	−70.872	−52.576	−120.287
Delphinidin	−70.457	−82.877	−68.376	−126.481
Di-hydrogossypetin	−56.359	−73.612	−48.949	−135.483
Di-hydromorin	−61.416	−66.071	−54.329	−131.088
Epicatechin	−66.996	−74.661	−53.054	−122.78
Eriodictyol	−66.790	−74.167	−55.545	−119.801
Europinidin	−75.421	−79.694	−74.993	−140.585
Fisetin	−67.182	−79.763	−64.252	−130.773
Fisetinidol	−64.279	−72.271	−59.406	−118.506
Fustin	−59.854	−76.510	−56.851	−135.63
Epicatechin gallate	−113.727	−98.330	−96.205	−174.333
Genistein	−68.316	−73.585	−58.867	−119.162
Gossypetin	−63.019	−75.620	−58.446	−139.059
Hesperidin	−101.446	−89.698	−65.656	−181.222
Hibiscetin	−71.879	−75.302	−60.718	−137.019
Homoeriodictyol	−75.599	−82.786	−62.698	−141.639
Isosakuranetin	−65.924	−71.351	−49.177	−131.514
Luteolinidin	−65.240	−80.031	−57.149	−122.481
Meciadanol	−73.596	−77.668	−55.342	−126.337
Mesquitol	−60.219	−74.776	−51.753	−128.058
Morin	−70.744	−84.587	−59.595	−139.778
Norartocarpetin	−67.527	−77.898	−60.514	−137.774
Pinocembrin	−56.707	−66.573	−46.254	−113.423
Procyanidin	−98.216	−130.002	−85.226	−88.460
Rhamnetin	−69.702	−83.582	−49.586	−142.785
Robinetinidol	−62.594	−78.967	−51.172	−125.203
Rosinidin	−83.735	−95.587	−63.376	−149.196
Sakuranetin	−70.695	−74.984	−51.408	−129.56
Sterubin	−69.560	−77.022	−56.015	−141.623
Taxifolin	−56.665	−69.743	−52.804	−126.612

epicatechin gallate (−98.330 kcal/mol), and rosinidin (−95.587 kcal/mol). For the flavonoids, hydrogen bonds were present for Lys43, Leu38, and Glu35. Key interactions were also observed for flavonoid activity in hydroxyl group steric interactions with residues Lys32, Lys43, and Glu35 considered key interactions for complex formation. These residues also appeared for the PDB ligand (Figure 2(b)).

Most COMT inhibitors have a catechol ring in their structure, such as entacapone and tolcapone, the most famous COMT inhibitor drugs. In our studies the enzyme COMT also presented flavonoid compound activity, being epicatechin gallate (−96.205 kcal/mol) a stronger interaction than the PDB ligand (BIA = −80.800 kcal/mol). For flavonoid activity, interactions with the active site presented eight residues, such as Asp141, Asn170, Lys144, Met40, and Glu199, forming hydrogen interactions with the catechol portions of the flavonoids. Residues Asn170, Glu199, Trp38, Leu198, Asp141, and Trp143 presented hydrophobic interactions with the hydroxyl portions of the flavonoids (Figure 2(c)). Similar results have been presented by Lee and Kim [144]

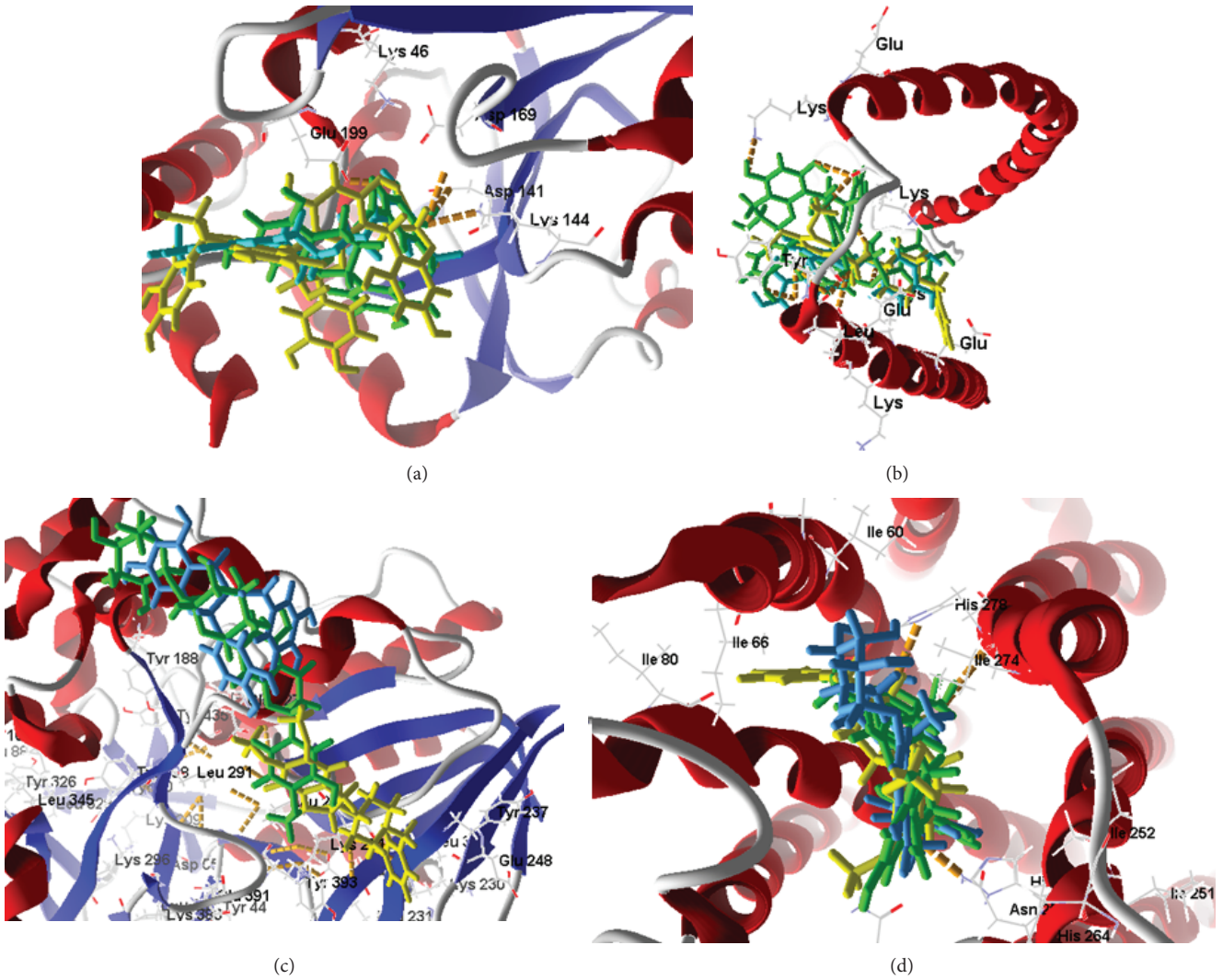

FIGURE 2: Molecular docking of flavonoids at the active site of Aden A_{2A} (PDB: 3UZA), α-synuclein (PDB: 1XQ8), COMT (PDB: 1H1D), and MAO-B (PDB: 2C65). (a) Docking of flavonoids at the active site of $Aden_{2A}$ (green to epicatechin gallate, yellow to procyanidin, and blue to hesperidin). (b) Docking of flavonoids at the active site of α-synuclein (green to procyanidin, yellow to epicatechin gallate, and blue to rosinidin). (c) Docking of flavonoids at the COMT active site (green to epicatechin gallate and yellow to procyanidin and blue to europinidin) (ligand PDB). (d) Docking of flavonoids at the active site of MAO-B (green to hesperidin, yellow to epicatechin, and blue to aspalathin).

and Tervo et al. [145], using molecular docking applied to compounds containing catechol and revealing potent COMT inhibition, which highlight the presence of these same interactions previously reported. The residues Asp141 and Asn170 were present for all of the flavonoids in our study, including the PDB ligand, making them key residues for the activity of these compounds.

MAO-B enzyme docking was performed at the two active PDB ligand sites. At the active site we saw that all of the flavonoids in the study were bound to the enzyme at both sites, with the same prevalence of compounds and presenting very close values at both sites. We also observed that the B subunit presents greater interaction with the compounds than subunit A (Table 3). Comparing the subunit B values, we found that the 10 flavonoid interactions were even more active than the PDB binder (4CR = −140 kcal/mol): 3-O-methylquercetin (−140.763 kcal/mol), 8-prenylnaringenin (−145.425 kcal/mol), aspalathin (−150.386 kcal/mol), capensinidin (−140.926 kcal/mol), europinidin (−140.585 kcal/mol), epicatechin gallate (−174.333 kcal/mol), hesperidin (−181.222 kcal/mol), homoeriodictyol (−141.639 kcal/mol), rosinidin (−149.196 kcal/mol), and sterubin (−141.623 kcal/mol). All these compounds presented steric interactions with residues Cys172, Tyr435, Leu171, Tyr435, Tyr326, Tyr60, and Gln206. Hydrogen bonds at Tyr398 and Met436 and Cys397 were presented with the hydroxyl portions of the flavonoids (Figure 2(d)). Similar results were also reported by Turkmenoglu et al. [39], using differing flavonoid derivatives in molecular docking (from a *Sideritis* species) for human monoamine oxidase (hMAO) isoform A and B, and by Shireen et al. [146] using flavonones from *Boesenbergia rotunda* for monoamine oxidase B, both of which presented interactions similar to our studied flavonoids, with docking results that presented significant hMAO-B inhibitory activity.

Table 4: Energy scores of flavonoids and control compounds against Alzheimer's disease.

Name	1Q5K	2FV5	3BKL	4DJU
3-O-Methylquercetin	−77.844	−137.815	−89.583	−81.959
8-Prenylnaringenin	−97.365	−132.520	−96.493	−85.052
Afzelechin	−69.480	−120.893	−79.982	−65.259
Ampelopsin	−71.079	−119.645	−83.823	−68.341
Aromadendrin	−65.678	−115.123	−81.374	−145.179
Aspalathin	−91.374	−153.001	−125.583	−92.594
Aurantinidin	−77.482	−113.425	−84.517	−60.915
Butin	−80.350	−132.235	−89.736	−110.684
Capensinidin	−77.262	−134.112	−108.407	−118.415
Chrysin	−77.346	−117.834	−88.051	−85.052
Delphinidin	−86.937	−132.828	−98.687	−73.381
Di-hydrogossypetin	−66.795	−120.679	−80.429	−72.832
Di-hydromorin	−67.026	−121.489	−87.870	−71.631
Donepezil*	−112.609	−154.722	−119.399	−83.404
Epicatechin	−72.393	−127.619	−83.552	−78.328
Eriodictyol	−74.681	−124.042	−87.631	−90.944
Europinidin	−85.511	−140.803	−108.977	−89.075
Fisetin	−81.627	−139.645	−95.587	−73.317
Fisetinidol	−74.131	−116.368	−83.084	−65.914
Fustin	−74.571	−116.130	−80.078	−74.650
Galantamine*	−84.430	−156.068	−93.838	−115.428
Epicatechin gallate	−105.952	−187.352	−114.841	−83.154
Genistin	−78.990	−127.356	−89.509	−90.625
Gossypetin	−69.944	−142.715	−84.131	−79.410
Hesperidin	−85.551	−145.093	−97.557	−80.780
Hibiscetin	−66.573	−144.530	−103.117	−81.446
Homoeriodictyol	−85.345	−134.677	−93.198	−82.368
Isosakuranetin	−76.492	−124.546	−81.779	−70.443
Luteolinidin	−76.499	−121.014	−84.251	−87.799
Meciadanol	−73.882	−127.300	−84.290	−74.119
Mesquitol	−81.114	−130.982	−92.321	−80.051
Morin	−79.444	−130.332	−97.326	−80.051
Norartocarpetin	−79.739	−128.750	−99.216	−106.335
Pinocembrin	−67.298	−113.647	−81.535	−56.405
Procyanidin	−115.164	−154.184	−113.990	−81.313
Rhamnetin	−81.950	−127.432	−89.885	130.736
Rivastigmine*	−76.582	−121.774	−85.559	186.829
Robinetidinol	−86.339	−124.910	−95.178	−136.143
Rosinidin	−96.375	−134.734	−111.602	266.611
Sakuranetin	−74.645	−118.156	−88.698	−89.075
Sterubin	−85.628	−124.397	−91.209	−145.179
Taxifolin	−69.263	−120.177	−77.806	−82.368

*Drugs used as a control for Alzheimer's molecular docking.

Such activity is recommended for first-line drugs to treat Parkinson's disease.

We observed that the interactions between flavonoids and the study proteins occurred close to the hydroxyl groups present in the ligand structure and a strong interaction with the catechol ring. It was also observed that molecules with greater molecular mass, and electron-donating hydrophilic hydroxyl groups in ring position B, were more reactive with the enzyme, this, given the greater number of steric and electrostatic interactions with the catalytic site. The

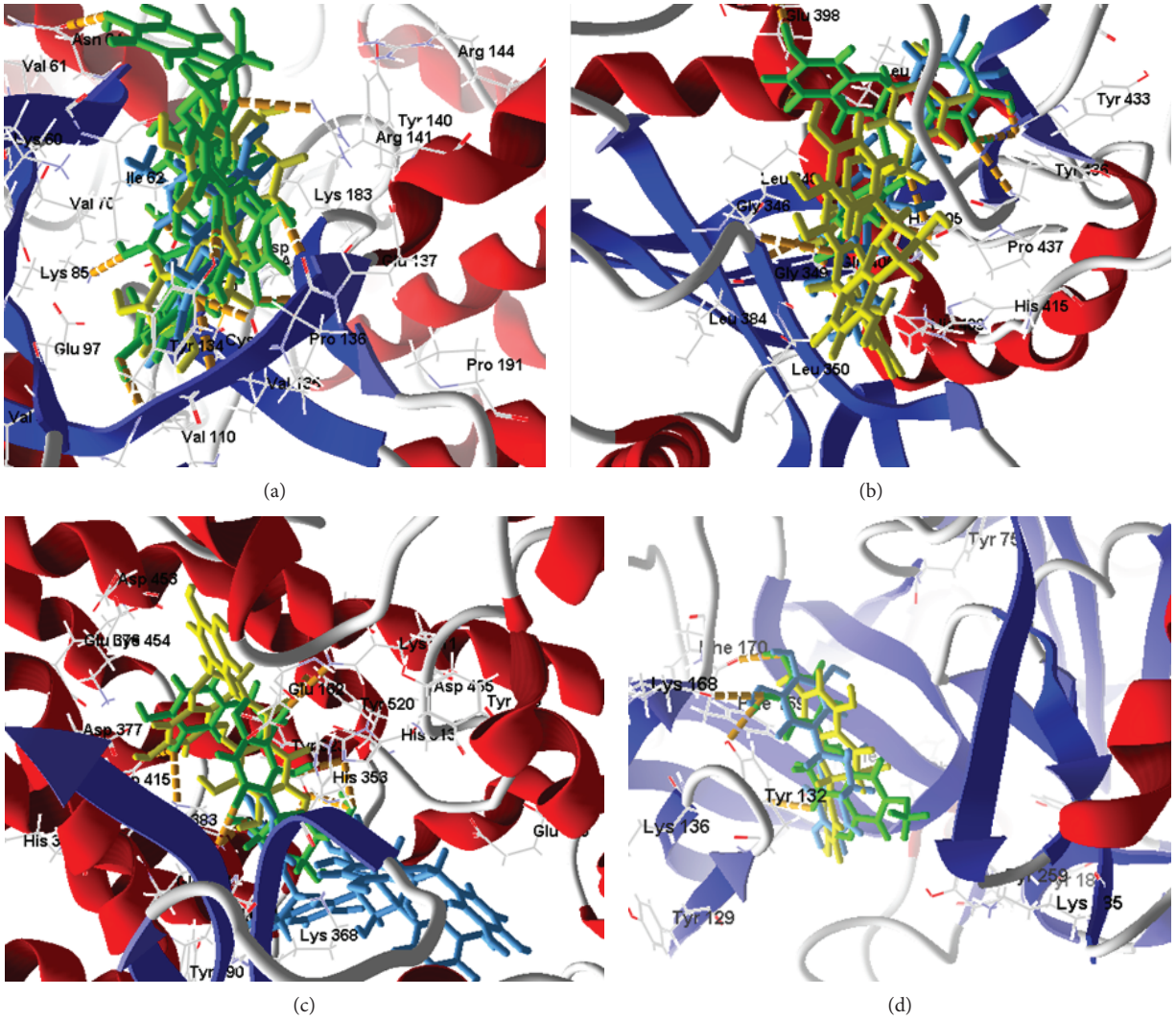

Figure 3: Molecular docking of flavonoids in the active site of GSK3 (PDB: 1Q5K), TACE (PDB: EFV5), ACE (PDB: 3BKL), and BACE1 (PDB: 4DJU). (a) Docking of flavonoids in the active site of GSK3 (green to procyanidin and yellow to epicatechin gallate). (b) Docking of flavonoids in the active site of TACE (green to epicatechin gallate, yellow to procyanidin, and blue to aspalathin). (c) Docking of flavonoids in the active site of ACE (green to aspalathin, yellow to epicatechin gallate, and blue to procyanidin). (d) Docking of flavonoids in the active site of BACE1 (green to sterubin, yellow to aromadendrin, and blue to robinetidinol).

observations led to the hypothesis that such clusters can be viewed as possible pharmacophores for the development of anti-PD drugs.

Our screening results (yielding the best values against the four studied proteins) indicated that 8-prenylnaringenin, europinidin, epicatechin gallate, homoeriodictyol, capensinidin, and rosinidin present structural characteristics which guarantee their potential pharmacological activity against PD.

5.3. Molecular Docking in Alzheimer's Disease. Molecular docking of the 39 flavonoids was performed to analyze ligand-receptor integration for AD targets; the total interaction energy values are presented in Table 4.

For the GSK-3 target, two flavonoids (procyanidin and epicatechin gallate) presented better receptor interaction results with respective energy values of −115.164 kJ/mol and− 105.952 kJ/mol. However, procyanidin presents toxicity risks to the reproductive system. Analyzing interactions with the amino acid residues, we perceived hydrogen bonds of hydroxyls at residue Val135, as well as Asp133, and discretely at Arg141, Pro136, and Try134 for most of the studied flavonoids. Comparing the common amino acid residues of the interaction of the complexed ligand with the crystalline target, we noticed the common contribution of two residues with hydrogen bonds, 2 interactions with residue Val135, and 1 interaction with Pro136, leading to the hypothesis that these residues contribute to GSK-3 inhibitory activity.

For the TACE target, three flavonoids presented interaction energies below 150.0000 kJ/mol (epicatechin gallate, procyanidin, and aspalathin) with respective interaction energies of −187.352 kJ/mol, −154.184 kJ/mol, and− 153.001 kJ/mol. In addition to the abovementioned

toxicity of procyanidin, there is little possibility for oral absorption since the %ABS = −5.241. For this target the molecules showed an interaction tendency for hydrogen bonding with Try433, Try436, and Pro437. For most of the compounds studied, the ligand when complexed with the PDB presented hydrogen-bonding interactions with residues Gly349, His409, His405, Glu406, Leu348, Gly349, and Asn447.

For the ACE target, thirteen compounds presented better interactions (below the median dock energy for each target studied) and hydrogen bond interactions with at least one of the amino acid residues: Tyr520, His513, Lys511, Tyr523, His353, Glu411, Glu384, and Ala356. Of these, five had molecular docking energies below −100.000 kJ/mol, aspalathin, epicatechin gallate, rosinidin, europinidin, and capensinidin.

Finally, for the BACE1 inhibition study, seventeen molecules presented satisfactory molecular docking energies, of which six (aromadendrin, sterubin, robinetidinol, capensidin, butin, and norartocarpetin) presented energies between −106.335 kJ/mol and −145.179 kJ/mol. The amino acid residues involved in the ligand-receptor interaction, with hydrogen bonds in important residues, Ile187, Glu95, Thr292, Asp289, Phe169, Thy132, Asn98, Trp137, Ser97, and Arg189, appeared with a high number of molecular bonds. In Figure 3, the docking of the 3 flavonoid enhancements for each target is presented.

By cross-checking the virtual screening data of the 39 flavonoids with the best interactions for each chosen PDB target, 7 flavonoids with the best results were obtained and are presented in this research: 8-prenylnaringenin, europinidin, epicatechin gallate, homoeriodictyol, aspalathin, butin, and norartocarpetin.

6. Conclusions

We conclude that the flavonoids of the study demonstrate potential neuroprotective activity by virtue of binding to certain key targets for Parkinson's and Alzheimer's. Based on our molecular docking studies, the flavonoids 8-prenylnaringenin, europinidin, epicatechin gallate, homoeriodictyol, capensinidin, and rosinidin present the best results for Parkinson's, whereas for Alzheimer's, the flavonoids 8-prenylnaringenin, europinidin, epicatechin gallate, homoeriodictyol, aspalathin, butin, and norartocarpetin present the best results. With lower and comparable binding energies (compared to crystallized binders), four flavonoids were observed in common for both diseases, presenting interactions and similarities consistent to those reported in the literature. For these flavonoid derivatives, it was observed that having greater flexibility together with hydrophobic hydroxyl groups facilitates interactions with hydrophobic regions of the target protein-binding sites.

Data Availability

The data used to support the findings of this study are available from the corresponding author upon request.

Conflicts of Interest

The authors declare that there is no conflict of interest regarding the publication of this paper.

Acknowledgments

The authors wish to acknowledge the Conselho Nacional de Desenvolvimento Científico e Tecnológico (CNPq). This study was financed in part by the Coordenação de Aperfeiçoamento de Pessoal de Nível Superior—Brasil (CAPES)—Finance Code 001.

References

[1] K. J. Barnham, C. L. Masters, and A. I. Bush, "Neurodegenerative diseases and oxidative stress," *Nature Reviews Drug Discovery*, vol. 3, no. 3, pp. 205–214, 2004.

[2] M. Fakhoury, "Role of immunity and inflammation in the pathophysiology of neurodegenerative diseases," *Neurodegenerative Diseases*, vol. 15, no. 2, pp. 63–69, 2015.

[3] M. T. Lin and M. F. Beal, "Mitochondrial dysfunction and oxidative stress in neurodegenerative diseases," *Nature*, vol. 443, no. 7113, pp. 787–795, 2006.

[4] G. G. Kovacs, "Current concepts of neurodegenerative diseases," *European Medical Journal of Neurology*, vol. 1, pp. 78–86, 2014.

[5] M. Hamer and Y. Chida, "Physical activity and risk of neurodegenerative disease: a systematic review of prospective evidence," *Psychological Medicine*, vol. 39, no. 1, pp. 3–11, 2009.

[6] P. I. Uriarte and M. I. Calvo, "Phytochemical study and evaluation of antioxidant, neuroprotective and acetylcholinesterase inhibitor activities of Galeopsis ladanum L. extracts," *Pharmacognosy Magazine*, vol. 5, no. 20, p. 287, 2009.

[7] A. Hosseini and A. Ghorbani, "Cancer therapy with phytochemicals: evidence from clinical studies," *Avicenna Journal of Phytomedicine*, vol. 5, no. 2, pp. 84–97, 2015.

[8] P. R. Dandawate, D. Subramaniam, R. A. Jensen, and S. Anant, "Targeting cancer stem cells and signaling pathways by phytochemicals: novel approach for breast cancer therapy," in *Seminars in Cancer Biology*, pp. 192–208, Academic Press, 2016.

[9] I. Sarfraz, A. Rasul, F. Jabeen et al., "Fraxinus: a plant with versatile pharmacological and biological activities," *Evidence-Based Complementary and Alternative Medicine*, vol. 2017, Article ID 4269868, 12 pages, 2017.

[10] N. Windayani, Y. Rukayadi, E. H. Hakim, K. Ruslan, and Y. M. Syah, "Antifungal activity of lignans isolated from Phyllanthus myrtifolius Moon. against Fusarium oxysporum," *Phytochemistry*, vol. 12, pp. 33–39, 2014.

[11] M. Mohamed Essa, M. Akbar, and G. Guillemin, *The benefits of Natural Products for Neurodegenerative Diseases*, Springer International Publishing, Switzerland, 2016.

[12] M. Sonee, T. Sum, C. Wang, and S. K. Mukherjee, "The soy isoflavone, genistein, protects human cortical neuronal cells from oxidative stress," *Neurotoxicology*, vol. 25, no. 5, pp. 885–891, 2004.

[13] W. Liao, G. Jin, M. Zhao, and H. Yang, "The effect of genistein on the content and activity of α- and β-secretase and protein kinase C in Aβ-injured hippocampal neurons,"

Basic & Clinical Pharmacology & Toxicology, vol. 112, no. 3, pp. 182–185, 2013.

[14] J. Cho, "Antioxidant and neuroprotective effects of hesperidin and its aglycone hesperetin," *Archives of Pharmacal Research*, vol. 29, no. 8, pp. 699–706, 2006.

[15] A. M. Sabogal-Guáqueta, J. I. Muñoz-Manco, J. R. Ramírez-Pineda, M. Lamprea-Rodriguez, E. Osorio, and G. P. Cardona-Gómez, "The flavonoid quercetin ameliorates Alzheimer's disease pathology and protects cognitive and emotional function in aged triple transgenic Alzheimer's disease model mice," *Neuropharmacology*, vol. 93, pp. 134–145, 2015.

[16] S. N. Wang, Q. Li, M. H. Jing et al., "Natural xanthones from Garcinia mangostana with multifunctional activities for the therapy of Alzheimer's disease," *Neurochemical Research*, vol. 41, no. 7, pp. 1806–1817, 2016.

[17] I. Solanki, P. Parihar, M. L. Mansuri, and M. S. Parihar, "Flavonoid-based therapies in the early management of neurodegenerative diseases," *Advances in Nutrition*, vol. 6, no. 1, pp. 64–72, 2015.

[18] H. Parhiz, A. Roohbakhsh, F. Soltani, R. Rezaee, and M. Iranshahi, "Antioxidant and anti-inflammatory properties of the citrus flavonoids hesperidin and hesperetin: an updated review of their molecular mechanisms and experimental models," *Phytotherapy Research*, vol. 29, no. 3, pp. 323–331, 2015.

[19] J. B. Harborne, *The Flavonoids: Advances in Research since 1980*, Springer, 2013.

[20] I. I. Abubakar, T. Tillmann, and A. Banerjee, "Mortality and causes of death collaborators. Global, regional, and national age-sex specific all-cause and cause-specific mortality for 240 causes of death, 1990-2013: a systematic analysis for the Global Burden of Disease Study 2013," *The Lancet*, vol. 385, no. 9963, pp. 117–171, 2015.

[21] A. J. Noyce, A. J. Lees, and A. E. Schrag, "The prediagnostic phase of Parkinson's disease," *Journal of Neurology, Neurosurgery, and Psychiatry*, vol. 87, no. 8, pp. 871–878, 2016.

[22] C. J. H. M. Klemann, G. J. M. Martens, M. Sharma et al., "Integrated molecular landscape of Parkinson's disease," *NPJ Parkinson's Disease*, vol. 3, no. 1, p. 14, 2017.

[23] D. Twelves, K. S. M. Perkins, and C. Counsell, "Systematic review of incidence studies of Parkinson's disease," *Movement Disorders*, vol. 18, no. 1, pp. 19–31, 2003.

[24] T. Pringsheim, N. Jette, A. Frolkis, and T. D. L. Steeves, "The prevalence of Parkinson's disease: a systematic review and meta-analysis," *Movement Disorders*, vol. 29, no. 13, pp. 1583–1590, 2014.

[25] E. R. Dorsey, R. Constantinescu, J. P. Thompson et al., "Projected number of people with Parkinson disease in the most populous nations, 2005 through 2030," *Neurology*, vol. 68, no. 5, pp. 384–386, 2007.

[26] S. Sveinbjornsdottir, "The clinical symptoms of Parkinson's disease," *Journal of Neurochemistry*, vol. 1, pp. 318–324, 2016.

[27] L. V. Kalia and A. E. Lang, "Parkinson's disease," *Lancet*, vol. 386, no. 9996, pp. 896–912, 2015.

[28] J. M. Shulman, P. L. de Jager, and M. B. Feany, "Parkinson's disease: genetics and pathogenesis," *Annual Review of Pathology*, vol. 6, no. 1, pp. 193–222, 2011.

[29] H. M. Gao, D. Tu, and Y. Gao, "Roles of microglia in inflammation-mediated neurodegeneration: models, mechanisms, and therapeutic interventions for Parkinson's disease," *Advances in Neurotoxicology*, vol. 1, pp. 185–209, 2017.

[30] N. L. Diaz and C. H. Waters, "Current strategies in the treatment of Parkinson's disease and a personalized approach to management," *Expert Review of Neurotherapeutics*, vol. 9, no. 12, pp. 1781–1789, 2014.

[31] T. Müller, H. Hefter, R. Hueber et al., "Is levodopa toxic?," *Journal of Neurology*, vol. 251, pp. 44–46, 2004.

[32] C. A. Tamminga, "Partial dopamine agonists in the treatment of psychosis," *Journal of Neural Transmission*, vol. 109, no. 3, pp. 411–420, 2002.

[33] Z. Shahpiri, R. Bahramsoltani, M. Hosein Farzaei, F. Farzaei, and R. Rahimi, "Phytochemicals as future drugs for Parkinson's disease: a comprehensive review," *Reviews in the Neurosciences*, vol. 27, no. 6, pp. 651–668, 2016.

[34] K. B. Magalingam, A. K. Radhakrishnan, and N. Haleagrahara, "Protective mechanisms of flavonoids in Parkinson's disease," *Oxidative Medicine and Cellular Longevity*, vol. 2015, Article ID 314560, 14 pages, 2015.

[35] L. Ferreira, R. dos Santos, G. Oliva, and A. Andricopulo, "Molecular docking and structure-based drug design strategies," *Molecules*, vol. 20, no. 7, pp. 13384–13421, 2015.

[36] F. F. Ribeiro, F. J. B. Mendonca Junior, J. B. Ghasemi, H. M. Ishiki, M. T. Scotti, and L. Scotti, "Docking of natural products against neurodegenerative diseases: general concepts," *Combinatorial Chemistry & High Throughput Screening*, vol. 21, no. 3, pp. 152–160, 2018.

[37] V. P. Lorenzo, M. F. Alves, L. Scotti, S. G. dos Santos, M. D. F. F. M. Diniz, and M. T. Scotti, "Computational chemistry study of natural alkaloids and homemade databank to predict inhibitory potential against key enzymes in neurodegenerative diseases," *Current Topics in Medicinal Chemistry*, vol. 17, no. 26, pp. 2926–2934, 2017.

[38] H. M. Ishiki, J. M. B. Filho, M. S. da Silva, M. T. Scotti, and L. Scotti, "Computer-aided drug design applied to Parkinson targets," *Current Neuropharmacology*, vol. 16, no. 6, pp. 865–880, 2018.

[39] F. Turkmenoglu, İ. Baysal, S. Ciftci-Yabanoglu et al., "Flavonoids from Sideritis species: human monoamine oxidase (hMAO) inhibitory activities, molecular docking studies and crystal structure of xanthomicrol," *Molecules*, vol. 20, no. 5, pp. 7454–7473, 2015.

[40] N. Desideri, A. Bolasco, R. Fioravanti et al., "Homoisoflavonoids: natural scaffolds with potent and selective monoamine oxidase-B inhibition properties," *Journal of Medicinal Chemistry*, vol. 54, no. 7, pp. 2155–2164, 2011.

[41] L. Scotti and M. Scotti, "Computer aided drug design studies in the discovery of secondary metabolites targeted against age-related neurodegenerative diseases," *Current Topics in Medicinal Chemistry*, vol. 15, no. 21, pp. 2239–2252, 2015.

[42] H. S. Baul and M. Rajiniraja, "Favorable binding of quercetin to α-synuclein as potential target in Parkinson disease: an insilico approach," *Research Journal of Pharmacy and Technology*, vol. 11, no. 1, p. 203, 2018.

[43] A. Madeswaran, M. Umamaheswari, K. Asokkumar, T. Sivashanmugam, V. Subhadradevi, and P. Jagannath, "Docking studies: in silico lipoxygenase inhibitory activity of some commercially available flavonoids," *Bangladesh Journal of Pharmacology*, vol. 6, no. 2, 2011.

[44] C. N. Wilson and S. J. Mustafa, *Adenosine Receptors in Health and Disease*, Springer, Berlin, Heidelberg, 2009.

[45] M. T. Armentero, A. Pinna, S. Ferré, J. L. Lanciego, C. E. Müller, and R. Franco, "Past, present and future of A2A

adenosine receptor antagonists in the therapy of Parkinson's disease," *Pharmacology & Therapeutics*, vol. 132, no. 3, pp. 280–299, 2011.

[46] M. Morelli, A. R. Carta, and P. Jenner, "Adenosine A2A receptors and Parkinson's disease," *Handbook of Experimental Pharmacology*, vol. 193, pp. 589–615, 2009.

[47] R. A. Cunha and J. A. Ribeiro, "Adenosine A2A receptor facilitation of synaptic transmission in the CA1 area of the rat hippocampus requires protein kinase C but not protein kinase A activation," *Neuroscience Letters*, vol. 289, no. 2, pp. 127–130, 2000.

[48] T. Shindou, H. Nonaka, P. J. Richardson, A. Mori, H. Kase, and M. Ichimura, "Presynaptic adenosine A2A receptors enhance GABAergic synaptic transmission via a cyclic AMP dependent mechanism in the rat globus pallidus," *British Journal of Pharmacology*, vol. 136, no. 2, pp. 296–302, 2002.

[49] S. L. Swope, S. J. Moss, L. A. Raymond, and R. L. Huganir, "3 Regulation of ligand-gated ion channels by protein phosphorylation," *Advances in Second Messenger and Phosphoprotein Research*, vol. 33, pp. 49–78, 1999.

[50] A. L. Carvalho, C. B. Duarte, and A. P. Carvalho, "Regulation of AMPA receptors by phosphorylation," *Neurochemical Research*, vol. 25, no. 9/10, pp. 1245–1255, 2000.

[51] A. Pinna, "Adenosine A2A receptor antagonists in Parkinson's disease: progress in clinical trials from the newly approved istradefylline to drugs in early development and those already discontinued," *CNS Drugs*, vol. 28, no. 5, pp. 455–474, 2014.

[52] B. B. Fredholm, M. P. Abbracchio, G. Burnstock et al., "Nomenclature and classification of purinoceptors," *Pharmacological Reviews*, vol. 46, no. 2, pp. 143–156, 1994.

[53] P. Svenningsson, R. Nergardh, and B. B. Fredholm, "Regional differences in the ability of caffeine to affect haloperidol-induced striatal c-fos mRNA expression in the rat," *Neuropharmacology*, vol. 37, no. 3, pp. 331–337, 1998.

[54] M. A. Schwarzschild, L. Agnati, K. Fuxe, J. F. Chen, and M. Morelli, "Targeting adenosine A2A receptors in Parkinson's disease," *Trends in Neurosciences*, vol. 29, no. 11, pp. 647–654, 2006.

[55] W. Bara-Jimenez, A. Sherzai, T. Dimitrova et al., "Adenosine A2Areceptor antagonist treatment of Parkinson's disease," *Neurology*, vol. 61, no. 3, pp. 293–296, 2003.

[56] R. A. Hauser, J. P. Hubble, D. D. Truong, and the Istradefylline US-001 Study Group, "Randomized trial of the adenosine A(2A) receptor antagonist istradefylline in advanced PD," *Neurology*, vol. 61, no. 3, pp. 297–303, 2003.

[57] T. Kondo, Y. Mizuno, and Japanese Istradefylline Study Group, "A long-term study of istradefylline safety and efficacy in patients with Parkinson disease," *Clinical Neuropharmacology*, vol. 38, no. 2, pp. 41–46, 2015.

[58] P. Jenner, "A2A antagonists as novel non-dopaminergic therapy for motor dysfunction in PD," *Neurology*, vol. 61, no. 11, Supplement 6, pp. S32–S38, 2003.

[59] M. Morelli, N. Simola, and J. Wardas, *The Adenosinergic System: A Non-Dopaminergic Target in Parkinson's Disease*, vol. 10, Springer, 2015.

[60] R. Jakes, M. G. Spillantini, and M. Goedert, "Identification of two distinct synucleins from human brain," *FEBS Letters*, vol. 345, no. 1, pp. 27–32, 1994.

[61] A. Iwai, E. Masliah, M. Yoshimoto et al., "The precursor protein of non-Aβ component of Alzheimer's disease amyloid is a presynaptic protein of the central nervous system," *Neuron*, vol. 14, no. 2, pp. 467–475, 1995.

[62] D. F. Clayton and J. M. George, "Synucleins in synaptic plasticity and neurodegenerative disorders," *Journal of Neuroscience Research*, vol. 58, no. 1, pp. 120–129, 1999.

[63] M. Farrer, K. Gwinn-Hardy, M. Muenter et al., "A chromosome 4P haplotype segregating with Parkinson's disease and postural tremor," *Human Molecular Genetics*, vol. 8, no. 1, pp. 81–85, 1999.

[64] M. H. Polymeropoulos, C. Lavedan, E. Leroy et al., "Mutation in the α-synuclein gene identified in families with Parkinson's disease," *Science*, vol. 276, no. 5321, pp. 2045–2047, 1997.

[65] C. W. Olanow and P. Brundin, "Parkinson's disease and alpha synuclein: is Parkinson's disease a prion-like disorder?," *Movement Disorders*, vol. 28, no. 1, pp. 31–40, 2013.

[66] M.-C. Chartier-Harlin, J. Kachergus, C. Roumier et al., "α-Synuclein locus duplication as a cause of familial Parkinson's disease," *The Lancet*, vol. 364, no. 9440, pp. 1167–1169, 2004.

[67] P. Ibáñez, A.-M. Bonnet, B. Débarges et al., "Causal relation between α-synuclein locus duplication as a cause of familial Parkinson's disease," *The Lancet*, vol. 364, no. 9440, pp. 1169–1171, 2004.

[68] P. T. Männisto and S. Kaakkola, "Catechol-O-methyltransferase (COMT): biochemistry, molecular biology, pharmacology, and clinical efficacy of the new selective COMT inhibitors," *Pharmacological Reviews*, vol. 51, no. 4, pp. 593–628, 1999.

[69] B. Zhu, "Catechol-O-methyltransferase (COMT)-mediated methylation metabolism of endogenous bioactive catechols and modulation by endobiotics and xenobiotics: importance in pathophysiology and pathogenesis," *Current Drug Metabolism*, vol. 3, no. 3, pp. 321–349, 2002.

[70] J. L. Martin and F. M. McMillan, "SAM (dependent) I AM: the S-adenosylmethionine-dependent methyltransferase fold," *Current Opinion in Structural Biology*, vol. 12, no. 6, pp. 783–793, 2002.

[71] S. Kaakkola, "Clinical pharmacology, therapeutic use and potential of COMT inhibitors in Parkinson's disease," *Drugs*, vol. 59, no. 6, pp. 1233–1250, 2000.

[72] E. Nissinen, P. Kaheinen, K. E. Penttila, J. Kaivola, and I. B. Linden, "Entacapone, a novel catechol-O-methyltransferase inhibitor for Parkinson's disease, does not impair mitochondrial energy production," *European Journal of Pharmacology*, vol. 340, no. 2-3, pp. 287–294, 1997.

[73] D. Offen, H. Panet, R. Galili-Mosberg, and E. Melamed, "Catechol-O-methyltransferase decreases levodopa toxicity in vitro," *Clinical Neuropharmacology*, vol. 24, no. 1, pp. 27–30, 2001.

[74] I. Reenilä and P. T. Männistö, "Catecholamine metabolism in the brain by membrane-bound and soluble catechol-o-methyltransferase (COMT) estimated by enzyme kinetic values," *Medical Hypotheses*, vol. 57, no. 5, pp. 628–632, 2001.

[75] M. Martínez-Jauand, C. Sitges, V. Rodríguez et al., "Pain sensitivity in fibromyalgia is associated with catechol-O-methyltransferase (COMT) gene," *European Journal of Pain*, vol. 17, no. 1, pp. 16–27, 2013.

[76] J. A. Badner and E. S. Gershon, "Meta-analysis of whole-genome linkage scans of bipolar disorder and schizophrenia," *Molecular Psychiatry*, vol. 7, no. 4, pp. 405–411, 2002.

[77] J. Chen, B. K. Lipska, N. Halim et al., "Functional analysis of genetic variation in catechol-O-methyltransferase (COMT): effects on mRNA, protein, and enzyme activity in postmortem human brain," *The American Journal of Human Genetics*, vol. 75, no. 5, pp. 807–821, 2004.

[78] J. B. Rowe, L. Hughes, C. H. Williams-Gray et al., "The val158met COMT polymorphism's effect on atrophy in healthy aging and Parkinson's disease," *Neurobiology of Aging*, vol. 31, no. 6, pp. 1064–1068, 2010.

[79] C. H. Williams-Gray, A. Hampshire, T. W. Robbins, A. M. Owen, and R. A. Barker, "Catechol O-methyltransferase Val158Met genotype influences frontoparietal activity during planning in patients with Parkinson's disease," *Journal of Neuroscience*, vol. 27, no. 18, pp. 4832–4838, 2007.

[80] M. B. H. Youdim and Y. S. Bakhle, "Monoamine oxidase: isoforms and inhibitors in Parkinson's disease and depressive illness," *British Journal of Pharmacology*, vol. 147, no. S1, pp. S287–S296, 2006.

[81] J. P. M. Finberg, "Update on the pharmacology of selective inhibitors of MAO-A and MAO-B: focus on modulation of CNS monoamine neurotransmitter release," *Pharmacology & Therapeutics*, vol. 143, no. 2, pp. 133–152, 2014.

[82] E. Rodriguez-Vieitez, L. Saint-Aubert, S. F. Carter et al., "Diverging longitudinal changes in astrocytosis and amyloid PET in autosomal dominant Alzheimer's disease," *Brain*, vol. 139, no. 3, pp. 922–936, 2016.

[83] J. Reis, F. Cagide, D. Chavarria et al., "Discovery of new chemical entities for old targets: insights on the lead optimization of chromone-based monoamine oxidase B (MAO-B) inhibitors," *Journal of Medicinal Chemistry*, vol. 59, no. 12, pp. 5879–5893, 2016.

[84] J. C. Shih, K. Chen, and M. J. Ridd, "Monoamine oxidase: from genes to behavior," *Annual Review of Neuroscience*, vol. 22, no. 1, pp. 197–217, 1999.

[85] R. B. Silverman, "Radical ideas about monoamine oxidase," *Accounts of Chemical Research*, vol. 28, no. 8, pp. 335–342, 1995.

[86] E. Grünblatt, S. Mandel, J. Jacob-Hirsch et al., "Gene expression profiling of parkinson substantia nigra pars compacta; alterations in ubiquitin-proteasome, heat shock protein, iron and oxidative stress regulated proteins, cell adhesion/cellular matrix and vesicle trafficking genes," *Journal of Neural Transmission*, vol. 111, no. 12, pp. 1543–1573, 2004.

[87] S. Harris, S. Johnson, J. W. Duncan et al., "Evidence revealing deregulation of the KLF11-MAO a pathway in association with chronic stress and depressive disorders," *Neuropsychopharmacology*, vol. 40, no. 6, pp. 1373–1382, 2015.

[88] O. Rascol, S. Perez-Lloret, and J. J. Ferreira, "New treatments for levodopa-induced motor complications," *Movement Disorders*, vol. 30, no. 11, pp. 1451–1460, 2015.

[89] D. Robakis and S. Fahn, "Defining the role of the monoamine oxidase-B inhibitors for Parkinson's disease," *CNS Drugs*, vol. 29, no. 6, pp. 433–441, 2015.

[90] H. H. Fernandez and J. J. Chen, "Monoamine oxidase-B inhibition in the treatment of Parkinson's disease," *Pharmacotherapy*, vol. 27, 12 Part 2, pp. 174S–185S, 2007.

[91] K. Teo and S.-L. Ho, "Monoamine oxidase-B (MAO-B) inhibitors: implications for disease-modification in Parkinson's disease," *Translational Neurodegeneration*, vol. 2, no. 1, p. 19, 2013.

[92] J. W. Choi, B. K. Jang, N. Cho et al., "Synthesis of a series of unsaturated ketone derivatives as selective and reversible monoamine oxidase inhibitors," *Bioorganic & Medicinal Chemistry*, vol. 23, no. 19, pp. 6486–6496, 2015.

[93] C. Binda, P. Newton-Vinson, F. Hubalek, D. E. Edmondson, and A. Mattevi, "Structure of human monoamine oxidase B, a drug target for the treatment of neurological disorders," *Nature Structural and Molecular Biology*, vol. 9, no. 1, pp. 22–26, 2001.

[94] G. C. Brown and P. H. St George-Hyslop, "Deciphering microglial diversity in Alzheimer's disease," *Science*, vol. 356, no. 6343, pp. 1123-1124, 2017.

[95] R. M. Ransohoff, "Specks of insight into Alzheimer's disease," *Nature*, vol. 552, no. 7685, pp. 342-343, 2017.

[96] A. Fitzpatrick, B. Falcon, S. He et al., "Cryo-Em structures of Tau filaments from Alzheimer's disease brain," *Alzheimer's & Dementia*, vol. 13, no. 7, p. P892, 2017.

[97] H. Y. Cai, J. T. Yang, Z. J. Wang et al., "Lixisenatide reduces amyloid plaques, neurofibrillary tangles and neuroinflammation in an APP/PS1/tau mouse model of Alzheimer's disease," *Biochemical and Biophysical Research Communications*, vol. 495, no. 1, pp. 1034–1040, 2018.

[98] P. C. Donaghy, J.-P. Taylor, J. T. O'Brien et al., "Neuropsychiatric symptoms and cognitive profile in mild cognitive impairment with Lewy bodies," *Psychological Medicine*, vol. 48, no. 14, pp. 2384–2390, 2018.

[99] K. G. Yiannopoulou and S. G. Papageorgiou, "Current and future treatments for Alzheimer's disease," *Therapeutic Advances in Neurological Disorders*, vol. 6, no. 1, pp. 19–33, 2012.

[100] S. M. Neuner, L. A. Wilmott, B. R. Hoffmann, K. Mozhui, and C. C. Kaczorowski, "Hippocampal proteomics defines pathways associated with memory decline and resilience in normal aging and Alzheimer's disease mouse models," *Behavioural Brain Research*, vol. 322, no. Part B, pp. 288–298, 2017.

[101] E. Andrade-Jorge, L. A. Sánchez-Labastida, M. A. Soriano-Ursúa, J. A. Guevara-Salazar, and J. G. Trujillo-Ferrara, "Isoindolines/isoindoline-1, 3-diones as AChE inhibitors against Alzheimer's disease, evaluated by an improved ultra-micro assay," *Medicinal Chemistry Research*, vol. 27, no. 9, pp. 2187–2198, 2018.

[102] A. Simchovitz, M. T. Heneka, and H. Soreq, "Personalized genetics of the cholinergic blockade of neuroinflammation," *Journal of Neurochemistry*, vol. 142, pp. 178–187, 2017.

[103] J. Yan, J. Hu, A. Liu, L. He, X. Li, and H. Wei, "Design, synthesis, and evaluation of multitarget-directed ligands against Alzheimer's disease based on the fusion of donepezil and curcumin," *Bioorganic & Medicinal Chemistry*, vol. 25, no. 12, pp. 2946–2955, 2017.

[104] L. Scotti, F. J. B. M. Junior, M. S. da Silva, I. R. Pitta, and M. T. Scotti, "Biochemical changes evidenced in Alzheimer's disease: a mini-review," *Letters in Drug Design & Discovery*, vol. 11, no. 2, pp. 240–248, 2014.

[105] E. F. Silva-Junior, P. H. Barcellos Franca, L. J. Quintans-Junior et al., "Dynamic simulation, docking and DFT studies applied to a set of anti-acetylcholinesterase inhibitors in the enzyme β-secretase (BACE-1): an important therapeutic target in Alzheimer's disease," *Current Computer-Aided Drug Design*, vol. 13, no. 4, pp. 266–274, 2017.

[106] T. D. Mai, D. Ferraro, N. Aboud et al., "Single-step immunoassays and microfluidic droplet operation: towards a versatile

approach for detection of amyloid-β peptide-based biomarkers of Alzheimer's disease," *Sensors and Actuators B: Chemical*, vol. 255, pp. 2126–2135, 2018.

[107] E. F. Silva-Junior, P. H. Barcellos Franca, L. J. Quintans-Junior et al., "A key role for MAM in mediating mitochondrial dysfunction in Alzheimer disease," *Cell Death & Disease*, vol. 9, no. 3, p. 335, 2018.

[108] D. Alcolea, E. Vilaplana, M. Suárez-Calvet et al., "CSF sAPPβ, YKL-40, and neurofilament light in frontotemporal lobar degeneration," *Neurology*, vol. 89, no. 2, pp. 178–188, 2017.

[109] G. Botteri, L. Salvadó, A. Gumà et al., "The BACE1 product sAPPβ induces ER stress and inflammation and impairs insulin signaling," *Metabolism*, vol. 85, pp. 59–75, 2018.

[110] F. Atlam, M. Awad, and R. Salama, "Factors influencing the potency of Alzheimer inhibitors: computational and docking studies," *American Journal of Alzheimer's Disease & Other Dementias®*, vol. 33, no. 3, pp. 166–175, 2018.

[111] P. Barai, N. Raval, S. Acharya, A. Borisa, H. Bhatt, and N. Acharya, "Neuroprotective effects of bergenin in Alzheimer's disease: investigation through molecular docking, in vitro and in vivo studies," *Behavioural Brain Research*, vol. 356, pp. 18–40, 2019.

[112] S. Das, M. A. Laskar, S. D. Sarker et al., "Prediction of anti-Alzheimer's activity of flavonoids targeting acetylcholinesterasein silico," *Phytochemical Analysis*, vol. 28, no. 4, pp. 324–331, 2017.

[113] H. Eldar-Finkelman and A. Martinez, "GSK-3 inhibitors: preclinical and clinical focus on CNS," *Frontiers in Molecular Neuroscience*, vol. 4, 2011.

[114] R. Bhat, Y. Xue, S. Berg et al., "Structural insights and biological effects of glycogen synthase kinase 3-specific inhibitor AR-A014418," *Journal of Biological Chemistry*, vol. 278, no. 46, pp. 45937–45945, 2003.

[115] W. Wang, M. Li, Y. Wang et al., "GSK-3β inhibitor TWS119 attenuates rtPA-induced hemorrhagic transformation and activates the Wnt/β-catenin signaling pathway after acute ischemic stroke in rats," *Molecular Neurobiology*, vol. 53, no. 10, pp. 7028–7036, 2016.

[116] A. Kremer, "GSK3 and Alzheimer's disease: facts and fiction…," *Frontiers in Molecular Neuroscience*, vol. 4, 2011.

[117] V. Nicolia, V. Ciraci, R. A. Cavallaro, I. Ferrer, S. Scarpa, and A. Fuso, "GSK3β 5′-flanking DNA methylation and expression in Alzheimer's disease patients," *Current Alzheimer Research*, vol. 14, no. 7, pp. 753–759, 2017.

[118] V. Chinchalongporn, M. Shukla, and P. Govitrapong, "Melatonin ameliorates Aβ42-induced alteration of βAPP-processing secretases via the melatonin receptor through the Pin1/GSK3β/NF-κB pathway in SH-SY5Y cells," *Journal of Pineal Research*, vol. 64, no. 4, article e12470, 2018.

[119] S. J. Tyler, D. Dawbarn, G. K. Wilcock, and S. J. Allen, "α-and β-secretase: profound changes in Alzheimer's disease," *Biochemical and Biophysical Research Communications*, vol. 299, no. 3, pp. 373–376, 2002.

[120] R. Chang, K. L. Yee, and R. K. Sumbria, "Tumor necrosis factor α inhibition for Alzheimer's disease," *Journal of Central Nervous System Disease*, vol. 9, 2017.

[121] D. W. Dickson, "The pathogenesis of senile plaques," *Journal of Neuropathology & Experimental Neurology*, vol. 56, no. 4, pp. 321–339, 1997.

[122] X. Cheng, L. Yang, P. He, R. Li, and Y. Shen, "Differential activation of tumor necrosis factor receptors distinguishes between brains from Alzheimer's disease and non-demented patients," *Journal of Alzheimer's Disease*, vol. 19, no. 2, pp. 621–630, 2010.

[123] R. Zhou and P. Bickler, "Interaction of isoflurane, tumor necrosis factor-α and β-amyloid on long-term potentiation in rat hippocampal slices," *Anesthesia & Analgesia*, vol. 124, no. 2, pp. 582–587, 2017.

[124] P. G. Kehoe, S. Wong, N. A. L. Mulhim, L. E. Palmer, and J. Scott Miners, "Angiotensin-converting enzyme 2 is reduced in Alzheimer's disease in association with increasing amyloid-β and tau pathology," *Alzheimer's Research & Therapy*, vol. 8, no. 1, p. 50, 2016.

[125] T. Ohrui, N. Tomita, T. Sato-Nakagawa et al., "Effects of brain-penetrating ACE inhibitors on Alzheimer disease progression," *Neurology*, vol. 63, no. 7, pp. 1324-1325, 2004.

[126] V. Mehta, N. Desai, A. Perwez, D. Nemade, S. Dawoodi, and S. B. Zaman, "ACE Alzheimer's: the role of vitamin A, C and E (ACE) in oxidative stress induced Alzheimer's disease," *Journal of Medical Research and Innovation*, vol. 2, no. 1, article e000086, 2018.

[127] X. Li and J. N. Buxbaum, "Transthyretin and the brain re-visited: is neuronal synthesis of transthyretin protective in Alzheimer's disease?," *Molecular Neurodegeneration*, vol. 6, no. 1, p. 79, 2011.

[128] H. Kölsch, F. Jessen, N. Freymann et al., "ACE I/D polymorphism is a risk factor of Alzheimer's disease but not of vascular dementia," *Neuroscience Letters*, vol. 377, no. 1, pp. 37–39, 2005.

[129] R. Monastero, R. Caldarella, M. Mannino et al., "Lack of association between angiotensin converting enzyme polymorphism and sporadic Alzheimer's disease," *Neuroscience Letters*, vol. 335, no. 2, pp. 147–149, 2002.

[130] C. Fridman, S. P. Gregório, E. D. Neto, and É. P. Benquique Ojopi, "Alterações genéticas na doença de Alzheimer," *Archives of Clinical Psychiatry (São Paulo)*, vol. 31, no. 1, pp. 19–25, 2004.

[131] R. Vassar, "BACE1 inhibitor drugs in clinical trials for Alzheimer's disease," *Alzheimer's Research & Therapy*, vol. 6, no. 9, pp. 89–89, 2014.

[132] G. Koelsch, "BACE1 function and inhibition: implications of intervention in the amyloid pathway of Alzheimer's disease pathology," *Molecules*, vol. 22, no. 10, p. 1723, 2017.

[133] C. Ridler, "Alzheimer disease: BACE1 inhibitors block new Aβ plaque formation," *Nature Reviews Neurology*, vol. 14, no. 3, p. 126, 2018.

[134] J. Bao, M. Qin, Y. A. R. Mahaman et al., "BACE1 SUMOylation increases its stability and escalates the protease activity in Alzheimer's disease," *Proceedings of the National Academy of Sciences*, vol. 115, no. 15, pp. 3954–3959, 2018.

[135] X. Hu, B. Das, H. Hou, W. He, and R. Yan, "BACE1 deletion in the adult mouse reverses preformed amyloid deposition and improves cognitive functions," *Journal of Experimental Medicine*, vol. 215, no. 3, pp. 927–940, 2018.

[136] A. V. Savonenko, T. Melnikova, F. M. Laird, K. A. Stewart, D. L. Price, and P. C. Wong, "Alteration of BACE1-dependent NRG1/ErbB4 signaling and schizophrenia-like phenotypes in BACE1-null mice," *Proceedings of the National Academy of Sciences*, vol. 105, no. 14, pp. 5585–5590, 2008.

[137] HyperChem, *Computational Chemistry*, Hypercube Inc, 2009.

[138] OSIRIS, *Property Explorer, Organic Chemistry Portal*, Idorsia pharmaceuticals ltd, Switzerland, http://www.organicchemistry.org/prog/peo/.

[139] H. M. Berman, J. Westbrook, Z. Feng et al., "The Protein Data Bank," *Nucleic Acids Research*, vol. 28, no. 1, pp. 235–242, 2000.

[140] X. Niu, S. Umland, R. Ingram et al., "IK682, a tight binding inhibitor of TACE," *Archives of Biochemistry and Biophysics*, vol. 451, no. 1, pp. 43–50, 2006.

[141] J. M. Watermeyer, W. L. Kröger, H. G. O'Neill, B. T. Sewell, and E. D. Sturrock, "Probing the basis of domain-dependent inhibition using novel ketone inhibitors of angiotensin-converting enzyme," *Biochemistry*, vol. 47, no. 22, pp. 5942–5950, 2008.

[142] J. N. Cumming, E. M. Smith, L. Wang et al., "Structure based design of iminohydantoin BACE1 inhibitors: identification of an orally available, centrally active BACE1 inhibitor," *Bioorganic & Medicinal Chemistry Letters*, vol. 22, no. 7, pp. 2444–2449, 2012.

[143] *Molegro Virtual Docker 2.3 Molegro ApS*, Aarhus, Denmark, 2007.

[144] J. Y. Lee and Y. M. Kim, "Comparative homology modeling and ligand docking study of human catechol-O-methyltransferase for antiparkinson drug design," *Bulletin of the Korean Chemical Society*, vol. 26, no. 11, pp. 1695–1700, 2005.

[145] A. J. Tervo, T. H. Nyrönen, T. Rönkkö, and A. Poso, "A structure-activity relationship study of catechol-O-methyltransferase inhibitors combining molecular docking and 3D QSAR methods," *Journal of Computer-Aided Molecular Design*, vol. 17, no. 12, pp. 797–810, 2003.

[146] P. Ajmala Shireen, K. Muraleedharan, and V. M. Abdul Mujeeb, "Identification of flavanones from Boesenbergia rotunda as potential antioxidants and monoamine oxidase B inhibitors," *Chemical Papers*, vol. 71, no. 12, pp. 2473–2483, 2017.

Hindawi
Oxidative Medicine and Cellular Longevity
Volume 2018, Article ID 8952646, 10 pages
https://doi.org/10.1155/2018/8952646

Research Article

Effect of Alkaloid Extract from African Jointfir (*Gnetum africanum*) Leaves on Manganese-Induced Toxicity in *Drosophila melanogaster*

Ganiyu Oboh,[1] **Opeyemi Babatunde Ogunsuyi**,[1,2] **Olatunde Isaac Awonyemi**,[3] **and Victor Ayomide Atoki**[1]

[1]*Department of Biochemistry, Federal University of Technology, P.M.B. 704 Akure, Nigeria*
[2]*Department of Biomedical Technology, Federal University of Technology, P.M.B. 704 Akure, Nigeria*
[3]*Central Research Laboratory, Federal University of Technology, P.M.B. 704 Akure, Nigeria*

Correspondence should be addressed to Ganiyu Oboh; goboh@futa.edu.ng

Received 2 May 2018; Accepted 1 October 2018; Published 30 December 2018

Guest Editor: Francisco J. B. Mendonça Júnior

Metal-induced toxicity in fruit fly (*Drosophila melanogaster)* is one of the established models for studying neurotoxicity and neurodegenerative diseases. Phytochemicals, especially alkaloids, have been reported to exhibit neuroprotection. Here, we assessed the protective effect of alkaloid extract from African Jointfir (*Gnetum africanum)* leaf on manganese- (Mn-) induced toxicity in wild type fruit fly. Flies were exposed to 10 mM Mn, the alkaloid extract and cotreatment of Mn plus extract, respectively. The survival rate and locomotor performance of the flies were assessed 5 days posttreatment, at which point the flies were homogenized and assayed for acetylcholinesterase (AChE) activity, nitric oxide (NO), and reactive oxygen species (ROS) levels. Results showed that the extract significantly reverted Mn-induced reduction in the survival rate and locomotor performance of the flies. Furthermore, the extract counteracted the Mn-induced elevation in AChE activity, NO, and ROS levels. The alkaloid extract of the African Jointfir leaf may hence be a source of useful phytochemicals for the development of novel therapies for the management of neurodegeneration.

1. Introduction

Manganese (Mn) is essential for a wide array of biochemical processes in the body [1]. However, exposure to excessive level of Mn through, for example, occupational means can induce neurodegenerative diseases with pathophysiological features similar to Parkinson's disease [2]. Neurodegenerative diseases are pathologies of multiple causative factors; examples include Alzheimer's disease (AD) and Parkinson's disease (PD). Studies reveal that these diseases are characterized by decline in neurotransmitters associated with the brain, such as acetylcholine and neuroactive amines, as well as oxidative stress caused by excessive levels of metal ions in the brain [3]. It has therefore become essential to develop holistic therapeutic approach for preventing and managing these diseases by focusing attention on the different risk factors. Cholinergic neurons make use of the neurotransmitter acetylcholine which is metabolized by cholinesterase enzymes [4–6]. Therefore, cholinesterase inhibitors such as galantamine and donepezil have been used as therapeutic intervention for AD [6, 7]. Over the years, cholinesterase and monoamine oxidase inhibitors have been used as therapeutic approach for managing these diseases. These interventions have, however, been shown to pose serious adverse effects. Therefore, the importance of complementary/alternative dietary/medicinal interventions as a managerial and preventive approach cannot be overemphasized.

The fruit fly (*Drosophila melanogaster)* has gained a lot of use as an alternative animal model for biomedical research, especially for unraveling the molecular mechanisms behind several human diseases. Furthermore, studies have shown that up to 75% of the human disease-causing genes are conserved in *Drosophila* [8]. The similarity between human and Drosophila genomes is not only limited to genetic

elements but also includes the relationship between them, with numerous examples of conserved biological mechanisms [9]. Metal-induced toxicity in *D. melanogaster* is an established model for studying neurotoxicity and neurodegenerative diseases. Previous studies have used metals such as Fe, Al, Cu, and Mn to induce neurotoxicity as models of neurodegeneration in *D. melanogaster*; Fe-, Cu-, and Mn-induced toxicity have been linked with PD and Parkinsonism [10], while Al is used to model Alzheimer-like pathology in *D. melanogaster* [11]. Specifically, the hallmark of Mn-induced neurotoxicity in *D. melanogaster* includes reduction in life span and locomotor performance, increased ROS generation, and impaired cholinergic and doperminergic systems [12–14].

Plant-based bioactive phytochemicals such as polyphenols and alkaloids have shown promising neuroprotective potentials in both *in vitro* [15] and *in vivo* rat [16, 17] and *drosophila* models [18, 19]. Green leafy vegetables form a major constituent of local diets and are the major sources of plant bioactive phytochemicals. They are desired not only for their nutritional benefits but also for their medicinal properties as reported in folklore. Notable among them is African Jointfir (*Gnetum africanum)*. African Jointfir (AFJ) is a leafy vegetable desired in different African countries and especially south-eastern Nigeria (where it is commonly referred to as "Okazi") for its nourishment and medicinal properties [14, 20, 21]. The leaves are reported to be abundant in alkaloid phytochemicals [22] and has been used traditionally for treatment of several diseases such as fever, ulcer, and diabetes [23]. The leaves are consumed as spice and in preparation of soups and stews [24]. Furthermore, the hypolipidermic, hyperglycemic, anti-inflammatory, and antioxidant properties of this vegetable has been previously reported [25, 26]. This study, therefore, evaluated some of the biochemical mechanisms behind the protective properties of alkaloid extract of AFJ against manganese-induced neurotoxicity model in *D. melanogaster*.

2. Materials and Method

2.1. Sample Collection and Extraction of Crude Alkaloids Compounds. Fresh sample of African Jointfir (*Gnetum africanum)* leaves was sourced from local market in Akure, (South West) Nigeria, during the raining season (May) of 2017. The sample was identified and authenticated at the Department of Biology, Federal University of Technology, Akure, Nigeria (identification number: FUTA/BIO/404). The leaves were carefully separated, rinsed under running tap water, and dried for twenty days at room temperature (under shade) to constant weight. The pulverized sample was kept in an airtight container prior the extraction of the alkaloids.

2.2. Reagents. Chemical reagents such as acetylthiocholine iodide, thiobarbituric acid, sulphanilamide, reduced glutathione, DEPPD, DMSO, DPPH, trichloroacetic acid, and sodium acetate were sourced from Sigma-Aldrich (now Merck KGaA, Darmstadt, Germany). Hydrogen peroxide, methanol, acetic acid, hydrochloric acid, aluminium chloride, potassium acetate, sodium dodecyl sulphate, iron (II) sulphate, manganese chloride, potassium ferrycyanide, and ferric chloride were sourced from BDH Chemicals Ltd., (Poole, England). Except stated otherwise, all other chemicals and reagents were of analytical grades and the water was glass distilled.

2.3. Fruit Fly (Drosophila melanogaster) Culturing. Wild type fruit fly (Harwich strain) stock culture (originally from the National Species Stock Centre (Bowling Green, OH, USA)) was obtained from the Drosophila Laboratory, Department of Biochemistry, University of Ibadan, Oyo State. The flies were maintained and reared on a normal diet made up of corn meal medium containing 1% *w*/*v* brewer's yeast and 0.08% *v*/*w* nipagin at room temperature under 12 h dark/light cycle conditions in the Drosophila Research Laboratory, Functional Foods and Nutraceutical Unit, Federal University of Technology, Akure, Nigeria. All the experiments were carried out with the same *D. melanogaster* strain.

2.4. Alkaloid Extract Preparation. Alkaloid extract of the sample was prepared according to the method of Harborne [27], with slight modifications [28]. This involved extracting 10 g of the samples in 100 mL of 10% alcoholic-acetic acid for 24 hours. The mixture was subsequently filtered to obtain clear filtrate. The filtrate was concentrated under a vacuum at 45°C in a rotary evaporator (Laborota 4000 Efficient, Heidolph, Germany), which was followed by NH_3OH precipitation. The precipitate was collected as the crude alkaloid extract, dried thoroughly at 45°C and stored in the refrigerator at 4°C for all subsequent analysis. The yield of the extract obtained was 95 mg/g of dried leaf sample of African Jointfir. The extracts were dissolved in 1% DMSO for all subsequent analysis.

2.5. In Vitro Analysis

2.5.1. Cholinesterase Activity Assay. The effect of the alkaloid extract on AChE activity was assessed by the modified Ellman colorimetric method [29]. The reaction consisted of 135 μL of distilled water, 20 μL of 100 mM sodium phosphate buffer (pH 8.0), 20 μL of 10 mM DTNB, fly homogenate in 0.1 M phosphate buffer (pH 8.0) (see below for details of tissue homogenate preparation), appropriate dilutions of extract, and 20 μL of 8 mM acetylthiocholine iodide as initiator. The reaction was monitored for 5 min (15 s intervals) at 412 nm using a spectrophotometer. A negative control assay was conducted to include the extract and homogenate, without the substrate. The AChE activity was thereafter expressed as percentage inhibition of the reference (homogenate AChE activity in the absence of the extract).

2.5.2. Free Radical Scavenging Ability. The ability of the extract to scavenge free radicals using the DPPH model was assessed by the method of Gyamfi et al. [30] as previously reported [31] in a reaction mixture consisting of the extract (0-1 mL) and 1 mL of 0.4 mM methanolic-DPPH solution. This was followed by incubation in the dark for 30 min, and the absorbance was measured at 516 nm. The radical scavenging ability was expressed as percentage of the reference (reaction mixture excluding the extract).

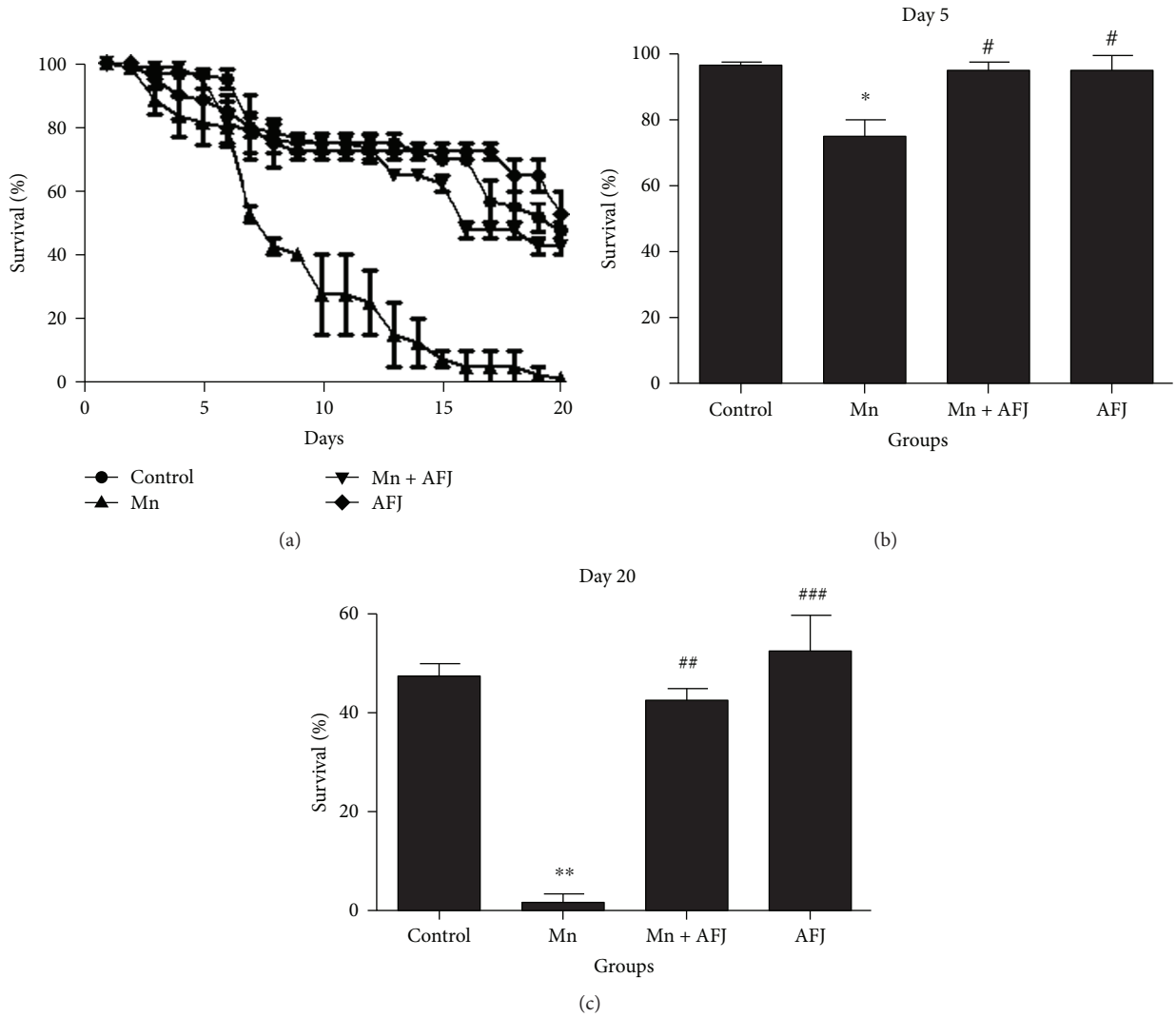

Figure 1: Effect of African Jointfir (AFJ) leaf alkaloid extract on: (a) survival, (b) day 5 survival rate, and (c) day 20 survival rate in Mn-induced toxicity in *Drosophila melanogaster*. Bars represent mean ± SEM. Mean values are significantly different at $P < 0.05^{*}$; $P < 0.01^{**}$ compared to control. Mean values are significantly different at $P < 0.05^{\#}$; $P < 0.01^{\#\#}$; $P < 0.001^{\#\#\#}$ compared to Mn-treated group.

2.5.3. Iron Chelation Assay. The chelating ability of the extract against iron was determined using the method of Puntel et al. [32]. An aliquot of 150 μL of 500 μM $FeSO_4$ which serve as the iron source was reacted with 168 μL 0.1 M Tris–HCl (pH 7.4), 218 μL saline, and the extract (0–25 μL). The reaction mixture was incubated for 5 min, before addition of 13 μL 0.25% 1, 10-phenanthroline (*w*/*v*). The absorbance was subsequently measured at 510 nm in a spectrophotometer. The Fe^{2+} chelating ability was expressed as percentage of the reference (reaction mixture excluding the extract).

2.6. In Vivo Analysis

2.6.1. Experimental Design. Harwich strain of *D. melanogaster* (both gender, 3–5 days old) was divided into 5 groups containing 50 flies each ($n = 3$). Group 1 was placed on a normal diet (without alkaloid), while groups 2–4 were placed on a diet containing 10 mM Mn (sourced as $MnCl_2$), Mn + AFJ alkaloid extract (final concentration of 2.5 mg/g of diet), and AFJ alkaloid extract alone, respectively. The flies were exposed to these treatments for 20 days and maintained at ambient temperature before being used for different assays. The choice of dose for Mn was based on preliminary survival study (data not shown) in which flies were exposed to varying concentrations of Mn (2–10 mM) supported by previously published data [14]. A preliminary study was conducted to ascertain that the dose of AFJ extract chosen and the vehicle (1% DMSO) showed no significant mortality to the flies (data not shown).

2.6.2. Lethality Response. The flies were observed daily for the incidence of mortality, and the survival rate was determined by counting the number of dead flies, while the survivors were transferred to a freshly prepared diet weekly. The data were subsequently analysed and plotted as cumulative mortality and percentage of live flies after the treatment period [13].

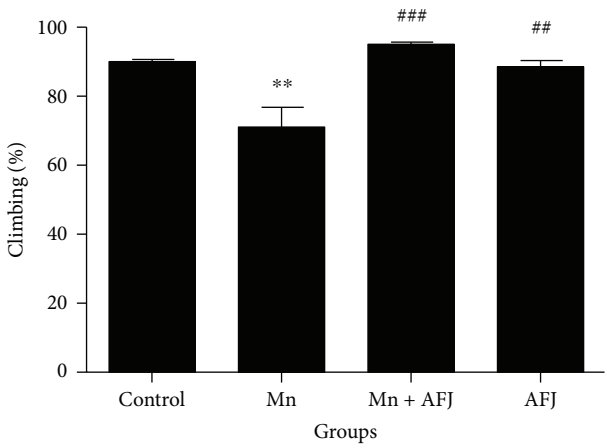

Figure 2: Effect of African Jointfir (AFJ) leaf alkaloid extract on: locomotor performance (climbing ability) in Mn-induced toxicity in *Drosophila melanogaster*. Bars represent mean ± SEM. Mean values are significantly different at $P < 0.01^{**}$ compared to control. Mean values are significantly different at $P < 0.01^{\#\#}$; $P < 0.001^{\#\#\#}$ compared to Mn-treated group.

2.6.3. Measurement of Locomotor Performance by Negative Geotaxis Assay. The negative geotaxis assay was used to evaluate the locomotor performance of flies [33]. In brief, after the treatment period of five days, the flies from each group were briefly immobilized in ice and transferred into a clean tube (11 cm in length and 3.5 cm in diameter) labelled accordingly. The flies were initially allowed to recover from immobilization for 10 min and thereafter were tapped at the bottom of the tubes. Observations that were made for the total number of flies that crossed the 6 cm line within a period of 6 s were recorded. The results are expressed as percentage of flies that escaped beyond a minimum distance of 6 cm in 6 s during three independent experiments.

2.6.4. Preparation of Tissue Homogenate. The flies were immobilized in ice and homogenized in 0.1 M phosphate buffer, pH 7.4. The resulting homogenates were centrifuged at 10,000 × g at 4°C for 10 minutes in a Kenxin refrigerated centrifuge Model KX3400C (KENXIN Intl. Co., Hong Kong). Subsequently, the supernatant was separated from the pellet into labelled Eppendorf microtubes and used for various biochemical assays.

2.7. Bioassays

2.7.1. Acetylcholinesterase (AChE) Activity Assay. AChE activity was assayed according to the method of Ellman [34], with slight modifications. The reaction mixture was made up of 195 μL of distilled water, 20 μL of 100 mM sodium phosphate buffer (pH 8.0), 20 μL of 10 mM DTNB, 5 μL of homogenate, and 20 μL of 8 mM acetylthiocholine (as initiator). Thereafter, reaction was monitored for 5 minutes (15-second intervals) at 412 nm. The AChE activity was thereafter calculated and expressed as mmolAcSch/h/mg protein.

2.7.2. Total Reactive Oxygen Species (ROS) Level. Total ROS level in the whole fly tissue homogenates was estimated as H_2O_2 equivalent according to a previously reported method [35], with slight modifications. The reaction mixture consist of 50 μL of tissue homogenate, 1400 μL of 0.1 M sodium acetate buffer (pH 4.8), and 1000 μL of reagent mixture of 6 mg/mL DEPPD and 4.37 μM of $FeSO_4$ dissolve in the sodium acetate buffer (1 : 25). The reaction was incubated at 37°C for 5 min, followed by absorbance measurement at 505 nm in a spectrophotometer. ROS levels were estimated from an H_2O_2 standard calibration curve and expressed as unit/mg protein, where 1 unit = 1 mg H_2O_2/L.

2.7.3. Measurement of Nitric Oxide (NO). NO content in the whole fly tissue homogenate was estimated using the Greiss reagent spectrophotometric based method [36] with slight modifications. Briefly, the reaction mixture consist of 150 μL of tissue homogenate, 50 μL of distilled water, and 600 μL of Greiss reagent (0.1% *N*-(1-naphthyl)-ethylenediamine dihydrochloride, 1% sulfanilamide, and 2.5% phosphoric acid). This was followed by 10 min incubation at room temperature in the dark and absorbance measurement at 540 nm. The concentration of nitrite and nitrate as a measure of NO level was determined from the sodium nitrate standard curve and expressed as μmol of NO/mg protein.

2.7.4. Determination of Total Protein. The Bradford method [37], with bovine serum albumin (BSA) as standard, was used to quantify the total protein content of fly homogenates.

2.8. GC-MS Characterization. A qualitative characterization analysis of possible compounds present in AFJ was carried out using GC-MS (using scan mode) as previously reported [28] with slight modifications. Briefly, an aliquot of samples (500 mg) was dissolved in 10 mL of methanol. Thereafter, the analysis was performed using 7890A gas chromatograph coupled to 5975C inert mass spectrometer with electron-impact source (Agilent Technologies). The stationary phase of separation of the compounds was HP-5MS capillary column coated with 5% phenyl methyl siloxane (30 m length × 0.32 mm diameter × 0.25 μm film thickness) (Agilent Technologies). The carrier gas was helium used at a constant flow of 1.0 mL/min at an initial nominal pressure of 19.6 MPa and average velocity of 33.425 cm/sec. An aliquot of the samples (1 μL) was injected in splitless mode at an injection temperature of 110°C. Purge flow was 3 mL/min with a total flow of 11.762 mL/min; gas saver mode was switched on. Oven was initially programmed at 110°C (2 min) then ramped at 10°C/min to 200°C (2 min) then 5°C/min to 280°C (9 min). Run time was 38 min with a 3 min solvent delay. The mass spectrometer was operated in electron ionization mode with ionization energy of 70 eV with ion source temperature of 230°C, quadrupole temperature of 150°C, and transfer line temperature of 280°C.

Prior to analysis, the MS was autotuned to perfluorotributylamine (PFTBA) using already established criteria to check the abundance of m/z 69, 219, 502, and other instrument optimal and sensitivity conditions.

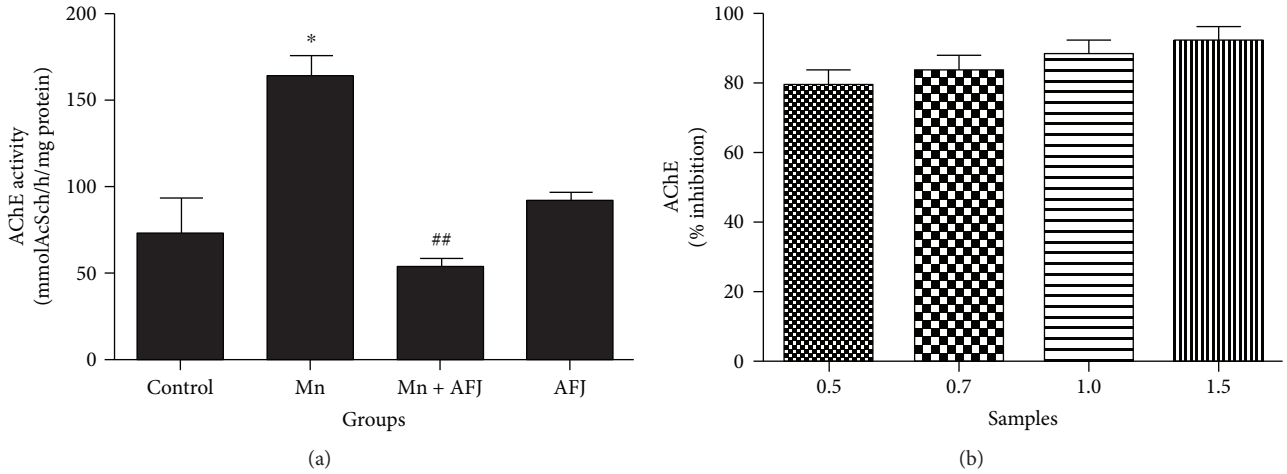

Figure 3: (a) Effect of African Jointfir (AFJ) leaf alkaloid extract on acetylcholinesterase (AChE) activity in Mn-induced toxicity in *Drosophila melanogaster*. (b) *In vitro* AChE inhibitory effect of AFJ leaf alkaloid extract. Bars represent mean ± SEM. Mean values are significantly different at $P < 0.05^{*}$ compared to control. Mean values are significantly different at $P < 0.01^{\#\#}$ compared to Mn-treated group.

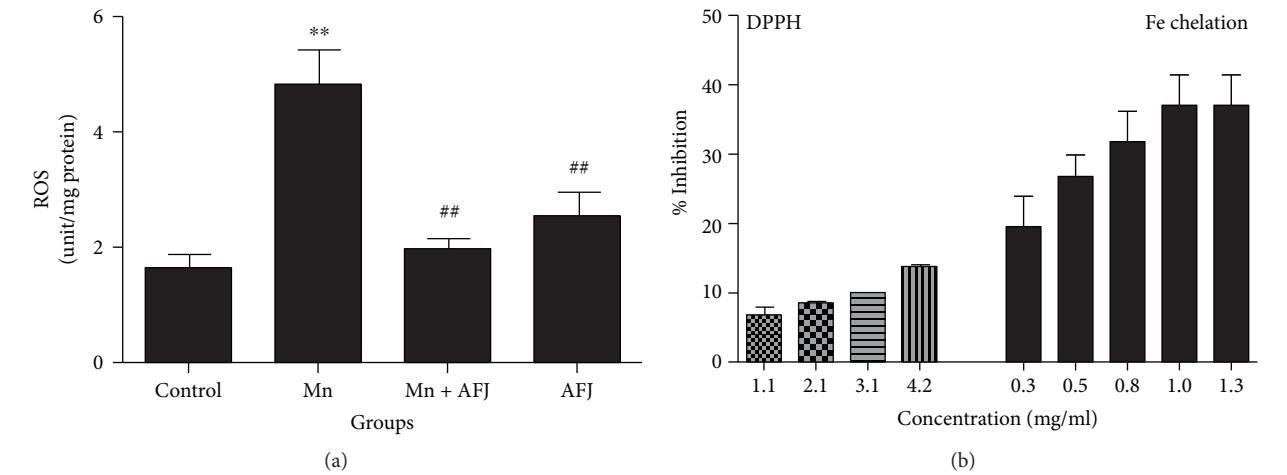

Figure 4: (a) Effect of African Jointfir (AFJ) leaf alkaloid extract on reactive oxygen species (ROS) level in Mn-induced toxicity in *Drosophila melanogaster*. (b) *In vitro* DPPH radical scavenging and Fe^{2+} chelating abilities of AFJ leaf alkaloid extract. Bars represent mean ± SEM. Mean values are significantly different at $P < 0.01^{**}$ compared to control. Mean values are significantly different at $P < 0.01^{\#\#}$ compared to Mn-treated group.

Analysis validation was conducted by running replicate samples in order to see the consistency of the constituent compound name, respective retention time, and molecular weight. These abundances were outputs from the *NIST 11 library search report* of the extracts constituents. Each compound identified via the NIST library search report has a corresponding mass spectrum showing the abundance of the possible numerous *m*/*z* peaks per compound.

2.9. Data Analysis. Data obtained were reported as mean ± standard error of mean (SEM) and appropriately analysed using one-way analysis of variance (ANOVA) with a subsequent Tukey's post hoc test (levels of significance were accepted at $p < 0.05$, $p < 0.01$, and $p < 0.001$). All statistical analysis was carried out using the software GraphPad PRISM (V.5.0).

3. Results and Discussion

In this present study, we assessed the mechanisms behind the protective ability of alkaloid extract of African Jointfir (AFJ) against manganese-induced neurotoxicity model in *D. melanogaster*. This study reveals that exposure of *D. melanogaster* to 10 mM of Mn for 20 days significantly ($P < 0.05$) reduced flies' survival rate (Figures 1(a)–1(c)) and locomotor performance (Figure 2). However, cotreatment with AFJ alkaloid extract significantly ameliorated the reduction in the survival rate and locomotor performance of Mn-induced flies. Previous studies have also reported that 10 mM Mn significantly reduced the survival rate and locomotor performance of *D. melanogaster*, and this could be associated with the cytotoxic effect of Mn [13]. Our findings also agree with earlier findings on the ability of plant alkaloid extracts to ameliorate Mn-

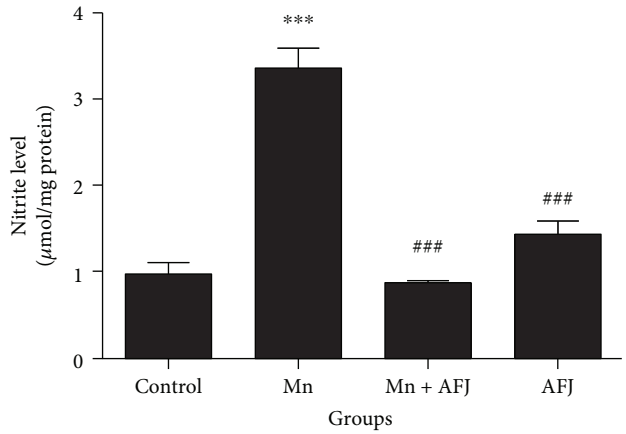

Figure 5: Effect of African Jointfir (AFJ) leaf alkaloid extract on: nitric oxide (NO) level in Mn-induced toxicity in *Drosophila melanogaster*. Bars represent mean ± SEM. Mean values are significantly different at $P < 0.001^{***}$ compared to control. Mean values are significantly different at $P < 0.001^{\#\#\#}$ compared to Mn-treated group.

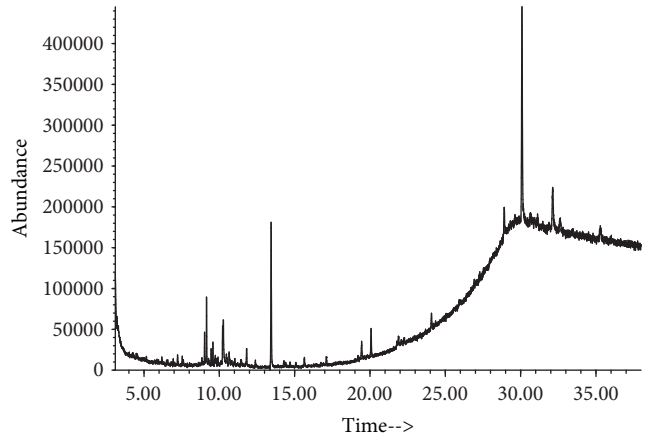

Figure 6: Total ion chromatogram (TIC) from GC-MS characterization of African Jointfir (*Gnetum africanum*) leaf alkaloid extract.

induced impairment in the locomotor performance and survival rate of *D. melanogaster* [14, 38]. Furthermore, it has also been reported that plant alkaloid extract ameliorated Mn-induced neurotoxicity in rats [39, 40].

Our findings showed that AFJ exhibit AChE inhibitory effect (*in vitro*) concentration dependently (Figure 3(b)) and also significantly ameliorate the elevation in the activity of AChE induced by Mn *in vivo* in Drosophila (Figure 3(a)). AChE catalyses the hydrolysis of acetylcholine to acetate and choline, thus regulating the cholinergic neuronal function [7]. Acetylcholine as a neurotransmitter is essential to regulate cognitive function, learning/memory, motor function, and locomotion [41]. Neurotoxic levels of Mn have been reported to impair the cholinergic system which is associated with Mn-induced impairments of motor function, locomotion, and cognitive dysfunction [41]. Therefore, as demonstrated in this present study, the increase in AChE activity after five days of exposure to Mn correlates to the significant decrease in their climbing abilities. The impairment observed in the climbing ability of the flies could be associated with a decrease in bioavailability of acetylcholine available for cholinergic neurotransmission [13, 42]. This phenomenon has been reported as a major risk factor in the development and progression of dementia [7]. Also, our findings are in agreement with earlier reports that short-term administration of Mn brought about a significant elevation in rat brain AChE activity [43, 44]. Another study revealed that exposure of rat to Mn caused an elevation in AChE activity in their serum and brain [45]. Consequently, the ability of AFJ alkaloid extract to ameliorate Mn-induced elevated AChE activity in flies, as well as increase the climbing ability of Mn-treated flies could suggest one of the mechanisms behind the protective effect of the extract against Mn-induced toxicity. In agreement with previous findings, anticholinesterase properties of plant extract have been substantially linked to their constituent phytochemicals including alkaloids; alkaloid extracts exhibit cholinesterase inhibitory properties *in vitro* [46, 47]. Konrath et al. reported that alkaloid extracts from Lycopodiaceae species from South America exhibited anticholinesterase activities *in vitro* and *in vivo* in the cerebral cortex, striatum, and hippocampus of rats following acute administration [48]. In addition, plant-derived alkaloids such as berberine, caffeine, evodiamine, isorhynchophylline, tetramethylpyrazine, and trigonelline have also been reported to show neuroprotective properties in various experimental models and are often associated with their anticholinesterase, antioxidant, and anti-inflammatory properties [49–54]. Therefore, AFJ alkaloid extracts also present a source of potent neuroprotective alkaloids. Generally, plant alkaloids are being promoted as drug leads for the management of neurodegenerative diseases owing to a number of their therapeutic mechanisms including anticholinesterase properties [55].

Earlier findings have implicated oxidative stress in Mn-induced neurotoxicity [13, 56, 57]. Oxidative stress, a consequence of ROS overload which cannot be effectively counteracted by the antioxidant defence mechanisms and hence, initiating cellular damage [58, 59]. In physiological systems, antioxidant enzymes including catalase, superoxide dismutase, and glutathione peroxidase are involved in preventing free radical overload and consequent oxidative stress. Results from this study showed that flies exposed to Mn exhibited a significant elevation in ROS level (Figure 4(a)) which is an indicator of oxidative stress. This is in agreement with earlier report on elevation of ROS level following Mn-induced toxicity in *Drosophila* [13, 60, 61]. However, cotreatment with AFJ alkaloid extract significantly ameliorated ROS level in Mn-intoxicate flies. This observation could be associated with the antioxidant properties of AFJ extract which can be further substantiated by their DPPH free radical scavenging and Fe^{2+} chelating abilities (Figure 4(b)). DPPH scavenging ability and Fe^{2+} chelation are two common assays carried out to assess the antioxidant potential of a test compound. Previous studies have shown that plant alkaloid extracts exhibit antioxidant properties which have been associated with their neuroprotective potentials [62]. The Fe^{2+} chelating

Table 1: Possible compounds from GC-MS characterization of African Jointfir (*Gnetum africanum*) leaf alkaloid extract.

S/N	Possible structure	RT (min)*	Molecular formula	MW**	Exact mass (g/mol)	CAS number	EN***
1	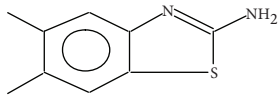	9.158	$[C_9H_{10}N_2S]$	178	178.056469	29927-08-0	291167
2	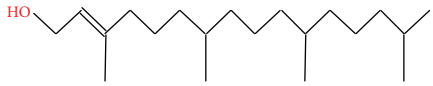	13.438	$[C_{20}H_{40}O]$	296	296.307917	150-86-7	375015

*RT (min) = retention time (min); **MW = molecular weight (g/mol); ***entry number in NIST 11 library.

ability of the extract in this study could be of significant therapeutic importance; first, excessive accumulation of Fe^{2+} could trigger chain redox reactions especially the Fenton reaction which can initiate the generation of cytotoxic ROS. Secondly, the chemical similarities between Mn and Fe have suggested that the neurotoxic effect of Mn is mediated by competing with Fe for "nonredox" domains in proteins [63]. Therefore, therapeutic agents with Fe chelating abilities are shown to be promising in ameliorating Mn-induced toxicity [41].

This study also shows that Mn was able to significantly elevate NO level in flies (Figure 5). This is similar to previous study which reported that Mn-induced toxicity caused elevation in NO level in rat brain cerebral cortex [2]. Nitric oxide is a diffusible signalling molecule in the nervous system of both vertebrates and insects [64]. In *D. melanogaster*, NO has been shown to mediate in cell proliferation and differentiation during fly developmental stages [65, 66]. NO also mediates in immune responses of the flies to pathogens and parasites [67, 68]. Generally, NO is reported to act as a proinflammatory mediator in which there is NO synthesis by inducible nitric oxide synthase (iNOS) that is significantly elevated [69]. Consequently, the ability of AFJ alkaloid extract to significantly ameliorate Mn-induced elevation in NO level in flies could suggest its potential anti-inflammatory property. In Figure 6 and Table 1, the result of the GC-MS characterization was presented, and the molecular structure of possible compounds in the extract were determined; this however demands further studies to fully elucidate the precise structural composition of constituent alkaloids in the extract for further pharmacological investigations.

Conclusion can therefore be drawn from this present study that alkaloid extract of AFJ was able to protect against manganese-induced toxicity by mechanisms including reducing oxidative stress, repressing AChE activity and pro-inflammatory mediator NO, and a consequent increase in climbing and locomotion activities in *Drosophila melanogaster*. Therefore, AFJ alkaloid extract could represent a novel source of neuroprotective compounds.

Abbreviations

AChE: Acetylcholinesterase
AFJ: African Jointfir
AD: Alzheimer's disease
DEPPD: *N,N*-diethyl-*para*-phenylenediamine
DPPH: 1,1-diphenyl–2 picrylhydrazyl
DMSO: Dimethyl sulfoxide
NO: Nitric oxide
PD: Parkinson's disease
ROS: Reactive oxygen species.

Data Availability

The data used to support the findings of this study are available from the corresponding author upon request.

Conflicts of Interest

The authors declare that they have no conflicts of interest.

Acknowledgments

This research was funded by The World Academy of Sciences (TWAS) Grant No: 16-500 RG/CHE/AF/AC_G – FR3240293300.

References

[1] R. B. Hernández, M. Farina, B. P. Espósito, N. C. Souza-Pinto, F. Barbosa Jr., and C. Suñol, "Mechanisms of manganese-induced neurotoxicity in primary neuronal cultures: the role of manganese speciation and cell type," *Toxicological Sciences*, vol. 124, no. 2, pp. 414–423, 2011.

[2] Y. Chtourou, H. Fetoui, M. Sefi et al., "Silymarin, a natural antioxidant, protects cerebral cortex against manganese-induced neurotoxicity in adult rats," *BioMetals*, vol. 23, no. 6, pp. 985–996, 2010.

[3] O. Bar-Am, T. Amit, L. Kupershmidt et al., "Neuroprotective and neurorestorative activities of a novel iron chelator-brain selective monoamine oxidase-A/monoamine oxidase-B inhibitor in animal models of Parkinson's disease and aging," *Neurobiology of Aging*, vol. 36, no. 3, pp. 1529–1542, 2015.

[4] J. L. Cummings, "Alzheimer's disease," *The New England Journal of Medicine*, vol. 351, no. 1, pp. 56–67, 2004.

[5] C. Humpel, "Chronic mild cerebrovascular dysfunction as a cause for Alzheimer's disease?," *Experimental Gerontology*, vol. 46, no. 4, pp. 225–232, 2011.

[6] E. E. Nwanna, S. I. Oyeleye, O. B. Ogunsuyi, G. Oboh, A. A. Boligon, and M. L. Athayde, "In vitro neuroprotective properties of some commonly consumed green leafy vegetables in Southern Nigeria," *NFS Journal*, vol. 2, pp. 19–24, 2016.

[7] H. W. Klafki, M. Staufenbiel, J. Kornhuber, and J. Wiltfang, "Therapeutic approaches to Alzheimer's disease," *Brain*, vol. 129, no. 11, pp. 2840–2855, 2006.

[8] M. D. Adams, S. E. Celniker, R. A. Holt et al., "The genome sequence of *Drosophila melanogaster*," *Science*, vol. 287, no. 5461, pp. 2185–2195, 2000.

[9] L. T. Reiter, L. Potocki, S. Chien, M. Gribskov, and E. Bier, "A systematic analysis of human disease-associated gene sequences in *Drosophila melanogaster*," *Genome Research*, vol. 11, no. 6, pp. 1114–1125, 2001.

[10] L. Bonilla-Ramirez, M. Jimenez-Del-Rio, and C. Velez-Pardo, "Acute and chronic metal exposure impairs locomotion activity in *Drosophila melanogaster*: a model to study Parkinsonism," *BioMetals*, vol. 24, no. 6, pp. 1045–1057, 2011.

[11] K. Prüßing, A. Voigt, and J. B. Schulz, "*Drosophila melanogaster* as a model organism for Alzheimer's disease," *Molecular Neurodegeneration*, vol. 8, no. 1, p. 35, 2013.

[12] A. Benedetto, C. Au, and M. Aschner, "Manganese-induced dopaminergic neurodegeneration: insights into mechanisms and genetics shared with Parkinson's disease," *Chemical Reviews*, vol. 109, no. 10, pp. 4862–4884, 2009.

[13] I. A. Adedara, A. O. Abolaji, J. B. T. Rocha, and E. O. Farombi, "Diphenyl diselenide protects against mortality, locomotor deficits and oxidative stress in *Drosophila melanogaster* model of manganese-induced neurotoxicity," *Neurochemical Research*, vol. 41, no. 6, pp. 1430–1438, 2016.

[14] M. C. Bianchini, C. O. A. Gularte, D. F. Escoto et al., "*Peumus boldus* (Boldo) aqueous extract present better protective effect than boldine against manganese-induced toxicity in *D. melanogaster*," *Neurochemical Research*, vol. 41, no. 10, pp. 2699–2707, 2016.

[15] S. F. Akomolafe, G. Oboh, A. A. Akindahunsi, A. J. Akinyemi, and O. G. Tade, "Inhibitory effect of aqueous extract of stem bark of *Cissus populnea* on ferrous sulphate- and sodium nitroprusside-induced oxidative stress in rat's testes in vitro," *ISRN Pharmacology*, vol. 2013, Article ID 130989, 7 pages, 2013.

[16] T. P. Stringer, D. Guerrieri, C. Vivar, and H. van Praag, "Plant-derived flavanol (−)epicatechin mitigates anxiety in association with elevated hippocampal monoamine and BDNF levels, but does not influence pattern separation in mice," *Translational Psychiatry*, vol. 5, no. 1, article e493, 2015.

[17] G. Oboh, O. B. Ogunsuyi, and O. E. Olonisola, "Does caffeine influence the anticholinesterase and antioxidant properties of donepezil? Evidence from in vitro and in vivo studies," *Metabolic Brain Disease*, vol. 32, no. 2, pp. 629–639, 2017.

[18] A. J. Akinyemi, G. Oboh, O. Ogunsuyi, A. O. Abolaji, and A. Udofia, "Curcumin-supplemented diets improve antioxidant enzymes and alter acetylcholinesterase genes expression level in *Drosophila melanogaster* model," *Metabolic Brain Disease*, vol. 33, no. 2, pp. 369–375, 2018.

[19] A. O. Abolaji, O. V. Babalola, A. K. Adegoke, and E. O. Farombi, "Hesperidin, a citrus bioflavonoid, alleviates trichloroethylene-induced oxidative stress in *Drosophila melanogaster*," *Environmental Toxicology and Pharmacology*, vol. 55, pp. 202–207, 2017.

[20] E. E. J. Iweala and A. O. Osundiya, "Biochemical, haematological and histological effects of dietary supplementation with leaves of *Gnetum africanum* Welw. on paracetamol-induced hepatotoxicity in rats," *International Journal of Pharmacology*, vol. 6, no. 6, pp. 872–879, 2010.

[21] R. U. Ebana, A. I. Essien, and O. D. Ekpa, "Nutritional and potential medicinal value of the leaves of *Lasianthera africana* (Beauv)," *Global Journal of Pure and Applied Sciences*, vol. 1, pp. 1–7, 1995.

[22] E. U. Onyeka and I. O. Nwambekwe, "Phytochemical profile of some green leafy vegetables in South East, Nigeria," *Nigerian Food Journal*, vol. 25, no. 1, pp. 67–76, 2007.

[23] J. E. Okokon, B. S. Antia, and G. A. Essiet, "Evaluation of in vivo antiplasmodial activity of ethanolic leaf extract of *Lasianthera africana*," *Research Journal of Pharmacology*, vol. 1, no. 2, pp. 30–33, 2007.

[24] A. F. Eleyinmi, "Chemical composition and antibacterial activity of *Gongronema latifolium*," *Journal of Zhejiang University SCIENCE B*, vol. 8, no. 5, pp. 352–358, 2007.

[25] O. Morebise, M. A. Fafunso, J. M. Makinde, O. A. Olajide, and E. O. Awe, "Antiinflammatory property of the leaves of *Gongronema latifolium*," *Phytotherapy Research*, vol. 16, no. S1, pp. 75–77, 2002.

[26] O. O. Ogundipe, J. O. Moody, T. O. Akinyemi, and A. Raman, "Hypoglycemic potentials of methanolic extracts of selected plant foods in alloxanized mice," *Plant Foods for Human Nutrition*, vol. 58, no. 3, pp. 1–7, 2003.

[27] A. J. Harborne, "Phytochemical methods a guide to modern techniques of plant analysis," Springer, 1998.

[28] A. O. Ademiluyi, O. B. Ogunsuyi, G. Oboh, and O. J. Agbebi, "Jimson weed (*Datura stramonium* L.) alkaloid extracts modulate cholinesterase and monoamine oxidase activities in vitro: possible modulatory effect on neuronal function," *Comparative Clinical Pathology*, vol. 25, no. 4, pp. 733–741, 2016.

[29] A. J. Akinyemi, G. Oboh, S. I. Oyeleye, and O. Ogunsuyi, "Anti-amnestic effect of curcumin in combination with donepezil, an anticholinesterase drug: involvement of cholinergic system," *Neurotoxicity Research*, vol. 31, no. 4, pp. 560–569, 2017.

[30] M. A. Gyamfi, M. Yonamine, and Y. Aniya, "Free-radical scavenging action of medicinal herbs from Ghana: Thonningia sanguinea *on experimentally-induced liver injuries*," *General Pharmacology: The Vascular System*, vol. 32, no. 6, pp. 661–667, 1999.

[31] S. F. Akomolafe, A. J. Akinyemi, O. B. Ogunsuyi et al., "Effect of caffeine, caffeic acid and their various combinations on enzymes of cholinergic, monoaminergic and purinergic systems critical to neurodegeneration in rat brain—in vitro," *NeuroToxicology*, vol. 62, pp. 6–13, 2017.

[32] R. L. Puntel, C. W. Nogueira, and J. B. T. Rocha, "Krebs cycle intermediates modulate thiobarbituric acid reactive species (TBARS) production in rat brain in vitro," *Neurochemical Research*, vol. 30, no. 2, pp. 225–235, 2005.

[33] E. Le Bourg and F. A. Lints, "Hypergravity and aging in *Drosophila melanogaster*. 4. Climbing activity," *Gerontology*, vol. 38, no. 1-2, pp. 59–64, 1992.

[34] G. L. Ellman, "Tissue sulfhydryl groups," *Archives of Biochemistry and Biophysics*, vol. 82, no. 1, pp. 70–77, 1959.

[35] I. Hayashi, Y. Morishita, K. Imai, M. Nakamura, K. Nakachi, and T. Hayashi, "High-throughput spectrophotometric assay of reactive oxygen species in serum," *Mutation Research*, vol. 631, no. 1, pp. 55–61, 2007.

[36] K. Soni and M. Parle, "*Trachyspermum ammi* seeds supplementation helps reverse scopolamine, alprazolam and electroshock induced amnesia," *Neurochemical Research*, vol. 42, no. 5, pp. 1333–1344, 2017.

[37] M. M. Bradford, "A rapid and sensitive method for the quantitation of microgram quantities of protein utilizing the

principle of protein-dye binding," *Analytical Biochemistry*, vol. 72, no. 1-2, pp. 248–254, 1976.

[38] G. F. Kwakye, R. A. McMinimy, and M. Aschner, "Disease-toxicant interactions in Parkinson's disease neuropathology," *Neurochemical Research*, vol. 42, no. 6, pp. 1772–1786, 2017.

[39] R. I. Nadeem, H. I. Ahmed, and B. M. El-Sayeh, "Protective effect of vinpocetine against neurotoxicity of manganese in adult male rats," *Naunyn-Schmiedeberg's Archives of Pharmacology*, vol. 391, no. 7, pp. 729–742, 2018.

[40] M. A. Rao, M. N. Palaksha, K. N. Sirisha, V. L. Bhargavi, and P. Manikandhar, "Effect of *Aerva lanata* on cisplatin induced neurotoxicity in rats," *World Journal of Pharmacy and Pharmaceutical Sciences*, vol. 3, no. 2, pp. 2431–2451, 2014.

[41] T. V. Peres, M. R. C. Schettinger, P. Chen et al., "Manganese-induced neurotoxicity: a review of its behavioral consequences and neuroprotective strategies," *BMC Pharmacology and Toxicology*, vol. 17, no. 1, p. 57, 2016.

[42] P. S. Oliveira, V. C. Chaves, N. P. Bona et al., "*Eugenia uniflora* fruit (red type) standardized extract: a potential pharmacological tool to diet-induced metabolic syndrome damage management," *Biomedicine & Pharmacotherapy*, vol. 92, pp. 935–941, 2017.

[43] C. Liapi, A. Zarros, P. Galanopoulou et al., "Effects of short-term exposure to manganese on the adult rat brain antioxidant status and the activities of acetylcholinesterase, (Na^+,K^+)-ATPase and Mg^{2+}-ATPase: modulation by L-cysteine," *Basic & Clinical Pharmacology & Toxicology*, vol. 103, no. 2, pp. 171–175, 2008.

[44] Y. Chtourou, H. Fetoui, E. M. Garoui, T. Boudawara, and N. Zeghal, "Improvement of cerebellum redox states and cholinergic functions contribute to the beneficial effects of silymarin against manganese-induced neurotoxicity," *Neurochemical Research*, vol. 37, no. 3, pp. 469–479, 2012.

[45] M. A. Lebda, M. S. El-Neweshy, and Y. S. El-Sayed, "Neurohepatic toxicity of subacute manganese chloride exposure and potential chemoprotective effects of lycopene," *NeuroToxicology*, vol. 33, no. 1, pp. 98–104, 2012.

[46] N. Cortes, R. Alvarez, E. H. Osorio, F. Alzate, S. Berkov, and E. Osorio, "Alkaloid metabolite profiles by GC/MS and acetylcholinesterase inhibitory activities with binding-mode predictions of five Amaryllidaceae plants," *Journal of Pharmaceutical and Biomedical Analysis*, vol. 102, pp. 222–228, 2015.

[47] C. L. Cespedes, C. Balbontin, J. G. Avila et al., "Inhibition on cholinesterase and tyrosinase by alkaloids and phenolics from *Aristotelia chilensis* leaves," *Food and Chemical Toxicology*, vol. 109, Part 2, pp. 984–995, 2017.

[48] E. L. Konrath, B. M. Neves, P. S. Lunardi et al., "Investigation of the in vitro and ex vivo acetylcholinesterase and antioxidant activities of traditionally used *Lycopodium* species from South America on alkaloid extracts," *Journal of Ethnopharmacology*, vol. 139, no. 1, pp. 58–67, 2012.

[49] S. K. Kulkarni and A. Dhir, "Berberine: a plant alkaloid with therapeutic potential for central nervous system disorders," *Phytotherapy Research*, vol. 24, no. 3, pp. 317–324, 2010.

[50] J. Y. Zhou and S. W. Zhou, "Isorhynchophylline: a plant alkaloid with therapeutic potential for cardiovascular and central nervous system diseases," *Fitoterapia*, vol. 83, no. 4, pp. 617–626, 2012.

[51] J. Zhou, L. Chan, and S. Zhou, "Trigonelline: a plant alkaloid with therapeutic potential for diabetes and central nervous system disease," *Current Medicinal Chemistry*, vol. 19, no. 21, pp. 3523–3531, 2012.

[52] G. Huang, B. Kling, F. H. Darras, J. Heilmann, and M. Decker, "Identification of a neuroprotective and selective butyrylcholinesterase inhibitor derived from the natural alkaloid evodiamine," *European Journal of Medicinal Chemistry*, vol. 81, pp. 15–21, 2014.

[53] M. Kim, S. O. Kim, M. Lee et al., "Tetramethylpyrazine, a natural alkaloid, attenuates pro-inflammatory mediators induced by amyloid β and interferon-γ in rat brain microglia," *European Journal of Pharmacology*, vol. 740, pp. 504–511, 2014.

[54] G. Oboh, A. J. Akinyemi, A. O. Ademiluyi, and F. O. Bello, "Inhibitory effect of some tropical green leafy vegetables on key enzymes linked to Alzheimer's disease and some pro-oxidant induced lipid peroxidation in rats' brain," *Journal of Food Science and Technology*, vol. 51, no. 5, pp. 884–891, 2014.

[55] Y. P. Ng, T. C. T. Or, and N. Y. Ip, "Plant alkaloids as drug leads for Alzheimer's disease," *Neurochemistry International*, vol. 89, pp. 260–270, 2015.

[56] D. S. Ávila, D. Colle, P. Gubert et al., "A possible neuroprotective action of a vinylic telluride against Mn-induced neurotoxicity," *Toxicological Sciences*, vol. 115, no. 1, pp. 194–201, 2010.

[57] E. N. Martins, N. T. C. Pessano, L. Leal et al., "Protective effect of *Melissa officinalis* aqueous extract against Mn-induced oxidative stress in chronically exposed mice," *Brain Research Bulletin*, vol. 87, no. 1, pp. 74–79, 2012.

[58] M. Valko, D. Leibfritz, J. Moncol, M. T. D. Cronin, M. Mazur, and J. Telser, "Free radicals and antioxidants in normal physiological functions and human disease," *The International Journal of Biochemistry & Cell Biology*, vol. 39, no. 1, pp. 44–84, 2007.

[59] E. O. Farombi, I. A. Adedara, A. B. Oyenihi, E. Ekakitie, and S. Kehinde, "Hepatic, testicular and spermatozoa antioxidant status in rats chronically treated with *Garcinia kola*seed," *Journal of Ethnopharmacology*, vol. 146, no. 2, pp. 536–542, 2013.

[60] M. Mora, E. Bonilla, S. Medina-Leendertz, Y. Bravo, and J. L. Arcaya, "Minocycline increases the activity of superoxide dismutase and reduces the concentration of nitric oxide, hydrogen peroxide and mitochondrial malondialdehyde in manganese treated *Drosophila melanogaster*," *Neurochemical Research*, vol. 39, no. 7, pp. 1270–1278, 2014.

[61] G. Mohandas, S. V. Rao, Muralidhara, and P. S. Rajini, "Whey protein isolate enrichment attenuates manganese-induced oxidative stress and neurotoxicity in *Drosophila melanogaster*. Relevance to Parkinson's disease," *Biomedicine & Pharmacotherapy*, vol. 95, pp. 1596–1606, 2017.

[62] E. E. Nwanna, A. A. Adebayo, G. Oboh, O. B. Ogunsuyi, and A. O. Ademosun, "Modulatory effects of alkaloid extract from Gongronema latifolium (Utazi) and Lasianthera africana (Editan) on activities of enzymes relevant to neurodegeneration," *Journal of dietary supplements*, pp. 1–13, 2018.

[63] M. Farina, D. S. Avila, J. B. T. da Rocha, and M. Aschner, "Metals, oxidative stress and neurodegeneration: a focus on iron, manganese and mercury," *Neurochemistry International*, vol. 62, no. 5, pp. 575–594, 2013.

[64] U. Müller, "The nitric oxide system in insects," *Progress in Neurobiology*, vol. 51, no. 3, pp. 363–381, 1997.

[65] G. Enikolopov, J. Banerji, and B. Kuzin, "Nitric oxide and *Drosophila* development," *Cell Death & Differentiation*, vol. 6, no. 10, pp. 956–963, 1999.

[66] J. S. Jaszczak, J. B. Wolpe, A. Q. Dao, and A. Halme, "Nitric oxide synthase regulates growth coordination during *Drosophila melanogaster* imaginal disc regeneration," *Genetics*, vol. 200, no. 4, pp. 1219–1228, 2015.

[67] A. J. Nappi, E. Vass, F. Frey, and Y. Carton, "Nitric oxide involvement in *Drosophila* immunity," *Nitric Oxide*, vol. 4, no. 4, pp. 423–430, 2000.

[68] I. Eleftherianos, K. More, S. Spivack, E. Paulin, A. Khojandi, and S. Shukla, "Nitric oxide levels regulate the immune response of *Drosophila melanogaster* reference laboratory strains to bacterial infections," *Infection and Immunity*, vol. 82, no. 10, pp. 4169–4181, 2014.

[69] E. O. Farombi, A. O. Abolaji, T. H. Farombi, A. S. Oropo, O. A. Owoje, and M. T. Awunah, "*Garcinia kola* seed biflavonoid fraction (Kolaviron), increases longevity and attenuates rotenone-induced toxicity in *Drosophila melanogaster*," *Pesticide Biochemistry and Physiology*, vol. 145, pp. 39–45, 2018.

Hindawi
Oxidative Medicine and Cellular Longevity
Volume 2018, Article ID 2131895, 12 pages
https://doi.org/10.1155/2018/2131895

Research Article

Anacardium microcarpum Promotes Neuroprotection Dependently of AKT and ERK Phosphorylation but Does Not Prevent Mitochondrial Damage by 6-OHDA

Illana Kemmerich Martins,[1] Nélson Rodrigues de Carvalho,[1,2] Giulianna Echeverria Macedo,[1] Nathane Rosa Rodrigues,[1,3] Cynthia Camila Ziech,[1] Lúcia Vinadé,[1] Valter Menezes Barbosa Filho,[4] Irwin Alencar Menezes,[4] Jeferson Franco,[1] and Thaís Posser[1]

[1]*Oxidative Stress and Cell Signaling Research Group, Centro Interdisciplinar de Pesquisa em Biotecnologia, Universidade Federal do Pampa, Campus São Gabriel, 97300-000 São Gabriel, RS, Brazil*
[2]*Instituto Federal Farroupilha, Campus Santo Ângelo, 98806-700 Santo Ângelo, RS, Brazil*
[3]*Departamento de Química, Programa de Pós-Graduação em Bioquímica Toxicológica, Universidade Federal de Santa Maria, 97105-900 Santa Maria, RS, Brazil*
[4]*Departamento de Química Biológica, Universidade Regional do Cariri, 63100-000 Crato, CE, Brazil*

Correspondence should be addressed to Thaís Posser; thaisposser@unipampa.edu.br

Received 12 June 2018; Revised 11 August 2018; Accepted 18 August 2018; Published 29 October 2018

Academic Editor: Francisco Jaime Bezerra Mendonça Júnior

Parkinson's disease is a degenerative and progressive illness characterized by the degeneration of dopaminergic neurons. 6-hydroxydopamine (6-OHDA) is a widespread model for induction of molecular and behavioral alterations similar to Parkinson and has contributed for testing of compounds with neuroprotective potential. The Brazilian plant *Anacardium microcarpum* is used in folk medicine for treatment of several illnesses; however, the knowledge about toxicology and biological effects for this plant is very rare. The neuroprotective effect from hydroalcoholic extract and methanolic and acetate fraction of *A. microcarpum* on 6-OHDA-induced damage on chicken brain slices was investigated in this study. 6-OHDA decreased cellular viability measured by MTT reduction assay, induced lipid peroxidation by HPLC, stimulated Glutathione-S-Transferase and Thioredoxin Reductase activity, and decreased Glutathione Peroxidase activity and the total content of thiols containing compounds. The methanolic fraction of *A. microcarpum* presented the better neuroprotective effects in 6-OHDA-induced damage in relation with hydroalcoholic and acetate fraction. The presence of AKT and ERK1/2 pharmacological inhibitors blocked the protective effect of methanolic fraction suggesting the involvement of survival pathways in the neuroprotection by the plant. The plant did not prevent 6-OHDA autoxidation or 6-OHDA-induced mitochondrial dysfunction. Thus, the neuroprotective effect of the methanolic fraction of *A. microcarpum* appears to be attributed in part to chelating properties of extract toward reactive species and is dependent on ERK1/2 and AKT phosphorylation. This study contributes to the understanding of biochemical mechanisms implied in neuroprotective effects of the vegetal species *A. microcarpum.*

1. Introduction

The Brazilian plant *Anacardium microcarpum*, popularly known as "cajui," belongs to the Anacardiaceae family. It is found in the Northeast Region of Brazil and is used in traditional folk medicine for treatment of infectious diseases, inflammation, rheumatism, and tumor. Phytochemical constitution of *A. microcarpum* stem bark crude extract and fractions demonstrating the presence of different flavonoids such as gallic acid, caffeic acid, and quercetin [1].

Although a limited number of studies on this plant is available, our group demonstrated *in vitro* antioxidant potential and antibacterial effect of this plant [2].

Parkinson's disease (PD), which was described by James Parkinson in 1817, is the second most frequent neurodegenerative disease after Alzheimer's disease and is characterized by a progressive nigrostriatal neurodegeneration. This illness reaches all ethnic groups and socioeconomic classes and is present in approximately 1% of the world population over the 60s [3]. PD symptoms include resting tremor, stiffness, bradykinesia, and gait impairment [4]. The symptoms onset indicates an advanced stage of disease, with a substantial loss of dopaminergic cells in the substantia nigra and an 80% depletion of striatum dopamine [5]. It is known that genetic, environmental, and aging factors contribute to the progression of disease [6]. Moreover, biochemical factors such as oxidative stress, mitochondrial dysfunction, inflammation, and apoptotic cell death play important roles in the pathogenesis of PD [7, 8].

Substances able to damage selectively dopaminergic neurons are useful tools to study molecular mechanisms implied in neurodegeneration in PD and for screening of neuroprotective potential of chemicals. Among those substances are MPTP, paraquat, rotenone, and 6-hydroxydopamine [9].

6-hydroxydopamine (6-OHDA) is a toxic dopamine metabolite which is rapidly and nonenzymatically oxidized by molecular oxygen to form *p*-quinone and hydrogen peroxide [10] and is proposed as a putative neurotoxic factor contributing for PD pathogenesis. The induction of reactive oxygen species (ROS) formation is a major mechanism implied in neurotoxicity of 6-OHDA. Some characteristics of the brain tissue make it very susceptible to oxidative stress such as the elevated consumption of oxygen, high content of unsaturated fatty acids, and iron levels [11].

The most effective drug in the treatment of PD is L-DOPA; however, its frequent use is associated with neurotoxicity once L-DOPA gives rise to 6-OHDA via nonenzymatic reactions [12]. It is important to consider that the therapies available for PD delay the progression of degeneration and symptoms instead of providing an effective treatment for the disease. Thus, the search for alternative therapies such as natural antioxidants has grown greatly over the years; besides, there are evidence that plant extracts have beneficial potential, attenuating the progression of PD, through antioxidant compounds present in extracts [13–15]. The model of brain slices has provided an important contribution for detailing of brain circuits and neurochemical mechanisms and testing of the neuroprotective potential of compounds. The main factor why this model is considered appropriate for studying biochemical events in the brain is the maintenance of extracellular matrix, neuronal connectivity, and neuronal-glial interactions [16].

This study is aimed at evaluating the neuroprotective potential and the mechanisms that mediate the neuroprotection of *A. microcarpum* hydroalcoholic extract (AMHE), methanolic (AMMF), and ethyl acetate (AMEAF) fractions against 6-hydroxydopamine- (6-OHDA-) induced damage on cortical slices.

2. Materials and Methods

2.1. Chemicals. Dimetil sulfoxide (DMSO), Folin-Ciocalteu, 2,2′-azino-bis(3-ethylbenzothiazoline-6-sulfonic acid diammonium salt, sodium acetate, HEPES minimum 99.5% titration, albumin from bovine serum (BSA), reduced glutathione (GSH), oxidized glutathione, tetramethylethylenediamine (TEMED), 3-(4,5-dimethylthiazol-2-yl)-2,5-diphenyltetrazolium bromide (MTT), D-Manitol, K_2HPO_4, KH_2PO_4, Triton X-100, β-mercaptoethanol, anti-rabbit immunoglobulin (HRP peroxidase-linked antibody), and carbonyl cyanide 4-(trifluoromethoxy) phenylhydrate (FCCP) were obtained from Sigma-Aldrich (São Paulo, SP, Brazil). SDS, acrylamide, bis-acrylamide, and hybond nitrocellulose were obtained from GE Healthcare Life Division (Uppsala, Sweden). Anti-phospho-p38 (Thr180/Tyr182) and total form, anti phospho-AKT (Thr308) and total form, anti-phospho PTEN, anti-phospho and total JNK1/2 (Thr183/Tyr185), anti-phospho ERK1/2 (Thr202/Tyr204) and anti-total-ERK1/2, and β-actin antibodies were purchased from Cell Signaling Technology (Danvers, MA). Poly (ADP)-ribose polymerase (PARP) antibody was obtained from Santa Cruz Biotechnology (Santa Cruz, CA). Kit Caspase-Glo 3/7 was obtained from Promega (Madison, WI). All other reagents were commercial products of the highest purity grade available.

2.2. Animals. For this study, it used chicks of *Gallus gallus* species from both genders with age among 5–15 days. The animals were maintained in the animal facility at controlled conditions of light and temperature with food and water ad libitum. All procedures were performed in accordance with the approval, under protocol no. 011/2012, of the CEUA/UNIPAMPA (Animal Ethics Committee from Universidade Federal do Pampa).

2.3. Plant Collection and Extractions. The stem barks of *A. microcarpum* were collected from Barreiro Grande, Crato-Ceará (7°22_S; 39°28_W; 892 m sea level), Brazil, in November 2011. The plant material was identified by Dr. Maria Arlene Pessoa da Silva of the herbarium Caririense Dárdano de Andrade-Lima (HCDAL) of the Regional University of Cariri (URCA), and a voucher specimen was deposited (n° 6702). The fresh barks of *A. microcarpum* were macerated with 99.9% of ethanol and water (1 : 1, v/v) for 3 days. The suspension was filtered, and the solvent evaporated and lyophilized under reduced pressure to obtain 490 g of hydroalcoholic extract. One hundred and fifty grams (150 g) of this was partitioned with ethyl acetate and methanol to obtain 12.5 g of ethyl acetate fraction and 105.23 g of the methanolic fraction. All fractions were stored in the freezer and resuspended in water prior to experiments.

2.4. Identification and Quantification of Phenolic Compounds and Flavonoids of Anacardium microcarpum by HPLC-DAD. The chemical composition of the *A. microcarpum* hydroalcoholic extract (AMHE), *A. microcarpum* methanolic fraction (AMMF), and *A. microcarpum* ethyl acetate fraction (AMEAF) was previously determined by our group [1] as shown in Table 1. The complete study can be found in literature where differences were verified between

Table 1: Phytochemical characterization of extract and fractions of *Anacardium microcarpum*. (Adapted from Barbosa-Filho et al., 2014.)

Compounds	AMHE (mg/g)	AMMF (mg/g)	AMEAF (mg/g)
Gallic acid	14.53 ± 0.02	7.13 ± 0.01	21.32 ± 0.04
Chlorogenic acid	5.83 ± 0.03	—	10.57 ± 0.03
Caffeic acid	19.36 ± 0.02	13.57 ± 0.05	27.19 ± 0.03
Ellagic acid	15.12 ± 0.01	13.19 ± 0.01	25.61 ± 0.05
Catechin	3.79 ± 0.01	3.05 ± 0.04	6.24 ± 0.02
Epicatechin	4.53 ± 0.01	3.11 ± 0.01	9.35 ± 0.01
Rutin	3.81 ± 0.03	9.86 ± 0.03	7.03 ± 0.01
Isoquercitrin	14.25 ± 0.01	15.79 ± 0.03	25.98 ± 0.02
Quercetrin	7.29 ± 0.02	13.20 ± 0.02	20.64 ± 0.02
Quercetin	28.03 ± 0.04	18.16 ± 0.01	27.02 ± 0.01
Kaempferol	3.54 ± 0.01	9.93 ± 0.02	11.25 ± 0.02
Kaempferol glycoside	9.06 ± 0.03	3.15 ± 0.04	3.47 ± 0.01

hydroalcoholic extract, methanolic, and ethyl acetate fractions, respectively.

2.5. Tissue Slice Preparation and Treatment. Animals were euthanized by decapitation under anesthesia. The brain was dissected and placed in cutting solution oxygenated at 4°C (110 mM sucrose, 60 mM NaCl, 3 mM KCl, 0.5 mM $CaCl_2$, 7 mM $MgSO_4$, 5 mM glucose, and 25 mM HEPES pH 7.4). The cortical region was separated, and 400 μm thickness slices were prepared in a McIlwain tissue slicer [17]. The diameter of slices was standardized using a 3 mm punch. Briefly, slices were transferred to 96-well plates containing HEPES-saline buffer (124 mM NaCl, 4 mM KCl, 1.2 mM $MgSO_4$, 12 mM glucose, 1 mM $CaCl_2$, and 25 mM HEPES pH 7.4) previously oxygenated during 30 minutes (200 μL/slice). After 30 min of preincubation, the buffer was removed, and fresh buffer was added. Tissue slices were subsequently incubated for 120 minutes at 37°C in the presence/absence of 6-OHDA 500 μM and/or hydroalcoholic extract (AMHE), methanolic (AMME), and ethyl acetate *A. microcarpum* fractions (AMEA) (concentrations among 0.1–1 mg/mL). All dissolved in the culture medium.

2.6. Cell Viability. Cell viability was determined by the reduction of 3-(4,5-dimethylthiazol-2-yl)-2,5-diphenyltetrazolium bromide (MTT) (0.05% HEPES-saline). After 120 minutes of treatment, slices were incubated for 30 minutes at 37°C in the presence of MTT [17]. Subsequently, MTT was removed, and samples were incubated in DMSO for 30 min (37°C). The absorbance resulted from formazan product diluted in DMSO was read at 540 nm in an EnsPire® multimode plate reader (PerkinElmer, USA).

2.7. Spectrophotometric Studies of 6-OHDA Autoxidation. The autoxidation of 6-OHDA was followed by monitoring the formation of *p*-quinone at 490 nm [10]. A Cary 60-UV-Visible Spectrophotometer by Agilent Technologies was used for the assay. The cuvette holder was thermostatically maintained at 37°C. For each assay, 1 mL of phosphate buffer (pH 7.4) was incubated in a quartz cuvette for 10 min to reach the set temperature. Then, the autoxidation was initiated with the addition of 5 μL of a stock solution of 6-OHDA (100 mM) at a final concentration of 0.5 mM. The monitoring of the corresponding kinetics was immediately initiated and maintained for subsequent 3 min. To verify if AMHE, AMMF, and AMEAF could prevent autoxidation of the compound, different concentrations of the plant extract or fractions (1 μg/mL, 10 μg/mL, and 100 μg/mL) were added in the presence or absence of 6-OHDA. GSH 10 mM was used as positive control.

2.8. Lipid Peroxidation. The final product from lipid peroxidation was determined with thiobarbituric acid as the reactive substance (TBARS) with some modifications [18]. Tissue slices were incubated for 120 minutes at 37°C in different extract concentrations (0.1–1 mg/mL) in the presence/absence of 6-OHDA (500 μM). For the next step, five slices per treatment group were homogenized in 150 μL of HEPES 20 mM buffer. Further, all content was incubated during 60 minutes at 95°C into acetic acid/HCl 0.45 M buffer, thiobarbituric acid 0.8% (TBA), SDS 8.1% to promote the coloring, and absorbance was measured at 532 nm.

2.9. Enzyme Assays. Glutathione S-transferase activity (GST) was assayed using 1-chloro 2,4-dinitrobenzene (CDNB) as substrate [19]. The assay is based on the formation of the conjugated complex of CDNB and GSH. The reaction was conducted in a mix consisting of 0.1 M phosphate buffer pH 7.0, 1 mM EDTA, 1 mM GSH, and 2.5 mM CDNB. Glutathione peroxidase activity (GPx) was measured and defined as the rate of NADPH oxidation by the coupled reaction with glutathione reductase [20]. One unit of GPx will consume 1.0 μmol of $NADP^+$ from NADPH per minute ($\varepsilon = 6.22\ M^{-1}\ cm^{-1}$). Thioredoxin reductase (Trx-R) activity consists in measuring the rate of reduction of DTNB by NADPH [21]. One unit of enzyme activity was considered the amount of enzyme that catalyzes the formation of 1.0 μmol of DTNB per minute at 25°C, pH 7.0 ($\varepsilon = 13.60\ M^{-1}\ cm^{-1}$). All spectrophotometric assays were performed at 340 nm in an Agilent Cary 60 UV/VIS spectrophotometer with an 18 cell holder accessory coupled to a Peltier Water System temperature controller (Santa Clara, CA).

2.10. Determination of Reduced (GSH) and Oxidized Glutathione (GSSG). For the measurement of GSH and GSSG levels, brain homogenate was treated with 0.5 mL of 13% trichloroacetic acid and centrifuged at 100.000 g for 30 min at 4°C. Aliquots (10 μL) of supernatant were mixed with 100 mM NaH_2PO_4 buffer, pH 8.0, containing 5 mM EDTA. *O*-phthalaldehyde (OPT) (1 mg/mL) was added, and fluorescence was measured 15 min later using the 350/420 nm excitation/emission wavelength pair in Perkin Elmer inspire [22]. For measurement of GSSG levels, brain supernatant was incubated at room temperature with N-ethylmaleimide (NEM) (0.04 M) for 30 min at room temperature, and after that, were added NaOH (0.1 N) buffer, following of added

OPT and incubated for 15 min in the dark, using the procedure outlined above for GSH assay. Results were presented as the GSH/GSSG ratio.

2.11. High-Resolution Respirometry (HRR) In Vitro. For respirometry determination, chick brain (400 mg) was weighed and transferred to 1 mL of cold homogenization buffer containing 5 mM Tris-HCl, 250 mM sucrose, and 2 mM EGTA (pH 7.4), and brain homogenate was used to the HRR. Oxygraph-2k (O2k, OROBOROS Instruments, Innsbruck, Austria) was employed for all respiration measurements. Experiments were performed in 2 mL of MiR05 buffer (110 mM sucrose, 60 mM K-lactobionate, 0.5 mM EGTA, 3 mM $MgCl_2$, 20 mM taurine, 10 mM KH_2PO_4, 20 mM HEPES pH 7.4, and 0.1% BSA) [23]. All experiments were performed at 37°C using DatLab 4.0 software (Oroboros Inc., Austria), with continuous stirring at 750 RPM, and all experiments started by registering the endogenous substrate supported respiration, following protocols established in the literature [24].

All experiments of mitochondrial bioenergetics analysis in brain homogenate were performed following [25] with minor modifications at the O2k-chamber. All concentrations of compounds (control group without treatment, 100 μg/mL of a methanolic fraction, 6-OHDA 500 μM in the absence or presence of methanolic fraction) were added at the O2k-chamber after signal stabilization of the basal respiration supported by endogenous substrates. Four individual preparations of the brain homogenate were performed per group.

2.12. Mitochondrial Respiration Assays. Titration protocols of multiple substrates and inhibitors were used to assess mitochondrial function in terms of different respiration states. The routine of electron transport system activities in brain homogenate was carried out according to literature [26]. Malate, glutamate, and succinate were used as oxidizable substrates in all experiments. Complex I- (CI-) mediated Leak (LEAK) respiration was determined using 2 mM malate and 10 mM glutamate. CI-mediated OXPHOS (OXPHOS) was determined using ADP (2.5 mM). Respiratory control ratios ($RCR = CI_{OXPHOS}/CI_{LEAK}$) were used as a quality control of isolated mitochondria. The convergent electron flow during the maximal OXPHOS respiration ($CI + CII_{OXPHOS}$) was determined with substrates of CI and CII (10 mM Succinate). CI + CII-mediated ETS (electron transfer system) ($CI + CII_{ETS}$) was determined using Carbonyl cyanide-4-(trifluoromethoxy) phenylhydrazone (FCCP) (optimum concentration reached between 0.5 and 1.5 μM). CII-mediated ETS respiration (CII_{ETS}) was determined with 0.5 μM rotenone. Addition of 2.5 μM antimycin A inhibited complex III, resulting in nonmitochondrial respiration (ROX) with small contributions from electron leak in the uncoupled state.

2.13. Western Blotting Analysis. Analysis of protein phosphorylation in cortical slices was performed using western blotting with slight modification [27]. Four slices were homogenized in 100 μL of 4% SDS stop solution (4% SDS, 50 mM Tris, 100 mM EDTA, pH 6.8), and 10 μL of sample was taken out for protein analysis. In the remaining sample was added 25% Glycerol sample and 8% β-mercaptoethanol. The proteins were separated by SDS–PAGE using 10% gels and then electrotransferred to nitrocellulose membranes. The membranes were washed in Tris-buffered saline with Tween-20 (100 mM Tris–HCl, pH 7.5, 0.9% NaCl, and 0.1% Tween-20) and incubated overnight at 4°C with primary antibodies anti-phospho p38, anti-total and phospho-ERK1/2, anti-total and phospho-JNK1/2, anti-phospho and total-AKT, anti-phospho PTEN. Subsequently, membranes were washed in Tris-buffered saline with Tween-20 and incubated for 1 hour at 25°C with horseradish peroxidase-linked anti-IgG secondary specific antibodies. The blottings were visualized on the IS4000MM Pro Bruker imaging system using ECL-detection reagent, and the band density was quantified using the Scion Image® software. The density of the bands was measured and expressed as a rate (%) of increase in relation to control (slices treated only with media).

2.14. PI3K/AKT and MEK Inhibitors. To determine the implication of signaling pathway involved in cell survival in the neuroprotective effect of *A. microcarpum* methanolic fraction, PI3K/AKT inhibitor LY294002 at final concentration of 20 μM and MEK/ERK inhibitor PD98059 at final concentration of 50 μM. PD98059 acts on inhibition of MEK1 in a reversible, allosteric, and noncompetitive manner with respect to ATP and ERK1/2 binding whereas LY294002 acts at an ATP-binding site of PI3K enzyme, thus selectively inhibiting the PI3K-Akt interaction. The inhibitors were added to the medium 30 min prior to the addition of 6-OHDA plus AMMF. After 2 hours of treatment, MTT assay was conducted to verify the slices viability as described above. Inhibitors were diluted in DMSO; the final concentration of DMSO in the wells was 0.5%.

2.15. Protein Quantification. The protein concentration in samples was estimated using BSA as standard [28, 29].

2.16. Statistical Analysis. All data were tested for normal distribution by Kolmogorov-Smirnov. Statistical analysis was performed using one-way analysis of variance (ANOVA) followed by Newman-Keuls post hoc analysis. Results were considered statistically significant when $p < 0.05$.

3. Results

3.1. Analysis of 6-Hydroxydopamine Autoxidation in the Presence of Extract and Fractions of A. microcarpum. 6-OHDA undergoes spontaneous autoxidation in the presence of oxygen under physiological conditions forming hydrogen peroxide (H_2O_2) and the corresponding *p*-quinone whose formation can be monitored spectrophotometrically at 490 nm [10]. The absorbance of 6-OHDA at the end of 3 min of incubation with phosphate buffer is visualized in the graph (Figures 1(a)–1(c)). The presence of fractions of *A. microcarpum* did not alter the 6-OHDA absorbance, whereas hydroalcoholic fraction decreased it partially. The antioxidant glutathione (GSH) was used as a positive control preventing 6-OHDA autoxidation due to the ability of

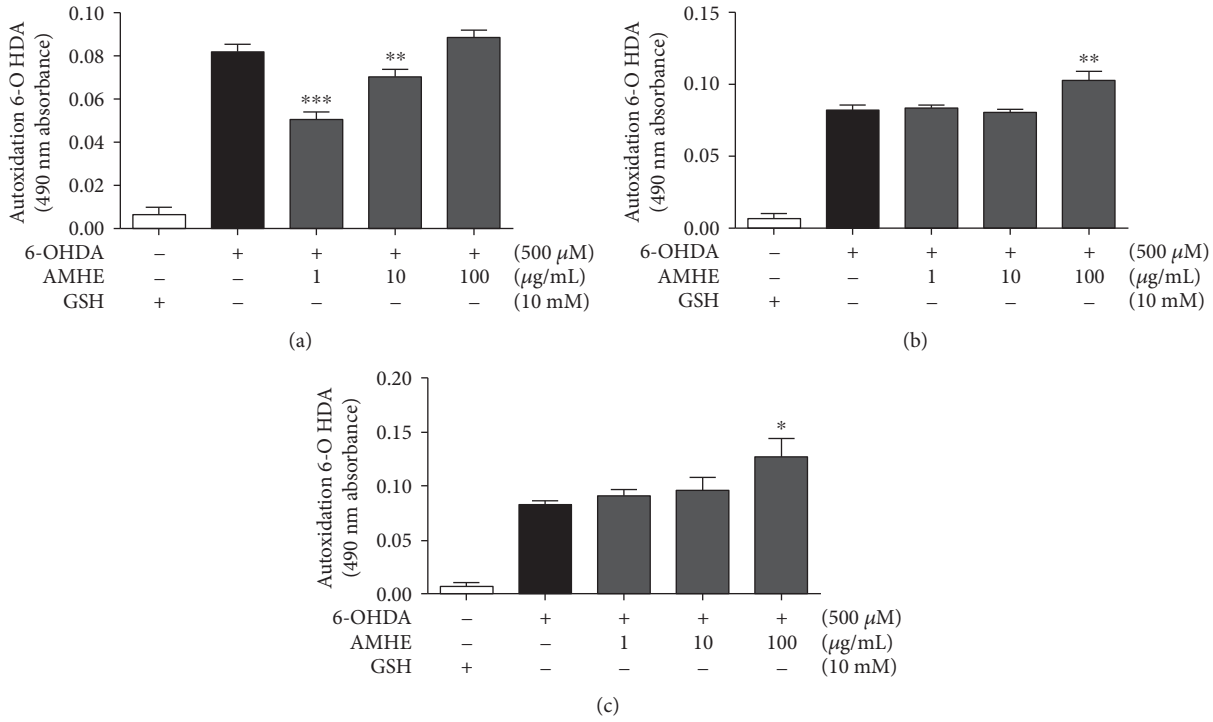

Figure 1: 6-OHDA autoxidation in the presence of *A. microcarpum* and GSH. The autoxidation of 6-OHDA (500 μM) was followed spectrophotometrically by monitoring the formation of *p*-quinone at 490 nm in the presence or absence of extract or fractions (a) 6-OHDA + AMHE, (b) 6-OHDA + AMMF, and (c) 6-OHDA + AMEAF. GSH 10 mM was used as positive control preventing 6-OHDA autoxidation. Data are expressed as percentage of the untreated control ± SE ($n = 3$). $^{***}p < 0.0001$ as compared to GSH control. $\#\#p < 0.001$ and $\#\#\#p < 0.0001$ as compared to 6-OHDA group.

sulfhydryl compounds to remove the H_2O_2 formed during the autoxidation reaction of 6-OHDA.

3.2. Evaluation of Toxicity and Neuroprotective Potential of A. microcarpum Hydroalcoholic Extract and Fractions. In order to investigate a possible neurotoxic effect of *A. microcarpum*, cortical slices were incubated for 2 hours with different concentrations of hydroalcoholic extract and fractions: 0, 1 μg/mL, 10 μg/mL, 100 μg/mL, and 1000 μg/mL. At the end of incubation period, cell viability assay was performed by MTT test. Our data showed that *A. microcarpum* per se was unable to affect the viability of slices (Figures 2(a)–2(c)).

To investigate the neuroprotective potential of *A. microcarpum*, slices were incubated with neurotoxin 6-OHDA 500 μM for 2 hours in the presence or absence of different extracts or fraction concentration (1–100 μg/mL). 6-OHDA concentration was defined in a dose-response curve, and the concentration able to decrease in approximately 30% the cell viability was chosen for further studies. The hydroalcoholic extract was unable to protect against damage caused by 6-OHDA (Figure 2(d)); however, AMMF and AMEAF reverted the drop in cell viability promoted by 6-OHDA at a concentration of 100 μg/mL ($p < 0.0001$) (Figures 2(e) and 2(f), respectively).

3.3. Lipid Peroxidation in Response to the Treatment with Methanolic and Acetate Fractions of A. microcarpum and 6-OHDA. Oxidative stress is implied in dopaminergic cell death induced by 6-OHDA [11]. AMMF and AMEAF but not AMHE presented neuroprotective potential in the MTT assay; thus, it was investigated a possible antioxidant potential of these fraction on slices exposed to 6-OHDA by its ability to prevent lipid peroxidation. 6-OHDA induced lipid peroxidation in 25% ($p < 0.0001$) when compared to control group. Only AMMF prevented this effect (Figures 3(a) and 3(b)); thus, further studies were conducted in the presence of methanolic fraction.

3.4. Analysis of ERK, AKT, PTEN Phosphorylation, and PARP Cleavage in Response to the Treatment with 6-OHDA and Methanolic Fraction of A. microcarpum. In this study, the effect of 6-OHDA on phosphorylation of proteins p38, JNK1/2, ERK1/2, AKT, cleavage of PARP protein, and phosphatase PTEN was analyzed by western blotting technique. No alterations in phosphorylation and total levels of p38 and JNK1/2 were detected (data not shown). The phosphorylation of ERK was increased in 30% only in the presence of extract and 6-OHDA (Figure 4(b)); no alterations were observed in the other groups. AKT phosphorylation (Figure 4(c)) was inhibited in approximately 25% by 6-OHDA treatment and remained at control level when fraction was present. The cleavage of PARP protein in an 89 kDa fragment was evaluated as an indicator of apoptotic cell death. No alteration in PARP cleavage was visualized by treatments as observed in the blotting. PTEN phosphorylation was unchanged by the treatments (Figure 4(d)).

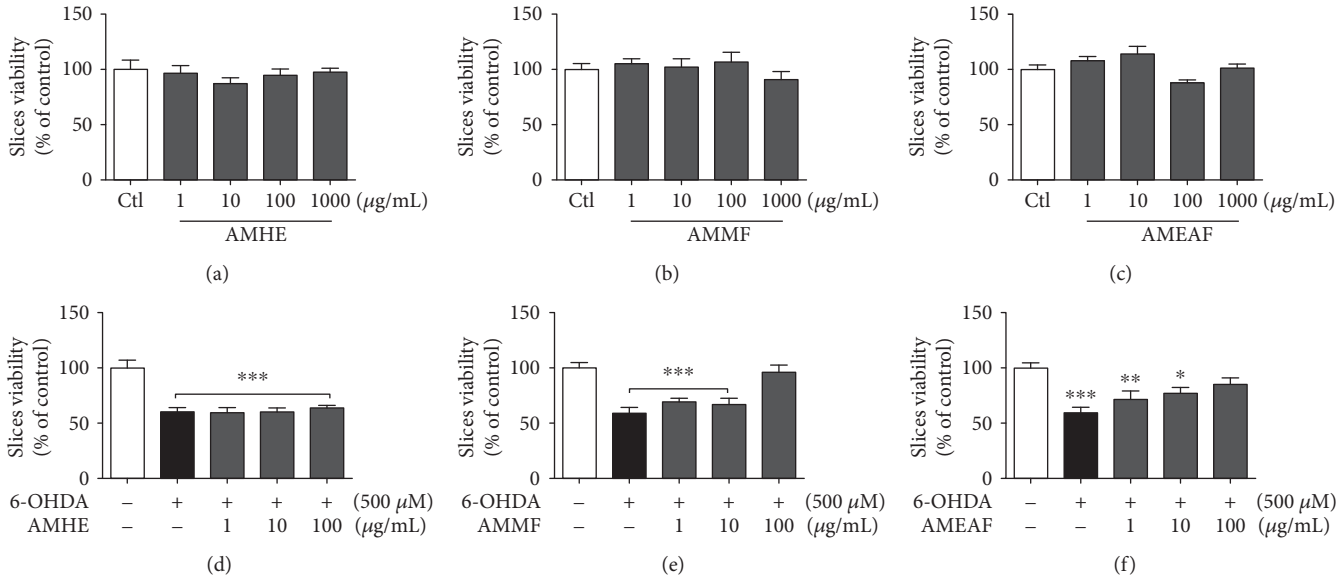

Figure 2: Effects of *A. microcarpum* and 6-OHDA on the viability of cortical slices. Cortical slices were incubated for 2 h in different concentrations (1–1000 μg/mL) of (a) AMHE, (b) AMMF, and (c) AMEAF and in the presence or absence of 6-OHDA (500 μM) during 2 h, (d) AMHE, (e) AMMF, and (f) AMEAF. Cell viability was measured by MTT test. Data are expressed as percentage of the untreated control ± SEM ($n = 3$). $^{*}p < 0.05$, $^{**}p < 0.001$, and $^{***}p < 0.0001$ different from control group.

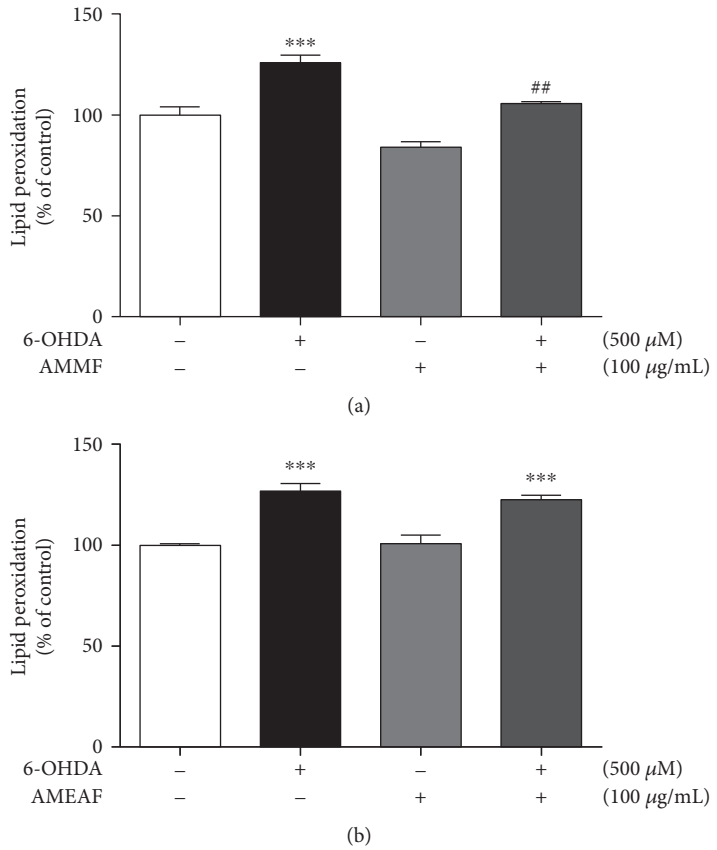

Figure 3: Effects of *A. microcarpum* on 6-OHDA (500 μM) induced lipid peroxidation (LPO) in cortical slices. Cortical slices were incubated with (a) AMMF and (b) AMEAF in the presence/absence of 6-OHDA for two hours, and lipid peroxidation was evaluated by formation of TBARS at 532 nm. Data are expressed as percentage of the untreated control ± SEM ($n = 3$). $^{***}p < 0.0001$ as compared to control. $^{\#\#}p < 0.001$ as compared to 6-OHDA group.

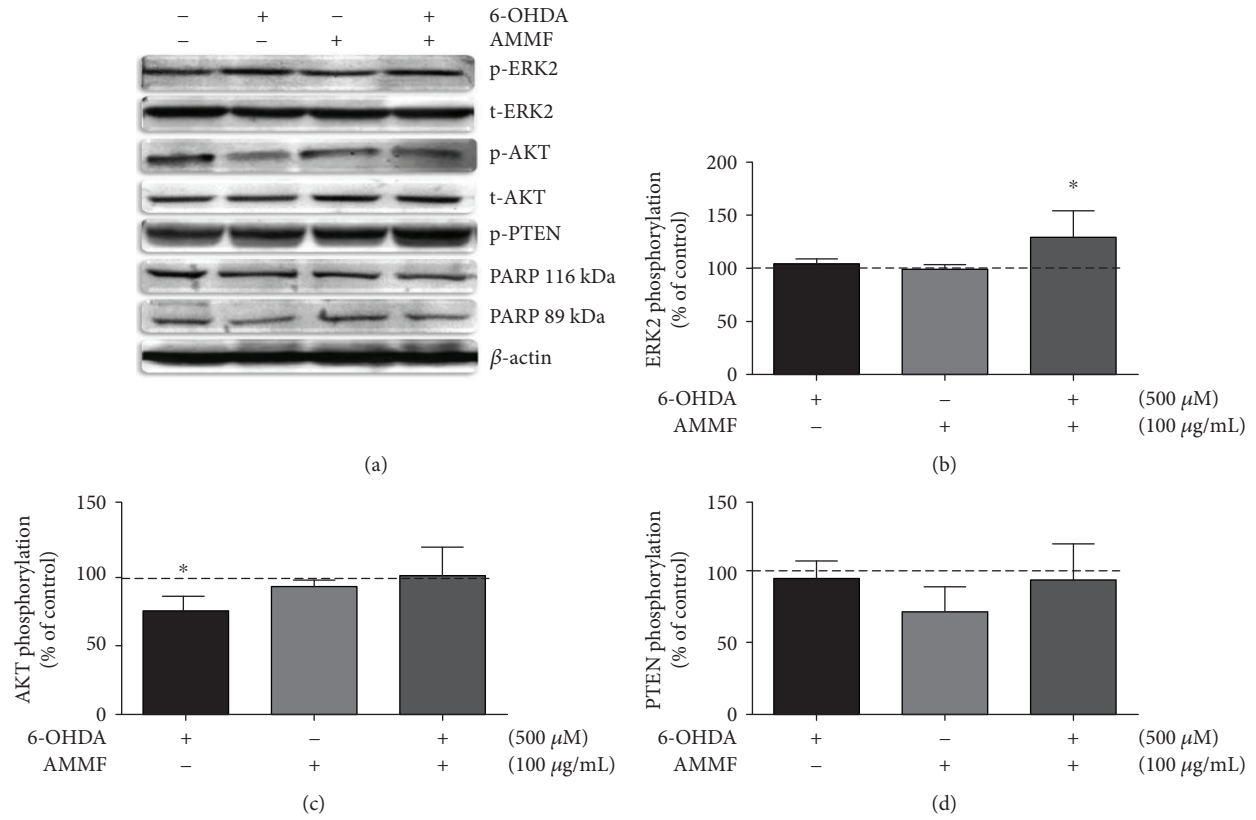

Figure 4: Modulation of ERK, AKT and PTEN phosphorylation, PARP cleavage in response to treatment with methanolic fraction of *A. microcarpum* and 6-OHDA in cortical slices. Proteins were separated by SDS–PAGE and transferred to nitrocellulose membrane. Total content and phosphorylation of proteins were detected by specific antibodies, and the reaction was developed by ECL. (a) Western blotting of phosphorylated and total forms of ERK2 and AKT phosphorylation and total forms and phospho-PTEN. (b) Quantitative analysis of ERK2 phosphorylation expressed as a ratio with its respective total form. (c) Quantitative analysis of AKT phosphorylation expressed as a ratio with its respective total form. (d) Quantitative analysis of PTEN phosphorylation expressed as a ratio with β-actin. The data are expressed as fold increase related to control group and represent mean ± SE of 4 independent experiments. Statistical analysis was performed by ANOVA, followed by the Newman-Keuls test. $^{*}p < 0.05$, $^{**}p < 0.001$, and $^{***}p < 0.0001$ different from control group. $\#p < 0.05$, $\#\#p < 0.001$, and $\#\#\#p < 0.0001$ when compared to 6-OHDA group.

3.5. Involvement of ERK and AKT Signaling Pathways in the Neuroprotective Mechanisms of Fraction. The participation of ERK1/2 and AKT in the protective potential of the methanolic fraction was investigated. Slices were incubated with synthetic inhibitors of ERK1/2 phosphorylation (PD98059) and AKT phosphorylation (LY294002) for 30 min prior to the addition of 6-OHDA or methanolic fraction. As shown in Figure 5, the inhibition of ERK and AKT blocked the protective effects of extract.

3.6. Activity of Antioxidant Enzymes and Redox State of Cells in Response to the Treatment with the Methanolic Fraction of A. microcarpum and 6-OHDA. As shown in Table 2, 6-OHDA caused a 1.68-fold increase in GST activity, and this effect was not observed in the presence of methanolic fraction and 6-OHDA. 6-OHDA induced TRx-R activity in 1.9-fold; this effect was not observed in the presence of methanolic fraction. On the other hand, GPx was inhibited in 1.71-fold by 6-OHDA when comparing to control, and this effect was not observed in the presence of methanolic fraction. The total glutathione content and oxidized glutathione were decreased by 34% and 39%, respectively, by 6-OHDA treatment, and the ratio GSH/GSSG was increased by 6-OHDA. This effect was not observed when 6-OHDA was present. The plant per se increased levels of reduced GSH (Table 3).

3.7. Mitochondrial Respiration in Response to 6-OHDA and A. microcarpum Methanolic Fraction. The mitochondrial respiration in response to 6-OHDA and methanolic fraction was measured in brain homogenate by cellular oxygen consumption. Basal respiration was unchanged in the brain by treatments (data not shown). After glutamate and malate substrate (CI_{Leak}) addition, a significant decrease ($p < 0.05$) on CI activity was induced by 6-OHDA. This drop in CI activity persisted when methanolic fraction was added ($p < 0.05$). AMMF per se did not change the activity of CI. In order to see CI_{OXPHOS}, it was added succinate and ADP (CI_{OXPHOS}); this parameter was also inhibited by 6-OHDA, and the fraction was unable to avoid it. The convergent electron flow during the maximal oxidative phosphorylation ($CI + CII_{OXPHOS}$) was also significantly decreased by 6-OHDA, and the fraction did not avoid this effect. Maximal mitochondrial respiration ($CI + CII_{ETS}$) was determined with

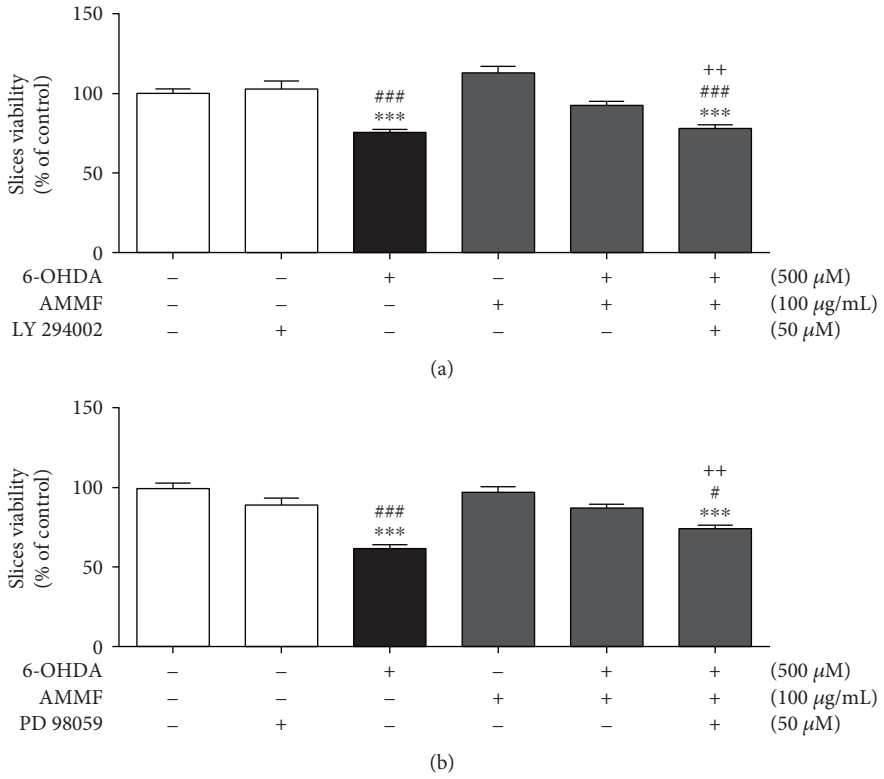

Figure 5: Effects of *A. microcarpum* and 6-OHDA on the viability of cortical slices in the presence of LY (294002) inhibitors and PD (98059). Slices were incubated with AMMF in the presence or absence of 6-OHDA (500 μM) and inhibitors for 2 h. The inhibitors were added 30 min prior to the addition of fraction and 6-OHDA and remained during all period of the treatment. Data are expressed as percentage of the untreated control ± SE ($n = 3$). $^{***}p < 0.0001$ as compared to control. $\#\#\#p < 0.0001$ as compared to only inhibitor treated group; $++p < 0.001$ as compared to cotreated group 6-OHDA + AMMF.

Table 2: Activity of antioxidant enzymes in cortical slices submitted to treatment with the neurotoxin 6-OHDA and *A. microcarpum* methanolic fraction.

	GST (mg/mU protein)	GPx (mg/mU protein)	TrxR (mg/mU protein)
Control	241.2 ± 8.49	41.37 ± 5.01	2.375 ± 0.342
6-OHDA 500 μM	406.4 ± 75.89*	23.82 ± 2.07*	4.675 ± 0.608*
AMMF 100 μg/mL	186.2 ± 42.13$^{\#}$	51.01 ± 4.04	2.459 ± 0.137$^{\#\#}$
AMMF 100 μg/mL + 6-OHDA 500 μM	251.5 ± 36.48$^{\#}$	46.29 ± 3.20$^{\#\#}$	3.164 ± 0.496$^{\#}$

Data are expressed as percentage of the untreated control ± SEM. $^{*}p < 0.05$ in relation to control group, $\#p < 0.05$ in relation to control group, $\#\#p < 0.001$ in relation to 6-OHDA group.

Table 3: Effect of treatment with 6-OHDA and *A. microcarpum* on GSH and GSSG levels and ratio GSH/GSSG.

	GSH (% of control)	GSSG (% of control)	Total glutathione (% of control)	GSH/GSSG (% of control)
Control	88.05 ± 6.73	90.60 ± 5.48	100.0 ± 10.66	100.0 ± 2.51
6-OHDA 500 μM	87.49 ± 5.41	61.61 ± 12.87*	66.56 ± 11.34*	168.1 ± 19.64**
AMMF 100 μg/mL	136.7 ± 6.54**	117.2 ± 10.04$^{\#\#}$	129.7 ± 4.18$^{\#\#}$	120.7 ± 9.21$^{\#\#}$
AMMF 100 μg/mL + 6-OHDA 500 μM	111.4 ± 13.28	111.9 ± 3.17$^{\#\#}$	111.8 ± 4.96$^{\#}$	99.61 ± 8.99$^{\#\#}$

Data are expressed as percentage of the untreated control ± SEM. $^{*}p < 0.05$; $^{**}p < 0.001$ in relation to control group. $\#\#p < 0.001$ when compared to 6-OHDA group.

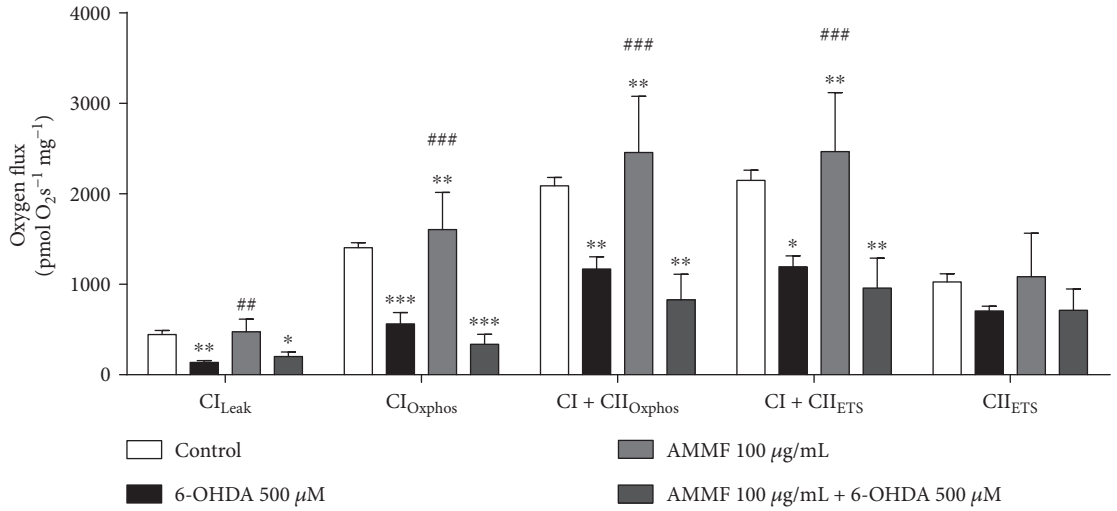

FIGURE 6: O_2 flux measured in the mitochondria of cortex homogenate exposed to 6-OHDA and/or *A. microcarpum.* Mitochondrial function is presented with the abbreviation(s) of the complex(es) involved followed by the state of respiration measured in the presence of glutamate + malate (CI_{LEAK}), +ADP (CI_{OXPHOS}), +succinate (CII_{OXPHOS}), +FCCP ($CI + II_{ETS}$), +rotenone (CII_{ETS}). Antimycin A was used to correct for residual O_2 consumption. Results are means ± SEM for 4 different preparations. $^{*}p < 0.05$, $^{**}p < 0.001$, and $^{***}p < 0.0001$ different from control group. $\#\#p < 0.001$ and $\#\#\#p < 0.0001$ when compared to 6-OHDA group.

the addition of the uncoupler FCCP. This parameter was inhibited by 6-OHDA and not avoided by the fraction ($p < 0.001$). CII_{ETS} activity was analyzed after inhibition of CI by rotenone, and no significant changes occurred by treatments. AMMF per se but not in the presence of 6-OHDA induced CI_{LEAK}, CI_{OXPHOS}, $CI + CII_{OXPHOS}$, and $CI + II_{ETS}$ (Figure 6).

4. Discussion

Oxidative stress, mitochondrial dysfunction, genetic, and environmental factors are mechanisms associated with neuronal damage observed in PD [30–32]. A number of studies have proposed antioxidant therapies to attenuate PD symptoms [33, 34]. In this study, methanolic and acetate fraction but not hydroalcoholic extract protected against neurotoxicity induced by 6-OHDA in brain slices, but methanolic fraction was more effective in protecting against induction in lipid peroxidation by 6-OHDA.

The cytotoxic effect of 6-OHDA is attributed to the formation of reactive species such as superoxide radical, *para*-quinone, and hydrogen peroxide from enzymatic and autoxidation reactions [35]. It this study, plant extract or fractions did not block effectively the autoxidation of 6-OHDA *in vitro*. With the base in this finding, it can be inferred that the mechanism implied in the protective effect of the plant is the neutralization of reactive species secondary to the autoxidation reaction and not a direct interaction with 6-OHDA molecule. In previous studies, 6-OHDA induced mitochondrial dysfunction by inhibition of I and IV complexes, disrupting the mitochondrial function, and producing superoxide anion, which in turn may form hydroxyl radicals which reacts with nitric oxide generating peroxynitrite [36–39]. In the present study, the 6-OHDA inhibited in 55% complex I activity in basal respiration around 75% the ATP production CI-dependent and compromise the mitochondrial electron transport system in 50%. This is in accordance with a similar work that showed a 20% of inhibition of complex I at a concentration of 100 μM, approximately [40]. This phenomenon was not blocked by *A. microcarpum.* Considering the inability of the plant to hamper the mitochondrial damage caused by 6-OHDA, it could be supposed that the neuroprotective effect by the plant is due to the neutralization of reactive species resulted from mitochondrial dysfunction.

Reactive oxygen species production, detoxification, and signaling pathways have been considered interesting targets for intervention in neurodegenerative diseases [41, 42]. Endogenous enzymatic and nonenzymatic antioxidants, such as GSH, glutathione S-transferase, glutathione peroxidase, and thioredoxin reductase (TRx-R), delay or prevent oxidative damage to proteins, lipids, and DNA [43, 44]. Glutathione peroxidase (GPx) is an intracellular antioxidant that reduces hydrogen peroxide to water at expenses of GSH and limits its harmful effect. In this study, 6-OHDA caused a substantial inhibition in GPx activity that was not observed in presence of methanolic fraction. Similar data were demonstrated in neuroblastoma cells treated with 6-OHDA [45]. In PD patients, the degree of symptom severity correlates with intracellular GSH loss in substantia nigra [46]. In our study, GSH content was not altered, and GSSG was decreased by 6-OHDA; this effect may be related to GPx inhibition and consequently a lower oxidation of GSH by this system. On the other hand, the TRx-R activity was stimulated by 6-OHDA, and the same data were observed in neuroblastoma cell line SH-SY5Y [47]. Our results suggest the participation of peroxiredoxins catalyzing peroxide reduction as a compensatory mechanism to replace the inhibited activity of GPx. Herein, 6-OHDA increased the activity of GST, which is implied in neuronal detoxification of quinones resulted

from catecholamine oxidation and free radicals [48], and this effect was not observed when plant was present. All these effects were prevented by the methanolic fraction of plant, showing a protective mechanism against oxidative stress induced by the 6-OHDA. Due to methodological issues, we were not able to detect quantifiable levels of the enzymes Superoxide Dismutase and Catalase, but their analysis will be considered in further studies.

Extracellular signal-regulated kinases (ERKs) have been implicated in the cellular response to reactive oxygen species [49–52]. Growth factors and other extracellular stimuli activate the kinase MEK1/2 by Ras/Raf pathway; MEK1/2 then phosphorylates and activates ERK1/2 [53]. ERK1/2 activates transcription factors such as cAMP response element–binding protein (CREB) and Elk, thereby increasing transcription of neurotrophic factors and prosurvival genes such as Bcl-2 [54]. In this study, the use of MEK1/2 inhibitor weakened the protective potential of methanolic fraction against the 6-OHDA, suggesting that the antioxidant potential of fraction per se is not enough to protect the brains slices, but the activation of prosurvival factors plays an important role in this effect. Experiments of western blotting showed that 6-OHDA did not alter ERK phosphorylation in brain slices after two hours of incubation with 6-OHDA. Previous studies reported an ERK1/2 phosphorylation peak after 10–15 min of exposure of dopaminergic cells to 6-OHDA; the phosphorylation of prosurvival protein CREB followed this temporal profile as well [54]. Authors showed that the inhibition of early phosphorylation of ERK1/2 abolished CREB activation and increased 6-OHDA toxicity. Thus, the possibility of an early activation of ERK1/2 in slices submitted to the treatment and the contribution of this activation for a self-protective response of cells that was prevented with use of inhibitors could not be discarded.

AKT is a serine/threonine kinase and its signaling pathway plays an important role in fundamental cellular functions, such as cell proliferation and survival, by phosphorylating a variety of enzymes, including proapoptotic regulators, antioxidant proteins, and transcription factors [55]. It is reported that AKT phosphorylation is reduced in the striatum of patients with PD, suggesting that its inactivation has an important role in PD [56]; being so, it is a substantial therapeutic target for treating neurodegenerative diseases, beyond other pathologies [57]. Herein, 6-OHDA inhibited phosphorylation level of AKT, and the plant prevented this effect. There was no alteration in phosphorylation level of PTEN (Phosphatase and tensin homolog deleted on chromosome ten), a negative regulator of AKT. Similar results were reported in SH-SY5Y and dopaminergic cell lines [58, 59]. In this study, AKT phosphorylation seems to display a role in neuroprotective effect of fraction against 6-OHDA, once the use of PI3K/AKT inhibitor blocked the protective effect of fraction. This result proposes that survival signaling pathways ERK and AKT contribute for neuroprotection by methanolic fraction of *A. microcarpum.*

Recent studies have suggested that several signal transduction pathways, including phosphatidylinositol 3 kinase (PI3K) pathways and MAPKs, are involved in releasing transcription factor Nrf2 from the complex Keap1-Nrf2 promoting Nfr2 translocation to the nucleus [60]. Nrf2 promotes transcriptional activation of a variety of antioxidant genes [61]. AMMF-mediated cytoprotection against 6-OHDA was abolished by ERK and AKT pathway inhibitors; these data support a possible involvement of Nrf2 activation leading to expression of downstream antioxidant genes through the modulation of AKT and ERK1/2 pathways by the fraction. According to another study, inhibition of AKT and ERK has also abolished the neuroprotective effect of a triterpenoid isolated from plant [62].

5. Conclusion

The present work shows for the first time the potential of the Brazilian plant *A. microcarpum* in protecting against 6-OHDA-induced damage in brain slices. Inhibition of mitochondrial complexes by 6-OHDA was not avoided by the extract. ERK and AKT phosphorylation display a role in the neuroprotective effect by the plant which was decreased by the presence of pharmacological inhibitors of those pathways.

Data Availability

The data used to support the findings of this study are available from the corresponding author upon request.

Conflicts of Interest

The authors declare that they have no conflicts of interest.

Acknowledgments

This study was supported by CNPq process #456207/2014-7, FAPERGS process # 2380-2551/14-8, and FAPERGS/PRONEX #16/25510000499-4. JLF is a recipient of CNPq fellowship. IKM, GEM and NRR are recipients of CAPES doctoral scholarship.

References

[1] V. M. B. Filho, E. P. Waczuk, J. P. Kamdem et al., "Phytochemical constituents, antioxidant activity, cytotoxicity and osmotic fragility effects of Caju (Anacardium microcarpum)," *Industrial Crops and Products*, vol. 55, pp. 280–288, 2014.

[2] H. Coutinho, V. Barbosa-Filho, E. Waczuk et al., "Phytocompounds and modulatory effects of *Anacardium microcarpum* (cajui) on antibiotic drugs used in clinical infections," *Drug Design, Development and Therapy*, vol. 9, pp. 5965–5972, 2015.

[3] T. Fritsch, K. A. Smyth, M. S. Wallendal, T. Hyde, G. Leo, and D. S. Geldmacher, "Parkinson disease: research update and clinical management," *Southern Medical Journal*, vol. 105, no. 12, pp. 650–656, 2012.

[4] R. Balestrino and P. Martinez-Martin, "Neuropsychiatric symptoms, behavioural disorders, and quality of life in Parkinson's disease," *Journal of the Neurological Sciences*, vol. 373, pp. 173–178, 2017.

[5] P. P. Michel, E. C. Hirsch, and S. Hunot, "Understanding dopaminergic cell death pathways in Parkinson disease," *Neuron*, vol. 90, no. 4, pp. 675–691, 2016.

[6] S. Fahn and D. Sulzer, "Neurodegeneration and neuroprotection in Parkinson disease," *NeuroRx*, vol. 1, no. 1, pp. 139–154, 2004.

[7] P. Bhattarai, A. K. Thomas, Y. Zhang, and C. Kizil, "The effects of aging on amyloid-β42-induced neurodegeneration and regeneration in adult zebrafish brain," *Neurogenesis*, vol. 4, no. 1, article e1322666, 2017.

[8] D. Kempuraj, R. Thangavel, P. A. Natteru et al., "Neuroinflammation induces neurodegeneration," *Journal of Neurology, Neurosurgery and Spine*, vol. 1, no. 1, 2016.

[9] J. Bové and C. Perier, "Neurotoxin-based models of Parkinson's disease," *Neuroscience*, vol. 211, pp. 51–76, 2012.

[10] R. Soto-Otero, E. Méndez-Álvarez, Á. Hermida-Ameijeiras, A. M. Muñoz-Patiño, and J. L. Labandeira-Garcia, "Autoxidation and neurotoxicity of 6-hydroxydopamine in the presence of some antioxidants: potential implication in relation to the pathogenesis of Parkinson's disease," *Journal of Neurochemistry*, vol. 74, no. 4, pp. 1605–1612, 2000.

[11] M. Shichiri, "The role of lipid peroxidation in neurological disorders," *Journal of Clinical Biochemistry and Nutrition*, vol. 54, no. 3, pp. 151–160, 2014.

[12] D. Blum, S. Torch, N. Lambeng et al., "Molecular pathways involved in the neurotoxicity of 6-OHDA, dopamine and MPTP: contribution to the apoptotic theory in Parkinson's disease," *Progress in Neurobiology*, vol. 65, no. 2, pp. 135–172, 2001.

[13] K. Komolafe, T. M. Olaleye, R. L. Seeger et al., "*Parkia biglobosa* improves mitochondrial functioning and protects against neurotoxic agents in rat brain hippocampal slices," *BioMed Research International*, vol. 2014, Article ID 326290, 15 pages, 2014.

[14] K. Gao, M. Liu, J. Cao et al., "Protective effects of *Lycium barbarum* polysaccharide on 6-OHDA-induced apoptosis in PC12 cells through the ROS-NO pathway," *Molecules*, vol. 20, no. 1, pp. 293–308, 2015.

[15] A. I. Abushouk, A. Negida, H. Ahmed, and M. M. Abdel-Daim, "Neuroprotective mechanisms of plant extracts against MPTP induced neurotoxicity: future applications in Parkinson's disease," *Biomedicine & Pharmacotherapy*, vol. 85, pp. 635–645, 2017.

[16] R. Rodnight, C. A. Gonçalves, R. Leal, E. Rocha, C. G. Salbego, and S. T. Wofchuk, "Chapter 11: regional distribution and properties of an enzyme system in rat brain that phosphorylates ppH-47, an insoluble protein highly labelled in tissue slices from the hippocampus," *Progress in Brain Research*, vol. 89, pp. 157–167, 1991.

[17] T. Posser, J. L. Franco, D. A. dos Santos et al., "Diphenyl diselenide confers neuroprotection against hydrogen peroxide toxicity in hippocampal slices," *Brain Research*, vol. 1199, pp. 138–147, 2008.

[18] H. Ohkawa, N. Ohishi, and K. Yagi, "Assay for lipid peroxides in animal tissues by thiobarbituric acid reaction," *Analytical Biochemistry*, vol. 95, no. 2, pp. 351–358, 1979.

[19] W. H. Habig and W. B. Jakoby, "[51] Assays for differentiation of glutathione S-transferases," *Methods in Enzymology*, vol. 77, pp. 398–405, 1981.

[20] A. Wendel, "[44] Glutathione peroxidase," *Methods in Enzymology*, vol. 77, pp. 325–333, 1981.

[21] A. Holmgren and M. Björnstedt, "Thioredoxin and thioredoxin reductase," *Methods in Enzymology*, vol. 252, pp. 199–208, 1995.

[22] P. J. Hissin and R. Hilf, "A fluorometric method for determination of oxidized and reduced glutathione in tissues," *Analytical Biochemistry*, vol. 74, no. 1, pp. 214–226, 1976.

[23] E. Gnaiger, "Capacity of oxidative phosphorylation in human skeletal muscle: new perspectives of mitochondrial physiology," *The International Journal of Biochemistry & Cell Biology*, vol. 41, no. 10, pp. 1837–1845, 2009.

[24] A. V. Kuznetsov, S. Schneeberger, R. Seiler et al., "Mitochondrial defects and heterogeneous cytochrome *c* release after cardiac cold ischemia and reperfusion," *American Journal of Physiology-Heart and Circulatory Physiology*, vol. 286, no. 5, pp. H1633–H1641, 2004.

[25] N. Pichaud, M. Messmer, C. C. Correa, and J. W. O. Ballard, "Diet influences the intake target and mitochondrial functions of Drosophila melanogaster males," *Mitochondrion*, vol. 13, no. 6, pp. 817–822, 2013.

[26] D. Pesta and E. Gnaiger, "High-resolution respirometry: OXPHOS protocols for human cells and permeabilized fibers from small biopsies of human muscle," *Methods in Molecular Biology*, vol. 810, pp. 25–58, 2012.

[27] T. Posser, M. T. De Paula, J. L. Franco, R. B. Leal, and J. B. T. Da Rocha, "Diphenyl diselenide induces apoptotic cell death and modulates ERK1/2 phosphorylation in human neuroblastoma SH-SY5Y cells," *Archives of Toxicology*, vol. 85, no. 6, pp. 645–651, 2011.

[28] M. M. Bradford, "A rapid and sensitive method for the quantitation of microgram quantities of protein utilizing the principle of protein-dye binding," *Analytical Biochemistry*, vol. 72, no. 1-2, pp. 248–254, 1976.

[29] G. L. Peterson, "A simplification of the protein assay method of Lowry et al. which is more generally applicable," *Analytical Biochemistry*, vol. 83, no. 2, pp. 346–356, 1977.

[30] V. Bellou, L. Belbasis, I. Tzoulaki, E. Evangelou, and J. P. A. Ioannidis, "Environmental risk factors and Parkinson's disease: an umbrella review of meta-analyses," *Parkinsonism & Related Disorders*, vol. 23, pp. 1–9, 2016.

[31] S. D. Ugarte, E. Lin, E. Klann, M. J. Zigmond, and R. G. Perez, "Effects of GDNF on 6-OHDA-induced death in a dopaminergic cell line: modulation by inhibitors of PI3 kinase and MEK," *Journal of Neuroscience Research*, vol. 73, no. 1, pp. 105–112, 2003.

[32] B. Uttara, A. Singh, P. Zamboni, and R. Mahajan, "Oxidative stress and neurodegenerative diseases: a review of upstream and downstream antioxidant therapeutic options," *Current Neuropharmacology*, vol. 7, no. 1, pp. 65–74, 2009.

[33] M. Solayman, M. Islam, F. Alam, M. Khalil, M. Kamal, and S. Gan, "Natural products combating neurodegeneration: Parkinson's disease," *Current Drug Metabolism*, vol. 18, no. 1, pp. 50–61, 2017.

[34] Q. Zhao, J. Ye, N. Wei, C. Fong, and X. Dong, "Protection against MPP^+-induced neurotoxicity in SH-SY5Y cells by tormentic acid via the activation of PI3-K/Akt/GSK3β pathway," *Neurochemistry International*, vol. 97, pp. 117–123, 2016.

[35] Y. Glinka, M. Gassen, and M. B. H. Youdim, "Mechanism of 6-hydroxydopamine neurotoxicity," *Journal of Neural Transmission. Supplementum*, vol. 50, pp. 55–66, 1997.

[36] Y. Y. Glinka and M. B. H. Youdim, "Inhibition of mitochondrial complexes I and IV by 6-hydroxydopamine," *European Journal of Pharmacology*, vol. 292, no. 3-4, pp. 329–332, 1995.

[37] G. C. Brown and V. Borutaite, "Inhibition of mitochondrial respiratory complex I by nitric oxide, peroxynitrite and

S-nitrosothiols," *Biochimica et Biophysica Acta (BBA) - Bioenergetics*, vol. 1658, no. 1-2, pp. 44–49, 2004.

[38] R. K. Chaturvedi and M. Flint Beal, "Mitochondrial diseases of the brain," *Free Radical Biology & Medicine*, vol. 63, pp. 1–29, 2013.

[39] M. Golpich, E. Amini, Z. Mohamed, R. Azman Ali, N. Mohamed Ibrahim, and A. Ahmadiani, "Mitochondrial dysfunction and biogenesis in neurodegenerative diseases: pathogenesis and treatment," *CNS Neuroscience & Therapeutics*, vol. 23, no. 1, pp. 5–22, 2017.

[40] J. Iglesias-González, S. Sánchez-Iglesias, E. Méndez-Álvarez et al., "Differential toxicity of 6-hydroxydopamine in SH-SY5Y human neuroblastoma cells and rat brain mitochondria: protective role of catalase and superoxide dismutase," *Neurochemical Research*, vol. 37, no. 10, pp. 2150–2160, 2012.

[41] E. K. Kim and E.-J. Choi, "Compromised MAPK signaling in human diseases: an update," *Archives of Toxicology*, vol. 89, no. 6, pp. 867–882, 2015.

[42] J. M. C. Gutteridge and B. Halliwell, "Antioxidants: molecules, medicines, and myths," *Biochemical and Biophysical Research Communications*, vol. 393, no. 4, pp. 561–564, 2010.

[43] J. Robaczewska, K. Kedziora-Kornatowska, M. Kozakiewicz et al., "Role of glutathione metabolism and glutathione-related antioxidant defense systems in hypertension," *Journal of Physiology and Pharmacology*, vol. 67, no. 3, pp. 331–337, 2016.

[44] H.-C. Kuo, H.-C. Chang, W.-C. Lan, F.-H. Tsai, J.-C. Liao, and C.-R. Wu, "Protective effects of *Drynaria fortunei* against 6-hydroxydopamine-induced oxidative damage in B35 cells *via* the PI3K/AKT pathway," *Food & Function*, vol. 5, no. 8, pp. 1956–1965, 2014.

[45] Y. Chandrasekhar, G. Phani Kumar, E. M. Ramya, and K. R. Anilakumar, "Gallic acid protects 6-OHDA induced neurotoxicity by attenuating oxidative stress in human dopaminergic cell line," *Neurochemical Research*, vol. 43, no. 6, pp. 1150–1160, 2018.

[46] P. Riederer, E. Sofic, W. D. Rausch et al., "Transition metals, ferritin, glutathione, and ascorbic acid in parkinsonian brains," *Journal of Neurochemistry*, vol. 52, no. 2, pp. 515–520, 1989.

[47] L. Arodin, A. Miranda-Vizuete, P. Swoboda, and A. P. Fernandes, "Protective effects of the thioredoxin and glutaredoxin systems in dopamine-induced cell death," *Free Radical Biology & Medicine*, vol. 73, pp. 328–336, 2014.

[48] A. P. Mazzetti, M. C. Fiorile, A. Primavera, and M. Lo Bello, "Glutathione transferases and neurodegenerative diseases," *Neurochemistry International*, vol. 82, pp. 10–18, 2015.

[49] K. Z. Guyton, Y. Liu, M. Gorospe, Q. Xu, and N. J. Holbrook, "Activation of mitogen-activated protein kinase by H_2O_2. Role in cell survival following oxidant injury," *The Journal of Biological Chemistry*, vol. 271, no. 8, pp. 4138–4142, 1996.

[50] A. Bonni, A. Brunet, A. E. West, S. R. Datta, M. A. Takasu, and M. E. Greenberg, "Cell survival promoted by the Ras-MAPK signaling pathway by transcription-dependent and -independent mechanisms," *Science*, vol. 286, no. 5443, pp. 1358–1362, 1999.

[51] H. Dudek, S. R. Datta, T. F. Franke et al., "Regulation of neuronal survival by the serine-threonine protein kinase Akt," *Science*, vol. 275, no. 5300, pp. 661–665, 1997.

[52] H. Harada, B. Quearry, A. Ruiz-Vela, and S. J. Korsmeyer, "Survival factor-induced extracellular signal-regulated kinase phosphorylates BIM, inhibiting its association with BAX and proapoptotic activity," *Proceedings of the National Academy of Sciences*, vol. 101, no. 43, pp. 15313–15317, 2004.

[53] R. Seger and E. G. Krebs, "The MAPK signaling cascade," *The FASEB Journal*, vol. 9, no. 9, pp. 726–735, 1995.

[54] E. Lin, J. E. Cavanaugh, R. K. Leak, R. G. Perez, and M. J. Zigmond, "Rapid activation of ERK by 6-hydroxydopamine promotes survival of dopaminergic cells," *Journal of Neuroscience Research*, vol. 86, no. 1, pp. 108–117, 2008.

[55] B. D. Manning and A. Toker, "AKT/PKB signaling: navigating the network," *Cell*, vol. 169, no. 3, pp. 381–405, 2017.

[56] L. A. Greene, O. Levy, and C. Malagelada, "Akt as a victim, villain and potential hero in Parkinson's disease pathophysiology and treatment," *Cellular and Molecular Neurobiology*, vol. 31, no. 7, pp. 969–978, 2011.

[57] M. P. Cunha, M. D. Martín-de-Saavedra, A. Romero et al., "Protective effect of creatine against 6-hydroxydopamine-induced cell death in human neuroblastoma SH-SY5Y cells: involvement of intracellular signaling pathways," *Neuroscience*, vol. 238, pp. 185–194, 2013.

[58] E. Amiri, R. Ghasemi, and M. Moosavi, "Agmatine protects against 6-OHDA-induced apoptosis, and ERK and Akt/GSK disruption in SH-SY5Y cells," *Cellular and Molecular Neurobiology*, vol. 36, no. 6, pp. 829–838, 2016.

[59] C. X. Tiong, M. Lu, and J.-S. Bian, "Protective effect of hydrogen sulphide against 6-OHDA-induced cell injury in SH-SY5Y cells involves PKC/PI3K/Akt pathway," *British Journal of Pharmacology*, vol. 161, no. 2, pp. 467–480, 2010.

[60] J. Kim, Y.-N. Cha, and Y.-J. Surh, "A protective role of nuclear factor-erythroid 2-related factor-2 (Nrf2) in inflammatory disorders," *Mutation Research/Fundamental and Molecular Mechanisms of Mutagenesis*, vol. 690, no. 1-2, pp. 12–23, 2010.

[61] S. E. Lacher, J. S. Lee, X. Wang, M. R. Campbell, D. A. Bell, and M. Slattery, "Beyond antioxidant genes in the ancient Nrf2 regulatory network," *Free Radical Biology & Medicine*, vol. 88, pp. 452–465, 2015.

[62] Z. Qi, X. Ci, J. Huang et al., "Asiatic acid enhances Nrf2 signaling to protect HepG2 cells from oxidative damage through Akt and ERK activation," *Biomedicine & Pharmacotherapy*, vol. 88, pp. 252–259, 2017.

Hindawi
Oxidative Medicine and Cellular Longevity
Volume 2018, Article ID 9595741, 16 pages
https://doi.org/10.1155/2018/9595741

Research Article

Formulated Chinese Medicine Shaoyao Gancao Tang Reduces Tau Aggregation and Exerts Neuroprotection through Anti-Oxidation and Anti-Inflammation

I-Cheng Chen,[1] **Te-Hsien Lin**,[2] **Yu-Hsuan Hsieh**,[2] **Chih-Ying Chao**,[1] **Yih-Ru Wu**,[1] **Kuo-Hsuan Chang**,[1] **Ming-Chung Lee**,[3] **Guey-Jen Lee-Chen**,[2] **and Chiung-Mei Chen**[1]

[1]*Department of Neurology, Chang Gung Memorial Hospital, Chang Gung University College of Medicine, Taipei 10507, Taiwan*
[2]*Department of Life Science, National Taiwan Normal University, Taipei 11677, Taiwan*
[3]*Sun Ten Pharmaceutical Co. Ltd., New Taipei City 23143, Taiwan*

Correspondence should be addressed to Guey-Jen Lee-Chen; t43019@ntnu.edu.tw
and Chiung-Mei Chen; cmchen@adm.cgmh.org.tw

Received 11 May 2018; Accepted 29 July 2018; Published 28 October 2018

Academic Editor: Francisco Jaime Bezerra Mendonça Júnior

Misfolded tau proteins induce accumulation of free radicals and promote neuroinflammation by activating microglia-releasing proinflammatory cytokines, leading to neuronal cell death. Traditional Chinese herbal medicines (CHMs) have been widely used in clinical practice to treat neurodegenerative diseases associated with oxidative stress and neuroinflammation. This study examined the neuroprotection effects of formulated CHMs Bai-Shao (made of *Paeonia lactiflora*), Gan-Cao (made of *Glycyrrhiza uralensis*), and Shaoyao Gancao Tang (SG-Tang, made of *P. lactiflora* and *G. uralensis* at 1 : 1 ratio) in cell model of tauopathy. Our results showed that SG-Tang displayed a greater antioxidative and antiaggregation effect than Bai-Shao and Gan-Cao and a stronger anti-inflammatory activity than Bai-Shao but similar to Gan-Cao. In inducible 293/SH-SY5Y cells expressing proaggregant human tau repeat domain (ΔK280 tau_{RD}), SG-Tang reduced tau misfolding and reactive oxygen species (ROS) level in ΔK280 tau_{RD} 293 cells and promoted neurite outgrowth in ΔK280 tau_{RD} SH-SY5Y cells. Furthermore, SG-Tang displayed anti-inflammatory effects by reducing nitric oxide (NO) production in mouse BV-2 microglia and increased cell viability of ΔK280 tau_{RD}-expressing SH-SY5Y cells inflamed by BV-2 conditioned medium. To uncover the neuroprotective mechanisms of SG-Tang, apoptosis protein array analysis of inflamed tau expressing SH-SY5Y cells was conducted and the suppression of proapoptotic proteins was confirmed. In conclusion, SG-Tang displays neuroprotection by exerting antioxidative and anti-inflammatory activities to suppress neuronal apoptosis in human tau cell models. The study results lay the base for future applications of SG-Tang on tau animal models to validate its effect of reducing tau misfolding and potential disease modification.

1. Introduction

Neurodegenerative diseases including Alzheimer's disease (AD) and tauopathy are characterized by the presence of hyperphosphorylated, insoluble, and filamentous tau protein, which leads to neuronal dysfunction and loss [1]. Tau is an ubiquitously distributed microtubule-associated protein that promotes and stabilizes microtubule assembly. Aside from helping microtubule assembly, tau also interacts with other cytoskeleton components to play a role in axonal transport [2]. Tau is encoded by *MAPT* (microtubule-associated protein tau) gene located on chromosome 17q21, containing 16 exons [3]. By alternative splicing, tau proteins exist as six different isoforms in human central nervous system (CNS). Exons 9–12 encode four C-terminal microtubule binding motifs which are imperfect copies of an 18-amino-acid tau repeat domain (tau_{RD}). Different point mutations found in tau_{RD} reduced the ability of tau to promote microtubule assembly [4] and accelerated aggregation of tau into filaments [5]. In addition, a single amino acid deletion

(ΔK280) was found in patients with frontotemporal dementia and AD [6–8]. ΔK280 is extremely fibrillogenic and frequently used to model tau aggregation [9–11].

Emerging evidence has shown protein aggregation as a trigger for inflammation and neurodegeneration [12]. Activated microglia are found in the postmortem brain tissues of human tauopathy, and microglial burden correlated with tau burden in most of the pathologically afflicted areas [13, 14]. Chronic activation of microglia may enhance the hyperphosphorylation of tau and the subsequent development of neurofibrillary tangles [15]. Activated microglia contribute to neurofibrillary pathology in AD through production of interleukin (IL)-1 and activation of neuronal p38-MAPK (mitogen-activated protein kinase 1) *in vitro* [16] and *in vivo* [17]. In transgenic mice that develop both tau and amyloid pathologies (3 × Tg-AD line), lipopolysaccharide-(LPS-) induced activation of glia exacerbates tau pathology [18]. Tau oligomers colocalize with astrocytes and microglia to induce inflammation, leading to neuronal damage and eventual cell death [19]. Being a critical component in pathogenesis, neuroinflammation provides an attractive therapeutic target in the treatment and prevention of AD and other tauopathy [20, 21].

Traditional Chinese herbal medicines (CHMs) have accumulated several lines of beneficial evidence in the treatment of AD [22–24]. However, treatment approaches addressing inflammatory processes in tauopathy have not been well investigated. Bai-Shao and Gan-Cao are formulated CHMs prepared from herbs *Paeonia lactiflora* (*P. lactiflora*) and *Glycyrrhiza uralensis* (*G. uralensis*), respectively. Total glucosides of paeony extracted from *P. lactiflora* may exert anti-inflammatory activities that contribute to its analgesic effect through modulating production of proinflammatory cytokines from macrophage-like synoviocytes [25]. In addition, ethanol extracts of *G. uralensis* possess inhibitory effects against NF-κB-mediated inflammatory response and strong activation of the Nrf2-ARE-antioxidative stress signaling pathways [26]. In this study, Bai-Shao, Gan-Cao, and Shaoyao Gancao Tang (SG-Tang), a formulated CHM made of *P. lactiflora* and *G. uralensis* at 1 : 1 ratio, were tested in a tau aggregation model [27] to reveal underlying pathogenesis and develop therapeutic strategy targeting neuroinflammation in tauopathy.

2. Materials and Methods

2.1. Preparation of Formulated CHMs. Bai-Shao (Code: 5722), Gan-Cao (Code: 5536), and SG-Tang (Code: 0703H) were provided by Sun Ten Pharmaceutical Co. Ltd. (New Taipei City, Taiwan). To prepare the CHM stock solution, 5 g powder was dissolved in 10 ml ddH_2O, vortexed to mix well, and then centrifuged at 4000 rpm for 10 min at room temperature. The supernatant was collected and used for further experiments.

2.2. HPLC Analysis. High-performance liquid chromatography (HPLC) was performed using a LaChrom Elite HPLC system (Hitachi, Tokyo, Japan) equipped with photodiode array detector. The chromatographic separation of Bai-Shao, Gan-Cao, and SG-Tang (500 mg/ml) was achieved using a Hypersil ODS (C18) column (250 × 4.6 mm, 5 μm). The mobile phase consisted of 0.1% phosphoric acid in water (A) and acetonitrile (B). The linear gradient elution was used as follows: 10~50% B (0~40 min), 50~90% B (40~45 min), 90% B (45~55 min), 90~10% B (55~60 min), and 10% B (60~70 min). The flow rate was 0.8 ml/min. The column and autosampler were maintained at 30°C and 20°C, respectively. Reference compounds were paeoniflorin and ammonium glycyrrhizinate (Sigma-Aldrich, St. Louis, MO, USA) and absorbance was monitored at 230 nm and 250 nm, respectively. The scan range for photo diode array was 190~600 nm. 3-(4,5-Dimethylthiazol-2-yl)-2,5-diphenyltetrazolium bromide (MTT), 1,1-diphenyl-2-picrylhydrazyl (DPPH), LPS, and Congo red were purchased from Sigma-Aldrich. Interferon- (IFN-) γ was obtained from Santa Cruz.

2.3. Cell Culture. Two mouse cell lines, RAW 264.7 macrophage (BCRC 60001, Food Industry Research and Development Institute, Taiwan) and BV-2 microglia (kind gift from Dr. Han-Min Chen, Catholic Fu-Jen University, New Taipei City, Taiwan), were used in this study. The murine RAW 264.7 and microglial BV-2 cells were routinely maintained in DMEM supplemented with 10% FBS (Invitrogen, Waltham, MA, USA) at 37°C under 5% CO_2 and 95% relative humidity.

Four human cell lines, HEK-293 cells (ATCC no. CRL-1573), SH-SY5Y neuronal cells (ATCC no. CRL-2266) and Tet-on ΔK280 tau_{RD}-DsRed 293/SH-SY5Y cells [27] were used. HEK-293 cells were grown in DMEM with 10% FBS, and SH-SY5Y cells were maintained in DMEM-F12 with 10% FBS. In addition to the basal media for HEK-293 and SH-SY5Y, 5 μg/ml blasticidin and 100 μg/ml hygromycin (InvivoGen, San Diego, CA, USA) were applied for Tet-On ΔK280 tau_{RD}-DsRed cells.

2.4. MTT Assay. To evaluate cell viability, 5×10^4 HEK-293/SH-SY5Y cells were plated into 48-well dishes, grown for 20 h, and treated with tested Chinese medicine formulas (0.1~1000 μg/ml Bai-Shao, Gan-Cao, or SG-Tang). After 1 day, 20 μl of 5 mg/ml MTT was added onto each 48-well containing cells with 200 μl of cultured medium at 37°C for 3 h. 200 μl of lysis buffer (10% Triton X-100, 0.1 N HCl, 18% isopropanol) was then added onto 48-well and the absorbance at OD 570 nm was read by a microplate reader (FLx800 fluorescence microplate reader, Bio-Tek, Winooski, VT, USA). The half maximal inhibitory concentration (IC_{50}) were calculated using the interpolation method.

2.5. DPPH Assay. The DPPH radical-scavenging activity was measured in a reaction mixture containing 0.1 ml of 0.2 mM DPPH radical solution and 0.1 ml of each tested formulas (100~1000 μg/ml). The solution was rapidly mixed and incubated for 30 min at 25°C. The scavenging capacity was measured by monitoring the absorbance at 517 nm with a microplate reader (Multiskan GO, Thermo Scientific, Waltham, MA, USA). The half maximal effective concentrations (EC_{50}) were calculated using the interpolation method.

2.6. Detection of Inflammatory Mediators. Murine RAW 264.7 macrophage cells were seeded in DMEM containing 1% FBS and pretreated with tested formulas (0.5~2 mg/ml) or celecoxib (50 μM) for 8 h followed by LPS (1 μg/ml) stimulation. The release of NO was evaluated by Griess assay according to the manufacturer's protocol (Sigma-Aldrich). The levels of tumor necrosis factor- (TNF-) α, IL-1β, and IL-6 were determined using a mouse enzyme-linked immunosorbent assay (ELISA) system (R&D Systems, Minneapolis, MN, USA) following the manufacturer's protocol. The optical density at 450 nm was detected using a microplate reader (ELISA Reader: SpectraMAX340PC; Molecular Devices, Sunnyvale, CA, USA). In addition, the immortalized murine microglial BV-2 cells, an alternative model system for primary microglia, were used. BV-2 cells were seeded in DMEM containing 1% FBS. Next day, cells were pretreated with SG-Tang for 8~24 h, stimulated with LPS (1 μg/ml) for 20 h, and released of NO in the media determined.

2.7. ΔK280 tau$_{RD}$-DsRed Fluorescence Assay. DsRed fluorescence was evaluated to reflect tau aggregation. On the first day, ΔK280 tau$_{RD}$-DsRed 293 cells were seeded into the 96-well dish in a density of 0.8×10^4 cells/well and one day after seeding, 5~20 μM Congo red or 50~200 μg/ml Bai-Shao, Gan-Cao, and SG-Tang were added. After 8 h of culture, doxycycline (1 μg/ml; Sigma-Aldrich) was added to induce misfolded tau expression. On the fifth day, cells were stained with Hoechst 33342 (0.1 μg/ml) for 30 min, and fluorescence intensities (543 nm excitation and 593 nm emission for DsRed; 377 nm excitation and 447 nm emission for Hoechst 33342) were measured using a high content analysis (HCA) system (ImageXpressMICRO, Molecular Devices). All images were analyzed by MetaXpress Image Acquisition and Analysis Software (Molecular Devices).

2.8. ROS Assay. Cellular ROS of the above Tet-On ΔK280 tau$_{RD}$-DsRed 293 cells was measured by fluorogenic reagent (CellROX™ Deep Red, Molecular Probes, Eugene, OR, USA) with final concentration of 5 μM and incubated at 37°C for 30 min. Then, cells were washed with PBS and analyzed by flow cytometer (Becton-Dickinson, Franklin Lakes, NJ, USA) with excitation/emission wavelengths at 640/665 nm. For each sample, 5×10^4 cells are analyzed.

2.9. Neurite Outgrowth Analysis. 3×10^4 of ΔK280 tau$_{RD}$-DsRed SH-SY5Y cells/well were seeded in a 24-well plate, and 10 μM retinoic acid (Sigma-Aldrich) was added to initiate neuronal differentiation. On the second day, cells were treated with SG-Tang (200 μg/ml) or Congo red (20 μM) for 8 h before tau expression induction by adding doxycycline (1 μg/ml). On day 9, cells were fixed in 4% paraformaldehyde in PBS for 15 min, permeabilized in 0.1% Triton X-100 in PBS for 10 min, and blocked in 3% bovine serum albumin (BSA) in PBS for 20 min. Primary TUBB3 antibody (1 : 1000 dilution in PBS with 1% BSA, 0.05% Tween 20, and 0.02% NaN_3; Covance, Princeton, NJ, USA) was used to stain neuronal cells, followed by secondary goat anti-rabbit Alexa Fluor ®555 antibody (1 : 1000 dilution; Molecular probes) at room temperature. After nuclei staining by 4′-6-diamidino-2-phenylindole (DAPI), images of cells were taken via the HCA system and analyzed as described.

2.10. Cell Viability/Cytotoxicity Assays of Inflamed SH-SY5Y Cells. Previously, cell-free media obtained from LPS/IFN-γ-exposed microglia-like cells resulted in the highest toxicity on cell viability of SH-SY5Y cells [28]. To prepare conditioned medium (CM) with inflammatory factors, BV-2 cells were stimulated with a combination of LPS (1 μg/ml) and IFN-γ (100 ng/ml) for 24 h. After morphology examination, the BV-2 CM were collected, pooled, and centrifuged to remove cell debris. The induced inflammation was confirmed by release of NO, TNF-α, IL-1β, and IL-6 in the media and increased Iba1 expression in the cell lysate.

For SH-SY5Y cell viability assay, DMEM-F12 was then mixed with two times volume of BV-2 CM (a final FBS concentration at 10%) and added to undifferentiated ΔK280 tau$_{RD}$-DsRed SH-SY5Y cells for 2 days to induce inflammation. Cell viability was determined by MTT assay as described. For SH-SY5Y cytotoxicity assay, neuronal-differentiated ΔK280 tau$_{RD}$-DsRed SH-SY5Y cells were treated with BV-2 CM for 5 days as described and media were collected. 100 μl of supernatant from each sample was transferred to 96-well plate to examine the release of lactate dehydrogenase (LDH) by using LDH cytotoxicity assay kit (Cayman, Ann Arbor, MI, USA). The absorbance was read at 490 nm with a microplate reader (Multiskan GO, Thermo Scientific).

2.11. Human Apoptosis Antibody Array. Protein samples from ΔK280 tau$_{RD}$-DsRed SH-SY5Y cells with different treatments (Dox uninduced/induced, CM unstimulated/stimulated, and SG-Tang unpretreated/pretreated) were prepared and incubated with apoptosis antibody array membranes (RayBiotech, Norcross, GA, USA). The relative levels of 43 apoptosis-related proteins in human cell lysates were measured with the array. The detected changes in protein levels were confirmed by Western blot or caspase 3 activity assay.

2.12. Western Blot Analysis. Cells were lysed in hypotonic buffer (20 mM HEPES pH 7.4, 1 mM $MgCl_2$, 10 mM KCl, 1 mM DTT, 1 mM EDTA pH 8.0) containing the protease inhibitor mixture (Sigma-Aldrich). After sonication and sitting on ice for 20 min, the lysates were centrifuged at $14000 \times g$ for 30 min at 4°C. Protein concentrations were determined using the Bio-Rad protein assay kit (Bio-Rad, Hercules, CA, USA), with albumin as standards. Total proteins (25 μg) were electrophoresed on 10% or 12% SDS-polyacrylamide gel and transferred onto nitrocellulose membrane (Bio-Rad) by reverse electrophoresis. After being blocked, the membrane is stained with Iba1 (1 : 500; Wako, Osaka, Japan), Tau (1 : 200; Dako, Santa Clara, CA, USA), p-Tau Ser202 (1 : 200; Fremont, CA, USA), p-Tau Thr231 (1 : 500, Invitrogen), p-Tau Ser396 (1 : 500; Invitrogen), BID (1 : 1000; Cell Signaling, Danvers, MA, USA), BAD (1 : 500; Santa Cruz, Dallas, TX, USA), CYCS (1 : 500; Biovision, Milpitas, CA, USA), CASP8 (1 : 1000; Cell Signaling), DsRed

(1 : 500; Santa Cruz), tubulin (1 : 1000; Sigma-Aldrich), or GAPDH (1 : 1000, MDBio) primary antibodies. The immune complexes are detected using horseradish peroxidase-conjugated goat anti-mouse (Jackson ImmunoResearch, West Grove, PA, USA) or goat anti-rabbit (Rockland, Pottstown, PA, USA) IgG antibody (1 : 10000 dilution) and ImmobilonTM Western Chemiluminescent HRP substrate (Millipore, Billerica, MA, USA).

2.13. Caspase 3 Activity Measurement. Cells were lysed in 1 × lysis buffer by repeated cycles of freezing and thawing. Caspase 3 activity was measured with the caspase 3 assay kit according to the manufacturer's instructions (Sigma-Aldrich).

2.14. Statistical Analysis. For each set of values, data are represented as mean ± SD of three independent experiments. Differences between groups were evaluated by two-tailed Student's *t*-test or ANOVA (one-way and two-way) with post hoc LSD test where appropriate. p values < 0.05 were considered significant.

3. Results

3.1. Formulated CHMs and Cytotoxicity. Three formulated CHMs, Bai-Shao, Gan-Cao, and SG-Tang were studied. To examine the cytotoxicity of these CHM formulas, MTT assay was performed on HEK-293 or SH-SY5Y cells after treatment with the tested formulas for 24 h. As shown in Figure 1(a), Bai-Shao, Gan-Cao, and SG-Tang exhibited very low cytotoxicity in HEK-293 and SH-SY5Y cells.

Next, the amounts of active constituents, paeoniflorin and ammonium glycyrrhizinate, in these CHM formulas were analyzed by full-spectrum analytic HPLC. As shown in Figure 1(b), chromatographic patterns showed peaks at 230 and 250 nm corresponding to the retention time compatible with paeoniflorin and ammonium glycyrrhizinate, respectively. The amounts of active constituents in these CHM formulas (0.5 g/ml) were 4.06% (42.25 mM) for paeoniflorin in Bai-Shao, 5.78% (34.41 mM) for ammonium glycyrrhizinate in Gan-Cao, and 2.81% (29.33 mM) for paeoniflorin and 2.43% (14.52 mM) for ammonium glycyrrhizinate in SG-Tang.

3.2. Radical-Scavenging Activity and Anti-Inflammatory Activity of the Tested Formulas. To evaluate the radical-scavenging activity of these CHM formulas, DPPH scavenging assay was conducted. As shown in Figure 2(a), Bai-Shao, Gan-Cao, and SG-Tang displayed free radical-scavenging activities with EC_{50} at 305 μg/ml, 794 μg/ml, and 292 μg/ml, respectively, indicating SG-Tang has a greater radical-scavenging activity than Bai-Shao or Gan-Cao. The anti-inflammatory responses of formulated CHMs were examined using RAW 264.7 cells, as LPS induced NO, TNF-α, and IL-6 production in murine macrophages [29, 30]. As shown in Figure 2(b), the exposure of RAW 264.7 cells to LPS resulted in a significant increase of NO, TNF-α, IL-1β, and IL-6 after 24 h of incubation (100% vs. 1~12%, $p < 0.001$). The elevations in NO, TNF-α, IL-1β, and IL-6 were reduced significantly in the presence of the nonsteroidal anti-inflammatory drug (NSAID) celecoxib (a selective cyclooxygenase (COX) inhibitor as a positive control) (NO: 39%, $p < 0.001$; TNF-α: 23%, $p = 0.003$; IL-1β: 20%, $p = 0.001$; IL-6: 29%, $p = 0.002$). Similar inhibitory phenomena were observed in the cells treated with Gan-Cao and SG-Tang (NO: 72~16%, $p = 0.023$~<0.001; TNF-α: 66~42%, $p = 0.044$~0.001; IL-1β: 44~26%, $p = 0.004$~<0.001; IL-6: 51~20%, $p = 0.003$ ~<0.001). Our results demonstrated that formulated CHMs Gan-Cao and SG-Tang possess anti-inflammatory effects by reducing production of inflammatory mediators.

3.3. Reduction of Tau Misfolding and Promotion of Neurite Outgrowth of the Tested Formulas. Previously, we generated a proaggregant (ΔK280) tau_{RD} cell model targeting tau misfolding [27]. Inhibition of tau aggregation may improve DsRed misfolding, leading to increased fluorescence in tau_{RD}-DsRed expressing cells. Utilizing the established Tet-on ΔK280 tau_{RD}-DsRed 293 cells, Bai-Shao, Gan-Cao, and SG-Tang were tested for effects of reducing tau misfolding and antioxidation (Figure 3(a)). Fluorescent images of the cells were automatically recorded by a HCA system. As a positive control, Congo red (5~20 μM) significantly increased the ΔK280 tau_{RD}-DsRed fluorescence compared to no treatment (113~127% vs. 100%, $p = 0.023$~0.004). Significantly increased DsRed fluorescence was observed with Bai-Shao (109~117% for 100~200 μg/ml treatment, $p = 0.028$~0.023), Gan-Cao (109~123% for 50~200 μg/ml treatment, $p = 0.017$ ~0.003), and SG-Tang (108~130% for 50~200 μg/ml treatment, $p = 0.003$~ < 0.001) compared to no treatment (Figure 3(b)). Representative fluorescent images of ΔK280 tau_{RD}-DsRed cells untreated or treated with Congo red (20 μM) or SG-Tang (200 μg/ml) are shown in Figure 3(c). The results indicated that Bai-Shao, Gan-Cao, and SG-Tang reduced tau misfolding in our tauopathy 293 cell model and SG-Tang demonstrated a better antiaggregation function than Bai-Shao or Gan-Cao.

Misfolded tau may increase the production of reactive oxygen species (ROS) [31]. To examine whether these CHM formulas display antioxidative effects, ROS level was evaluated in Tet-On ΔK280 tau_{RD}-DsRed 293 cells. As Figure 3(d) shows, pretreatment with Congo red (10 μM, a positive control) or formulas (100 μg/ml) significantly reversed the ROS level elevated by misfolded tau production compared to no treatment (88~95% vs. 100%, $p = 0.045$ ~<0.001). These data showed the anti-oxidative effects of Bai-Shao, Gan-Cao, and SG-Tang, and SG-Tang possesses a greater anti-oxidative effect than Bai-Shao or Gan-Cao.

Since our study showed that SG-Tang has greater effects in free radical scavenging, antioxidation, and antiaggregation than Bai-Shao or Gan-Cao, we focused on SG-Tang treatment in subsequent experiments. The neuroprotective potential of SG-Tang was examined (Figure 4(a)). As Figure 4(b) shows, misfolded tau induction significantly reduced the length of neurites as compared to the absence of induction (93% vs. 100%, $p = 0.030$) and 20 μM Congo red (positive control) or 200 μg/ml SG-Tang pretreatment ameliorated this negative effect (103% vs. 93%, $p = 0.041$ for Congo red; 101% vs. 93%, $p = 0.039$ for SG-Tang). Representative neurite outgrowth images uninduced (− Dox), untreated

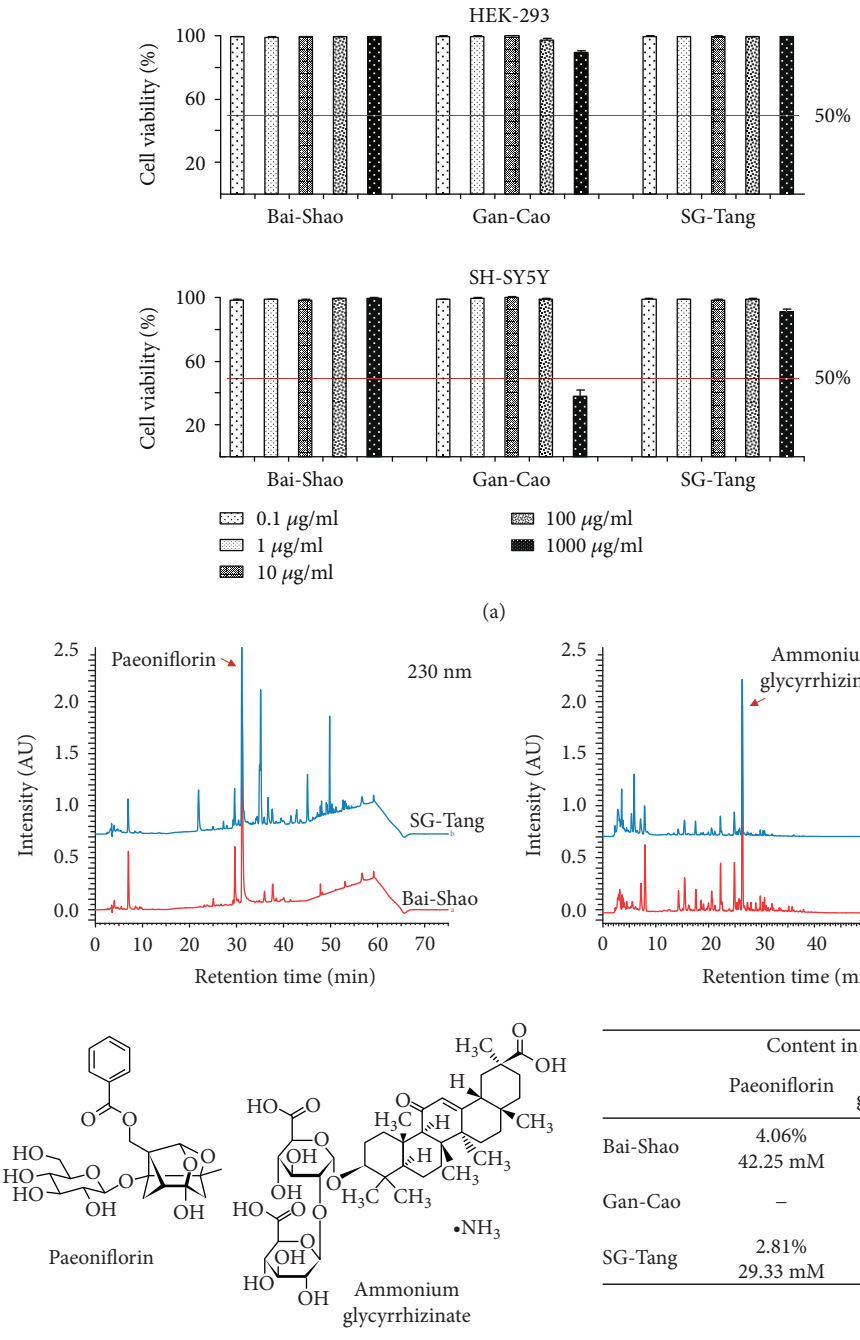

	Content in 0.5 g/ml	
	Paeoniflorin	Ammonium glycyrrhizinate
Bai-Shao	4.06% 42.25 mM	–
Gan-Cao	–	5.78% 34.41 mM
SG-Tang	2.81% 29.33 mM	2.43% 14.52 mM

Figure 1: Cytotoxicity and chemical profiles of Bai-Shao, Gan-Cao, and SG-Tang. (a) MTT cell viability assay of HEK-293 and SH-SY5Y cells after treatment with Bai-Shao, Gan-Cao, and SG-Tang (0.1~1000 μg/ml) for 24 h. To normalize, the relative viability of untreated cells was set as 100%. The red line represents 50% viability. (b) HPLC analysis of Bai-Shao, Gan-Cao, and SG-Tang. Chromatographic patterns (230 and 250 nm) show peaks compatible with paeoniflorin and ammonium glycyrrhizinate. Also shown below are chemical structures of paeoniflorin and ammonium glycyrrhizinate and the relative amounts (in % and mM) of these molecules in Bai-Shao, Gan-Cao, and SG-Tang (0.5 g/ml).

(+ Dox), and after treatment with Congo red and SG-Tang are shown in Figure 4(c). Thus, SG-Tang exerts neuroprotective effect by rescuing the reduction of neurite outgrowth induced by tau misfolding.

3.4. Anti-Inflammatory Effects of SG-Tang in LPS-Stimulated BV-2 Microglia. In the brain, activated microglia release proinflammatory mediators such as NO and cytokines as a response to inflammation [32]. Thus, the anti-inflammatory effects of SG-Tang were determined using LPS-stimulated BV-2 microglia (Figure 5(a)). Figure 5(b) demonstrates that NO production of BV-2 cells significantly increased by LPS stimulation (33.9 μM vs. 4.8 μM, $p < 0.001$) and pretreatment of 100~500 μg/ml SG-Tang for 8~24 h significantly reduced

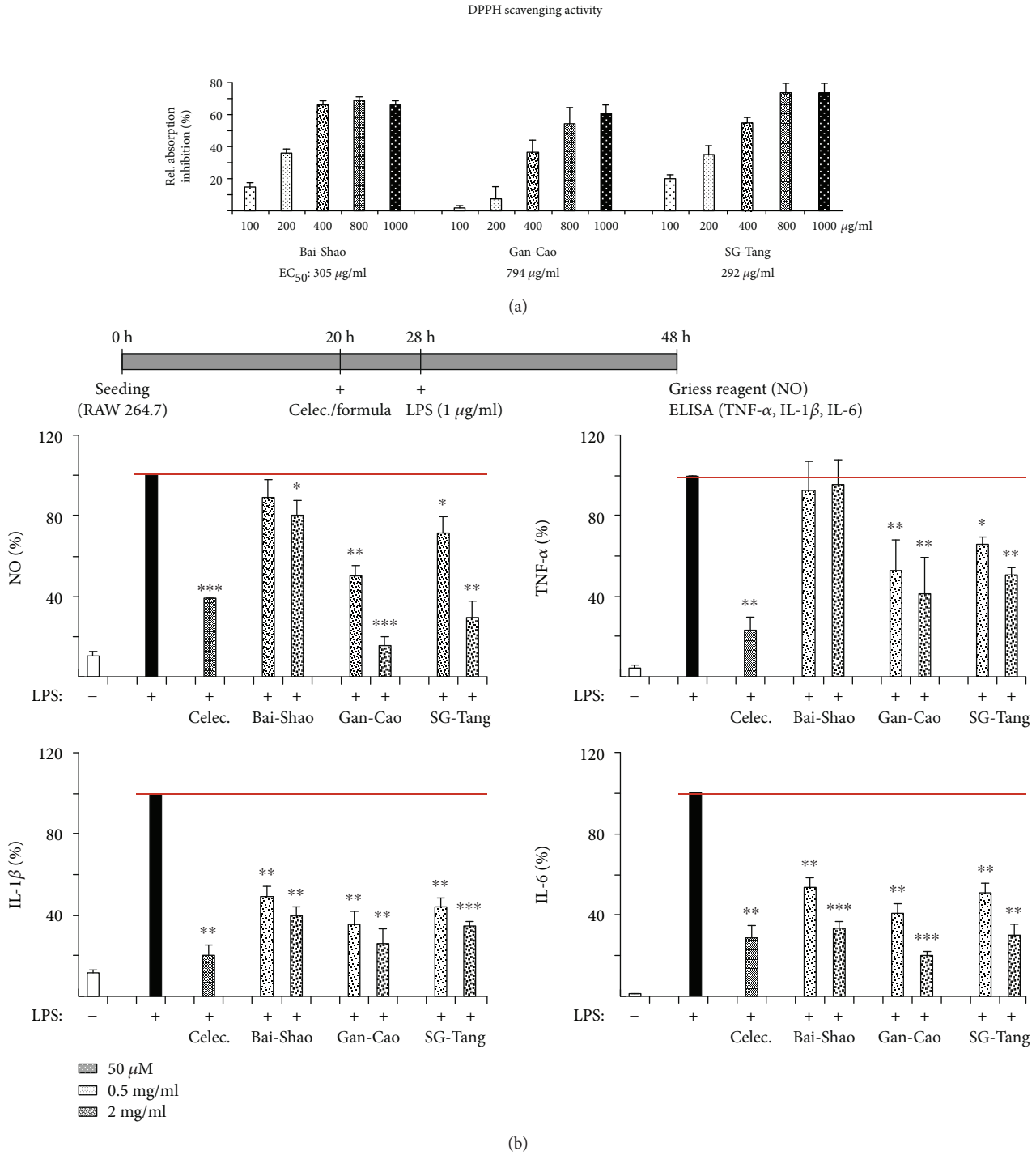

Figure 2: Antioxidative and anti-inflammatory activities of Bai-Shao, Gan-Cao, and SG-Tang. (a) DPPH radical-scavenging activities of the tested CHM formulas (100~1000 μg/ml). The EC_{50} of each formula is shown under the columns. (b) Anti-inflammatory activities of the tested formulas on RAW 264.7 macrophages. Cells (10^6) were pretreated with formulas (0.5~2 mg/ml) or compound celecoxib (Celec., 50 μM) as a positive control for 8 h, and LPS (1 μg/ml) was applied to induce inflammation. After 20 h, the levels of NO (assessed by Griess reagent), TNF-α, IL-1β, and IL-6 (assessed by ELISA) released into cultured media were determined ($n = 3$). For normalization, the relative NO, TNF-α, IL-1β, and IL-6 levels of LPS-treated cells were set as 100%. $^*p < 0.05$, $^{**}p < 0.01$, and $^{***}p < 0.001$, celecoxib/formulas treated vs. untreated cells.

NO production (100 μg/ml for 8 h: 23.7 μM, $p = 0.008$; 500 μg/ml for 8 h: 19.4 μM, $p = 0.002$; 100 μg/ml for 24 h: 17.5 μM, $p = 0.001$; 500 μg/ml for 24 h: 12.2 μM, $p = 0.002$). The results indicate that SG-Tang displayed anti-inflammatory effects by reducing NO production in microglia. We then applied LPS and IFN-γ to BV-2 cells for 24 h for

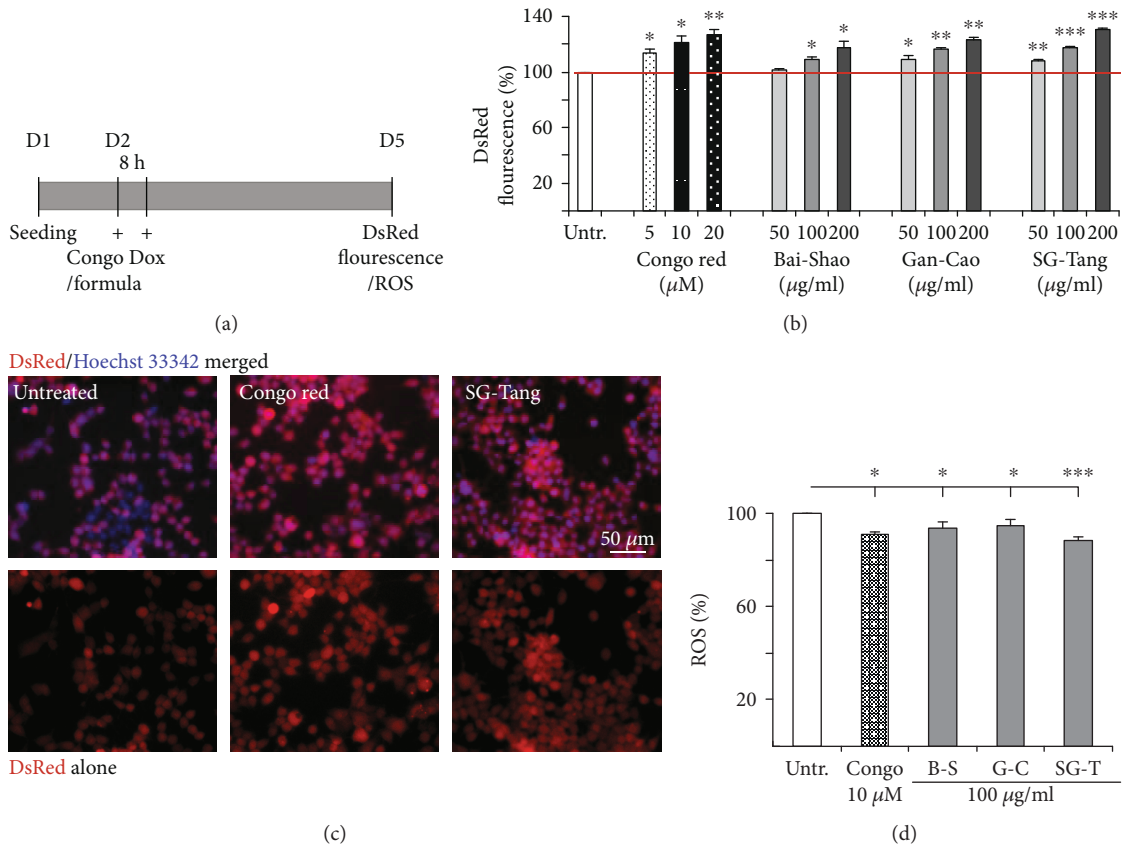

FIGURE 3: The effects of Bai-Shao, Gan-Cao, and SG-Tang on tau misfolding and ROS production in Tet-on ΔK280 tau_{RD}-DsRed 293 cells. (a) Experiment flow chart. ΔK280 tau_{RD}-DsRed 293 cells were pretreated with the tested formulas or Congo red (Congo, as a positive control) for 8 h before misfolded tau induction by doxycycline (Dox, 1 μg/ml) for three days. (b) DsRed fluorescence analysis with Congo red (5~20 μM) or the Chinese medicine formulas Bai-Shao, Gan-Cao, and SG-Tang (50~200 μg/ml) treatment ($n = 3$). The relative DsRed fluorescence of untreated cells is normalized (100%). $^{*}p < 0.05$, $^{**}p < 0.01$, and $^{***}p < 0.001$, treated vs. untreated cells. (c) Representative microscopy images (upper row: merged DsRed and Hoechst 33342 signals; low row: DsRed signal alone) of ΔK280 tau_{RD}-DsRed 293 cells untreated or treated with Congo red (20 μM) or SG-Tang (200 μg/ml). (d) ROS assay of ΔK280 tau_{RD}-DsRed 293 cells untreated or treated with Congo red (10 μM) or the tested formulas Bai-Shao (B-S), Gan-Cao (G-C), and SG-Tang (SG-T) (100 μg/ml) ($n = 3$). The relative ROS of untreated cells was normalized as 100%. $^{*}p < 0.05$ and $^{***}p < 0.001$, treated vs. untreated cells.

conditioned medium (CM) collection (Figure 5(b)). The resting BV-2 microglia showed a ramified morphology but more extended processes with elongated morphology were observed after LPS/IFN-γ treatment for 24 h (Figure 5(d)). As shown in Figures 5(e) and 5(f), elevated Iba1 (induction of brown adipocytes 1, a microglial marker) expression in inflamed BV-2 cells (100% vs. 240%, $p = 0.042$) and increased release of NO, TNF-α, IL-1β, and IL-6 in BV-2 CM (NO: 0.5 μM vs. 49.6 μM, $p = 0.001$; TNF-α: 0.9 ng/ml vs. 28.1 ng/ml, $p = 0.002$; IL-1β: 2.9 pg/ml vs. 8.9 pg/ml, $p < 0.001$; IL-6: 0 ng/ml vs. 33.6 ng/ml, $p = 0.021$) were confirmed. The collected CM was then used to provide inflammatory mediators to ΔK280 tau_{RD}-DsRed SH-SY5Y cells.

3.5. Effects of SG-Tang on BV-2 Conditioned Medium-Inflamed ΔK280 tau_{RD}-DsRed SH-SY5Y Cells. Undifferentiated (without retinoic acid, − RA) or differentiated (with retinoic acid, + RA) ΔK280 tau_{RD}-DsRed SH-SY5Y cells were pretreated with SG-Tang (200 μg/ml) for 8 h before misfolded tau induction and then BV-2 CM was added to provoke inflammatory damage on SH-SY5Y cells for two days (Figure 6(a)). Figure 6(b) shows that misfolded tau induction reduced the viability of ΔK280 tau_{RD}-DsRed SH-SY5Y cells (− RA: 91% vs. 100%, $p = 0.012$; + RA: 90% vs. 100%, $p = 0.035$) and application of SG-Tang rescued the decreased cell viability caused by misfolded tau induction and BV-2 CM addition (− RA: 122% vs. 88%, $p = 0.015$; + RA: 122% vs. 91%, $p = 0.014$). Thus, the reduced viability of inflamed ΔK280 tau_{RD}-DsRed SH-SY5Y cells was not influenced by retinoic acid.

Differentiated SH-SY5Y cells expressing ΔK280 tau_{RD}-DsRed were further evaluated on day 8 for LDH release, neurite outgrowth, and tau phosphorylation (Figure 6(c)). Both addition of Dox (118% vs. 100%, $p = 0.019$) and BV-2 CM (184% vs. 118%, $p < 0.001$) increased the LDH release of ΔK280 tau_{RD}-DsRed SH-SY5Y cells and application of SG-Tang attenuated the LDH release (156% vs. 184%, $p = 0.010$) (Figure 6(d)). Misfolded tau induction significantly reduced the length of neurites compared to the uninduced cells (94% vs. 100%, $p = 0.005$), and addition of BV-2 CM

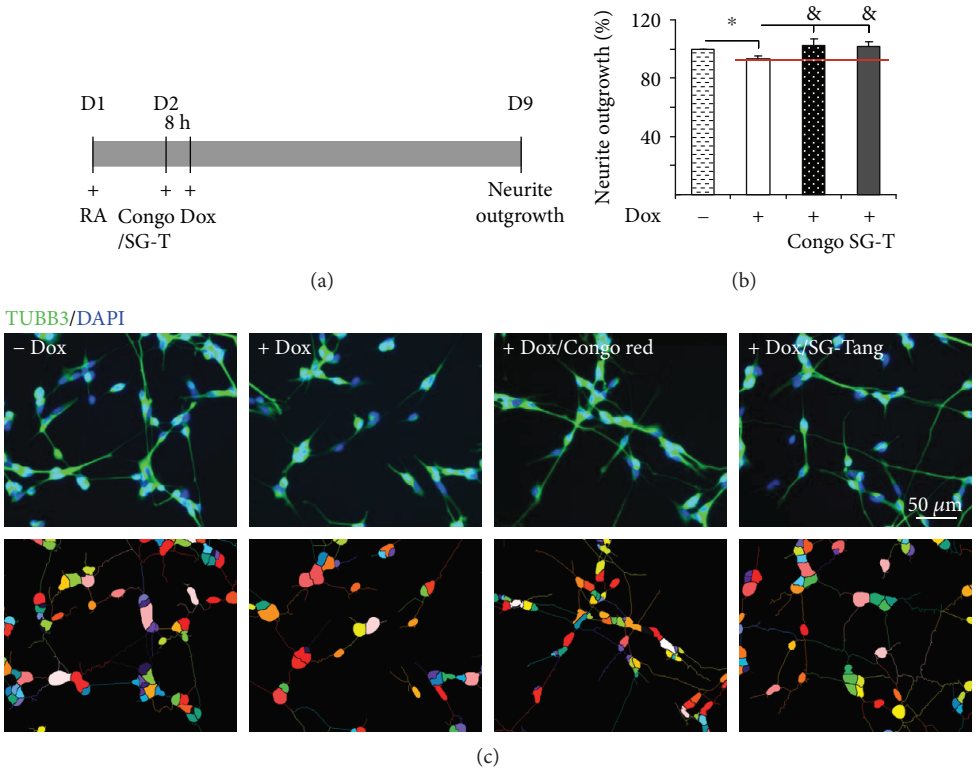

FIGURE 4: The effects of Bai-Shao, Gan-Cao and SG-Tang on neurite outgrowth in Tet-on ΔK280 tau_{RD}-DsRed SH-SY5Y cells. (a) Experiment flow chart. ΔK280 tau_{RD}-DsRed SH-SY5Y cells were seeded in 24-well (3×10^4/well) plate with all *trans* retinoic acid (RA, 10 μM). On day 2, cells were treated with Congo red (20 μM) or SG-Tang (200 μg/ml) for 8 h, induced tau_{RD}-DsRed expression with doxycycline (Dox, 1 μg/ml), and neurite outgrowth assayed on day 9. (b) Neurite outgrowth assay ($n = 3$) with Congo red or SG-Tang (SG-T) treatment. To normalize, the relative neurite outgrowth of untreated cells is set as 100%. $^*p < 0.05$, induced vs. un-induced cells; $^\&p < 0.05$, treated vs. untreated cells. (c) Representative microscopy images of neuronally differentiated ΔK280 tau_{RD}-DsRed SH-SY5Y cells uninduced (– Dox), untreated (+ Dox), and after treatment with Congo red (+ Dox/Congo red) or SG-Tang (+ Dox/SG-Tang). Neurites were stained with TUBB3 (neuronal class III β-tubulin, green) antibody. Nuclei were detected using (DAPI, blue). Upper row, merged TUBB3 and DAPI signals; lower row, images of the neurites and the body of individual cells being outlined by the same color for outgrowth quantification.

aggravated this condition (88% vs. 94%, $p < 0.001$). Pretreatment of SG-Tang resulted in significant increase of neurite outgrowth (98% vs. 88%, $p = 0.004$) (Figure 6(e)). Representative images of neurite outgrowth of the above cells are shown in Figure 6(f).

The abnormal hyperphosphorylation of tau plays a role in the molecular pathogenesis of AD and other tauopathies. Therefore, the amount of phosphorylated tau was examined and Western blot showed that misfolded tau induction increased tau phosphorylation at residue Ser202, Thr231, and Ser396 compared to uninduced cells (Ser202: 130% vs. 100%, $p = 0.020$; Thr231: 119% vs. 100%, $p = 0.016$; Ser396: 127% vs. 100%, $p = 0.012$). Although addition of BV-2 CM in misfolded tau-expressing cells did not cause further increase of tau phosphorylation at Ser202, Thr231, and Ser396, pretreatment of SG-Tang could reverse abnormal tau hyperphosphorylation at Ser202 (76% vs. 107%, $p = 0.022$) and Thr231 (79% vs. 122%, $p = 0.021$) (Figure 6(g)). Our results demonstrate that SG-Tang could protect cells from cell death, increase neurite outgrowth, and reduce hyperphosphorylation of tau in inflamed misfolded tau-expressing ΔK280 tau_{RD}-DsRed cells.

3.6. Identification of SG-Tang Targets by Human Apoptosis Antibody Array. TNF-α has been long considered as an effecter of inflammation-induced cell death. It has been shown that TNF-α binds to receptor TNFR1 to permit the release of silencer of death domain (SODD) and the recruitment of intracellular death signaling inducing signaling complex (DISC) proteins, including TNFR-associated death domain protein (TRADD) and Fas-associated protein with death domain (FADD), which then activates caspase 8 leading to apoptosis [33]. Caspase 8 is also a key mediator of inflammation and processing of pro-IL-1β to IL-1β [34]. Since we have found SG-Tang decreased TNF-α and IL-1β in CM of BV-2, we proposed that SG-Tang may also act on the inflammation-induced cell death. To elucidate the molecular mechanisms underlying the rescue from inflammation-induced cell death by SG-Tang, proteins from uninduced (– Dox), induced (+ Dox), inflamed (+ Dox/CM), and SG-Tang-pretreated inflamed (+ Dox/CM/SG-Tang) ΔK280 tau_{RD}-DsRed SH-SY5Y cells were examined by using human apoptosis array to evaluate expression levels of 43 apoptosis-related proteins (Figure 7(a)). Among these targets, expression of proapoptotic Bcl2-associated agonist of cell death

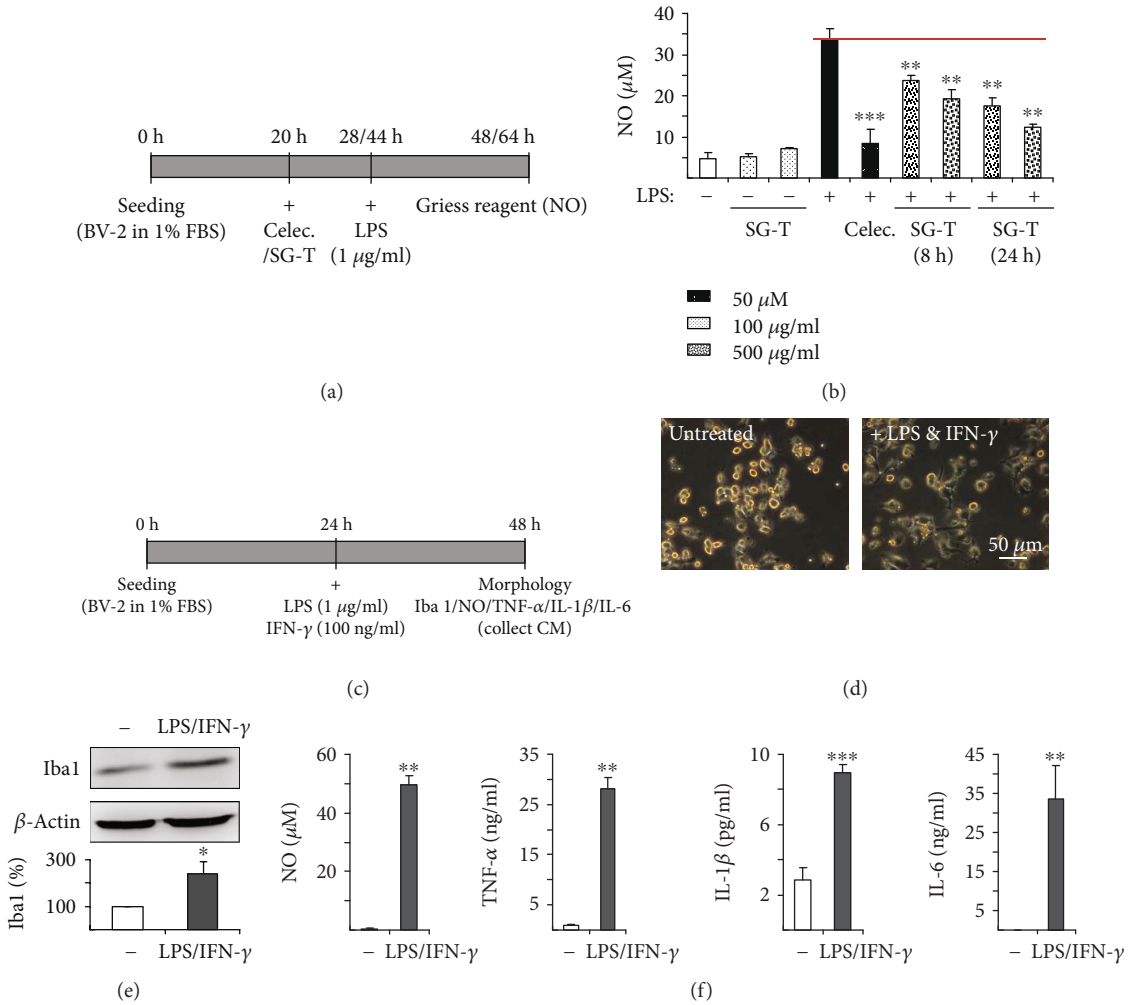

Figure 5: Anti-inflammatory effects of SG-Tang and BV-2 conditioned medium preparation. (a) Experiment flow chart for LPS stimulation. BV-2 cells were seeded in 1% fetal bovine serum (FBS) and pretreated with 50 μM celecoxib (Celec.) for 8 h or 100~500 μg/ml SG-Tang (SG-T) 8~24 h followed by 1 μg/ml LPS stimulation 20 h. NO level was evaluated with Griess reagent. (b) Anti-inflammatory effect of celecoxib (Celec.) and SG-Tang (SG-T) on BV-2 cells ($n = 3$). ** $p < 0.01$ and *** $p < 0.001$, treated vs. untreated cells. (c) Experiment flow chart for LPS/IFN-γ stimulation. For preparation of BV-2 conditioned medium (CM), BV-2 cells were seeded in Dulbecco's modified Eagle's medium (DMEM) with 1% FBS medium. Next day, cells were stimulated with a combination of LPS (1 μg/ml) and IFN-γ (100 ng/ml). After 24 h stimulation, the BV-2 CM was collected and examined for inflammation by morphology, Iba1 Western blotting and NO/TNF-α/IL-1β/IL-6 determination. (d) Morphology of BV-2 cells. (e) Western blot analysis of Iba1 expression in inflamed BV-2 cells ($n = 3$). To normalize, Iba1 expression level in uninflamed cells was set as 100%. * $p < 0.05$, stimulated vs. unstimulated cells. (f) Secretion of NO, TNF-α, IL-1β, and IL-6 in BV-2 CM. ** $p < 0.01$ and *** $p < 0.001$, stimulated vs. unstimulated cells.

(BAD), BH3-interacting domain death agonist (BID), caspase 3 (CASP3), caspase 8 (CASP8) and cytochrome c, and somatic (CYCS) were apparently reduced by SG-Tang treatment (Table 1). Western blot analysis of BAD, BID, CASP8, and CYCS expression changes and caspase 3 activity assay further confirmed that pretreatment of SG-Tang could significantly decrease these identified targets (BAD: from 228% to 157%, $p = 0.023$; BID: from 139% to 110%, $p = 0.038$; CASP8: from 118% to 104%, $p = 0.024$; CYCS: from 163% to 96%, $p = 0.040$; caspase 3 activity: from 165% to 103%, $p = 0.005$). Moreover, addition of SG-Tang improved ΔK280 tau$_{RD}$-DsRed misfolding and enhanced soluble tau$_{RD}$-DsRed protein level in inflamed ΔK280 tau$_{RD}$-DsRed SH-SY5Y cells (from 90% to 115%, $p = 0.004$) (Figure 7(b)). Our results indicated that SG-Tang may protect inflamed ΔK280 tau$_{RD}$-DsRed SH-SY5Y cells by inhibiting production of proapoptotic proteins.

4. Discussion

In this study, we demonstrated neuroprotection, antioxidative and anti-inflammatory effects of formulated CHM SG-Tang. Our results showed that SG-Tang displayed a greater antioxidative and antiaggregation effect than Bai-Shao and Gan-Cao and a stronger anti-inflammatory activity than Bai-Shao but similar to Gan-Cao (Figures 2 and 3). Moreover, SG-Tang showed neuroprotective effect of promoting neurite outgrowth probably by ameliorating tau misfolding and oxidative stress in our tauopathy model (Figures 3 and 4). The anti-inflammatory effects of SG-Tang were further

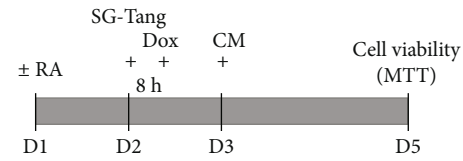

(a)

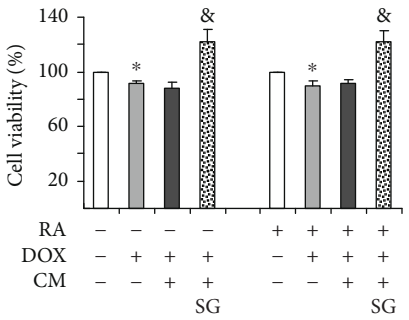

(b)

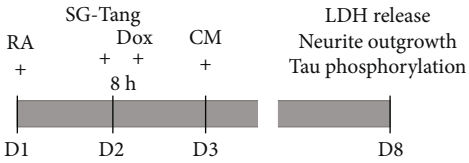

(c)

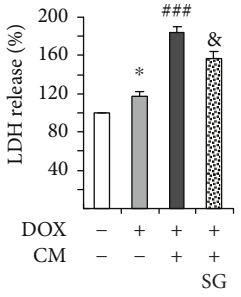

(d)

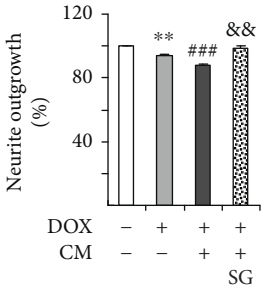

(e)

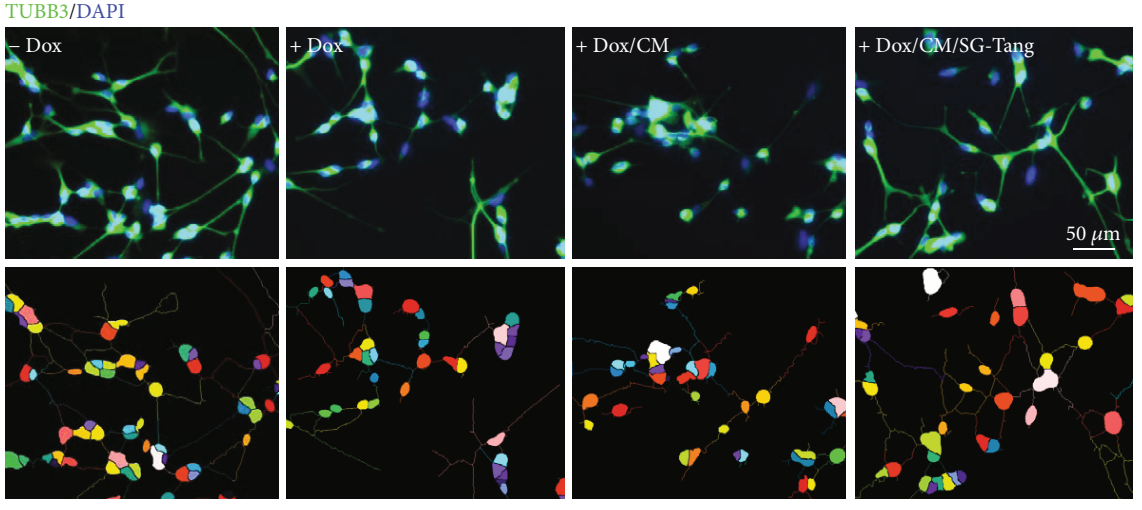

(f)

Figure 6: Continued.

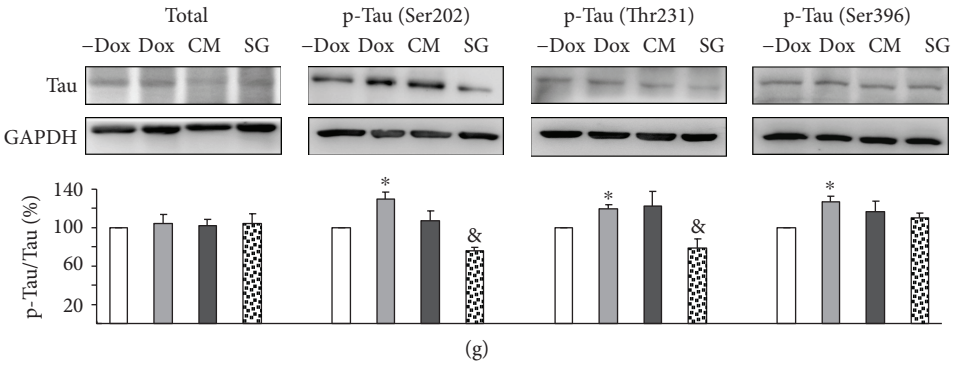

Figure 6: Neuroprotection of SG-Tang on ΔK280 tau_{RD}-DsRed SH-SY5Y cells from BV-2 conditioned medium-induced cell death. (a) Experiment flow chart for cell viability assay. ΔK280 tau_{RD}-DsRed SH-SY5Y cells were plated in media with/without retinoic acid (± RA, 10 μM) on day 1 and pretreated with SG-Tang the next day for 8 h, followed by doxycycline addition (Dox, 1 μg/ml) to induce misfolded tau expression. On day 3, DMEM-F12 media was mixed with BV-2 CM and cell viability was assessed by MTT assay on day 5. (b) Cell viability assay ($^{*}p < 0.05$, − Dox vs. + Dox; $^{\&}p < 0.05$, + Dox/CM vs. + Dox/CM/SG-Tang-treated cells) ($n = 3$). (c) Experiment flow chart for LDH release, neurite outgrowth, and tau phosphorylation assays. RA (10 μM, present in cultures throughout) differentiated ΔK280 tau_{RD}-DsRed SH-SY5Y cells were pretreated with SG-Tang (200 μg/ml) on day 2 for 8 h, followed by inducing ΔK280 tau_{RD}-DsRed expression (+ Dox, 1 μg/ml). On day 3, DMEM-F12 was mixed with BV-2 CM and added to the cells. After five days, media were collected for LDH release examination. In addition, cells were examined for neurite outgrowth and tau phosphorylation. (d) LDH assay ($^{*}p < 0.05$, − Dox vs. + Dox; $^{\#\#\#}p < 0.001$, + Dox vs. +Dox/CM; $^{\&}p < 0.05$, + Dox/CM vs. + Dox/CM/SG-Tang treated cells) ($n = 3$). (e) Neurite outgrowth assay ($n = 3$). To normalize, the relative neurite outgrowth of uninduced cells is set as 100%. $^{**}p < 0.01$, − Dox vs. + Dox; $^{\#\#\#}p < 0.001$, + Dox vs. + Dox/CM; $^{\&\&}p < 0.01$, + Dox/CM vs. + Dox/CM/SG-Tang-treated cells. (f) Representative microscopy images of differentiated ΔK280 tau_{RD}-DsRed SH-SY5Y cells uninduced (− Dox), induced (+ Dox), inflamed (+ Dox/CM), or treated with SG-Tang (+ Dox/CM/SG-Tang). Neurites were stained with TUBB3 (green) antibody. Nuclei were detected using DAPI (blue). Upper row, merged TUBB3 and DAPI signals; lower row, images of the neurites and the body of a cell being outlined by the same color for outgrowth quantification. (g) Western blot analysis of total and phosphorylated (Ser202, Thr231, and Ser396) tau (normalized to GAPDH internal control, $n = 3$). $^{*}p < 0.05$, − Dox vs. + Dox; $^{\&}p < 0.05$, + Dox/CM vs. + Dox/CM/SG-Tang-treated cells.

demonstrated by using LPS-stimulated BV-2 microglia (Figure 5). Targets identified from human apoptosis protein array indicate SG-Tang may suppress the expression levels of proapoptotic proteins in inflamed ΔK280 tau_{RD}-DsRed SH-SY5Y cells and thus elevate the cell viability (Figures 6 and 7).

In human tauopathy, substantial activated microglia are found in regions of phosphorylated tau accumulation [35]. In tau P301S transgenic mice, prominent glial activation precedes tangle formation and the pattern of activated glia correlates closely with the distribution and density of NFTs [36]. As neuroinflammation is linked to the progression of tauopathy, anti-inflammatory strategy may be effective at reducing tau-related pathology. Indeed, FK506 attenuates tau pathology and increased lifespan in tau P301S mouse model [36]. Treatment of 3xTg-AD mice with anti-inflammatory drug ibuprofen reduces tau phosphorylation and memory impairment [37]. Administration of potent anti-inflammatory minocycline reduces the development of disease-associated tau species in the htau mouse model [38] by reducing several inflammatory factors [39]. In the present study, we applied BV-2 conditioned medium to proaggregant ΔK280 tau_{RD}-DsRed 293/SH-SY5Y cells to mimic neuroinflammation. The study results reveal that CHM formula SG-Tang displays neuroprotection by exerting anti-inflammatory and antiapoptotic activities.

Inflammation is a double-edged sword. Inflammatory response could lead to activation of immune system and elimination of pathogens thereby reducing further cell loss. Although inflammation might be protective and beneficial to cells, prolonged or dysregulated inflammatory process could also result in production of neurotoxic factors that exacerbate neurodegenerative pathology and cause cell death [12]. Thus, a potential strategy for treating tauopathies is to intervene in microglial activation and neuroinflammation. NSAID has been commonly used as treatment of inflammation and known to be neuroprotective [40]. The mechanism of NSAID has been shown to inhibit the synthesis or activity of inflammatory mediators such as prostaglandin and COX isoforms 1 and 2. Although NSAID could effectively suppress the inflammatory symptoms, these agents may also induce significant side effects such as increased risk of thrombotic cardiovascular and cerebrovascular events [41]. Therefore, more safely, anti-inflammatory drugs need to be explored and developed.

There is a growing interest in natural compounds/products with anti-inflammatory activities which have long been used for treating inflammation-related diseases. In this study, SG-Tang used was formulated with Bai-Shao (*P. lactiflora*) and Gan-Cao (*G. uralensis*) and analyzed by HPLC using two main active constituents, paeoniflorin and ammonium glycyrrhizinate (Figure 1). Both paeoniflorin and glycyrrhizinic acid were demonstrated to be able to cross the blood-brain barrier (BBB) in middle cerebral artery occlusion rats [42]. However, multiplicity of the components *in P. lactiflora and G. uralensis* contributes to the effects *of* antioxidation and anti-inflammation. In the root of *P. lactiflora*, a total of 40 components including 29 monoterpene glycosides,

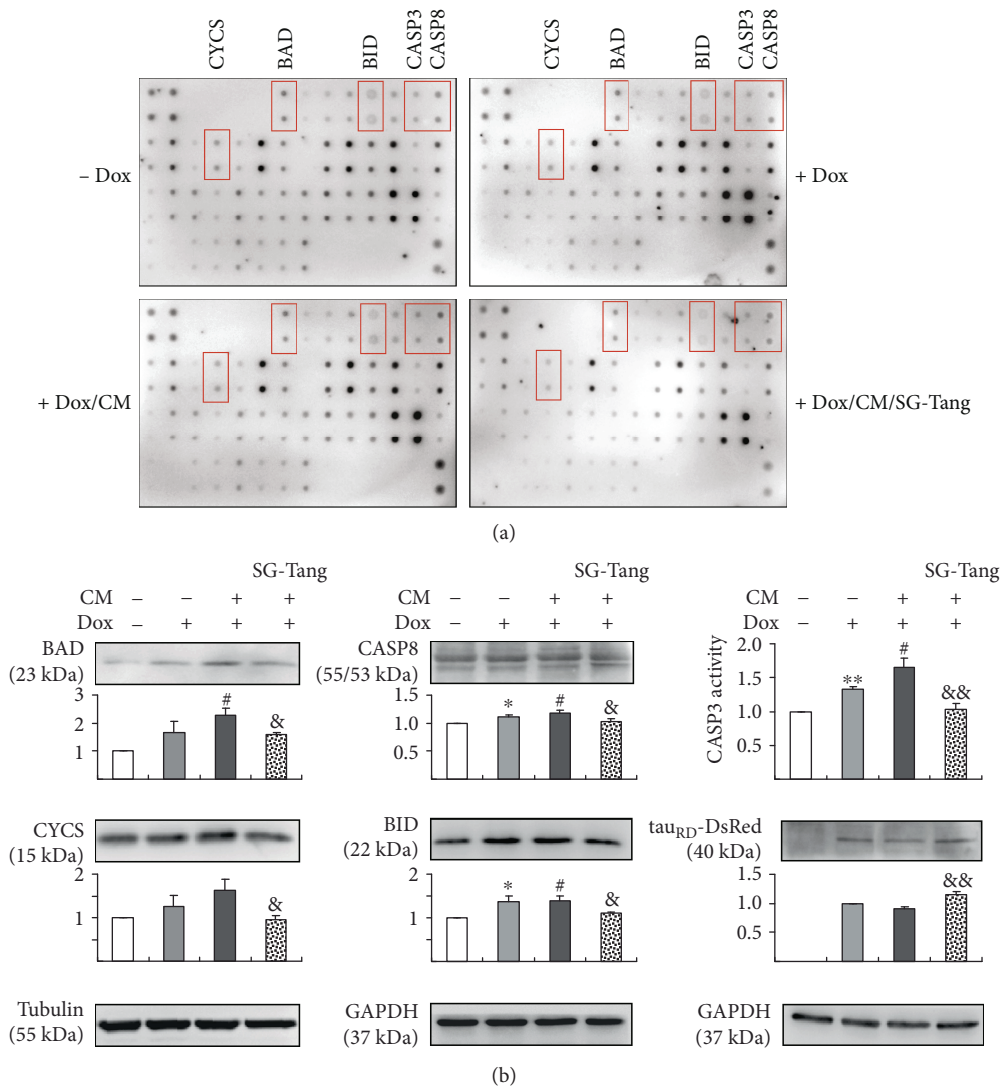

Figure 7: Apoptosis-related protein targets of SG-Tang in BV-2 conditioned medium-stimulated ΔK280 tau_{RD}-DsRed SH-SY5Y cells. (a) Representative images of apoptosis antibody array of proteins collected from Figure 6(c). (b) Western blot analysis of BAD, CYCS, CASP8, BID, and tau_{RD}-DsRed protein levels (normalized to tubulin or GAPDH internal control, $n = 3$) and caspase 3 activity assay from each sample. $^{*}p < 0.05$ and $^{**}p < 0.01$, – Dox vs. + Dox; $^{\#}p < 0.05$, + Dox vs. + Dox/CM; $^{\&}p < 0.05$ and $^{\&\&}p < 0.01$, + Dox/CM vs. + Dox/CM/SG-Tang-treated cells.

Table 1: Proteins identified by human apoptosis antibody array.

Gene symbol	UniProt accession number	Protein	Fold change (+ Dox/CM vs. – Dox)	Fold change (+ Dox/CM/SG-T vs. + Dox/CM)
BAD	Q92934	Bcl2-associated agonist of cell death	1.16	0.63
BID	P55957	BH3-interacting domain death agonist	1.33	0.41
CASP3	P42574	Caspase 3	1.49	0.71
CASP8	Q14790	Caspase 8	1.34	0.62
CYCS	P99999	Cytochrome c, somatic	0.92	0.62

8 galloyl glucoses, and 3 phenolic compounds were identified [43]. Among them, paeoniflorin, a monoterpene glycoside, is known to possess anti-inflammatory effect and has been applied to cerebral ischemic injury [44]. Paeoniflorin also exhibits neuroprotective effects via inhibiting neuroinflammation in APP/PS1 and in PS2 mutant mice [45, 46]. Paeoniflorin and the isomer albiflorin attenuated neuropathic pain by inhibiting the activation of p38 MAPK pathway in spinal microglia and subsequent upregulated IL-1β and TNF-α [47]. Benzoylpaeoniflorin, another

paeoniflorin-related glycoside in *P. lactiflora* root, protected primary rat cortical cells against H_2O_2-induced oxidative stress [48]. In addition to monoterpene glycosides, gallic acid, a phenolic compound in *P. lactiflora* root, displayed antioxidative effect by scavenging free radicals, inhibiting lipid peroxidation, and protecting against oxidative DNA damage [49]. Paeonol, another phenolic compound in *P. lactiflora* root, exerted neuroprotective effect in the model of ischemia through reducing proinflammatory receptors/mediators [50].

The main bioactive components of *G. uralensis* are triterpene saponins and various types of flavonoids, including glycyrrhetinic acid, glycyrrhizic acid, liquiritigenin, isoliquiritigenin, liquiritin, and licochalcone A [51]. Glycyrrhizin and related compounds were found to show anti-inflammatory activity *in vitro* [52] and *in vivo* [53]. Although diammonium glycyrrhizinate rescues neurotoxicity in $A\beta_{1-42}$-induced mice [54], its effect in tauopathy models is not known. Isoliquiritigenin, isoliquiritin, and liquiritigenin significantly suppressed iNOS, TNF-α, and IL-6 expression in IL-1β-treated rat hepatocytes [55]. Interestingly, the purified glycyrrhiza polysaccharides increased the pinocytic activity, the production of NO, IL-1, IL-6, and IL-12 in macrophages of mice [56]. Glycyrrhetinic acid, liquiritigenin, isoliquiritigenin, and liquiritin were also found to be all potent NRF2 inducers [57]. Moreover, Calzia et al. has shown that polyphenolic phytochemicals displayed a potent antioxidant action by modulating the ectopic F_0F_1-ATP synthase activity of the rod outer segments of the retina and prevented the induction of apoptosis [58]. Therefore, polyphenolic compounds from Bai-Shao and Gan-Cao may also exert antioxidative activities not only in but also outside of mitochondria. Given that multiple different compounds in both Bai-Shao and Gan-Cao are exerting effects on different pathways, the combination of Bai-Shao and Gan-Cao may thus have additive protection effects than each alone, which is supported by our study results.

The anti-inflammatory effect of Jakyakgamcho-tang, a formulated *P. lactiflora* and *G. uralensis* in Korea, has been shown by inhibiting the NF-κB signaling pathway in keratinocytes [59]. Aberrant activation of NF-κB signaling may lead to apoptosis and cell death [60]. We found that several proapoptotic proteins including BAD, BID, CASP3, CASP8, and CYCS were induced by misfolded tau expression and/or caused by LPS/IFN-γ-stimulated BV2 microglia. BAD protein is a proapoptotic member of the Bcl-2 gene family involved in initiating apoptosis [61]. BID is also a proapoptotic protein which plays a role as a sentinel for protease-mediated death signals [62]. Caspases are well-studied important mediators of apoptosis. CYCS is known to be released from mitochondria into cytosol to stimulate cell apoptosis [63]. Administration of SG-Tang decreased the production of these proapoptotic proteins, indicating that SG-Tang may target on inhibiting proapoptotic proteins to protect neuron cells from inflammatory damage.

Finally, pretreatment of SG-Tang reversed abnormal hyperphosphorylation at tau Ser202 and Thr231 in inflamed misfolded tau-expressing SH-SY5Y cells (Figure 6). Tau function is regulated by phosphorylation at specific sites, and tau phosphorylation plays both physiological and pathological roles in the cells. Tau Ser199/202 and Thr205 were found to be locally phosphorylated along the nascent axon during axonogenesis [64]. Phosphorylation of tau Thr231 inhibited tau to bind and stabilize microtubules [65]. Both Ser202 and Thr231 are hyperphosphorylated in degenerating AD brain [66]. Among kinases that regulate tau Ser202 and Thr231 phosphorylation, cyclic AMP-dependent protein kinase (PKA) and cyclin-dependent kinase 2 (CDC2) might be the potential targets of SG-Tang, and SG-Tang treatment may result in activity suppression of these two kinases [66, 67]. The exact mechanism for PKA or CDC2 regulation by SG-Tang remains to be determined in our future work.

5. Conclusions

Plant-derived natural medications have been used for centuries and becoming more popular because of their low side effects. Despite the fact that natural compounds are relatively safe, the complexity of natural products makes nutraceutical preparations difficult to be appropriately designed. In this study, we showed antioxidative and anti-inflammatory effects of SG-Tang as a potential agent for treatment or prevention of neuroinflammation-associated tauopathy. In future, studies of main active compounds paeoniflorin and ammonium glycyrrhizinate in SG-Tang, separately or in combination, in tauopathy cell model are warranted to provide a novel avenue for protection against tauopathy.

Abbreviations

AD: Alzheimer's disease
BAD: Bcl2-associated agonist of cell death
BBB: Blood-brain barrier
BID: BH3-interacting domain death agonist
BSA: Bovine serum albumin
CASP3: Caspase 3
CASP8: Caspase 8
CDC2: Cyclin-dependent kinase 2
CHM: Chinese herbal medicine
CM: Conditioned medium
CNS: Central nervous system
COX: Cyclooxygenase
CYCS: Cytochrome c, somatic
DAPI: 4′-6-Diamidino-2-phenylindole
Dox: Doxycycline
DMEM: Dulbecco's modified Eagle's medium
DPPH: 1,1-Diphenyl-2-picrylhydrazyl
EC_{50}: Half maximal effective concentration
ELISA: Enzyme-linked immunosorbent assay
FBS: Fetal bovine serum
HCA: High-content analysis
HPLC: High-performance liquid chromatography
Iba1: Induction of brown adipocytes 1
IC_{50}: Half maximal inhibitory concentration
IFN: Interferon
IL: Interleukin
LDH: Lactate dehydrogenase
LPS: Lipopolysaccharide

MTT: 3-(4,5-Dimethylthiazol-2-yl)-2,5-diphenyltetrazolium bromide
NO: Nitric oxide
NSAID: Nonsteroidal anti-inflammatory drug
PKA: Cyclic AMP-dependent protein kinase
ROS: Reactive oxygen species
SG-Tang: Shaoyao Gancao Tang
tau_{RD}: Tau repeat domain
TNF: Tumor necrosis factor.

Data Availability

The data used to support the findings of this study are available from the corresponding author upon request.

Conflicts of Interest

The authors declare no conflicts of interest.

Authors' Contributions

Guey-Jen Lee-Chen and Chiung-Mei Chen designed the research and revised the paper. I-Cheng Chen performed the experiments, analyzed the data, and wrote the manuscript. Te-Hsien Lin conducted experiments and analyzed the data. Yu-Hsuan Hsieh and Chih-Ying Chao performed experiments and assisted in the technical work. Yih-Ru Wu and Kuo-Hsuan Chang commented on the experiment design. Ming-Chung Lee provided CHM materials for this study. All authors approved the final version of the manuscript. I-Cheng Chen and Te-Hsien Lin contributed equally to this work.

Acknowledgments

This work was supported by the grants from the Ministry of Science and Technology (105-2325-B-003-001) and Chang Gung Memorial Hospital (CMRPG3F136, CMRPG3F1611-2, and CMRPG3G052). We thank the Molecular Imaging Core Facility of National Taiwan Normal University for the technical assistance.

References

[1] D. R. Williams, "Tauopathies: classification and clinical update on neurodegenerative diseases associated with microtubule-associated protein tau," *Internal Medicine Journal*, vol. 36, no. 10, pp. 652–660, 2006.

[2] G. Lee and C. J. Leugers, "Tau and tauopathies," *Progress in Molecular Biology and Translational Science*, vol. 107, pp. 263–293, 2012.

[3] R. L. Neve, P. Harris, K. S. Kosik, D. M. Kurnit, and T. A. Donlon, "Identification of cDNA clones for the human microtubule-associated protein tau and chromosomal localization of the genes for tau and microtubule-associated protein 2," *Brain Research*, vol. 387, no. 3, pp. 271–280, 1986.

[4] M. Hasegawa, M. J. Smith, and M. Goedert, "Tau proteins with FTDP-17 mutations have a reduced ability to promote microtubule assembly," *FEBS Letters*, vol. 437, no. 3, pp. 207–210, 1998.

[5] P. Nacharaju, J. Lewis, C. Easson et al., "Accelerated filament formation from tau protein with specific FTDP-17 missense mutations," *FEBS Letters*, vol. 447, no. 2-3, pp. 195–199, 1999.

[6] I. D'Souza, P. Poorkaj, M. Hong et al., "Missense and silent tau gene mutations cause frontotemporal dementia with parkinsonism-chromosome 17 type, by affecting multiple alternative RNA splicing regulatory elements," *Proceedings of the National Academy of Sciences of the United States of America*, vol. 96, no. 10, pp. 5598–5603, 1999.

[7] P. Rizzu, J. C. van Swieten, M. Joosse et al., "High prevalence of mutations in the microtubule-associated protein tau in a population study of frontotemporal dementia in the Netherlands," *The American Journal of Human Genetics*, vol. 64, no. 2, pp. 414–421, 1999.

[8] P. Momeni, A. Pittman, T. Lashley et al., "Clinical and pathological features of an Alzheimer's disease patient with the *MAPT* ΔK280 mutation," *Neurobiology of Aging*, vol. 30, no. 3, pp. 388–393, 2009.

[9] S. Barghorn, Q. Zheng-Fischhöfer, M. Ackmann et al., "Structure, microtubule interactions, and paired helical filament aggregation by tau mutants of frontotemporal dementias," *Biochemistry*, vol. 39, no. 38, pp. 11714–11721, 2000.

[10] V. Vogelsberg-Ragaglia, J. Bruce, C. Richter-Landsberg et al., "Distinct FTDP-17 missense mutations in tau produce tau aggregates and other pathological phenotypes in transfected CHO cells," *Molecular Biology of the Cell*, vol. 11, no. 12, pp. 4093–4104, 2000.

[11] M. von Bergen, S. Barghorn, L. Li et al., "Mutations of tau protein in frontotemporal dementia promote aggregation of paired helical filaments by enhancing local β-structure," *The Journal of Biological Chemistry*, vol. 276, no. 51, pp. 48165–48174, 2001.

[12] P. J. Khandelwal, A. M. Herman, and C. E. H. Moussa, "Inflammation in the early stages of neurodegenerative pathology," *Journal of Neuroimmunology*, vol. 238, no. 1-2, pp. 1–11, 2011.

[13] P. L. DiPatre and B. B. Gelman, "Microglial cell activation in aging and Alzheimer disease: partial linkage with neurofibrillary tangle burden in the hippocampus," *Journal of Neuropathology and Experimental Neurology*, vol. 56, no. 2, pp. 143–149, 1997.

[14] K. Ishizawa and D. W. Dickson, "Microglial activation parallels system degeneration in progressive supranuclear palsy and corticobasal degeneration," *Journal of Neuropathology and Experimental Neurology*, vol. 60, no. 6, pp. 647–657, 2001.

[15] M. Kitazawa, T. R. Yamasaki, and F. M. Laferla, "Microglia as a potential bridge between the amyloid β-peptide and tau," *Annals of the New York Academy of Sciences*, vol. 1035, no. 1, pp. 85–103, 2004.

[16] Y. Li, L. Liu, S. W. Barger, and W. S. T. Griffin, "Interleukin-1 mediates pathological effects of microglia on tau phosphorylation and on synaptophysin synthesis in cortical neurons through a p38-MAPK pathway," *The Journal of Neuroscience*, vol. 23, no. 5, pp. 1605–1611, 2003.

[17] K. Bhaskar, M. Konerth, O. N. Kokiko-Cochran, A. Cardona, R. M. Ransohoff, and B. T. Lamb, "Regulation of tau pathology by the microglial fractalkine receptor," *Neuron*, vol. 68, no. 1, pp. 19–31, 2010.

[18] M. Kitazawa, S. Oddo, T. R. Yamasaki, K. N. Green, and F. LaFerla, "Lipopolysaccharide-induced inflammation exacerbates tau pathology by a cyclin-dependent kinase 5-mediated

pathway in a transgenic model of Alzheimer's disease," *Journal of Neuroscience*, vol. 25, no. 39, pp. 8843–8853, 2005.

[19] A. N. Nilson, K. C. English, J. E. Gerson et al., "Tau oligomers associate with inflammation in the brain and retina of tauopathy mice and in neurodegenerative diseases," *Journal of Alzheimer's Disease*, vol. 55, no. 3, pp. 1083–1099, 2017.

[20] P. D. Wes, F. A. Sayed, F. Bard, and L. Gan, "Targeting microglia for the treatment of Alzheimer's disease," *Glia*, vol. 64, no. 10, pp. 1710–1732, 2016.

[21] A. Ardura-Fabregat, E. W. G. M. Boddeke, A. Boza-Serrano et al., "Targeting neuroinflammation to treat Alzheimer's disease," *CNS Drugs*, vol. 31, no. 12, pp. 1057–1082, 2017.

[22] J. Gao, Y. Inagaki, X. Li, N. Kokudo, and W. Tang, "Research progress on natural products from traditional Chinese medicine in treatment of Alzheimer's disease," *Drug Discoveries & Therapeutics*, vol. 7, no. 2, pp. 46–57, 2013.

[23] Z. Y. Wang, J. G. Liu, H. Li, and H. M. Yang, "Pharmacological effects of active components of Chinese herbal medicine in the treatment of Alzheimer's disease: a review," *The American Journal of Chinese Medicine*, vol. 44, no. 08, pp. 1525–1541, 2016.

[24] T. Y. Wu, C. P. Chen, and T. R. Jinn, "Traditional Chinese medicines and Alzheimer's disease," *Taiwanese Journal of Obstetrics & Gynecology*, vol. 50, no. 2, pp. 131–135, 2011.

[25] Y. Q. Zheng and W. Wei, "Total glucosides of paeony suppresses adjuvant arthritis in rats and intervenes cytokine-signaling between different types of synoviocytes," *International Immunopharmacology*, vol. 5, no. 10, pp. 1560–1573, 2005.

[26] T.-Y. Wu, T. O. Khor, C. L. L. Saw et al., "Anti-inflammatory/anti-oxidative stress activities and differential regulation of Nrf2-mediated genes by non-polar fractions of tea *Chrysanthemum zawadskii* and licorice *Glycyrrhiza uralensis*," *The AAPS Journal*, vol. 13, no. 1, pp. 1–13, 2011.

[27] K.-H. Chang, I.-C. Chen, H.-Y. Lin et al., "The aqueous extract of *Glycyrrhiza inflata* can upregulate unfolded protein response-mediated chaperones to reduce tau misfolding in cell models of Alzheimer's disease," *Drug Design, Development and Therapy*, vol. 10, pp. 885–896, 2016.

[28] D. Brown, A. Tamas, D. Reglodi, and Y. Tizabi, "PACAP protects against inflammatory-mediated toxicity in dopaminergic SH-SY5Y cells: implication for Parkinson's disease," *Neurotoxicity Research*, vol. 26, no. 3, pp. 230–239, 2014.

[29] Y. C. Park, C. H. Lee, H. S. Kang, H. T. Chung, and H. D. Kim, "Wortmannin, a specific inhibitor of phosphatidylinositol-3-kinase, enhances LPS-induced NO production from murine peritoneal macrophages," *Biochemical and Biophysical Research Communications*, vol. 240, no. 3, pp. 692–696, 1997.

[30] H. Fang, R. A. Pengal, X. Cao et al., "Lipopolysaccharide-induced macrophage inflammatory response is regulated by SHIP," *Journal of Immunology*, vol. 173, no. 1, pp. 360–366, 2004.

[31] M. Cente, P. Filipcik, M. Pevalova, and M. Novak, "Expression of a truncated tau protein induces oxidative stress in a rodent model of tauopathy," *The European Journal of Neuroscience*, vol. 24, no. 4, pp. 1085–1090, 2006.

[32] P. L. McGeer, T. Kawamata, D. G. Walker, H. Akiyama, I. Tooyama, and E. G. McGeer, "Microglia in degenerative neurological disease," *Glia*, vol. 7, no. 1, pp. 84–92, 1993.

[33] L. M. Sedger and M. F. McDermott, "TNF and TNF-receptors: from mediators of cell death and inflammation to therapeutic giants - past, present and future," *Cytokine & Growth Factor Reviews*, vol. 25, no. 4, pp. 453–472, 2014.

[34] T. P. Monie and C. E. Bryant, "Caspase-8 functions as a key mediator of inflammation and pro-IL-1β processing via both canonical and non-canonical pathways," *Immunological Reviews*, vol. 265, no. 1, pp. 181–193, 2015.

[35] A. Sasaki, T. Kawarabayashi, T. Murakami et al., "Microglial activation in brain lesions with tau deposits: comparison of human tauopathies and tau transgenic mice TgTauP301L," *Brain Research*, vol. 1214, pp. 159–168, 2008.

[36] Y. Yoshiyama, M. Higuchi, B. Zhang et al., "Synapse loss and microglial activation precede tangles in a P301S tauopathy mouse model," *Neuron*, vol. 53, no. 3, pp. 337–351, 2007.

[37] A. C. McKee, I. Carreras, L. Hossain et al., "Ibuprofen reduces Aβ, hyperphosphorylated tau and memory deficits in Alzheimer mice," *Brain Research*, vol. 1207, pp. 225–236, 2008.

[38] W. Noble, C. Garwood, J. Stephenson, A. M. Kinsey, D. P. Hanger, and B. H. Anderton, "Minocycline reduces the development of abnormal tau species in models of Alzheimer's disease," *The FASEB Journal*, vol. 23, no. 3, pp. 739–750, 2009.

[39] C. J. Garwood, J. D. Cooper, D. P. Hanger, and W. Noble, "Anti-inflammatory impact of minocycline in a mouse model of tauopathy," *Frontiers in Psychiatry*, vol. 1, p. 136, 2010.

[40] M. A. Ajmone-Cat, A. Bernardo, A. Greco, and L. Minghetti, "Non-steroidal anti-inflammatory drugs and brain inflammation: effects on microglial functions," *Pharmaceuticals (Basel)*, vol. 3, no. 6, pp. 1949–1965, 2010.

[41] J. C. Maroon, J. W. Bost, and A. Maroon, "Natural anti-inflammatory agents for pain relief," *Surgical Neurology International*, vol. 1, no. 1, p. 80, 2010.

[42] H. Li, M. Ye, Y. Zhang et al., "Blood-brain barrier permeability of Gualou Guizhi granules and neuroprotective effects in ischemia/reperfusion injury," *Molecular Medicine Reports*, vol. 12, no. 1, pp. 1272–1278, 2015.

[43] S. L. Li, J. Z. Song, F. F. K. Choi et al., "Chemical profiling of Radix Paeoniae evaluated by ultra-performance liquid chromatography/photo-diode-array/quadrupole time-of-flight mass spectrometry," *Journal of Pharmaceutical and Biomedical Analysis*, vol. 49, no. 2, pp. 253–266, 2009.

[44] Y. Zhang, H. Li, M. Huang et al., "Paeoniflorin, a monoterpene glycoside, protects the brain from cerebral ischemic injury via inhibition of apoptosis," *The American Journal of Chinese Medicine*, vol. 43, no. 03, pp. 543–557, 2015.

[45] H. R. Zhang, J. H. Peng, X. B. Cheng, B. Z. Shi, M. Y. Zhang, and R. X. Xu, "Paeoniflorin atttenuates amyloidogenesis and the inflammatory responses in a transgenic mouse model of Alzheimer's disease," *Neurochemical Research*, vol. 40, no. 8, pp. 1583–1592, 2015.

[46] X. Gu, Z. Cai, M. Cai et al., "Protective effect of paeoniflorin on inflammation and apoptosis in the cerebral cortex of a transgenic mouse model of Alzheimer's disease," *Molecular Medicine Reports*, vol. 13, no. 3, pp. 2247–2252, 2016.

[47] J. Zhou, L. Wang, J. Wang et al., "Paeoniflorin and albiflorin attenuate neuropathic pain via MAPK pathway in chronic constriction injury rats," *Evidence-Based Complementary and Alternative Medicine*, vol. 2016, Article ID 8082753, 11 pages, 2016.

[48] S. H. Kim, M. K. Lee, K. Y. Lee, S. H. Sung, J. Kim, and Y. C. Kim, "Chemical constituents isolated from *Paeonia lactiflora* roots and their neuroprotective activity against oxidative stress

in vitro," *Journal of Enzyme Inhibition and Medicinal Chemistry*, vol. 24, no. 5, pp. 1138–1140, 2009.

[49] S. C. Lee, Y. S. Kwon, K. H. Son, H. P. Kim, and M. Y. Heo, "Antioxidative constituents from *Paeonia lactiflora*," *Archives of Pharmacal Research*, vol. 28, no. 7, pp. 775–783, 2005.

[50] W. Y. Liao, T. H. Tsai, T. Y. Ho, Y. W. Lin, C. Y. Cheng, and C. L. Hsieh, "Neuroprotective effect of paeonol mediates anti-inflammation via suppressing toll-like receptor 2 and toll-like receptor 4 signaling pathways in cerebral ischemia-reperfusion injured rats," *Evidence-Based Complementary and Alternative Medicine*, vol. 2016, Article ID 3704647, 12 pages, 2016.

[51] Q. Zhang and M. Ye, "Chemical analysis of the Chinese herbal medicine Gan-Cao (licorice)," *Journal of Chromatography. A*, vol. 1216, no. 11, pp. 1954–1969, 2009.

[52] S. Matsui, H. Matsumoto, Y. Sonoda et al., "Glycyrrhizin and related compounds down-regulate production of inflammatory chemokines IL-8 and eotaxin 1 in a human lung fibroblast cell line," *International Immunopharmacology*, vol. 4, no. 13, pp. 1633–1644, 2004.

[53] T. Genovese, M. Menegazzi, E. Mazzon et al., "Glycyrrhizin reduces secondary inflammatory process after spinal cord compression injury in mice," *Shock*, vol. 31, no. 4, pp. 367–375, 2009.

[54] H. Zhao, S. L. Wang, L. Qian et al., "Diammonium glycyrrhizinate attenuates $A\beta_{1\text{-}42}$-induced neuroinflammation and regulates MAPK and NF-κB pathways *in vitro* and *in vivo*," *CNS Neuroscience & Therapeutics*, vol. 19, no. 2, pp. 117–124, 2013.

[55] R. Tanemoto, T. Okuyama, H. Matsuo, T. Okumura, Y. Ikeya, and M. Nishizawa, "The constituents of licorice (*Glycyrrhiza uralensis*) differentially suppress nitric oxide production in interleukin-1β-treated hepatocytes," *Biochemistry and Biophysics Reports*, vol. 2, pp. 153–159, 2015.

[56] A. Cheng, F. Wan, J. Wang, Z. Jin, and X. Xu, "Macrophage immunomodulatory activity of polysaccharides isolated from *Glycyrrhiza uralensis* fish," *International Immunopharmacology*, vol. 8, no. 1, pp. 43–50, 2008.

[57] H. Gong, B. K. Zhang, M. Yan et al., "A protective mechanism of licorice (*Glycyrrhiza uralensis*): isoliquiritigenin stimulates detoxification system via Nrf2 activation," *Journal of Ethnopharmacology*, vol. 162, pp. 134–139, 2015.

[58] D. Calzia, M. Oneto, F. Caicci et al., "Effect of polyphenolic phytochemicals on ectopic oxidative phosphorylation in rod outer segments of bovine retina," *British Journal of Pharmacology*, vol. 172, no. 15, pp. 3890–3903, 2015.

[59] S. J. Jeong, H. S. Lim, C. S. Seo et al., "Traditional herbal formula Jakyakgamcho-tang (*Paeonia lactiflora* and *Glycyrrhiza uralensis*) impairs inflammatory chemokine production by inhibiting activation of STAT1 and NF-κB in HaCaT cells," *Phytomedicine*, vol. 22, no. 2, pp. 326–332, 2015.

[60] B. Kaltschmidt, C. Kaltschmidt, T. G. Hofmann, S. P. Hehner, W. Droge, and M. L. Schmitz, "The pro- or anti-apoptotic function of NF-κB is determined by the nature of the apoptotic stimulus," *European Journal of Biochemistry*, vol. 267, no. 12, pp. 3828–3835, 2000.

[61] E. Yang, J. Zha, J. Jockel, L. H. Boise, C. B. Thompson, and S. J. Korsmeyer, "Bad, a heterodimeric partner for Bcl-XL and Bcl-2, displaces Bax and promotes cell death," *Cell*, vol. 80, no. 2, pp. 285–291, 1995.

[62] K. Wang, X. M. Yin, D. T. Chao, C. L. Milliman, and S. J. Korsmeyer, "BID: a novel BH3 domain-only death agonist," *Genes & Development*, vol. 10, no. 22, pp. 2859–2869, 1996.

[63] X. Liu, C. N. Kim, J. Yang, R. Jemmerson, and X. Wang, "Induction of apoptotic program in cell-free extracts: requirement for dATP and cytochrome c," *Cell*, vol. 86, no. 1, pp. 147–157, 1996.

[64] J. W. Mandell and G. A. Banker, "A spatial gradient of tau protein phosphorylation in nascent axons," *The Journal of Neuroscience*, vol. 16, no. 18, pp. 5727–5740, 1996.

[65] J.-H. Cho and G. V. W. Johnson, "Glycogen synthase kinase 3β phosphorylates tau at both primed and unprimed sites: differential impact on microtubule binding," *Journal of Biological Chemistry*, vol. 278, no. 1, pp. 187–193, 2003.

[66] J. Z. Wang and F. Liu, "Microtubule-associated protein tau in development, degeneration and protection of neurons," *Progress in Neurobiology*, vol. 85, no. 2, pp. 148–175, 2008.

[67] D. P. Hanger, B. H. Anderton, and W. Noble, "Tau phosphorylation: the therapeutic challenge for neurodegenerative disease," *Trends in Molecular Medicine*, vol. 15, no. 3, pp. 112–119, 2009.

Hindawi
Oxidative Medicine and Cellular Longevity
Volume 2018, Article ID 9089016, 14 pages
https://doi.org/10.1155/2018/9089016

Research Article

Effects of the *Aphanizomenon flos-aquae* Extract (Klamin®) on a Neurodegeneration Cellular Model

D. Nuzzo,[1] **G. Presti**,[2] **P. Picone**,[1] **G. Galizzi**,[1] **E. Gulotta**,[2] **S. Giuliano**,[2] **C. Mannino**,[2] **V. Gambino**,[2] **S. Scoglio**,[3] **and M. Di Carlo**[1]

[1]*Istituto di Biomedicina ed Immunologia Molecolare (IBIM) "Alberto Monroy", CNR, Via Ugo La Malfa 153, 90146 Palermo, Italy*
[2]*Chemical Laboratory of Palermo, Italian Agency of Customs and Monopolies, Via Crispi, 143, 90133 Palermo, Italy*
[3]*Nutritherapy Research Center, 61029 Urbino, Italy*

Correspondence should be addressed to M. Di Carlo; di-carlo@ibim.cnr.it

Received 19 June 2018; Accepted 30 July 2018; Published 17 September 2018

Academic Editor: Francisco Jaime Bezerra Mendonça Júnior

Cyanobacteria have been recognized as a source of bioactive molecules to be employed in nutraceuticals, pharmaceuticals, and functional foods. An extract of *Aphanizomenon flos-aquae* (AFA), commercialized as Klamin®, was subjected to chemical analysis to determine its compounds. The AFA extract Klamin® resulted to be nontoxic, also at high doses, when administered onto LAN5 neuronal cells. Its scavenging properties against ROS generation were evaluated by using DCFH-DA assay, and its mitochondrial protective role was determined by JC-1 and MitoSOX assays. Klamin® exerts a protective role against beta amyloid- (Aβ-) induced toxicity and against oxidative stress. Anti-inflammatory properties were demonstrated by NFβB nuclear localization and activation of IL-6 and IL-1β inflammatory cytokines through ELISA. Finally, by using thioflavin T (ThT) and fluorimetric measures, we found that Klamin® interferes with Aβ aggregation kinetics, supporting the formation of smaller and nontoxic structures compared to toxic Aβ aggregates alone. Altogether, these data indicate that the AFA extract may play a protective role against mechanisms leading to neurodegeneration.

1. Introduction

Blue-green algae, including *Aphanizomenon flos-aquae* (AFA), are unicellular prokaryotic microorganism belonging to the Cyanobacteria (Cyanophyta) phylum. These bacteria are among the oldest life forms, are the only microorganisms to achieve oxygenic photosynthesis, and probably have been the main biotic source of oxygen on early Earth [1]. These microorganisms are widely diffused, colonizing both salt- and freshwater around the world, alone or in a symbiotic relationship with plants or fungi [2]. Cyanobacteria are a source of bioactive compounds such as polyunsaturated fatty acids, proteins, pigments, and minerals and are rich in substances with anti-inflammatory and antioxidant properties [3–8].

The Aphanizomenon genus includes several species including the flos-aquae. AFA is a cyanobacterial unicellular organism endowed with several health-enhancing properties that, unlike other commercial "microalgae," spontaneously grows in Upper Klamath Lake (southern Oregon, USA) where it also inhibits, when in bloom, the growth of other cyanobacterial species. Upper Klamath Lake is an ideal natural ecosystem, in which the AFA microalga finds the perfect conditions that allow its proliferation, especially between late summer and early fall, while going quiescent in the winter. The 300 days of sunshine that characterize the Klamath Basin favor its intense photosynthetic activity, managed by the microalga through various pigments, including its unique type of phycocyanins. Being placed at 1300 meters of height, in the winter, the lake freezes over, a condition which stimulates the production of fatty acids, including omega 3, by the AFA microalgae. AFA contains a high concentration of vitamins, especially of the B group. Vitamin B12 is essential for the synthesis of nucleic acids, of erythrocytes, and for myelin formation. B12 deficiency can cause a series of more or less severe nervous system-associated symptoms [9, 10].

Due to the volcanic origin of the lake, AFA contains a wide and complete spectrum of minerals and trace minerals [11]. It is also rich in pigments such as carotene, beta-carotene, and chlorophylls [12]. Of particular relevance are its phycocyanins, which have a particular structure [13] and have proven to have significant antioxidant [14], anti-inflammatory [15], and antiproliferative [16] properties.

Furthermore, AFA contains significant amounts of phenylethylamine (PEA), an endogenous molecule that is considered a general neuromodulator [17] and which is lacking in certain forms of depression and affective disturbances [18, 19]. Klamin® is an AFA extract which concentrates phenylethylamine, as well as other molecules, such as AFA-phycocyanins and the mycosporine-like amino acids (MAAs) porphyra and shinorine, which act as powerful MAO-B inhibitors [20]. Klamin® has proven to be effective in countering depression, anxiety, and other pathologies [21–23]. This is why Klamin® is emerging as a nutritional supplement supporting the correct functioning of the neurological system, and its role in neurodegenerative diseases has been reported [24]. The PEA contained in Klamin® has also been shown to play a role in modulating the immune system response [25]. All these properties make Klamin® a potential therapeutic agent, especially for those pathologies in which oxidative stress, inflammation, and mitochondrial and neurological dysfunction play a relevant role.

With the increase of the life expectancy, the number of people affected by neurodegenerative diseases is growing. Among these diseases, Alzheimer's disease (AD) is the most diffuse form of dementia [26–29]. Currently, no effective treatment is available. Hence, there is a great interest in studying natural bioactive compounds to use as neuroprotective and neuroregenerative agents. One of the histopathological hallmarks of AD is the amyloid plaque formation in the brain. These plaques are mainly constituted by aggregates of the Aβ peptide, a peptide generated by proteolytic cleavage of the amyloid precursor protein (APP) [30]. At the molecular level, Aβ induces oxidative stress, inflammation, mitochondrial dysfunction associated with specific signaling impairment, and apoptosis [31–36]. Antioxidant molecules, such as ferulic acid, have been successfully employed to inhibit oxidative stress, mitochondrial dysfunction, and apoptosis in an *in vitro* model of Alzheimer's [37–39]. An attractive approach for preventing or reducing neurodegeneration could consist in introducing dietary supplements with antioxidant, anti-inflammatory, and neuromodulating properties. Antioxidant and anti-inflammatory substances from natural, food-derived sources display elevated bioavailability and a higher efficacy than synthetic antioxidants that do produce scarce if any effect [40]. Thus, a proper intake of natural, food-derived antioxidant and anti-inflammatory substances can play an important role in preventing and controlling diseases. Some studies have shown that the AFA extract Klamin® can improve mood, reduce anxiety, and enhance attention and learning, suggesting that it could have a role in clinical areas including mood disorders and neurodegenerative diseases [20, 21].

In the present study, we investigate some biological properties of Klamin®'s compounds, thus evaluating the possibility to use it as a dietary supplement playing a protective role against neurodegenerative disease. A soluble preparation of the AFA extract Klamin® was used to identify the antioxidant properties in a neuronal LAN5 cell model and its protective effect on neurodegeneration by biochemical assay and inhibition of Aβ fibrillogenesis kinetics.

2. Materials and Methods

2.1. Solubilization of Klamin®. The Klamin® extract was kindly provided by Nutrigea Research s.r.l. (Republic of San Marino). Klamin® tablets were pulverized using a mortar and pestle and 10 mg of powder was dissolved in 10 ml of PBS (pH = 7.4; 137 mM NaCl, 2.7 mM KCl, 8 mM Na_3PO_4). The solution was sonicated (70% of the maximum power, twice for 30 seconds) and magnetically stirred for an hour. The insoluble faction was removed by centrifugation at 14,000 rpm for 30 min at 4°C. The supernatant was collected, filtered by using a 0.45 μm Sartorius filter, aliquoted (1 ml/vial), and stored at −20°C. We will call this fraction "AFA extract."

2.2. Chemical Analysis. The solubilized Klamin® (1 : 100) was loaded on a cuvette and measured by using a spectrophotometer in the range between 310 and 360 nm for mycosporine-like amino acid (MAA) identification and in the spectrum range of 400–600 nm for carotenoid, phycoerythrin, and phycocyanin identification. Phyco-complexes were visualized by using a fluorescence microscope (ZEISS) and specific excitation filters for UV (blue emission), FITC (green emission), and Texas Red (red emission). Phenolic compounds were determined according to Ignat et al. [41] and Naczk and Shahidi [42] and by employing reverse-phase high-performance liquid chromatography (HPLC) combined with a photodiode array detector (DAD) (Accela Thermo Fisher Scientific) and UV detection at 280 nm wavelength (Zang et al., 2013) and by using 3-hydroxytyrosol (Sigma), caffeic acid (Fluka), and vanillic acid (Fluka) as standard. The column was a C18 THERMO Accucore (2.1 mm × 100 mm, particle size 2.6 μm) thermostated at 30°C. The mobile phase was obtained by a gradients composed by 50% methanol/50% acetonitrile (solution A) and H_2O/0.2% H_3PO_4 (solution B). The flow rate is 450 μl/min. The identity of the phenolic compounds was ascertained by comparing their retention times and UV–Vis spectra with that of authentic standards. Carbohydrates were analyzed according to Rojas-Escudero et al. [43] and by using a gas chromatography-mass spectrometry (GC-MS) (GC-MS ISQ LT 300 Thermo Fisher Scientific) instrument and D-Pinitol (Sigma) and inositol (Sigma) as standard. The solubilized Klamin® sample (1 ml) was submitted to the derivatization method to increase its volatility by using SYLON HTP kit HDMS+TMCS+PYRIDINE 3 : 1 : 9 Supelco at 80°C for 1 hour. Then, the sample was centrifuged at 5000 rpm for 30 minutes and the supernatant was freeze-dried in nitrogen. After the addition of hexane (1 ml), the sample was analyzed by GC-MS. Mineral compounds were evaluated by inductively coupled plasma-mass spectrometry (ICP-MS) (ICP X-SERIES 2 Thermo Scientific Instrument). The AFA extract (5 gr) was ionized by microwave digestion by using a MARS Xpress instrument

(CEM) and in the presence of nitric acid (10 ml) at 400 W for 15 minutes and at 800 W for additional 15 minutes. After digestion, 500 ml of H_2O was added to the sample for qualitative and quantitative mineral determinations by mass spectrometry.

2.3. Folin-Ciocalteu Colorimetric Assay. Hydrosoluble biophenolic content was determined by using Folin-Ciocalteu colorimetric assay.

An aliquot (0.2 ml) of the AFA hydrosoluble extract was diluted with distilled water to a total volume of 5 ml, and 0.5 ml of the Folin-Ciocalteu reagent was added. After 3 min, 1 ml of Na_2CO_3 (20% *w*/*v*) was added to the reaction mixture that was mixed and diluted with water to 10 ml. The samples were stored for 2 hours at room temperature, and the absorbance of the solution was measured at 765 nm by using a spectrophotometer (Shimadzu) and quantified by using a gallic acid standard curve.

2.4. Oxygen Radical Absorbance Capacity (ORAC) Assay of Klamin®'s Phenolic Extract. The ORAC assay was performed according to Ninfali et al. [44] and Cao et al. [45], slightly modified. The reaction was carried out using a 96-well plate: 160 μl of 0.04 μM fluorescein in 0.075 M Na-K phosphate buffer (pH 7.0), 20 μl of the diluted phenolic extract, or 20 μl of 100 μM Trolox. The mixture was incubated for 10 min at 37°C in the dark; after this incubation, 20 μl of 40 mM 2,2′-Azobis-(2-methylpropionamidine) dihydrochloride (AAPH) solution was added. The microplate was immediately placed in a microplate reader (Thermo Scientific Fluoroskan Ascent F2 Microplate) and the fluorescence recorded (excitation and emission wavelengths of 485 and 527 nm, respectively) every five minutes for 60 min. The ORAC value refers to the net area under the curve of fluorescein decay in the presence of the Klamin® phenolic extract or Trolox, minus the blank area. The activity of the sample was expressed by μmol of Trolox equivalents (TE)/g of Klamin®, with the following equation:

$$\mathrm{ORAC}(\mu\mathrm{mol\,TE/g}) = kah\left[\frac{(S_{\mathrm{sample}} - S_{\mathrm{blank}})}{(S_{\mathrm{Trolox}} - S_{\mathrm{blank}})}\right], \quad (1)$$

where k is the final dilution of the water soluble extract, a is the ratio between the volume (liters) of the water soluble extract and grams of Klamin®, h is the final concentration of Trolox expressed as μmol/l, and S is the area under the curve of fluorescein in the presence of sample, Trolox, or buffer solution. All the reaction mixtures were prepared in triplicate, and at least three independent assays were performed for each sample.

2.5. Cell Cultures and Treatment. Cells were cultured with RPMI 1640 medium (Celbio srl, Milan, Italy) supplemented with 10% fetal bovine serum (Gibco-Invitrogen, Milan, Italy) and 1% antibiotics (50 mg ml^{-1} penicillin and 50 mg ml^{-1} streptomycin). Cells were maintained in a humidified 5% CO_2 atmosphere at 37 ± 0.1°C. For dose- and time-dependent assay, LAN5 cells were treated with 50, 100, 200, 400, and 800 ng/μl of extract for 3, 24, 48, and 72 hours. For the DCFH-DA, MitoRed, and JC-1 assays and immunofluorescence experiment, the AFA extract was utilized at 800 ng/μl for 24 h. The treated and control cells were analyzed by using microscopy (Axio Scope 2 microscope; Zeiss, Germany). In the experiments in which the Aβ peptide effect was analyzed, 40 μM of a recombinant peptide produced according to Carrotta et al. [46] was utilized.

2.6. Determination of Cell Viability. Cell viability was measured by MTS assay (Promega Italia S.r.l., Milan, Italy). MTS was utilized according to the manufacturer's instructions. After cell treatments, the incubation was continued for 3 hours at 37°C in 5% CO_2. The absorbance was read at 490 nm on the Microplate reader WallacVictor 2 1420 Multilabel Counter (Perkin Elmer Inc., Monza, Italy). Results were expressed as the percentage MTS reduction with reference to the control cells.

2.7. Oxidation Kinetics. LAN5 cells were treated with 1 mM TBH or 40 μM Aβ to induce oxidative stress and cotreated with five different concentrations of the AFA extract (50, 100, 200, 400, and 800 ng/μl). The production of reactive oxygen species (ROS) was evaluated using 2′,7′-dichlorodiidrofluorescineacetate (DCFH-DA) (Molecular Probes, Eugene, OR). The oxidation kinetics was evaluated using the GloMax® Discover System (Promega) in a 96-multiwell plate incubated for 2 hours at 37°C at the excitation wavelength of 475 nm and emission wavelength 555 nm. After treatment, cells were analyzed with the microscope Leica Microsystems (Leica, Heidelberg, Germany). Results were compared with untreated cells, used as control.

2.8. ROS Generation and Mitochondrial Transmembrane Potential Modification. To assess ROS generation, the cells were incubated as mentioned above. Afterwards, cells were incubated with 1 mM DCFH-DA in PBS for 10 min at room temperature in the dark. After washing with PBS, the cells were analyzed by a fluorescence microscope (Axio Scope 2 microscope; Zeiss, Oberkochen, Germany) and a fluorimeter (Microplate reader WallacVictor 2 1420 Multilabel Counter; PerkinElmer Inc.) for fluorescence intensity. Then, cells were treated with 800 ng/μl of the AFA extract and incubated for 30 min at 37°C with 2 mM JC-1 using the MitoProbe JC-1 assay kit (Molecular Probes, Eugene, OR, USA) fluorescent dye. CCCP (carbonyl cyanide 3-chlorophenylhydrazone) (50 μm), a mitochondrial membrane potential disrupter, was used as positive control. Fluorescence emission shift of JC-1 from red (590 nm) to green (529 nm) was evaluated by fluorimeter (Microplate reader WallacVictor 2 1420 Multilabel Counter; PerkinElmer, Inc.) and fluorescence microscope (Axio Scope 2 microscope; Zeiss) equipped with 488 nm excitation laser. The mitochondrial production of superoxides was analyzed by fluorescence using the MitoSOX Red reagent. After the treatment, the cells were washed with PBS and incubated with 5 μM MitoSOX reagent working solution for 10 min at 37°C in the dark. At the end of the incubation, cells were washed in PBS and analyzed by fluorimeter. MitoSOX fluorescence was measured using supercontinuum white laser (Leica Microsystems CMS,

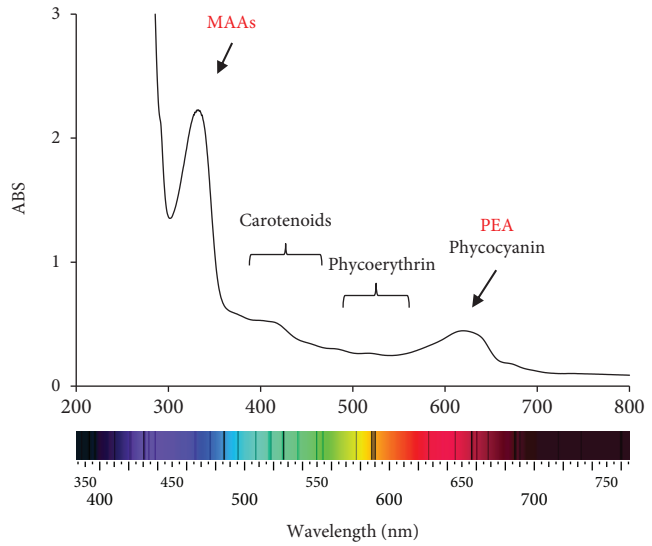

(a)

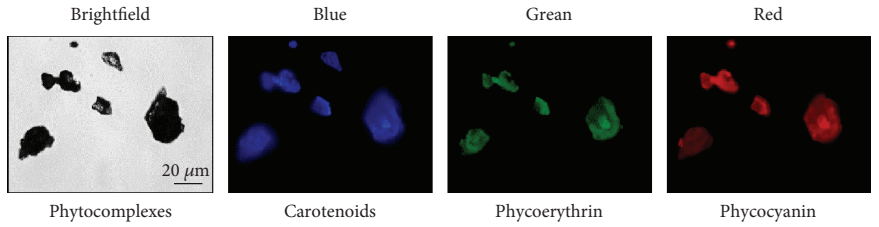

(b)

Elemets	AFA (ppm)
Ti	0.4
Mo	0.5
W	0.2
B	0.6
Al	1.5
Mn	2.2
Co	0.1
Ni	0.3
Zn	0.15
Cu	0.2
As	0.4
Se	0.06
Rb	0.25
Sr	4.5
Ba	0.5

(c)

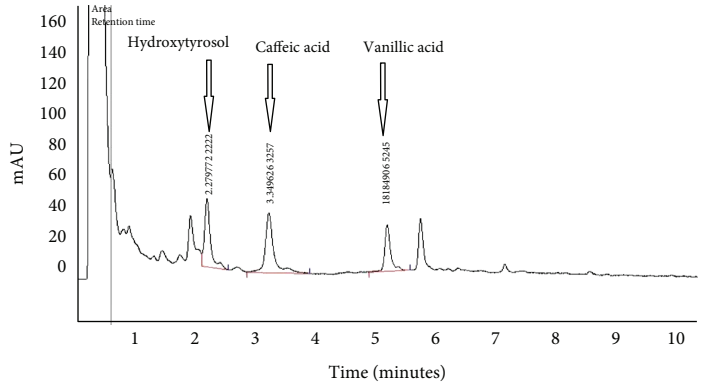

(d)

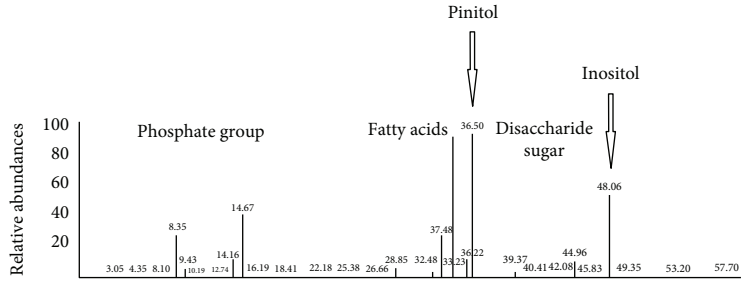

(e)

Figure 1: Hydrosoluble Klamin® extract compounds. (a) Spectrophotometric measure of the extract presenting different peaks of absorption both in the spectrum range between 310 and 360 nm (MAAs) and in the spectrum range of 400–600 nm. (b) Fluorescence analysis of phyco-complexes. (c) Spectrum of minerals obtained by ICP-MS analysis. (d) Phenolic components separated by HPLC. (e) Spectrum of carbohydrate obtained by GC-mass analysis.

Mannheim, Germany) at the excitation wavelength of 514 nm and recording the emission spectrum in the range 540–640 nm.

2.9. Immunofluorescence. 10^6/ml LAN5 cells were cultured on Lab-Tek II Chambered Coverglass (Nunc) and treated as described above. After washing in PBS, the cells were fixed in 4% paraformaldehyde for 30 min and stored at 4°C. After incubation with 3% BSA/PBS for 1 h, the cells were immunostained with anti-phosphorylated-NFκB (1 : 100; Cell Signaling) antibody at 4°C overnight. After washing in PBS, the samples were incubated with anti-rabbit Cy3-conjugate secondary antibody (1 : 500; Sigma). For nuclear staining, the cells were incubated with Hoechst 33258 (5 μg/ml) for 20 minutes. After washing, the cells were visualized by using a Leica DM5000 upright microscope (Leica Microsystems, Heidelberg, Germany) at 20x magnification.

2.10. ELISA. Supernatant of LAN5 cultured cells was centrifuged at 14,000 rpm for 30 min at 4°C. 100 μl of the supernatant were used to measure interleukin-1β and interleukin-6 (Cloud-Clone Corp) according to manufacturer's instructions. The samples were red on iMark™ Microplate Absorbance Reader at 450 nm.

2.11. Kinetics of Aβ Aggregation. Samples containing Aβ (40 μM) alone and Aβ with AFA extract (Aβ-AFA) (800 ng/μl) were placed in a 96 black multiwell plate at which thioflavin T (8 μM) was added. The kinetics was followed by using a fluorimeter at the wavelength of 485 nm at 37°C for 8 hours until the samples arrived to the plateau. The formation and mean size of Aβ aggregates was evaluated by using a fluorescence microscope (Leica Microsystems, Heidelberg, Germany).

2.12. Statistical Analysis. All experiments were repeated at least three times and each experiment was performed in triplicate. The results are presented as mean + SD. A one-way ANOVA was performed, followed by Bonferroni post hoc test for analysis of significance. Results with a p value < 0.05 were considered statistically significant.

3. Results

3.1. Characterization of the Water-Soluble Klamin® Extract. With the aim to test the biological effect of AFA compounds on *in vitro* cell culture, the extract was dissolved in PBS and submitted to different chemical analyses. Spectrophotometer absorption measures in the range between 310 and 360 nm indicated the presence of mycosporine-like amino acids (MAAs), whereas absorption in the spectrum range between 400 and 600 nm indicated the presence of carotenoids, phycoerythrins, and phycocyanins (Figure 1(a)). The presence of phyco-complexes was confirmed by using fluorescence microscope at different wavelengths, by using appropriate excitation and emission filters (Figure 1(b)).

By ICP-MS, a spectrum of minerals was identified and an unusual presence of molybdenum and tungsten was revealed (Figure 1(d)). The polyphenolic component was separated by HPLC, and peaks corresponding to hydroxytyrosol, vanillic acid, and caffeic acid were detected (Figure 1(d)). Presence of inositol and pinitol was revealed by GC-Mass spectrum (Figure 1(e)). Thus, the hydrosoluble Klamin® extract contains molecules with potential bioactive activity.

Table 1: Antioxidant capacity of the hydrosoluble Klamin® extract assayed by ORAC and F–C reducing capacity.

Test	Value
ORAC	86.54 ± 15.6 μmol TE/g
FOLIN	86 ± 11.4 mg/l

AFA extract antioxidant activity expressed as μmol of Trolox equivalents (TE) per gr of extract for ORAC assays and as mg of gallic acid equivalents per gr of extract for the Folin-Ciocalteu (F-C) assay are reported in Table 1.

3.2. Klamin® Is Not Cytotoxic. To evaluate the possible toxicity of the AFA extract, different concentrations were added to LAN5 cells, and after incubation at different times, an MTS assay was performed. Figure 2(a) shows that no toxicity was detected at all concentrations and times compared with the control. The result was confirmed by the morphological observation of the cells treated with the highest AFA extract concentration and incubated at different times (Figure 2(b)). Correct cell shape was observed and measures of the cell body confirmed the absence of any cell damage (Figure 2(c)).

3.3. Klamin® Prevents Oxidative Stress. The AFA extract protective property was evaluated by treating LAN5 cells with TBH alone or in combination with increasing concentrations of the AFA extract and after 3 hours of incubation. As detected by MTS assay, the AFA extract is able to inhibit TBH-induced toxicity at 50 ng/μl in a dose-dependent manner (Figure 3(a)); the results were also confirmed by microscopic observation in which a significant recovery of the altered cell morphology was observed (Figure 3(b)). Furthermore, Klamin® antioxidant ability was analyzed by using DCFH-DA assay. Presence of Klamin® decreases TBH-induced ROS generation at 800 ng/μl (Figure 3(c)). The result was also confirmed by fluorescence microscope inspection (Figure 3(d)), in which untreated, or AFA extract treated cells, did not show any fluorescence; in contrast, cells treated with TBH showed green fluorescence due to ROS generation. The result suggests that the components of AFA extract, such as carotenoids, phycoerythrins, phycocyanins, MAAs, and polyphenols, play a significant role as antioxidant agents.

The possible protective effect of the AFA extract on mitochondrial dysfunction was also evaluated. LAN5 cells treated with TBH and CCCP, as positive control, show an intense green fluorescence indicating that a high depolarization of the mitochondrial membrane is occurred. Cells cotreated with TBH and AFA extract, or alone with AFA extract, showed instead a higher red fluorescence emission similar to the untreated control (Figure 3(e)). The red/green fluorescence ratio is represented in the histogram in Figure 3(f).

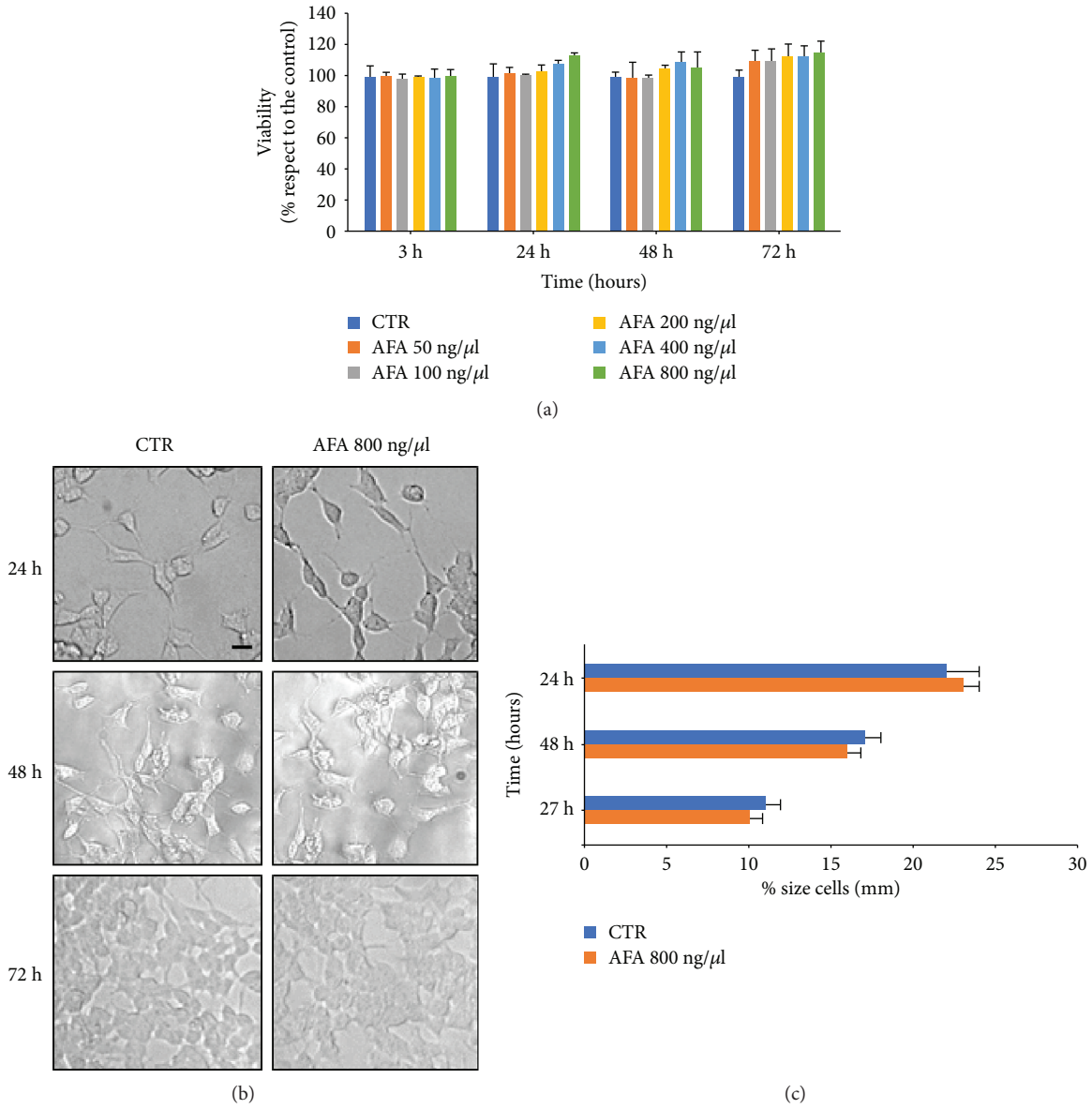

Figure 2: Cytotoxicity of the AFA extract on LAN5 cells. (a) MTS cell viability assay. (b) Representative morphological images of untreated cells (CTR) and after 24, 48, and 72 hours from the addition of 800 ng/μl of the extract. (c) Analysis of the body size of untreated cells (CTR) and cells treated with the AFA extract at different concentrations and times. Bar: 50 μm.

The ability of the AFA extract in counteracting the mitochondrial superoxide ions, generated as byproducts of oxidative phosphorylation, was investigated through MitoSOX assay. LAN5 cells treated with TBH exhibited a high fluorescence intensity. On the contrary, the cells treated with the AFA extract alone, or with TBH and Klamin®, do not show any fluorescent signal (Figure 3(g)). The fluorescence was quantified by fluorimeter analysis and illustrated in the relative histogram (Figure 3(h)). This data is in agreement with the presence of biomolecules such as hydroxytyrosol, vanillic acid, and caffeic acid in the AFA extract, whose antioxidant properties are well known, plus carotenoids and the specific cyanobacterial antioxidant molecules such as phycocyanins and phycoerythrins.

3.4. Klamin® Protects LAN5 Cells from Toxicity and Oxidative Stress Induced by Aβ. The potential neuroprotective effect of the AFA extract was evaluated by treating LAN5 cells with Aβ peptide alone and with two AFA extract concentrations and submitted to MTS assay. The Aβ-induced toxicity was inhibited by the coadministration of the AFA extract between 100 ng/μl and 800 ng/μl (Figure 4(a)). Observation of cell morphology confirmed the viability assay results (Figure 4(b)). The antioxidant capacity of AFA extract against the Aβ peptide-induced oxidative stress was evaluated by DCFH-DA assay. Fluorescence analysis indicated that cells treated with Aβ alone exhibit high levels of ROS generation, whereas cotreatment of Aβ and AFA extract (Aβ-AFA) did not produce any fluorescent

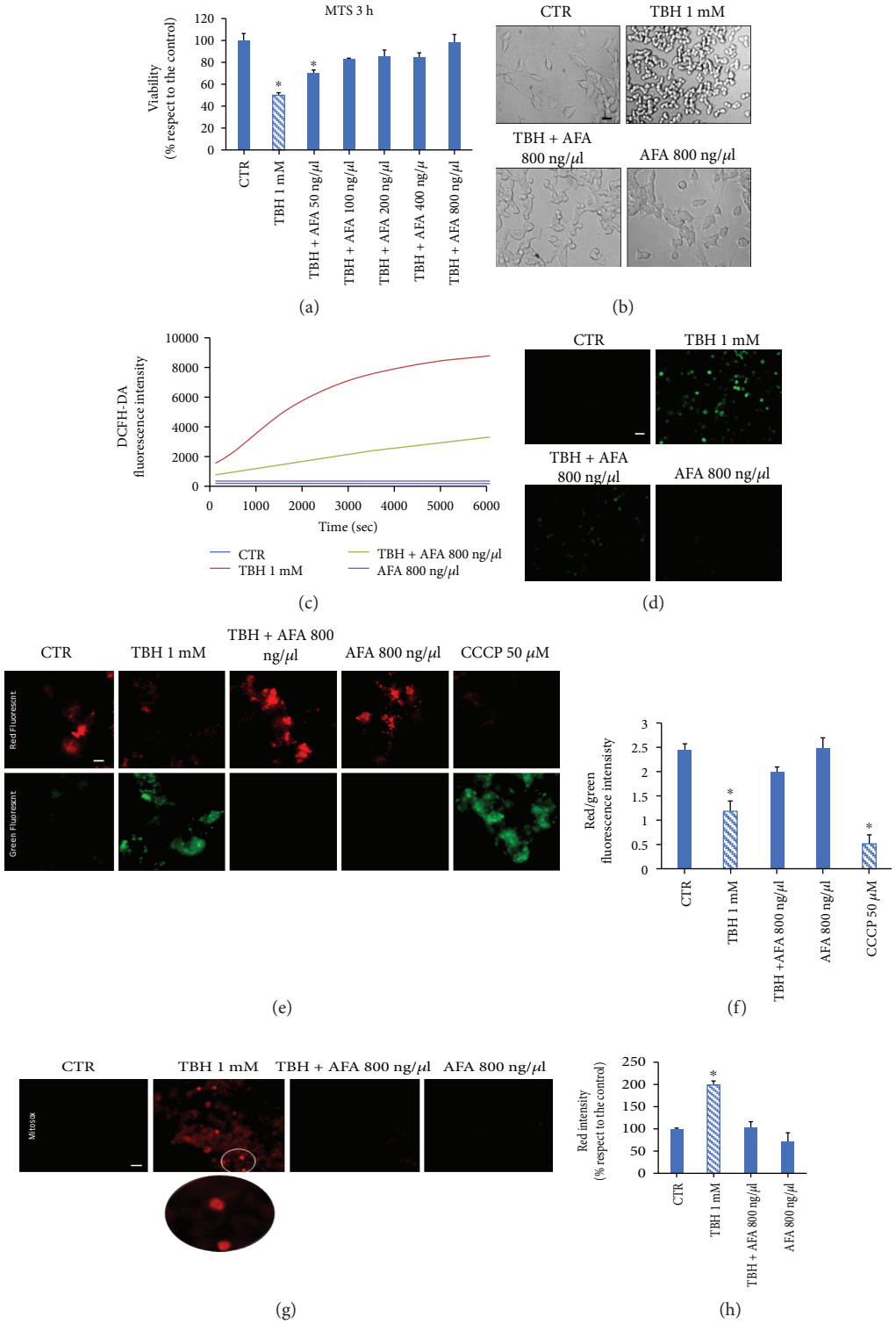

Figure 3: AFA extract protects LAN5 cells from oxidative insult. (a) Viability assay on untreated cells (CTR) or cells treated with TBH or cotreated with TBH and AFA extracts at increasing concentrations for 3 hours. (b) Representative morphological images of untreated cells (CTR) or cells treated with TBH or cotreated with TBH and the AFA extract and treated with the AFA extract. (c) Oxidation kinetics of LAN5 cells alone (CTR) or in the presence of TBH or TBH and AFA at two concentrations measured by the DCFH-DA assay. (d) Fluorescence microscopy images of untreated cells (CTR) and cells treated with TBH or cotreated with TBH and the AFA extract. Bar: 50 μm. AFA extract protects against mitochondrial damage. (e) Fluorescence microscope images of cells untreated (CTR) or treated with TBH alone or with the AFA extract or with CCCP and submitted to JC-1. (f) Values of the ratio between the red and green fluorescence intensities as compared with the control. (g) MitoSOX assay on control cells (CTR) and cells treated with TBH, with TBH and the AFA extract, with AFA alone, and with CCCP. (h) Histogram representing the red fluorescence intensity. Bar: 50 μm.

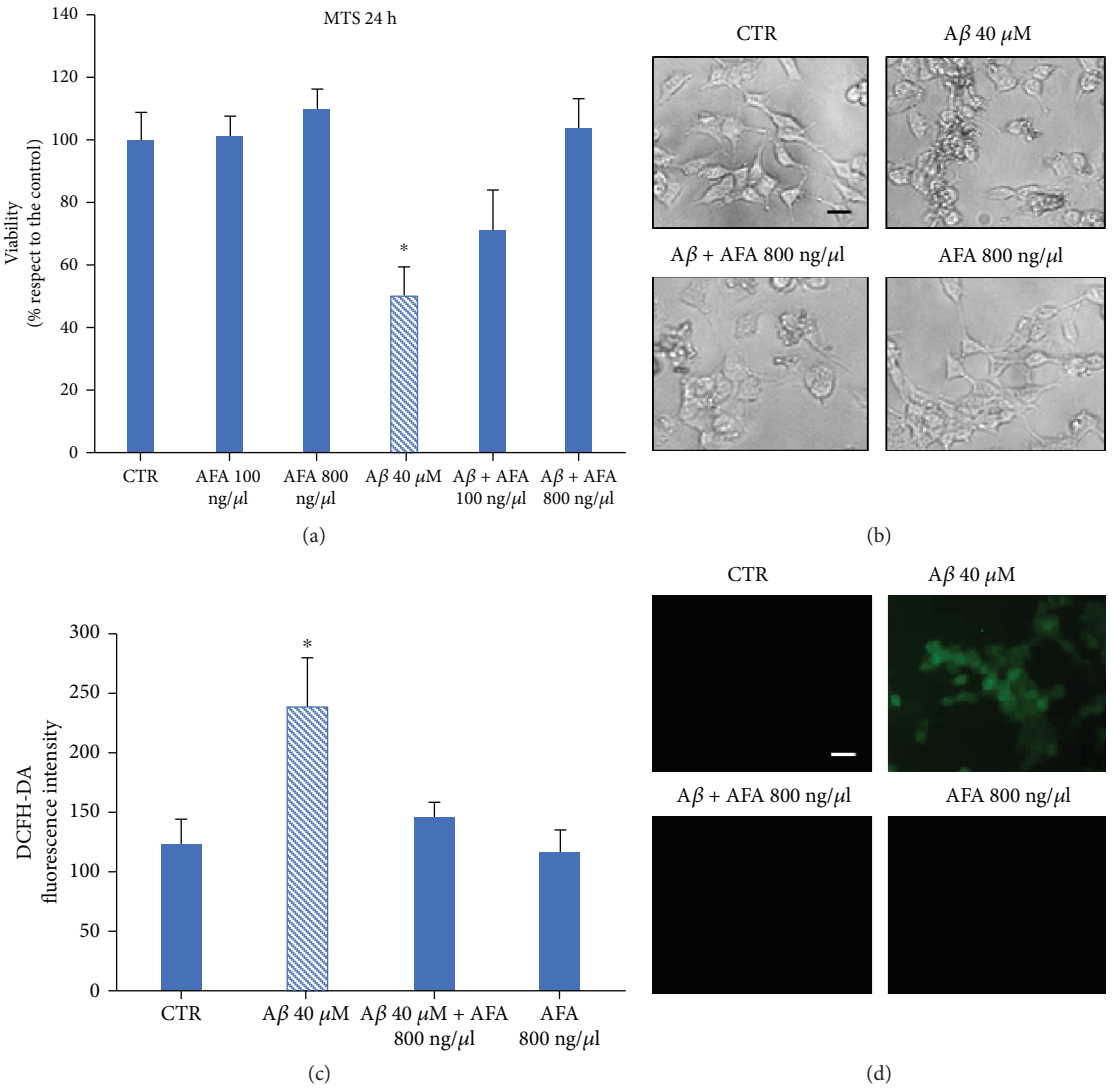

Figure 4: AFA protects against Aβ-induced toxicity. (a) MTS of untreated LAN5 cells (CTR) or cells treated with the AFA extract at two concentrations, with Aβ alone, or with Aβ-AFA at two concentrations for 24 hours. (b) Morphological representative images of samples indicated in (a). (c) DCFH-DA assay of untreated LAN5 cells (CTR) or cells treated with Aβ alone or with Aβ-AFA at two concentrations. (d) Fluorescence representative images of samples indicated in (c). Bar: 50 μm.

signal (Figure 4(d)). The same samples were observed at fluorescent microscopy (Figure 4(d)).

3.5. Neuroinflammation. NFκB is a transcription factor that under stimulation is phosphorylated and translocates from the cytoplasm to the nucleus where several genes including those triggering inflammation responses are activated. We assessed the ability of AFA to inhibit Aβ-induced inflammation by analyzing activated NFκB (p-NFκB) localization. Immunofluorescence analysis showed that after LAN5 Aβ stimulation, p-NFκB was localized in the nucleus, whereas after AFA or Aβ-AFA treatment, no presence of p-NFκB in the nuclei of the cells (Figure 5(a)) was detected. In addition, to take another evidence that Klamin® protects the cells against Aβ inflammatory response activation, the expression of cytokines1β and 6 (IL1β and IL6) was measured. The data shown in Figures 5(b) and 5(c) indicate that, in agreement with NFκB activation, the AFA extract significantly reduces the expression of proinflammatory cytokines.

3.6. Klamin® Affects Aβ Peptide Aggregation. The effect of the AFA extract on the aggregation kinetics of Aβ peptide was measured in presence of thioflavin T (ThT). Results, showed in Figure 6, indicated that the AFA extract interferes with the Aβ aggregation kinetics. Fluorescence microscopy analysis on samples containing Aβ alone, or Aβ plus AFA extract, was done at time O ($t = 0$ and after 8 hours ($t = 8$). At $t = 0$, no signal was detected in any samples (Figure 6(a)). At $t = 8$ in Aβ sample, a diffuse fluorescence is detectable and objects with an average size of about 90 μm were present (Figure 6(b)). On the contrary, a slight fluorescence was visible in Aβ + AFA extract sample in which

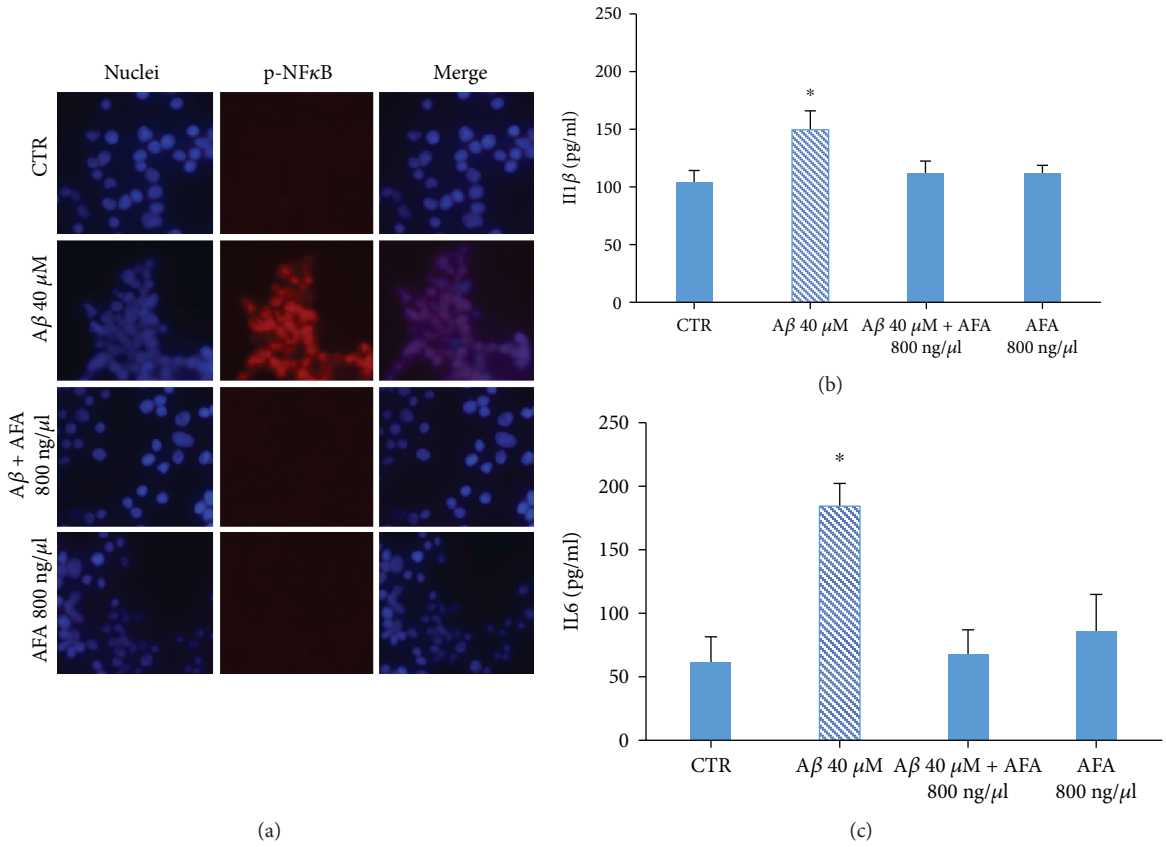

Figure 5: AFA extract inhibits Aβ-induced NFκB nuclear translocation. (a) Immunofluorescence of untreated LAN5 cells (CTR) or cells treated with Aβ, with Aβ-AFA, or AFA alone and incubated with an antibody against p-NFκB. (b–c) Measurement of the level of expression of IL-1β and IL-6 in untreated LAN5 cells (CTR) or cells treated with Aβ, with Aβ-AFA, or AFA alone, by the ELISA test.

objects having mean size of 50 μm was present (Figure 6(c)). These results reveal that the AFA extract affects Aβ aggregation inducing formation of smaller aggregates.

Furthermore, the toxicity and antioxidant ability of the Aβ aggregates formed in the absence or in the presence of the AFA extracts on LAN5 cells was evaluated through MTS (Figure 7(a)) and DCFH-DA assay (Figure 7(b)). Aggregates of Aβ peptide (A*βag*) caused a reduction of about 40% of cell viability when compared with the control. On the contrary, the addition of Aβ + Klamin® aggregates (Aβ-AFA*ag*) did not significantly affect cell viability. Microscope fluorescence images performed after DCFH-DA assay showed that a diffuse green fluorescent signal was mainly present in cells treated with A*βag* while no signal was revealed after treatments with Aβ + AFA*ag*. Furthermore, no significant morphological differences were observed from cells incubated with Aβ + AFA*ag* or control cells or cells treated with the AFA extract (Figure 7(b)).

4. Discussion

Cyanobacteria are a source of structurally different bioactive compounds with potential nutraceutical, pharmaceutical, and cosmeceutical employment [47]. The AFA extract Klamin® contains secondary metabolites such as MMAs, polyphenols, sugars, and different minerals. By spectrophotometer analysis, MMAs were detected in the UV absorbing range of 310–360 nm and carotenoids, phycoerythrins, and phycocyanins in the visible spectrum of light between 400 and 650 nm. MMAs are synthesized and accumulated by the algae as defense against exposition to environmental UV [48]. Use of high-resolution nuclear magnetic resonance (NMR) has evidenced in Klamin® a high concentration of MAAs and in particular of porphyra-334 (P334) and shinorine (Shi), two monoamine oxidase (MAO) inhibitors [49]. These molecules can cross the blood-brain barrier (BBB) and express their MAO-B inhibitory potential in the brain [20]. Most of the mycosporines exhibit high antioxidant activity by scavenging large amounts of reactive oxygen such as superoxide anions and hydroxyl radicals [50]. Thus, their antioxidant properties, born to contrast environmental stress, can be exploited to enhance human health. Molybdenum and tungsten, two transition metals, also known as enzymes cofactors [51, 52] were found in high concentration in Klamin® and, even though additional studies would be required, we can plausibly expect that they can activate biochemical pathways with a beneficial effect. Presence of polyphenols such as hydroxytyrosol, vanillic acid, caffeic acid; of phytosynthetic pigments such as carotenoids and phycoerythrins, endowed with well-known antioxidant properties: and most of all of the AFA-phycocyanins, which have shown to be the most powerful

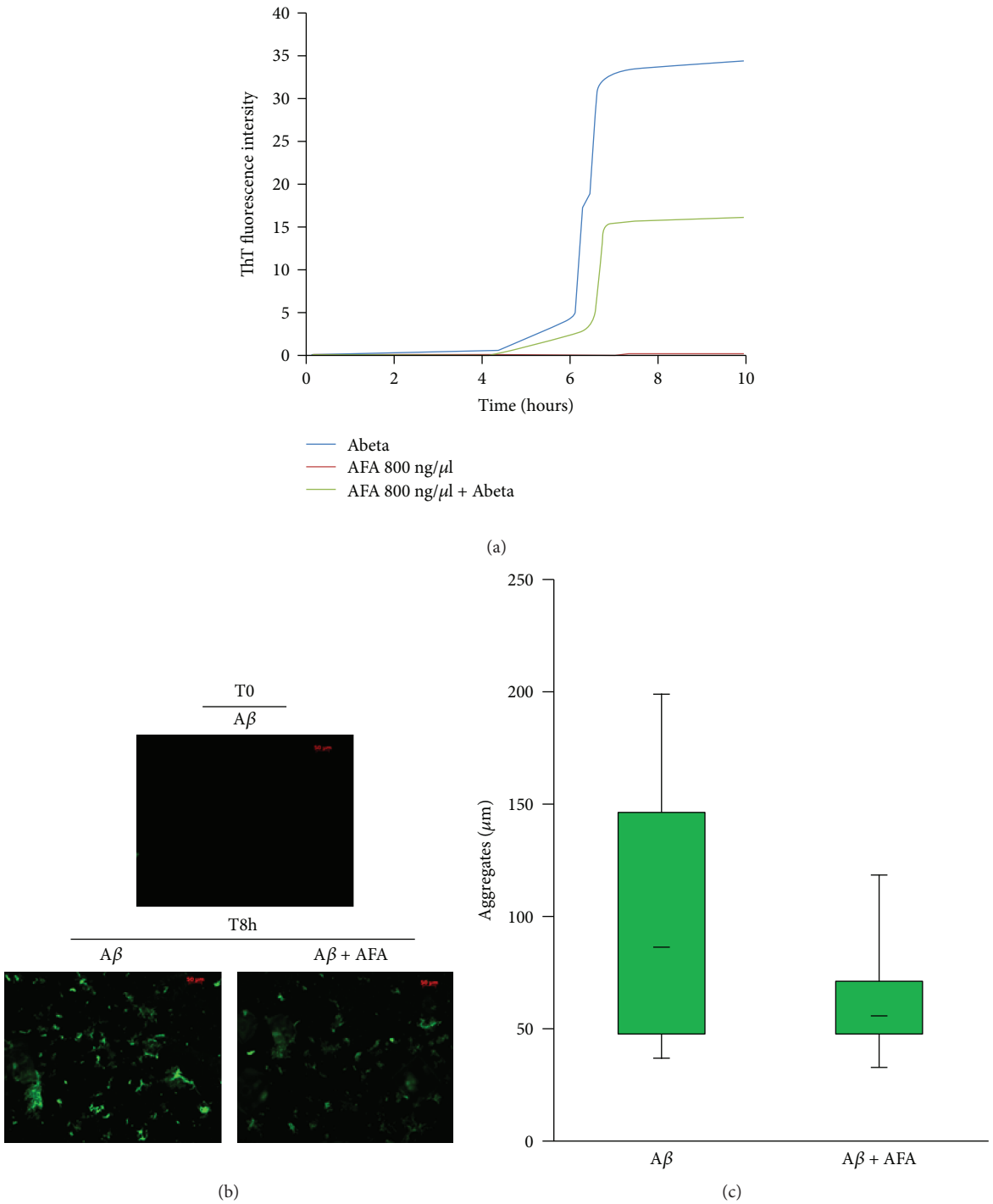

Figure 6: Effects of the AFA extract on Aβ aggregation. (a) Kinetics of Aβ aggregation alone or with AFA incubated with ThT. (b) Fluorescence microscopic images representing size and morphology of Aβ aggregates at $t = 0$ and $t = 8$ in the absence or presence of AFA. (c) Histogram of medium size of Aβ aggregates formed in the absence or presence of AFA at $t = 8$.

antioxidants among all purified molecules [14], suggests that the AFA extract can be regarded as a valuable resource for human nutrition and health.

Klamin® does not show any toxicological risks on the LAN5 cell line even at high doses, indicating that it does not contain any unhealthy by-products for this test. The radical scavenging activity of the AFA extract was confirmed by *in vitro* experiments in which an oxidant agent was used. The antioxidant activity found with the AFA extract is probably particularly strong thanks to the synergic effect of all its various components. TBH-induced mitochondrial dysfunction was also prevented by the administration of Klamin®, indicating that its scavenging effect is also extended to mitochondrial ROS. TBH-induced mitochondrial membrane damage is inhibited by Klamin®, indicating that it exerts a protective role in the

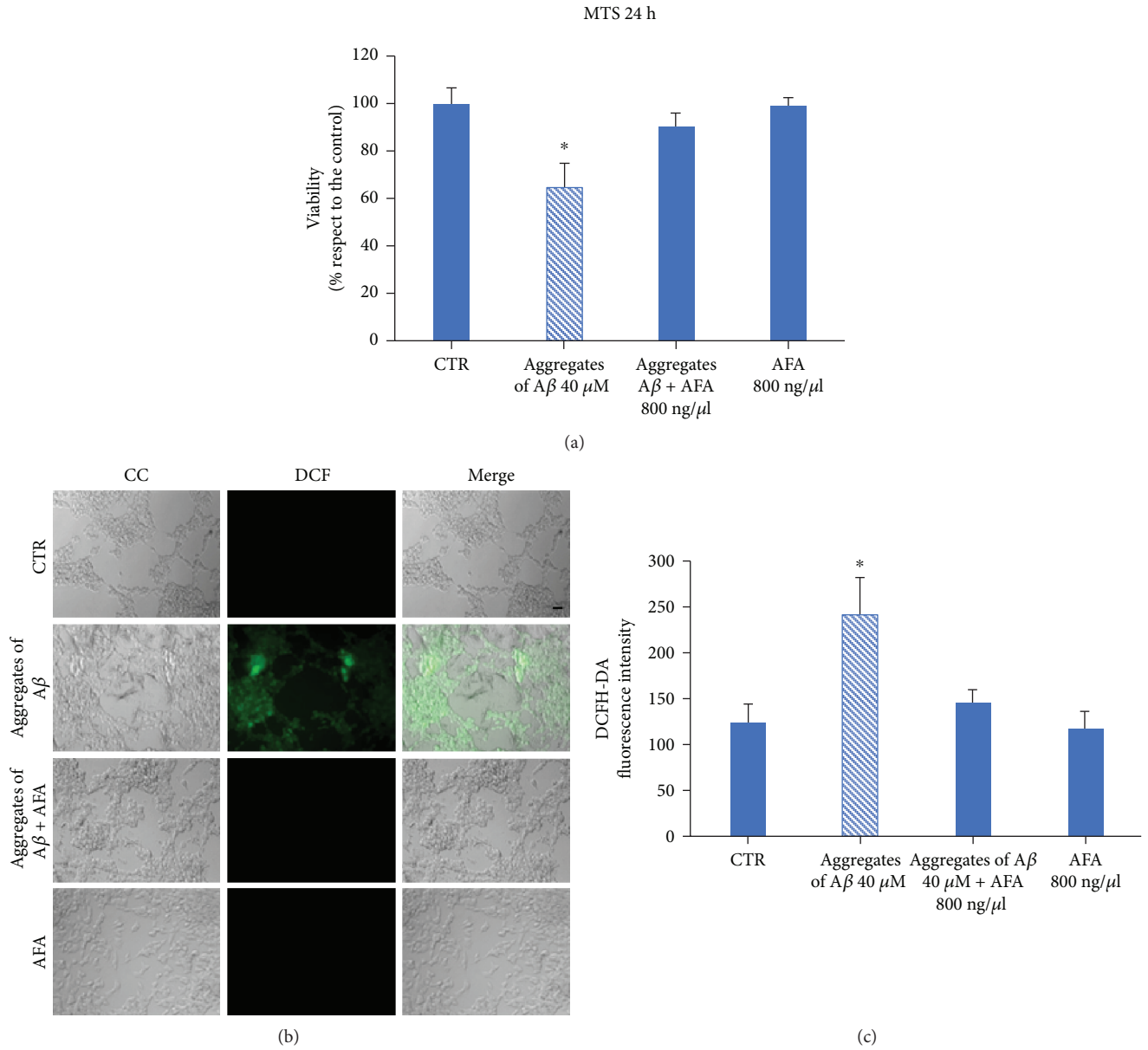

Figure 7: Aβ-AFA aggregates do not affect toxicity and oxidative stress. (a) MTS assay of untreated LAN5 cells (CTR) or cells treated with Aβ*ag*, Aβ-AFA*ag*, or AFA alone for 24 hours. (b) DCFH-DA assay of untreated LAN5 cells (CTR) or cells treated with Aβ*ag*, Aβ-AFA*ag*, or AFA alone. (c) Fluorescence intensity of the samples shown in (b). Barr: 20 μm.

cell's fundamental organelle, involved in several pathological dysfunctions.

Free radical generation is one of the main causes of aging and aging-related diseases in humans, and antioxidants may have a positive antiaging effect [53]. The use of natural nutritional supplement could be an important milestone for the prevention and treatment of neurodegenerative diseases. Here, we found, for the first time, that the AFA extract Klamin® has a beneficial effect on neurons in which toxicity was induced by Aβ peptide, suggesting that the AFA extract, consumed as a nutraceutical, could play a significant neuroprotective role. Furthermore, the AFA extract exerts anti-inflammatory activity as a response to Aβ toxic stimulus. Inflammation is a pathological mechanism underlying many chronical diseases, including neurodegenerative diseases, and chronic inflammation have been found in the brain of early AD [54]. The anti-inflammatory function of the molecular components of Klamin® is mediated by its inhibition of the nuclear factor kappa B (NFκB) activation and by its decreasing the production of proinflammatory cytokines such as IL-6 and IL-1β. However, we cannot exclude that Klamin® neuroprotective activity can be exerted through other components. By molecular docking, simulation studies have been demonstrated that phlorotannins derived from Eisenia bicyclis, a Japanese alga, can be a potential inhibitor of β-amyloid cleavage enzyme (BACE1) activity, a protease involved in Aβ formation [55].

Fibrillogenesis of Aβ is a relevant event, leading to deposition of amyloid plaques in AD brain. Use of inhibitors can prevent this process [56]. Klamin® interferes on Aβ aggregation stabilizing Aβ aggregates in a protective way to reduce oxidative stress. The kinetics of amyloid formation can be described in a sigmoid curve subdivided in three stages: (a) the slow lag nucleation phase, (b) the fast-exponential elongation phase, and (c) the saturation phase. Klamin® blocks the elongation phase, producing aggregates of shorter dimensions. We can suppose that the various antioxidant components of AFA extract, from its polyphenols to its phycocyanins, interact with Aβ, inhibiting its extension and destabilizing the preformed fibrils. It is known that antioxidants, containing one or more phenolic rings, are able to interact with the aromatic residues of the amyloid peptides, destabilizing their well-ordered self-assembly process [37]. Thus, Klamin® could have a disaggregating activity on Aβ.

In conclusion, Klamin® is a reservoir of effective molecules with numerous health benefits. The intrinsic antioxidant, anti-inflammatory, and antifibrillogenesis properties of its compounds suggest that it could be used as an innovative approach for the treatment and/or prevention of neurodegenerative disease.

Data Availability

The data used to support the findings of this study are available from the corresponding author upon request.

Disclosure

Neither the funding agency nor any outside organization has participated in the study design or have any competing of interest.

Conflicts of Interest

The authors declare that there is no conflict of interests regarding the publication of this paper. Dr. Stefano Scoglio is the owner and manager of the Nutrigea company that provided us the Klamath. The research was funded by Nutrigea. Nutrigea had the final approval of the manuscript.

Acknowledgments

The authors wish to thank Dr. Alessia Provenzano and Mister Luca Caruana for their useful technical support.

References

[1] T. L. Hamilton, D. A. Bryant, and J. L. Macalady, "The role of biology in planetary evolution: cyanobacterial primary production in low-oxygen Proterozoic oceans," *Environmental Microbiology*, vol. 18, no. 2, pp. 325–340, 2016.

[2] W. K. Dodds, D. A. Gudder, and D. Mollenhauer, "The ecology of Nostoc," *Journal of Phycology*, vol. 31, no. 1, pp. 2–18, 1995.

[3] H. Choi, S. J. Mascuch, F. A. Villa et al., "Honaucins A–C, potent inhibitors of inflammation and bacterial quorum sensing: synthetic derivatives and structure-activity relationships," *Chemistry & Biology*, vol. 19, no. 5, pp. 589–598, 2012.

[4] E. Christaki, P. Florou-Paneri, and E. Bonos, "Microalgae: a novel ingredient in nutrition," *International Journal of Food Sciences and Nutrition*, vol. 62, no. 8, pp. 794–799, 2011.

[5] C. S. Ku, Y. Yang, Y. Park, and J. Lee, "Health benefits of blue-green algae: prevention of cardiovascular disease and nonalcoholic fatty liver disease," *Journal of Medicinal Food*, vol. 16, no. 2, pp. 103–111, 2013.

[6] C. M. Reddy, V. B. Bhat, G. Kiranmai, M. N. Reddy, P. Reddanna, and K. M. Madyastha, "Selective inhibition of cyclooxygenase-2 by C-phycocyanin, a biliprotein from Spirulina platensis," *Biochemical and Biophysical Research Communications*, vol. 277, no. 3, pp. 599–603, 2000.

[7] C. Romay, J. Armesto, D. Remirez, R. González, N. Ledon, and I. García, "Antioxidant and anti-inflammatory properties of C-phycocyanin from blue-green algae," *Inflammation Research*, vol. 47, no. 1, pp. 36–41, 1998.

[8] C. Romay, N. Ledón, and R. González, "Further studies on anti-inflammatory activity of phycocyanin in some animal models of inflammation," *Inflammation Research*, vol. 47, no. 8, pp. 334–338, 1998.

[9] L. Baroni, S. Scoglio, S. Benedetti et al., "Effect of a Klamath algae product ("AFA-B12") on blood levels of vitamin B12 and homocysteine in vegan subjects: a pilot study," *International Journal for Vitamin and Nutrition Research*, vol. 79, no. 2, pp. 117–123, 2009.

[10] R. Pawlak, S. E. Lester, and T. Babatunde, "The prevalence of cobalamin deficiency among vegetarians assessed by serum vitamin B12: a review of literature," *European Journal of Clinical Nutrition*, vol. 68, no. 5, pp. 541–548, 2014.

[11] R. I. Kushak, C. Drapeau, and H. D. Winter, "The effect of blue-green algae *Aphanizomenon Flos Aquae* on nutrient assimilation in rats," *JANA*, vol. 3, pp. 35–39, 2001.

[12] J. P. Kamat, K. K. Boloor, and T. P. A. Devasagayam, "Chlorophyllin as an effective antioxidant against membrane damage in vitro and ex vivo," *Biochimica et Biophysica Acta (BBA) - Molecular and Cell Biology of Lipids*, vol. 1487, no. 2-3, pp. 113–127, 2000.

[13] S. Rinalducci, P. Roepstorff, and L. Zolla, "*De novo* sequence analysis and intact mass measurements for characterization of phycocyanins subunit isoforms from the blue-green alga *Aphanizomenon flos-aquae*," *Journal of Mass Spectrometry*, vol. 44, no. 4, pp. 503–515, 2009.

[14] S. Benedetti, F. Benvenuti, S. Scoglio, and F. Canestrari, "Oxygen radical absorbance capacity of phycocyanin and phycocyanobilin from the food supplement *Aphanizomenon flos-aquae*," *Journal of Medicinal Food*, vol. 13, no. 1, pp. 223–227, 2010.

[15] A. Cavalchini and S. Scoglio, "Complementary treatment of psoriasis with an AFA-phyocyanins product: a preliminary 10-cases study," *International Medical Journal*, vol. 16, pp. 221–224, 2009.

[16] S. Scoglio, V. Lo Curcio, S. Catalani, F. Palma, S. Battistelli, and S. Benedetti, "Inhibitory effects of *Aphanizomenon flos-aquae* constituents on human UDP-glucose dehydrogenase activity," *Journal of Enzyme Inhibition and Medicinal Chemistry*, vol. 31, no. 6, pp. 1492–1497, 2016.

[17] M. Federici, R. Geracitano, A. Tozzi et al., "Trace amines depress $GABA_B$ response in dopaminergic neurons by inhibiting G-$\beta\gamma$-gated inwardly rectifying potassium channels," *Molecular Pharmacology*, vol. 67, no. 4, pp. 1283–1290, 2005.

[18] H. C. Sabelli and A. D. Mosnaim, "Phenylethylamine hypothesis of affective behavior," *American Journal of Psychiatry*, vol. 131, no. 6, pp. 695–699, 1974.

[19] H. Sabelli, P. Fink, J. Fawcett, and C. Tom, "Sustained antidepressant effect of PEA replacement," *The Journal of Neuropsychiatry and Clinical Neurosciences*, vol. 8, no. 2, pp. 168–171, 1996.

[20] S. Scoglio, Y. Benedetti, F. Benvenuti, S. Battistelli, F. Canestrari, and S. Benedetti, "Selective monoamine oxidase B inhibition by an *Aphanizomenon flos-aquae* extract and by its constitutive active principles phycocyanin and mycosporine-like amino acids," *Phytomedicine*, vol. 21, no. 7, pp. 992–997, 2014.

[21] A. D. Genazzani, E. Chierchia, C. Lanzoni et al., "Effects of Klamath algae extract on psychological disorders and depression in menopausal women: a pilot study," *Minerva Ginecologica*, vol. 62, no. 5, pp. 381–388, 2010.

[22] P. Bellingeri, M. Bonucci, and S. Scoglio, "Complementary treatment of mood disturbances in terminally ill oncological patients with the Aphanizomenon flos aquae extract Klamin®," *Advances in Complementary and Alternative Medicine*, vol. 1, pp. 1–5, 2018.

[23] M. Cremonte, D. Sisti, I. Maraucci et al., "Complementary and alternative supplementation with the Klamath algae extract Klamin® on attention deficit/hyperactivity disorder," *Journal of Medicinal Food*, vol. 20, pp. 1233–1239, 2017.

[24] S. Sedriep, X. Xia, F. Marotta et al., "Beneficial nutraceutical modulation of cerebral erythropoietin expression and oxidative stress: an experimental study," *Journal of Biological Regulators and Homeostatic Agents*, vol. 25, no. 2, pp. 187–194, 2011.

[25] A. Babusyte, M. Kotthoff, J. Fiedler, and D. Krautwurst, "Biogenic amines activate blood leukocytes via trace amine-associated receptors TAAR1 and TAAR2," *Journal of Leukocyte Biology*, vol. 93, no. 3, pp. 387–394, 2013.

[26] M. Robinson, B. Y. Lee, and F. T. Hane, "Recent progress in Alzheimer's disease research, part 2: genetics and epidemiology," *Journal of Alzheimer's Disease*, vol. 57, no. 2, pp. 317–330, 2017.

[27] M. D. Hurd, P. Martorell, A. Delavande, K. J. Mullen, and K. M. Langa, "Monetary costs of dementia in the United States," *The New England Journal of Medicine*, vol. 368, no. 14, pp. 1326–1334, 2013.

[28] T. Rapp, B. H. Apouey, C. Senik, and REAL.FR/DSA group, "The impact of institution use on the wellbeing of Alzheimer's disease patients and their caregivers," *Social Science & Medicine*, vol. 207, pp. 1–10, 2018.

[29] J. M. Zissimopoulos, B. C. Tysinger, P. A. St.Clair, and E. M. Crimmins, "The impact of changes in population health and mortality on future prevalence of Alzheimer's disease and other dementias in the United States," *The Journals of Gerontology: Series B*, vol. 73, Supplement 1, pp. S38–S47, 2018.

[30] W. L. Klein, W. B. Stine Jr., and D. B. Teplow, "Small assemblies of unmodified amyloid β-protein are the proximate neurotoxin in Alzheimer's disease," *Neurobiology of Aging*, vol. 25, no. 5, pp. 569–580, 2004.

[31] R. Castellani, K. Hirai, G. Aliev et al., "Role of mitochondrial dysfunction in Alzheimer's disease," *Journal of Neuroscience Research*, vol. 70, no. 3, pp. 357–360, 2002.

[32] P. Picone, R. Carrotta, G. Montana, M. R. Nobile, P. L. San Biagio, and M. di Carlo, "Aβ oligomers and fibrillar aggregates induce different apoptotic pathways in LAN5 neuroblastoma cell cultures," *Biophysical Journal*, vol. 96, no. 10, pp. 4200–4211, 2009.

[33] P. Picone, D. Giacomazza, V. Vetri et al., "Insulin-activated Akt rescues Aβ oxidative stress-induced cell death by orchestrating molecular trafficking," *Aging Cell*, vol. 10, no. 5, pp. 832–843, 2011.

[34] P. Picone, D. Nuzzo, L. Caruana, V. Scafidi, and M. di Carlo, "Mitochondrial dysfunction: different routes to Alzheimer's disease therapy," *Oxidative Medicine and Cellular Longevity*, vol. 2014, Article ID 780179, 11 pages, 2014.

[35] D. Nuzzo, L. Inguglia, J. Walters, P. Picone, and M. Di Carlo, "A shotgun proteomics approach reveals a new toxic role for Alzheimer's disease Aβ peptide: spliceosome impairment," *Journal of Proteome Research*, vol. 16, no. 4, pp. 1526–1541, 2017.

[36] D. Nuzzo, P. Picone, L. Caruana et al., "Inflammatory mediators as biomarkers in brain disorders," *Inflammation*, vol. 37, no. 3, pp. 639–648, 2014.

[37] A. Sgarbossa, D. Giacomazza, and M. Di Carlo, "Ferulic acid: a hope for Alzheimer's disease therapy from plants," *Nutrients*, vol. 7, no. 7, pp. 5764–5782, 2015.

[38] P. Picone, M. L. Bondi, P. Picone et al., "Ferulic acid inhibits oxidative stress and cell death induced by Ab oligomers: improved delivery by solid lipid nanoparticles," *Free Radical Research*, vol. 43, no. 11, pp. 1133–1145, 2009.

[39] P. Picone, D. Nuzzo, and M. Di Carlo, "Ferulic acid: a natural antioxidant against oxidative stress induced by oligomeric A-beta on sea urchin embryo," *The Biological Bulletin*, vol. 224, no. 1, pp. 18–28, 2013.

[40] R. Kahl and H. Kappus, "Toxicology of the synthetic antioxidants BHA and BHT in comparison with the natural antioxidant vitamin E," *Zeitschrift für Lebensmittel-Untersuchung und -Forschung*, vol. 196, no. 4, pp. 329–338, 1993.

[41] I. Ignat, I. Volf, and V. I. Popa, "A critical review of methods for characterisation of polyphenolic compounds in fruits and vegetables," *Food Chemistry*, vol. 126, no. 4, pp. 1821–1835, 2011.

[42] M. Naczk and F. Shahidi, "Extraction and analysis of phenolics in food," *Journal of Chromatography A*, vol. 1054, no. 1-2, pp. 95–111, 2004.

[43] E. Rojas-Escudero, A. L. Alarcón-Jiménez, P. Elizalde-Galván, and F. Rojo-Callejas, "Optimization of carbohydrate silylation for gas chromatography," *Journal of Chromatography A*, vol. 1027, no. 1-2, pp. 117–120, 2004.

[44] P. Ninfali, A. Chiarabini, and D. Angelino, "The ORAC/kcal ratio qualifies nutritional and functional properties of fruit juices, nectars, and fruit drinks," *International Journal of Food Sciences and Nutrition*, vol. 65, no. 6, pp. 708–712, 2014.

[45] G. Cao, H. M. Alessio, and R. G. Cutler, "Oxygen-radical absorbance capacity assay for antioxidants," *Free Radical Biology & Medicine*, vol. 14, no. 3, pp. 303–311, 1993.

[46] R. Carrotta, M. Di Carlo, M. Manno et al., "Toxicity of recombinant β-amyloid prefibrillar oligomers on the morphogenesis of the sea urchin *Paracentrotus lividus*," *The FASEB Journal*, vol. 20, no. 11, pp. 1916-1917, 2006.

[47] J. T. Hafting, J. S. Craigie, D. B. Stengel et al., "Prospects and challenges for industrial production of seaweed bioactives," *Journal of Phycology*, vol. 51, no. 5, pp. 821–837, 2015.

[48] J. M. Shick and W. C. Dunlap, "Mycosporine-like amino acids and related gadusols: biosynthesis, accumulation, and

UV-protective functions in aquatic organisms," *Annual Review of Physiology*, vol. 64, no. 1, pp. 223–262, 2002.

[49] S. Scoglio, F. Canestrari, S. Benedetti, Y. Benedetti, and M. Delgado-Esteban, "Alphanizomenon flos aquae preparation, extracts and purified components thereof for the treatment of neurological, neurodegenerative and mood disorders," US Patent WO2008000430, 2008.

[50] N. Wada, T. Sakamoto, and S. Matsugo, "Multiple roles of photosynthetic and sunscreen pigments in cyanobacteria focusing on the oxidative stress," *Metabolites*, vol. 3, no. 2, pp. 463–483, 2013.

[51] R. Hille, "Molybdenum and tungsten in biology," *Trends in Biochemical Sciences*, vol. 27, no. 7, pp. 360–367, 2002.

[52] M. J. Pushie and G. N. George, "Spectroscopic studies of molybdenum and tungsten enzymes," *Coordination Chemistry Reviews*, vol. 255, no. 9-10, pp. 1055–1084, 2011.

[53] D. Harman, "Aging: a theory based on free radical and radiation chemistry," *Journal of Gerontology*, vol. 11, no. 3, pp. 298–300, 1956.

[54] I. Blasko, M. Stampfer-Kountchev, P. Robatscher, R. Veerhuis, P. Eikelenboom, and B. Grubeck-Loebenstein, "How chronic inflammation can affect the brain and support the development of Alzheimer's disease in old age: the role of microglia and astrocytes," *Aging Cell*, vol. 3, no. 4, pp. 169–176, 2004.

[55] H. A. Jung, S. H. Oh, and J. S. Choi, "Molecular docking studies of phlorotannins from *Eisenia bicyclis* with BACE1 inhibitory activity," *Bioorganic & Medicinal Chemistry Letters*, vol. 20, no. 11, pp. 3211–3215, 2010.

[56] D. M. Walsh, A. Lomakin, G. B. Benedek, M. M. Condron, and D. B. Teplow, "Amyloid β-protein fibrillogenesis. Detection of a protofibrillar intermediate," *Journal of Biological Chemistry*, vol. 272, no. 35, pp. 22364–22372, 1997.